U.S.NRC
United States Nuclear Regulatory Commission
Protecting People and the Environment

NUREG/CR-7153, Vol. 2
ORNL/TM-2013/532

Expanded Materials Degradation Assessment (EMDA)

Volume 2: Aging of Core Internals and Piping Systems

Office of Nuclear Regulatory Research

AVAILABILITY OF REFERENCE MATERIALS IN NRC PUBLICATIONS

NRC Reference Material

As of November 1999, you may electronically access NUREG-series publications and other NRC records at NRC's Public Electronic Reading Room at http://www.nrc.gov/reading-rm.html. Publicly released records include, to name a few, NUREG-series publications; *Federal Register* notices; applicant, licensee, and vendor documents and correspondence; NRC correspondence and internal memoranda; bulletins and information notices; inspection and investigative reports; licensee event reports; and Commission papers and their attachments.

NRC publications in the NUREG series, NRC regulations, and Title 10, "Energy," in the *Code of Federal Regulations* may also be purchased from one of these two sources.

1. The Superintendent of Documents
   U.S. Government Printing Office
   Mail Stop SSOP
   Washington, DC 20402–0001
   Internet: bookstore.gpo.gov
   Telephone: 202-512-1800
   Fax: 202-512-2250
2. The National Technical Information Service
   Springfield, VA 22161–0002
   www.ntis.gov
   1–800–553–6847 or, locally, 703–605–6000

A single copy of each NRC draft report for comment is available free, to the extent of supply, upon written request as follows:

Address: U.S. Nuclear Regulatory Commission
Office of Administration
Publications Branch
Washington, DC 20555-0001
E-mail: DISTRIBUTION.RESOURCE@NRC.GOV
Facsimile: 301–415–2289

Some publications in the NUREG series that are posted at NRC's Web site address http://www.nrc.gov/reading-rm/doc-collections/nuregs are updated periodically and may differ from the last printed version. Although references to material found on a Web site bear the date the material was accessed, the material available on the date cited may subsequently be removed from the site.

Non-NRC Reference Material

Documents available from public and special technical libraries include all open literature items, such as books, journal articles, transactions, *Federal Register* notices, Federal and State legislation, and congressional reports. Such documents as theses, dissertations, foreign reports and translations, and non-NRC conference proceedings may be purchased from their sponsoring organization.

Copies of industry codes and standards used in a substantive manner in the NRC regulatory process are maintained at—

The NRC Technical Library
Two White Flint North
11545 Rockville Pike
Rockville, MD 20852–2738

These standards are available in the library for reference use by the public. Codes and standards are usually copyrighted and may be purchased from the originating organization or, if they are American National Standards, from—

American National Standards Institute
11 West 42nd Street
New York, NY 10036–8002
www.ansi.org
212–642–4900

Legally binding regulatory requirements are stated only in laws; NRC regulations; licenses, including technical specifications; or orders, not in NUREG-series publications. The views expressed in contractor-prepared publications in this series are not necessarily those of the NRC.

The NUREG series comprises (1) technical and administrative reports and books prepared by the staff (NUREG–XXXX) or agency contractors (NUREG/CR–XXXX), (2) proceedings of conferences (NUREG/CP–XXXX), (3) reports resulting from international agreements (NUREG/IA–XXXX), (4) brochures (NUREG/BR–XXXX), and (5) compilations of legal decisions and orders of the Commission and Atomic and Safety Licensing Boards and of Directors' decisions under Section 2.206 of NRC's regulations (NUREG–0750).

U.S.NRC
United States Nuclear Regulatory Commission
Protecting People and the Environment

NUREG/CR-7153, Vol. 2
ORNL/TM-2013/532

Expanded Materials Degradation Assessment (EMDA)

Volume 2: Aging of Core Internals and Piping Systems

Manuscript Completed: October 2013
Date Published: October 2014

Prepared by Expert Panel
Peter Andresen, General Electric; Koji Arioka, Institute of Nuclear Safety Systems; Steve Bruemmer, Pacific Northwest National Laboratory; Jeremy Busby, Oak Ridge National Laboratory; Robin Dyle, Electric Power Research Institute; Peter Ford, General Electric-Retired, Karen Gott, Swedish Nuclear Power Inspectorate-Retired; Amy Hull, U.S. Nuclear Regulatory Commission; and Roger Staehle, Staehle Consulting

On behalf of
Oak Ridge National Laboratory
Managed by UT-Battelle, LLC

J. T. Busby, DOE-NE LWRS EMDA Lead

P. G. Oberson and C. E. Carpenter, NRC Project Managers
M. Srinivasan, NRC Technical Monitor

Office of Nuclear Regulatory Research

ABSTRACT

In NUREG/CR-6923, "Expert Panel Report on Proactive Materials Degradation Assessment," referred to as the PMDA report, NRC conducted a comprehensive evaluation of potential aging-related degradation modes for core internal components, as well as primary, secondary, and some tertiary piping systems, considering operation up to 40 years. This document has been a very valuable resource, supporting NRC staff evaluations of licensees' aging management programs and allowing for prioritization of research needs.

This report describes an expanded materials degradation assessment (EMDA), which significantly broadens the scope of the PMDA report. The analytical timeframe is expanded to 80 years to encompass a potential second 20-year license-renewal operating-period, beyond the initial 40-year licensing term and a first 20-year license renewal. Further, a broader range of structures, systems, and components (SSCs) was evaluated, including core internals, piping systems, the reactor pressure vessel (RPV), electrical cables, and concrete and civil structures. The EMDA uses the approach of the phenomena identification and ranking table (PIRT), wherein an expert panel is convened to rank potential degradation scenarios according to their judgment of susceptibility and current state of knowledge. The PIRT approach used in the PMDA and EMDA has provided the following benefits:

- Captured the status of current knowledge base and updated PMDA information,
- Identified gaps in knowledge for a SSC or material that need future research,
- Identified potential new forms of degradation, and
- Identified and prioritized research needs.

As part of the EMDA activity, four separate expert panels were assembled to assess four main component groups, each of which is the subject of a volume of this report.

- Core internals and piping systems (i.e., materials examined in the PMDA report) – Volume 2
- Reactor pressure vessel steels (RPV) – Volume 3
- Concrete civil structures – Volume 4
- Electrical power and instrumentation and control (I&C) cabling and insulation – Volume 5

This volume summarizes the results of expert panel assessment of the aging and degradation of core internals and piping materials of nuclear power plants (NPPs). The work was conducted via a partnership between the NRC and the DOE's Light Water Reactor Sustainability (LWRS) program to extend NRC's Proactive Materials Degradation Assessment (PMDA), NUREG/CR-6923. The main objective of the work described herein was to identify core internal and primary piping components of NPPs where degradation is likely to occur, or may have occurred, to define relevant aging and degradation modes and mechanisms, and to perform systematic assessment of the effects of this aging related degradation on the future life of those components, drawing on the knowledge and expertise of the above-cited panel. The approach adopted by the panel is based on the Phenomena Identification and Ranking Table (PIRT) process.

FOREWORD

According to the provisions of Title 10 of the *Code of Federal Regulations* (CFR), Part 54, "Requirements for Renewal of Operating Licenses for Nuclear Power Plants," licensees may apply for twenty-year renewals of their operating license following the initial forty-year operating period. The majority of plants in the United States have received the first license renewal to operate from forty to sixty years and a number of plants have already entered the period of extended operation. Therefore, licensees are now assessing the economic and technical viability of a second license renewal to operate safely from sixty to eighty years. The requirements of 10 CFR, Part 54 include the identification of passive, long-lived structures, systems, and components which may be subject to aging-related degradation, and the development of aging management programs (AMPs) to ensure that their safety function is maintained consistent with the licensing basis during the extended operating period. NRC guidance on the scope of AMPs is found in NUREG-1800 "Standard Review Plan for Review of License Renewal Applications for Nuclear Power Plants" (SRP-LR) and NUREG-1801, "Generic Aging Lessons Learned (GALL) Report."

In anticipation to review applications for reactor operation from sixty to eighty years, the Office of Nuclear Reactor Regulation (NRR) requested the Office of Nuclear Regulatory Research (RES) to conduct research and identify aging-related degradation scenarios that could be important in this timeframe, and to identify issues for which enhanced aging management guidance may be warranted and allowing for prioritization of research needs. As part of this effort, RES agreed to a Memorandum of Understanding with the U.S. Department of Energy (DOE) to jointly develop an Expanded Materials Degradation Assessment (EMDA) at Oak Ridge National Laboratory (ORNL). The EMDA builds upon work previously done by RES in NUREG/CR-6923, "Expert Panel Report on Proactive Materials Degradation Assessment." Potential degradation scenarios for operation up to forty years were identified using an expert panel to develop a phenomena identification and ranking table (PIRT). NUREG/CR-6923 mainly addressed primary system and some secondary system components. The EMDA covers a broader range of components, including piping systems and core internals, reactor pressure vessel, electrical cables, and concrete structures. To conduct the PIRT and to prepare the EMDA report, an expert panel for each of the four component groups was assembled. The panels included from 6 to 10 members including representatives from NRC, DOE national laboratories, industry, independent consultants, and international organizations. Each panel was responsible for preparing a technical background volume and a PIRT scoring assessment. The technical background chapters in each volume summarizes the current state of knowledge concerning degradation of the component group and highlights technical issues deemed to be the most important for subsequent license renewal.

Detailed background discussions, PIRT findings, assessments, and comprehensive analysis for each of these component groups are presented in the following chapters.

CONTENTS

FIGURES

TABLES

ACKNOWLEDGMENTS

This work was performed jointly under contract with the U.S. Nuclear Regulatory Commission (NRC) Office of Nuclear Regulatory Research (RES) and under the U.S. DOE Office of Nuclear Energy Light Water Reactor Sustainability Program. The authors thank R. Reister, the DOE-NE LWRS Program Manager; K. McCarthy, the DOE-NE LWRS Technical Integration Office Lead, and J. Busby, the DOE-NE LWRS Technical Manager; P. G. Oberson and C. E. Carpenter, the NRC Project Managers; M. Srinivasan, the NRC Technical Monitor; and J. Stringfield, the Oak Ridge National Laboratory (ORNL) NRC Program Manager for support and guidance. J. Busby, T. Rosseel, and D. Williams at ORNL provided helpful suggestions that were essential in the execution of the panel discussion and incorporation of the results into the report. Many valuable review comments were received from NRC staff members of RES and the Division of Engineering. The authors also wish to thank W. Koncinski, A. Harkey, K. Jones, and S. Thomas at ORNL for assistance in formatting and preparing the final document. G. West at ORNL deserves special attention and thanks for his assistance in developing a database to compile, sort, and format the extensive data generated in the PIRT process. Professor G. Was at the University of Michigan was a key participant in the writing of the technical background assessments and his contribution to this work is greatly appreciated.

ABBREVIATED TERMS

%, percent

°C, degrees Celsius

°F, degrees Fahrenheit

γ, gamma

γ′, gamma prime

Δ, delta; denotes change

$\Delta\sigma_y$, change in yield strength

σ, sigma; denotes variability

τ, UMD recovery time

ϕ, flux

ϕt, fluence

$<T_{dam}>$, total average damage energy per atom

0.5T, ½T compact tension specimen

1TC(T), 1T compact tension specimen

3/4-t, three-quarters of the way through the vessel

3DAP, three-dimensional atom probe

41J, 41 joules (absorbed energy level in which Charpy v-notch specimen reaches the ductile-to-brittle transition temperature)

AAR, alkali-aggregate reaction

ADP, annealing demonstration project

AERE, Atomic Energy Research Establishment (UK)

AFCEN, French Society for Design and Construction and In-Service Inspection Rules for Nuclear Islands

AMP, aging management program

AMR, aging management review

ANO-1, Arkansas Nuclear One Unit 1

APT, atom probe tomography

ASME, American Society of Mechanical Engineers

ASTM, American Society for Testing and Materials

at %, atomic percent

ATI, ATI Consulting

ATR, Advanced Test Reactor

B&W, Babcox and Wilcox

BAC, boric acid corrosion

BR3, Belgian reactor 3

BWR, boiling water reactor

C, carbon

C&LAS, carbon and low alloy steels

CASS, cast austenitic stainless steel

CFR, *Code of Federal Regulations*

Cl^-, chloride ion

cm, centimeter

Cr, chromium

CR, cold rolled

CRD, control rod drive

CRDM, control rod drive mechanism

CREEP, thermal creep

CREV, crevice corrosion

CRIEPI, Central Research Institute of Electric Power Industry (Japan)

CRP, Cu-rich precipitates

Cu, copper

CUF, cumulative fatigue usage factor

CVCS, chemical and volume control system

CVN, Charpy V-notch

CW, cold-worked

DBTT, ductile-to-brittle transition temperature

DEBOND, debonding

DH, dissolved hydrogen

DOE, U.S. Department of Energy

dpa, displacements per atom

E, neutron spectrum flux

EBSD, electron backscatter diffraction

EC, erosion–corrosion

ECCS, emergency core cooling system

ECP, electric chemical potential

E_d, displacement threshold energy

EDF, Electricite de France

EDS, energy-dispersive X-ray spectroscopy

EK, Erickson Kirk

Emb., Embrittlement

EMDA, Extended Materials Degradation Assessment

Env., environmental

EONY, Eason, Odette, Nanstad, and Yamamoto

EPMDA, Extended Proactive Materials Degradation Assessment

EPR, electrochemical potentiokinetic reactivation

EPRI, Electric Power Research Institute

eV, electron volt

FAC, flow-accelerated corrosion

FAT, corrosion fatigue

Fe, iron

f_p, volume fraction

FR, fracture resistance

GALL, generic aging lessons learned

GALV, galvanic corrosion

GC, general corrosion

h, hour

HAZ, heat-affected zone

HC, high cycle

HSSI, Heavy-Section Steel Irradiation

HSST, Heavy Section Steel Technology

HWC, hydrogen water chemistry

HWR, heavy water reactor

I&C, instrumentation and controls

IA, irradiation assisted

IAEA, International Atomic Energy Agency

IASCC, irradiation-assisted stress corrosion cracking

IC, irradiation creep

IG, intergranular

IGC, intergranular corrosion

IGF, intergranular fracture

IGSCC, intergranular stress corrosion cracking

IMP, Implementation

IMT, Issue Management Table

in., inch

INL, Idaho National Laboratory

IPA, integrated plant assessment

IVAR, irradiation variables

JAEA, Japan Atomic Energy Agency

JAERI, Japan Atomic Energy Research Institute

JMTR, Japan Materials Testing Reactor

JNES, Japan Nuclear Safety Organization

JPDR, Japan Power Demonstration Reactor

K, stress intensity

keV, thousand electron volt

K_{Ia}, crack-arrest toughness

K_{Ic}, fracture toughness

K_{Jc}, elastic-plastic fracture toughness at onset of cleavage fracture

LAS, low alloy steel

LBP, late-blooming phase

LC, low cycle

LMC, lattice Monte Carlo

LRO, long-range ordering

LTCP, low-temperature crack propagation

LTO, long-term operation

LWR, light water reactor

LWRS, Light-Water Reactor Sustainability

LWRSP, Light Water Reactor Sustainability Program

MA, mill-anneal

MDM, materials degradation matrix

MeV, million electron volts

MIC, microbially induced corrosion

MF, matrix feature

MIG, metal inert gas (welding)

Mn, manganese

MO, Mader and Odette

Mo, molybdenum

MOU, memorandum of understanding

MOY, Mader, Odette, and Yamamoto

MPa√m, stress intensity factor; fracture toughness in units of megapascal square root meter

MPC, Materials Properties Council

n/cm², fluence

n/cm²·s, flux

NE, DOE Office of Nuclear Energy

NEI, Nuclear Energy Institute

Ni, nickel

NMCA, noble metal chemical addition

NOSY, Nanstad, Odette, Stoller, and Yamamoto

NPP, nuclear power plant

NRC, U.S. Nuclear Regulatory Commission

NWC, normal water chemistry

ORNL, Oak Ridge National Laboratory

P, phosphorous

PA, proton annihilation

PIA, postirradiation annealing

PIRT, phenomenon identification and ranking technique

PIT, pitting

PLIM, Nuclear Power Plant Integrity Management

PMDA, Proactive Materials Degradation Assessment

PMMD, proactive management of materials degradation

PNNL, Pacific Northwest National Laboratory

PRA, primary recoil atom

PRE, Prediction of Radiation Embrittlement

PREDB, Power Reactor Engineering Database

PSF, Poolside Facility

PT, penetration test

PTS, pressurized thermal shock

PWHT, post-weld heat treatment

PWR, pressurized water reactor

PWROG, Pressurized Water Reactor Owners Group

PWSCC, primary water stress corrosion cracking

R&D, research and development

RADAMO, SCK-CEN TR model and corresponding TR database

RCS, reactor coolant system

RES, NRC Office of Nuclear Research

RHRS, residual heat removal system

RIS, radiation-induced segregation

RPV, reactor pressure vessel

RSE-M, Rules for In-Service Inspection of Nuclear Power Plant Components (France)

RT, reference temperature

SA, solution anneal

SANS, small-angle neutron scattering

SCC, stress corrosion cracking

SCK-CEN, Studiecentrum voor Kernenergie—Centre d'Etude de l'Énergie Nucléaire (Belgian Nuclear Research Centre)

SE(B), single-edge, notched bend

SEM, scanning electron microscopy

SG, steam generator

SIA, self-interstitial atom

SIS, safety injection system

SM, Stationary Medium Power

SMF, stable matrix feature

SR, stress relaxation

SS, stainless steel

SSC, system, structure, and component

SSRT, slow strain rate test

SW, swelling

$\mathbf{T_0}$, fracture toughness reference temperature

$\mathbf{T_{41J}}$, ductile-to-brittle transition temperature measured at 41 joules of Charpy impact energy

TEM, transmission electron microscopy

TG, transgranular

Th, thermal

$\mathbf{T_i}$, irradiation temperature

TIG, tungsten inert gas (welding)

TiN, titanium nitride

TLAA, time-limited aging analysis

TMS, The Minerals, Metals and Materials Society

TR, test reactor

TT, reference transition temperature; thermal treatment

TTS, transition temperature shift

UCSB, University of California, Santa Barbara

UK, United Kingdom

UMD, unstable matrix defect

UNS, Unified Numbering System

U.S., United States

USE, upper-shelf energy

UT, ultrasonic test

VS, void swelling

VVER, Voda-Vodyanoi Energetichesky Reaktor (Water-Water Energetic Reactor)

WEAR, fretting/wear

Wstg., wastage

wt %, weight percent

Zn, zinc

1. INTRODUCTION

Ensuring safe operation of NPPs for a first, and any subsequent, license renewal period (i.e., 60–80+ years) will require an in-depth knowledge of the various modes of materials degradation that could impact the long-lived systems, structures, and components (SSC) of concern. Identifying and evaluating the effects of emerging degradation mechanisms on the expected service life is vital. The key to any adequate aging management program (AMP) is identifying and controlling the degradation of the constituent materials of the SSC. The U.S. Nuclear Regulatory Commission (NRC) Office of Nuclear Regulatory Research (RES) agreed to a memorandum of understanding (MOU) [1] with the U.S. Department of Energy (DOE) Office of Nuclear Energy (NE) to cooperate on research activities related to the long-term operation of licensed commercial nuclear power plants (NPPs). The NRC and DOE have now completed an Expanded Materials Degradation Assessment (EMDA), involving a comprehensive analysis of degradation mechanisms that may affect the functionality of (i) primary and secondary piping materials and core internals, (ii) concrete civil structures, (iii) reactor pressure vessels (RPVs), and (iv) electrical power and instrumentation and control (I&C) cable insulations during the second, and further subsequent periods of extended operation. The outcome of this research is prioritization of needed research to inform the development of technical basis for such extended reactor operation. The main objective of the EMDA report is to provide a technical basis for regulatory assessments and safety evaluations regarding subsequent license renewal. The EMDA was performed using the same methodology, including an expert panel discussion and PIRT scoring process, as in the original Proactive Materials Degradation Assessment (PMDA), formally presented in *Expert Panel Report on Proactive Materials Degradation Assessment,* NUREG/CR-6923 [2].

1.1 MATERIALS DEGRADATION IN CORE INTERNALS AND PIPING SYSTEMS

Aging-related materials degradation can lead to increased maintenance, downtime, and economic uncertainty for the nuclear power industry as well as increased oversight for the regulatory authorities. Thus, there is a need to resolve materials issues for reactor pressure vessels (RPV) and primary piping, core internals, secondary systems, weldments, concrete, electrical power and instrumentation and control cable insulation, and buried piping. This report deals with core internals and piping systems.

The components, structures and systems of nuclear reactors are exposed to very harsh environments during their service. Components within a reactor core must tolerate high temperature water, stress, vibration, and an intense neutron field. Degradation of materials in this environment can lead to reduced performance, and in some cases, unexpected early failure. Materials degradation within a nuclear power plant is very complex. There are many different types of materials within the reactor itself: over 25 different metal alloys can be found within the primary and secondary systems, not to mention the concrete containment vessel, instrumentation and control, and other support facilities. When this diverse set of materials is placed in the complex and harsh environment coupled with load, degradation over an extended life is indeed quite complicated.

Clearly, materials degradation will impact reactor reliability, availability and, potentially, safe operation. Routine surveillance and component replacement can mitigate these factors, although failures still occur. With reactor life extensions to 60 years or beyond many components must

tolerate the reactor environment for even longer times and when coupled with power uprates reactor conditions may also become more severe (e.g. higher temperatures, increased flow, or higher neutron fluxes). This may increase susceptibility of most components and may introduce new degradation modes. While all components (except perhaps the reactor vessel) can be replaced, it may not be economically favorable. Therefore, understanding, detecting, mitigating, and preventing materials degradation processes with adequate repair and replacement are key priorities for extended reactor operation and power uprate considerations.

The reactor core is a very adverse environment, combining the effects of stress, corrosion, and irradiation. Components in this environment are also often the most critical for safe and reliable operation as the failure of a core internal component may have very severe consequences. Service life beyond 60 years will increase time at temperature and neutron fluence, in general leading to increased susceptibility and severity with respect to known degradation mechanisms (although new mechanisms are also possible). Therefore, understanding the materials performance and degradation mechanisms is one of the key elements for aging management. The issues described below represent those that may warrant additional attention for life beyond 60 years and are grouped into three key areas: corrosion, thermal aging embrittlement and fatigue, and irradiation-induced aging effects. While the material susceptibilities to these key aging effects are highly dependent upon specific material and environment combinations, these aging effects have been observed in service for many key components. These elements are described in considerably more detail in following chapters, organized by key classes of materials.

1.1.1 Corrosion and Stress Corrosion Cracking

In addition to elevated temperatures, intense neutron fields, and stress, components must also be able to withstand a corrosive environment. Temperatures typically range from 288 ºC (550 ºF) in a BWR up to 360 ºC (680 ºF) in a PWR, although other water chemistry variables differ more significantly between the BWR and PWRs.

Corrosion is a complex form of degradation that is strongly dependent on temperature, material condition, material composition, water purity, water pH, water impurities, and gas concentrations. The operating corrosion mechanism will vary from location to location within the reactor vessel and piping system and a number of different mechanisms may be operative simultaneously. These may include general corrosion mechanisms such as uniform corrosion, boric acid corrosion (BAC), flow-accelerated corrosion (FAC), and/or erosion corrosion. Generally speaking, material degradation due to these corrosion mechanisms occurs over a reasonably large area in a fairly homogenous manner. By contrast, localized corrosion modes occurs over much smaller areas, but at much higher rates than general corrosion and includes crevice corrosion, pitting, galvanic corrosion, and microbially-induced corrosion (MIC). Finally, environmentally assisted cracking (EAC) includes other forms of degradation, which are assisted by localized or general corrosion with the additional contribution of stress. In a LWR, a number of different environmentally assisted cracking mechanisms are observed: intergranular stress corrosion cracking (IGSCC), transgranular stress corrosion cracking (TGSCC), primary water stress corrosion cracking (PWSCC), irradiation-assisted stress corrosion cracking (IASCC) and low-temperature crack propagation (LTCP).

While all forms of corrosion are important in developing an appropriate aging management program, IASCC has received considerable attention over the last four decades due to both its severity and unpredictability. Despite over thirty years of international study, the underlying mechanism of IASCC is still unknown, although more recent work led by groups such as the

Cooperative IASCC Research Group* has identified important controlling parameters. This will be discussed in considerably more detail below.

Clearly, unmonitored corrosion (in all the various forms) is not acceptable for the safe and reliable operation of a reactor. With extended lifetimes, components must resist degradation due to additional time in contact with the coolant. As a result, the various corrosion mechanisms must all be understood and evaluated for different reactor component and sub-systems to ensure safe extended service. The *NUREG/CR-6923* report provides a clear and in-depth review of all these mechanisms for the current LWR fleet. Additional effort is required to evaluate the importance of each with further license renewal.

Components in the secondary (steam generator) side of a PWR are also subject to degradation. While the secondary side of the reactor does not have the added complications of an intense neutron irradiation field, the combined action of corrosion and stress can create many different forms of failure. The majority of steam generator systems in U.S. power plants today originally used Alloy 600 (a Ni-Cr-Fe alloy) for tubes and some other components, although service experience showed many failures in tubes through the 1970s. In the last 20 years, most steam generators with Alloy 600 tubes have been replaced with units that have Alloy 690 tubes, which contain higher Cr content and exhibits more resistance SCC. In addition to the base material, there are weldments, joints, and varying water chemistry conditions leading to a very complex component. Indeed, the array of modes of degradation varies with location. In a single steam generator examined by Staehle and Gorman [3], twenty-five different modes of corrosion degradation were identified. Stress corrosion cracking is found in several different forms, and may be the limiting factor for extended service. The integrity of these components is critical for reliable power generation in extended operation, and as a result, understanding and mitigating these forms of degradation is important. Adding additional service period to these components will allow more time for corrosion to occur. The various forms of corrosion must be evaluated as in the PMDA report, with a special attention to those that may be life limiting in extended service.

1.1.2 Thermal Aging and Fatigue

The effects of elevated temperature service in metal alloys have been examined for many years. Possible effects include phase transformations that can adversely affect mechanical properties. Extended time at elevated temperature may permit even very slow phase transformations to occur. This is of particular concern for cast stainless steel components where the formation of a brittle alpha-phase can result in a loss of fracture toughness and lead to brittle failure. The effects of aging on other components are also of concern and should be examined. The effort required for identifying possible problems can be reduced, though, by using modern materials science modeling techniques and experience from other industries.

Fatigue refers to an aging degradation mechanism where components undergo cyclic stress. Typically, these are either low-load, high frequency stresses or high-load, low frequency stresses generated by thermal cycling, vibration, seismic events, or loading transients. Environmental factors may accelerate fatigue and eventually may result in a component failure. In a light water reactor, components such as the pressure vessel, pressurizer, steam generator shells, steam separators, pumps, and piping are among the components that may be affected. The PMDA

* An international collaboration, based in Halden, Norway, among utilities, vendors, regulators, and research organizations to develop IASCC data.

report identified fatigue as an issue for a number of different components and subsystems for both PWR and BWR. This area of degradation was also identified by the panelists of this effort and is discussed in considerable detail in the background Chapters in this Volume..

Due to the potential for thermal aging and fatigue damage during extended lifetimes, the assumptions and limits considered at the design phase for core internal structures should also be examined. During the initial plant design, each component was designed with a load to expected and specific lifetimes and operating conditions using established guidelines (typically those in Section III of the ASME Boiler and Pressure Vessel Code). An 80-year reactor period of operation corresponds to over 600,000 hours of service (at a 90% service factor) while most long-term mechanical performance data used in design comes from tests operating much less than 100,000 hours. The extension of period of operations beyond these initial design considerations should be carefully examined.

1.1.3 Irradiation-induced Effects

Over the forty-year lifetime of a light water reactor, internal structural components may experience neutron flux to ~10^{22} n/cm^2/s in a BWR and ~10^{23} n/cm^2/s in a PWR (E > 1 MeV), corresponding to accumulated neutron dose of ~7 displacements per atom (dpa) and 70 dpa, respectively. Extending the operating period of a reactor will increase the total neutron fluence to each component. Fortunately, radiation effects in stainless steels (the most common core constituent) are also the most examined as these materials are also of interest in fast-spectrum fission and fusion reactors where higher fluences are encountered. A brief summary of key irradiation-induced changes is listed below, however a much more detailed assessment is provided in Chapter 8 below.

The neutron irradiation field can produce large property and dimensional changes in materials. This occurs primarily via one of five radiation damage processes: Radiation-induced hardening and embrittlement, phase instabilities from radiation-induced or -enhanced segregation and precipitation, irradiation creep due to unbalanced absorption of interstitials vs. vacancies at dislocations, volumetric swelling from cavity formation, and high temperature helium embrittlement due to formation of helium-filled cavities on grain boundaries. For light water reactor systems, high temperature embrittlement and creep are not common problems due to the relatively (for creep) lower reactor operating temperature. However, radiation embrittlement, phase transformation, segregation, and swelling have all been observed in reactor components.

Radiation-induced segregation and phase transformations: Under irradiation, the large concentrations of radiation-induced defects will diffuse to defect sinks such as grain boundaries and free surfaces. These concentrations are far in excess of thermal-equilibrium values and can lead to coupled-diffusion with particular atoms. In engineering metals such as stainless steel, this results in radiation-induced segregation of elements within the steel. For example, in Type 316 stainless steel (SS), chromium (important for corrosion resistance) can be depleted at areas while elements like nickel and silicon are enriched to levels well above the starting, homogenous composition. While radiation-induced segregation does not directly cause component failure, it can influence corrosion behavior in a water environment. Further, this form of degradation can accelerate the thermally-driven phase transformations mentioned above and also result in phase transformations that are not favorable under thermal aging (such as gamma or gamma-prime phases observed in stainless steels). Additional fluence may exacerbate radiation-induced phase transformations and should be considered. The wealth of data generated for fast-breeder reactor studies and more recently in LWR-related analysis will be beneficial in this effort.

Radiation-induced swelling and creep: The diffusion of radiation-induced defects can also result in the clustering of vacancies, creating voids. If gas atoms such as He enter the void, it becomes a bubble. While swelling is typically a greater concern for fast reactor applications where it can be life-limiting, voids have recently been observed in LWR components such as baffle bolts. The motion of vacancies can also greatly accelerate creep rates, resulting in stress relaxation and deformation. Irradiation-induced swelling and creep effects can be synergistic and their combined influence must be considered. Longer reactor component lifetimes may increase the need for a more thorough evaluation of swelling as a limiting factor in LWR operation. As above, data, theory, and simulations generated for fast reactor and fusion applications can be used to help identify potentially problematic components.

Radiation-induced embrittlement: Irradiation may lead to a change in material properties, characterized by a loss of fracture toughness and resistance to crack growth. Radiation embrittlement is typically concurrent with in an increase in the yield and ultimate tensile strength of the material. This increase in strength comes with a corresponding decrease in ductility. This hardening and embrittlement can be caused by the changes in the alloy's microstructure including radiation-induced segregation, phase transformations, and swelling. Although they are different measures of material properties or performance, the irradiation effects community often refers to hardening and embrittlement synonymously, due to their concurrent occurrence and root causes. Extended reactor lifetimes may lead to increased embrittlement issues.

1.2 EMDA PROCESS AND IDENTIFICATION OF RESEARCH NEEDS FOR EXTENDED OPERATING PERIODS

As noted above, materials degradation in the core and primary piping is complex and involves many variables including alloy, environment, stress state, irradiation, and time. The *NUREG/CR-6923* effort provided a systematic and detailed assessment of the susceptibility and knowledge for many of those material, environment, and degradation combinations. When evaluating service to potential 80 years, a similar systematic analysis is required to highlight key needs in research. This document provides an expert panel assessment of corrosion, stress corrosion cracking, thermal effects and irradiation for key material systems in core internal and piping systems. Here, an expanded PMDA methodology was again utilized to provide systematic assessment of aging-related degradation for the extended period of operation up to 80 years. This approach benefits all stakeholders in providing a comprehensive analysis of degradation modes and identifying potential gaps, which may need to be addressed by further research to provide additional data and information for assurance of safe and efficient extended operation.

The expert elicitation process conducted for each expert panel in the EMDA project is based on the Phenomena Identification and Ranking Table (PIRT) process. This process has been used in many nuclear applications for ranking and prioritizing any number of issues. The PIRT process provides a systematic means of obtaining information from experts by generating and analyzing lists (tables) of degradation phenomena. In this process, "phenomena" can refer to a particular reactor condition, a physical or engineering approximation, a reactor component or parameter, or anything else that might influence some relevant figure-of-merit, which is related to reactor safety. The process usually involves the ranking of these phenomena using a series of scoring criteria. The results of the scoring can be assembled to lead to a quantitative ranking of issues or needs.

Each PIRT application has been unique in some respect and the current project is unique in its application. The current PIRT can be described in terms of several key steps. These are

described for the generic process below, although each expert panel made minor adjustments, based on the needs of that material system, and such adjustments will also be described below.

As part of this activity, an expert panel was assembled and, included up to 9 leading experts with a variety of perspectives (including regulatory, academia, industry, and international experience). The panelists selected for this core internals and piping panel had an average of over 40 years experience in the field and many had participated earlier in the NUREG/CR-6923 activity. Selection and assembly of panel experts was performed with NRC and DOE input and approval.

Initial technical background assessments of key degradation modes were then developed and used as a starting foundation for broader discussion, evaluation, and ranking. For this volume, the existing *NUREG/CR-6923* was used as a starting point and additional discussion on the potential changes that might be experienced during subsequent operating periods. Each chapter of the technical background assessment was written by a single panelist and then peer-reviewed by the entire panel. Subsequent discussion amongst the entire panel was also used to identify key themes and revisions to the technical background assessments were made accordingly.

It is important to note that these background assessments are not intended to encompass all of the particular degradation modes or material systems. Detailed texts and background assessments exist in other publications and it is beyond the scope of this project to reproduce them here. Rather, the discussions presented in this report are intended to introduce the subject and context for the evaluation of key modes of degradation for subsequent operating periods.

Based on the input from the technical background chapters (Chapters 2-8 of this volume) the panel then developed a PIRT matrix with a list of degradation scenarios to score. A degradation scenario generally encompasses a particular material, system, component, or subcomponent (depending on the categorization scheme devised by the panel), the environmental condition to which that material is exposed, and the degradation mode, which that material may experience, based on laboratory and operational data. If a certain material is exposed to multiple environments or may experience multiple degradation modes, those are listed and scored as distinct scenarios.

After the scoring matrix was developed, panelists independently scored the degradation scenarios in three categories: Susceptibility, Confidence, and Knowledge. These categories are the same as were used for *NUREG/CR-6923*. Subsequent to the completion of panelists scoring, all scores were compiled and the average of Susceptibility and Knowledge were calculated. Since Confidence is a measure of personal confidence, the average is less meaningful and was not calculated.

After completion of scoring and identification of “outliers,” the panels were reassembled for discussion of the scoring. During this discussion, each degradation mode and related scoring was discussed with the “outliers” being of highest priority. In these discussions, the scoring panelist presented rationale for any scores that differed from the average. The objective was not to develop a consensus score or force conformity among the panelists. The primary goal of this discussion was to foster comprehensive assessments and exchange differing points of view. This discussion among panelists was an important part of the process to ensure all points of view were considered, including consideration of any new information on the subject area which was not previously considered, and accounted for in the final scoring. After compiling any changes in scoring following this debate, the PIRT scoring was tabulated to determine relative research needs and priorities.

Finally, the results of the PIRT scoring were compared to the background technical chapters to ensure all of the important modes of degradation and technical discussion points were captured. Revisions were then made to the supporting chapters and analysis to ensure adequate discussion of key topics, outcomes, and underlying causes. Thus, the technical basis information for conducting PIRT and the results of the PIRT were re-iterated to ensure that coverage and consistency is maintained in the various PIRT subject areas.

1.3 ORGANIZATION OF THIS EMDA VOLUME

This EMDA volume on core internals and piping systems is broad and is an extension of *NUREG/CR-6923*, which covered the same material systems. These material systems include low alloy and carbon steels, wrought stainless steels (SS), Alloy 600 and its weldments, Alloy 690 and its weldments, CASS, and liner materials. These materials serve in a variety of environments spanning a broad range of water chemistry and stress conditions. For many components, irradiation may also occur. The expert panel considered and scored over 1,000 different material/environment/degradation combinations (451 for PWR and 599 for BWR). This document represents the expert panel deliberations and PIRT findings for reactor core internals and primary piping systems.

Chapters 2 through 7 present the technical background assessments for key material systems. These include chapters covering

- Alloy 600 and its weldments
- Alloy 690 and its weldments
- Low alloy and carbon steels
- Wrought stainless steels
- Cast-austenitic stainless steels
- Containment liners

In addition, a separate assessment (Chapter 8) covering irradiation effects is presented as a crosscutting issue covering many of the specific material systems. Each technical background assessment provides a limited amount of background into key material specifications and operating regimes along with an assessment of key degradation modes. Each background assessment also includes a summary of key modes of degradation or knowledge gaps that may exist for subsequent operating periods.

Chapter 9 provides a more detailed description of the PIRT process used by this panel. The overlap and differences with the original PMDA in *NUREG/CR-6923* is also provided. The findings of the PIRT scoring are presented and the results are compared with the findings of the technical background assessments.

Finally, Chapter 10 provides a summary of key knowledge gaps that were identified by the expert panel as well as recommendations and conclusions.

1.4 REFERENCES*

1. NRC, "Memorandum of Understanding between U.S. Nuclear Regulatory Commission and U.S. Department of Energy on Cooperative Nuclear Safety Research," ADAMS ML083370612, U.S. Nuclear Regulatory Commission, April 20, 2009.
2. P. L. Andresen et al., *Expert Panel Report on Proactive Materials Degradation Analysis,* NUREG/CR-6923 (BNL-NUREG-77111-2006), U.S. Nuclear Regulatory Commission, February 2007.
3. R. W. Staehle and J. A. Gorman, "Quantitative Assessment of Submodes of Stress Corrosion Cracking on the Secondary Side of Steam Generator Tubing in Pressurized Water Reactors: Part 2," *Corrosion* **60**(1): 5–63 (2004).

* Inclusion of references in this report does not necessarily constitute NRC approval or agreement with the referenced information.

2. WROUGHT STAINLESS STEELS

Koji Arioka
Institute of Nuclear Safety Systems, Inc.*

2.1 INTRODUCTION

There are over 150 different grades of stainless steel in current commercial use, of which 15 are commonly used in LWRs. Of these, 304 SS and 316 SS are the most common with specific applications of 308 SS, 309 SS, 321 SS, and 347 SS. Both 304 SS and 316 SS are widely used in nuclear reactor applications as well as 321 SS and 347 SS grades. Decades of experience in both commercial LWRs and fast breeder reactors have resulted in further refinement of stainless steel compositions for reactor applications. Past experience in both LWRs and fast breeder reactors has shown that 316 SS offers higher performance and greater reliability than 304 SS, particularly in aqueous corrosion and radiation damage resistance, which will be discussed in more detail in a later chapter.

Type 316 and 304 SS are used for pressure-retaining piping for primary and secondary systems in PWRs. Stabilized stainless steel (Type 347 SS) was used in steam generator tubing in PWRs during the 1960s and is still used in stems of reactor coolant pumps. Types 308L SS and 316L SS are used as the filler metals between stainless steels components and stainless steel piping. The chemical compositions of the Fe-based stainless steels used in LWRs are described in Table 2.1. In BWRs, type 304 SS and 316 SS are utilized as core internal structures including core shrouds, guides, plates, and supports. These grades are also utilized as pressure-retaining piping and coolant pumps. As in PWRs, Type 308 SS and 309 SS are used as weld filler metals (316 SS is used as weld filler in some applications in other countries). Types 308 SS and 309 SS are also utilized for vessel cladding applications.

The background on the choice of these materials is described in the *Corrosion and Wear Handbook for Water-Cooled Reactors* [1], which contains a materials database and explains the concept for material selection for the first nuclear-powered submarine (USS *Nautilus*) and the first commercial PWR (Shippingport, Pennsylvania). The main criteria for the material selection were (a) high corrosion resistance in a readily available alloy for the small purification system needed in a submarine; (b) good fabrication characteristics; and (c) extensive experience with the alloys in other industries, such as petrochemical and fossil power, to avoid unexpected failures and fully leverage the previous research and literature review results.

* Wholly owned by Kansai Electric Power Co., Inc. (KEPCO), Japan.

Table 2.1. Chemical compositions of stainless steels used in LWRs (wt %) (balance is Fe)

	C	Nb	Cr	Cu	Mn	Mo	Ni	P	S	Si
Type 316	0.08 max.	—	16.0-18.0	—	2.0 max.	2.0-3.0	10.0-14.0	0.045 max.	0.03 max.	1.0 max.
Type 316L	0.03 max.	—	16.0-18.0	—	2.0 max.	2.0-3.0	10.0-14.0	0.045 max.	0.03 max.	1.0 max.
Type 304	0.08 max.	—	18.0-20.0	—	2.0 max.	—	8.0-10.5	0.045 max.	0.03 max.	1.0 max.
Type 304L	0.03 max.	—	18.0-20.0	—	2.0 max.	—	8.0-12.0	0.045 max.	0.03 max.	1.0 max.
Type 347	0.08 max.	10xC min.	17.0-19.0	—	2.0 max.	—	9.0-13.0	0.045 max.	0.03 max.	1.0 max.
Type 308L	0.04 max.	—	18.0-21.0	0.75 max.	0.5-2.5	0.75 max.	9.0-11.0	0.04 max.	0.03 max.	0.90 max.
Type 309L	0.04 max.	—	22.0-25.0	0.75 max.	0.5-2.5	0.75 max.	12.0-14.0	0.04 max.	0.03 max.	0.90 max.
Type 403	0.15 max.	—	11.5-13.0	—	1.0 max.	—	—	0.04 max.	0.03 max.	0.5 max
Type 410	0.15 max.	—	11.5-13.5	—	1.0 max.	—	—	0.04 max.	0.03 max.	1.0 max
Type 630	0.07 max.	0.15-0.45	15.0-17.5	3.0-5.0	1.0 max.	—	3.0-5.0	0.04 max.	0.03 max.	1.0 max.

Reproduced from [1].

The stainless steels listed in Table 2.1 are used in the primary systems in a variety of forms, including seamless piping, forgings, castings, and plates. The specific stainless steel–component combinations vary among reactor designs and manufacturers but in general share the following traits:

- Main coolant piping and elbows for PWR primary circuits are cast 316 SS (CF8M). Seamless Type 316 SS is also used for main coolant piping in some PWRs. Cast grades are discussed in detail in Chapter 7 below.
- The inner surfaces of the RPV, pressurizer, and steam generator channel head are clad with Type 308L SS; they are then stress-relieved during a post-weld heat treatment (PWHT) at 595 °C (1,103 °F) to 620 °C (1,148 °F) for 1 hour per 25 mm thickness of steel.
- Pump and valve casings are generally made of cast stainless steel (CF8). Type 410 and Type 630 SS is used for the valve stem. Type 347 SS is used for the reactor coolant pump stem.
- Type 410 and Type 403 SS are used for stem and parts of the control rod drive mechanism, such as the plunger.
- Main coolant piping, elbows, joints and elbows for BWR circuits are comprised for 304 and 316 SS grades.
- Like PWRs the inner surfaces of the RPV are clad with stainless steel, typically 309 or 308L SS grades.
- Core internal structures in BWRs are made of wrought 304 SS and 316 SS.

The history of material degradation in LWRs supports the need for proactive research to identify potential problems before they manifest in the field, and sharing the research results among the stakeholders enables appropriate countermeasures to be taken. Various types of corrosion, such as general corrosion, crevice corrosion, SCC, and corrosion product transport in the primary

system, were studied in the stainless steels described above in hydrogenated and oxygenated high-temperature water to determine their suitability for use in the *Nautilus* and in the first commercial PWRs. The following recommendations were made with regard to expected material degradation at the time of the first commercial nuclear power plants.

2.1.1 Effect of Cold Work on SCC in Primary Systems

Before 1957, SCC had been found in non-sensitized and cold-worked >10% Type 304 SS that had been exposed to oxygenated pure water at 316 °C (601 °F) (see Table 2.2). However, at that time, SCC had not been found in cold-worked non-sensitized Type 304 SS, 310 SS, 316 SS, or 347 SS in hydrogenated pure water after testing for 120 days. Based on those results, it was recommended that cold-worked stainless steels not be used as spring materials in primary systems.

2.1.2 Effect of Secondary Water Chemistry and Sensitization on SCC of Steam Generator Tubing

An initial major concern was cracking in the secondary side of steam generator tubing made of stainless steel when exposed to seawater, especially onboard a submarine. To reduce SCC, non-sensitized stainless steel (Type 347 SS) was recommended as a less susceptible tubing material. Water treatments with phosphate (PO_4^{3-}) as an inhibitor and sulfite ($Na_2SO_3^{2-}$) as an oxygen scavenger were recommend for the secondary water based on the results described in Tables 2.3 and 2.4.

The U.S. Navy decided to change the steam generator tubing material to a Ni-based alloy (Alloy 600) in 1962 to minimize the occurrence of SCC on the secondary side. However, before then in 1959, Coriou et al. [2] reported experimental results to show the SCC susceptibility of Alloy 600 in high-temperature deuterated pure water environments. At present, the materials used to make steam generator tubing are Alloy 690, Alloy 800, and Alloy 600. Alloy 600 is now being phased out in commercial power plants because of IGSCC occurrence on both the primary and secondary sides.

Table 2.2. Influence of cold work and oxygen concentration on SCC susceptibility of austenitic stainless steels in high temperature water

Autoclave SCC tests in Primary water with simple beam specimens of AISI austenitic stainless steels

Water condition			AISI Type	Condition	Stress (psi)	Days	SCC
Temp. (°F)	Gas content	Velocity (ft/sec)					
500	5-10 ppm O2	0	302	Annealed	10,000	90	No
500	do	0	302	do	30,000	90	No
500	do	0	302	do	> yield stress	90	No
500	do	0	302	Sensitized 2h, 1200°F	10,000	90	No
500	do	0	302	do	30,000	90	No
500	do	0	302	do	>yield stress	90	No
500	0.5-4.6 ml/liter O2	11	304	Annealed	30,000	90	No
500	20-30 ml/liter O2	11	304	do	30,000	120	No
600	5-10 ppm O2	0	304	10% Cold worked, annealed	30,000	74	Yes
600	do	0	304	do	50,000	74	Yes
600	do	0	304	50% Cold worked, annealed	30,000	74	Yes
600	do	0	304	do	50,000	74	No
600	do	0	304	10% Cold worked	60,000	74	Yes
600	do	0	304	do	80,000	74	Yes
600	do	0	304	20% Cold worked	70,000	30	No
600	do	0	304	do	90,000	74	Yes
600	do	0	304	30% Cold worked	95,000	30	Yes
600	do	0	304	do	110,000	30	No
600	do	0	304	40% Cold worked	110,000	30	No
600	do	0	304	do	125,000	30	Yes
600	do	0	304	50% Cold worked	130,000	30	No
600	do	0	304	do	150,000	30	No
600	200 ml/ liter H2	0	304	10% Cold worked	60,000	38	No
600	do	0	304	do	80,000	38	No
600	do	0	304	20% Cold worked	70,000	38	No
600	do	0	304	do	90,000	38	No
600	do	0	304	30% Cold worked	95,000	38	**
600	do	0	304	do	110,000	38	**
600	do	0	304	40% Cold worked	110,000	38	No
600	do	0	304	do	125,000	38	**
600	do	0	304	50% Cold worked	130,000	38	No
600	do	0	304	do	150,000	38	No
500	0.5-4.6 ml/liter O2	11	310	Annealed	29,800	30	No
500	20-30 ml/liter O2	11	310	do	29,800	120	No
500	0.5-4.6 ml/liter O2	11	316	do	28,300	30	No
500	20-30 ml/liter O2	11	316	do	28,300	120	No
500	0.5-4.6 ml/liter O2	11	347	do	31,500	30	No
500	20-30 ml/liter O2	11	347	do	31,500	120	No
600	Degassed *	25	347	do	22,400	34	No

Water velocity obtained by rotation of specimens in water or circulating of water past specimen.

* : Degassed means air purge by boiling autoclave before sealing

** : Slight defect parallel to direction of stress; Apparantly associated with a rolling seam ; doubtful if associated with stress corrosion

Reproduced from [1].

Table 2.3. Influence of phosphate treatment on SCC susceptibility of austenitic stainless steels in high temperature water

Autoclave SCC tests of AISI type austenitic stainless steel U-Bend specimens submerged in various alkaline phosphase treated waters (steels annealed before testing)

Cl (ppm)	Nominal O2 ppm	AISI type	Days of test in water with pH *			Total days in tests	Temp, °F	Number of specimens	SCC
			10.6	11	11.3				
High **	Degassed	347	14			14	500	2	No
High **	do	347			14	14	500	2	No
553	Saturated	347	15			15	467	2	No
553	30	347	7			7	500	3	No
553	0.1-0.7	347	30			30	467	2	No
553	0.06	347	7			7	500	3	No
553	Degassed	347	15			15	467	4	No
550	0.05-0.5	304	7		55	62	500	40	No
550	do	347	7	24	51	82	500	50	No
530	Saturated	304	15			15	500	1	Yes ***
530	do	305	15			15	500	1	Yes ***
530	do	347	15			15	500	1	Yes ***
530	do	304			15	15	500	1	No
530	do	347			15	15	500	1	No
530	Aerated	304	90			90	500	1	No
530	do	347	90			90	500	2	No
530	Degassed	347	14			14	470	1	No
500	do	347	15			15	467	1	No
400	do	347	15			15	467	1	No
350	<1.0	347	15			15	500	2	No
350	Degassed	347	15			15	467	1	No
336	Aerated	347			30	30	500	2	No
336	Degassed	347			30	30	470	1	No
336	do	347			30	30	500	2	No
300	do	347	15			15	467	1	No
200	0.05-0.5	304	21	9	35	65	500	40	No
200	do	347	21	53	31	105	500	50	No
150	Degassed	347	15			15	467	1	No
100	<1.0	347	15			15	500	2	No
50	0.05-0.5	304	35		43	78	500	40	No
50	do	347	49	39	52	140	500	50	No
10	do	304	33		83	116	500	40	No
10	do	347	42		74	116	500	50	No
2	do	304	36		67	103	500	40	No
2	do	347	59	14	66	139	500	50	No
1	200	347	15			15	500	2	No
1	30	347	15			15	500	2	No
total								495	Yes : 3 No : 492

Degassed means oxygen removed by boiling and venting autoclave. Aerated means no atempt was made to remove air before sealing autoclave.
Saturatede means oxygen was bubbled through autoclave before sealing. Actual or calculated oxygen contents are given where data are available.
* Water conposition were: pH 10.6 : 50 ppm PO4, pH 11 : 120 ppm PO4, pH 11.3 : 200 ppm PO4
** Exact cholide unknown. High chlorode contained by boiling off to full saturation a solution originally containinng 530 ppm Cl, 50 ppm PO4, and pH 10
*** Vessel was inverted momentarily twice each day, thus exposing the specimens to the vapor phase for short periods.

Reproduced from [1].

Table 2.4. Influence of sensitization on SCC susceptibility under phosphate treatment of austenitic stainless steels

Autocleva SCC tests of sensitized type 304 stainless steel, U bend specimens submerged in 500°F Alkaline-Phosphate treated water containing 0.05-0.5 ppm oxygen

Time sensitized at 1,200F, hr	Cl, ppm	Days of test in water with pH *			Total days in tests	Number of specimens	Number of specimens with IGSCC
		10.6	11	11.3			
1	550	7			7	10	10
1	200	21	9	35	65	10	2
1	50	7		35	42	10	10
1	10	33		69	102	10	None
1	2	36		67	103	10	None
2	550			40	40	4	4
2	550			28	28	10	6
2	50			29	29	10	None

* : Water compositions were, pH 10.6 : 50 ppm PO4, pH 11 : 120 ppm PO4, pH 11.3 : 200 ppm PO4

Reproduced from [1].

2.1.3 Crevice Corrosion in Primary Systems

Crevice corrosion has not yet been experienced in crevice joints, such as socket welds or flange joints, in the presence of hydrogen-bearing water.

2.1.4 Key Modes of Degradation of Stainless Steel in Water Reactor Applications

The degradation of stainless steel in water reactors has been examined for decades and many forms of degradation are well known. Irradiation effects for austenitic stainless steels are well studied and material changes can occur in a number of forms. These are described in detail in Chapter 8 below.

Environmentally assisted cracking (EAC) is also a known form of degradation for stainless steels provided the material is in a susceptible state, a corrosive environment, and under stress. In LWR conditions, the coolant can be very aggressive with high temperatures, high electrochemical potentials [in BWR normal water chemistry (NWC)], with the potential for impurities in sufficient concentration to alter corrosion processes. Stress states are typically complex for most reactor components. Stainless steel is also known to be susceptible to several forms of degradation caused by cold working, embrittlement, sensitization, and weldments and heat-affected zones. For stainless steels in an LWR, a number of different cracking mechanisms are observed: intergranular stress corrosion cracking (IGSCC), transgranular stress corrosion cracking (TGSCC), primary water stress corrosion cracking (PWSCC) and irradiation-assisted stress corrosion cracking (IASCC) have all been observed.

2.2 POTENTIAL FOR DEGRADATION OF STAINLESS STEELS IN LWRS BEYOND 60 YEARS OF OPERATION

Overall, the service experience with wrought stainless steel has been positive to date, although there have been a number of degradation issues in the past.

As noted widely in the open literature, conventional wrought austenitic stainless steels such as 304 SS and 316 SS are susceptible to IGSCC in BWRs when the material was sensitized during

fabrication (either through heat treatment or welding processes), particularly in the high electrochemical potential in NWC environments for BWRs. Proactive countermeasures to reduce the electrochemical potential of the environment and improve the resistance of the alloy via refined alloy chemistry and management of residual stress have greatly reduced cracking observations in BWR piping. Incidents of IGSCC in stainless steel piping in BWRs are now rare.

While IGSCC in BWR piping is well known and largely addressed in the U.S. fleet, EAC in BWR reactor core internals is still observed today. A number of ongoing industry, regulatory, and academia programs are underway around the world to understand the mechanisms and key factors driving susceptibility. Mitigation techniques such as hydrogen water chemistry (HWC) are being utilized to reduce the potential of BWR water and reduce cracking. Noble metal chemical additions have also been successful in reducing cracking incidence in austenitic stainless steel core internals. The long-term effectiveness of these techniques in core internal environments is still being evaluated.

Wrought stainless steels used in PWR reactor coolant systems and reactor internals have an excellent history of service performance. The absence of systematic IGSCC in piping in PWR applications is different than experience in BWR systems and this difference is attributed to the low oxygen content and hydrogen overpressure in PWR reactor coolant. Indeed, this observation was a key motivation for the development of HWC in BWR applications. The relatively limited numbers of problems that have occurred in stainless steel parts in PWRs have generally been due to either mechanical or thermal fatigue, to high levels of cold work, or to the development in stagnant areas of aggressive environments with chlorides, concentrated boric acid and entrapped oxygen.

When considering the potential for operation beyond 60 years of service, there are a number of possible EAC degradation factors and open questions that must be addressed. EAC in oxidizing, high-potential environments like BWR-NWC are well-known phenomena and currently well mitigated for piping applications. Mitigation results from operation in lower electrochemical corrosion potential (ECP) environments such as PWR or even BWR-HWC environments. The following sections are primarily focused on low-ECP hydrogenated water environments, as they will be the most common for extended operating periods.

Potential for the degradation of stainless steel reactor components beyond 60 years of operation may occur due to following phenomena (which are also discussed in more detail in later sections of this document):

- SCC in a low-electrochemical-potential environment typically requires a long-term incubation time or a precursor, becoming apparent after extended times.

- SCC in a high-electrochemical-potential environment (such as oxygen-stagnant areas in PWRs) and possibly impurities such as chloride. Such conditions may occur during plant start-up because the residual air might not be adequately removed before plant start-up. Therefore, the cumulative number of times permitted under such an aggressive environment might exceed after extended operation.

- Potential for the acceleration in more mechanistic degradation processes and ultimately, SCC susceptibility might occur due to a change in the local grain boundary or surface properties during long-term operation, such as chemical composition changes (primarily driven by radiation-induced segregation although thermal processes are also possible) or cavity formation.

Two degradation modes for stainless steels are addressed in the following sections in terms of (a) the past and current plant experience; (b) the current prediction capabilities (e.g., parametric dependency, mechanistic-based models) that expand the analysis time; and based on (c) the long-term (beyond 60 years) concerns that address both the onset of new degradation modes and/or inadequacies in the current mitigation/plant management actions, based on information from both current plant experience and prediction capabilities.

2.2.1 SCC in a Low-Electrochemical-Potential Environment

2.2.1.1 Past and current plant experience

There have been a few reports of PWR component failures due to SCC: canopy seal welds resulting from SCC of austenitic stainless steel in oxygen-stagnant areas [3], the upstream side of the final check valve in the Safety Injection System (SIS) [4], and IASCC [5–9]. The main cause of SCC is assumed to be degradation under high-electrochemical-potential environments due to the residual oxygen in case of the first two incidents. Moreover, the main cause of IASCC is usually assumed to be material irradiation in low-electrochemical-potential environments. To date, the number of incidents caused by SCC in low-electrochemical-potential environments is very few. However, the following incidents caused by SCC on cold-worked 316 SS were reported recently in low-electrochemical-potential environments in PWR primary systems besides IASCC.

SCC in the HAZ of the safe end welded with steam generator inlet nozzle and main coolant piping

Circumferential shallow intergranular cracking was identified in Mihama unit 2 in 2008 [10]. The cracks were located at the safe end made from forged 316 SS. The safe end was welded with the steam generator inlet nozzle and main coolant piping in the primary system. The temperature at the inlet nozzle is about 320 °C (608 °F) during operation. The inner surface was machined and surface-ground after welding. The surface hardness was reported to be ~400 (H_v 1g load) [10]. The maximum depth of the cracking was 0.9 mm. The cracking was located about 3 to 5 mm away from the weld fusion line. An example of the fracture surface and cross-sectional view of the cracking is shown in Figure 2.1. The steam generator in Mihama unit 2 was replaced in the beginning of 1990. The replacement was outfitted with Alloy 690TT tubing. The plant resumed operation in 1994. Therefore, the cracking near the safe end weld is thought to have developed between 1994 and 2008. Significant sensitization was not observed by electrochemical potentiokinetic reactivation method (EPR) and by transmission electron microscope (TEM) observation. Since before 1994, the diaphragm of the make-up tank in Mihama unit 2 has been covered by N_2 gas to keep the oxygen concentration low. Consequently, the influence of oxygen ingress on the cracking of Mihama unit 2 is not postulated to be very significant.

Figure 2.1. Fracture surface and cross-sectional view of the cracking observed at the safe end in Mihama unit 2, after [10].

SCC on the heater sheath in the pressurizer

Since 1997, several occurrences of longitudinal IGSCC have been identified in France on the heater sheaths in pressurizers. Some of them had leaked [11]. The heater sheaths were made from 316L SS and 304L SS, and the cracking initiated from the cold-worked surface. The reported surface hardness via Vickers hardness testing was between 280 and 411 (Hv 0.05g load). No trace of impurity was identified for the removed heater sheath. Based on field results and on laboratory tests, Electricite de France (EdF) concluded that strain localization and associated cold working are necessary conditions for SCC and that IGSCC may be promoted by low strain rate and an increase of alkalinity. EDF developed the stress-relieved heater sheath to decrease the surface hardness, which occurred during manufacturing process. EDF has used the alternative heater sheaths as replacements since the beginning of 2011 [12]. Similar stress-relieving heater sheaths have been used in other countries, such as Japan.

2.2.1.2 Current prediction capabilities

The dependency of a variety of variables on SCC growth behavior has been researched [13–17] in PWR primary water coolant environments using cold-worked austenitic stainless steels and weld metals. The dependence of variables on SCC growth, such as cold work, temperature, stress intensity factor, material composition of forged materials (316, 304 SS) and weld metals (308L SS, 316L SS), electrochemical potential, the extent of sensitization, and rolling direction have been examined. Furthermore, water chemistry variables, such as hydrogen, lithium, and boron concentration, have also been examined [15, 18]. With such information, dissimilarities and similarities in SCC growth behaviors in PWRs and BWRs could be compared, factoring the possible inadequacy of sources and the amount of data.

However, there has been little research to date on the crack initiation phenomena of stainless steels in BWR or PWR primary systems. Lifetime prediction depends on an understanding of the processes occurring during crack initiation and propagation. Consequently, detailed studies on the processes of crack initiation are necessary for reliable estimates of cracking susceptibility during long-term operation.

Present knowledge on the important factors on growth of SCC is summarized as follows to assess the present prediction capabilities and limitations.

Cold work and electrochemical potential

Dependence of electrochemical potential on SCC growth was observed on cold-worked non-sensitized 316 SS and 304 SS in high-temperature water. This trend is quite similar to the results shown in Table 2.1. However, significant IGSCC growth did occur, even in hydrogenated PWR primary water on cold-worked non-sensitized 316 SS and 304 SS, as shown in Figure 2.2.

The growth rate of IGSCC increased with an increasing degree of cold work (which leads to an increase in YS). This result suggested that the growth rate of SCC increases with increasing the residual strain in the materials, such as in the HAZ, heater sheath, and cold-worked piping.

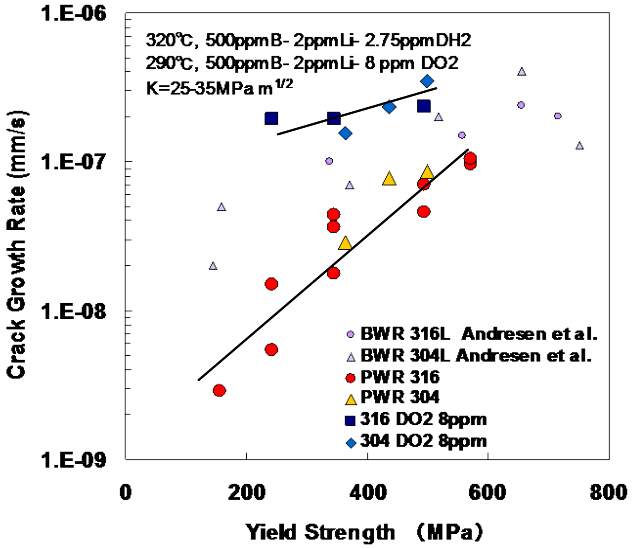

Figure 2.2. Dependence of cold work (measured by yield stress here) and potential on growth of IGSCC of non-sensitized 316 SS and 304 SS [15].

The residual strain caused by shrinkage during the welding process is considered to be strongly dependent on the heat input and the number of passes made during welding. Therefore, the residual strain at weld HAZs is dependent on the thickness or diameter of the piping. Consequently, the rate of SCC growth at the weld HAZ is affected by the pipe diameter and heat input. Examples of major piping in PWR systems and their respective outer diameters are given in Table 2.5.

Table 2.5 Key piping in PWR systems

System piping	Outer Diameter (mm)
Reactor coolant system and safe end	800
Safety injection	165
Residual heat removal	165
Chemical and volume control	89

Given the test results shown in Figure 2.2 and the information on the size of the piping used in PWRs, the weld HAZ in the Reactor Coolant System (RCS) and safe end might show high SCC susceptibility in PWRs. In other words, the SCC susceptibility in the other systems is assumed to be lower. The residual strain also depends on the manufacturing process. The degree of cold work of the through-wall cracked heater sheath was reported as around 30%, judging from its hardness measurement. Given this operating information and results shown in Figure 2.2, one of the major causes of the failure of the heater sheath is considered to be the heavy cold work during manufacturing. A stress-relieved heater sheath is recommended to maintain reliability. Stress-relieved heater sheaths have been put into service in some countries (e.g., Japan and France).

The growth rate of SCC in PWRs is low compared with that in high potential environment such as under NWC condition in BWRs judging from the literature data, such as shown in Figure 2.2. Furthermore, the number of incidents caused by SCC is a few in PWRs except for the cases described in above, to date. However, a few field experiences described here suggested that it is necessary to recognize that it is not immune even in low potential environment such as BWR HWC or PWRs, if material was heavily cold worked. Therefore, detailed studies of SCC initiation are important for precise prediction after long-term operation to keep reliability of components made from heavily cold-worked stainless steels after long-term operation in high tensile stress conditions.

Temperature and cold work

The effect of temperature on IGSCC growth of cold-worked austenitic stainless steels exposed to PWR primary water is shown in Figure 2.3. The growth rate of IGSCC of non-sensitized 20% cold worked 316 [20% cold-worked (CW) 316 SS] increased with increasing temperature in the range 250 °C (482 °F) to 340 °C (644 °F) and then decreased at 360 °C (680 °F) in a PWR primary environment. Also, the growth rate of IGSCC of non-sensitized 10% CW and 15% CW 316 SS increased with increasing temperature up to 330 °C (626 °F) and then decreased at 340 °C (644 °F) and 360 °C (680 °F). However, the detailed mechanism is not clear on this temperature dependence with peak. Simple 1/T type temperature dependence is observed below 330 °C (626 °F) in either case, the apparent activation energy is about 100 kJ/mol. The results seem to suggest that significant crack growth does not occur in the pressurizer [~343 °C (650 °F)], if the degree of cold work does not exceed 20%. Considering the small diameter and thin thickness of the piping in the pressurizer, the residual strain at the weld HAZ is assumed to be low, so the SCC susceptibility and growth rate are assumed to be low in the pressurizer except for heavily cold-worked heater sheath that has not been stress-relieved. The highest operating temperature in Chemical Volume Control System (CVCS) is about 290 °C from the outlet of RCS until the first regenerative heater, and then the temperature decreased. The highest temperature is also about 290 °C in Safety Injection System (SIS) and Residual Heat Removal System (RHRS), even if cavity flow occurs from the RCS, and then temperature decreases. On the upstream side of the separator valve of RHR system, the operating temperature is usually less than about 177 °C (351 °F). Given the operating temperature in CVCS, SIS and RHRS, the SCC susceptibility and SCC growth rate at the weld HAZ in those systems are assumed to be low compared with the hot-leg side of the RCS [~320 °C (608 °F)] based on the literature data such as shown in Figure 2.3. Furthermore, the size and thickness of the piping in CVCS, SIS, and RHRS is smaller and thinner than main coolant piping in RCS, consequently the residual strain caused by welding is assumed to be smaller in weld HAZ in CVCS, SIS, and RHRS than that in RCS. These results suggested that SCC susceptibility in these systems (CVCS, SIS, RHRS) will be lower than that of the safe end welded area in main coolant piping, which was described in Section 1.2.1.1.

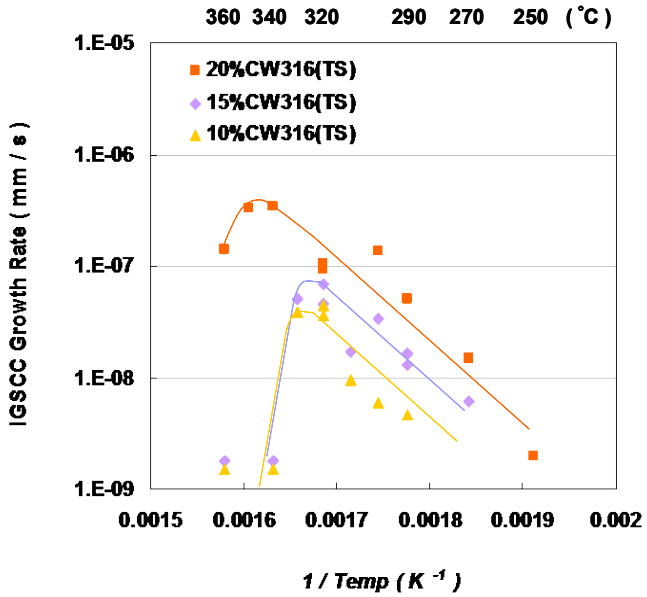

Figure 2.3. Dependence of temperature and cold work on the growth of IGSCC of non-sensitized 316 SS [16]. "TS" in the legend refers to cold-work direction.

Stress intensity factor and cold work

The effect of the stress intensity factor (K) on the crack growth rate of IGSCC in the PWR primary environment is shown in Figure 2.4. Within the test period (~2 months), no significant growth was observed for 15% and 20% cold-worked 316 SS with a K of less than 10 MPa $m^{1/2}$ at 320 °C (608 °F), or for 5% and 10% cold-worked 316 SS with a K of less than 20 MPa $m^{1/2}$ at 320 °C. The results indicated that the growth rate of SCC was insignificant in the HAZ of piping under low-K conditions.

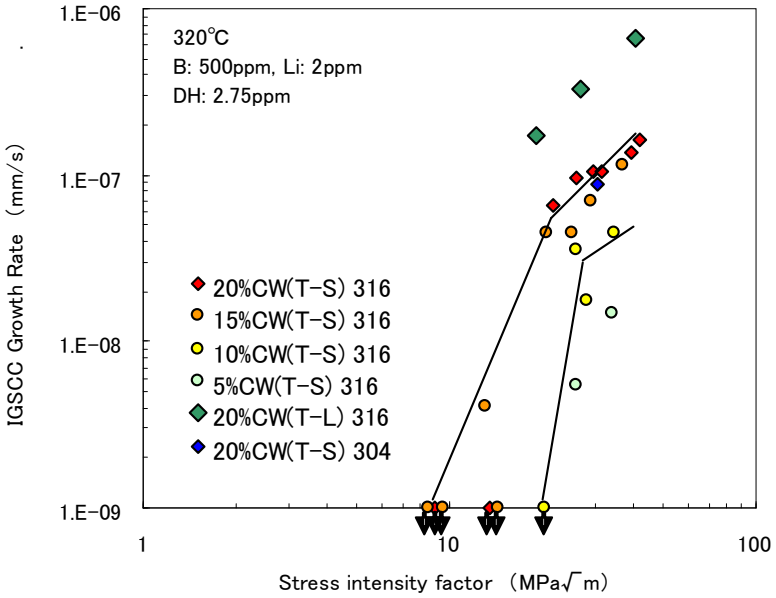

Figure 2.4. Dependence of IGSCC growth rate on stress intensity factor for non-sensitized 316 SS and 304 SS [15].

Sensitization and electrochemical potential

Significant IGSCC growth was not observed for sensitized 20% cold-worked 316 SS in a PWR primary environment in the temperature range between 250 °C (482 °F) and 340 °C (644 °F), as shown in Figure 2.5. This trend is completely different from the IGSCC behavior in high-potential environments such as in BWRs. Furthermore, a similar trend was observed in the hydrogen range between 0 and 30 cc/kg of H_2O, as shown in Figure 2.6. This result suggested that stress relieving does not have any harmful effect on IGSCC propagation in stainless steels in a PWR primary coolant environment except for case in oxygen stagnant area.

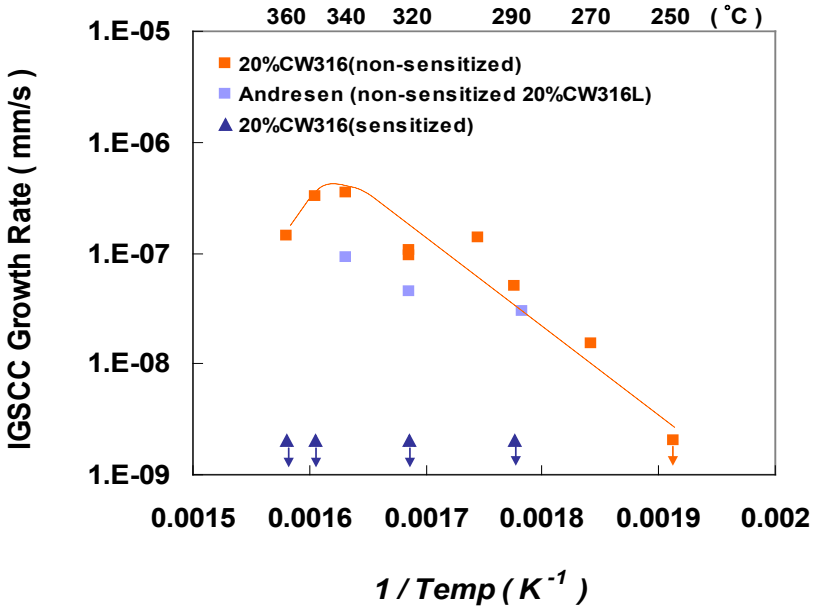

Figure 2.5. Influence of sensitization on IGSCC growth in the PWR primary environment [16].

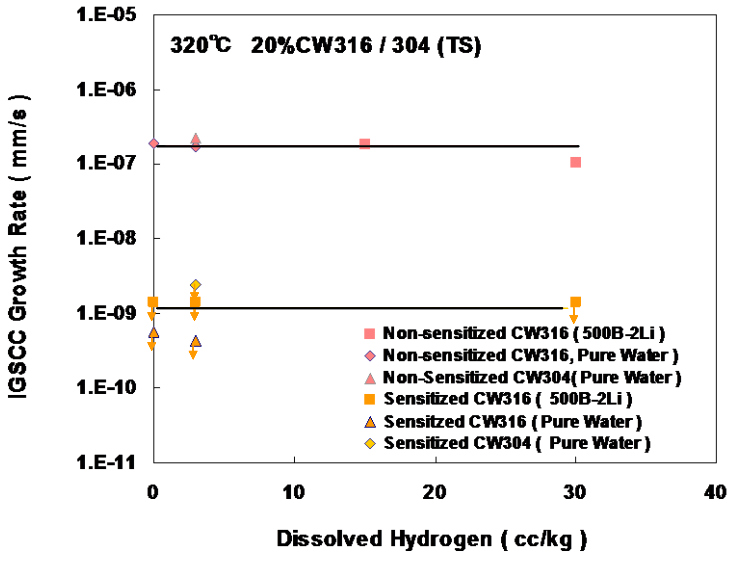

Figure 2.6. Influence of sensitization on IGSCC growth in the PWR primary environment [16].

In other words, this result seems to suggest that stress relieving might become a future countermeasure to retard IGSCC susceptibility in low-potential environments by removing any residual stresses in a component. However, much more fundamental information is necessary, including the mechanistic cause of the effect of sensitization on IGSCC growth in a low-potential environment.

Weld metal and electrochemical potential

High SCC resistance of weld metal (308L SS, 316L SS) was reported [17] for samples exposed to low-potential PWR primary water, although so far the data are limited. Significant SCC growth was not observed for a 10% CW weld metal (308L SS, 316L SS) specimen in a PWR primary environment at 320 °C (608 °F). This behavior is different from that observed forged austenitic stainless steels as discussed above. On the other hand, SCC growth was observed at ferrite and austenite boundaries for 10% cold-worked 308 SS and 316L SS specimens in oxygenated high-temperature water containing lithium and boric acid. Preferential oxidation was observed in the ferrite phase in a high-potential environment although it is not clear whether this is one of the causes of SCC in a high-potential environment. A significant difference in the growth rate in the high-potential environment was not observed between weld metal (308L SS and 316L SS) and forged 316 SS and 304 SS specimens in the high-potential environment. Furthermore, the effect of spinodal decomposition during long term operation on SCC growth was reported [17] using weld and cast stainless steel in both a high- and a low-potential environment. These research data on weld stainless steels has indicated a high resistance to SCC in a low-potential PWR primary environment. However, the data is very limited to data for the precise prediction. To improve the prediction capability on SCC behavior of stainless steel weld metals and cast stainless steels, many more studies are needed. In addition, mechanistic knowledge, such as the mechanistic cause of the difference in SCC susceptibility between stainless steel forgings and stainless steel welds in a low-potential environment and the reason why SCC growth rates are dependent on the potential could potentially enable informed understanding for taking corrective measures

The probability that IGSCC will occur in low potential environment is relatively low for both of non-sensitized and sensitized stainless steels, mainly due to the differences in the electrochemical potential in the respective environments judging from the data shown in Figures 2.2 through 2.6. However, the combined knowledge, based on laboratory data and a few recent field experiences, indicates that heavily cold-worked non-sensitized stainless steels under conditions of high tensile stress condition and high temperature are not immune to SCC, even in a low-potential PWR environment.

When cracking has been observed, it has been related to the combined effects of

- heavy cold work and high residual stress and strain due to high heat input during welding,
- high tensile residual stress and/or stress concentration due to poor weld design, and
- lack of effective stress-relief treatment.

2.2.1.3 Long-term concerns

As described in previously, the probability of occurrence of IGSCC in a low-potential environment is low for both sensitized and non-sensitized stainless steel. However, we should realize that these grades of steel are not immune even in PWR primary low potential environment, if material was heavily cold worked. Therefore, there are concerns for operation extended for more than 60

years. A maintenance program based on information that addresses those concerns should be established to maintain the reliability of components made with these materials in BWRs and PWRs. Those concerns are detailed in the following sections.

Crack initiation process during long-term operation

Steady IGSCC propagation is assumed to start with shallow cracking (~50 to 100 μm deep), although the depth may depend on a number of variables, such as the type of material, degree of cold work, presence of residual stress, and environmental conditions (e.g. service temperature, and coolant chemistry). In other words, even though SCC may be observed in some area in some system (such as safe end weld HAZ), SCC may not occur in piping in other systems (such as SIS, CVCS and RHRS). However, studies on SCC initiation processes in LWR environments are limited to date. From an engineering point of view, detailed studies to consider what locations are susceptible and not susceptible to SCC would be beneficial.

Criteria for arresting the IGSCC propagation

In some cases, the surfaces of HAZ in the welded zone are machined and surface-ground. Shallow local oxidation penetration may occur in these cold-worked regions exposed to PWR environments during long-term operation as judged from the results of removed piping examination [10]. It might be difficult to control the local penetration of corrosion into the cold-worked layer beyond 60 years. However, some cracks are likely to stop growing, even after shallow oxide penetration into the cold-worked layer; in other cases, cracking may continue to grow after shallow crack penetration into the cold worked layer. These different growth behaviors are assumed to depend on the difference in the residual stress and residual strain in the material.

Residual stress and strain in the HAZ strongly depend on the welding procedures, such as the number of passes of welding and heat input. Consequently, if the residual stress in the HAZ is low enough, the crack stops growing, even after shallow crack penetration into the cold-worked surface layer. If the residual stress is high, the crack could potentially grow just after shallow crack penetration into the cold-worked surface layer. Therefore, studies to focus on the criteria for arresting IGSCC propagation would be useful for establishing a reasonable maintenance program to extend reliability beyond 60 years.

Crack growth behavior in weld metal after long-term operation

Hardness and mechanical strength of the ferrite phase change with time due to the spinodal decomposition during operation. Consequently, the local stress and local chemical composition can be expected to change with time. Thermal aging and potential influences on SCC were studied using thermal aged 316L SS, 308L SS, and CF8M test coupons [17–19]. An increase in SCC growth rates was observed after long term aged cast stainless steel (40,000 h at 400 °C (752 °F) in comparison with the crack growth rate of non-aged cast stainless steel in a high potential environment with B and Li at 320 °C (608 °F). On the other hand, no SCC growth was observed in low potential PWR primary environment in the same aged material. However, the data are very limited, especially for the PWR primary environment (service stress, temperature, and coolant chemistry and its composition). Furthermore, the cause of the difference in SCC growth between stainless steel weld and forged stainless steel materials is not well known. More detailed studies on SCC growth and initiation in weld stainless steels may provide technical data and basis to provide the material and component performance assessments for reactor operation beyond 60 years.

Potential for change in local grain-boundary and surface properties during long-term operation

In general, the lattice diffusivity in face centered cubic materials (fcc) is slower than that of body centered cubic material (bcc) such as steel. Therefore, the influence of lattice diffusion on changes in local chemical composition in fcc is assumed to be low at LWR operating temperatures. On the other hand, it's well known that cold work enhances the lattice diffusivity. However, little has been published describing the effect of cold work on diffusivity of austenitic stainless steel and other fcc materials at low temperature less than 600 °C (1,112 °F), and thus not enough information is available about the local change in the materials at PWR operating temperatures. Estimating the possible change in local properties such as the local chemical composition of grain boundaries during long-term operation (beyond 60 years) is not presently available.

Cavity formation was identified at grain boundaries not only for bcc material but also for fcc materials in recent research using cold-worked Alloy 690 (fcc), cold-worked Alloy 600 (fcc), and cold-worked carbon steel (bcc) after testing in the temperature range between 360 °C (680 °F) to 475 °C (887 °F) [20, 21]. An example is shown in Figure 2.7. These cavities are proposed to form as a result of the diffusion of vacancies induced by cold work and driven by a stress gradient. Targeted research may provide information on the possibility that changes in the grain boundary properties (such as changes in grain boundary bonding strength and in chemical composition of grain boundary) have an effect on IGSCC initiation and growth during long-term operation, especially for cold-worked materials.

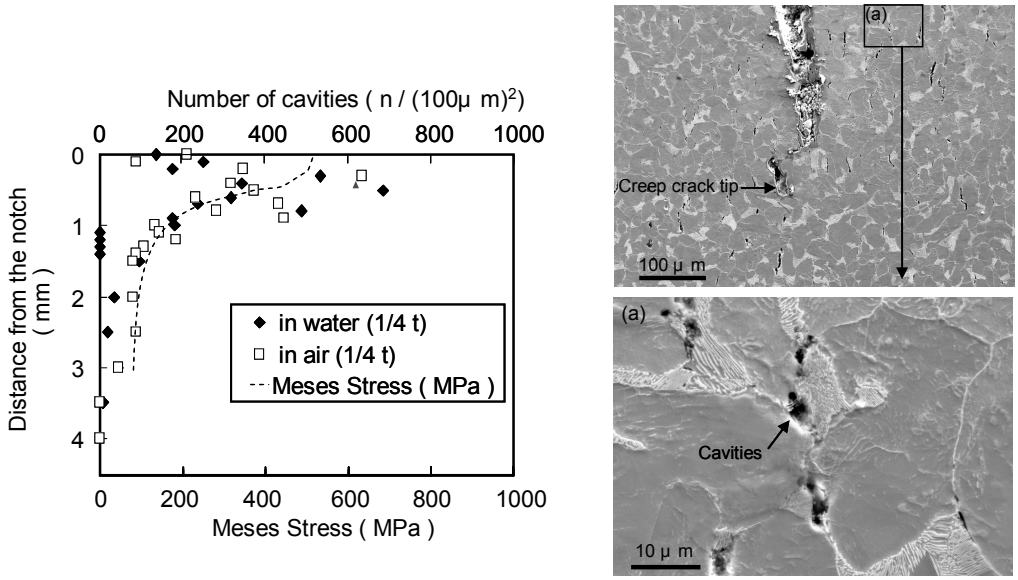

Figure 2.7. Cavity formation at grain boundaries of 30% cold-worked carbon steel after test in at 360 °C [20].

2.2.2 SCC in a High-Electrochemical-Potential Environment (Oxygen-Stagnant Area)

2.2.2.1 Past and current plant experience

There have been some reports of incidents in PWR components resulting from SCC of austenitic stainless steel in oxygen-stagnant areas, such as canopy seal welds [3], the upstream side of the final check valve in the safety injection line [4], and the heater sleeve of the pressurizer [22]. The major cause of the SCC was due to the presence of residual oxygen in the affected area. In these cases, the affected area was exposed to a high electrochemical potential during every plant start-up due to the presence of air in the crevice unless a special plant start-up procedure was applied, such as an air removal procedure using vacuum pumping before plant start-up. Consequently, cracking occurs if the cumulative number of times that an aggressive environment forms during plant start-up exceeds some threshold quantity. Therefore, this type of SCC in an oxygen stagnant area in low-potential environments is one of concerns when determining how to maintain reliability for more than 60 years.

Stress corrosion cracking at the canopy seal weld in the control rod drive mechanism

Small leakage occurred at the lower canopy seal of some PWR plants in 1980 [3]. The canopy seal ensures the leak tightness of threaded joints between the top of the vessel head penetrations and the CRDM housing and is typically fabricated from Type 304. Destructive examination of the affected seals was performed on five PWR plants. In almost all cases, TGSCC from the inside the canopy seal was found. It was concluded that the cause of the cracking was a combination of a corrosive medium, most likely chloride, and oxygen in the “dead end cavity” that is formed by the canopy seal.

Stress corrosion cracking at the heater sleeve in the pressurizer

During a 2006 outage at Braidwood Unit 1, a leak was detected in the upper socket weld connected to a pressurizer heater [22]. The sleeve material was Type 316 SS with 0.08% C. Based on destructive examination, the leak was determined to be the result of circumferential IGSCC, which initiated from the inner surface. The crack propagated through the HAZ of the multipass socket weld. Significant sensitization was confirmed, and it was reported that qualitative energy-dispersive X-ray spectroscopy (EDS) evaluations identified high oxygen content on the crack deposits, indicating that the crevice was exposed to an oxygenated environment. Given the structure of the heater sleeve, it is not easy to remove all the residual air before plant start-up. Based on the observed structure, the cause of the cracking was concluded to be due to a combination of the presence of residual oxygen in the socket weld during start-up and high degree of sensitization of the material.

Stress corrosion cracking at the upstream side of the final check valve in the SIS

Cracking was found by routine ultrasonic examination at Sequoyah Unit 2 during an outage in 1996 [4]. IGSCC was located at the HAZ adjacent to the weld in the piping on the upstream side of the final check valve between SIS and RCS. The piping was made from 316 SS with 0.077% C. The results of examination conducted according to ASTM test standard A262 [23] revealed that the HAZ was sensitized to high levels. No evidence of contaminants or aggressive elements, such as chlorine, was reported; it was concluded that the IGSCC was caused by the exposure to the oxygenated water and a high concentration of boric acid in the SIS.

2.2.2.2 Current prediction capabilities

The slow strain rate test (SSRT) has been used in an environment that simulates the oxygen-stagnant areas in PWR primary systems to investigate the susceptibility of austenitic stainless steels to SCC. The essential variables, such as temperature, electrochemical potential, sensitization, and the effect of lithium and boron were examined [24–27].

The current knowledge of these important variables affecting susceptibility to SCC is summarized in the following subsections of this chapter to assess the current capabilities and limitations to predict potential occurrence of SCC during extended reactor operation.

Effect of temperature, LiOH, and boric acid

The susceptibility of sensitized 304 SS to IGSCC in oxygenated water with LiOH and boric acid below 200 °C (392 °F) increases with increasing temperature. Below 150 °C (302 °F), sensitized 304 SS is less susceptible to IGSCC in water containing 2 ppm Li than it is in pure water without Li and B or in water containing low concentrations of B (500 ppm). Below 200 °C, the IGSCC susceptibility of sensitized 304 SS is also suppressed by B concentrations greater than 1,500 ppm B (Figure 2.8). However, no significant difference in IGSCC susceptibility was identified at high temperature (above 200 °C) in a high-potential environment.

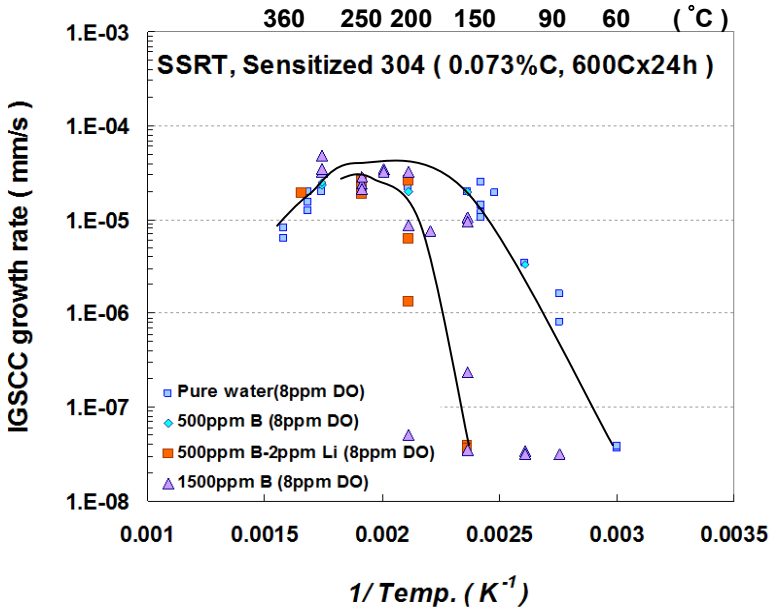

Figure 2.8. Influence of temperature and LiOH and $B(OH)_3$ concentrations on IGSCC susceptibility in an oxygen-stagnant environment [26].

Generally, LiOH and boric acid additions retard the IGSCC susceptibility of sensitized stainless steels compared with that in oxygenated pure water at temperature less than 150 °C. However, no significant effect of LiOH and B addition was observed at high temperature (above 200 °C). This result suggests that the probability of IGSCC occurrence in an oxygen-stagnant area in PWRs is low at temperatures <150 °C compared with that in oxygenated pure water. This result also suggests that it could be difficult to prevent SCC occurrence in an oxygen-stagnant area in PWRs during long-term operation especially at high temperature (>200 °C) conditions, such as canopy seal weld and heater sleeve. Consequently, to improve the prediction capability on SCC

occurrence during extended service, detailed evaluations of the SCC susceptibility for each stagnant area are necessary to consider the measures to keep reliability during extended operation. In addition, based on the results of the evaluation described above, applications of appropriate countermeasures, such as residual air removal, would likely benefit maintaining reliability of PWRs for long-term operation.

Effect of sensitization

The effect of sensitization on SCC was examined to consider the potential SCC in simulated oxygen-stagnant areas. The sensitization of the materials was measured by EPR method. The result is shown in Figure 2.9. This trend is quite similar to that in BWR environment. Similar sensitization dependence was also observed at low temperature [100 °C (212 °F)]. In addition, the critical potential for the IGSCC susceptibility of sensitized 304 SS and 316 SS was studied in a B-Li environment [24, 25] and was summarized as a function of temperature.

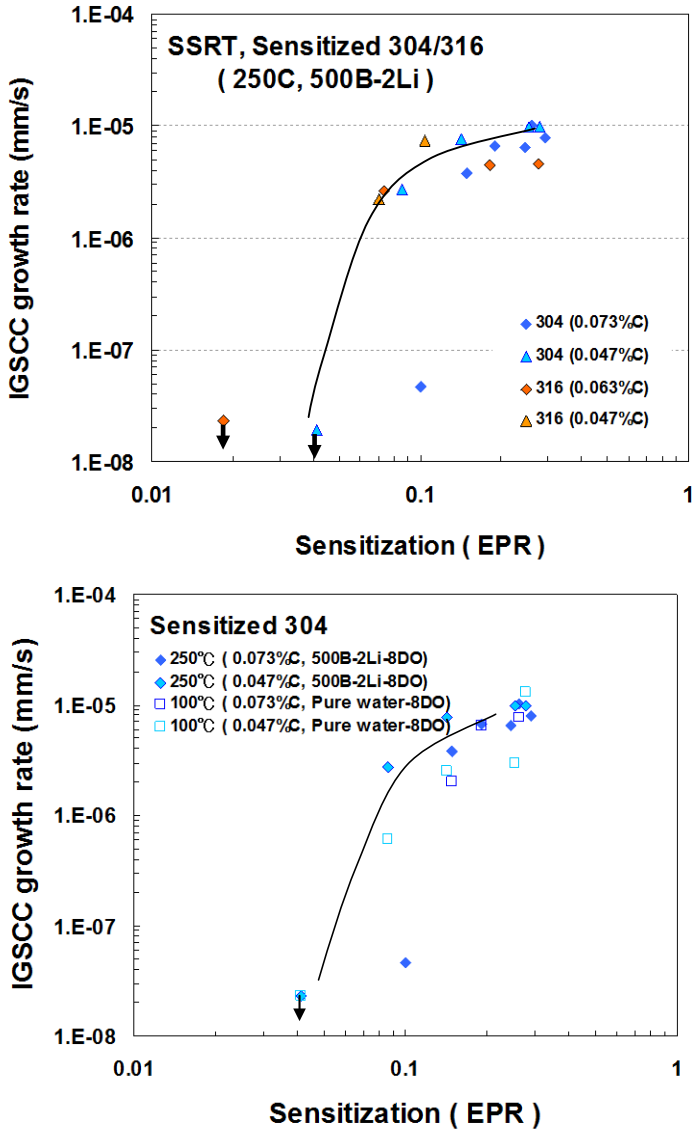

Figure 2.9. Sensitization-dependence on IGSCC-susceptibility in an oxygen-stagnant environment [26].

These test results suggested that sensitization enhanced the IGSCC susceptibility in an oxygen-stagnant areas in PWR piping and internals at high and low temperatures. These results suggest that replacement of the sensitized stainless steels with sensitization-resistant stainless steels will mitigate IGSCC in the oxygen-stagnant areas of PWR piping systems.

Effect of oxygen and hydrogen on electrochemical potential

Hydrogen addition affects electrochemical potential significantly, mainly due to its high exchange current density (Figure 2.10). This result suggests that the potential in oxygen-stagnant areas is controlled by the combination of the concentrations of hydrogen and oxygen, and the temperature. In other words, the potential is controlled by how rapidly hydrogen was supplied to the oxygen stagnant area during plant start-up as shown in Figure 2.10. Therefore, one of the ways for evaluation of SCC susceptibility in an oxygen stagnant area is to evaluate the local potential and then to compare it with the critical potential for the occurrence of SCC [25, 27]. Dotted lines in Figure 2.10 are the calculated results of the potential based on the revised mix potential model [18]. In other words, the change in potential during plant start-up could be estimated using this type of calculation model if we can better determine the oxygen and hydrogen concentration behavior in the stagnant area.

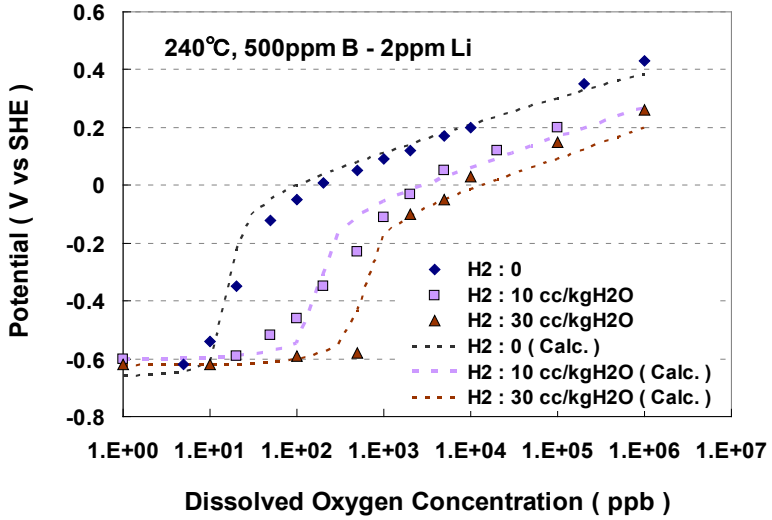

Figure 2.10. Influence of hydrogen concentration on the potential of stainless steel at 240 °C [18].

One example, the potential for the upper part of a canopy sealed crevice, is shown in Figure 2.11. The calculated result suggests that the potential exceeds the critical potential for IGSCC in about 300 h beginning from start-up for a plant, if residual air is not removed before plant start-up. A comparison of the results for the upper part of a canopy sealed crevice with the results for the lower part is shown in Figure 2.12. The duration exceeding the critical potential is much longer in the lower part. Thus, the duration exceeding the critical potential seems to depend on the design and manufacturing process, such as length of diffusion pass of oxygen and hydrogen and temperature. However, past operational experience, has shown that it is difficult to remove residual oxygen in such stagnant areas before plant start-up.

In essence, based on the combined knowledge of operating experience, laboratory results, and mechanistic understanding, detailed studies would inform proper evaluation of the possibility of

crack initiation and propagation beyond 60 years in the oxygen-stagnant areas in PWRs if residual air is not adequately removed before plant start-up. Furthermore, some studies on appropriate countermeasures, such as residual air removal or replacement of the non-sensitized stainless steels, might provide additional information to help maintain the reliability of LWRs for long-term operation.

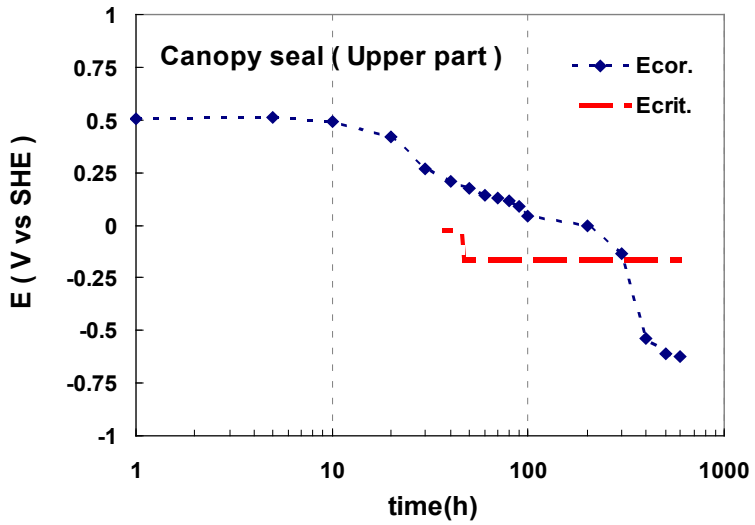

Figure 2.11. Assumed electrochemical potential behavior during plant start-up in canopy seal [18].

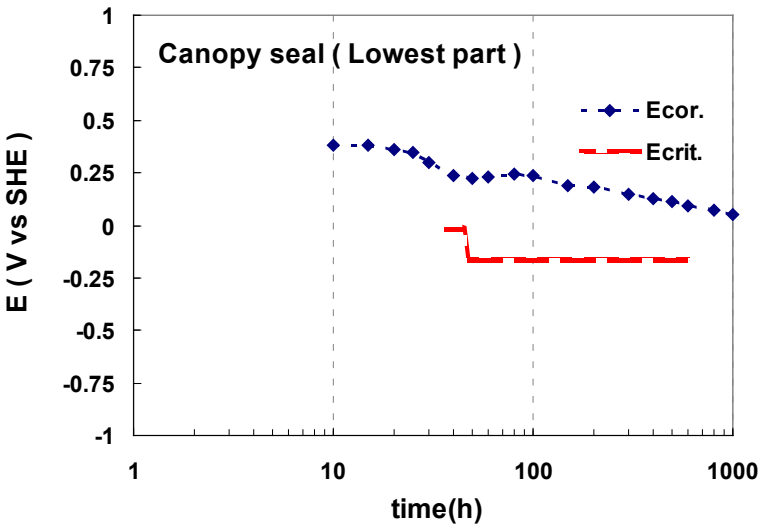

Figure 2.12. Assumed electrochemical potential behavior during plant start-up in canopy seal [18].

2.2.2.3 Long-term concerns

Based on information presented above, some potential technical issues for extended operations to beyond 60 years have been identified. These issues are as follows.

- ***Detailed evaluation of SCC susceptibility in each stagnant area.*** Studies on the SCC susceptibility in each stagnant area will inform a complete evaluation of the possibility of SCC occurrence during extended operation to maintain reliability.
- ***Effective residual air removal procedure before plant start-up.*** Studies for effective residual air removal procedure before plant start-up would provide additional information to maintain the stagnant area.
- ***Stress relief.*** Stress relieving and replacement with non-sensitized materials are considered to be other types of countermeasures to retard SCC susceptibility in oxygen stagnant areas.

2.3 REFERENCES*

1. D. J. DePaul (ed.), *Corrosion and Wear Handbook for Water-Cooled Reactors,* United States Atomic Energy Commission, McGraw-Hill, New York, 1957.
2. H. Coriou, L. Grall, and V. Gall, *Colloque de Metallugie, Sacley (1959)*, North Holland Publishing, Amsterdam, 1960, pp.161–169.
3. C. M. Pezze and I. L. W. Wilson, *Proc. 4th Int. Symp. Environmental Degradation of Materials in Nuclear Power Systems—Water Systems,* Jekyll Island, Aug. 6–10, 1989, D. Cubicciotti (ed.), National Association of Corrosion Engineers, 1990, p. 4-164.
4. G. V. Rao, D. E. Boyle, and R. Phillips, *Proc. Fontevraud 4 Int. Symp.: Contribution of Materials Investigation to the Resolution of Problems Encountered in Pressurized Water Reactors*, F. de Keroulas and Ph. Berge (Meeting Chairs), Société Française d'Energie Nucléaire, Paris, Sept. 14–18, 1998.
5. R. Cauvin, O. Goltrant, Y. Rouillon, E. Cazus, P. Dubuisson, P. Poitrenaud, and S. Bellet, *Proc. Fontevraud 3 Int. Symp.: Contribution of Materials Investigation to the Resolution of Problems Encountered in Pressurized Water Reactors,* F. de Keroulas and Ph. Berge (Meeting Chairs), Société Française d'Energie Nucléaire, Paris, Sept. 12–16, 1994, p. 54.
6. G. Pironet, A. Heuze, O. Goltrant, and R. Cauvin, *Proc. Fontevraud 4 Int. Symp.: Contribution of Materials Investigation to the Resolution of Problems Encountered in Pressurized Water Reactors*, F. de Keroulas and Ph. Berge (Meeting Chairs), Société Française d'Energie Nucléaire, Paris, Sept. 14–18, 1998, p. 195.
7. M. Nakano, K. Fukuya, K. Fujii, M. Kodama, and T. Torimaru, *Proc. 11th Int. Symp. Environmental Degradation of Materials in Nuclear Power Systems—Water Reactor,* Stevenson, Aug. 10–14, 2003, Gary S. Was and L. Nelson (eds.), American Nuclear Society, 2003.
8. T. Yonezawa, K. Arioka, H. Kanasaki, K. Fujimoto, S. Urata, and H. Mizuta, *Proc. Fontevraud 4 Int. Symp.: Contribution of Materials Investigation to the Resolution of Problems Encountered in Pressurized Water Reactors*, F. de Keroulas and Ph. Berge (Meeting Chairs), Société Française d'Energie Nucléaire, Paris, Sept. 14–18, 1998, p. 237.
9. T. Yonezawa, K. Arioka, H. Kanasaki, K. Fujimoto, K. Ajiki, T. Matsuoka, S. Urata, and H. Mizuta, "Intergranular cracking mechanism in baffle former bolt materials for PWR core internals," *Journal of the Atomic Energy Society of Japan* **42,** 212–217 (2000).

* Inclusion of references in this report does not necessarily constitute NRC approval or agreement with the referenced information.

10. T. Shoji, K. Sakaguchi, Z. Lu, S. Hirano, Y. Hasegawa, T. Kobayashi, K. Fujimoto, and Y. Nomura, *Proc. Fontevraud 7 Int. Symp.: Contribution of Materials Investigations to Improve the Safety and Performance of LWRs,* Société Française d'Energie Nucléaire, Avignon, Sept. 26–30, 2010.

11. T. Couvant, P. Moulart, L. Legras, P. Bordes, J. Capelle, Y. Rouillon, and T. Balon, *Proc. Fontevraud 6 Int. Symp.: Contribution of Materials Investigations to Improve the Safety and Performance of LWRs,* Société Française d'Energie Nucléaire, Paris, Sept. 18–22, 2006, p. 67.

12. J. Champredonde, Y. Thebault, P. Moulart, T. Couvant, K. Dubourgnoux, Y. Neau, J. Fageon, D. Lecharpetier, A. Breiul, and V. Derouet, *Proc. 15th Int. Conf. Environmental Degradation in Nuclear Power Systems—Water Reactors,* Colorado Springs, J. Busby and G. Ilevbare (eds.), The Metallurgical Society, 2011.

13. K. Arioka, Y. Yamada, T. Terachi, and Roger W. Staehle, "Intergranular Stress Corrosion Cracking Behavior of Austenitic Stainless Steels in Hydrogenated High-Temperature Water," *Corrosion* **62,** 74 (2006).

14. K. Arioka, T. Yamada, T. Terachi, and G. Chiba, "Influence of Carbide Precipitation and Rolling Direction on Intergranular Stress Corrosion Cracking of Austenitic Stainless Steels in Hydrogenated High-Temperature Water," *Corrosion* **62,** 568 (2006).

15. K. Arioka, T. Yamada, T. Terachi, and G. Chiba, "Cold Work and Temperature Dependence of Stress Corrosion Crack Growth of Austenitic Stainless Steels in Hydrogenated and Oxygenated High-Temperature Water," *Corrosion* **63,** 1114 (2007).

16. K. Arioka, T. Yamada, T. Terachi, and T. Miyamoto, "Dependence of Stress Corrosion Cracking for Cold-Worked Stainless Steel on Temperature and Potential, and Role of Diffusion of Vacancies at Crack Tips," *Corrosion* **64,** 691 (2008).

17. T. Yamada, T. Terachi, K. Arioka, Proc. *14th Int. Conf. Environmental Degradation in Nuclear Power Systems—Water Reactors,* Virginia Beach, T. Allen and J. Busby (eds.), American Nuclear Society, 2010.

18. K. Arioka, T. Yamada, T. Terachi, and T. Fukumura, *SCC Behaviors of Stainless Steels in PWR Primary Environments*, INSS Monograph No. 5, Institute of Nuclear Safety Systems, Japan (2012).

19. K. Arioka, *Proc. Fontevraud 5 Int. Symp.: Contribution of Materials Investigation to the Resolution of Problems Encountered in Pressurized Water Reactors,* F. de Keroulas and F. Hedin (Meeting Chairs), Société Française d'Energie Nucléaire, Paris, Sept. 23–27, 2002.

20. K. Arioka, T. Miyamoto, T. Yamada, and T. Terachi, "Formation of Cavities Prior to Crack Initiation and Growth on Cold-Worked Carbon Steel in High-Temperature Water," *Corrosion* **66,** 015008 (2010).

21. K. Arioka, T. Miyamoto, T. Yamada, and T. Terachi, "Dependence of Stress Corrosion Cracking of Alloy 690 on Temperature, Cold Work, and Carbide Precipitation—Role of Diffusion of Vacancies at Crack Tips," *Corrosion* **67,** 035006 (2011).

22. NRC, *Circumferential Cracking in the Stainless Steel Pressurizer Heater Sleeves of Pressurized Water Reactors,* NRC Information Notice 2006-27, ADAMS ML062500219, U.S. Nuclear Regulatory Commission, Dec. 11, 2006.

23. ASTM, *Standard Practices for Detecting Susceptibility to Intergranular Attack in Austenitic Stainless Steels,* ASTM A262–10, ASTM International.

24. K. Arioka, M. Hourai, S. Okamoto, and K. Onimura, “The effects of boric acid, solution temperature, and sensitization on SCC behavior under elevated temperature water,” *Corrosion’83,* Paper 135, National Association of Corrosion Engineers, USA, 1983.

25. K. Arioka, T. Nojima, T. Kanechiku, C. G. Schmidt, and D. D. Macdonald, “Critical potential of IGSCC for sensitized stainless steels under PWR environment,” *3rd Int. Conf. Nuclear Engineering,* Kyoto, Japan, 1995.

26. K. Arioka, M. Hourai, S. Noguchi, and K. Onimura, “Studies on analytical method and non-destructive measurement method for sensitization of 304 and 316 stainless steels,” *Corrosion’83,* Paper 134, National Association of Corrosion Engineers, USA, 1983.

27. H. C. Park, G. Cragnolino, and D. D. Macdonald, *1st Int. Conf. Environment Degradation of Materials in Nuclear Power Systems—Water Reactors,* Myrtle Beach, Aug. 22–25, 1983, J. Roberts and W. Berry (eds.), National Association of Corrosion Engineers, 1984.

3. DEGRADATION VULNERABILITIES OF ALLOY 600 AND ALLOY 182/82 WELD METALS IN LIGHT WATER REACTORS

Peter Andresen
General Electric Global Research, Niskayuna, New York

3.1 INTRODUCTION

Nickel alloys and weld metals were chosen for LWR components because of low corrosion rate, resistance to SCC, and thermal expansion coefficient that is similar to that of low alloy RPV steel. Components containing Alloy 600 and Alloy 182 and 82 weld metals are listed in Figure 3.1 and Table 3.1 for BWRs, and in Figure 3.2 and Table 3.2 for PWRs. Table 3.3 contains data on the compositions of Alloy 600 and its weld metals, and Alloy X-750. Alloy 800 is preferred to Alloy 600 in Canadian and some German steam generators, and it possesses some attractive properties. However, it is an iron-base alloy (30Ni-21Cr) and is not covered in this section.

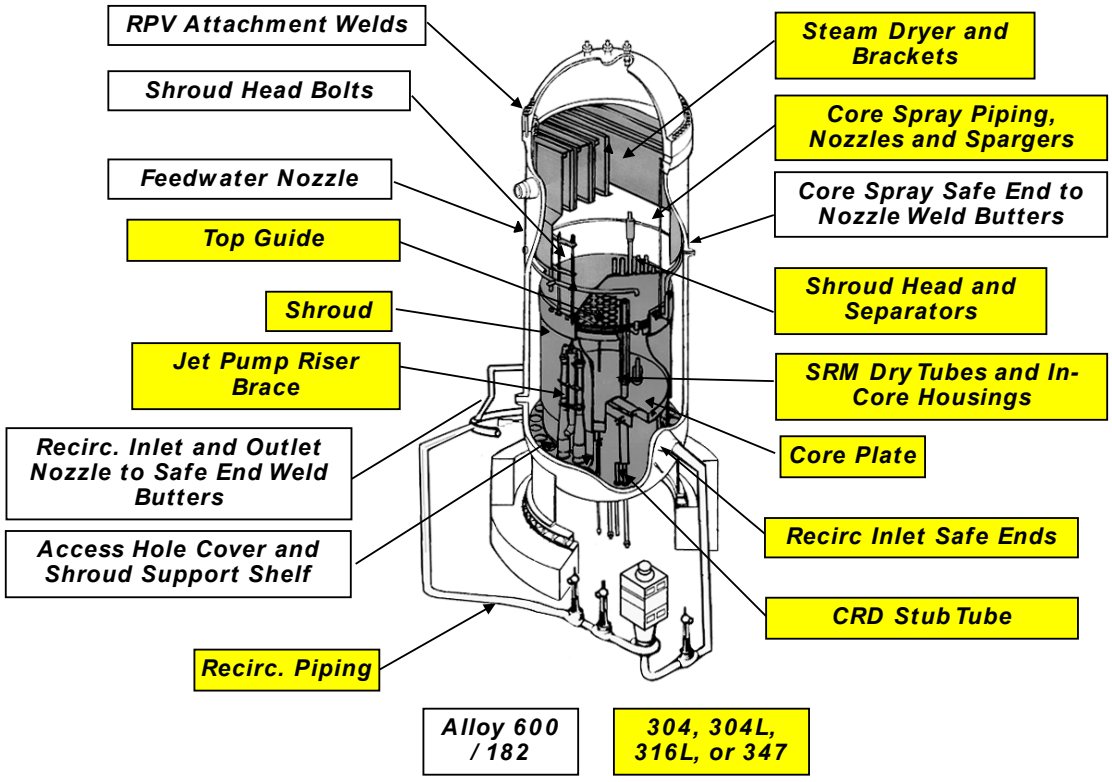

Figure 3.1. BWR components containing Alloy 600 and alloy 182 and 82 weld metals (white boxes). Austenitic stainless steels are shown in yellow boxes.

Table 3.1. BWR components fabricated from Ni alloys

BWR Component	Nickel Alloy Designation
BWR shroud head bolts	Alloy 600
Pressure vessel attachment pads	Alloy 182
Control rod penetrations	Alloy 600
Control rod penetration welds	Alloy 182
Core shroud support welds	Alloy 182
Pressure vessel nozzles	Alloys 182 and 82
Safe ends	Alloy 600
Weld metal deposits	Alloys 82 and 182
Jet pump beams	Alloy X-750
Fuel rod spacers	Alloy X-750

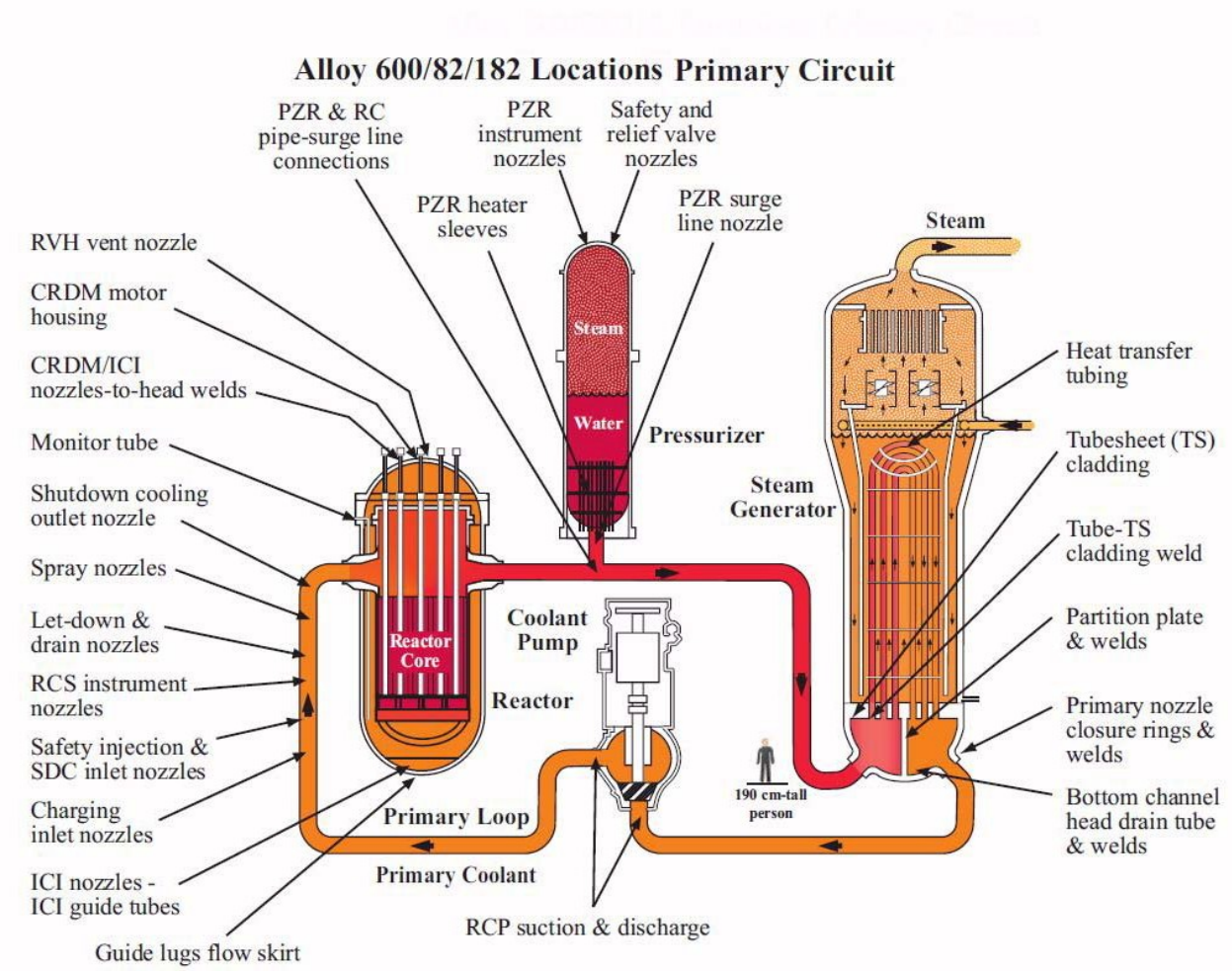

Figure 3.2. PWR components containing Alloy 600 and Alloy 182 and 82 weld metals [1, 2].

Table 3.2. PWR components fabricated from Ni alloys

PWR Component	Nickel Alloy Designation
Steam generator tubes	Alloy 600 (mill annealed and thermally treated)
Steam generator divider plates	Alloy 600
Upper head penetrations	Alloy 600
Lower head penetrations	Alloy 600
Core supports	Alloy 600
Pressurizer nozzles	Alloy 600
Safe ends	Alloy 600
Weld metal deposits	Alloys 82 and 182

Table 3.3. Compositions of common Ni alloys used in LWRs

	Alloy 600	Alloy 182	Alloy 82	Alloy X-750
Nickel (Ni)	Bal.	Bal.	Bal.	Bal.
Chromium (Cr)	14-17	13-17	18-22	15-17
Iron (Fe)	6-10	≤10.0	≤3.00	8-9
Titanium (Ti)		≤1.0	≤0.75	2.5-3.0
Aluminum (Al)				0.7-1.0
Niobium (Nb) plus tantalum (Ta)		1.0-2.5	2.0-3.0	0.8-1
Carbon (C)	≤0.05	≤0.10	≤0.10	0.05-0.08
Manganese (Mn)	≤1.0	5.0-9.5	2.5-3.5	0.1
Sulfur (S)	≤0.015	≤0.015	≤0.015	<0.03
Phosphorous (P)		≤0.030	≤0.030	<0.03
Silicon (Si)	≤0.5	≤1.0	≤0.50	0.1-0.2
Copper (Cu)	≤0.5	≤0.50	≤0.50	<0.50
Cobalt (Co)	≤0.10	≤0.12	≤0.10	<0.10

Degradation modes and related concerns in Ni alloys and weld metals include:

- SCC
- environmentally assisted fatigue, and
- environmentally assisted fracture.

For weld metals, potential issues also include:

- welding defects, such as hot cracking, ductility dip cracking, and lack of fusion;
- thermal aging;
- dilution effects (and cracking along the weld interface); and
- the growth of cracks through weld metal attachment pads and interface and into the underlying low alloy steel.

Significant cracking of Ni alloys was discovered in BWR components in the 1970s, and SCC has become the primary materials issue for Ni alloys in LWRs [1, 3–10]. Although cracking occurred initially in crevices and/or cold-worked components, it has spread to other areas and components, and has especially manifested in Alloy 182 welds. The SCC growth rates of Alloy 82 weld are not consistently different from Alloy 182 weld metal.

In PWR water (deaerated and/or hydrogenated), the susceptibility of Alloy 600 to intergranular stress corrosion cracking (IGSCC) was first revealed in laboratory testing in 1959 and then surfaced in operational service in plant in the early 1970s. IGSCC that occurs during exposure to PWR primary water is today commonly referred to as primary water stress corrosion cracking (PWSCC) [3, 4]. Highly cold-worked components were affected earlier, including the tight U-bends in steam generator tubes and cold-worked expansion of the tubes within the tube sheet [5]. IGSCC of steam generator tubing became prevalent in the 1980s, leading to steam generator retirement and replacement. PWSCC of pressurizer nozzles and control rod drive mechanism (CRDM) nozzles in the upper heads of PWR RPVs was observed in the late 1980s and has continued for more than two decades [6, 7].

SCC exhibits an intergranular morphology (Figure 3.3), both in base metal and weld metals. The cracking morphology in weld metals is often referred to as interdendritic, but it occurs primarily along the grain boundaries of packets of dendrites and not necessarily along all dendritic boundaries. The IGSCC susceptibility of these alloys was recognized in laboratory testing more than 50 years ago [3]. Important variables that affect SCC include stress intensity factors (Figure 3.4), corrosion potential (Figures 3.5–3.7), water purity, temperature, cold work, composition [especially chromium (Cr) content] (Figures 3.8 and 3.9), and microstructure (including grain boundary carbides and other particles) [1, 7–17].

The historical incidence of SCC is not always a good predictor of future problems, partly because inspections are incomplete and detection is insensitive to incipient cracking, and partly because aging and its synergy with degradation phenomena can lead to unexpected cracking. For Ni alloy base metals, the opportunity for aging is small, but for Alloy 182 and 82 weld metals, some microstructural evolution may occur. This may produce an increase in yield strength, changes in grain boundary composition and structure, and other factors that could alter susceptibility to SCC and environmentally assisted fracture.

The historical incidence of SCC is also dependent on various operational factors, including low leakage core operation (where cooler and hotter water mix and can produce thermal fluctuations and cyclic thermal fatigue loading on surface of the component). Also, the increasing use of non-deaerated make-up water might expose components to high corrosion potential conditions that can greatly increase crack growth rates (Figures 3.5, 3.6, and 3.10).

Most of this section will address SCC vulnerabilities, but there is growing concern for environmentally assisted fracture, a reduction in J-R tearing resistance [18, 19], and sudden fracture [20, 21]. The reduction in J-R tearing resistance can be very high under certain conditions of temperature or environment (Figure 3.11). In the high-temperature BWR and PWR environments, sudden fracture (Figure 3.12) has been observed in Ni alloy weld metals at stress intensity factors as low as 86 MPa$\sqrt{m}$ (78 ksi$\sqrt{in}$). In many but not all cases, the sudden fracture is consistent with plastic instability.

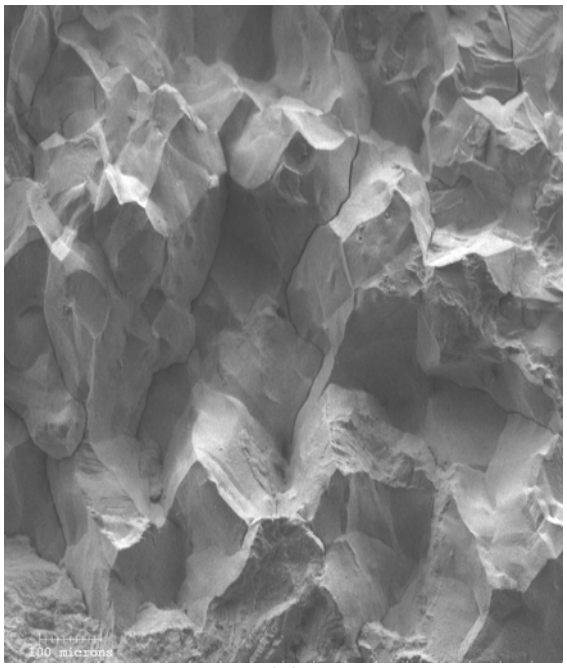

(a)

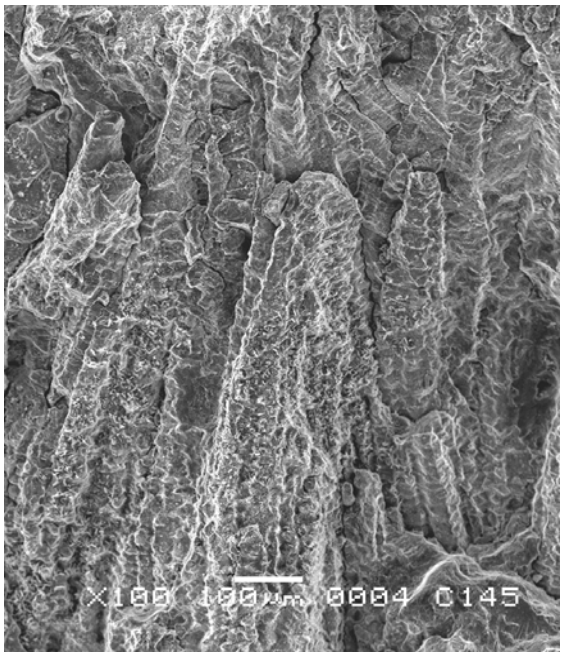

(b)

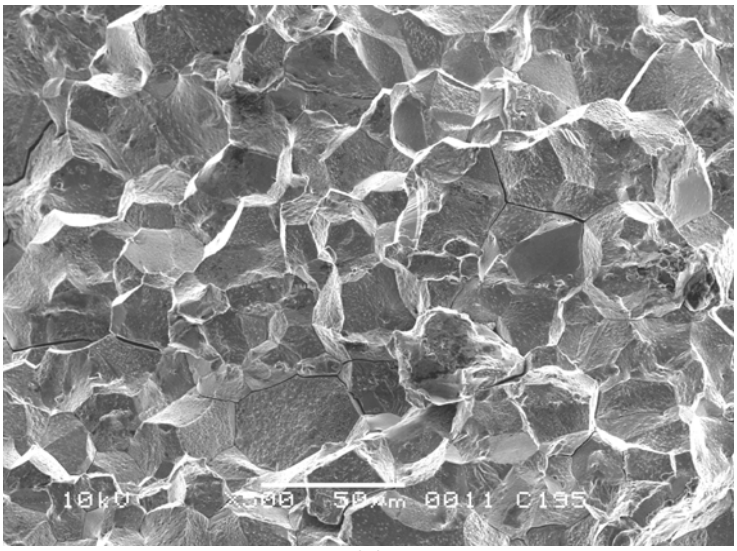

(c)

Figure 3.3. Scanning electron micrographs showing the intergranular fracture morphology of (a) Alloy 600, (b) Alloy 182 weld metal, and (c) alloy X-750 when tested in high-temperature water.

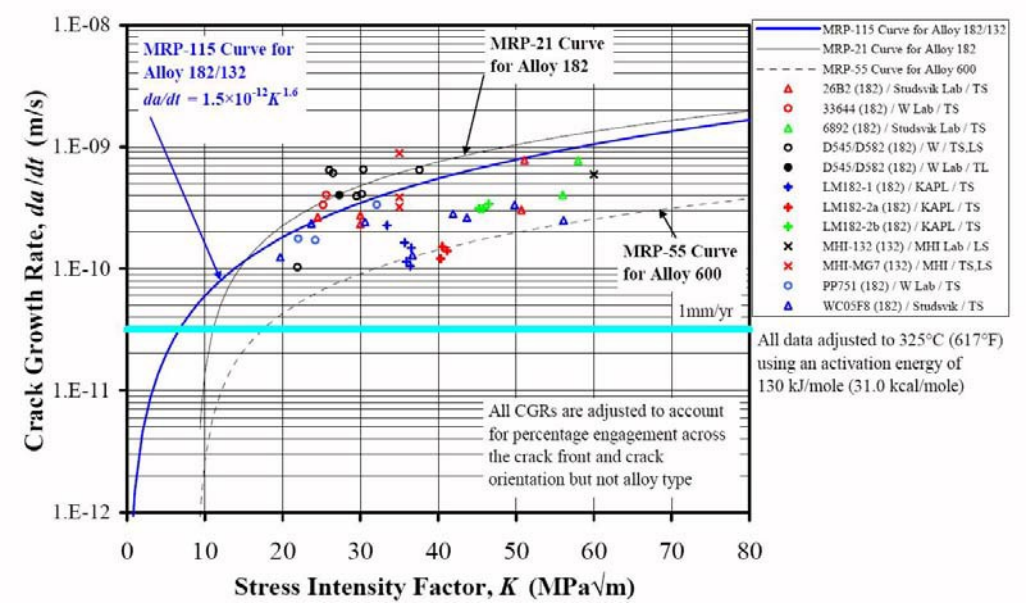

Figure 3.4. Crack growth rate of Alloy 182 and 132 weld metals in PWR primary water along with disposition curves for Alloy 182 weld metal (MRP-115 [22]) and Alloy 600 (MRP-55 [23]). Cold work and temperature cause an increase in crack growth rate.

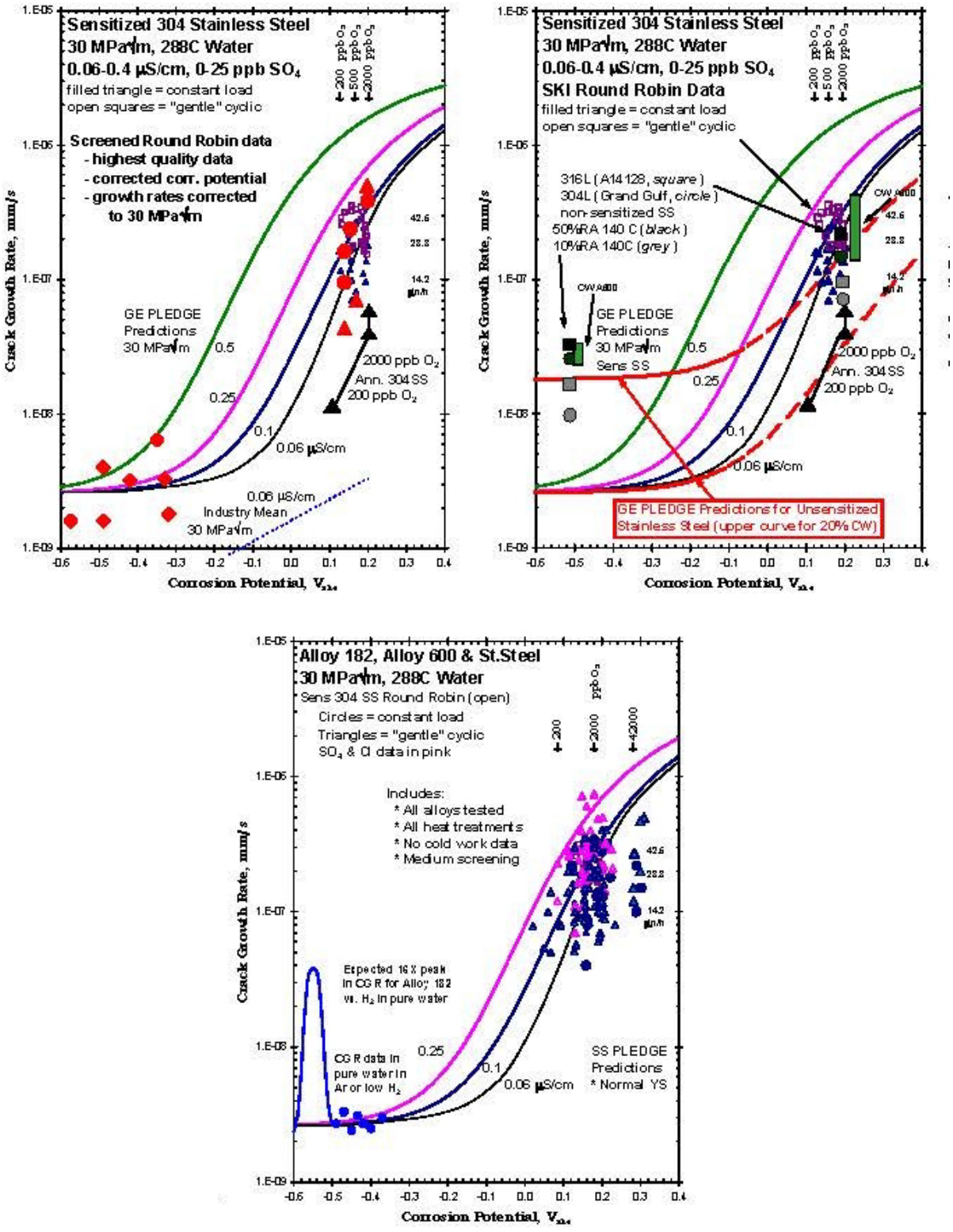

Figure 3.5. SCC growth rate vs. corrosion potential for stainless steels *(top)* and Ni alloys *(bottom)* tested in 288 °C (550 °F) high-purity water containing 2,000 ppb O_2 and 95–3,000 ppb H_2.

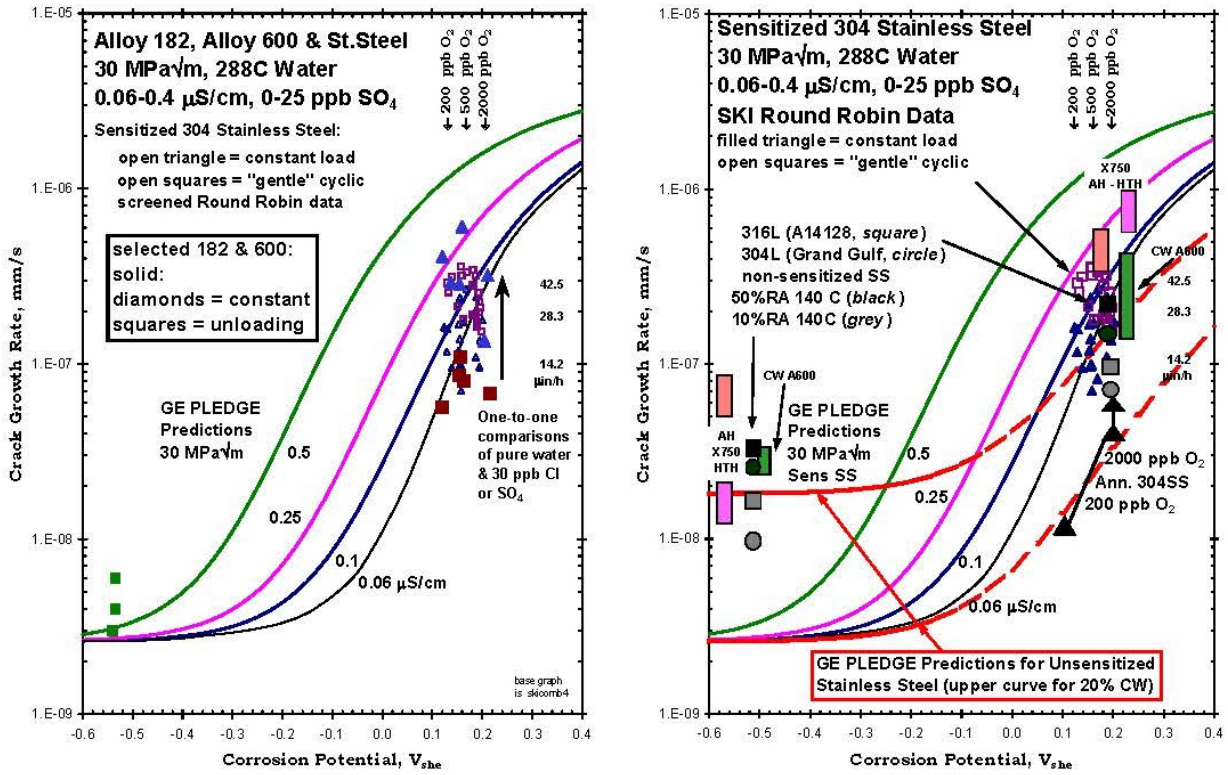

Figure 3.6. ***(Left)*** **The growth rates in high purity water at high corrosion potential fall within the observations for sensitized stainless steel (open symbols), and the effect of low potential or additions of 6 × 10^{-7} N SO_4 or Cl are consistent with the SCC behavior of sensitized stainless steel.** ***(Right)*** **SCC growth rate vs. corrosion potential for stainless steels in various conditions, 20% cold-worked alloys 600 and X-750 tested in 288 °C (550 °F) high-purity water containing 2 ppm O_2 and 95–3,000 ppb H_2 [24].**

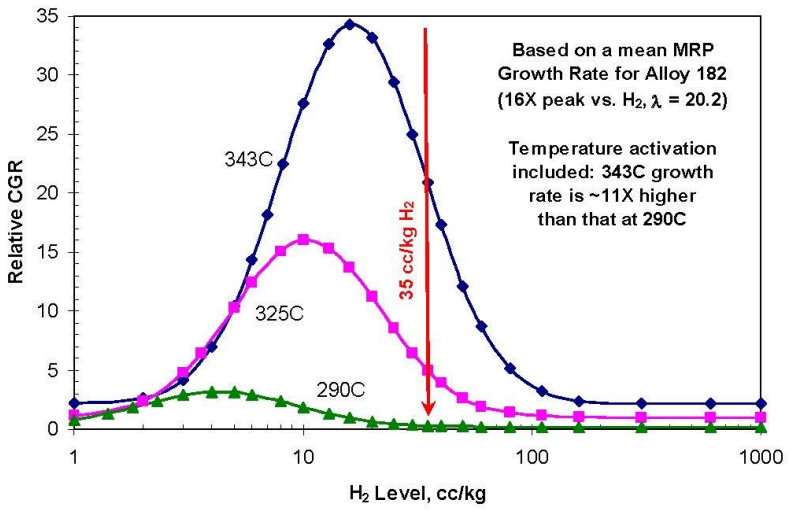

Figure 3.7. Predicted effect of H_2 on the relative crack growth rate of Ni alloy weld metals based on a 16× crack growth rate peak height at 290 °C, 325 °C, or 343 °C, (554 °F, 617 °F, or 650 °F) with the effect of temperature activation on crack growth rate factored in. From a H_2 level of 35 cc/kg, shifting to higher H_2 will monotonically decrease crack growth rate. For lower H_2, no benefit will occur until the H_2 level is below about 0.52, 3.1 and 7.7 cc/kg H_2 for 290 °C, 325 °C, and 343 °C, respectively. While the peak height is 16× at all temperatures, the crack growth rate is much higher at 343 °C.

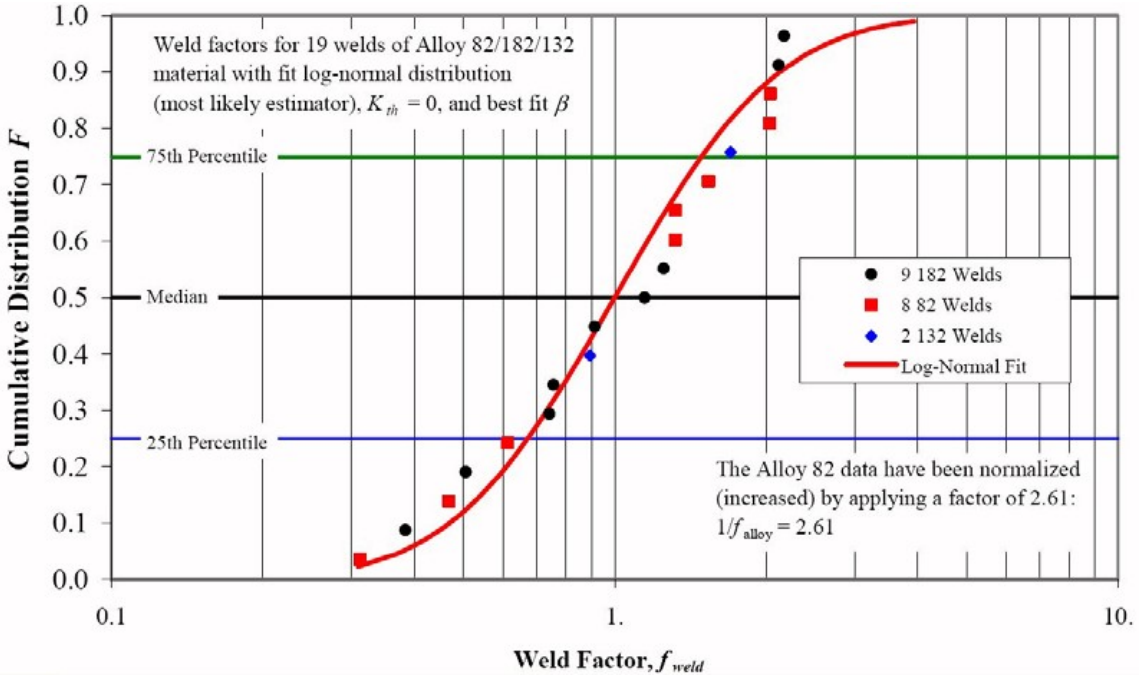

Figure 3.8. Analysis of the crack growth rate response in PWR primary water for alloys 182 and 132 and Alloy 82 weld metals. Recognizing that the Alloy 82 data have been increased by 2.6×, the cumulative distributions for these materials are intertwined, indicating identical response. Note that the Alloy 82 data in the plot indicate somewhat better SCC resistance [22].

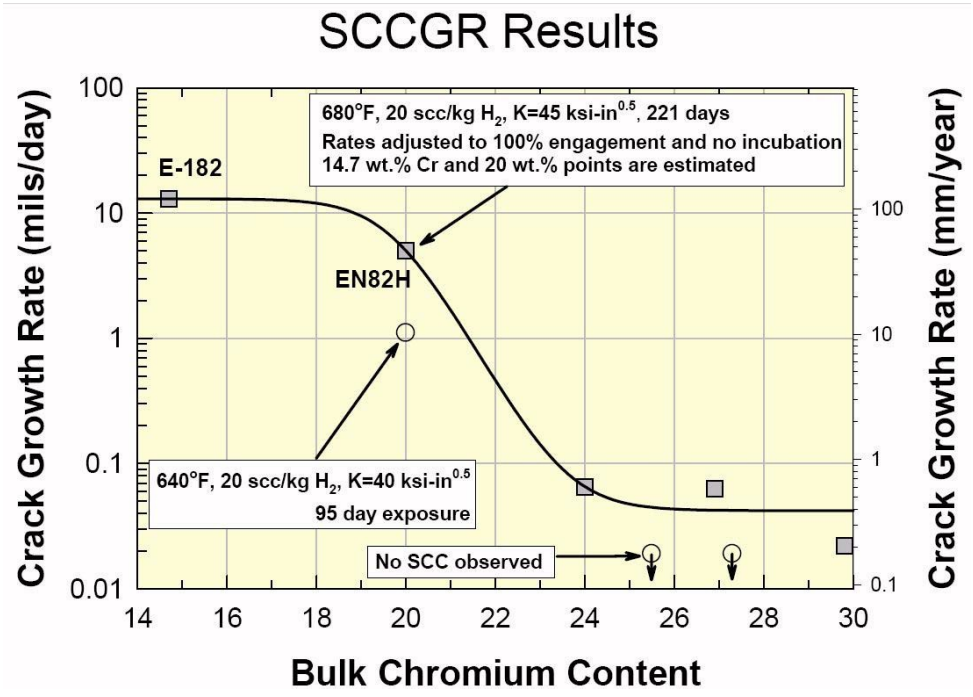

Figure 3.9. SCC growth rate vs. bulk Cr content of Ni alloy weld metals tested in 360 °C (680 °F) hydrogenated water [25–28].

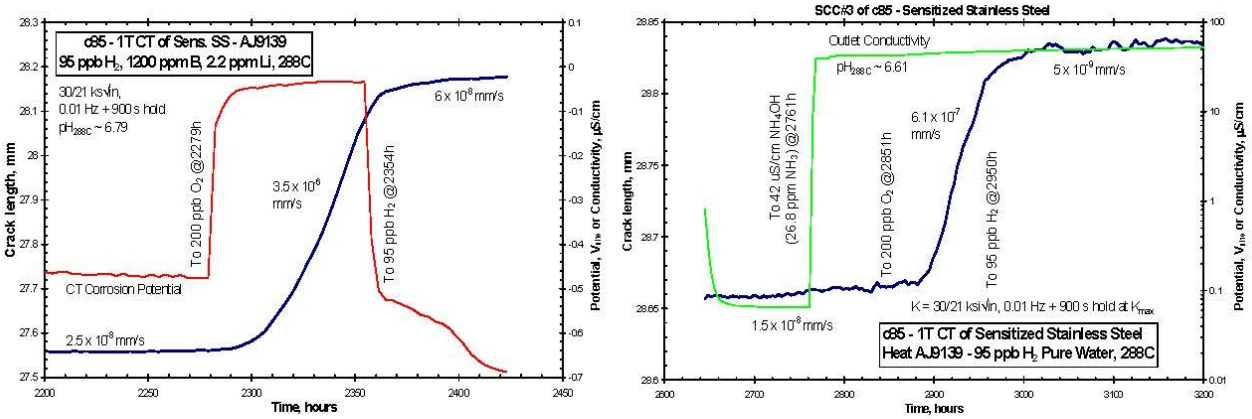

(a) (b)

Figure 3.10. SCC crack length vs. time of sensitized stainless steel in 288 °C (550 °F) showing that the presence of (a) 1,200 ppm B as H_3BO_3 and 2.2 ppm Li as LiOH, or (b) 26.8 ppm NH_3, results in a low growth rate until the corrosion potential becomes elevated at 2,279 h by the addition of 200 ppb O_2 [15, 16].

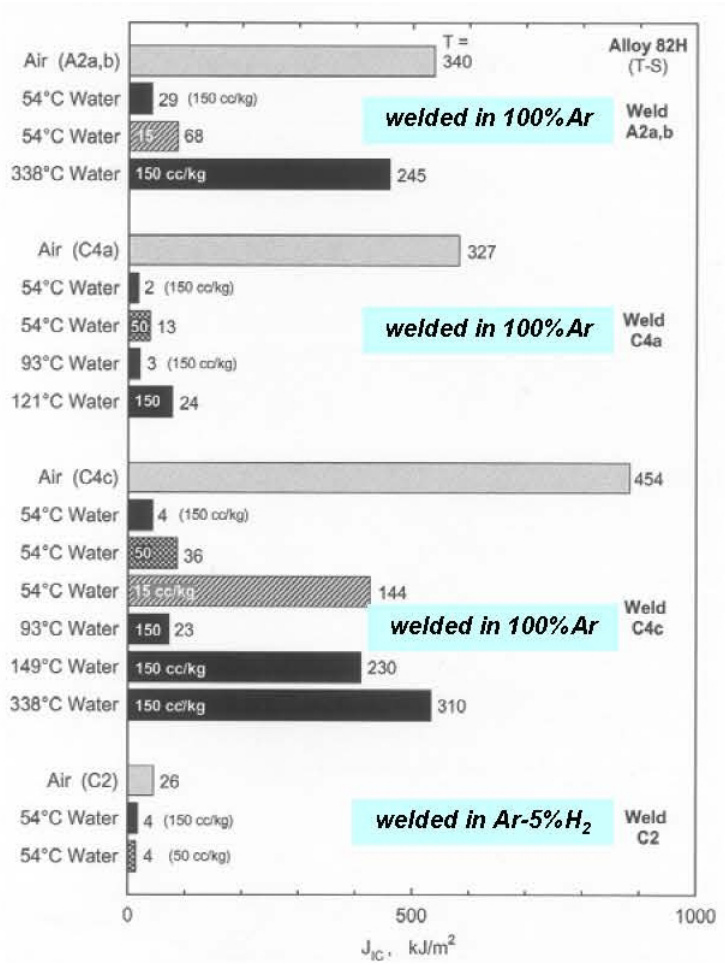

Figure 3.11. J-R data of Mills et al. on various Ni Alloy 82H weld metals showing a large reduction in fracture resistance in water versus air [18, 19]. Reprinted with permission of The Minerals, Metals & Materials Society.

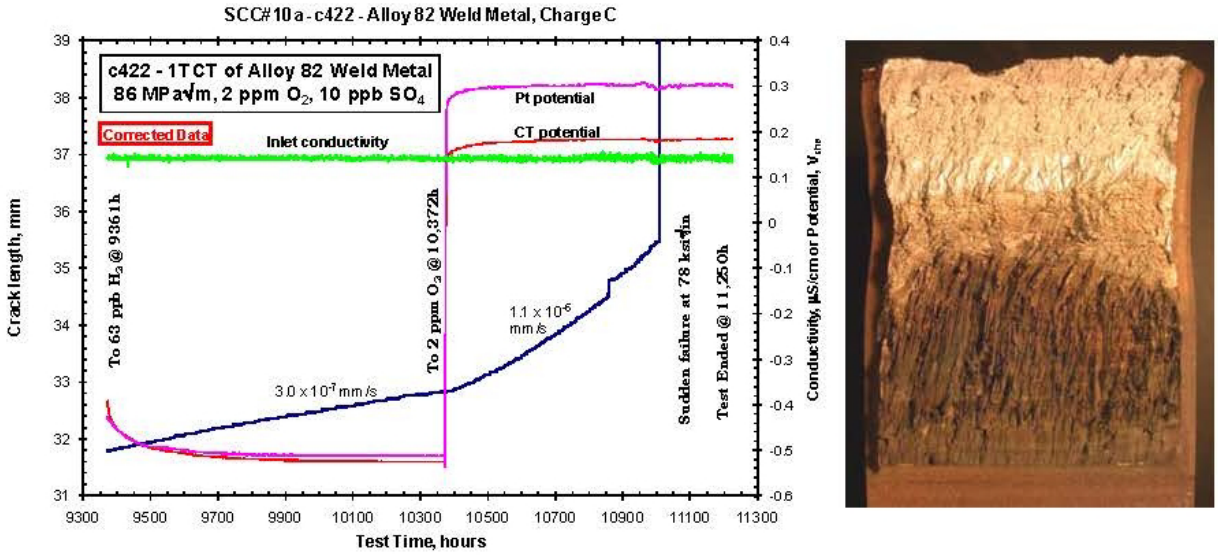

Figure 3.12. Examples of sudden failure of Alloy 182 weld metal tested in 288 °C (550 °F) water at increasing stress intensity factor (K) until failure occurred. The load and the crack depth at failure are very well defined, and the resulting "K_{IC}" is relatively low [20, 21]. Some of these rapid fracture events are consistent with plastic instability, others may not be.

3.2 PERSPECTIVE ON SCC DEPENDENCIES AND MECHANISMS

Until recently, the SCC of Ni alloys in PWRs has been considered a distinct and different phenomenon from SCC of nickel alloys in BWRs. However, there is increasing evidence that SCC follows a smooth transition between traditional BWR (most U.S. BWRs now operate at low corrosion potential using NobleChem™) and PWR primary water, with many common dependencies as a function of temperature, oxidant level, H_2 level, and water purity [8–17]. For example, as the corrosion potential is changed by varying the dissolved O_2 and H_2 level, a well-behaved transition in SCC growth rate is observed, both for Ni alloys and stainless steels (Figures 3.5 and 3.6).

Under deaerated conditions, the corrosion potential is controlled by the H_2–H_2O reaction, which is parallel to the Fe, Ni, and Cr metal-oxide phase boundaries in Pourbaix (pH-potential) diagrams (Figure 3.13). Changing pH in the mid-range of ~5–8 (pH at temperature) has little effect on SCC response, and more than three dozen on-the-fly chemistry changes (where the experimental conditions remain stable apart from the controlled change) were observed to have no effect on SCC growth rates in Ni alloys, even from pure water to elevated levels of H_3BO_3 and LiOH (Figure 3.14) [15]. Even the effect of H_2 on SCC is observed to be similar for BWR and PWR water [16, 17], which is unsurprising given the similarity between the two environments. The similarities in the two reactor types is more evident for BWRs that employ NobleChem™ to catalytically achieve low corrosion potentials that are very close to the H_2O/H_2 line (Figure 3.13).

This non-oxidizing condition is quite similar to the primary environment of PWRs, with three significant differences: solution pH, H_2 fugacity, and temperature.

Many of the factors used to distinguish SCC response in BWRs vs. PWRs have proven to be artificial [8, 10, 12, 24]. The positive experience of thermally treated Alloy 600 in PWRs was

considered to contradict the deleterious role of grain boundary carbides and Cr depletion in BWRs. However, grain boundary carbides are in fact beneficial in both environments, although when accompanied by Cr depletion at the grain boundary, SCC susceptibility increased in oxidizing environments. This is widely attributed to the slower repassivation rates at lower Cr concentrations in the pH-shifted chemistries that form when oxidants are present [8–10].

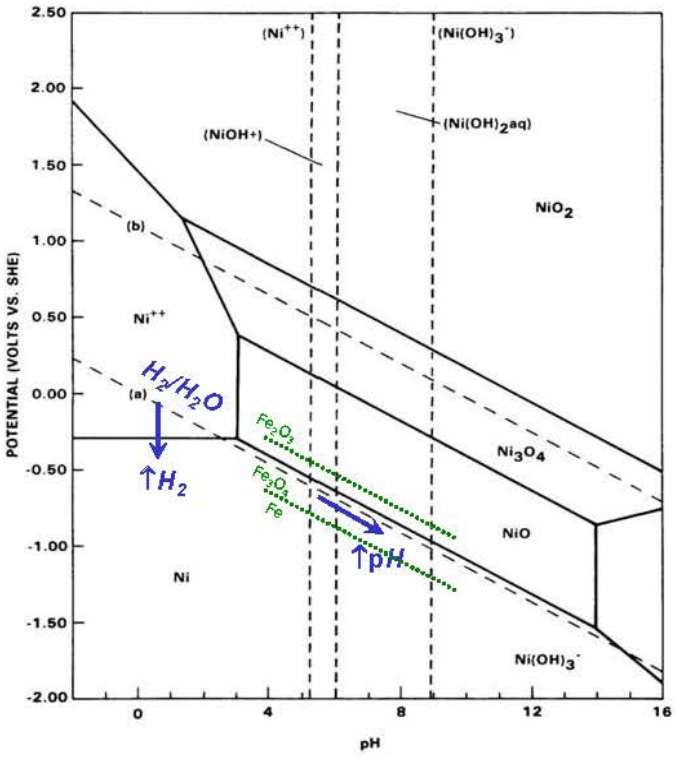

Figure 3.13. Ni–H_2O Pourbaix diagram at 300 °C (572 °F).

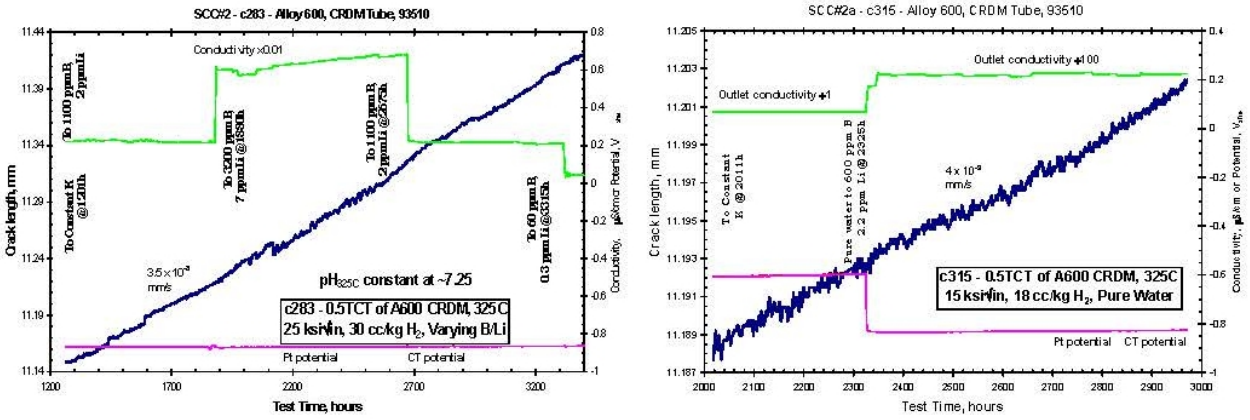

Figure 3.14. Crack length vs. time for Alloy 600 and tested in 325 °C water containing 30 cc/kg H_2 under constant K conditions showing that extensive variations in B and Li content in produced no change in crack growth rate [15].

Solution pH variations in the near-neutral regime have little effect on SCC in deaerated (e.g., PWR) water (Figure 3.14) [15], although they have some effect on the corrosion potential [112 mV / pH unit at 288 °C (550 °F)] because the corrosion potential under deaerated conditions is

controlled by the H_2O/H_2 reaction (this is the slope of the H_2O/H_2 line in Figure 3.13). Both pH and solution conductivity are higher in the PWRs as a result of H_3BO_3 and LiOH additions. The pH_{290C} is now typically in the range from 6.8 to 7.2 in PWRs (pH_{290C} represents 1,100 ppm B and 2 ppm Li, which gives a pH_{325C} = 7.25 and a pH_{340C} = 7.58) vs. 5.65 for pure (BWR) water, and the conductivity is 166 μS/cm vs. 5 μS/cm. There is a change in corrosion potential as a function of pH, but this difference is unimportant because there is no difference in potential relative to the metal – metal oxide phase transitions. Also, in the absence of oxidants, there is no potential gradient in the crack and therefore no aggressive crack chemistry develops.

Second, the difference in H_2 fugacity is only ~70×, from ~40 ppb H_2 in BWRs to ~3,000 ppb in PWRs. This produces only a small change in corrosion potential of about 100 mV, which can nevertheless be important to SCC of Ni alloys. Its role is related to a shift in the stability of Ni vs. NiO, which is affected by both H_2 and temperature (Figure 3.15). No potential gradient forms in the crack because H_2 (unlike oxidants) is not consumed, so no aggressive crack chemistry forms whether the H_2 level is high or low.

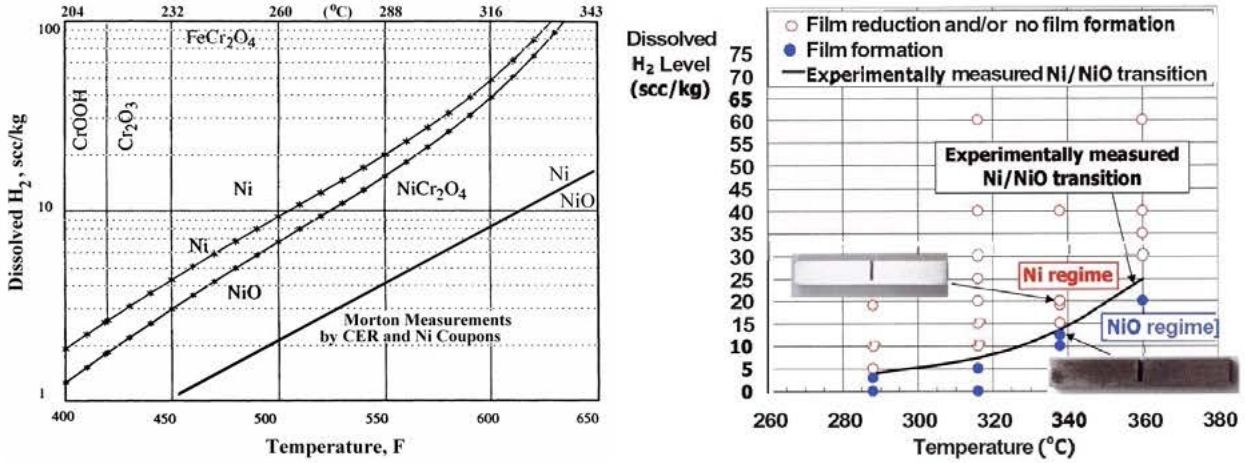

Figure 3.15. Ni/NiO phase boundary as a function of H_2 fugacity and temperature [29]. Copyright 2003 by the American Nuclear Society.

The third difference is temperature. The temperature of most structural components is 274 °C (525 °F) in a BWR [the feed water reduces the recirculating core outlet water from 288 °C (550 °F) to 274 °C]; thus, this is the temperature in the recirculation and cleanup piping, the annulus between the shroud and the pressure vessel, and the lower plenum region. In a PWR, the core inlet temperature is about 286 °C (547 °F), core outlet temperature is typically 323 °C [ranging from ~316 °C to 323 °C (601 °F to 613 °F)], and the pressurizer is ~343 °C (650 °F), nearly 70 °C (158 °F) hotter than most structural components in a BWR. For Ni alloys, this difference (323 vs. 274 °C) leads to a significant increase in crack growth rate of about 14× [23, 24, 30, 31]; compared to the 343 °C PWR pressurizer, the difference is about 40×.

Both crack initiation and crack growth rate are important factors in the emergence of SCC in plant components. Crack initiation can be viewed as dominant for non-structural components, such as the thin-walled steam generator tubing, and crack growth can account for a significant fraction of life in larger structural components. Crack growth can be quantified with greater precision, and the bulk characteristics of components are much better known than the highly variable surface characteristics, although modern steam generator fabrication can produce very well controlled surfaces. For structural components, there are many examples of *claims* of excellent surface

fabrication controls in components that were later proven to possess severely cold-worked and defected surfaces from which extensive cracking nucleated and grew.

Because there are many possible mechanisms of crack initiation (e.g., intergranular corrosion, pitting, pre-existing defects, mechanical cracks, and severely cold-worked/damaged surfaces), it can be very difficult to identify what initiated cracking. Even without visible problems, after extended service (e.g., a license extension of > 20 years), components that were viewed as not susceptible to SCC have experienced cracking. Thus, the evolving perspective is that it is necessary not only for component design and surface characteristics to be optimized to minimize the probability of crack initiation, but to also be inherently resistant to crack growth to ensure plant lifetimes commensurate with the desired 60–80+ year range.

3.3 NICKEL ALLOY COMPONENTS AND WELDS IN BWRS

Nickel-base weld materials are used extensively in BWRs [32] and are more prevalent than wrought Ni alloy components (Table 3.1). Alloy 182 and 82 weld metals are used to join the low alloy steel pressure vessel and pressure vessel nozzles to wrought Ni alloys and austenitic stainless steel components. Alloy 182 is typically used as a coated stick electrode designed for manual welding, whereas Alloy 82 is typically used in wire form for automated tungsten inert gas or metal inert gas welding. Figures 3.1 and 3.16 show the key components and their locations in GE BWRs, and Figures 3.17–3.20 show the configurations of some locations where Alloy 182 and 82 welds exist.

Different vessel fabricators used different nozzle-to-safe-end weld configurations, but Alloy 182 weld metal was used for the nozzle butter and/or the weld joint. These include the recirculation inlet and outlet nozzles, core spray nozzles, jet pump instrumentation nozzles, and feed water nozzles. Figures 3.17 and 3.18 show the details typical of the weld buildup with alloys 182 and 82 common in many BWRs. Alloy 182 was often used to butter the safe end, after which the vessel was heat treated (tempered) to restore its properties. Following this post-weld heat treatment (PWHT), the subsequent weld to the safe end was typically made with an Alloy 82 root pass then completed with Alloy 182. The dendritic structure shown in Figure 3.3 develops during weld solidification of both Alloy 182 and 82 welds, with the dendrites growing toward the top of the weld (opposite the direction of heat flow). Even when the entire weld was nominally made with Alloy 82, weld repair records at some plants indicate manual welding using Alloy 182 because of the repair geometry or limited access. Weld repairs are suspected of being the origin of preferred crack initiation and faster crack growth. Unfortunately, many weld repairs were poorly documented. The start and end point of welds are also areas of concern, especially for manual welds.

Essentially all internal attachments to the pressure vessel are made using Alloy 182 pads that are welded directly onto the pressure vessel after the 308/L SS cladding is applied and before the PWHT. Stainless steel weld metal has proved to be more resistant to SCC than Alloy 182 weld metal. The Alloy 182 attachments include the steam dryer hold down brackets, core spray brackets, and shroud support structures. The latter were typically constructed of wrought Alloy 600, with Alloy 182 welds used for its construction and attachment to the vessel (Figure 3.19). This represents the largest circumference of Ni base weld. Legs welded to the bottom head of the RPV support the structure in many cases. Alloy 182 and 82 welds were used for many of the penetrations through the bottom of the pressure vessel—the most numerous welds being in the control rod drive (CRD) housings (Figure 3.20). Finally, in most BWRs, water is pumped through the core using jet pumps, which require circular openings in the Alloy 600 support ledge and are attached using Alloy 182 and 82 welds.

In the standard BWR environment (normal water chemistry, or NWC), the water chemistry is oxidizing and Alloy 182 is susceptible to SCC. Alloy 182 cracking was first discovered during replacement of weld sensitized stainless steel recirculation piping. Since then, there have been continuing instances of cracking in Alloy 182. This section discusses the field cracking characteristics of Alloy 182, SCC dependencies, mitigation techniques, and improved materials.

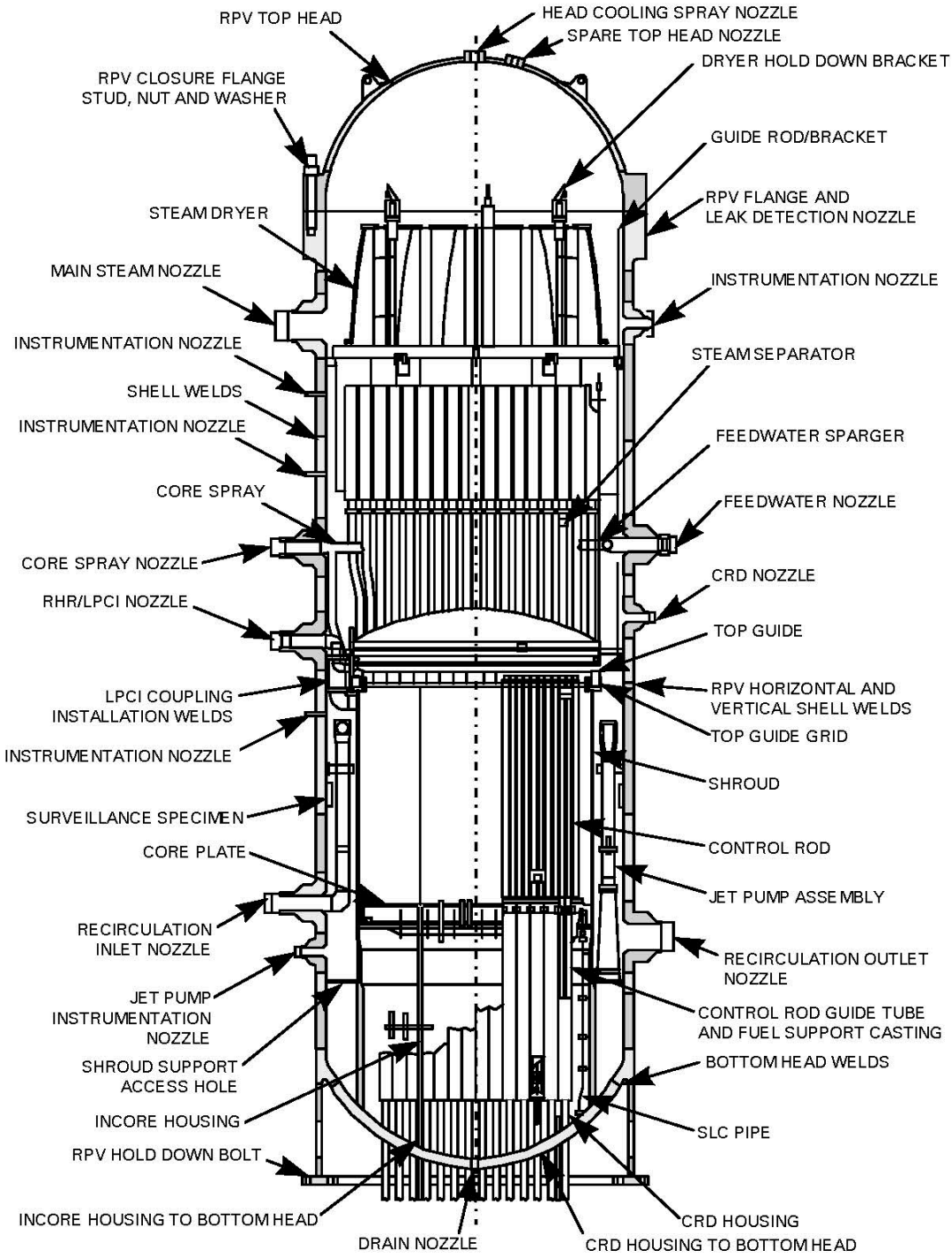

Figure 3.16. Schematic of typical BWR RPV, nozzles, and attachments.

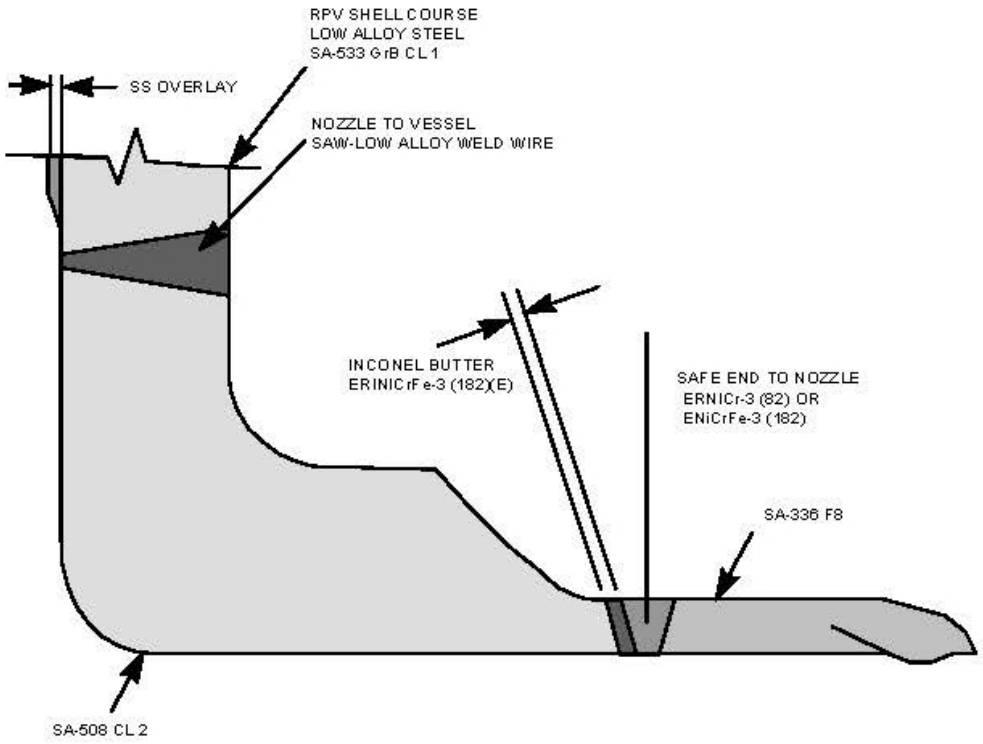

Figure 3.17. Typical BWR recirculation outlet nozzle, nozzle butter, weld, and safe end.

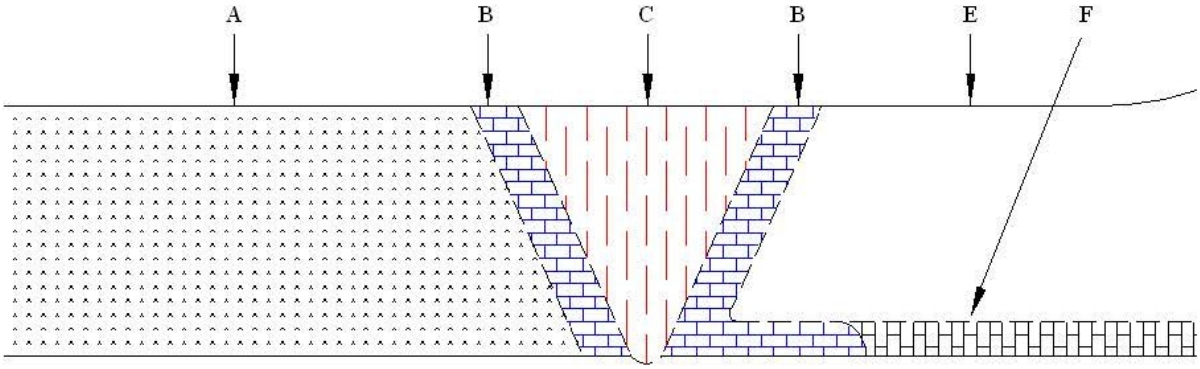

A) Stainless Steel Safe End
B) Alloy 182 Weld Butter
C) Alloy 182 or Alloy 82 Weld Metal
B) Alloy 182 Weld Butter
D) Low Alloy Steel Nozzle
E)··Low·Alloy·Steel¶
F)··Stainless·Steel·Cladding¶

Figure 3.18. Enlargement of safe end to nozzle weld region in BWRs using Alloy 182 and 82 weld metals.

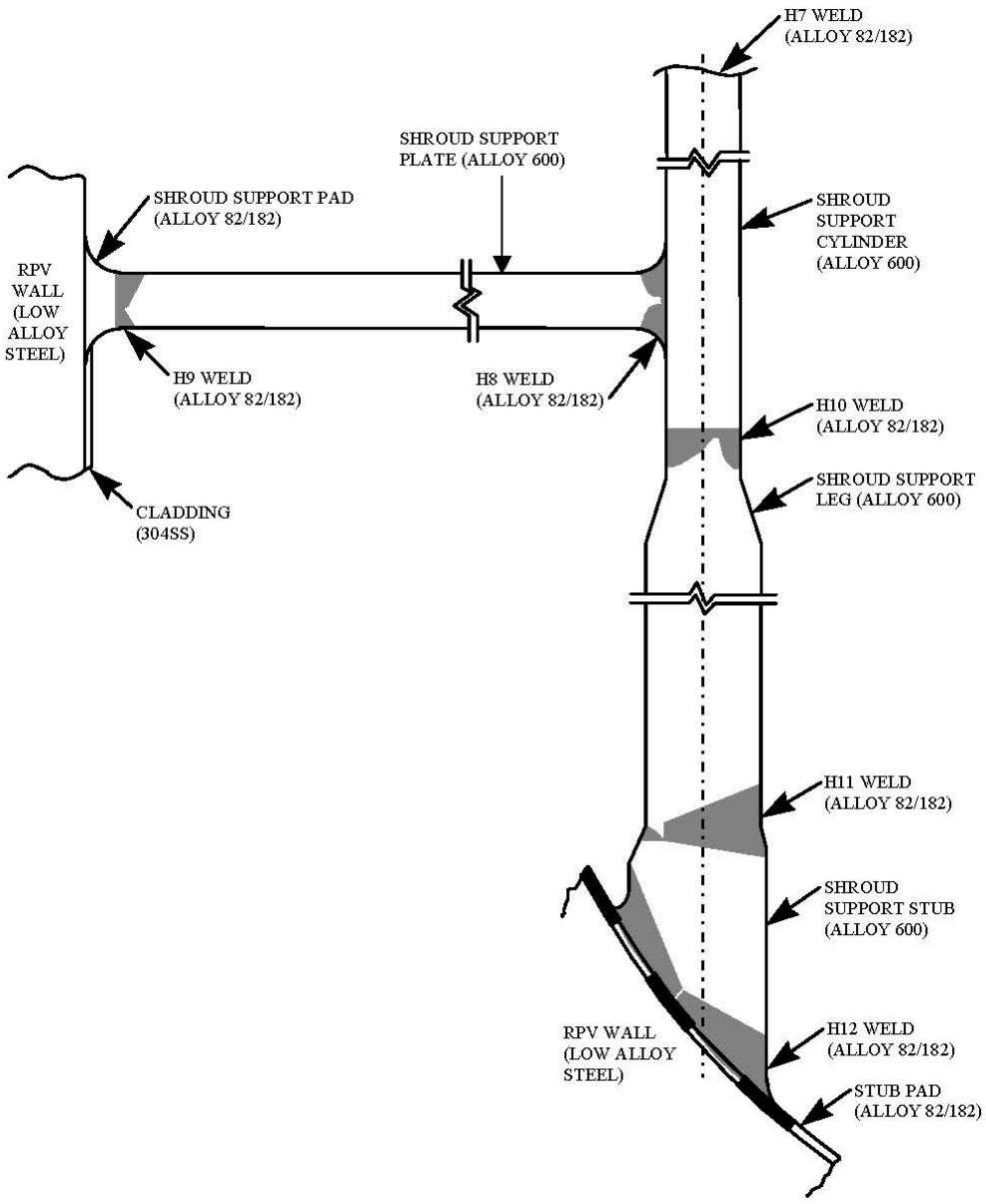

Figure 3.19. Typical BWR shroud support structure of the leg design with Alloy 182 used throughout. Also shown are the H9 and H12 welds that join the component to the RPV.

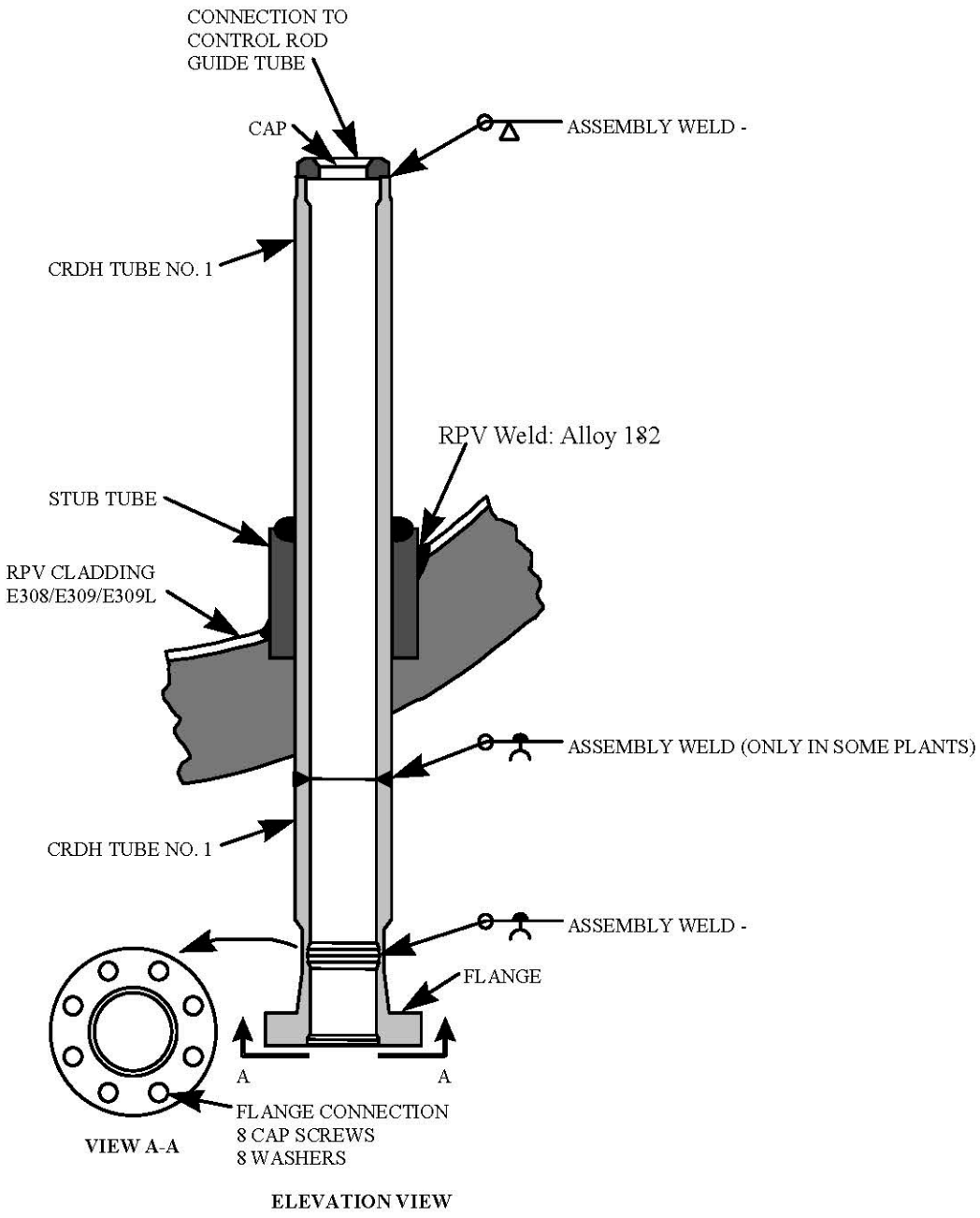

Figure 3.20. Typical CRD stub tube and CRD housing configurations. Alloy 182 used in stub tube to RPV weld.

3.4 SCC OPERATING EXPERIENCE OF NICKEL ALLOYS IN BWRS

The BWR Ni alloy components and welds listed in Tables 3.1, 3.4, and 3.5 have experienced SCC. There has also been extensive cracking of creviced Alloy 600, primarily in components, such as shroud head bolts, safe ends, and ledge and access hole covers. For Ni alloys and stainless steels, a high initial incidence of cracking occurred, primarily due to poor water chemistry management during the early operation of most BWRs (Figure 3.21). While dramatic

improvements were made in water purity, once cracks nucleated, growth was readily sustained even with good water chemistry. Figure 3.21 shows the correlation between BWR water purity and incidence of cracking in Alloy 600 shroud head bolts. In addition to the important effect of *average* water purity, both prediction and plant data show that very high conductivity early in life produced a different population of more severe cracking than is reflected by the plant *average* conductivity.

The overall experience with wrought Ni alloys in BWRs has been better than with welded austenitic stainless steels, where IGSCC has been widely observed in the heat affected zone of types 304 SS and 316 SS (but rarely in type 308L SS weld metal). This is especially true for furnace or weld-sensitized stainless steels, but unsensitized stainless steel has also cracked extensively, primarily due to the combination of weld residual stresses and weld shrinkage strains. Residual strains peak at the weld fusion line and are generally equivalent to 15–20% room temperature tensile strain [33, 34].

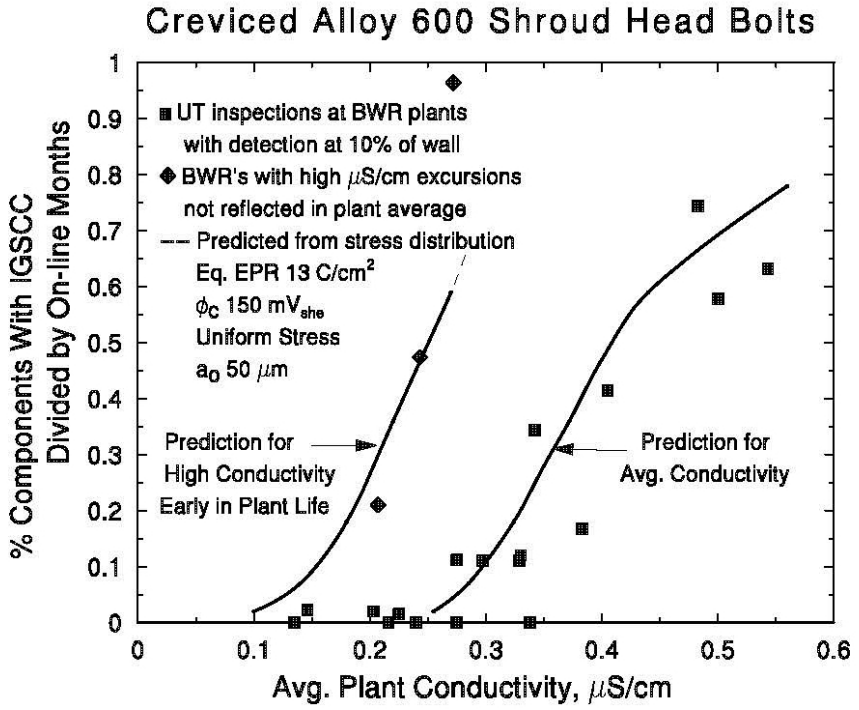

Figure 3.21. Observation and prediction of the incidence of SCC in Alloy 600 shroud head bolts as a function of average plant conductivity. An unusual population of bolts from three plants showed a much greater incidence of SCC because these plants had poor water chemistry early in their life, typical of most BWRs.

Table 3.4. Alloy 82 and 182 field cracking in one set of BWRs

Material	Component	Part	BWR Type	First Synch	Find Date	Cause
Alloy 182	Feed water sparger	End bracket	2	Sep-69	Oct-2000	IGSCC
Alloys 82 and 182	In-core monitor	Penetration		May-84	Aug-97	Most likely original fabrication weld defects (possible exception on 08-41)
Alloy 182	RPV head	Bracket	Non-GE BWR	Jan-81	Jan-95	IGSCC
Alloy 182	RPV head	Bracket	Non-GE BWR	Jun-80	Jan-95	IGSCC
Alloy 182	Shroud support	Leg	3	Mar-71	Dec-99	Probable IGSCC

Table 3.5. Alloy 182 field cracking in a second set of BWRs

Plant	System	Year of Detection	Location of Indication
E-1	Recirc	1990	Main loop
E-2	Recirc	1985	Flange
E-2	Core spray	1999	Brackets
E-3	Recirc	1996	Pipe weld
E-4	Recirc	1997	Pipe weld
E-4	Core spray	1999	Brackets
E-5	Core spray	1999	Brackets
E-6	Feed water	1985	Nozzle
E-6	RPV	1986	Head spring beams
E-6	RPV	1986	Flange
E-6	Feed water	1997	Nozzle
E-6	RHR	1997	Safe end
E-7	RPV	1985	Head spring beams
E-7	RPV	1990	Flange
E-7	Feed water	1995	Nozzle
E-8	RPV	1994	Head spring beams
E-8	Core cooling	1991	Nozzle
E-8	RPV	1995	Head spring beams

While extensive SCC of Alloy 600 has occurred in the crevices of components, there has been very good experience with Alloy 600 in the welded, non-crevice regions, particularly in the bottom-head region. Alloy 182 weld metal has not performed nearly as well. Initial concerns for the high probability of SCC for Alloy 182 were initially raised because of the laboratory test data from the United States [35] and subsequently confirmed internationally [11, 13, 14, 36]. This led to recommendations to inspect weld metal butters during the replacement of recirculation piping

that was necessitated by the IGSCC occurrence in weld sensitized, large diameter Type 304 SS pipes. The first inspection, performed at a BWR/3 around 1984, revealed cracking in several welds. Inspections were performed in the recirculation inlet and outlet safe ends during the piping replacement [37]. Cracking was detected using dye penetrant testing in 3 of 10 inlet nozzles and 1 of 2 outlet nozzles. The cracking was axial in all nozzle butters, with a maximum depth of about 70% of wall thickness. Boat samples were removed from one weld that attached the stainless steel safe end to the outlet nozzle. Metallography examination verified that the cracking was confined to the Alloy 182 weld and did not extend into the low alloy steel; it also established that cracking was interdendritic along intergranular dendrite grain boundaries and did not penetrate into the Alloy 82 root pass (corroborating the higher SCC resistance of Alloy 82 weld metal shown in laboratory data). Many axial segments initiated in the Alloy 182, with several circumferential segments that followed the fusion line.

Subsequently, cracking was detected in other BWRs. The number of affected nozzle-to-safe end welds varied from plant to plant, with one plant having six cracked nozzles. The frequency of cracking has now decreased, but leakage has occurred in some smaller diameter pipes. Some observations were associated with weld repair locations and the improper classification of inspection findings as weld geometry or internal weld defects. The cracked nozzles included recirculation inlet and outlet, core spray, and feed water nozzles. The cracking has remained primarily axial in nature, although there are some instances of circumferential cracking. Many of these cracked welds have been overlay repaired with a structural build-up of SCC resistant material to restore structural margin/integrity.

Knowledge of cracking in BWR core internal structures was very limited until the late 1990s, primarily because only a limited number of inspections were performed. The first components to be evaluated were the access hole covers, which were welded during plant construction after access was no longer needed to the lower plenum region. These welds were particularly susceptible because crevices existed where the cover recessed into the ledge. While cracking occurred in the creviced wrought Alloy 600 in many plants, it also initiated and/or propagated in the Alloy 182 weld metal. This heightened the concern for the occurrence of SCC for Alloy 182 in other locations.

The first instances of SCC in non-creviced attachment welds were found in hold-down brackets on the reactor vessel head that restrained the dryer assembly. These locations were inspected soon after SCC was first observed, and subsequent metallurgical evaluations confirmed the extent and morphology of cracking. The extent of cracking could not be accurately detected visually; only a penetration test (PT) examination or proper ultrasonic test (UT) interrogation could accurately characterize the extent of the tight weld cracks. While the cracked areas could be removed or repaired, their proximity to the RPV material heightened the need for periodic inspection of Alloy 182 welds in the reactor. Improved inspection approaches were developed by the EPRI's BWR Vessel and Internals Project between 1995 and 1998.

Subsequently, extensive SCC was discovered in Alloy 182 welds in the shroud support structure of a BWR/2 during a core shroud replacement in 1999. Visual inspections and liquid penetrant examinations were performed on the shroud support structure, revealing cracks in the attachment welds joining the conical support structure to the reactor vessel wall (Figure 3.22). This cracking was found in the weld build-up pad on the vessel wall (designated the H9 weld), as well as in other Alloy 182 welds and adjacent Alloy 600 in the lower conical section. Of greatest interest was the cracking found on the inside part (the lower bottom side) of the H9 weld, where nearly 300 individual cracks were found in 34 locations. These cracks were largely axial in nature (~90%); however, none entered the RPV low alloy steel. Since cracking was associated solely

with the underside of the actual core support structure, it was not detected during routine visual in-service inspection from the top surface. This led to inspections at other BWRs, and similar cracking was detected in another BWR/2 at the same H9 weld [38]. While the inspection technique was focused on circumferentially oriented cracking because the UT system was deployed from inside the vessel, the cracking appeared to be primarily axial.

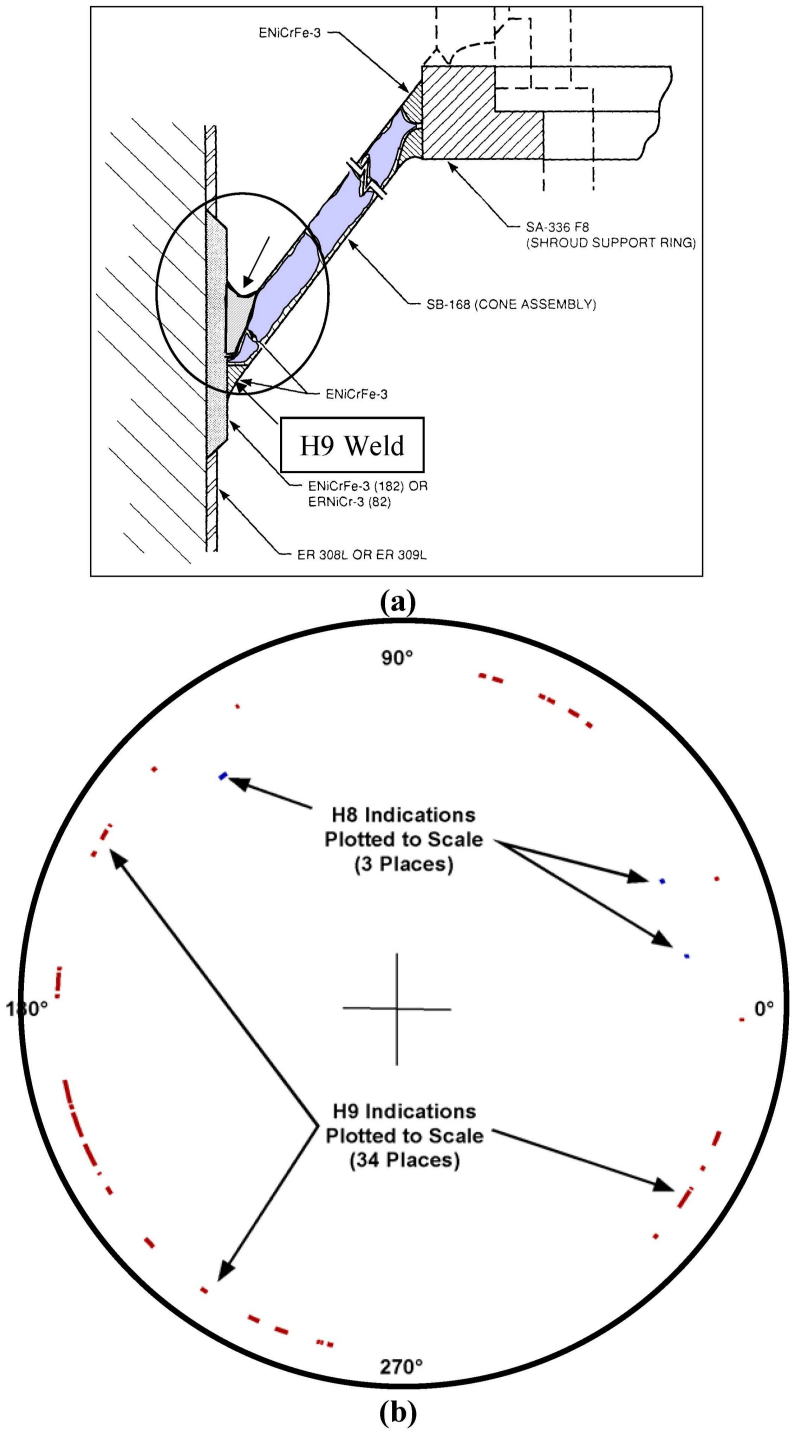

Figure 3.22. (a) Cross section of BWR/2 H9 weld and (b) schematic of the azimuthal orientation and length of the H8 and H9 indications (around vessel circumference) as determined by UT inspection.

3.5 OPERATING EXPERIENCE IN PWR PRIMARY SYSTEMS

Cracking was identified in thick section, forged, Alloy 600 components beginning in the mid-1980s with cracking first detected in the hottest components, i.e., pressurizer nozzles (Figure 3.2) [1, 2]. At all French PWRs, Alloy 600 pressurizer nozzles were replaced with stainless steel. In 1989, the first cracking of Alloy 600 upper head CRDM nozzles (Figures 3.23 and 3.24) occurred at Bugey 2, a first-generation French plant. Initially considered an isolated incident, this cracking was attributed to a stress concentration from a counter bore in the nozzles just below the level of the J-groove seal weld with the upper head combined with a relatively high operating temperature that was believed to be closer to that of the hot leg. However, CRDM nozzles at other plants in France exhibited the same type of cracking; however, in these subsequent episodes, the nozzles had no counter bores and their design was different (no tapered lower section). Furthermore, the upper head temperatures were the same as the inlet cold leg temperatures [39, 40].

These incidents of cracking in upper head CRDM nozzles shared three common features: (1) the presence of a significant cold-worked layer due to machining or grinding on the internal bore, (2) some distortion or ovalization (out-of-roundness) induced by the fabrication of the J-groove seal welds, and (3) a tendency to occur much more frequently in the outer set-up circles where the angles between the vertical CRDM nozzle and the domed upper head were greatest. The combination of these three features plus the fact that the upper head is stress relieved before the CRDM nozzles are welded in place pointed to high residual stresses being responsible for these premature failures.

Although the generic problem of Alloy 600 CRDM nozzle cracking first appeared in France, only sporadic instances of similar cracking were observed in other countries until the beginning of the 21st century, when numerous other incidents began to be reported. In some cases, where cracking was allowed to develop to the point of leaking primary water into the crevice between the CRDM nozzle and the upper head, circumferential cracks initiated on the outer surface of the CRDM nozzle at the root of the J-groove seal weld (U.S. experience, Davis Besse Nuclear Plant) [41]. This latter instance was also observed in 1989 at Bugey 2 but only to a minor extent. No further leaks of primary water due to CRDM nozzle cracking have occurred in France because of an inspection regime adopted to avoid them and a decision to replace all upper heads using thermally treated Alloy 690 CRDM nozzles [39, 40]. This same strategy, more economical than the cost of repairs and repeat inspections, has often been adopted elsewhere. The dangers of allowing primary water leaks to continue over several years so that extensive boric acid deposits accumulate was amply demonstrated by the discovery of very severe corrosion (wastage) of the low alloy steel of the upper head at the Davis Besse Nuclear Plant in Ohio in 2002 [7, 41].

The history of PWSCC in Alloy 600 and similar Ni base alloys has continued in recent years with the discovery of cracked Alloy 182 welds in several PWRs around the world (Figure 3.25) [41, 42]. This has occurred on the primary water side of the J-groove welds that seal the CRDM nozzles in the upper head and also in a few cases in the safe end welds of the RPV or pressurizer (Figure 3.26). One case has also occurred in the J-weld of a lower head instrumentation penetration [43]. Cracking seems to be significantly exacerbated by the presence of weld defects and weld repairs made during fabrication, usually to eliminate indications due to hot cracking, or slag inclusions, thus again implicating high residual stress in the failures observed to date. The cracking has often been described as interdendritic, but recent work shows that it is in fact intergranular. Incubation periods before detectable cracking seem to be on the order of twenty years.

It should be noted that all the Ni base weld metal cracking observed to date has involved welds that have not experienced the stress relief given to adjacent low alloy steel pressure vessel components [42]. Although the stress relief temperature is clearly not optimized for Ni base alloys (or stainless steels), it has been shown on mockups that such the surface residual stress of the welds is very significantly reduced and doubtless imparts greater resistance to PWSCC in PWR primary water.

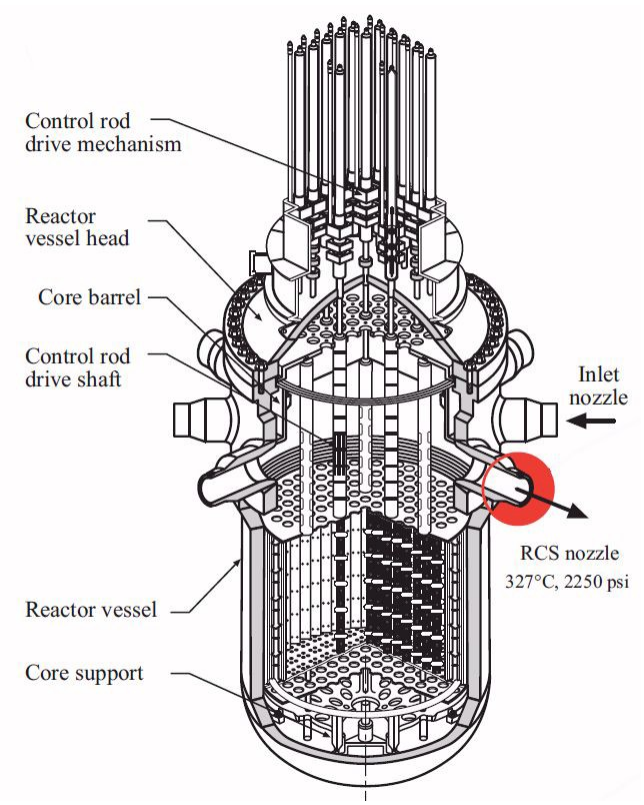

Figure 3.23. Schematic of a PWR pressure vessel and related structures.

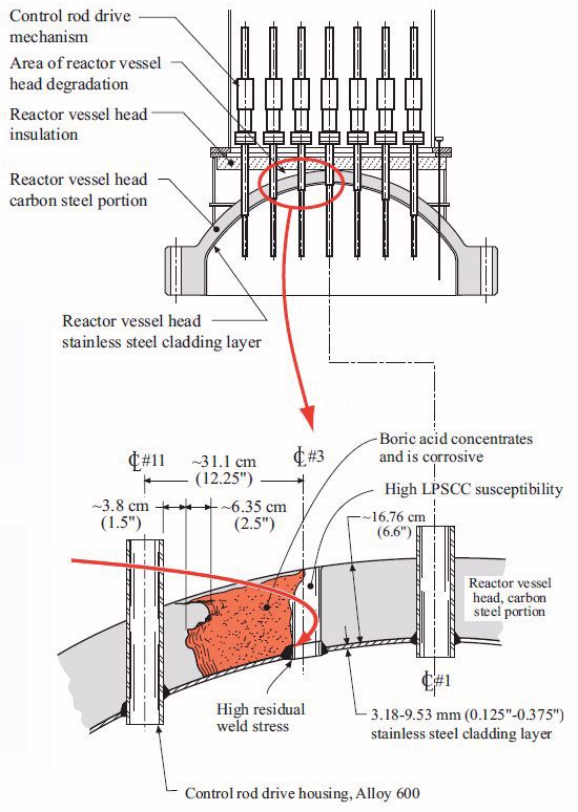

Figure 3.24. Schematic of the PWR CRDM penetrations.

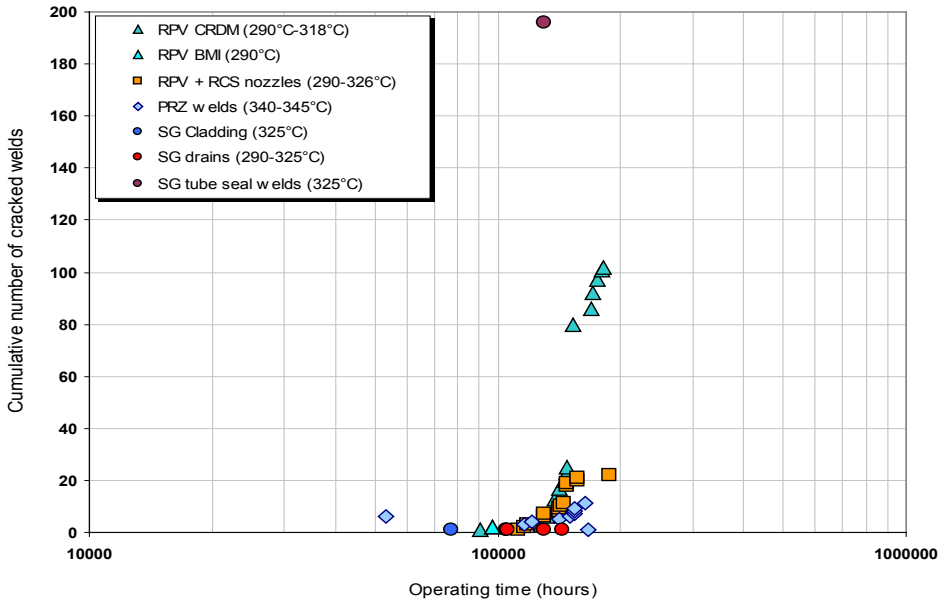

Figure 3.25. Time of detection of SCC in Alloy 182 welds in PWRs [41, 42].

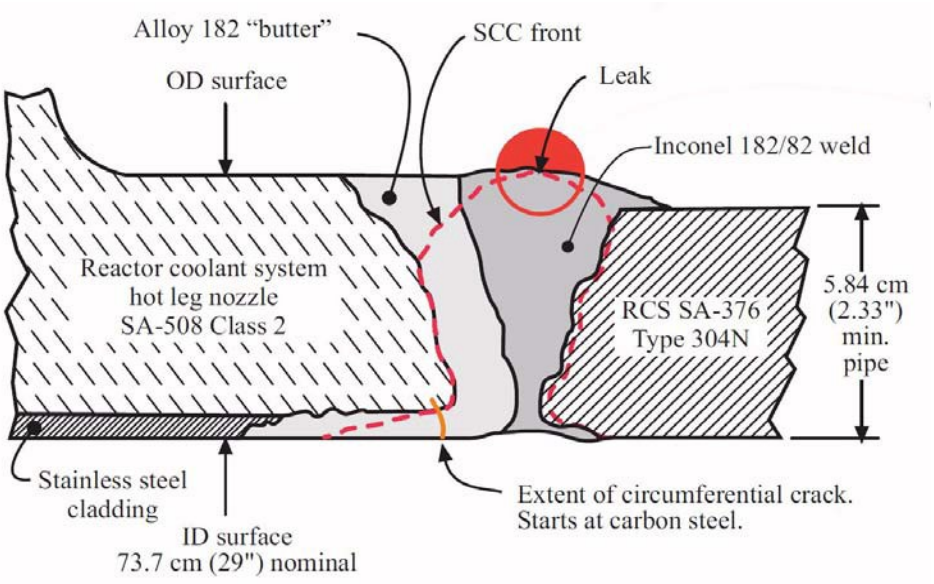

Figure 3.26. Schematic of the Alloy 182 weld used to join stainless steel piping to the RPV nozzle.

3.6 OPERATING EXPERIENCE OF PWR SECONDARY SYSTEMS

Most PWR steam generators are recirculating designs, although some are once-through designs where all of the secondary water entering the steam generator is transformed into steam. Most in-service PWSCC has occurred in recirculating steam generators (Figures 3.27 and 3.28). An important difference between the two with respect to the occurrence of PWSCC is that the once-through steam generators were subjected to a pre-service stress relief of the whole steam

generator at a temperature of about 610 °C (1,130 °F). In addition to contributing to grain boundary carbide precipitation in Alloy 600, some grain boundary Cr depletion (sensitization) also occurred. The lower strength and grain boundary carbide precipitation in once-through steam generators tubes has been beneficial to resist PWSCC on the primary side, despite the sensitization; however, even these steam generators are now being steadily replaced after typically 20 to 25 years of service [44]. In one case, an unintended ingress of thiosulfate into the once-through steam generators led (predictably) to extensive intergranular attack of the sensitized tubes.

PWSCC of Alloy 600 steam generator tubing in the mill-annealed condition became a major degradation mechanism from the 1970s onward for recirculating steam generators [45]. In 1971, the first confirmed primary side cracking of mill annealed Alloy 600 tubes of recirculating steam generators occurred when leakage at U-bends occurred in the Obrigheim, Germany after only two years of operation [4]. Cracking occurred in the tight U-bends, mainly on the inner two rows at the apex and at the tangent points and in the tube sheet at the transition expansion or roll expansion tube regions. This latter occurrence has been responsible for premature steam generator replacement at numerous plants.

The first roll transitions experiencing PWSCC were located on the hot leg side, where the temperature is typically around 320 °C and is 30 to 40 °C hotter than the cold leg inlet at 280 °C (536 °F). Thus, it was clear that temperature had a significant influence on PWSCC, indicating a thermally activated mechanism. The apparent activation energy, calculated from fitting the temperature dependence to the Arrhenius equation is rather high (~180 kJ/mole) so that a typical temperature difference of 30 °C (54 °F) between hot and cold legs could easily account for a factor of four to five increase in the time to the onset of detectable cracking. Thus, a reduction of hot leg temperature was employed for mitigation. Hot leg temperature reductions from 4 °C (7.2 °F) to even 10 °C (18 °F) have been applied.

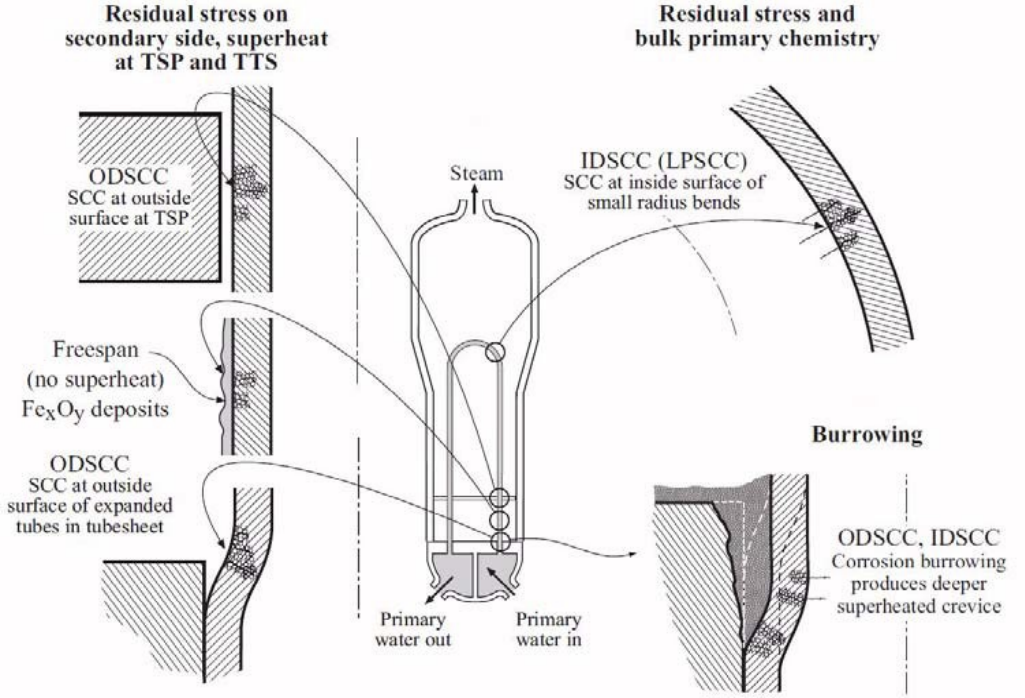

Figure 3.27. Schematic of locations where SCC most often occurs in Alloy 600 steam generator tubing.

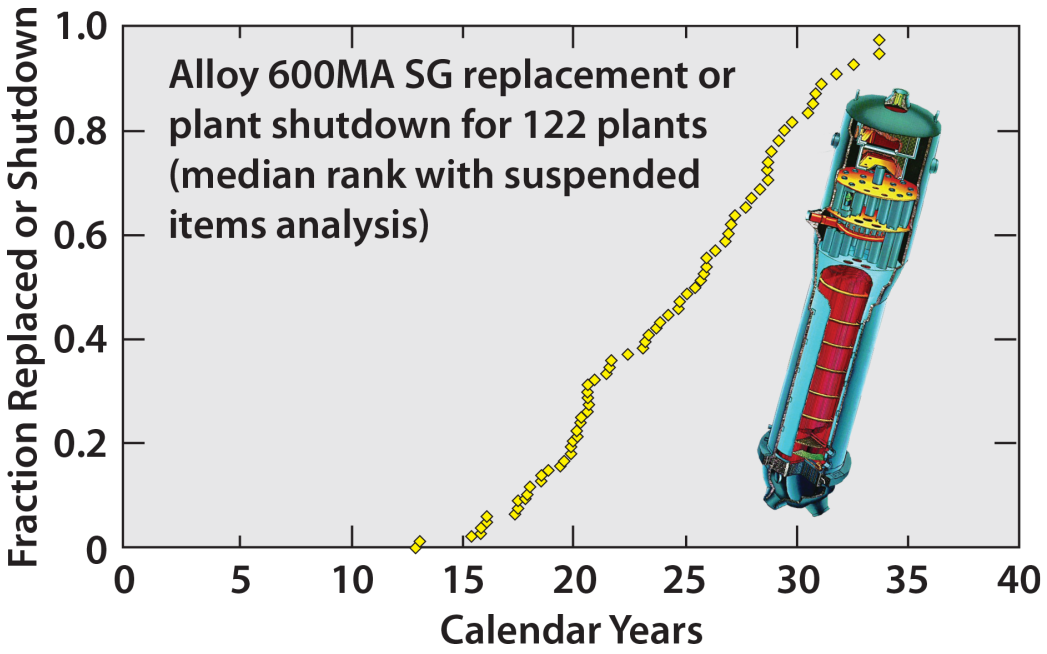

Figure 3.28. Fraction of Alloy 600 steam generators replaced per calendar years of operation.

The magnitude of the tensile residual stress from fabrication has also had a major impact on the time for detectable PWSCC to develop; only the most highly strained regions of steam generator tubing (i.e., first and second row U-bends, roll transition regions, expanded regions, and dented areas) have exhibited PWSCC. Consequently, several stress mitigation techniques have been developed, such as local stress relief of first and second row U-bends by resistance or induction heating, and shot peening or roto-peening to induce compressive stresses on the internal surface of roll transitions [46, 47]. While peening helps to prevent initiation of new cracks, it cannot prevent the growth of existing cracks whose depth is greater than that of the induced compressive layer, typically 100 to 200 μm (approximately 0.004 to 0.008 in.). Thus, peening has been most effective when most tubes have either no cracks or only very shallow ones (i.e., when practiced before service or very early in life) [47, 48].

Material susceptibility, in combination with the factors mentioned above, is also a major factor affecting the occurrence of PWSCC in service. Most PWSCC has occurred in mill-annealed tubing. However, it is important to emphasize that there is not a single product called “mill-annealed” Alloy 600 tubing since each tubing manufacturer has different production processes. Whereas some mill-annealed tubing has never experienced PWSCC over many years, other mill-annealed tubing has undergone PWSCC after only 1 to 2 years of service, particularly at roll transitions. This variability of PWSCC susceptibility can be seen even between heats from the same manufacturer in the same steam generator [1]. The variation in susceptibility to PWSCC of the heats of Alloy 600 typically fits approximately a lognormal distribution, perhaps indicating that a rather small fraction of Alloy 600 heats may be responsible for a disproportionately high number of tubes affected by primary side PWSCC. The reasons for this variability are only partly understood, as explained below.

This microstructural aspect of susceptibility to PWSCC is strongly affected by the final mill annealing temperature, which determines whether carbide precipitation occurs predominantly on grain boundaries or within the grains (intragranular). The most susceptible microstructures are those produced by low mill annealing temperatures, typically around 980 °C (1,796 °F) that

develop fine grain sizes (ASTM 9 to 11), copious quantities of intragranular carbides, and, usually, few to no grain boundary carbides [49, 50]. Higher mill annealing temperatures in the range of 1,040 °C (1,904 °F) to 1,070 °C (1,958 °F) avoid undue grain growth and leave enough dissolved carbon (C) so that intergranular carbide precipitation occurs more readily during cooling.

A further development to exploit the apparent advantages of grain boundary carbides for PWSCC resistance was to thermally treat the tubing for ~15 h at 705 °C (1,301 °F) after mill annealing. This heat treatment increases the density of intergranular carbides and provides enough time so that most of the C in solution is consumed and the Cr can diffuse to grain boundaries, thus eliminating depletion of carbide avoiding sensitization [50]. The beneficial influence of grain boundary Cr carbides on primary side PWSCC resistance has been extensively evaluated in laboratory studies; the results showed an improvement in life of thermally treated tubing of between 2 and 5 times relative to the mill annealed condition. In fact, primary side PWSCC resistance is improved with or without grain boundary Cr depletion, as also deduced from the generally much better operating experience of Alloy 600 tubing of once-through steam generators [44, 49, 50]. However, even thermally treated Alloy 600 tubing has cracked in service, but much less frequently than mill annealed Alloy 600. This has usually been attributed to a failure of the thermal treatment to produce the desired intergranular carbide microstructure either due to insufficient C or factors such as tube straightening prior to thermal treatment, which favors carbide precipitation on dislocations instead of grain boundaries.

Steam generator tubes with PWSCC detectable by non-destructive testing have usually been preventively plugged either to avoid leakage or before the crack length reaches some predefined conservative fraction of the critical size for ductile rupture. Sleeving has sometimes been deployed as a repair method in operating PWRs to avoid plugging and maintain the affected tubes in service. The sleeves bridge the damaged area and are welded to material ground beyond the damage. The ends of the sleeves may be expanded hydraulically or explosively and are in most cases sealed by rolling, welding, or brazing [5].

Modern (usually replacement) steam generators have been fabricated using Alloy 690 tubes thermally treated for 5 hours at 715 °C. As well as being highly resistant in severe laboratory tests to PWSCC in PWR primary water compared to either mill annealed or thermally treated Alloy 600, the lead steam generators with thermally treated Alloy 690 tube bundles have to date passed about 16 years of service with no known tube failures, related to PWSCC.

3.7 IMPROVED NICKEL ALLOYS AND WELD METALS

Efforts to improve Ni alloy resistance to SCC have focused on *incremental* improvements and *major* improvements. Incremental tuning includes additions of stabilizing elements [such as niobium (Nb), tantalum (Ta), and titanium (Ti)] and control of C levels, which minimizes the likelihood of grain boundary Cr depletion and creates a dispersion of MC-type carbides, where M represents the alloying element. An empirically-derived N-bar parameter has been used to assess the SCC susceptibility for Alloy 182 [51], represented by: N-bar = 0.13×(Nb+Ti)/(2×C) (in weight percent), with values below 12 indicating moderate susceptibility. A more recent measure is the stress corrosion resistance index, which includes Cr level in the assessment [52].

$$SCRI = Cr + (Nb+Ta)\times 5 + Ti\times 10 - 116.5\times C \quad \text{(in weight percent)} \qquad (1)$$

A value below 30 represents susceptibility. Higher crack growth rates have also been measured in tests performed to evaluate SCC susceptibility due to other alloying impurities, such as

phosphorous (P), sulfur (S), and silicon (Si), but this may be due to synergistic effects with Cr-depleted boundaries. These elements, especially elevated Si and lower manganese (Mn), adversely affect weldability by leading to a higher propensity for hot cracking that could accelerate crack advance. Vendor specifications have been adapted to account for these factors.

More significant improvements have been achieved by markedly increasing the Cr content, e.g., from 15–20% Cr to 27–30% Cr. Examples are Alloy 690 base metal (~30% Cr), Alloy 152/52 weld metals (~30% Cr), and Alloy 52i weld metal (~27% Cr). The higher Cr content imparts greater resistance to SCC (Figures 3.9, 3.29, and 3.30), but also brings some challenges. The higher Cr content of Alloy 690 makes it more prone to segregation and banding, thus requiring controlled processing. Alloy 152 and 52 weld metals are more prone to hot cracking and ductility dip cracking, and the very extensive efforts to improve their weldability have only been partly successful.

The PWR industry has shifted to Alloy 52 and 152 weld metal, and Alloy 600 has been replaced with Alloy 690. In general, the SCC susceptibility is significantly reduced. However, many Alloy 690 heats have exhibited high SCC growth rates when cold worked in laboratory experiments, and welds—especially if they have been repaired—can have residual strains greater than 25%. Issues with Alloy 690, and Alloy 152/52 materials will be discussed in the following Chapter. Some in the BWR industry still consider Alloy 82 an adequate choice when fabrication concerns are included in the decision process. But both PWR and BWR data (Figures 3.8 and 3.31) [25–28] indicate that the distinction between Alloy 182 and 82 weld metals is not very significant in laboratory experiments involving crack growth studies.

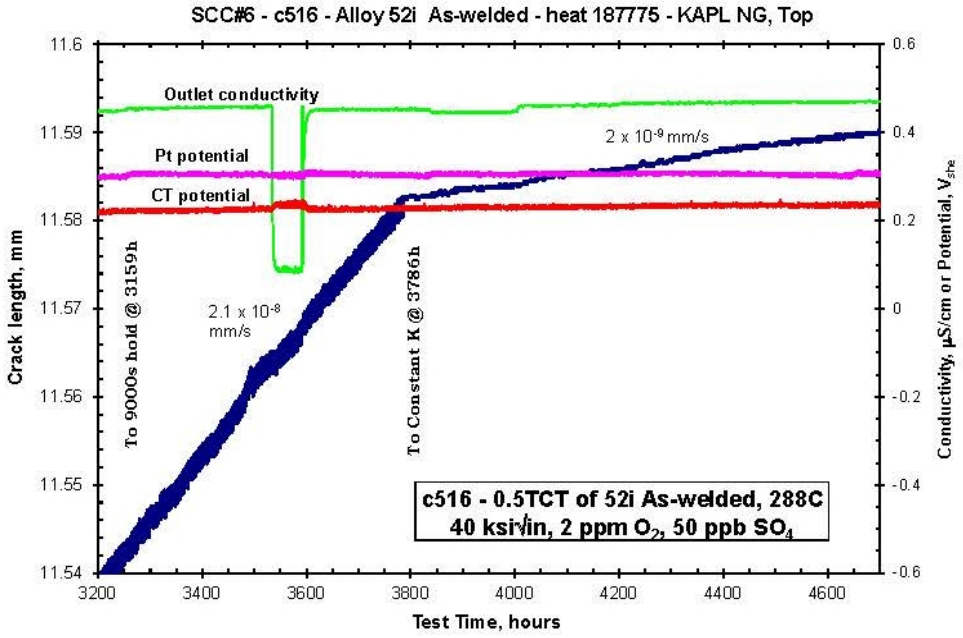

Figure 3.29. SCC response of 27% Cr, Alloy 52i weld metal in BWR water chemistry with 2 ppm O_2 and high levels of acid sulfate.

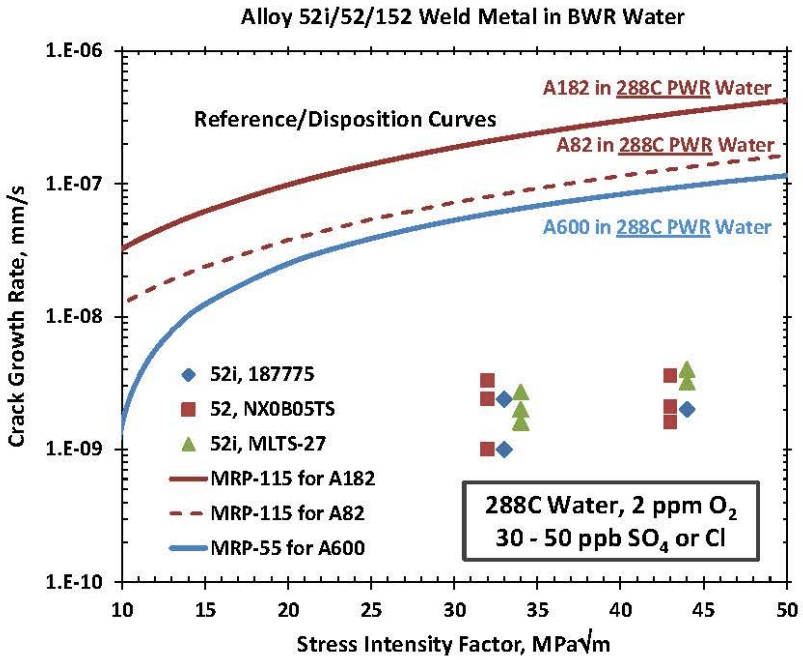

Figure 3.30. Summary of crack growth rates on Alloy 52 and 152 weld metals in BWR water with 2 ppm O_2 and high levels of acid sulfate or chloride. The growth rates in BWR water are ~50× lower than the disposition curve for Alloy 82 weld metal in PWR primary water (low corrosion potential) at 288ºC (550 °F) (dashed curve).

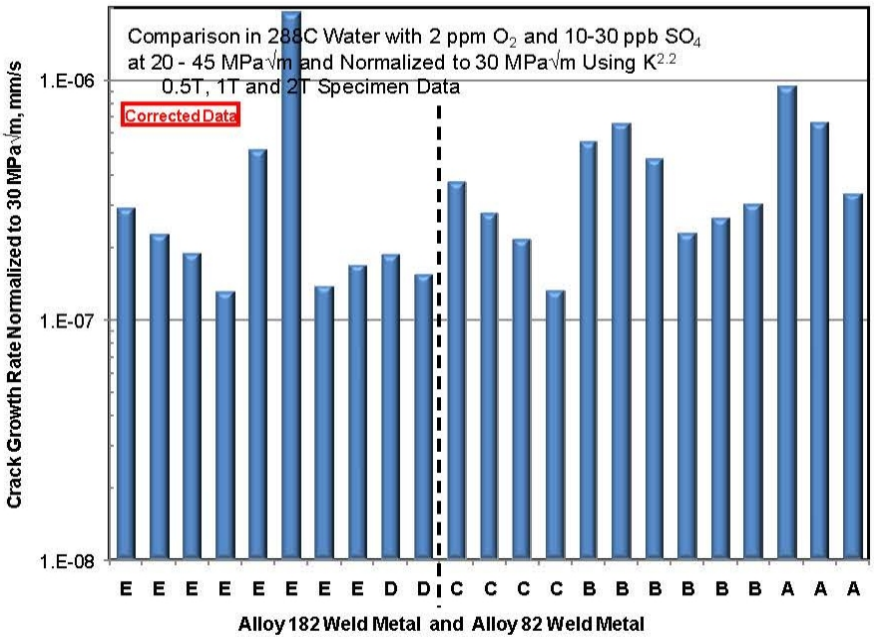

Figure 3.31. Overview of SCC growth rate data on five heats of Alloy 182 and 82 weld metal in 288 °C BWR water showing the lack of a distinctive difference between them, as well as their fairly high crack growth rates [25–28].

3.8 REFERENCES*

1. P. M. Scott, “Stress Corrosion Cracking in Pressurized Water Reactors—Interpretation, Modeling and Remedies,” *Corrosion* **56**(8), 771–782 (2000).
2. Ph. Berge, “Importance of Surface Preparation for Corrosion Control in Nuclear Power Stations,” *Materials Performance* **36**(11), 56 (1997).
3. J. Blanchet, H. Coriou, L. Grall, C. Mahieu, C. Otter, G. Turluer, “Historical Review of the Principal Research Concerning the Phenomena of Cracking of Nickel Base Austenitic Alloys,” pp. 1149–1160 in *Proc. NACE-5 Stress Corrosion Cracking and Hydrogen Embrittlement of Iron Base Alloys,* National Association of Corrosion Engineers, 1977.
4. H. J. Schenk, “Investigation of Tube Failures in Inconel 600 Steam Generator Tubing at KWO Obrigheim,” *Materials Performance* **15**(3), 25–33 (1976).
5. S. J. Green, “Steam Generator Failure or Degradation,” pp. 937–945 in “Corrosion in the Nuclear Power Industry,” *ASM Handbook, Vol. 13, Corrosion,* 1987.
6. W. Bamford and J. Hall, “A Review of Alloy 600 Cracking in Operating Nuclear Plants: Historical Experience and Future Trends,” pp. 1071–1079 in *Proc. 11th Int. Conf. Environmental Degradation of Materials in Nuclear Power Systems—Water Reactors,* Stevenson, Aug. 10–14, 2003, G. Was and L. Nelson (eds.), American Nuclear Society, 2003.
7. W. H. Cullen, Jr., and T. S. Mintz, *A Survey of Worldwide Experience with the Cracking Susceptibility of Alloy 600 and Associated Welds,* ADAMS ML040910354, Office of Nuclear Regulatory Research, U.S. Nuclear Regulatory Commission, Washington, DC, March 2004.
8. F. P. Ford and P. L. Andresen, “Development and Use of a Predictive Model of Crack Propagation in 304/316L, A533B/A508 and Inconel 600/182 in 288 °C Water,” pp. 789–800 in *3rd Int. Symp. Degradation of Materials in Nuclear Power Industry,* The Minerals, Metals &Materials Society, 1988.
9. P. L. Andresen and F. P. Ford, “Life Prediction by Mechanistic Modeling and System Monitoring of Environmental Cracking of Fe and Ni Alloys in Aqueous Systems,” *Materials Science and Engineering* **A103,** 167–183 (1988).
10. F. P. Ford and P. L. Andresen, “Corrosion in Nuclear Systems: Environmentally Assisted Cracking in Light Water Reactors,” pp. 501–546 in *Corrosion Mechanisms,* P. Marcus and J. Ouder (eds.), Marcel Dekker, 1994.
11. P. L. Andresen, “Fracture Mechanics Data and Modeling of Environmental Cracking of Nickel-Base Alloys in High Temperature Water,” *Corrosion* **47,** 917–938 (December 1991).
12. P. L. Andresen, “Conceptual Similarities and Common Predictive Approaches for SCC in High Temperature Water Systems,” Paper 96258, *Corrosion/96,* National Association of Corrosion Engineers, 1996.
13. P. L. Andresen, L. M. Young, P. W. Emigh, and R. M. Horn, “Stress Corrosion Crack Growth Rate Behavior of Ni Alloys 182 and 600 in High Temperature Water,” Paper 02510, *Corrosion/02,* National Association of Corrosion Engineers, 2002.

* Inclusion of references in this report does not necessarily constitute NRC approval or agreement with the referenced information.

14. P. L. Andresen, “SCC of Alloy 182 and 82 Weld Metals in BWR Water,” *Corrosion/10,* National Association of Corrosion Engineers, Houston, 2010.

15. P. L. Andresen, J. Hickling, K. S. Ahluwalia, and J. A. Wilson, “Effects of PWR Primary Water Chemistry on PWSCC of Ni Alloys,” *Proc. 13th Int. Symp. Environmental Degradation of Materials in Nuclear Power Systems,* Whistler, Aug. 19–23, 2007, P. King and T. Allen (eds.), The Canadian Nuclear Society, 2008.

16. P. L. Andresen, J. Hickling, K. S. Ahluwalia, and J. A. Wilson, “Effects of Hydrogen on SCC Growth Rate of Ni Alloys in High Temperature Water,” *Corrosion* **64**(9), 707 (2008).

17. P. L. Andresen and P. Chou, “Effects of Hydrogen on SCC Growth Rate of Ni Alloys in BWR Water,” *Proc. 15th Int. Symp. Environmental Degradation of Materials in Nuclear Power Systems—Water Reactors,* Colorado Springs, Aug. 7–11, 2011, J. Busby and G. Ilevbare (eds.), The Minerals, Metals & Materials Society, 2012.

18. C. M. Brown and W. J. Mills, “Load Path Effects on the Fracture Toughness of Alloy 82H and 52 Welds in Low Temperature Water,” *Proc. 12th Int. Symp. on Environmental Degradation of Materials in Nuclear Power Systems—Water Reactors*, Salt Lake City, Aug. 14–18, 2005, L. Nelson, P. King, and T. R. Allen (eds.), The Minerals, Metals &Materials Society, 2007.

19. C. M. Brown and W. J. Mills, “Fracture Toughness of Alloy 690 and EN52 Welds in Air and Water,” *Metallurgical Transactions A* **33A,** 1725 (June 2002).

20. P. L. Andresen and M. M. Morra, “Emerging Issues in Environmental Cracking in Hot Water,” *Proc. 13th Int. Symp. Environmental Degradation of Materials in Nuclear Power Systems,* Whistler, Aug. 19–23, 2007, P. King and T. Allen (eds.), The Canadian Nuclear Society, 2008.

21. P. L. Andresen, “Observations of Environmental Effects on Rapid Fracture,” unpublished data, GE Global Research Center, Schenectady, NY, 2010.

22. *Materials Reliability Program: Crack Growth Rates for Evaluating Primary Water Stress Corrosion Cracking (PWSCC) of Alloy 82, 182, and 132 Welds,* Report 1006696 (MRP-115), Electric Power Research Institute, 2004.

23. *Materials Reliability Program (MRP) Crack Growth Rates for Evaluating Primary Water Stress Corrosion Cracking (PWSCC) of Thick-Wall Alloy 600 Materials (MRP-55) Revision 1,* Final Report 1006695, Electric Power Research Institute, November 2002.

24. P. L. Andresen, P. W. Emigh, and M. M. Morra, “SCC of High Strength Ni-base Alloys in High Temperature Water,” Paper 04675, *Corrosion/04,* National Association of Corrosion Engineers, 2004.

25. G. A. Young, R. A. Etien, M. J. Hackett, J. D. Tucker, and T. E. Capobianco, “Physical Metallurgy, Weldability and In-Service Performance of Nickel-Chromium Filler Metals Used in Nuclear Power Systems,” *Proc. 14th Environmental Degradation of Materials in Nuclear Power Systems,* Virginia Beach, Aug. 23–27, 2009, T. Allen and J. Busby (eds.), American Nuclear Society, 2010.

26. R. A. Etien III, G. A. Young, T. E. Capobianco, J. V. Mullen, S. Leveillee, and P. C. Sander, “Development of a Corrosion Resistant and Highly Weldable Filler Metal For Use With Alloy 690,” Paper 08597, *Corrosion/2008,* National Association of Corrosion Engineers, Houston, TX, 2008.

27. G. A. Young, T. E. Capobianco, R. Etien III, J. V. Mullen, L. L. D’Amore, and S. Leveillee, “Development of a Highly Weldable and Corrosion Resistant Ni-Cr Filler Metal,” *Proc. 11th Environmental Degradation of Materials in Nuclear Power Systems—Water Reactors,*

Stevenson, Aug. 10–14, 2003, G. Was and L. Nelson (eds.), American Nuclear Society, 2003.

28. P. L. Andresen, "SCC of High Cr Alloys in BWR Environments," *Proc. 15th Int. Symp. Environmental Degradation of Materials in Nuclear Power Systems—Water Reactors,* Colorado Springs, Aug. 7–11, 2011, J. Busby and G. Ilevbare (eds.), The Minerals, Metals & Materials Society, 2012.
29. S. A. Attanasio and D. S. Morton, "Measurement of the Ni/NiO Transition in Ni-Cr-Fe Alloys and Updated Data and Correlation to Quantify the Effect of Aqueous Hydrogen on Primary Water SCC," *Proc. 11th Int. Symp. Environmental Degradation of Materials in Nuclear Power Systems—Water Reactors,* Stevenson, Aug. 10–14, 2003, G. Was and L. Nelson (eds.), American Nuclear Society, 2003.
30. D. S. Morton, S. A. Attanasio, and G. A. Young, "Primary Water SCC Understanding and Characterization Through Fundamental Understanding in the Vicinity of the Ni/NiO Phase Transition," *Proc. 10th Int. Symp. Environmental Degradation of Materials in Nuclear Power Systems—Water Reactors,* Lake Tahoe, Aug. 5–9, 2001, F. P. Ford and G. Was (eds.), National Association of Corrosion Engineers, 2002.
31. D. Morton, S. Attanasio, E. Richey, G. Young, and R. Etien, "Updated Data and Correlation to Quantify the Effect of Aqueous Hydrogen and Low Temperature on the SCC Growth Rate of Nickel-base Alloys in Primary Water," *Proc. Alloy 600 Conference,* Atlanta, June 2007, Electric Power Research Institute, 2007.
32. *BWR RPV License Renewal Industry Report, Revision 1,* Report TR-103836, Electric Power Research Institute, July 1994.
33. T. M. Angeliu, P. L. Andresen, E. Hall, J. A. Sutliff, and S. Sitzman, "Strain and Microstructure Characterization of Austenitic Stainless Steel Weld HAZs," Paper 00186, *Corrosion/2000,* National Association of Corrosion Engineers, 2000.
34. P. L. Andresen, T. M. Angeliu, L. M. Young, W. R. Catlin, and R. M. Horn, "Mechanisms and Kinetics of SCC in Stainless Steels," *Proc. 10th Int. Symp. Environmental Degradation of Materials in Nuclear Power Systems—Water Reactors,* Lake Tahoe, Aug. 5–9, 2001, F.P. Ford and G. Was (eds.), National Association of Corrosion Engineers, 2002.
35. A. Page, *Stress Corrosion Cracking of Alloys 600 and 690 and Weld Metals No. 82 and 182 in High Temperature Water,* EPRI NP-2617, Electric Power Research Institute, September 1982.
36. L. G. Ljungberg, *Stress Corrosion Cracking of Alloys 600 and 182 in BWRs,* EPRI/SKI Research Project 2293-1, interim reports, Electric Power Research Institute, 1991–1994.
37. *Reactor Pressure Vessel Attachment Welds: Degradation Assessment,* EPRI-NP-7139-D, Final Report, Electric Power Research Institute, May 1991.
38. H. S. Mehta, R. M. Horn, and G. B. Inch, "A Fracture Mechanics Evaluation of Observed Cracking at a BWR-2 Reactor Pressure Vessel Weld," *2002 ASME PVP Conference,* Aug. 4–8, 2002, Vancouver, B.C., Canada.
39. F. Champigny, F. Chapelier, and C. Amzallag, "Maintenance Strategy of Inconel Components in PWR Primary Systems in France," *Proc. Conf. Vessel Penetration Inspection, Cracking and Repairs,* Gaithersburg, MD, Sept. 29–Oct. 2, 2003, U.S. Nuclear Regulatory Commission, 2004.
40. P. Chartier, D. Edmond, and G. Turluer, "The French Regulatory Experience and Views on Nickel-base Alloy PWSCC Prevention," *Proc. Conf. Vessel Penetration Inspection, Cracking*

and Repairs, Gaithersburg, MD, Sep. 29–Oct. 2, 2003, U.S. Nuclear Regulatory Commission, 2004.

41. A. Hiser, "US Regulatory Experience and Prognosis with RPV Head Degradation and VHP Nozzle Cracking," *Proc. Conf. Vessel Penetration Inspection, Cracking and Repairs,* Gaithersburg, MD, Sept. 29–Oct. 2, 2003, U.S. Nuclear Regulatory Commission, 2004.
42. C. Amzallag, J-M. Boursier, C. Pagès, and C. Gimond, "Stress Corrosion Life Assessment of 182 and 82 Welds Used in PWR Components," *Proc. 10th Int. Conf. Environmental Degradation of Materials in Nuclear Power Systems—Water Reactors,* Lake Tahoe, Aug. 5–9, 2001, F. P. Ford and G. Was (eds.), National Association of Corrosion Engineers, 2002.
43. S. Thomas, "Bottom Mounted Instrumentation Penetration Condition Resolution," *Proc. Conf. Vessel Penetration Inspection, Cracking and Repairs,* Gaithersburg, MD, Sept. 29–Oct. 2, 2003, U.S. Nuclear Regulatory Commission, 2004.
44. P. A. Sherburne, "OTSG Materials Performance—25 Years Later," pp. 529–540 in *Proc. Fontevraud 4 Int. Symp.,* Société Française d'Energie Nucléaire, 1998.
45. D. R. Diercks, W. J. Shack, and J. Muscara, "Overview of Steam Generator Tube Degradation and Integrity Issues," *Nuclear Engineering and Design* **194,** 19–30 (1999).
46. G. Frederick and P. Hernalsteen, "Generic Preventive Actions for Mitigating MA Inconel 600 Susceptibility to Pure Water Stress Corrosion Cracking," presented at The Specialist Meeting on Steam Generators, Stockholm, Sweden, NEA/CSNI-UNIPEDE, October 1984.
47. P. Saint-Paul and G. Slama, "Steam Generator Materials Degradation," pp. 39–49 in *Proc. 5th Int. Symp. Environmental Degradation of Materials in Nuclear Power Systems—Water Reactors,* Monterey, Aug. 25–29, 1991, D. Cubicciotti and E. Simonen (eds.), American Nuclear Society, 1992.
48. P. Pitner and T. Riffard, "Statistical Evaluation of the Effects of Shot-Peening on Stress Corrosion of Alloy 600 in PWR Steam Generators," pp. 707–712 in *Proc. 6th Int. Symp. Environmental Degradation of Materials in Nuclear Power Systems–Water Reactors,* San Diego, Aug. 1–5, 1993, E. Simonen and R. Gold (eds.), The Minerals, Metals & Materials Society, 1993.
49. G. P. Airey, "The Stress Corrosion Cracking (SCC) Performance of Inconel Alloy 600 in Pure and Primary Water Environments," pp. 462–476 in *Proc. 1st Int. Symp. Environmental Degradation of Materials in Nuclear Power Systems—Water Reactors,* Myrtle Beach, Aug. 22–25, 1983, J. Roberts and W. Berry (eds.), National Association of Corrosion Engineers, 1984.
50. A. A. Stein and A. R. McIlree, "Relationship of Annealing Temperature and Microstructure to Primary Side Cracking of Alloy 600 Steam Generator Tubing and the Prediction of Stress Corrosion Cracking in Primary Water," pp. 47–51 in *Proc. of 2nd Int. Symp. Environmental Degradation of Materials in Nuclear Power Systems—Water Reactors,* Monterey, Sept. 9–12, 1985, J. Roberts and J. Weeks (eds.), American Nuclear Society, 1986.
51. M. Akashi, "Effects of Cr and Nb Contents on the Susceptibility of Alloy 600 Type Ni-base Alloys to Stress Corrosion Cracking in a Simulated BWR Environment," *Corrosion/95,* Orlando, FL, March 1995, National Association of Corrosion Engineers.
52. D. Sandusky, T. Okada, and T. Saito, "Advanced Boiling Water Reactor Materials Technology," *Materials Performance* **29**(1), 66–71 (1990).

4. POTENTIAL VULNERABILITIES OF ALLOY 690 AND ALLOY 152/52 WELD METALS IN PRESSURIZED WATER REACTORS

Steve Bruemmer
Pacific Northwest National Laboratory, Richland, Washington

4.1 INTRODUCTION

Wrought Alloy 690 and its associated weld metals (Alloys 152, 52, 52M, and other variants) have become the common replacement and repair materials for Alloy 600 and Alloy 182/82 weld metals with lower chromium content in PWRs, primarily due to their superior resistance to primary side SCC. Although SCC susceptibility of Alloy 600 in hydrogenated water at high-temperature was identified by laboratory testing in 1959, its significance on PWR components performance was not fully recognized until the 1980s, when cracking of Alloy 600 tubing prompted the need to replace or retire steam generators. In addition to primary-side and secondary-side steam generator tubing degradation, cracking of other Alloy 600 PWR components has been documented, including pressurizer heater sleeves and welds, pressurizer instrument nozzles, reactor vessel closure head nozzles and welds, reactor vessel outlet nozzle welds, and reactor vessel head instrumentation nozzle and welds. Pressurizer nozzles operating at the highest temperature were the first thick-section Alloy 600 component identified to crack in service and were typically replaced with austenitic stainless steels. More serious concerns emerged when through-wall SCC was found in control rod drive mechanism (CRDM) nozzles in the upper head of the PWR pressure vessels. Following the practice for steam generator tubing, Alloy 690 was selected as the replacement material for the nozzles; Alloys 152, 52, and 52M were used as associated welds.

This chapter is different from others in the compendium of LWR materials issues because Alloy 690 and its weld metals have not experienced significant degradation in service. On the contrary, successful performance of these alloys in PWRs has been noticed for about two decades as effective replacement materials for Alloys 600, 182, and 82 in PWRs. In addition, the high-Cr weld metals have also been used extensively and without incident as a corrosion-resistant overlay for component repair. In general, potential degradation modes of concern for Alloy 690 are similar to Alloy 600, including SCC, corrosion fatigue, and environment-induced fracture at high and low temperatures. The high-Cr weld metals encounter similar issues along with a susceptibility to ductility dip and hot cracking during welding plus significant dilution effects for dissimilar metal welds. Vulnerabilities to corrosion and cracking have only been identified in laboratory experiments, and typically during testing in off-normal material conditions and/or in severe environments. Many of these observations will be summarized here with a focus on SCC in PWR primary water environment along with a discussion of technical issues where the available knowledge is insufficient to properly confirm the extent of degradation resistance for Alloy 690 and its weld metals at this time.

4.2 COMPOSITION, PROPERTIES, AND METALLURGY OF ALLOY 690 AND ITS WELD METALS

4.2.1 Alloy 690 Material Specifications

Inco Alloys International originally developed Alloy 690 under the trade name Inconel Alloy 690; it is now owned by Special Metals Corporation [1]. Although this alloy is listed under the Unified Numbering System (UNS) designation in American Society for Testing and Materials (ASTM) and in American Society of Mechanical Engineers (ASME) standards, it is generically referred to as Alloy 690 in the nuclear power industry, as is Alloy 600. The most commonly used product forms in the *ASME Boiler and Pressure Vessel Code* for wrought Alloy 690 materials are seamless pipe, tubing, rod, bar, wire, plate, sheet, and strip. Because Alloy 690 was developed to replace Alloy 600 for light water nuclear power reactors, both are listed in the same ASME Code material specification.

The ASME Code chemical composition requirements (given in weight percent) for Alloy 690 are: 58.0 Ni (min), 27.0–31.0 Cr, 7.0–11.0 Fe, 0.05 C (max), 0.5 Mn (max), 0.5 Si (max), 0.015 S (max), and 0.5 Nb+Ta (max). However, more conservative requirements on chemical composition, processing, mechanical properties, and heat treatment are imposed on Alloy 690 by utilities and vendors for PWR applications. For example, the Electric Power Research Institute (EPRI) guidelines [2] require the carbon content to be between 0.015 and 0.025 wt % for Alloy 690 steam generator tubing in an attempt to optimize the distribution of carbide precipitates in the final microstructure. Slightly different carbon concentration ranges have been identified for thick-wall PWR components [3] with 0.015–0.035 wt % for Alloy 690 RPV head penetrations, whereas 0.01–0.04 wt % has been routinely specified for bars, plates, and heavy section tubing.

The most critical difference between Alloy 690 and Alloy 600 chemical requirements is for Cr; Alloy 600 requires a much lower concentration, 14–17 wt %. This change in Cr level in Alloy 690 is compensated for by a decrease in the Ni concentration. All other elements are similar in the basic ASME specification, although Fe is slightly higher and Mn and Si are slightly lower in Alloy 690 than in Alloy 600. Minimum ASTM specifications [4] for Alloy 690 mechanical properties at room temperature are yield strength, 205 MPa; tensile strength, 586 MPa; and total elongation, 35%.

4.2.2 Key Aspects of Alloy 690 Metallurgy and Microstructure

Alloy 690 is fully austenitic up to its melting temperature, which ranges from 1,343 °C (2,449 °F) to 1,377 °C (2,511 °F). The predominant second phase is a Cr-rich carbide that precipitates both at grain boundaries and in the matrix, depending on final processing and heat treatment. The type of Cr carbide that forms in Alloy 690 is $Cr_{23}C_6$, while Cr_7C_3 and $Cr_{23}C_6$ are common in Alloy 600. Grain boundary carbide precipitates typically form as discrete particles during cooling from the mill-anneal (MA) temperature or during thermal treatment (TT) from the solution-anneal (SA) temperature. The much higher Cr concentration in Alloy 690 promotes carbide nucleation at higher temperatures and during more rapid cooling rates than Alloy 600 [5, 6]. Carbide precipitate distributions can be quite variable in MA materials but should be semi-continuous to continuous along grain boundaries in an alloy given a proper SA and TT, as illustrated in Figure 4.1. Significant Cr depletion develops during the growth of intergranular (IG) Cr carbides, but minimum Cr concentrations in Alloy 690 tend to be 20 wt % or greater for TT temperatures and treatment durations [7–13]. Several corrosion studies have been performed documenting the

excellent resistance of Alloy 690 to IG corrosion (due to sensitization) after heat treatments consistent with the TT condition.

Discontinuous, cellular precipitation of $Cr_{23}C_6$ also occurs in Alloy 690 due to grain boundary migration [9] (example shown in Figure 4.1b) and can produce local regions of more extensive Cr depletion. This has been identified in several Alloy 690TT extruded tubing heats produced for PWR upper head penetrations [12, 13], but it does not influence the minimum Cr level adjacent to the carbide.

Titanium nitride (TiN) and Ti carbo-nitrides are typically minor phases in Alloy 690, but their shape, size, and distribution can be highly variable, depending on processing history and heat chemistry. Certain Alloy 690 plate heats have exhibited large TiN particles in the matrix, often associated with compositional banding. Isolated, small TiN precipitates have also been discovered at grain boundaries [12] in both plate and extruded tubing heats. They are smaller and well spaced in comparison to Cr carbides formed during thermal treatment. Interestingly, these small IG TiN particles remained after solution annealing at 1,100 °C (2,012 °F) followed by water quenching while $Cr_{23}C_6$ precipitates were removed [12, 13].

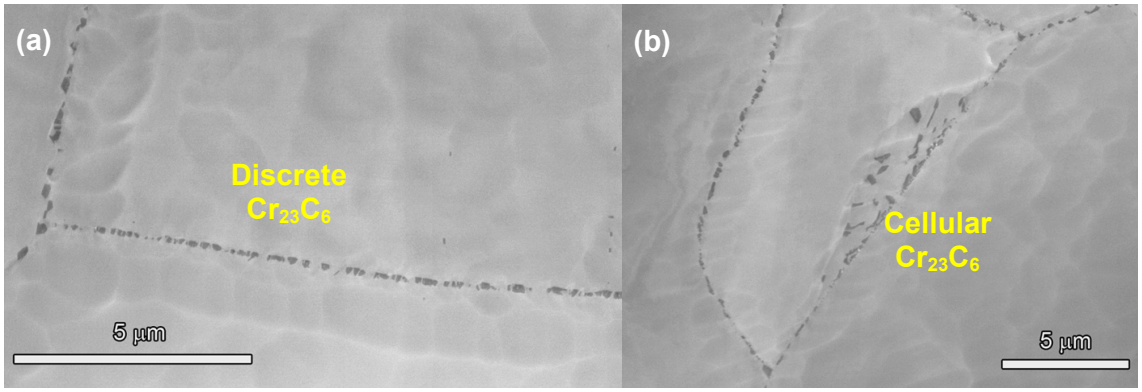

Figure 4.1. Scanning electron micrographs illustrating semi continuous Cr carbide precipitation in a thermally treated Alloy 690: (a) distribution of discrete IG $Cr_{23}C_6$ carbides and (b) distribution of discrete carbides along with a local region of boundary migration and cellular carbide growth [9]. Reprinted with permission of The Minerals, Metals & Materials Society.

Compositional banding can occur in this high Cr alloy [14] and can produce large variations in grain size and precipitate distributions. Banding can be present in the billet and can persist through very extensive processing steps (e.g., the steps required to produce plate and tubing products). Melting practice, homogenization, and critical strain during early working will affect the extent of banding. As a result, bands of fine grains with high densities of carbides and nitrides can exist within the microstructure along with areas of extremely large grains with few second phases. An example of this microstructural inhomogeneity in an Alloy 690 plate material is given in Figure 4.2.

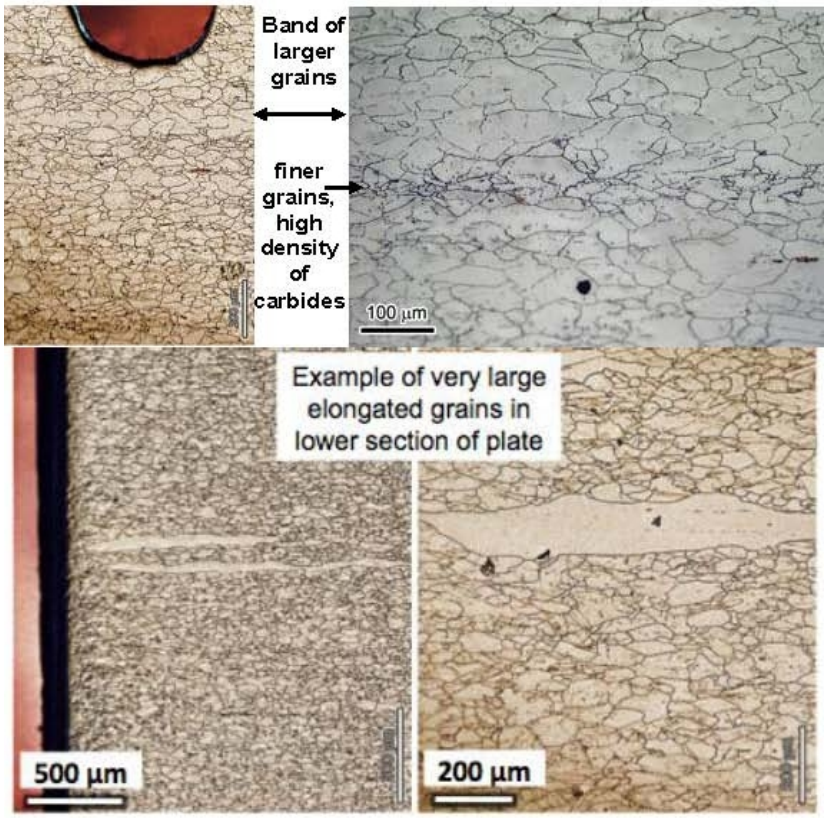

Figure 4.2. Optical micrographs illustrating microstructural variations due to compositional banding in an Alloy 690 plate material [14].

Carbide and nitride precipitation distributions have been found to play an important role in the evolution of deformation microstructures in Alloy 690 during cold work. High-resolution scanning and transmission electron microscopy (TEM) characterizations of heavily deformed Alloy 690 materials [12, 15, 16] have revealed small IG voids and cracked precipitates (primarily carbides) at grain boundaries as well as cracked particles (primarily larger nitrides) in the matrix. So far, extensive permanent (sub-micron size) damage of this type has only been documented in tubing and plate heats unidirectionally cold rolled (CR) to reductions greater than ~20%. Comparisons among cold-rolled materials indicate that void formation and precipitate cracking at grain boundaries directly depend on the starting distribution of IG precipitates. As noted earlier, the predominant precipitate formed is $Cr_{23}C_6$ with semi-continuous carbide distributions commonly found in Alloy 690TT materials and in Alloy 690MA materials. An example of the permanent damage that forms during CR is presented in Figure 4.3 for a 26% cold-rolled Alloy 690MA plate. A regular distribution of cracked carbides and voids along grain boundaries can be seen in Figures 4.3(b–d). The typical permanent damage spacing on many boundaries was on the order of 1 µm. Larger TiN particles in the matrix, often present in clusters extending for >50 µm, were also extensively cracked [Figure 4.3(e)]. This plate also exhibited compositional banding where an even higher density of cracked IG carbides and IG/matrix nitrides was indicated. Very limited research has been done to assess the threshold level of deformation that promotes this permanent damage, nor has work been done to investigate heat-to-heat and the starting microstructure effects.

This high level of cold work represents an extreme condition that is not representative of any Alloy 690 in reactor operation. However, such studies identify the need to better quantify

microstructures resulting from variations in processing and component fabrication procedures, including welding, straightening, and surface grinding. This research should be performed in tandem with the improved understanding of Alloy 690 processing and fabrication practices [17]. Key areas of study include: the mapping of precipitation, deformation structures, and damage in Alloy 690 weldments. Weld metal, fusion line, and heat affected zone (HAZ) regions exposed to complex temperature and strain cycles need to be better characterized. These regions develop low-to-moderate tensile strains from warm/cold work [18], and comparisons need to be made to the cold-work damage in Alloy 690 base metal described above. Electron backscatter diffraction (EBSD) has shown great promise in documenting general and local plastic strain distributions [19]. The degree of plastic strain can be indicated through characterization of local grain misorientations, and comparisons can be made among different materials, deformation levels, and microstructural regions such as a banded region or the HAZ. Although limited, EBSD has been applied effectively to assess the influence of thermomechanical treatments on microstructures of Alloy 690 materials and welds and SCC [12, 18, 20].

Another second phase in Alloy 690 worth identifying is the ordered intermetallic Ni_2Cr. It was hypothesized that formation of this phase is possible during extended reactor operation. The possibility that Ni_2Cr could form raised concerns that it might produce significant matrix hardening and embrittlement. Several extensive studies [21–24] have been conducted with the general conclusion that long-range ordering and Ni_2Cr formation can occur in a Ni-30%Cr alloy, but a minimum of 7 wt % Fe is sufficient to inhibit formation of this NiCr phase in Alloy 690. However, the EPRI guidelines for steam generator tubing [2] and pressure vessel nozzles [3] require a higher minimum content of 9 wt % Fe for a greater safety margin. Additional research on long-range ordering in Alloy 690 is still needed to verify and confirm that Ni_2Cr will not form during extended reactor operation (60–80 years), with potential adverse effects on reactor component performance.

There are other aspects of Alloy 690 microstructure and metallurgy, but these are not believed to be needed to underpin the key issues for the long-term degradation resistance in LWR service and so are not reviewed here. More detailed background information on Alloy 690 is given in reviews in EPRI Materials Reliability Program documents [25, 26].

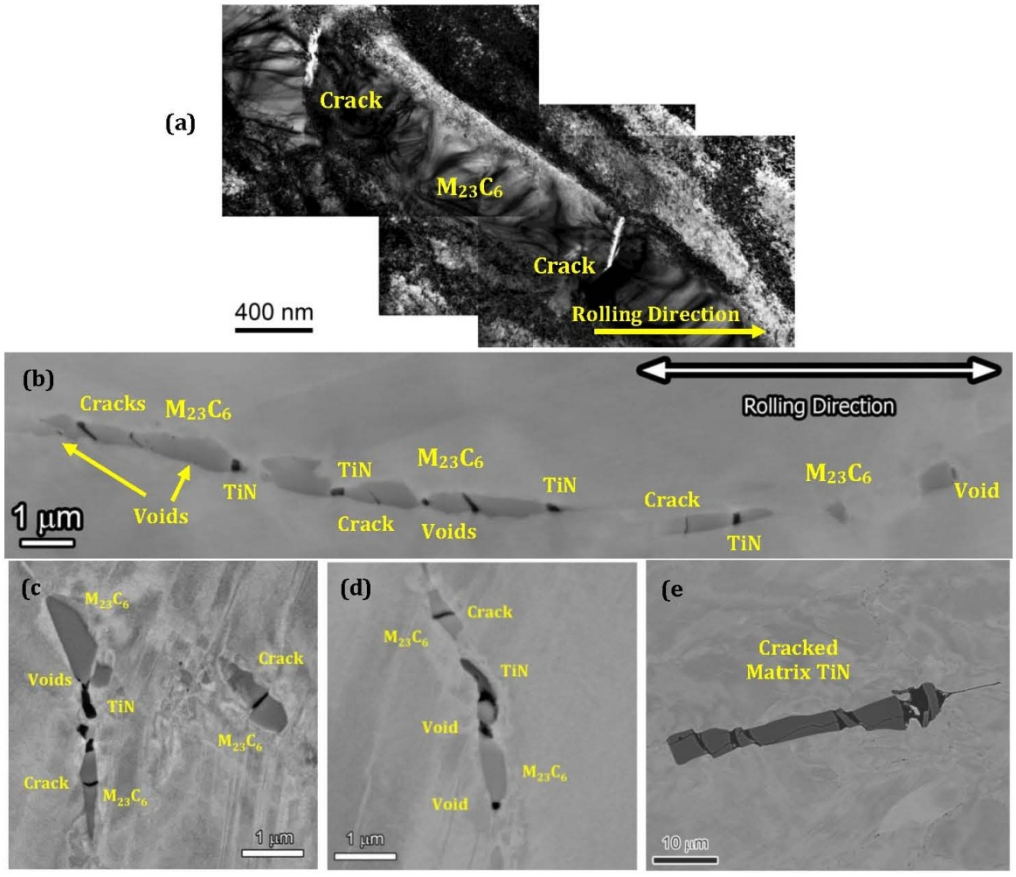

Figure 4.3. Transmission electron brightfield micrograph (a) showing a cracked IG carbide and high strain contrast in the adjacent matrix along with scanning electron micrographs illustrating grain boundary damage (voids and cracks) associated with carbide precipitates (b, c, and d) in a 26% CR Alloy 690 plate material. Cracking of larger matrix TiN particles (e) was also common in this plate material [12, 15, 16].
Reprinted with permission of The Minerals, Metals & Materials Society.

4.2.3 Material Specifications, Metallurgy, and Microstructure for Alloy 690 Weld Metals

The replacement of Alloy 600 with Alloy 690 prompted a change in welding products from Alloy 182 and 82 to higher chromium versions, Alloy 152 (shielded metal arc welding electrode) and Alloy 52 (gas tungsten and gas-metal welding filler metal). Based on specification sheets from Special Metals Corporation [27], several compositional differences can be seen among the three primary weld filler metals. Chemical composition requirements (weight percentages) for Alloy 152 are 28.0–31.5 Cr, 7.0–12.0 Fe, 0.05 C (max), 5.0 Mn (max), 0.50 Si (max), 0.015 S (max), 0.50 Mo (max), 0.50 Cu (max), 0.50 Ti (max), 0.50 Al (max), 0.03 P (max), and 1.0–2.5 Nb+Ta. Slightly different composition requirements (weight percentages) were established for Alloy 52: 28.0–31.5 Cr, 7.0–11.0 Fe, 0.04 C (max), 1.0 Mn (max), 0.75 Si (max), 0.015 S (max), 0.50 Mo (max), 0.30 Cu (max), 1.0 Ti (max), 1.10 Al (max), 1.5 Al+Ti (max), 0.02 P (max), and 0.1 Nb+Ta. Somewhat later, a modified Alloy 52 weld metal was developed and was identified as Alloy 52M. The overall composition is very similar to Alloy 52 except for the addition of B and Zr to improve

resistance to ductility dip cracking and to reduce inclusions. The Alloy 52M composition requirements (weight percentages) are 28.0–31.5 Cr, 7.0–11.0 Fe, 0.04 C (max), 1.0 Mn (max), 0.50 Si (max), 0.015 S (max), 0.50 Mo (max), 0.30 Cu (max), 1.0 Ti (max), 1.10 Al (max), 0.02 P (max), 0.5–1.0 Nb, 0.02 Zr (max), and 0.005 B (max). It is interesting that only maximum and no minimum concentrations are identified for the key additions of B and Zr. In addition, a few other differences in composition requirements can be identified for Ti, Al, and Nb.

Much less metallurgical and microstructural detail is available for the various Alloy 690 weld metals. Additional characterization is needed to better understand variability among the different weld metals and among welding practices. An important concern for welding of these high chromium, nickel alloys has been the formation of weld cracks [27–38].

Plant experience has shown that Alloys 152, 52, and 52M can be difficult to weld and are susceptible to weld cracking. Welding problems and cracking that occurred during manufacture and repair of PWR components have prompted considerable effort to develop specialized welding equipment and to optimize welding process parameters along with minor modifications to the base weld metal composition. Overall, these changes have significantly improved weldability of these high chromium nickel alloys; however, technical issues remain with the formation of weld defects, particularly with respect to ductility dip cracking in Alloy 52 and 52M welds.

Examples of ductility dip cracks discovered in an Alloy 52 mockup weld [29] are shown in Figure 4.4. The EBSD image enables a better visual image of the individual weld metal grains and highlights areas of plastic deformation. The typical large, elongated grains can be seen along with a collection of very fine grains along certain grain boundaries. The fine grains associated with the IG cracks suggest that local recrystallization may play some role in the cracking process. High strains depicted by large changes in crystal orientation within a grain are found at many of the high-angle grain boundaries and within the interior of many of the grains. Other regions examined also showed a mixture of large, elongated grains and local regions of very fine, recrystallized grains. As expected, high strains were found associated with cracks and grain boundaries in this entire region. Although some fundamental research has been performed [32–34, 38], there is no agreement on the root cause for cracking in these complex weld metals.

The microstructures and microchemistries developed within Alloy 152/52/52M welds that are representative of PWR plant components can be quite variable across the weld, and certainly at interfaces with base metals such as Alloy 690, low alloy steel, and stainless steel. In the weld metal, large, elongated grains containing a cellular dendritic solidification substructure are present along with areas of finer grains, often at weld pass boundaries and near the weld metal to base metal fusion lines. An example of the microstructural distribution across an Alloy 152 weld is presented in Figure 4.5. The orientation and size of the Alloy 152 grains can be seen to change as the fusion line with the Alloy 690 base metal is approached. Some degree of macro-segregation of Nb and Mn is typically seen [12, 29, 35–37 with the Nb-rich carbides forming at interdendritic sites. High-energy grain boundaries do not appear to exhibit strong segregation but often have a distribution of Nb (Ti) and Cr-rich $M_{23}C_6$ carbides. In many areas, the small Nb-rich carbides appear to locally pin the grain boundaries and promote a wavy morphology that has been suggested to improve resistance to the initiation of weld cracks [32–34]. The EBSD examinations have indicated that plastic strain is associated with high-energy grain boundaries and with some low-energy interdendritic boundaries; however much higher strains can be present at weld pass boundaries and near dissimilar metal interfaces [12, 18, 20, 35–37]. Recent work by Morra [20] has indicated the presence of relatively high strain in the weld metal transition region (partially melted and unmixed zones) adjacent to the fusion line with the

base metal. In nearly all cases, additional characterization and analyses are needed to better understand microstructures and microchemistries throughout those welds and to relate the analyses to degradation susceptibility.

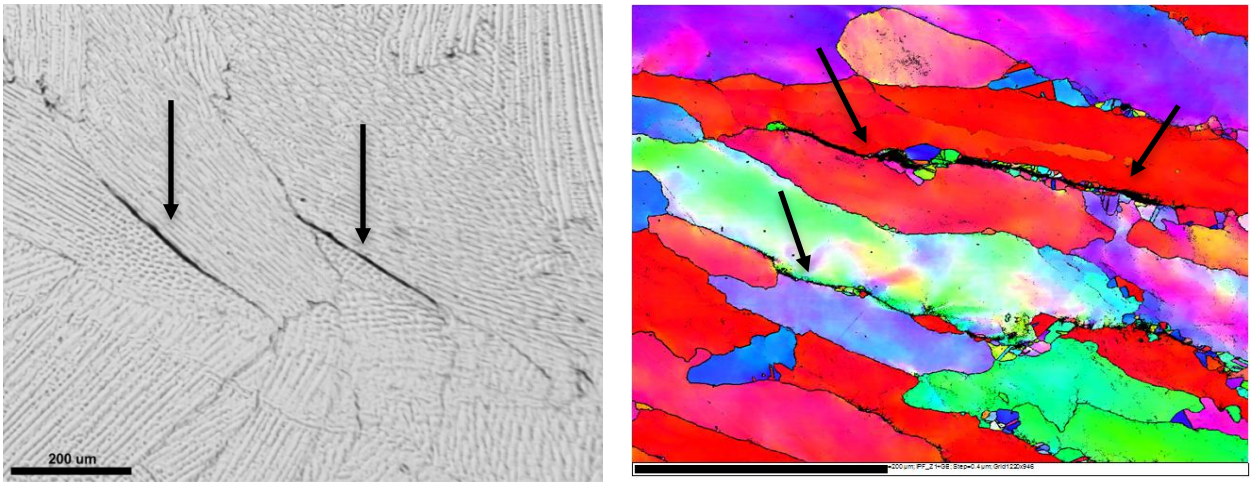

Figure 4.4. SEM (a) and EBSD inverse pole (b). Images showing ductility dip microcracks (locations are indicated by arrows) in an Alloy 52 mockup weld [29]. Fine grains can be seen associated with the cracks in the EBSD image.

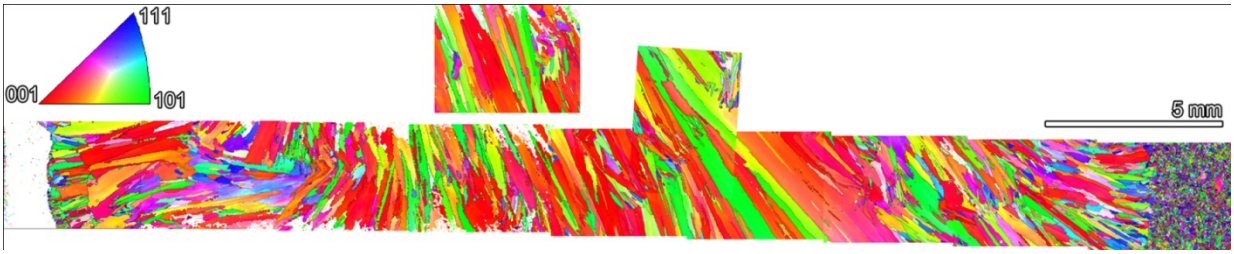

Figure 4.5. Montage of EBSD inverse pole. Images illustrate the grain microstructure changes across an Alloy 152 weld. The transition from Alloy 152 weld metal to Alloy 690 base metal is on the far right of the montage.

4.3 CORROSION, STRESS CORROSION, AND CORROSION FATIGUE OF ALLOY 690 AND ITS WELD METALS IN PWR PRIMARY WATER

4.3.1 Service Experience

The primary applications of Alloy 690 in PWRs have been as thin-wall (steam generators) or thick-wall (reactor pressure vessel head penetrations) tubing components to replace Alloy 600. PWR steam generator tubing is exposed to a challenging environment, including high temperatures, high stresses/strains, and a primary water environment that produced extensive IGSCC in Alloy 600 materials. The large number of tubes in each steam generator provides many different conditions to exist and/or develop promoting SCC initiation and growth.

Eighty-nine steam generators manufactured with Alloy 690TT tubing material were in international service as of 2008 with no reported primary-water SCC indications [26]. This excellent performance has now continued for more than 20 years in a few generators and for more than 15 years in approximately 40 generators. Although important improvements have been made to steam generator design and fabrication, service experience for Alloy 690 steam generator tubing confirms the considerable SCC resistance in PWR primary water.

The second major PWR component where SCC of Alloy 600 prompted replacement by Alloy 690 was for reactor pressure vessel head penetrations. The initial observation of primary water SCC was in the early 1990s and led to the replacement of 33 vessel heads in France by 2000 and nearly 30 vessel heads in the United States by 2008 [26]. Consistent with steam generator tube experience, no cracking has been identified for the Alloy 690 penetration nozzles or associated Alloy 152/52 welds after more than a decade of service. Alloy 690 has also been used in several other Alloy 600 component replacements in U.S. plants (e.g., pressurizer heater sleeve) without reported service failures.

4.3.2 Corrosion and Surface Oxidation Issues

Alloy 690 exhibits excellent resistance to both general and IG corrosion in PWR primary water environments. Many investigators have examined oxide film formation on Alloy 690 over the last decade and have compared it to that for Alloy 600. High-resolution characterizations have been limited [39–41] but suggest the formation of a continuous, high-Cr content protective film. The most comprehensive analysis on Alloy 690 has been conducted by Combrade and co-workers [39]. They concluded surface oxidation in PWR primary water occurs by this kinetic sequence:

1. selective oxidation of Cr and rapid initial growth of a thin Cr_2O_3 oxide layer,
2. restricted oxide growth due to near-surface Cr depletion allowing Ni and Fe transport through the film,
3. resumption of Cr-rich oxide growth with logarithmic kinetics, and
4. development of the bilayer oxide with Ni/Fe spinels forming on top of the Cr_2O_3 inner oxide layer.

Quite different corrosion/oxidation structures have recently been discovered [42] to form at both Alloy 690 crack surfaces and on polished surfaces during exposure to 360 °C (680 °F) PWR primary water. Nanoscale localized oxidation occurs from the surface and appears to follow dislocation substructures into the alloy matrix. Penetrative oxidation starts as shallow, well-spaced, small diameter (<5 nm), filaments after short exposure time and evolves to dense filaments that consume most of the remaining metallic matrix to a depth of several hundred nanometers. The oxide filaments have been characterized at near-atomic resolution by TEM and atom probe tomography to reveal a core structure of small chromia platelets surrounded by a nanocrystalline MO-structure oxide.

Alloy 690 grain boundaries intersecting the surface show no sign of localized oxidation; degradation appears to be limited to the dislocation structures [42]. Moreover, significant depletion of Cr is observed at grain boundaries to several micrometers below the surface along with evidence of boundary migration during the exposure to PWR primary water. A detailed understanding of surface oxidation processes and the stability of corrosion layer is expected to enable informed assessment of the long-term stability of the protective oxide film and the resistance of Alloy 690 to localized corrosion, SCC initiation, and SCC growth. This includes

corrosion and oxidation reactions with, and degradation of, the preexisting dislocation structures (due to both bulk deformation and surface preparation) and grain boundaries.

4.3.3 Stress Corrosion Crack Initiation

Laboratory SCC initiation testing for Alloy 690 has primarily focused on thin-wall tubing, typically reverse U-bend, double U-bend, constant load tensile, four-point bend, and steam generator tubing mock-up specimens. Investigations have been performed under a variety of environmental conditions described as simulated PWR primary water (often outside the normal operational range for temperature, Li, B, and dissolved hydrogen) along with some tests in higher-temperature doped-steam. The basic result from nearly all early Alloy 690 testing was the lack of any observable SCC. As more severe loading conditions and environments were applied, a few investigators reported limited IG cracking. Those results have been reviewed in some detail [25, 26] and have been linked to off-normal testing conditions not relevant to PWR service. Initiation testing on thick-walled tubing materials in simulated PWR primary water has been limited. The exception has been research [43] on Alloy 690 nozzle heats using uniaxial tensile specimens under constant, active load in primary water at 360 °C (680 °F) for duration approaching 10 years. The most recent report has indicated no cracking; however, results of high-resolution ex situ characterizations of these specimens have not been published to confirm whether finer cracks might be present.

Stress corrosion crack initiation remains one of the most significant unknowns for potential failure time range prediction in LWR structural alloys, including highly resistant Alloy 690 materials. As discussed in the previous section, surface corrosion/oxidation in PWR primary water is another key aspect but many other materials variables must be considered. It is pertinent to evaluate the influence of microstructure damage due to cold work or surface grinding on SCC nucleation. Carefully planned and conducted crack initiation tests on the same Alloy 690 heats and under conditions where SCC susceptibility has been seen in crack growth tests (described in the following section) may be of considerable value. Such tests have recently been started at General Electric Global Research [44] using blunt-notch specimens and at Pacific Northwest National Laboratory [45] using uniaxial tensile specimens under active constant load.

4.3.4 Stress Corrosion Crack Growth in Alloy 690

The early belief that Alloy 690 was essentially immune to SCC in representative PWR primary water was dispelled by crack-growth testing results [46] on cold-worked material about 10 years ago. The measured growth rates were quite low, but they identified the need for evaluations of heat-to-heat differences and the influence of thermo-mechanical processing. Quite a different concern was created when investigators at Bettis released data [47, 48] showing extremely high SCC growth rates in pertinent hydrogenated water environments on both cold-rolled and tensile-strained Alloy 690 plate materials when tested in the S-L or S-T orientation. For reference, the S-L orientation (or rolling direction) is parallel to the cold-rolling direction, while the S-T orientation (or transverse direction) is perpendicular to the cold-rolling direction. This information prompted considerable expansion of crack-growth testing on Alloy 690 and has led to an improved understanding of the influence of cold work.

Improvements in laboratory crack-growth testing and in-situ crack length detection have enabled remarkably low SCC rates to be measured in as-received, non-cold-worked Alloy 690. The approach for such tests is illustrated in Figure 4.6 for two extruded Alloy 690TT materials representative of CRDM tubing. Multiple evaluations of SCC response are made after a series of

transitioning steps resulting in long test times of a year or more. Maximum crack-growth rates under constant stress intensity (K) conditions for these materials was ~9 × 10^{-10} mm/s (3.5 × 10^{-11} in./s). Overall, the number of tests and measured SCC propagation rates at constant K or load on non-cold-worked Alloy 690 remain limited. A recent summary of published results includes data from tests on Alloy 690 HAZ specimens (Figure 4.7). In general, most crack growth rates at constant K are below 10^{-9} mm/s (4 × 10^{-11} in./s) for as-received materials and range from ~10^{-9} to 10^{-8} mm/s (4× 10^{-10} to 4 x0 10^{-9} in./s) for the HAZ specimens.

Research at many different laboratories [47–58] has clearly demonstrated the influence of cold work on SCC susceptibility in Alloy 690. A systematic evaluation has been conducted investigating the effects of the percentage of CR, specimen orientation, heat treatment condition, and microstructure on the SCC response for a single CRDM Alloy 690TT tubing heat [52–54, 57]. Cold rolling to 17% and 31% reductions and testing in the S-L orientation produced a consistent increase in measured SCC propagation rate to 3 × 10^{-9} mm/s (1.1 × 10^{-10} in./s) (Figure 4.8) and 1 × 10^{-7} mm/s (4× 10^{-9} in./s) (Figure 4.9), respectively. This change, (Figure 4.10), documents a 500× increase in the measured crack growth rate compared to non-cold-rolled material. Cold rolling promotes IGSCC with morphology of cracking completely IG for the 31% specimen, but only partial IG engagement is seen for the 17% specimen.

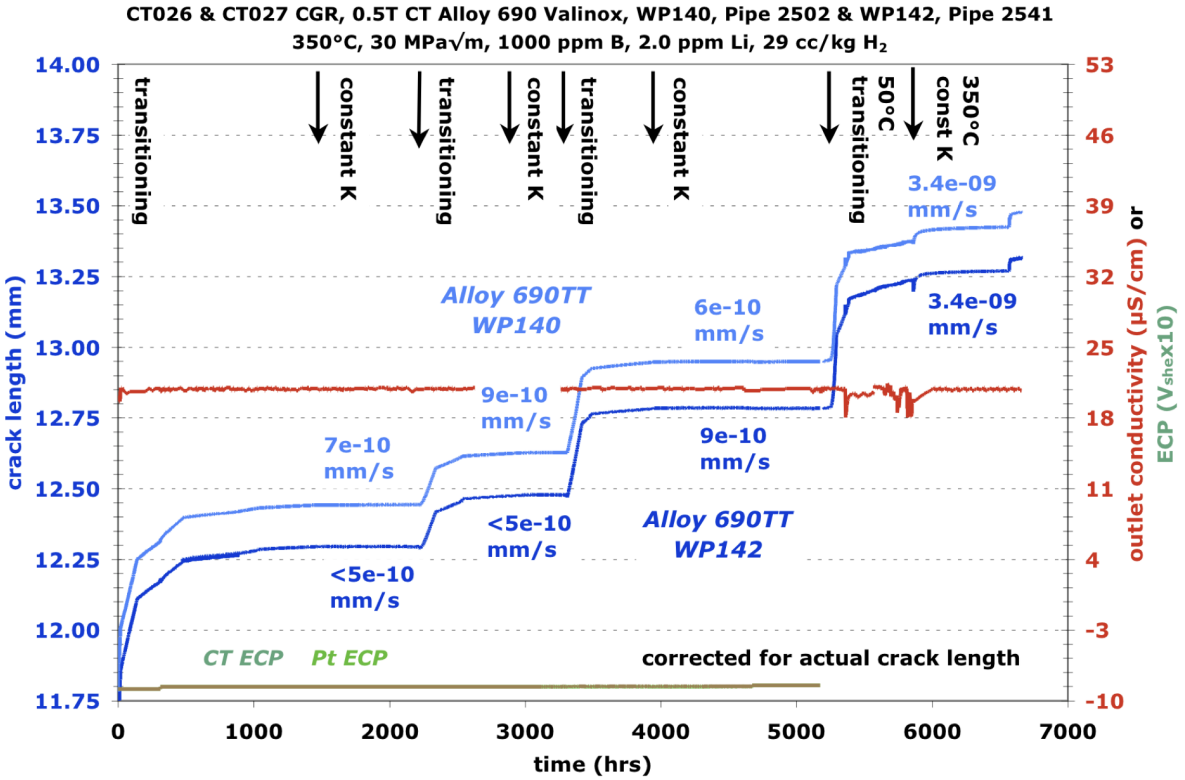

Figure 4.6. Overview of crack-growth test for two as-received Alloy 690TT materials in simulated PWR primary water at 350 °C (662 °F).

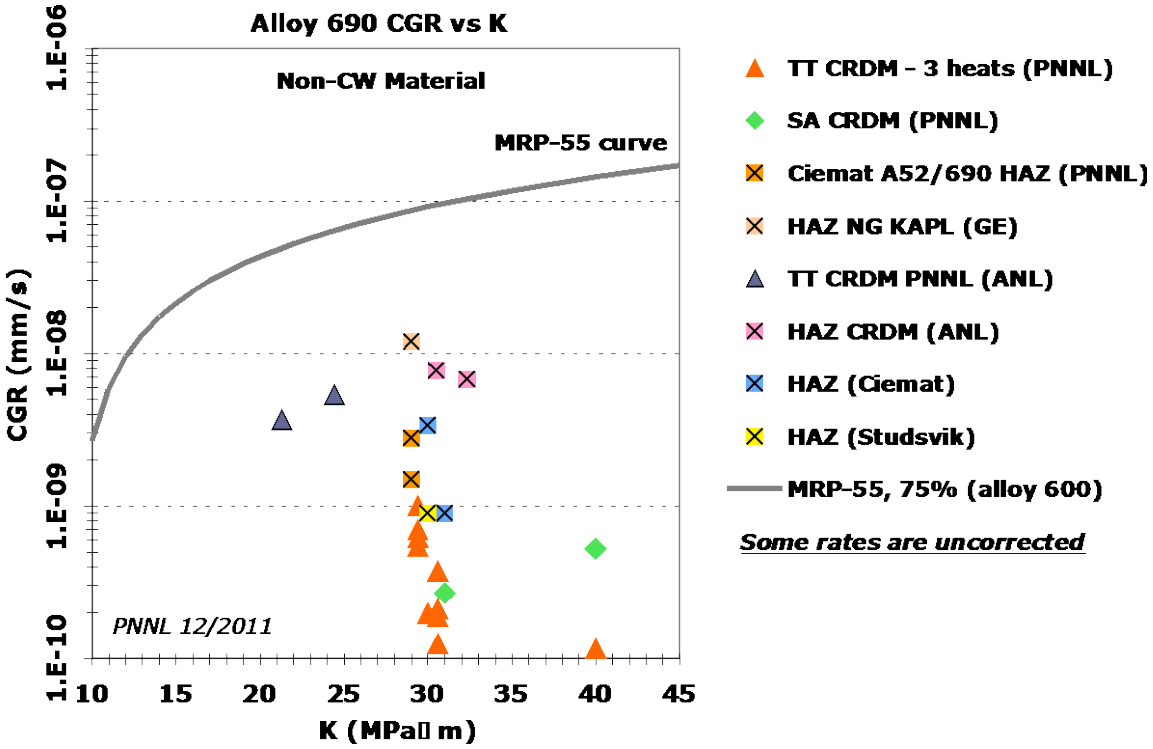

Figure 4.7. Summary of crack-growth test for as-received Alloy 690TT CRDM materials and Alloy 690 HAZ specimens in simulated PWR primary water.

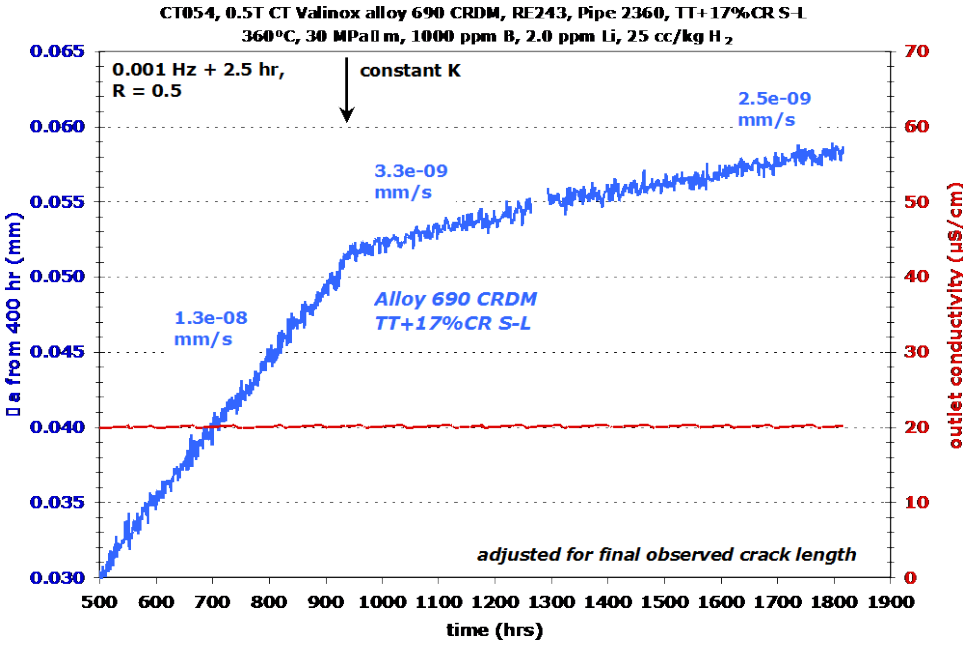

Figure 4.8. Crack growth response at 360 °C (680 °F) during cycle + hold and constant K of TT+17% CR S-L Alloy 690 CRDM.

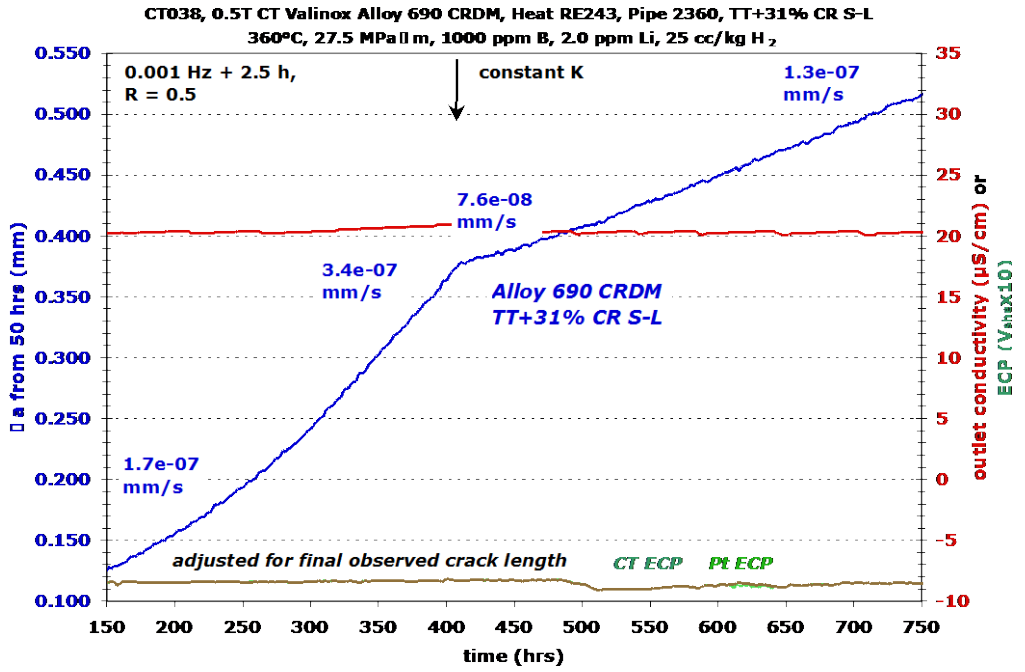

Figure 4.9. Crack growth response during cycle + hold and constant K of TT+31% CR S-L Alloy 690 CRDM.

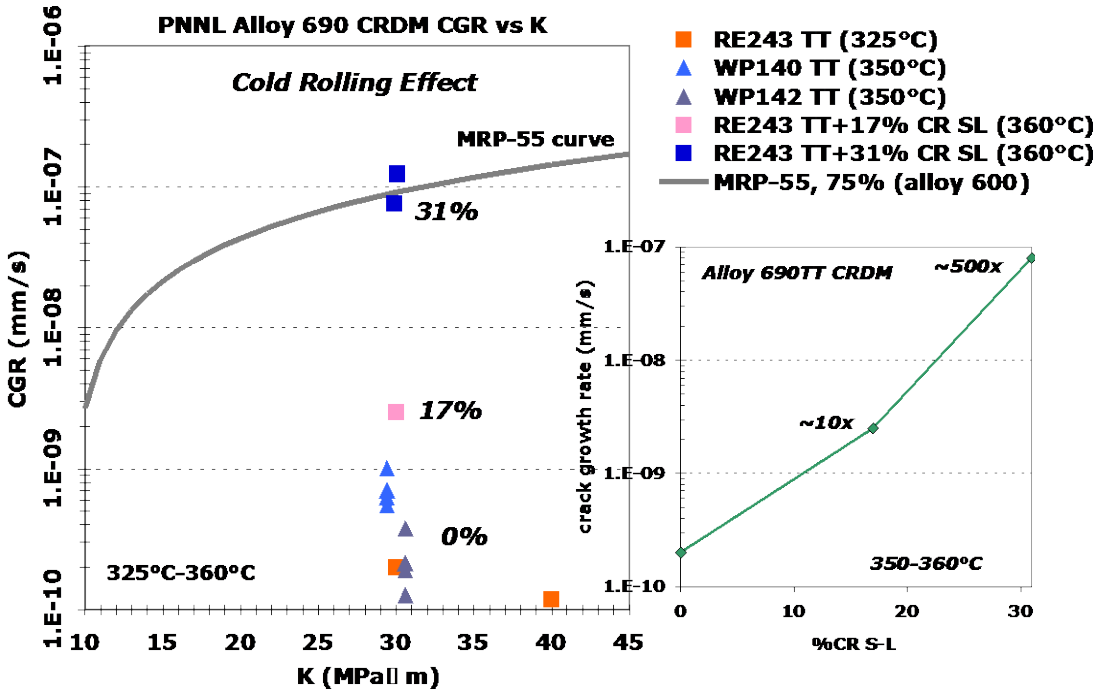

Figure 4.10. Crack growth response as a function of K level for the TT specimens and plotted as a function of the percentage of CR and testing in S-L orientation.

The most extensive crack-growth testing on cold-worked Alloy 690 materials has been performed at General Electric Global Research [49, 50, 55, 58] examining a wide range of tubing and plate heats in the cold-rolled and cold-forged condition. This research has substantiated that the primary factors controlling IGSCC susceptibility in PWR primary water are the degree and

nature of cold work along with the microstructural homogeneity of the alloy. In particular, extremely high SCC propagation rates (up to 10^{-6} mm/s, similar to those observed at Bettis Laboratory) were observed in a heavily banded Alloy 690 plate heat after significant cold work by rolling or forging. A summary of all Alloy 690 experimental data reported as of August 2011 is given in Figure 4.11 and illustrates a continuum of response from limited if any SCC growth at low levels of cold work to propagation rates more than a 1,000× higher in certain cold-worked heats.

A few recent tests have revealed very high crack growth rates. However, the earlier results from Bettis Laboratory investigation [47, 48] found these rates at lower levels of K and percentage of CR. In addition, they also measured high SCC propagation rates in tensile-strained Alloy 690 that is more relevant to a possible service condition (e.g., the Alloy 690 weld HAZ). Although it seems likely that a banded microstructure can be detrimental and increase SCC susceptibility, one of the Bettis Alloy 690 heats showing high growth rates was reported to have a homogeneous, non-banded microstructure, and several highly banded and cold-forged Alloy 690 heats have shown only moderate crack growth rates [55]. A final observation of importance for this issue is that the materials showing *very high* crack growth rates that do not change (remain very high) as a function of test temperature or hydrogen concentration [47, 48, 55]. By comparison, materials exhibiting low-to-high *SCC rates* in crack growth tests do show growth rates that depend directly on both test temperature (similar to Alloy 600 activation energy) and hydrogen concentration (rates decrease at dissolved hydrogen levels below the Ni/NiO stability line) [54]. Additional research is needed to assess the reasons why certain cold-worked heats exhibit very high versus moderate-to-high SCC rates, including the influence of compositional banding on Alloy 690 SCC susceptibility.

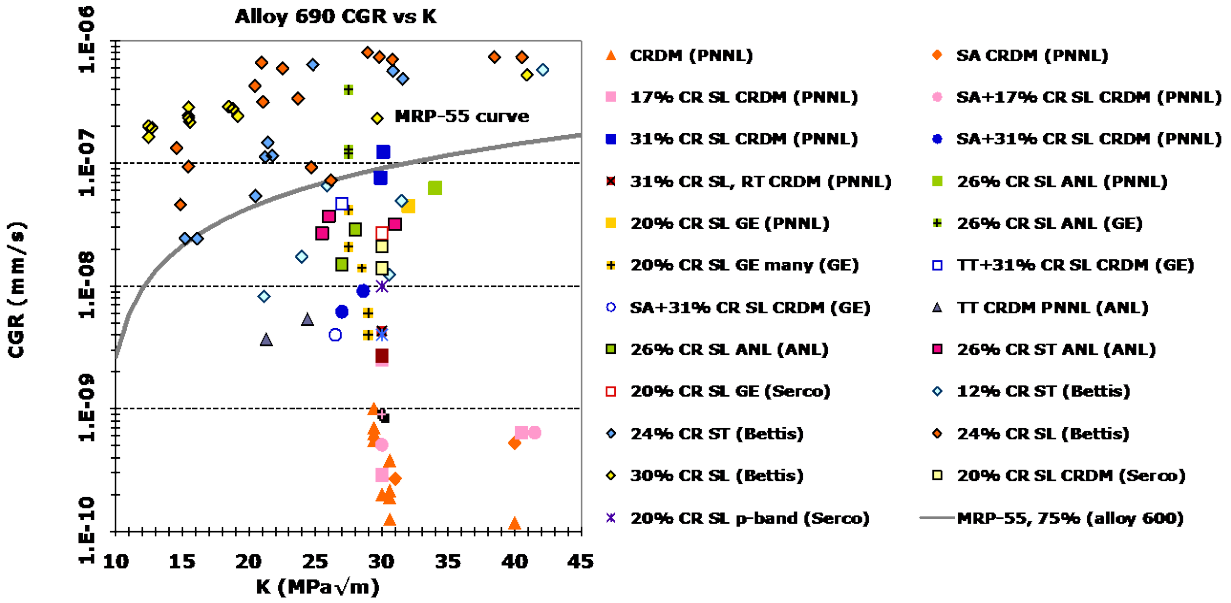

Figure 4.11. Summary of crack growth rate measurements [47–58] on Alloy 690 plate and tubing materials illustrating cold-rolling effects on SCC susceptibility.

The starting matrix and grain boundary microstructures will clearly influence the development of damage during cold working and IGSCC susceptibility. In order to evaluate the influence of IG carbides, the same Alloy 690TT tubing heat was solution annealed and water quenched to remove the semicontinuous $M_{23}C_6$ at grain boundaries. As discussed in the section on Alloy 690

metallurgy and microstructure, quite different IG permanent damage structures were observed between the TT and SA materials after CR. However, the average hardness and EBSD-measured average matrix strains (from misorientation) were nearly identical [49]. Crack-growth testing [54] revealed an order-of-magnitude lower SCC rate for the 30% to 31% cold-rolled SA materials than that measured for the TT materials. An example of this behavior is shown for the 30% cold-rolled materials tested in S-L orientation in Figure 4.12, while the SA and TT response for the different cold-rolled conditions are summarized in Figure 4.13. No influence of initial material condition is observed for the 0% and 17% cold-rolled materials, but a difference of ~10× is observed for the highly strained materials when tested in either the S-L or T-L orientations. This observation suggests that the TT condition may not be an optimal condition for Alloy 690 SCC resistance, at least in highly cold-worked materials. Additional research is needed to confirm SCC behavior as a function of heat treatment condition and to determine the role of grain boundary precipitates and their nature. One additional heat treatment condition was evaluated in this Alloy 690 CRDM tubing heat to modify the rolling-induced dislocation structure while leaving the permanent grain boundary damage (i.e., moderate density of IG voids and few cracked carbides). The 31% cold-rolled Alloy 690TT material was given a short duration (<5 hours) anneal at 700 ºC (1,292 ºF) that resulted in a 25× decrease in measured SCC propagation rate [53, 54].

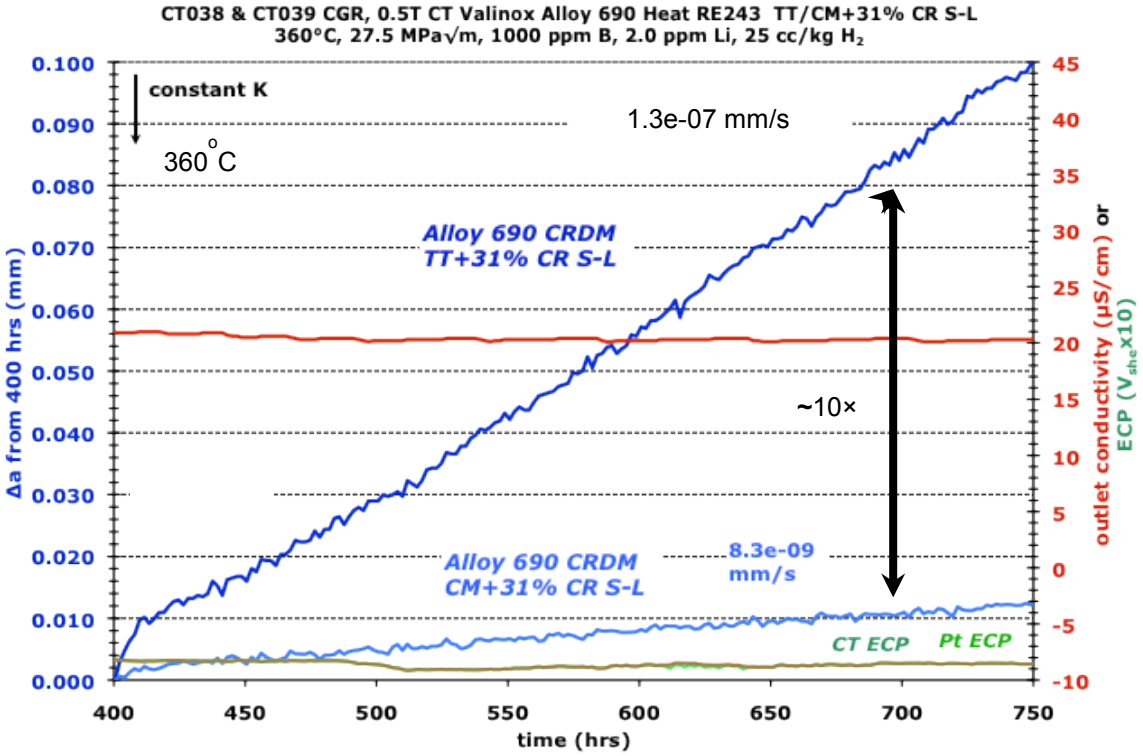

Figure 4.12. Crack growth response at constant K comparing the TT+31% CR S-L Alloy 690 CRDM to the SA+31% CR S-L Alloy 690 CRDM. These specimens were tested in series [54]. Reprinted with permission of The Minerals, Metals & Materials Society.

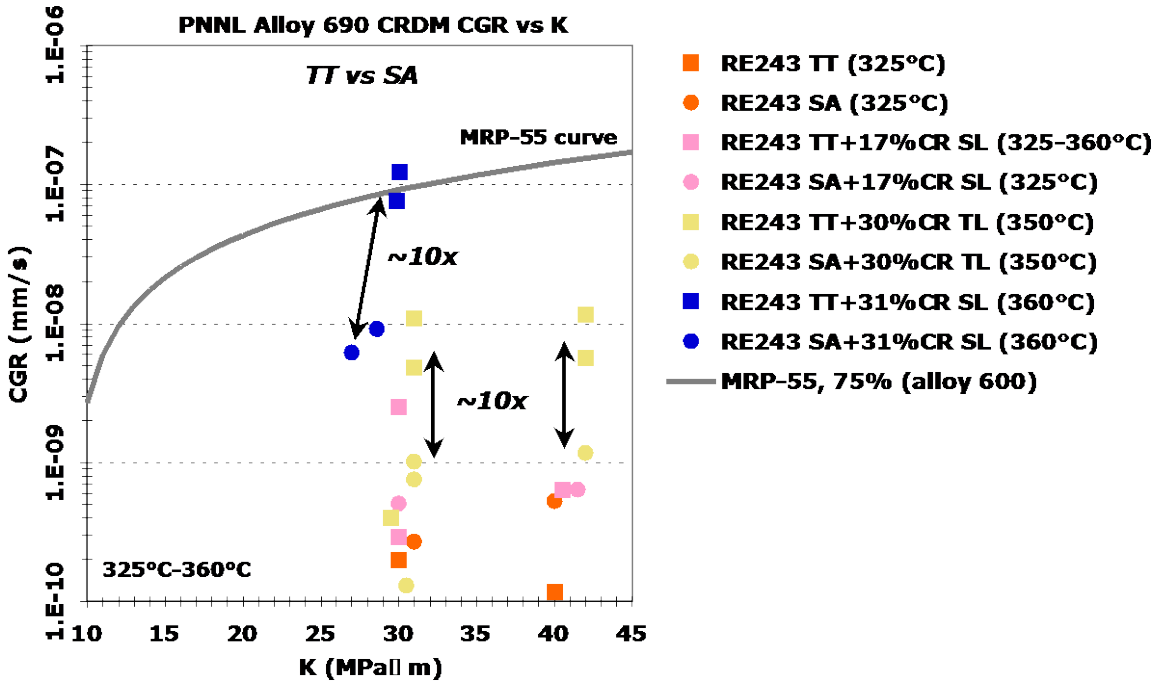

Figure 4.13. Crack growth rate of the thermally treated and solution annealed materials plotted as a function of stress intensity [54].
Reprinted with permission of The Minerals, Metals & Materials Society.

In order to provide insights on the influence of the rolling-induced permanent damage (grain boundary containing cracked carbides and voids) on IGSCC propagation, several high-resolution characterizations [53] have been performed on areas adjacent to cracks and crack tips produced in crack-growth test specimens. Several preliminary conclusions were made from the observations that are worth mentioning because of their implications on the mechanisms controlling SCC susceptibility in cold-worked Alloy 690 in PWR primary water environment. Scanning electron microscopy (SEM) observations indicated that the preexisting cracked carbides and voids at grain boundary did not accelerate environment-induced crack growth. The SCC path consistently follows the grain boundaries and did not "jump" between perpendicular cracks across carbides or between voids at carbide interfaces. The most significant observed interaction with the preexisting permanent damage is that many IGSCC cracks end at the cracked carbides. These crack-tip locations are often open and blunted as the SCC crack terminates at the crack across the carbide that is oriented perpendicular to the grain boundary propagation path. IG carbides clearly enhance localized grain boundary deformation during CR and produce permanent damage. Based on these limited observations and on the significant effect of the recovery anneal on the SCC crack growth response for the 31% cold-rolled Alloy 690TT material, it was suggested that localized grain boundary strains and stresses promote IGSCC susceptibility and not the cracked carbides and voids [53].

In addition to the crack examinations in the SEM, more detailed crack-tip characterizations were also performed on these same materials using TEM techniques [13, 53]. In general, the main observations were the presence of:

- loose crystallites of Ni/Fe-rich spinel in open cracks,
- fine polycrystalline Ni/Cr/Fe spinel and/or MO-structure oxide (not Cr rich) on the crack surfaces,

- penetrative oxidized filaments into the Alloy 690 matrix off crack surfaces, and
- very narrow (<10 nm) crack tips with oxide present.

No evidence for preferential grain boundary oxidation or enhanced void formation was found in regions beyond the open crack tips. Key differences for the Alloy 690 were identified versus prior examinations on Alloy 600 crack tips produced in PWR primary water [59–61] and on stainless steel tips produced in BWR or PWR environments [61–63]. No evidence for penetrative IG oxidation in the Alloy 690 samples has been found, while it is one of the defining crack-tip characteristics for Alloy 600. Grain boundaries do not appear to be an active path for oxidation in the 30% Cr Alloy 690 as they are in the 16% Cr Alloy 600 when exposed to PWR primary water environment. Surprisingly, penetrative oxidation was detected off the crack surfaces and into the matrix grains. Results indicate that the primary mechanism promoting IGSCC in PWR primary water for Alloy 690 is not a stress-assisted, grain boundary oxidation process as proposed for Alloy 600. Alloy 690 SCC cracks were open to their tips (similar to stainless steels) in both oxygenated and hydrogenated water, but a thin, protective, Cr-rich film is not found on the crack surfaces to the crack tips for Alloy 690. Therefore, preliminary observations are different from stainless steels that form Cr-rich spinel films to the tips consistent with a slip oxidation mechanism for SCC propagation. This brief description of the initial crack-tip characterizations illustrates the need for more detailed examinations on tailored materials to define important grain boundary microstructural/microchemical aspects and processes controlling IGSCC.

Even though SCC service failures have not been detected in Alloy 690 components, proactive confirmatory research is needed to understand underlying causes of IGSCC being seen in laboratory tests and to ensure the presence of adequate technical data supporting cracking resistance for long-term reactor operation. Additional materials testing and characterizations may permit parametric limits to be established for SCC susceptibility in PWR primary water environment and to determine material modifications that could ensure adequate performance.

Stress corrosion of Alloy 152/52/52M weld metals in PWR primary water

In nearly all cases, as-welded Alloy 152, 52, and 52M materials have exhibited excellent SCC resistance and low crack-growth rates in laboratory tests. Most crack-growth data have been generated at either General Electric [49, 55, 57, 64] or Pacific Northwest National Laboratory [65, 66]. Results for many different weld metals and more than 15 welds demonstrate that IGSCC occurs, but IG engagement is limited, resulting in propagation rates less than 5×10^{-9} mm/s (2×10^{-10} in./s). An example illustrating the range in observed SCC response is given in Figure 4.14 for two Alloy 52M welds. The Alloy 52M V-groove weld exhibits a constant K crack growth rate of 4×10^{-9} mm/s (1.6×10^{-10} in./s), while the Alloy 52M narrow groove weld shows very little crack growth with a rate of ~8×10^{-10} mm/s (3×10^{-11} in./s) Significant IG areas were observed ahead of and along the crack front of the V-groove specimen, providing confirmation for the higher measured SCC propagation rate. Several other weld metal specimens have shown slightly higher rates when switching from cycle + hold transitioning, but in these cases the measured rate decreases with time at constant K, reaching much lower stable values. Figure 4.15 summarizes the reported SCC measurements from various laboratories on Alloy 152 and 52 type welds and illustrates crack growth rates below 5×10^{-9} mm/s (2×10^{-10} in./s) for all but one Alloy 152 weld [45, 61] and an Alloy 52M overlay at a high K value [66]. The 1×10^{-8} mm/s (4×10^{-10} in./s) propagation rate measured in the Alloy 52M overlay was found to occur in a lower Cr (~24 wt %) weld layer, and rates measured in the Alloy 52M overlay layers with the proper 30 wt % Cr were ~3×10^{-9} mm/s (1×10^{-10} in./s). The one exception that has not been explained is the comparatively high constant load crack growth rates [up to ~6×10^{-8} mm/s (2.4×10^{-9} in./s)]

reported by Argonne National Laboratory on an Alloy 152 weld [51, 67]. Three specimens have now been tested and are reported to give consistent crack growth results and a high degree of IG engagement, suggesting that this weld is more susceptible to IGSCC.

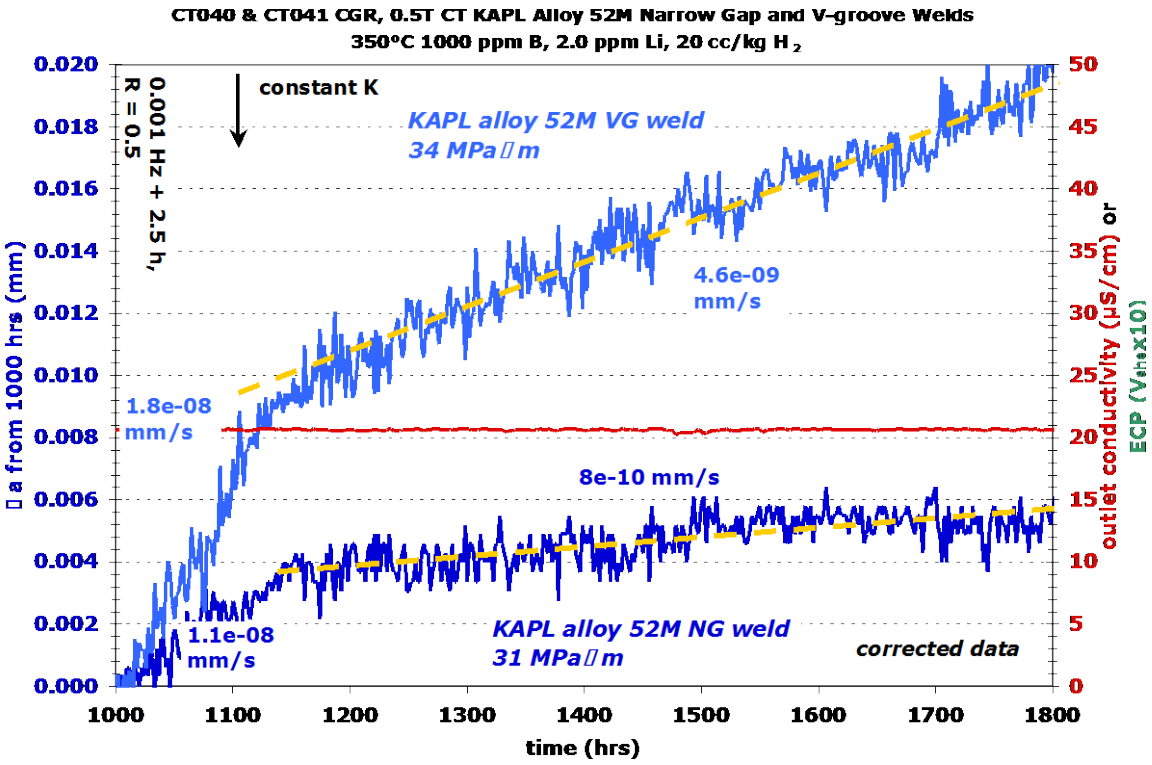

Figure 4.14. Measurements of constant K crack growth for two Alloy 52M welds showing low to very low propagation rates [64].

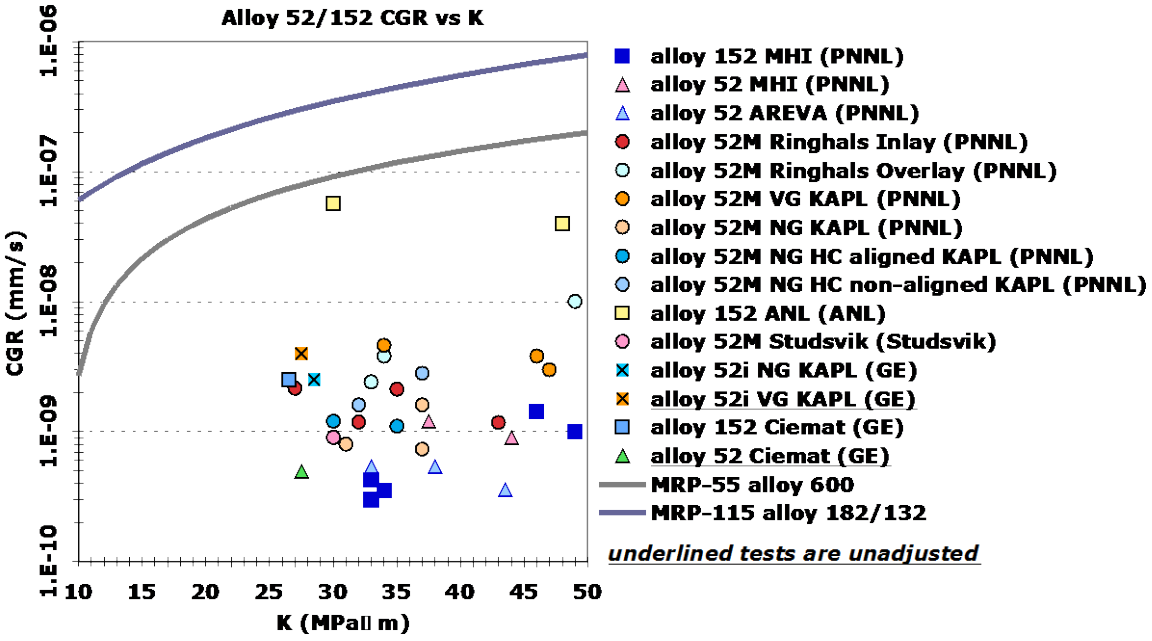

Figure 4.15. Summary of reported SCC propagation rates at constant K or constant load on alloy 152 and 52 type welds [64].

All but one of the welds were tested in the as-welded condition. One alloy 152 weld was evaluated at Pacific Northwest National Laboratory [65], both in the as-welded condition and after a low alloy steel stress relief annealing treatment. No influence on the SCC response was observed. Recently, General Electric also cold-forged an Alloy 152 weld in an attempt to simulate a high-strain condition. As might be expected from the results on cold-worked Alloy 690, preliminary results have indicated higher SCC growth rates. A key concern is the potential damage created during weld repairs, and this represents an essential need to be evaluated and characterized along with more diverse welds (e.g., heats, weld types, weld parameters, constraint) representing industry practice. It is also worthwhile to identify the potential effects of preexisting weld defects and cracks on subsequent SCC susceptibility. These flaws could create or enhance the opportunity for easier SCC initiation and growth due to the local microstructure and microchemistry plus its effect on the effective crack tip K level if the flaw is relatively deep. A few attempts have been made to evaluate the influence of weld cracks on SCC initiation [35–37] and propagation [66] with no indication of increased susceptibility. Although these limited studies have provided some initial information, additional experimentation is needed on well-controlled and characterized materials to properly assess the effects of weld defects on SCC response in PWR primary water environment.

4.3.5 Stress Corrosion of Weld Heat Affected and Dilution Zones in PWR Primary Water

The primary justification for the examination of cold-work effects on Alloy 690 microstructure evolution and SCC behavior is that weld shrinkage induces tensile plastic strain in the HAZ. As a result, crack growth along the HAZ is best represented by the S-L orientation with the plane of deformation that exhibits the highest SCC propagation rates. A few estimates of Alloy 690 HAZ plastic strain have been made based on EBSD measurements of misorientation [18, 46, 68]. These suggest that strains are somewhat lower than seen for stainless steel welds (less than ~15%) and are localized near the fusion line. As mentioned earlier, slightly higher strains have been identified in the partially melted zone.

A limited number of tests have been conducted to assess Alloy 690 HAZ SCC growth rates using compact tension (CT) specimens aligned with the weld fusion line and the HAZ. The best procedure seems to be carefully polish and etch the side surfaces of the CT specimen blank and to then to machine the notch and side grooves. Unfortunately, the weld fusion line typically meanders with depth through the specimen thickness, and the initial precrack during aggressive cycling can drive the crack outside the HAZ. These issues present challenges to a successful test in welds produced, particularly when the HAZ is not highly susceptible to SCC. In most cases, companion baseline tests have not been performed on the Alloy 690 base metal for a direct comparison to the HAZ results. Perhaps not surprisingly, crack-growth tests on Alloy 690 HAZs have not produced conclusive results. The limited data reveals low rates ($1–5 \times 10^{-9}$ mm/s ($0.4–2 \times 10^{-10}$ in./s) similar to that reported for base metal specimens, although isolated measurements [69, 70] have approached ~1×10^{-8} mm/s (4×10^{-10} in./s). The implications of these slightly higher rates are uncertain, especially considering the statistics in sampling, minor variations in test variables and the sparse data. It appears that additional testing and evaluation would better establish SCC behavior in the HAZ and adjacent areas of the weld fusion line. Integrated research is required that combines continued tests on representative mockup heats, tailored thermo-mechanical treatments to produce microstructures consistent with the HAZ, partially melted zone and the unmixed zone, and detailed characterizations of SCC interactions with these fusion line microstructures.

Dissimilar metal welds present an even more complicated fusion zone region, where unique microstructures and microchemistries are created between the alloy 152/52/52M weld metal and either low alloy steel or stainless steel. This reaction zone between the Ni-30%Cr alloy and the Fe-based steels produces significant dilution zone of complex composition along with the potential for new phase formation. Detailed characterizations and SCC evaluations of these dissimilar metal weld regions have not been reported. They represent another unknown for the long-term SCC resistance in PWR service, and research is needed to understand the characteristics of growing crack in the fusion zone region.

4.3.6 Corrosion Fatigue in PWR Primary Water

Just as SCC evaluations on Alloy 690 were concluded to be limited in the previous sections, it appears that focused corrosion fatigue testing has not been conducted on wide variety of materials and material conditions. Hickling [26], who reviewed several testing programs [71–74], concluded that sufficient data had been generated on prototypic reactor materials. Thick-walled Alloy 690 showed a reduction in fatigue life and an increase in cyclic crack-growth rates when tested in a simulated PWR primary water environment. However, this behavior was about the same as or somewhat better than that of other Ni-base alloys, such Alloy 600. All of these test results were obtained from Alloy 690, which is highly resistant to SCC. The limited testing that has been done on cold-worked materials as part of SCC crack-growth tests reveals accelerated cyclic crack growth, particularly under gentle cycling conditions. Of particular interest is the assessment of environmental enhancement (based on the comparison of crack-growth rates measured in PWR primary water versus estimated growth rates in air) routinely performed at Argonne National Laboratory [75, 76]. Results on as-received CRDM Alloy 690 materials showed little or no environmental enhancement, while significant enhancement, consistent with high SCC propagation rates, was observed in highly cold-rolled plate. Similar enhancements of cyclic crack growth rates have been seen at other laboratories during SCC tests on highly cold-worked Alloy 690 materials. Those materials that exhibit high SCC propagation rates also often show higher cyclic rates. Therefore, a similar issue exists for corrosion fatigue as discussed at some length in the previous section for SCC in PWR primary water.

4.4 CORROSION AND STRESS CORROSION CRACKING OF ALLOY 690 IN SECONDARY WATER

Research directed at providing information on the corrosion and SCC resistance of Alloy 690 in both nominal and faulted PWR secondary water chemistry has been significant due to the early use of Alloy 690 as steam generator tubing [28]. The water chemistry on the PWR secondary side is quite different from that on the primary side, including the chemical composition (with the absence of Li, B, and H_2 additions, and the presence of volatile alkalizing agents and possible impurities) and a higher, less-stable electrochemical potential. Gorman [77] has reviewed the international experience as of 2003 and examined probable causes for corrosion and cracking. The focus was on the degradation observed for mill-annealed Alloy 600 tubing, with some discussion addressing replacement tubing materials Alloy 600TT and Alloy 690TT. No known examples of degradation have been reported for Alloy 690TT, and, in general, laboratory tests have shown it to be highly resistant to corrosion and SCC in normal and most faulted secondary-side environments.

The most significant issue observed for Alloy 690TT has been the SCC in Pb-contaminated secondary water environments. Results show that the high-chromium Alloy 690 is susceptible to degradation in Pb-doped environments. Corrosion and transgranular SCC of Alloy 690TT

materials has been seen in the laboratory [78–86] for tests in neutral, acidic, caustic, and AVT (all-volatile-treated) water doped with Pb. Alloy 690 is most prone to PbSCC in high pH conditions (>9 at 330C), where it is more susceptible to cracking than Alloy 600.

It is important to note that even though the laboratory test results suggest SCC susceptibility, no secondary-side steam generator tube failures have been reported for Alloy 690TT, due to this cause. Considering the high number of corrosion and SCC failures in Alloy 600 tubing directly linked to Pb [78, 87, 88], service experience indicates that Alloy 690TT tubing has a significantly improved resistance to degradation. However, a recent review by Staehle [89] makes the case that Alloy 690TT tubing is likely to show secondary-side PbSCC during extended service. Pb greatly concentrates on surfaces of tubing in the superheated crevices either in drilled holes or in line contact geometries. High Pb concentrations (up to ~10%) have been observed even though trace Pb levels (parts per trillion) are present in the feedwater. These high surface Pb levels are expected in crevice regions of replacement Alloy 690 steam generators along with alkaline chemistries, creating conditions where severe PbSCC has been observed in laboratory tests. Staehle [89] also points out that Alloy 690 is prone to scale formation in the presence of Pb contamination, and local scale growth may accelerate SCC propagation.

Another secondary-side impurity of concern is the sulfur species on outer-diameter SCC of steam generator tubing [90, 91]. Alloy 690TT has been included in selected general corrosion and static SCC tests performed in complex sulfur-containing environments without any significant degradation reported. Limited evaluations of SCC propagation rates have also been performed [92, 93] in severely faulted secondary water (both highly acidic and highly alkaline), and again, no cracking was discovered for Alloy 690TT. More discerning crack-growth testing has not been conducted in secondary-side environments as has been done for primary-side environments. As a result, it seems likely that higher SCC susceptibility for cold-worked Alloy 690 would also be observed in AVT water and faulted secondary-side environments under similar test conditions. The most important impurity concern is Pb, and additional testing is needed to ensure long-term degradation resistance in service. If the opportunity occurs, it would be very useful to perform detailed examinations of corrosion and surface films in pulled tubes. Critical evaluations of secondary-side water chemistry on SCC behavior of Alloy 690TT using crack-growth testing techniques are also recommended, even though the PWR application is for thin-walled tubing. The direct measurement of corrosion products in secondary-side crevices will identify local impurity environments in the modern Alloy 690 steam generators and help specify conditions for laboratory tests to confirm long-term corrosion and SCC resistance.

Although not directly relevant to the PWR secondary-side environments, selected tests have been performed on Alloy 152 and 52 welds in oxidizing BWR water with impurities [94]. Crack-growth tests were performed at moderate-to-high K levels and very aggressive water chemistry conditions (2 ppm O_2 and 50 ppb SO_4 or Cl). In all cases, growth rates were low and the difference between 360 °C (680 °F) PWR primary water and BWR water at 288 °C (550 °F) was small. In any event, the BWR tests strongly support the excellent SCC resistance of the high-Cr weld metals in high-temperature water.

4.5 ENVIRONMENT-INDUCED FRACTURE AT LOW TEMPERATURES

Another potential issue of concern is a reduction in the fracture resistance of Alloy 690 and its weld metals during long-term exposure and dynamic straining in reactor water environments. This issue was first revealed by research of Mills [95–97] who observed large reductions in

fracture resistance in nickel-base alloys when tests were performed in low temperature water. Other researchers [98–101] have now confirmed this response in Alloy 690 and in alloy 152 and 52 weld metals. The phenomenon is often referred to as low-temperature crack propagation (LTCP), and it is not yet clear whether it represents a genuine reduction in fracture properties of the material or a form of rapid subcritical crack growth due to the environment. Both aspects may be involved. A typical feature of LTCP is the transition from ductile dimple fracture to brittle IG cracking; the alloy microstructure and probably grain boundary microchemistry have a crucial effect on susceptibility to SCC. The controlling mechanism of this "embrittlement" is clearly a form of hydrogen cracking with hydrogen ingress during prior exposure in high-temperature water and crack-tip corrosion during straining at lower temperature. Some data exist to characterize elements of the problem, but the detailed understanding to predict effects of material and environmental variables is lacking. It represents another area where additional research is needed, not only on the LTCP mechanisms, but also on interrelationships between IGSCC at high temperatures and IG crack extension at low temperatures during outages.

4.6 SUMMARY

Relevant properties and characteristics have been reviewed for Alloy 690 and its weld metals (Alloys 152, 52, and 52M) in relation to potential degradation issues for long-term LWR service. Alloy 690 and its associated weld metals have been effective replacement materials for Alloys 600, 182, and 82 in PWRs with no significant degradation identified (except tied to manufacturing or operation problems). Potential degradation modes of concern were evaluated, focusing on environment-assisted cracking, because SCC susceptibility has been identified in laboratory tests. For the most part, vulnerabilities have only been discovered during testing using off-normal material conditions (e.g., highly cold-worked Alloy 690) or in severe environments (e.g., Pb-containing secondary water). While these observations indicate the need for additional research to understand mechanisms promoting SCC and to establish limiting material–environmental conditions for susceptibility, excellent resistance has been documented for tests under representative service conditions. Recommended proactive research should include detailed evaluations of primary water SCC of cold-worked Alloy 690, as-welded alloy 152/52/52M, Alloy 690 HAZ (including the partially melted and unmixed zones), and dilution zone regions in dissimilar metal welds. Comprehensive characterizations are recommended in combination with SCC testing on multiple heats and welding conditions. Corrosion fatigue of Alloy 690 and its weld metals was not discussed in detail, but it presents many of the same questions as for SCC, and material effects on susceptibility are expected to be similar. While laboratory tests in PWR primary water only reveal SCC susceptibility under certain more-aggressive material conditions, Pb-containing secondary-side environments have been shown to produce extensive cracking of as-received Alloy 690. Steam generator experience with Alloy 690TT tubing has not yet identified this problem (as was found for Alloy 600 tubing); however, it represents a potential long-term vulnerability. Additional research is recommended, including secondary-side examinations of Alloy 690TT tubes removed from service. Several other material (e.g., weld cracking) and service degradation (e.g., LTCP) issues were also briefly discussed to identify aspects of the current understanding as well as interrelationships to other long-term degradation concerns.

The key concerns for Alloy 690 and its weld metals during extended PWR service to greater than 60 years discussed above are summarized here.

- Secondary-side SCC of Alloy 690TT steam generator tubing associated with Pb concentration particularly at line contact crevices. This issue may be observed much sooner

than 60 years, but has the potential to develop into a significant and widespread degradation mode during long-term operation.

- SCC of Alloy 690TT vessel penetrations and steam generator tubing in PWR primary water environments due to cold/warm work or mechanical damage. Deformation-induced high strength regions can exhibit significant SCC susceptibility with important heat-to-heat and microstructural effects. Even though such high strain regions do not appear to be likely in typical weld HAZs, the potential concern remains for off-normal microstructures including those created by compositional banding.

- SCC of alloy 152/52 welds and overlays particularly in high-strength regions created during welding and repair welding. Detailed understanding of strain and microstructural variability in service welds/overlays is limited, and direct assessment of effects on SCC susceptibility is needed.

- Weld defects, ductility dip, and hot cracking for alloy 152/52 weld metals and dissimilar metal dilution zones. A significant variability is expected for plant welds, and detailed characterizations are lacking. Evaluations of weld defect effects on SCC initiation and growth are needed.

- SCC of dissimilar metal welds of alloy 152/52 and LAS/SS, which represent an important issue for dilution zones (Cr depletion and Fe enrichment) and interface regions. Detailed understanding of strain and microstructural variability in limited and direct assessment of effects on SCC susceptibility is needed.

- Long-range ordering and Ni_2Cr precipitation. Although this does not appear to be an issue for service temperatures over 40 years, matrix strength increase, particularly for SCC susceptibility of Alloy 690 and weld metals, may be a potential long-term issue.

- While not discussed explicitly above, wear of steam generator tubing is a known operational issue and is typically a result of design issues rather than specific material conditions. However, if conditions for wear develop, this material will be susceptible to this form of degradation, although this is not unique to extended operating periods.

4.7 REFERENCES*

1. *INCONEL Alloy 690,* Publication SMC-079, Special Metals Corporation, 2002.
2. *Guidelines for PWR Steam Generator Tubing Specification and Repair," Vol. 2, Rev. 1: Guidelines for Procurement of Alloy 690 Steam Generator Tubing,* EPRI TR-016743-V2R1, Electric Power Research Institute, 1999.
3. A. McIlree and G. Ilevbare, *Materials Reliability Program: Guidelines for Thermally Treated Alloy 690 Pressure Vessel Nozzles (MRP-241),* 1015007, Electric Power Research Institute, 2008.

* Inclusion of references in this report does not necessarily constitute NRC approval or agreement with the referenced information.

4. ASME SB-167, “Specification for Nickel-Chromium-Iron Alloys (UNS N06600, N06601, N00690, N06025, and N06045) Seamless Pipe and Tube,” *ASME Boiler & Pressure Vessel Code,* Section II Material Specifications, Part B, 2001.

5. J. M. Sarver, J. R. Crum, and W. L. Mankins, “Carbide Precipitation and the Effect of Thermal Treatments on the SCC Behavior of Inconel Alloy 690,” p. 581 in *Proc. 3rd Int. Symp. Environmental Degradation of Materials in Nuclear Power Systems—Water Reactors,* Traverse City, Aug. 30–Sept. 3, 1987, G. J. Theus and J. Weeks (eds.), The Metallurgical Society, 1987.

6. T. Yonezawa et al., “Effect of Heat Treatment on Corrosion Resistance of Alloy 690,” p. 593 in *Proc. 2nd Int. Symp. Environmental Degradation of Materials in Nuclear Power Systems—Water Reactors,* Monterey, Sept. 9–12, 1985, J. Roberts and J. Weeks (eds.), American Nuclear Society, 1986.

7. K. Norring, K. Stiller, and J. Nilsson, “Grain Boundary Microstructure, Chemistry, and IGSCC in Alloy 600 and Alloy 690,” *Proc. 5th Int. Symp. Environmental Degradation of Materials in Nuclear Power Systems—Water Reactors,* Monterey, Aug. 25–29, 1991, D. Cubicciotti and E. Simonen (eds.), American Nuclear Society, 1992.

8. K. Stiller, J. Nilsson, and K. Norring, “Structure, Chemistry and Stress Corrosion Cracking of Grain Boundaries in Alloys 600 and 690,” *Metallurgical and Materials Transactions A* **27A**(2) (1996).

9. T. M. Angeliu and G. S. Was “Behavior of Grain Boundary Chemistry and Precipitates upon Thermal Treatment of Controlled Purity Alloy 690,” *Metallurgical Transactions A* **21,** 2097 (1990).

10. J. J. Kai, G. P. Yu, C. H. Tsai, M. N. Liu, and S. C. Yao, “The Effects of Heat Treatment on the Chromium Depletion, Precipitate Evolution and Corrosion Resistance of Inconel Alloy 690,” *Metallurgical Transactions A* **20A,** 2057 (1989).

11. R. S. Dutta, R. Tewari, and P. K. De, “Effects of heat-treatment on the extent of chromium depletion and caustic corrosion resistance of Alloy 690,” *Corrosion Science* **49,** 303 (2007).

12. S. M. Bruemmer and M. B. Toloczko, *Pacific Northwest National Laboratory Investigation of Stress Corrosion Cracking in Nickel-Base Alloys,* NUREG-CR-7103 Volume 2, U.S. Nuclear Regulatory Commission, January 2012.

13. S. M. Bruemmer, M. Olszta, L. E. Thomas, and M. B. Toloczko, “Linking Grain Boundary Microstructure to Stress Corrosion Cracking of Cold Rolled Alloy 690 in PWR Primary Water,” *Corrosion 2012,* National Association of Corrosion Engineers, 2012.

14. M. Morra, J. Grande, M. Othon, and E. Willis, “Quantification of Grain Size and Banding in Differently Thermo-Mechanical-Processed Heats of Alloy 690 Using Image Analysis,” *MRP Alloy 690/152/52 Research Collaboration Meeting,* Electric Power Research Institute, December 2010.

15. S. M. Bruemmer, M. J. Olszta, and M. B. Toloczko, “Cold Rolling Effects on Grain Boundary Damage and Stress Corrosion Crack Growth in Alloy 690,” Paper A062-T04, *Proc. Fontevraud 7 Int. Symp.: Contribution of Materials Investigation to Improve the Safety and Performance of LWRs,* Société Française d'Energie Nucléaire, Avignon, Sep. 26–30, 2010.

16. S. M. Bruemmer, M. J. Olszta, M. B. Toloczko, and L. E. Thomas, “High Resolution Characterization of Grain Boundary Damage and Stress Corrosion Cracks in Cold-Rolled Alloy 690,” p. 301 in *Proc. 15th Int. Conf. Environmental Degradation of Materials in*

Nuclear Power Systems—Water Reactors, Colorado Springs, Aug. 7–11, 2011, J. Busby and G. Ilevbare (eds.), The Minerals, Metals & Materials Society, 2012.

17. G. Theus et al., *Materials Reliability Program: Material Production and Component Fabrication and Installation Practices for Alloy 690 Replacement Components in Pressurized Water Reactor Plants (MRP-245),* 1016608, Electric Power Research Institute, 2008.
18. M. Morra, M. Othon, D. Wark, P. Chou, and E. Willis, "Characterization of Alloy 690 to 52-Type Welds, Weld Interfaces and Base Metal Interfaces," NRC–Industry 2011 Meeting on Alloy 690 Research, June 2011.
19. E. M. Lehockey, Y-P. Lin, and O. E. Lepik, "Mapping Residual Plastic Strain in Materials Using Electron Backscatter Diffraction," p. 247 in *Electron Backscatter Diffraction in Materials Science,* Schwartz et al. (eds.), Springer, 2000.
20. M. Morra, M. Othon, and D. Wark, "Macro and Microstructural Mapping and Residual Plastic Strains Analysis of Alloy 690 Base Metals and HAZ of Weldments," MRP Alloy 690/152/52 Research Collaboration Meeting, December 2010.
21. K. Smith, A. Klein, P. Saint-Paul, J. Blanchet, "Inconel 690, A Material with Improved Corrosion Resistance for PWR Steam Generator Tubes," p. 319 in *Proc. 2nd Int. Symp. Environmental Degradation of Materials in Nuclear Power Systems—Water Reactors,* Monterey, Sept. 9–12, 1985, J. Roberts and J. Weeks (eds.), American Nuclear Society, 1986.
22. A. Marucco, "Atomic Ordering in the Ni-Cr-Fe System," *Materials Science and Engineering* **A189,** 267 (1994).
23. T. Larsson, J. O. Nilsson, and J. Frodigh, "On the Possibility of Forming Ordered Ni2Cr in Alloy 690," p. 143 in *Proc. 9th Int. Symp. Environmental Degradation of Materials in Nuclear Power Systems—Water Reactors*, Newport Beach, Aug. 1–5, 1999, S. Bruemmer, F. P. Ford and G. Was (eds.), The Minerals, Metals & Materials Society, 1999.
24. F. Delabrouille et al., "Long range ordering in Ni Alloys containing 30% Cr," p. 888 in *Proc. 14th Int. Symp. Environmental Degradation of Materials in Nuclear Power Systems*, Virginia Beach, Aug. 23–27, 2009, T. Allen and J. Busby (eds.), American Nuclear Society, 2010.
25. H. Xu S. Fyfitch, P. Scott, M. Foucault, R. Killian, and M. Winters, *Materials Reliability Program, Resistance to Primary Water Stress Corrosion Cracking of Alloys 690, 52, and 152 in Pressurized Water Reactors (MRP-111),* 1009801, Electric Power Research Institute, 2004.
26. J. Hickling, *Materials Reliability Program, Resistance to Primary Water Stress Corrosion Cracking of Alloys 690 in Pressurized Water Reactors (MRP-258),* 1019086, Electric Power Research Institute, 2009.
27. S. D. Kiser, E. B. Hinshaw, J. R. Crum, and L. E. Shoemaker, "Nickel Alloy Welding Requirements for Nuclear Service," p. 21 in *Focus on Nuclear Power Generation* 2005, Special Metals Corporation.
28. Special Metals Corporation, *Product Datasheets for Inconel Alloy 152, 52 and 52M Weld Metals*, www.specialmetals.com/products.
29. S. M. Bruemmer, M .B. Toloczko, M. J. Olszta, R. J. Seffens, and P. G. Efsing, "Characterization of Defects in Alloy 152, 52 and 52M Welds," p. 319 in *Proc. 14th Int.*

Symp. Environmental Degradation of Materials in Nuclear Power Systems, Virginia Beach, Aug. 23–27, 2009, T. Allen and J. Busby (eds.), American Nuclear Society, 2010.

30. B. Hood and W. Lin, "Weldability Testing of Inconel Filler Materials," p. 69 in *Proc. 7th Int. Symp. Environmental Degradation of Materials in Nuclear Power Systems—Water Reactors,* Breckenridge, Aug. 7–12, 1995, R. Gold and A. McIlree (eds.), National Association of Corrosion Engineers, 1995.
31. W. Wu and C. Tsai, "Hot Cracking Susceptibility of Fillers 52 and 82 in Alloy 690," *Metall. Trans.* **30A,** 417 (1999).
32. M. Collins and J. Lippold, "An Investigation of Ductility Dip Cracking in Nickel-Based Filler Materials—Part I," *Welding Journal* **82**(10), 288s (2003).
33. M. Collins, A. Ramirez, and J. Lippold, "An Investigation of Ductility Dip Cracking in Nickel-Based Filler Materials—Part II," *Welding Journal* **82**(12), 348s (2003).
34. M. Collins, A. Ramirez, and J. Lippold, "An Investigation of Ductility Dip Cracking in Nickel-Based Filler Materials—"Part III," *Welding Journal* **83**(2), 39s (2004).
35. H. Hanninen, A. Toivonen, A. Brederholm, T. Saukkonen, U.Ehrnsten, and P. Aaltonen, "Environment-Assisted Cracking and Hot Cracking of Ni-Base Alloy Dissimilar Metal Welds," Paper 17, *Proc. 13th Int. Conf. Environmental Degradation of Materials in Nuclear Power Systems*, Whistler, Aug. 19–23, 2007, P. King and T. Allen (eds.), The Canadian Nuclear Society, 2008.
36. H. Hanninen, A. Toivonen, A. Brederholm, T. Saukkonen, U. Ehrnsten, and P. Aaltonen, "EAC Crack Initiation in Nickel-Based Dissimilar Metal Welds Using Doped Steam Test," p. 333 in *Proc. 14th Int. Symp. Environmental Degradation of Materials in Nuclear Power Systems*, Virginia Beach, Aug. 23–27, 2009, T. Allen and J. Busby (eds.), American Nuclear Society, 2010.
37. H. Hanninen, A. Toivonen, A. Brederholm, T. Saukkonen, W. Karlsen, U.Ehrnsten, and P. Aaltonen, "Effects of Hot Cracks on EAC Crack Initiation and Growth in Nickel-Base Alloy Weld Metals," p. 197 in *Proc. 15th Int. Conf. Environmental Degradation of Materials in Nuclear Power Systems—Water Reactors,* Colorado Springs, Aug. 7–11, 2011, J. Busby and G. Ilevbare (eds.), The Minerals, Metals and Materials Society, 2012.
38. G. A. Young, T. E. Capabianco, M. A. Penik, B. W. Morris, and J. J. McGee, "Mechanism of Ductility Dip Cracking in Nickel-Chromium Alloys," *Welding Journal* **87**(2), 31s (2008).
39. P. Combrade, P. M. Scott, M. Foucault, E. Andieu, and P. Marcus, "Oxidation of Ni Base Alloys in PWR Water: Oxide layers and Associated Damage to the Base Metal," p. 883 in *Proc. 12th Int. Conf. Environmental Degradation of Materials in Nuclear Power Systems—Water Reactors,* Salt Lake City, Aug. 14–18, 2005, L. Nelson, P. King and T. R. Allen (eds.), The Minerals, Metals and Materials Society, 2007.
40. M. Sennour, L. Marchetti, F. Martin, S. Perrin, R. Molins, and M. Pijolat, "A detailed TEM and SEM study of Ni-base alloys oxide scales formed in primary conditions of pressurized water reactors," *Journal of Nuclear Materials* **402,** 147 (2010).
41. J. B. Ferguson and H. F. Lopez, "Oxidation Products of Alloy 600 and 690 in PWR Environments and Their Role in Intergranular Stress Corrosion Cracking." *Metallurgical Transactions* **37A,** 2471 (2006).
42. M. J. Olszta, D. K. Schreiber, L. E. Thomas, and S. M. Bruemmer, "Penetrative Internal Oxidation from Alloy 690 Surfaces and Stress Corrosion Crack Walls during Exposure to PWR Primary Water," p. 331 in *Proc. 15th Int. Conf. Environmental Degradation of*

Materials in Nuclear Power Systems—Water Reactors, Colorado Springs, Aug. 7–11, 2011, J. Busby and G. Ilevbare (eds.), The Minerals, Metals and Materials Society, 2012.

43. S. Asada et al., "PWSCC Life Time Evaluation on Alloy 690, 52 and 152 for PWR Materials," *PWSCC of Alloy 600 Int. Conf. & Exhibition,* Atlanta, Electric Power Research Institute, June 2007.

44. P. L. Andresen, M. Morra and K. Ahluwalia, "SCC of Alloy 690 and Its Weld Metals," *Int. Boiling Water Reactor and Pressurized Water Reactor Materials Reliability Conference,* July 2012.

45. M. B. Toloczko, M. Olszta and S.M. Bruemmer, "Stress Corrosion Crack Initiation Testing on Nickel-Base Alloys in PWR Primary Water," International Cooperative Group on Envirnment-Assisted Cracking, Quebec City, Canada, May 2012.

46. P. L. Andresen, *Development of Advanced Testing Techniques to Quantify the Improved PWSCC Resistance of Alloy 690 and its Weld Metals (MRP-123),* Technical Report 1010269, Electric Power Research Institute, 2004.

47. D. J. Paraventi and W. C. Moshier, "Alloy 690 SCC Growth Rate Testing," *Workshop on Cold Work in Iron- and Nickel-Base Alloys,* Electric Power Research Institute, June 2007.

48. D. J. Paraventi and W. C. Moshier, "Alloy 690 SCC Growth Rate Testing," *Proc. EPRI Alloy 690 Workshop,* Atlanta, October 2007, Electric Power Research Institute.

49. P. L. Andresen, M. M. Morra, J. Hickling, A. Ahluwalia, and J. Wilson, "PWSCC of Alloys 690, 52 and 152," Paper 97 in *Proc. 13th Int. Conf. Environmental Degradation of Materials in Nuclear Power Systems*, Whistler, Aug. 19–23, 2007, P. King and T. Allen (eds.), The Canadian Nuclear Society, 2008.

50. P. L. Andresen, M. M. Morra, J. Hickling, K. Ahluwalia, and J. A. Wilson, "Effect of Deformation and Orientation on SCC of Alloy 690," p. 846 in *Proc. 14th Int. Symp. Environmental Degradation of Materials in Nuclear Power Systems*, Virginia Beach, Aug. 23–27, 2009, T. Allen and J. Busby (eds.), American Nuclear Society, 2010.

51. B. Alexandreanu, "The Stress Corrosion Cracking Behavior of Alloys 690 and 152 Weld in a PWR Environment," p. 239 in *Proc. 14th Int. Symp. Environmental Degradation of Materials in Nuclear Power Systems*, Virginia Beach, Aug. 23–27, 2009, T. Allen and J. Busby (eds.), American Nuclear Society, 2010.

52. M. B. Toloczko and S. M. Bruemmer, "Crack Growth Response of Alloy 690 in Simulated PWR Primary Water," p. 706 in *Proc. 14th Int. Symp. Environmental Degradation of Materials in Nuclear Power Systems*, Virginia Beach, Aug. 23–27, 2009, T. Allen and J. Busby (eds.), American Nuclear Society, 2010.

53. S. Bruemmer, M. Olszta, D. Edwards, and M. Toloczko, "Microstructural Effects on IGSCC of Cold-Rolled Alloy 690," *MRP Alloy 690/152/52 Research Meeting,* Electric Power Research Institute, December 2011.

54. M. B. Toloczko and S. M. Bruemmer, "One Dimensional Cold Rolling Effects on Stress Corrosion Crack Growth in Alloy 690 Tubing and Plate Materials," p. 91 in *Proc. 15th Int. Conf. Environmental Degradation of Materials in Nuclear Power Systems—Water Reactors,* Colorado Springs, Aug. 7–11, 2011, J. Busby and G. Ilevbare (eds.), The Minerals, Metals & Materials Society, 2012.

55. P. L. Andresen, M. M. Morra, and K. Ahluwalia, "SCC of Alloy 690 and Its Weld Metals," p. 161 in *Proc. 15th Int. Conf. Environmental Degradation of Materials in Nuclear Power*

Systems—Water Reactors, Colorado Springs, Aug. 7–11, 2011, J. Busby and G. Ilevbare (eds.), The Minerals, Metals & Materials Society, 2012.

56. D. R. Tice, S. L. Medway, N. Platts, and J. W. Stairmand, “Crack Growth Testing on Cold Worked Alloy 690 in Primary Water Environment,” p. 71 in *Proc. 15th Int. Conf. Environmental Degradation of Materials in Nuclear Power Systems—Water Reactors,* Colorado Springs, Aug. 7–11, 2011, J. Busby and G. Ilevbare (eds.), The Minerals, Metals & Materials Society, 2012.

57. S. M. Bruemmer and M. B. Toloczko, “Update on PNNL SCC Growth Rate Testing on Alloy 690 Materials,” *MRP Alloy 690/152/52 Research Collaboration Meeting,* Electric Power Research Institute, December 2011.

58. P. L. Andresen, M. M. Morra, and K. S. Ahluwalia, “SCC of Alloy 690 and Its Weld Metals,” Paper A010-T04, *Proc. Fontevraud 7 Int. Symp.: Contribution of Materials Investigation to Improve the Safety and Performance of LWRs,* Société Française d'Energie Nucléaire, Avignon, Sept. 26–30, 2010.

59. L. E. Thomas and S. M. Bruemmer, “High-Resolution Characterization of Intergranular Attack and Stress Corrosion Cracking of Alloy 600 in High-Temperature Primary Water," *Corrosion Journal* **56**(7), 572 (2000).

60. S. M. Bruemmer and L. E. Thomas, “Crack-Tip Examinations of Primary-Water Stress Corrosion Cracking in Alloy 600,” p. 603 in *Proc. Fontevraud 6 Int. Symp.: Contributions of Materials Investigations to Improve the Safety and Performance of LWRs,* Société Française d'Energie Nucléaire, Paris, Sept. 18–22, 2006.

61. S. M. Bruemmer and L. E. Thomas, “Insights into Stress Corrosion Mechanisms from High Resolution Measurements of Crack-Tip Structures and Compositions,” Paper 1264-BB01-09, *Proc. 2010 MRS Spring Meeting,* Vol. 1264, Materials Research Society, 2010.

62. S. M. Bruemmer and L. E. Thomas, “High-Resolution Characterizations of Stress-Corrosion Cracks in Austenitic Stainless Steel from Crack Growth Tests in BWR-Simulated Environments,” p. 189 in *Proc. 12th Int. Conf. Environmental Degradation of Materials in Nuclear Power Systems—Water Reactors,* Salt Lake City, Aug. 14–18, 2005, L. Nelson, P. King and T.R. Allen (eds.), The Minerals, Metals & Materials Society, 2007.

63. S. M. Bruemmer and L. E. Thomas, “Comparison of IGSCC Crack-Tip Characteristics in BWR Oxidizing Water and BWR Hydrogen Water Chemistry Conditions,” Paper 144, *Proc. EPRI Alloy 690 Workshop,* Atlanta, October 2007.

64. P. L. Andresen and M. Morra, “SCC Growth Rates of Alloy 152/52/52i Welds,” *MRP Alloy 690/152/52 Research Collaboration Meeting,* Electric Power Research Institute, December 2011.

65. M. B. Toloczko and S. M. Bruemmer, “Crack-Growth Response of Alloy 152 and 52 Weld Metals in Simulated PWR Primary Water,” p. 690 in *Proc. 14th Int. Symp. Environmental Degradation of Materials in Nuclear Power Systems—Water Reactors*, Virginia Beach, Aug. 23–27, 2009, T. Allen and J. Busby (eds.), American Nuclear Society, 2010.

66. M. B. Toloczko, M. Olszta, and S. M. Bruemmer, “Stress Corrosion Crack Growth of Alloy 52M in Simulated PWP Primary Water,” p. 225 in *Proc. 15th Int. Conf. Environmental Degradation of Materials in Nuclear Power Systems—Water Reactors,* Colorado Springs, Aug. 7–11, 2011, J. Busby and G. Ilevbare (eds.),The Minerals, Metals & Materials Society, 2012.

67. B. Alexandreanu, Y. Chen, K. Natesan, and W. Shack, “SCC Behavior of Alloy 152 Weld in PWR Environment,” p. 179 in *Proc. 15th Int. Conf. Environmental Degradation of Materials in Nuclear Power Systems—Water Reactors,* Colorado Springs, Aug. 7–11, 2011, J. Busby and G. Ilevbare (eds.), The Minerals, Metals & Materials Society, 2012.

68. G. Young, M. J. Hackett, J. D. Tucker, and J. M. Pyle, “Ni-Cr Weld Characterization,” *Alloy 690 Experts Meeting,* Electric Power Research Institute, December 2009.

69. P. L. Andresen, M. Morra, and A. Ahluwalia, “SCC Growth Rates of Alloy 690 and HAZ,” *NRC/Industry Alloy 690 Expert Meeting,* U.S. Nuclear Regulatory Commission, June 2011.

70. B. Alexandreanu, Y. Chen, K. Natesan, and W. Shack, “Cyclic and SCC Behavior of Alloy 690 HAZ in PWR Environment,” p. 109 in *Proc. 15th Int. Conf. Environmental Degradation of Materials in Nuclear Power Systems—Water Reactors,* Colorado Springs, Aug. 7–11, 2011, J. Busby and G. Ilevbare (eds.), The Minerals, Metals and Materials Society, 2012.

71. M. Higuchi et al., “Revised and new proposal of environmental fatigue life correction factor for carbon and low alloy steels and nickel base alloys in LWR water environments,” *Proc. ASME Pressure Vessels and Piping Division Conference,* PVP2006-ICPVT-11-93194, 2006.

72. R. Etien et al., “EAC Behavior and Mechanical Properties of Improved Alloy 690 Filler Metals,” *MRP PWSCC Expert Panel Meeting,* Electric Power Research Institute, November 2007.

73. A. Jenssen, K. Norring, and P. Efsing, “Swedish Activities on Alloy 690 and its Weld,” *MRP PWSCC Expert Panel Meeting*, Electric Power Research Institute, November 2008.

74. K. Tsutsumi, “Fatigue Crack Growth Rate Curve for Nickel Based Alloys in PWR Environment,” *Proc. Fontevraud 7 Int. Symp.: Contribution of Materials Investigations to Improve the Safety and Performance of LWRs,* Société Française d'Energie Nucléaire, Avignon, Sept. 26–30, 2010.

75. W. J. Shack and T. F. Kassner, *Review of Environmental Effects on Fatigue Crack Growth of Austenitic Stainless Steels*, NUREG/CR-6176, ANL-94/1, U.S. Nuclear Regulatory Commission, May 1994.

76. B. Alexandreanu, “SCC CGRs of Alloys 690 and 52/152 Welds in PWR Water,” *Alloys 690/52/152 PWSCC Research Test Materials Meeting,* Industry/NRC RES, U.S. Nuclear Regulatory Commission, July 2008.

77. J. A. Gorman, J. E. Harris, R. W. Staehle, and K. Fruzzetti, “Secondary Side Corrosion of 600MA Tubing in PWR Steam Generators—Causes, Implications for Alloys 600TT and 690TT and Need Research,” p. 362 in *Proc. 11th Int. Conf. Environmental Degradation of Materials in Nuclear Power Systems—Water Reactors,* Stevenson, Aug. 10–14, 2003, G. Was and L. Nelson (eds.), American Nuclear Society, 2003.

78. R. W. Staehle, “Clues and Issues in the SCC of High Nickel Alloys with Dissolved Lead,” *MRP Alloy 690/152/52 Research Collaboration Meeting,* EPRI, December 2011, p. 1163; and “Assessment of and Proposal for a Mechanistic Interpretation of the SCC of High Nickel Alloys in Lead-Containing Environments,” p. 381 in *Proc. 14th Int. Symp. Environmental Degradation of Materials in Nuclear Power Systems*, Virginia Beach, Aug. 23–27, 2009, T. Allen and J. Busby (eds.), American Nuclear Society, 2010.

79. T. Sakai, T. Senjuh, K. Aoki, T. Shigemitsu, and Y. Kishi, “Study on Corrosion Resistance of Alloy 600 and 690 in High Temperature Water Containing Lead,” p. 83/1 in *Corrosion 1992*, National Association of Corrosion Engineers, 1992.

80. K. K. Chung, J. K. Lim, S. Moriya, Y. Watanabe, and T. Shoji, “Lead Induced Stress Corrosion Cracking of Alloy 690 in High Temperature Water,” p. 233 in *Proc. 7th International Symposium on Environmental Degradation of Materials in Nuclear Power Systems—Water Reactors*, Breckenridge, Aug. 7–12, 1995, R. Gold and A. McIlree (eds.), National Association of Corrosion Engineers, 1995.

81. F. Vaillant, D. Buisine, B. Prieux, D. Gomez Briceno, and L. Castano, “Influence of Lead on the Secondary Side Cracking of Alloys 600, 690 and 800,” p. 13/1 in *Eurocorr’96*, Centre Francais de L’Anticorrosion Societe de Chimie Industrielle, Nice, 1996.

82. H. Takamatsu, B. P. Miglin, P. A. Sherburne, and K. Aoki, “Study on Lead-induced Stress Corrosion Cracking of Steam Generator Tubing under AVT Water Chemistry Conditions,” p. 216 in *Proc. 8th Int. Symp. Environmental Degradation of Materials in Nuclear Power Systems—Water Reactors*, Amelia Island, Aug. 10–14, 1997, A. McIlree and S. Bruemmer (eds.), American Nuclear Society, 1997.

83. J. M. Sarver, “IGSCC of Nickel Alloys in Lead Contaminated High Purity Water,” p. C11/1 in *1987 EPRI Workshop on Secondary Side Intergranular Corrosion Mechanisms*; NP-5971, Electric Power Research Institute, 1987.

84. J. Lumsden and A. R. McIlree, “Factors Affecting PbSCC in Alloy 600 and Alloy 690 Steam Generator Tubing,” PWR Secondary-III, Paper 40, *Proc. Fontevraud 7 Int. Symp.,* Société Française d'Energie Nucléaire, Avignon, Sept. 26–30, 2010.

85. H. Kim, S. Hwang, J. Kim, and J. Hong, “Stress Corrosion Cracking of Steam Generator Tubing Materials in Lead Containing Solution,” PWR Secondary-III, Paper 38, *Proc. Fontevraud 7 Int. Symp.,* Société Française d'Energie Nucléaire, Avignon, Sept. 26–30, 2010.

86. M. G. Burke et al., Evidence for a Corrosion Slot/Tunneling Mechanism for Lead-Induced Transgranular SCC of Alloy 690 in PbO + 10% NaOH Solution,” PWR Secondary-III, Paper 37 in *Proc. Fontevraud 7 Int. Symp.: Contribution of Materials Investigations to Improve the Safety and Performance of LWRs,* Société Française d'Energie Nucléaire, Avignon, Sept. 26–30, 2010.

87. L. E. Thomas and S. M. Bruemmer, “Observations and Insights into Pb-Assisted Stress Corrosion Cracking of Alloy 600 Steam Generator Tubes,” p. 1143 in *Proc. 13th Int. Conf. Environmental Degradation of Materials in Nuclear Power Systems*, Whistler, Aug. 19–23, 2007, P. King and T. Allen (eds.), The Canadian Nuclear Society, 2008.

88. L. E. Thomas and S. M. Bruemmer, *Summary of Analytical Electron Microscopy Observations of Intergranular Attack and Stress Corrosion Cracks in Alloy 600 Steam Generator Tubing,* Topical Report 1011683, Electric Power Research Institute, April 2005.

89. R. W. Staehle, “Reasonably Expected Performances of Alloy 690 and 800 Based on their Properties and Environment,” *7th CNS Int. Steam Generator Conference,* Toronto, November 2012.

90. *Pressurized Water Reactor Secondary Water Chemistry Guidelines—Revision 6,* Report 1008224, Electric Power Research Institute, 2004.

91. C. Mansour, “Behavior of Sulfur Species in Steam Generator Conditions of PWRs,” PWR Secondary 1, paper 10, *Proc. Fontevraud 7 Int. Symp.,* Société Française d'Energie Nucléaire, Avignon, Sept. 26–30, 2010.

92. Y. Yamamoto et al., “Evaluation of Crack Growth Rate for Alloy 600TT Steam Generator Tubing in Primary and Faulted Secondary Water Environments,” p. 1243 in *Proc. 14th Int.*

Symp. Environmental Degradation of Materials in Nuclear Power Systems, Virginia Beach, Aug. 23–27, 2009, T. Allen and J. Busby (eds.), American Nuclear Society, 2010.

93. O. de Bouvier et al., "Stress Corrosion Cracking of Nickel Alloys in Complex (Liquid and Vapor) Environments," p. 1255 in *Proc. 14th Int. Symp. Environmental Degradation of Materials in Nuclear Power Systems*, Virginia Beach, Aug. 23–27, 2009, T. Allen and J. Busby (eds.), American Nuclear Society, 2010.

94. P. L. Andresen, "SCC of High Cr Alloys in BWR Environments," p. 267 in *Proc. 15th Int. Conf. Environmental Degradation of Materials in Nuclear Power Systems—Water Reactors,* Colorado Springs, Aug. 7–11, 2011, J. Busby and G. Ilevbare (eds.), The Minerals, Metals & Materials Society, 2012.

95. C. M. Brown, and W. J. Mills, "Effect of Water on Mechanical Properties and Stress Corrosion Behavior of Alloy 600, Alloy 690, EN82H Welds, and EN52 Welds," *Corrosion Journal* **55,** 173 (1999).

96. W. J. Mills and C. M. Brown, "Fracture Behavior of Ni-Base Alloys in Water," p.167 in *Proc. 9th Int. Symp. Environmental Degradation of Materials in Nuclear Power Systems—Water Reactors*, Newport Beach, Aug. 1–5, 1999, S. Bruemmer, F. P. Ford and G. Was (eds.), The Minerals, Metals & Materials Society, 1999.

97. C. M. Brown and W. J. Mills, "Fracture Toughness of Alloy 690 and EN52 Welds in Air and Water," *Metallurgical and Materials Transactions A* 33, 1725 (2002).

98. A. Demma, A. McIlree, J. Peng, and P.J. King, "Effects of Dissolved Hydrogen and Hydrogen Peroxide on the Fracture Resistance of Weld Metals 182, 52, and 152 in Simulated PWR Shutdown Environment," Paper 32 in *Proc. 13th Int. Conf. Environmental Degradation of Materials in Nuclear Power Systems*, Whistler, Aug. 19–23, 2007, P. King and T. Allen (eds.), The Canadian Nuclear Society, 2008.

99. K. Tsutsumi, Y. Nomura, H. Kanasaki and S. Asada, "Intergranular Cracking Susceptibility of Alloy 152 in Low Temperature Water with Hydrogen," *Transactions of the Japan Society of Mechanical Engineers A* **726,** 265 (2007).

100. M. Ahonen, U. Ehrnstén, and H. Hanninen, "Low Temperature Crack Propagation of Nickel-Based Weld Metals in Hydrogenated PWR Primary Water," Paper A016-T04, *Proc. Fontevraud 7 Int. Symp.,* Société Française d'Energie Nucléaire, Avignon, Sept. 26–30, 2010.

101. T. Shoji, Y. Ito, Zhanpeng Lu, and T. Yonezawa, "Mechanistic Understanding of Low Temperature Crack Propagation for Alloy 690 in Hydrogenated Water," p. 98 in *Proc. 13th Int. Conf. Environmental Degradation of Materials in Nuclear Power Systems*, Whistler, Aug. 19–23, 2007, P. King and T. Allen (eds.), The Canadian Nuclear Society, 2008.

5. CARBON AND LOW ALLOY STEELS

Peter Ford
General Electric Global Research, Niskayuna, New York – Retired

5.1 OVERALL INTRODUCTION AND CURRENT CONCERNS

Carbon and low alloys steels serve in a variety of locations within the nuclear power generating fleet. These ductile structural materials are used as pressure boundary materials in pressure vessels and piping in the RCS, ECCS, secondary water and service water systems of LWRs. These alloys are attractive for this use due to their relatively low cost, good mechanical properties in thick sections and good weldability. In reactor coolant system components, such as the pressure vessel, pressurizer and some piping, the carbon and low alloy steels are clad on the inside wetted surface with corrosion resistant materials such as austenitic stainless steels or nickel-base alloys.

This background paper covers stress corrosion cracking (SCC) of ductile carbon and low alloy steel components and their associated weldments, with a special focus on extended operation degradation. Stress corrosion cracking, corrosion fatigue cracking, and flow-accelerated corrosion (FAC) are the primary modes of degradation discussed and presented. Specific areas of concern for extended service are identified. Irradiation effects and thermal aging for these alloys are also covered in considerably more detail in Volume III of this EMDA report (i.e., NUREG/CR-7153).

5.1.1 Steel Compositions and Applications

Carbon and low alloy steels (Table 5.1) are used for pressure-retaining components in the primary, secondary, and tertiary systems of both BWRs and PWRs.

These steels are used in the reactor in a variety of forms, including seamless piping, forgings, castings, plate, and bolting. The specific carbon or low alloy steel/component combinations that are used in a particular reactor vary between reactor designs and manufacturers, but in general, the reactor components include the following:

- Reactor pressure vessel vertical sections in both PWRs and BWRs are manufactured from rolled low alloy steel A533 Gr. B Class 1 plates, which are then welded to form a cylinder. The cylinder is clad on the internal surface with a 5 mm layer of Type 308 SS, and then tempered during a post weld heat treatment (PWHT) at 595 °C (1,103 °F) to 620 °C (1,148 °F) for one hour per 25 mm thickness of steel. The composition of this C-Mn-Mo low alloy steel has more severe limitations on the Cu, S, P, and V contents for plates in the high-flux beltline region since these elements increase the extent of irradiation embrittlement.

- The top and bottom heads of the pressure vessel in BWRs and PWRs are generally clad[*] low alloy steel A508 Gr. 2 Class 1 forgings using the same cladding/heat treatment conditions as for the vertical sections. After the vertical sections and the top and bottom

[*] Note that in some BWR designs the top head may be unclad.

heads are fabricated, all three subassemblies are welded together to form the primary pressure vessel and are then given a further PWHT.

- Steam generator shells of PWRs are low alloy steel A533 Gr. A Class 1 or Class 2 plates, which, like the pressure vessel, are heat-treated after subassembly. The secondary side of the steam generator is not usually clad.

- Steam generator tube sheets in PWRs are generally A508 Gr. 2 Class 1 or A508 Gr. 2 Class 2, with cladding on the primary side of the bottom head.

- Steam generator channel heads in PWRs are generally A216 Gr.

- The pressurizer shells in PWRs are generally low alloy steel A516 Gr.70 or A533 Gr. B plate with internal stainless steel cladding.

Table 5.1. ASTM compositional specifications for ferritic and bainitic carbon and low alloy steel concentrations given as weight percentages. Balance is Fe.

ASME/ASTM	C max	Mn	P max	S max	Si	Cu max	Ni	Cr	Mo	V max
					Ferritic Steels					
A105	0.035	0.6–1.05	0.035	0.04	0.1–0.35	0.4(1)	0.4 max[a]	0.3 max[a]	0.12 max[a]	0.05
A106 GrB	0.3	0.29–1.06	0.035	0.035	0.1 min	0.4 (2)	0.4 max[b]	0.4 max[b]	0.15 max[b]	0.08[b]
A216 Gr WCB	0.3	1.0 max	0.04	0.045	0.6 max	0.3(3)	0.5 max[c]	0.5 max[c]	0.2 max[c]	0.03[c]
A302 GrB	0.25	1.15–1.50	0.035	0.035	0.15–0.4				0.45–0.6	
A333 Gr6	0.3	0.29–1.06	0.035	0.035	0.1 max					
A508 Gr3	0.25	1.2–1.5	0.025	0.025	0.15–0.4		0.4–1.0	0.25 max	0.45–0.6	0.05
A516 Gr70	*d*	0.85–1.2	0.035	0.035	0.15–0.4					
A533 Type A	0.25	1.15–1.5	0.035[e]	0.035	0.15–0.4				0.45–0.6	
A533 Type B	0.25	1.15–1.5	0.035	0.035	0.15–0.4		0.4–0.7		0.45–0.6	
					Bainitic Steels					
1Cr1Mo0.25V	0.33	0.85			0.25			1.0	1.25	0.25
2Cr1Mo Gr22	0.026	0.49	0.012	0.009	0.28	0.05		2.42	0.98	
NiCrMoV (A469 Cl8)	0.28	0.6	0.015	0.018	0.15–0.3		3.25–4.0	1.25–2.0	0.3–0.6	0.15
NiCrMoV (A470 Cl8)	0.35	1.0	0.015	0.018	0.15–0.35		0.75	0.9–1.5	1.0–1.5	0.3
NiCrMoV (A471 Cl8)	0.28	0.7	0.015	0.015	0.15–0.35		2.0–4.0	0.7–2.0	0.2–0.7	0.05

[a] Sum of Cu, Ni, Cr, and Mo shall be <1.00%; sum of Cr and Mo shall not exceed 0.32%.
[b] Limits for V and Nb may be increased to 0.1% and 0.05%, respectively.
[c] Sum of Cr and Ni shall not exceed 0.32%.
[d] Carbon max. varies with thickness of plate; 0.5–2 in., 0.28% max; 2–4 in., 0.30% max; 4–8 in., 0.31% max.
[e] For reactor beltline: Cu < 0.1% max, P < 0.012% max, S < 0.015% max, and V < 0.05% max.

- Reactor coolant piping for PWR primary circuits may be seamless carbon steel with, in some designs, austenitic stainless steel cladding. Alternatively, a higher-cost option of using cast stainless steel (CF8M) has been used for the main coolant piping. The recirculation piping in BWRs is usually stainless steel (Types 304 SS, 316 SS, 304L SS, 316L SS), although unclad A333 Gr. 6 carbon steel piping may be used in the main steam and the feedwater lines. The piping in the lower-temperature emergency core cooling and auxiliary/support systems is usually seamless A105 or A106 Gr. B carbon steel.

5.1.2 Initial Concerns

It was recognized initially by the reactor designers that two problems could occur if carbon steels and low alloy steels were used in water-cooled nuclear reactors. First, irradiation embrittlement of the pressure vessel steel would occur in high-neutron-flux regions over time, and, second, corrosion products could be irradiated during passage through the core region and would create radioactive “crud” that could hamper maintenance operations.

The first problem was addressed by monitoring the extent of irradiation embrittlement in low alloy steel surveillance samples placed adjacent to a reactor pressure vessel (RPV) wall in the high neutron flux “beltline” region. This embrittlement is, along with fatigue usage calculations, an input to the regulatory “time limited aging analyses” (TLAA) required for license renewal (sometimes referred to more commonly as “life extension”) for up to 60 years.

The crud/radioactivity issue was addressed by cladding the inside of the RPV with stainless steel (e.g., Type 308 SS), thereby reducing the inventory of corrosion product that could become irradiated.

5.1.3 Subsequent Concerns

Unfortunately, environmentally assisted degradation has been observed [1–8] in carbon and low alloy steel components of LWRs by degradation modes that were not assessed at the early design stage. The degradation modes were:

- “High-cycle” (i.e., low strain amplitude/high frequency) fatigue due to flow-induced vibration or thermal stress cycles (e.g., in dead legs and in feedwater nozzles).

- “Low-cycle” (i.e., high strain amplitude/low frequency) fatigue (e.g., due to start-up and shutdown cycles).

- Pitting of carbon steel components, usually under oxidizing conditions at temperatures <150 °C (302 °F). Such degradation often acts as a precursor to stress corrosion cracking (SCC) and corrosion fatigue (CF) during subsequent operation at higher temperatures.

- Corrosion of carbon steel tube support plates in the secondary side of PWR steam generators due to complex concentrated environments occurring at heat transfer surfaces in the tube/support plate crevice.

- Transgranular stress corrosion cracking (TGSCC) of BWR carbon steel piping and low alloy steel PWR steam generator shells in situations involving dynamic loading, oxidizing environments, and high service stress.

- Intergranular stress corrosion cracking (IGSCC) at elevated temperatures of components such as Canada Deuterium Uranium (CANDU) PWR steam generator inlet piping that had been cold formed.

- IGSCC of welded carbon steel piping in low-temperature [<90 °C (194 °F)], closed-coolant water (CCW) systems containing inhibitors.

- IGSCC in low alloy steel steam turbine components operating at temperature-pressure combinations associated with the Wilson line.*

- Microbially-induced corrosion (MIC) of carbon steel piping in tertiary systems such as the service water and fire suppression systems.

- Flow-accelerated corrosion (FAC) of carbon steel components (e.g., the PWR steam generator tube support plates and steam/condensate piping, and in BWR feedwater, main steam line, and auxiliary systems).

- Boric acid corrosion (BAC) of low alloy steel components exposed to coolant from leaks in the PWR primary system.

- Hydrogen embrittlement of high-strength martensitic and low alloy steel bolting largely used in air environments (e.g., vessel head, pump casings).

These incidences have been reported in conferences focused on the degradation of materials in water-cooled reactors [5], in EPRI reports and workshops [4, 6–8], and in NRC publications; these latter publications include generic letters and periodic revisions of the "Generic Aging Lessons Learned" (GALL) report [3].

The consequences of these material failures have been primarily economic, in that the failures have led to forced and extended plant outages, thereby entailing the cost of replacement power together with the cost of component repair or replacement. Rarely has there been a significant safety issue quantified, for instance, by an unacceptable increase in the core damage frequency (ΔCDF). However, these cumulative effects may contribute to the general obsolescence of the plant over the long-term and should be considered. On the other hand, these incidents have had a significant impact on the public perception of plant safety in some notable cases (e.g., FAC at Mihama).

5.1.4 Degradation Assessments for 60 Year Operational Times

As a result of these "unexpected" material degradation incidents, both the NRC [1] and EPRI [2, 4, 6–8] conducted analyses to assess the future modes of material degradation of the reactor structural materials that might be expected during a 40 year operational lifetime. These particular assessments were based on engineering judgment. For instance, the NRC analysis [1] was based on the "likelihood of degradation" and the "state of knowledge (of the controlling factors)"

* The Wilson line appears on the enthalpy/entropy chart for steam and is associated with the condition for condensation of water droplets. It corresponds to approximately 1–3% moisture in the equilibrium mixture. These droplets may undergo drying/evaporation cycles, leading to salt concentrations that result in accelerated and localized corrosion phenomena such as stress corrosion cracking on turbine discs and blades.

for various alloy/environment/degradation mode combinations. EPRI conducted similar analyses to assess technology gaps, and, subsequently, risk-based decisions were made by EPRI (e.g., [7, 8]) regarding the prioritization of research and development resources required to mitigate the degradation for a particular component.

Similar assessments have been conducted in Japan under the sponsorship of the Nuclear and Industrial Safety Agency (NISA), where the focus has been on the basic science questions associated with materials degradation [9].

On the basis of such evaluations, most of the degradation issues observed in carbon and low alloy steels in LWRs listed above have been judged to be manageable over the an extended license period of 40 years, provided the inspection and mitigation actions in the individual licensee's aging management programs (AMPs) were judged adequate during the NRC license renewal examination process.

5.2 CONCERNS RELATED TO DEGRADATION OF CARBON AND LOW ALLOY STEELS AT TIMES BEYOND 60 YEARS

Engineering judgments may offer some justification for reactor operation up to 60 years, since that judgment is based largely on the extrapolation of *known* phenomena after operating lives of 35–40 years. There are concerns, however, regarding the potential degradation of carbon steels and low alloy steels if the operating license was extended a further 20 years to 80 years since this may lead to events associated with time-limiting degradation modes (such as fatigue or thermal aging) and synergisms between different degradation modes (such as irradiation and SCC). These concerns are amplified by (a) aleatory uncertainties associated with the stochastic, random nature of some of the degradation modes (pitting, intergranular attack, FAC, fatigue) and (b) epistemic uncertainties arising out of the incompleteness of the various life prediction models, and the accuracy of the inputs to these models. Such epistemic uncertainties will impact on both the "likelihood of degradation" and the "state of knowledge (of the controlling factors)" referred to above.

In this chapter these concerns relating to operational lives of 60 to 80 years are discussed for the following degradation modes:

- Corrosion fatigue crack initiation
- FAC
- Enhanced SCC due to synergistic interactions with other degradation modes

These degradation modes are now discussed in terms of the current experience and the availability of life prediction models (e.g., parametric dependencies, mechanistically based models) that allow predictions out to 80 years.

5.2.1 Fatigue Crack Initiation

Fatigue life is based on strain-amplitude vs. cycles to crack initiation data obtained in air at 25 °C (77 °F) for polished cylindrical specimens, cyclically loaded under strain control. "Initiation" in this case is defined as a drop in maximum load by 25%, which physically corresponds to a crack depth of approximately 1 to 2 mm (0.04 to 0.08 in). Examples of these strain amplitude vs. crack

initiation relationships are given in Figures 5.1(a) and 5.1(b) for carbon steels and low alloy steels respectively.

It was recognized that these testing conditions on polished specimens in air were not necessarily relevant to the behavior of engineering structures, and, consequently, the fatigue cycles for crack initiation were decreased from those denoted by the "air" data lines in Figure 5.1, in order to take into account unknown (at that time) effects of temperature, surface roughness, or "industrial environment." The extent of this cycle decrease was based on engineering judgment, and the "design curve" in Figure 5.1 was displaced from the room temperature air data curve by a factor of 2 (on stress/strain amplitude) or 20 (on fatigue life), whichever was the more conservative [11]. The origin of the factor of "20" arose out of speculated effects of the variables such as data scatter, specimen size, and surface finish (Table 5.2).

The specific environmental or "atmospheric adjustment factor" was less than a factor of four and was originally meant to cover only the effect of an "industrial environment" compared to a "laboratory environment." It was left up to the reactor designer or licensee to determine the specific adjustment factor for his particular reactor environment [11]. In spite of that expectation, it is the "2 and 20" design curves shown in Figure 5.1 that are used for water-cooled reactors, and the licensee has to demonstrate for safety-significant components that, during the proposed operational life, the cumulative cycles will be within the bounds defined by the ASME Section III design curve at a given strain amplitude. In other words, the summation of the individual usage factors (defined as the ratio of the expected cycles to the design cycles) for an individual component must be less than 1.0.*

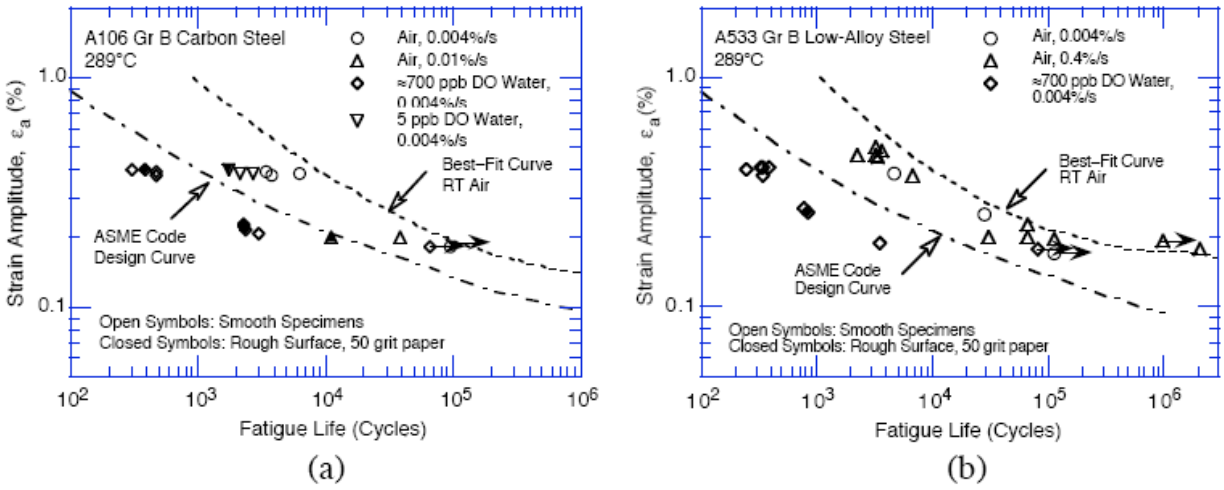

Figure 5.1. Effect of surface roughness and oxygen content on the fatigue life of (a) A106–Gr B carbon steel and (b) A533–Gr B low alloy steel in air and high-purity, oxygenated water at 289 °C (552 °F) [10].

* This summation is known as the "cumulative usage factor" (CUF).

Table 5.2. Design correction factors for ASME Section III fatigue cycles to crack initiation, N_{init} (measured in room temperature air) at a given strain amplitude [11]

Physical Phenomenon	Factor of Reduction in N Initial Values
Scatter in data	2.0
Component size	2.5
Surface finish, atmosphere, temperature, etc.	4.0
Total	**20**

5.2.1.1 Current state of knowledge of fatigue crack initiation in carbon and low alloy steels

Much discussion has taken place internationally about the appropriateness of this "2 and 20" design guidance, especially when the specific reactor environmental conditions need to be accounted for [10–31]. For instance, it is seen in Figure 5.1 that combinations of surface roughness and elevated concentrations of dissolved oxygen content may lead to cycles to crack initiation less than the design value. In fact, the cycles to corrosion fatigue initiation are a function of not just dissolved oxygen content but are controlled by the interactions between various material, environmental, and straining parameters. Examples include the following:

- For there to be a decrease in cycles to initiation due to the environment, the strain amplitude under fully reversed loading (for R = -1.0)* must exceed a critical value in the range 0.0015 to 0.003 [19–21], and/or the maximum tensile stress must exceed the high-temperature yield stress [22]. The magnitude of the critical strain amplitude [19] is a function of the sulfur content of the steel.

- The cycles to crack initiation, once the critical strain amplitude is exceeded, are markedly decreased by
  - increasing temperature above 150 °C (302 °F) [17, 23];
  - increasing oxygen content [17, 21, 23];
  - increasing water conductivity [24];
  - increasing sulfur content in the steel [21, 23]; and
  - decreasing strain rate [25, 18, 21, 23, 26].

- There is evidence that the strain-rate induced degradation may saturate [27] or even decrease at very low strain rates and/or long hold times [18] during trapezoidal loading.

- Various combinations of these system parameters can give rise to the situation where the number of cycles to crack initiation (N_i) is less than the N_i value prescribed by the ASME Section III design code relationship. The critical system conditions for this to occur are conjoint. In other words, for N_i to be less than the ASME Section III design value for a carbon

* The "R ratio" is defined as the ratio of the minimum stress (or strain) to the maximum stress (or strain). Thus a value of 1.0 is equivalent to constant stress (or strain), a value of zero is equivalent to stress (or strain) cycling between zero and a maximum tensile value. Conversely a value of -1.0 is equivalent to stress (or strain) cycling between equal maximum tensile and compressive values.

steel containing 0.015% S, the strain amplitude must exceed 0.0015, the strain rate must be $<10^{-4}$ s^{-1}, the oxygen content must be ~8 ppm, and the temperature must be ~288 °C (550 °F). If the oxygen content drops to 200 ppb, then, for the same steel at 288 °C, the critical strain rate drops to $<10^{-5}$ s^{-1}.

- The extent of environmental degradation is adversely affected by the presence of notches [49, 22, 28] and pits [21, 22, 28].

Thus, under particular straining, material, and environmental conditions, the cycles to crack initiation may be markedly less than those given by the current ASME Section III design life, and this will present increasing regulatory concern as the number of applied cycles increases with extended operational lives.

There are two approaches to managing these complicated interacting effects of the system parameters on fatigue crack initiation, and on redefining design curves that are more relevant to the system conditions in water-cooled reactor environments over extended operational periods.

The first approach involves an experimental redefinition of the design curves by conducting corrosion fatigue tests under very specific material, environmental, and straining conditions that are relevant to specific component operations.

The second approach is to reformulate the design life on the basis of an "environmental correction factor" (F_{env}) [18]. This factor is defined as the ratio of the fatigue life in room-temperature air to that in water for specific combinations on material (sulfur content), strain history (strain amplitude and frequency), and environment (dissolved oxygen content, temperature). Examples of the F_{env} equations based on correlations with laboratory data are shown in Table 5.3 for two data bases; one by Higuchi [29] and the other by Chopra and Shack [30]. The specific variations in F_{env} values as a function of strain rate, temperature, and dissolved oxygen content are illustrated in Figures 5.2 and 5.3. Although the difference between the results of these two analyses is not major, the NRC has adopted the formulations by Chopra and Shack [30, 31] and has incorporated them into Regulatory Guide 1.207 [32].

It should be noted that the current ASME Section III design value corresponds to an F_{env} of 20. Thus there are predictable combinations of applied strain rate, temperature, dissolved oxygen content, etc. when the ASME Section III design life for a particular strain amplitude is either greater or less than the observed crack initiation value.

Obviously, this analytical approach based on laboratory data is an improvement over the engineering judgment used to derive the "2 and 20" design life in the ASME Section III code, since it allows the licensee to determine the increment in corrosion fatigue damage (compared to that in air) that is associated with system parameters such as strain rate, dissolved oxygen content, temperature, etc. that are specific to his particular plant.

Table 5.3. Environmental correction factors for carbon steels and low alloy steels formulated by Higuchi [29] and at Argonne National Laboratory (ANL) by Chopra and Shack [30]

Japanese Latest Model (by Higuchi)	US ANL Model (by Chopra)
(Carbon & Low Alloy Steels) $\ln(F_{en})$=-(0.199 T^* O^* + 0.112) S^* ε'^* ε'^*= 0 (ε' > 1.0%/s) ε'^*= ln(ε') (1.0 ≥ ε' ≥ 0.0004%/s) ε'^*=ln(0.0004) (ε'<0.0004%/s) T^* =0.00531T-0.7396 (T ≥ 180°C) T^* =0.216 (T < 180°C) O^* =ln(DO/0.03) (0.03 ≤ DO ≤ 0.5 ppm) O^* =0 (DO < 0.03 ppm) O^* =ln(0.5/0.03) (DO < 0.5 ppm) S^* =17.23S+0.777 F_{en} = 1.0 (ε_a ≤ 0.042%) (ε_a of 0.042% is the same strain amplitude at 10^6 cycles in the design fatigue curve)	**(Carbon Steel)** : $\ln(F_{en})$ = 0.554 - 0.101 $S^*T^*O^*\varepsilon'^*$ **(Low Alloy Steel)**: $\ln(F_{en})$ = 0.898 - 0.101 $S^*T^*O^*\varepsilon'^*$ S^* = 0.015 (DO > 1.0 ppm or S > 0.015%) S^* = S (DO ≤ 1.0 ppm & S ≤ 0.015 %) T^* = 0 (T < 150°C) T^* = T-150 (150 ≤ T ≤ 350°C) O^* = 0 (DO < 0.04 ppm) O^* = ln(DO/0.04) (0.04 ≤ DO ≤ 0.5 ppm) O^* = ln(12.5) (DO > 0.5 ppm) ε'^* = 0 (ε' > 1%/s) ε'^* = ln(ε') (0.001 ≤ ε' ≤ 1%/s) ε'^* = ln(0.001) (ε' < 0.001%/s) F_{en} = 1.0 (ε_a ≤ 0.07%)

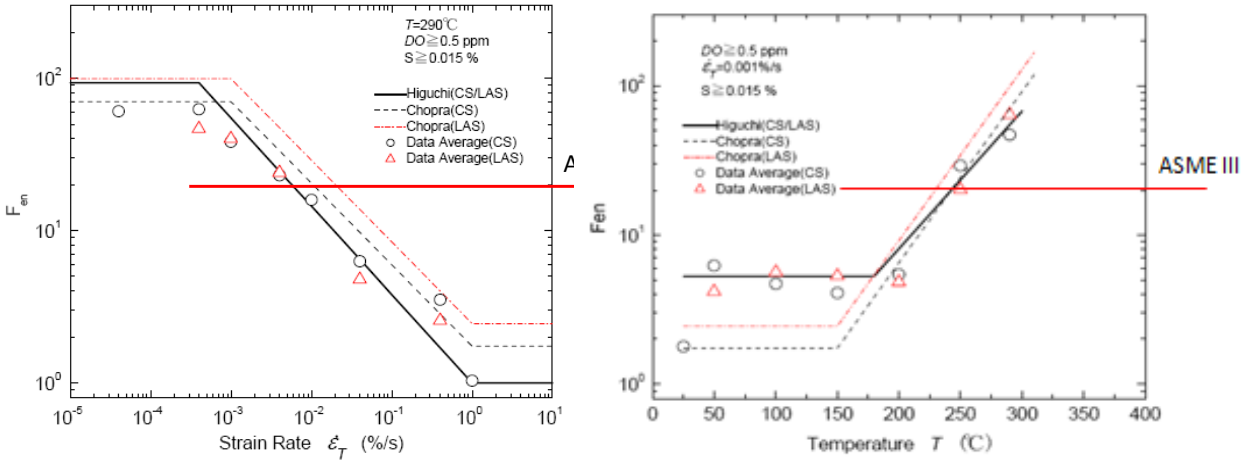

(a) (b)

Figure 5.2. F_{env} calculations of Higuchi and Chopra for the effect of (a) loading strain rate on fatigue life for carbon and low alloy steels at 290 °C (554 °F), and (b) temperature on fatigue life for carbon and low alloy steels at an applied strain rate of 0.001%/s [29, 30].

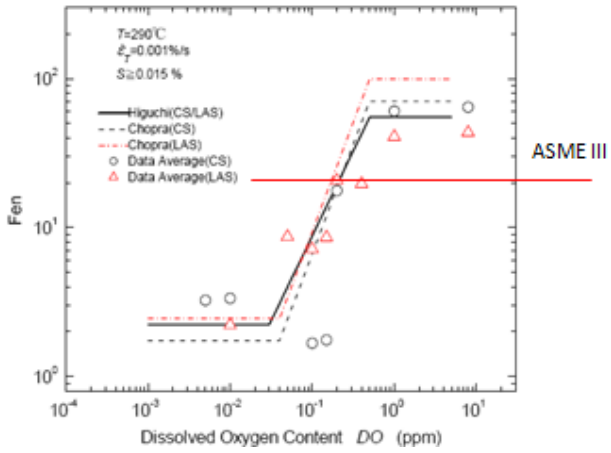

Figure 5.3. F_{env} calculations of Higuchi and Chopra for the effect of dissolved oxygen content on fatigue life for carbon and low alloy steels at an applied strain rate of 0.001%/s [29, 30].

5.2.1.2 Concerns regarding fatigue crack initiation over 60+ years operation

It is apparent, however, that even with this improvement in analytical approach, there are outstanding uncertainties that will become critical as the number of operational cycles increases. These concerns may affect the “Likelihood of Degradation” and the “State of Knowledge" scoring in the Assessment analysis reported in [1].

These uncertainties are associated with the following factors.

- The MnS inclusion size and distribution are parameters of importance, not the sulfur content of the steel.

- The parameter of prime importance is the corrosion potential, not the dissolved oxygen content. The relationship between corrosion potential and dissolved oxygen, hydrogen peroxide, and other oxidizing species is not linear at high LWR temperatures. Thus the "correction factor" to the F_{en} algorithms is not a simple relationship.

- No account is given to the effect of water flow rate, in spite of its considerable effect on the crack initiation and propagation rate. Two competing outcomes are possible: a decrease in the environmental effect due to convection of deleterious anionic species (e.g., S^{2-}) out of the embryonic crack, and an increase in the dissolved oxygen reduction kinetics that will increase the corrosion potential.

- No account is taken of the corrosion fatigue damage associated with complex strain /time patterns expected under reactor operating conditions, compared with the relatively simple strain patterns used in the laboratory.

- The water purity is not taken into account in spite of the high sensitivity of the environmentally assisted cracking sensitivity to sulphate and, especially, chloride concentrations. For instance [Figure 5.4(a)], decreasing the water purity leads to a significant decrease in the cycles to crack “initiation” for a WB36 low alloy steel in 220 °C (428 °F) water containing 200 ppb oxygen [33]. Such water purity effects are neither part of the current ASME Section III design life evaluations nor the improved RG 1.207 approach.

Moreover, corrosion fatigue cracks in carbon steels and low alloy steels in high-temperature water can initiate at pits [33] and then propagate, slow down, coalesce, and then accelerate. Thus, from a practical viewpoint, pitting of such steels, which may occur under low-temperature, oxygenated conditions (e.g., reactor shutdown), will lower the fatigue cycles to failure during subsequent cyclic loading at higher temperatures. This effect is illustrated in Figure 5.4(b) for a WB36 low alloy steel cyclically strained in high-purity 220 °C (428 °F) water containing 200 ppb oxygen; under these loading conditions, the cycles to initiation (associated with a 25% load drop) would be 450. However, if, at the beginning of life, the steel was cycled in impure 8 ppm oxygenated water (a situation that often happens in practice during early reactor operations) for only 25 cycles, then the total cycles to crack initiation when subsequently loaded in high purity water at 220 °C (428 °F) drops significantly, to 310 cycles, which is far less than the amount predicted via the linear Miner’s rule.

The fact that these factors are not addressed in the current approaches to CUF calculations raises some uncertainty about the quantification accuracy of corrosion fatigue crack initiation over extended operational times, when the number of actual cycles approaches the calculated maximum design value.

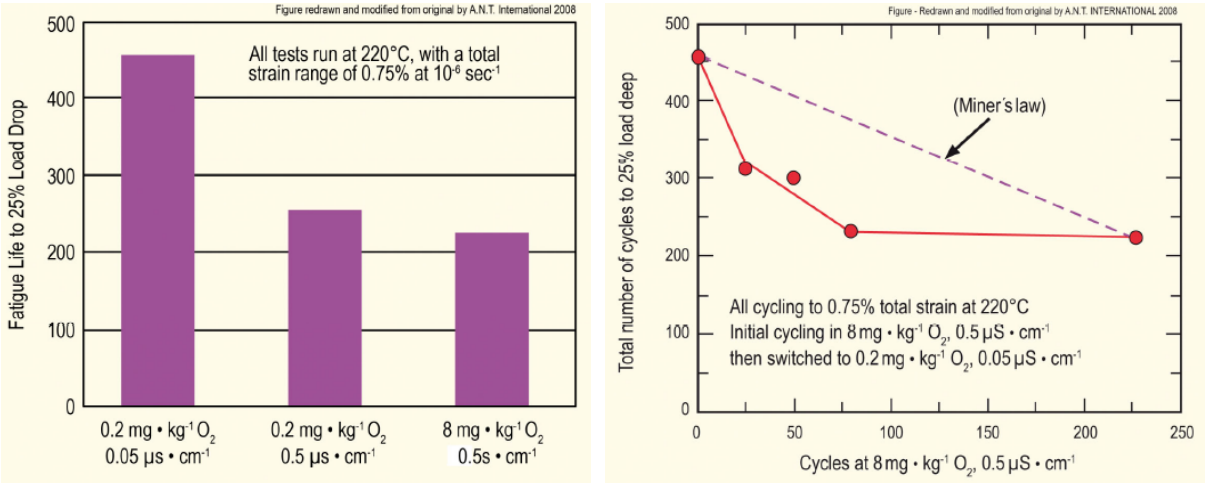

(a) (b)

Figure 5.4. (a) Effect of oxygen and conductivity transients on the low cycle fatigue behavior of low alloy steels in LCF tests, and (b) effect of initial cycling in impure water on total number of fatigue cycles to crack "initiation" defined by 25% load drop in a strain controlled test [33]. Reprinted with permission of The Minerals, Metals & Materials Society.

5.2.2 Flow-Accelerated Corrosion (FAC)

The term "flow-accelerated corrosion" covers enhanced corrosion that can occur on copper-base alloys and carbon steels in LWRs in flowing water or steam under single- or two-phase conditions. It is associated with changes in the mass-transport-controlled oxidation and reduction electrochemical reaction rates occurring on an oxidized surface and is most commonly observed in carbon steel used in feedwater, extraction steam, and drain lines. The impact of water droplets on the surface of main steam lines, upper support plates in PWR steam generators, or cross-around piping in turbines can enhance metal removal. This form of degradation is often associated with geometrical discontinuities or abrupt changes in flow direction, where high turbulence is encountered. As an example, typical metal losses from carbon steels can be more than 1 mm/year (0.04 in./year) for single-phase flow velocities of 6 to 10 m/s at 200 °C (392 °F).

The consequences of FAC include

- failure of the component due to thinning until system pressure or stress can no longer be supported;
- significant contribution to the iron content in the coolant and, therefore, an increase in radiation levels in the balance-of-plant of BWRs; and
- the fouling of flow measurement devices and ion exchange resins by released iron oxides.

Examples of operating experience on the consequences of FAC are the ruptures of an 46 cm (18 in.) diameter carbon steel condensate line on the secondary side of the Surry-2 PWR in 1986 [34] and a 61 cm (24 in.) diameter (carbon steel steam line between the low pressure heater and deaerator at the Mihama-3 PWR in 2004 [35].

Carbon steel feedwater systems for both BWRs and PWRs are particularly at risk from FAC and are typically inspected on a routine basis to ensure that wall thinning is monitored. In unfavorable conditions, metal loss rates up to 10 mm/year (0.39 in./year) have been observed [36]. This is of

significance for LWR operators applying for power uprates because the extra power can be achieved, among other things, by increasing the coolant and feedwater flow rates.

5.2.2.1 Current state of knowledge of FAC in carbon and low alloy steels

The extent of FAC of carbon and low alloy steels in water-cooled reactors depends on the interactions between the following parameters: (a) temperature, (b) oxygen concentration (corrosion potential), (c) water chemistry and pH, (d) chemical composition of the substrate metal, and (e) single- or two-phase flow and turbulence [37, 38].

Temperature

The FAC of carbon steel depends strongly on the temperature and tends to reach its maximum at around 130 °C (266 °F) to 150 °C (302 °F), as shown in Figure 5.5. In two-phase flow conditions, the maximum is typically at 180 °C (356 °F).

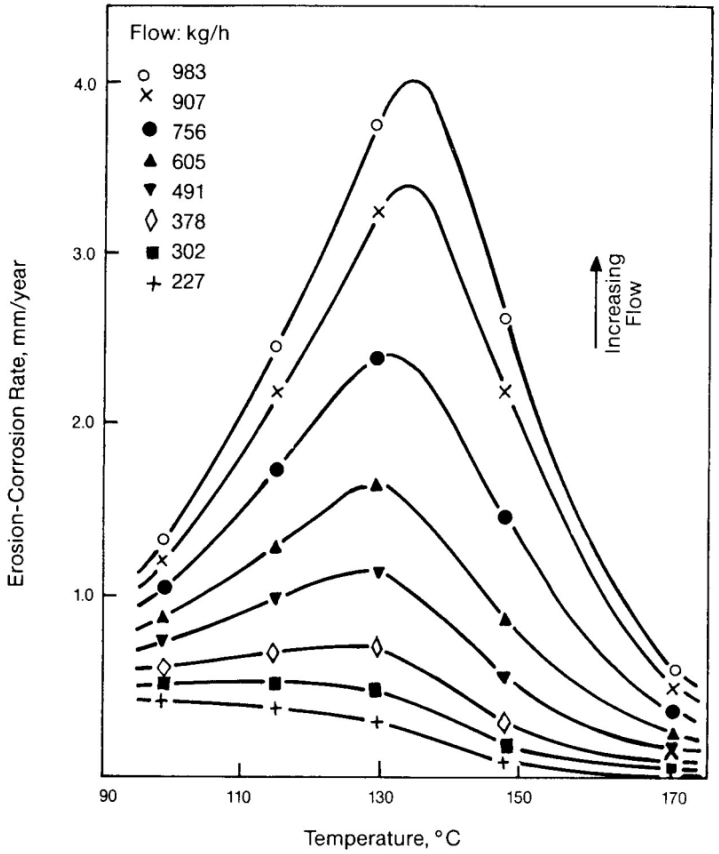

Figure 5.5. Effect of temperature on the flow-accelerated corrosion rate of carbon steel in deoxygenated ammonia all volatile treatment water [39].

The specific dependency of FAC on temperature is influenced by the values of the pH, single- or two-phase flow, and fluid velocity. Although FAC rates decrease at temperatures on either side of the peak temperature, FAC is often very localized because of mass transfer effects. Consequently, the rates of metal loss at higher or lower temperatures may still be sufficient to result in wall thinning and piping failure in thin-walled pipes. Operating experience with PWR steam generators shows, for example, that feedwater distribution J-tubes fabricated from carbon

steel can lose metal at up to 1 mm/year in single-phase water at 220 °C (428 °F) flowing at 8 to 9 m/s (26.2 to 29.5 ft/s) [40].

Dissolved oxygen content (corrosion potential)

Oxygen at concentrations ranging from a few ppb to a few tens of parts per billion, depending on the flow rate (which affects the efficiency of mass transport of the corroding species to and from the corroding surface), can have an adverse effect on increasing the corrosion potential by about 600 to 700 mV, and on decreasing very significantly the solubility of the iron oxides. Hematite (Fe_2O_3), the oxide of iron that forms at high corrosion potential, is several orders of magnitude less soluble in water than magnetite (Fe_3O_4), which forms at low corrosion potential. This has led to the practice of adding oxygen to feedwater in BWRs as well as in conventional boilers in Germany and the once-through boilers of the British Advanced Gas Cooled Reactors [41–44]. Figure 5.6 illustrates the advantage of using a dissolved oxygen content of >20 to 30 ppb to minimize the FAC damage in BWR feedwater systems.

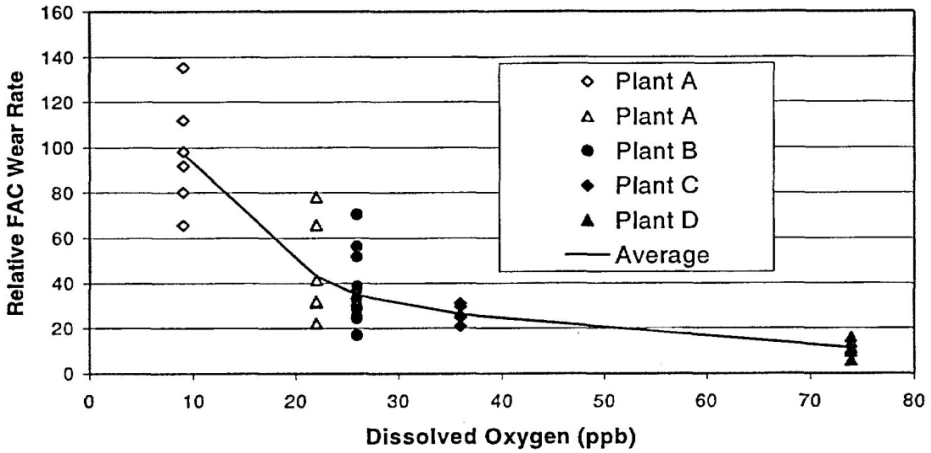

Figure 5.6. FAC data for condensate and moisturizer separator reheater drain systems in four BWR plants as a function of the local dissolved oxygen contents [41].

The amount of oxygen required to minimize FAC in two-phase wet steam lines of BWRs is a function of the amount of radiolysis occurring in the reactor core, the degree of hydrogen water chemistry/ Noblechem™, and the extent of venting applied in the moisture separators.

In PWR steam generators, the oxygen concentration in the secondary water is typical of most conventional boilers (<5 ppb). Hydrazine is added as an oxygen scavenger because the presence of oxidizing species is believed to have a detrimental effect on the resistance of Alloy 600 steam generator tubes to secondary side IGA/IGSCC. Thus, alternative measures are necessary to minimize metal loss from carbon steels. In fact, a considerable excess of hydrazine relative to the dissolved oxygen concentration is often added to PWR steam generator secondary feedwater, and in some cases the hydrazine concentration has been up to 400 ppb. In several cases, carbon steel support plates have disintegrated, with the use of high hydrazine concentrations (100 to 200 ppb) being concluded a significant factor [37].

Effect of water chemistry and pH

For carbon steels, the pH at 25 °C (77 °F) (the conventional temperature at which PWR secondary water pH is specified) should be between 9 and 10 to minimize corrosion in water due

to the minimum in-oxide solubility of carbon steels in that range [37, 45]. On the secondary side of PWR steam generators, this is usually achieved using an all-volatile treatment (AVT) with ammonia/hydrazine and/or organic amines such as morpholine or ethanolamine.

Another factor that can influence metal loss rates by FAC in PWR secondary circuits, particularly of carbon steel support plates in the steam generator, is the presence of impurities and their concentration in the liquid phase as the steam quality increases. Leaks of seawater through condenser tubes can allow the concentration of chloride in the liquid phase to increase and to acidify, especially due to hydrolysis of magnesium chloride. This can then increase the FAC rate of carbon steel support plates to a greater or lesser extent, depending on whether ammonia or organic amines are in use, the latter being in principle more effective in the presence of acidic impurities.

Effect of substrate metal composition

Material properties have a significant impact on FAC rates, as shown both by operating experience and in laboratory testing. The most important alloy variable affecting FAC of carbon steels is the chromium content of the alloy, as would be expected, given the protective nature of oxides that form on chromium-containing alloys. Chromium levels as low as 0.05 wt % have been shown to be beneficial, and levels >0.1 wt % appear largely sufficient to avoid the problem of FAC in single-phase conditions in PWR steam generator J-tubes, for example [39]. Stainless steel has also been used in PWR steam generator feedwater piping in newer plants, for example in all the Konvoi units in Germany.

One adverse effect of chromium on FAC behavior has been observed on several components. A characteristic groove has appeared just downstream of butt welds when the latter was resistant to FAC because it contained traces of chromium and the downstream material did not [46]. The phenomenon is known as the “entrance effect.” Similar situations can arise when FAC-susceptible carbon steel piping is replaced by a more resistant alloy and some of the less-resistant material is left in place downstream, either by accident or design.

Copper and molybdenum alloying additions have also been shown to have beneficial effects on reducing FAC in carbon and low alloy steels. However, the effects are typically small relative to that of chromium.

Effect of single- or two-phase flow and turbulence

As previously alluded to, FAC of carbon steels depends strongly on the steam quality of two-phase flows [39]. The rate of FAC increases very quickly when the moisture content attains 20% to 40% and is maximum between 40 and 80%. It is also observed that the range of temperatures normally associated with FAC in single-phase water extends to higher temperatures in two-phase flow. FAC has been seen at temperatures as high as those associated with the secondary side of PWR steam generators, where significant loss has been observed in upper support plates, steam separators, and blowdown piping [37]. The deleterious effect of two-phase flow is more exaggerated as the pH of the feedwater decreases, or with increasing partition of the AVT base to the vapor phase.

The rate of FAC in smooth straight tubes increases generally as a function of $Re^{0.8}$, whereas in straight tubes with a rough surface, the FAC rate is directly proportional to the fluid velocity. These dependencies have been verified in the laboratory for single-phase flow mainly in the

temperature range 150 °C (302 °F) to 250 °C (482 °F). However, the results for two-phase flow are consistent with the dependencies for single-phase flow.

Despite these well-characterized dependencies of FAC on hydraulic flow parameters, greater-than-predicted metal losses have been observed, particularly in single-phase flow conditions where the mass transfer coefficient is very high or in two-phase annular flow [44, 47]. The interpretation of these results has been controversial. The role of surface roughness under high mass transfer conditions has been emphasized by certain authors [39], whereas others have focused on the effect of fluid flow on the cathodic reaction rate in the corrosion process [44], which is usually neglected in most attempts to quantify FAC kinetics. The latter approach has the advantage of explaining locally increased solubility of magnetite due to a decrease in local corrosion potential caused by the effect of flow on the rate of the cathodic hydrogen evolution reaction. In this case, FAC is seen to accelerate as a function of high mass transfer rates after initially following the $Re^{0.8}$ dependence at lower mass transfer rates.

Prediction and management of FAC

Although there is extensive knowledge of the underlying principles affecting the kinetics of FAC of carbon steels, approaches have varied between different investigators in attempts to formulate predictive algorithms from the purely empirical through to a detailed understanding of the effect of flow on the oxidation and reduction kinetics as a function of various thermal-hydraulic parameters.

An empirical approach to FAC analysis and management of inspection priorities is based on observed parametric relationships [48], and these are encapsulated in the CHECWORKS™ prediction code [39, 49]. For each of the parameters affecting the phenomenology of FAC described earlier, empirical predictive algorithms were developed. The code is widely used by LWR operators to predict the most likely areas that may experience FAC as well as the rate of metal loss in order to fix inspection priorities. CHECWORKS™ is claimed to be accurate to within a factor of 2 when compared with plant measurements, with a confidence level of 98%.

The accuracy of such predictions has been questioned more recently by Garud [50] (Figure 5.7), where the poor reliability of predictive models is partly attributed to an oversimplified estimation of temperature effects and, more importantly, to a lack of reliable evaluation of mass transport in complex geometries.

The approach practiced in Japan has also been empirical, being based on thinning rates [51] observed in ~20,000 components at 23 PWRs. The inspection criteria were based solely on combinations of temperature, steam quality, and coolant velocity. With very few exceptions, the inspection guidelines, developed as early as 1990, were found to be conservative. The BWR data were also examined and found to exhibit lower corrosion rates than PWRs. This was attributed to water chemistry differences. Based on the PWR inspections, the 1990 inspection rules were endorsed by NISA until the Japan Society of Mechanical Engineers establishes standards. It should be pointed out, however, that a significant amount of work related to understanding the underlying mechanisms in support of this empirical approach has been undertaken by Uchida et al. [52] and by Satoh and colleagues [53].

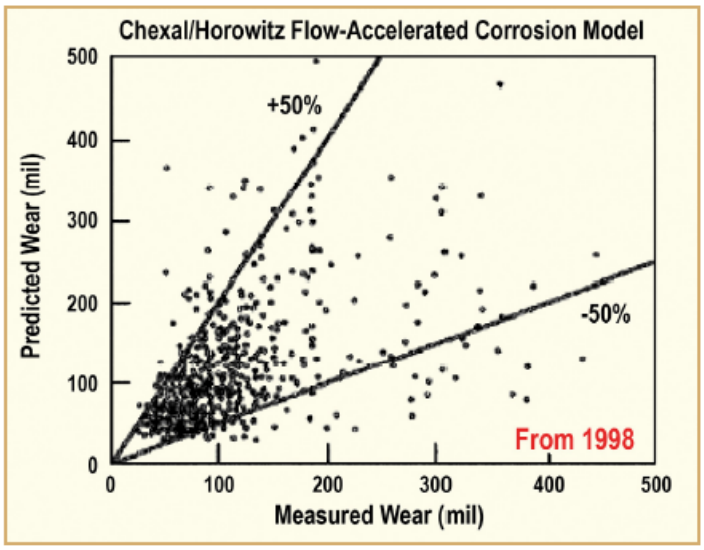

Figure 5.7. Measured vs. calculated wall thinning according to the Chexal-Horowitz model [50].

The COMSY code, used in Germany, is based on the known experimental and plant data on FAC [54]. This code incorporates detailed modeling of the plant geometry and thermal hydraulic characteristics and then, based on the water chemistry and material compositions, evaluates the zones at risk from FAC. For subsystems identified as vulnerable to FAC, a detailed analysis is performed to provide life predictions for individual components. An integrated inspection management module enables inspection data to be incorporated as they become available and the inspection scope, locations, and intervals optimized.

The BRT-CICERO software developed in France by EdF is based on a physical model of ferrous ion transfer between the boundary layer in equilibrium with magnetite reduction and the ferrous ion concentration in the bulk water [55]. The water chemistry and temperature are taken into account through the equilibrium ferrous ion concentrations in the boundary layer and that in the bulk water as well as the thermal hydraulic parameters via the mass transfer coefficient. Material composition parameters affect primarily the oxide thickness and porosity in the model. The BRT-CICERO model was used experimentally by EdF on a few plants in the early 1990s but became mandatory for all EdF PWRs after the discovery in 2001 of severe FAC on a reducer at the Fessenheim Unit 2 that had been correctly predicted by the model. Since then, the model has been tested on over 6,000 individual pipe thickness measurements taken over the last 20 years on nearly 4,800 different pipe elements in 58 plants. The results of a statistical analysis have shown that conservative predictions were made in 99.8% of cases, leaving only 11 non-conservative predictions (in over 6,000) (Figure 5.8). Surprisingly, the highest rate of nonconservatism was for straight tubes. The average deviation between the measured and calculated thickness was -1.07 mm.

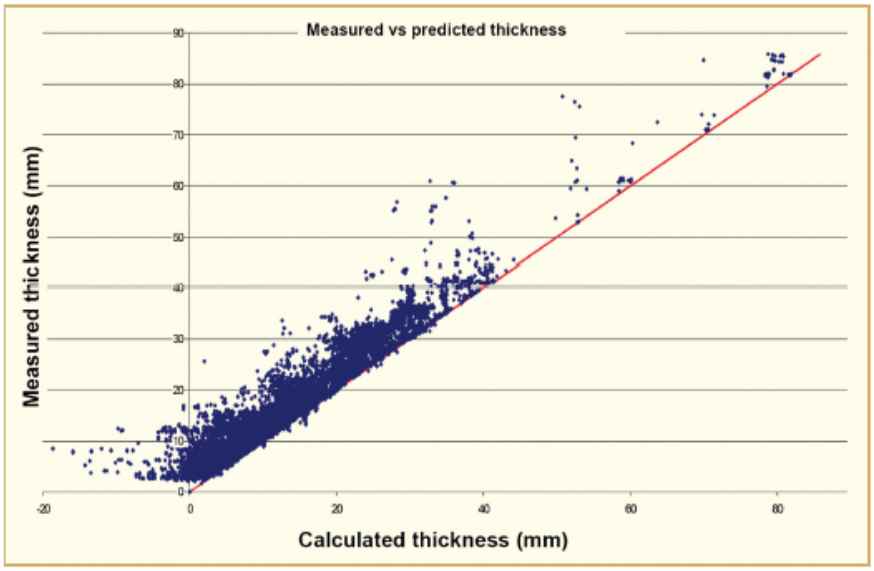

Figure 5.8. Measured vs. calculated component thicknesses using BRT-CICERO™ 3.1.b version, after [56].

A less-well-known physical model originally developed for the British Central Electricity Generating Board to address FAC issues in the once-through boilers of Advanced Gas Cooled reactors has been pressed into service again more recently by the owners, British Energy (and, more recently EdF) [43, 44, 57]. It has much the same features as the EdF model, but crucially also takes into account the effect of flow on the cathodic reaction rate and the lowering of corrosion potential that ensues at high fluid velocities.

5.2.2.2 Concerns regarding carbon steels and low alloy steels FAC beyond 60 years operation

The long-term concerns hinge around the accuracy of the FAC prediction algorithms [38], since these determine the adequacy of identifying regions in the reactor circuit that merit timely and focused inspections. Clearly, the FAC phenomenon is complex, involving interactions between numerous system parameters. As indicated above there are discrepancies between observation and predictions, especially when those predictions depend solely on empirical life prediction models. For the long term , therefore, there is a need to compare and qualify (i.e., assess the comparison between observation and prediction) the various life prediction models based on correlations with laboratory and plant observations (CHECWORKS™, COMSY) and those that draw primarily on fundamental principles (BRT-CICERO, EdF*).*

5.2.3 Stress Corrosion Cracking of Carbon and Low Alloy Steels

Stress corrosion cracking is one end of a spectrum of EAC modes that spans conditions where the stress or strain is: (1) constant (SCC); (2) monotonically increasing, as in strain-induced corrosion cracking; or (3) cyclic, as in corrosion fatigue.

Attention in this chapter is focused on SCC, since it is a dominant degradation mode encountered in LWR structures and balance of plant (e.g., steam turbines)

5.2.3.1 Current observations of SCC in carbon and low alloy steel components

Stress corrosion cracking of carbon and low alloy steels has been observed in BWR and PWR structures at temperatures as low as 54 °C in closed coolant water (CCW) systems to the more elevated temperatures in the primary reactor circuits and steam turbines. The material microstructures vary from ferritic to pearlitic to bainitic, and the crack morphologies have been transgranular or intergranular down prior austenite grain boundaries. Moreover, cracking may occur over a wide corrosion potential range, as seen in BWR structures, or be confined to a narrow potential range for cracking in wheels of steam turbines in PWR (and fossil) plants when concentrated environments (e.g., hydroxide) may exist in occluded regions such as wheel keyways and blade attachment geometries.

The Blunting Criterion

In spite of this wide variety of characteristics, there is one attribute that governs whether crack initiation and propagation in carbon and low alloy steels can be sustained in operating plant. That criterion is that the corrosion rate at the crack tip must be considerably greater than that on the crack sides. If that criterion cannot be met, then the embryonic crack will degrade to a blunt pit.* This is especially the case at temperatures below 150 °C, at which the solubility of the magnetite on the crack sides is high. It is for this rather obvious reason that several observations of component failures may be explained. For example, BWR carbon steel feedwater lines operating at about 200 °C (392 °F) [Figure 5.9(a)], may exhibit signs of localized corrosion/pitting, leading to crack blunting, but in adjacent regions, crack propagation has occurred. At lower temperatures, less than 150 °C, it is difficult to initiate and maintain a sharp crack in water [Figure 5.9(b)].

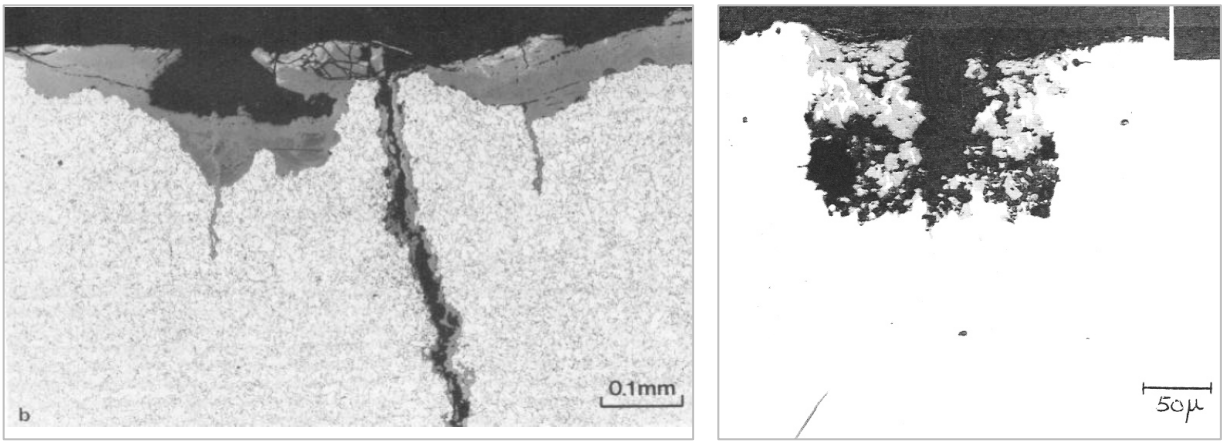

(a) (b)

Figure 5.9. (a) Incipient stress corrosion cracks in carbon steels BWR feedwater line [59].
(b) Transgranular cracking and pitting in SA333Gr6 carbon steel in water containing 1.8 ppm oxygen at 150 °C (302 °F) [58].
Reprinted from J. Hickling and D. Blind, "Strain-induced corrosion cracking of low alloy steels in LWR systems—Case histories and identification of conditions leading to susceptibility," *Nuclear Engineering and Design* 91, 305–330 (1986), with permission from Elsevier.

* This is not a limiting factor in nickel-base alloys and stainless steels in neutral environments because in these alloy-environment systems a protective oxide film is stable over the relatively wide pH/potential conditions expected in the crack enclave and the bulk environment in LWR systems.

It is possible, however, to counter this “blunting criterion” and sustain crack initiation and propagation in carbon steels and low alloy steels in low-temperature [<150 °C (302 °F)] water or condensing steam. This may be accomplished by either decreasing the corrosion rate of the crack sides or by increasing the crack tip propagation rate. The former is usually related to alloying additions (e.g., Cr) or potential/pH conditions leading to a protective oxide [50–75], whereas the latter may be related to material conditions that lead to enhanced plasticity at the crack tip.

Examples of such situations leading to cracking in LWRs are observed in CCW systems and in steam turbines. In the former case [76] the protection on the crack sides is provided by inhibitors added to the water for general corrosion protection, and in the latter case [77–82] the crack side protection may be associated with Cr, Mo and Ni alloying additions to the turbine wheel steel.

Stress corrosion cracking of carbon and low alloy steel components at elevated temperatures

At elevated temperatures (where the blunting criterion does not apply because of the low solubility of the oxide), cracking of unclad steam, feedwater, and condensate piping systems has been extensively analyzed [59, 83, 84] for German BWRs, where these components have been fabricated with relatively fine-grained, higher-strength steels (WB35, WB36) that allow the use of thinner walled piping without stress relief treatment of the welds. The features that aggravated the cracking susceptibility in these incidents were dynamic straining, high local stress, and oxidizing conditions.

Dynamic stress is associated with, for instance, changing loads during reactor start-up or thermal stratification during low feedwater flow or hot standby conditions. Such operations lead to a wide range of applied strain rates [12] that may be as high as 10^{-4} s^{-1} and would be expected to increase the crack propagation rate.

High local stresses at or above the high-temperature yield stress have been attributed in the failure analyses to weld defects (e.g., misalignment of weld edges, presence of root notches), piping fit-up stresses, and, in some cases, inadequate pipe support at elbows. The combination of this high stress adjacent to the weld and the high-applied strain rate led to a distribution of multiple cracks around the circumference of the pipe that was no longer confined by the asymmetric azimuthal distribution of weld residual stresses. The cracks propagated on separate planes and did not interlink, thereby potentially alleviating concerns about “leak before break” safety analyses that would be raised for a fully circumferential crack propagating evenly through the pipe wall.

Oxidizing conditions have a deleterious effect when they occur in conjunction with intermediate temperatures and anionic impurities. The affected piping generally operates in the temperature region 220 °C (428 °F) to 250 °C (482 °F). Moreover, cracking was often observed in stagnant areas of steam lines, where the dissolved oxygen concentration may be in excess of 100 ppb, which is well in excess of the 30 ppb “threshold” value, above which strain-induced cracking can be expected in these steels at 250 °C [85]. This conjunction of environmental factors was further aggravated by the fact that during reactor shutdown, stagnant water was sometimes left exposed to air in horizontal portions of piping. Pitting and general corrosion occurred under those low-temperature conditions, and the pits were observed to act as crack initiators during subsequent operation at more elevated temperatures.

Similar contributors to SCC susceptibility have been observed in transgranular cracking incidents in Model 44 and 51 designs of Westinghouse steam generators. This was initially noted in Europe, followed in 1982 by a well-analyzed cracking incident at the Indian Point-3 PWR [86] after approximately three effective full-power years. This cracking occurred at the upper shell-to-cone girth weld and was extensive, with over a hundred circumferential cracks propagating to a maximum depth of 25 mm. The cracking was attributed primarily to fatigue and SCC. Similar incidents were subsequently observed at other U.S. and European PWR plants [87].

As in the case discussed above for the higher-strength steels in German BWRs, the cracking in the PWR steam generators manufactured with lower-strength SA 302 grade B weldments and SA 533 grade B plate steels was aggravated by the fact that the weld was subjected to significant dynamic thermal stresses. In that case, the thermal stresses were due to the fact that the incoming feedwater at 204 °C (399 °F) to 227 °C (441 °F) came in contact with the hotter steam generator shell before mixing with the steam generator recirculating water.

Moreover, in the affected plants, this particular weld was the final closure weld, with a localized stress relief heat treatment being applied. However, subsequent hardness measurements indicated that the stress relief had not been fully effective. With respect to the stress/strain rate conditions, there had been extensive weld repairs applied at Indian Point-3, an operation that has been widely associated with premature cracking in, for instance, nickel base alloys in PWR primary components due to the attendant weld residual stresses.

Start-up operations, for instances where cracking in components were observed, involved the introduction of auxiliary feedwater from the condensate storage tank into the steam generator. Unfortunately, the water was aerated (a nitrogen blanket had not been applied to the condensate storage tank). This deleterious oxidizing condition was exacerbated by the presence of reducible Cu^{2+} cations associated with corrosion of the brass condenser tubes. Such oxidizing conditions promoted pitting; the pits in turn acted as initiation sites for the stress corrosion cracks. Poor chemistry control may also have increased the crack propagation rate.

Thus, the circumstances behind the cracking in these PWR steam generator incidences were the conjoint presence of oxidizing secondary water conditions and high residual stress, plus a component of dynamic straining and high hardness due to inadequate stress relief.

In summary, cracking has been observed on unclad components due to the combined effects of

- cold work and/or high yield stress,
- high tensile residual stress and/or stress concentration due to poor weld design,
- lack of effective stress relief heat treatment,
- dynamic loading due to thermal cyclic stress or mechanical vibrations, and
- elevation of the corrosion potential due to oxygen or other reducible species such as Cu^{2+}.

5.2.3.2 Current state of knowledge of predicting SCC in carbon and low alloy steels in LWRs

It is necessary to have a SCC prediction capability in order to assess the potential for EAC of carbon steels and low alloy steels in passive LWR components over the current 40 to 60 year

license period. That proven capability may then be used to assess the potential areas of concern for 60+ years of operation.

There is a pragmatic argument that the prediction capability should be based primarily on plant experience such as that described in the section above "because that represents the 'real world'." Such an approach has not proven to be practical for EAC of carbon steels and low alloy steels in LWRs because of the varying definitions of "failure" and, as illustrated in the section above, the large number of interacting material, stress, and environmental variables. The variables, which can have a significant effect on the cracking susceptibility, are not always adequately defined for a specific plant component. Moreover, there is not a large database of plant cracking incidents for carbon steels and low alloy steels under similar conditions that would allow a probabilistic analysis of future behavior, as has been done for cracking of Alloy 600 PWR steam generator tubes [88].

An alternative approach is to develop relationships between crack depth and time based on controlled laboratory conditions. This could make practical sense because the most sensitive system variables may be determined, and a mitigation strategy can be formulated. However, this approach to life prediction has proven to be difficult because of the extreme scatter in crack propagation rate data (Figure 5.10), which questions the validity of any disposition of formulated empirical relationship.

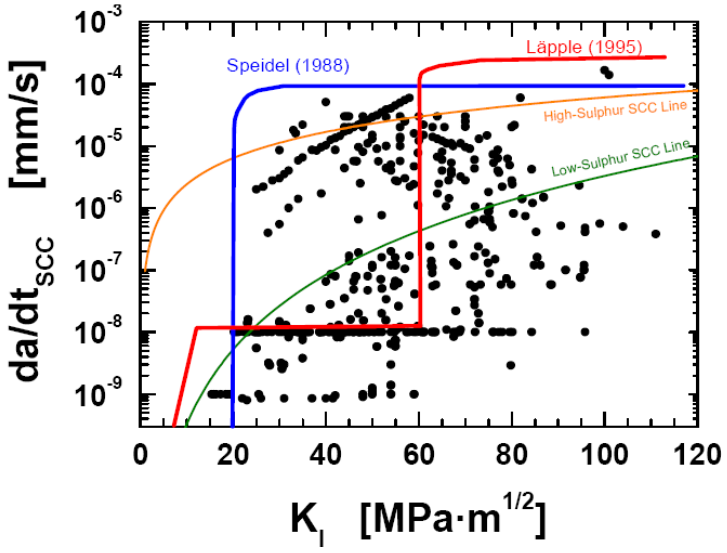

Figure 5.10. Bounding disposition relationships [89, 90] together with theoretical "high" and "low" sulfur relationships. Reprinted from M. O. Speidel and R. Magdowski, *International Journal of Pressure Vessels and Piping* 34, 119–142 (1988), with permission from Elsevier.

The reason for this variability can be attributed to inadequate control of a wide number of variables, such as the following:

- stress intensity and mode of stressing (e.g., constant load, constant displacement, loading rate, periodic unloading)
- test temperature
- MnS inclusion morphology and dispersion with respect to the crack plane

- corrosion potential as controlled by the coolant flow rate, alloy surface composition, dissolved hydrogen in the coolant, and the presence of oxidants such as oxygen, hydrogen peroxide, or cupric cations
- solution flow rate past the crack mouth (or, more specifically, the extent to which hydrodynamic conditions permit flushing out of the internal crack environment)
- anionic activity, especially sulfur (SO_4^{2-}, HS^-, S^{2-}) and chloride anions
- extent of crack tip constraint (i.e., plane stress vs. plane strain)
- yield stress of the material
- testing time and sequence of loading changes made during the test

There is no empirical relationship that correlates the crack propagation rate to all these variables. Thus another approach is needed. That approach is to develop an understanding of the mechanism of cracking that will provide a sufficient context in which to interrelate the observed cracking in the plant with the laboratory observations. Prime guidance is placed on the fact that most of the critical components are either clad with Type 308 SS or are shielded from the environment by Alloy 182 welds that attach, for instance, core shroud support plates to the pressure vessel. The practical question therefore is, “How rapidly would a crack propagate in the low alloy steel from a preexisting stress corrosion crack in the stainless steel cladding or Alloy 182 weldment?” Thus the emphasis has been on crack propagation in the carbon and low alloy steels rather than crack initiation.

A description of the research quantifying the effect of the individual system variables listed above on the crack propagation rate is well outside the scope of this chapter. The publication of that research has, however, been extensive [25, 58, 91–96] and covers the relationship between the crack propagation rate under constant stress and cyclic loading conditions.

In brief, the crack propagation hypothesis is that crack advance in the ductile structural alloys used in LWRs is related to Faraday’s electrochemical relationship between the advance of a crack tip and the oxidation charge density, Q_f . As illustrated in Figure 5.11, the propagation rate depends on (1) the oxide repassivation rate (*n*) following the rupture of the crack tip oxide; and (2) the periodicity of oxide rupture, which depends on the fracture strain of the crack tip oxide ε_f and the strain rate at the crack tip ($d\varepsilon/dt$).

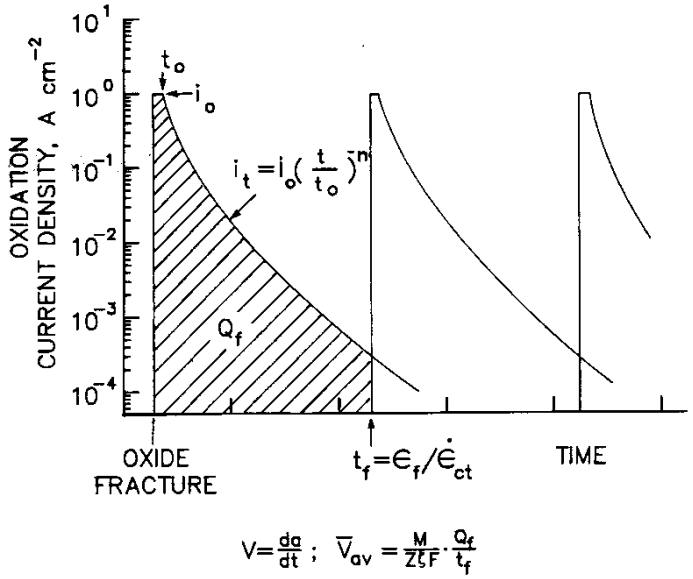

Figure 5.11. Elements of the slip-oxidation mechanism for crack propagation involving changes in oxidation current density following the rupture of the oxide at the crack tip [97, 98]. Reprinted with permission of The Minerals, Metals & Materials Society.

The average crack propagation rate can be characterized by the following general formula:

$$da/dt = A(d\varepsilon/dt)^{-n} , \quad (1)$$

where *n* is a function of the oxidation rate as the thermodynamically stable oxide re-forms at the strained crack tip (Figure 5.11) and is a function of the corrosion potential, material composition, and anionic activity at the crack tip.

There was extensive research during the 1980s to reformulate this general prediction formula in terms of “engineering parameters” such as the bulk environment (e.g., corrosion potential, anionic activity, flow rate) [92, 97, 98] the bulk material composition and heat treatment, and the stress or applied strain rate. Initial attention was focused on stainless steels under BWR conditions. This theory was appropriately modified to account for nickel-base alloys [99], the effect of irradiation on EAC propagation of stainless steels in BWR core components [95, 96], and carbon and low alloy steels [91, 93–96].

It was hypothesized that there were two major material and environmental differences from an EAC perspective between the austenitic alloys and carbon and low alloy steels. In the case of the austenitic alloys, the intergranular cracks were associated with grain boundary chromium depletion and the oxidation rate transients in crack tip environments that had enhanced chloride and sulfate concentrations.

By contrast, the transgranular cracking in the carbon and low alloy steels in high temperature water was associated with the dissolution of MnS inclusions (Figure 5.12) and the resultant S^{2-} and HS^{-} activity at the crack tip. These anions increased the oxidation rate transients at the crack tip such that the value of "n" in Figure 5.11 changed from a 0.3 in “high sulfur” concentrations to 1.0 in “low sulfur” concentrations. Physically these concentrations at the crack tip were determined by a balance between the various diffusion mechanisms (Fickian, potential, and

convection) that controlled the flux of these anions into and away from the crack tip region. Both the potential-driven diffusion and the crack propagation rate (which, depending on the density and size of the MnS inclusions, controlled the rate at which the MnS particles were exposed to the crack tip) could increase the S^{2-}/HS^{-} anionic activity at the crack tip (Figure 5.13).

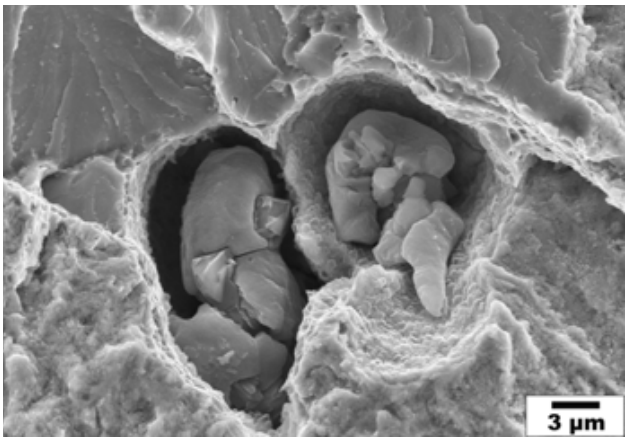

Figure 5.12. Partially dissolved MnS inclusions on the crack surface [100].

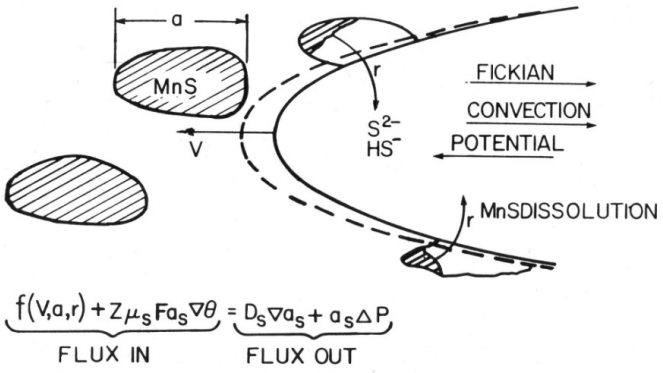

Figure 5.13. Schematic of crack tip illustrating the relationship between the MnS precipitate morphology and the advancing crack tip, and the various mass transport phenomena that control the anionic activity at the crack tip [94].

Experiments involving simultaneous microsampling of the crack tip liquid and the crack propagation rate with changes in corrosion potential [95, 96] confirmed the relationship between the crack propagation rate and the sulfur anionic activity at crack tip. This was important from a modeling perspective because separate experiments on simulated crack tip systems indicate that the bare surface oxidation rates increase as the dissolved sulfur anion activity increases from $<10^{-2}$ ppm ("low sulfur") to >10 ppm ("high sulfur").

Based on these observations, theoretical bounding crack propagation rate vs. crack tip strain rate relationships were formulated for "high sulfur" and "low sulfur" conditions and were compared with the observed crack propagation rates from tests in a variety of loading conditions (Figure 5.14) and environmental conditions (dissolved oxygen content, flow rate) that would influence whether the sulfur activity at the crack tip was "high" or "low."

The observed crack propagation rates agreed with the predicted rates for “high sulfur” conditions in 8 ppm oxygenated water over a wide crack tip strain rate range. However, as expected from the rationale associated with Figure 5.13, these high propagation rates could not be sustained when the crack propagation rate decreased below a critical value (which depended on conditions such as the dissolved oxygen content, and flow rate) because of the inability to introduce new soluble MnS inclusions to the crack tip enclave at a high enough rate. Consequently, below these critical propagation rates, the cracks slowed down and were subsequently arrested (Figure 5.15).

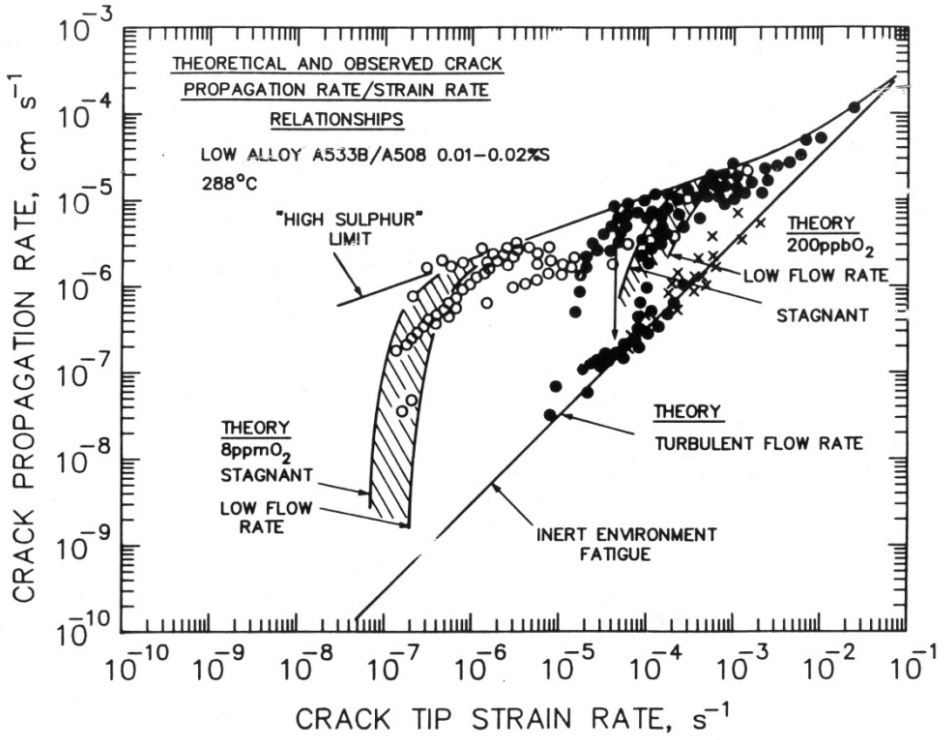

Figure 5.14. Observed and theoretical crack propagation rate/crack tip strain rate relations for low alloy steel in 288 °C water at various corrosion potentials [93, 94].The strain rate values are pertinent to tests conducted under corrosion fatigue (at the higher end), slowly increasing applied strain, and constant load creep (at the lower end).

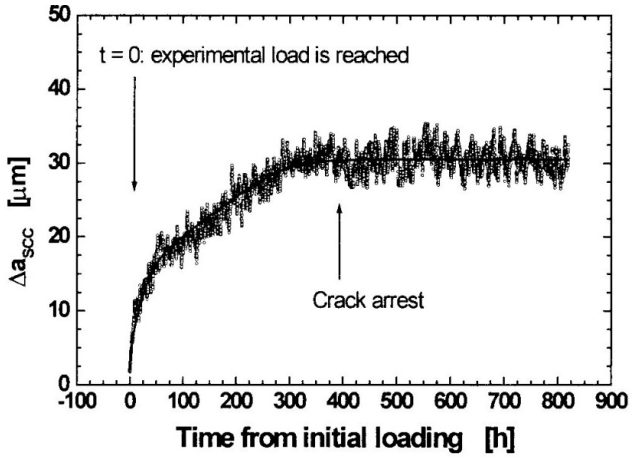

Figure 5.15. Crack length as a function of time for a low alloy steel specimen under constant load in high-temperature water [101].

Based on these results, two disposition crack propagation rate vs. stress intensity relationships were formulated for constant load stress corrosion conditions, depending on the system conditions that would lead to "high" [Equation (2)] or "low" [Equation (3)] sulfur conditions at the crack tip.

$$V = 9.6 \times 10^{-8} K^{1.4} \text{ mm·s}^{-1} , \quad (2)$$

$$V = 3.29 \times 10^{-14} K^{4} \text{ mm·s}^{-1} , \quad (3)$$

where K is in units of MPa√m. The maintenance of crack propagation rates associated with the "high" sulfur rates depends not only on the maintenance of a high crack tip sulfur activity but also on the maintenance of a sustainable crack tip strain rate. Thus the engineering system conditions that meet all these criteria for "high sulfur" propagation rates are combinations of the following:

- high-sulfur-content steels (>0.02 wt %) with the MnS inclusions in a segregated "banded" structure
- high corrosion potentials, >100 mV_{SHE}
- stagnant or low flow rate water
- highly impure water conditions, primarily >5 ppb chloride and, to a lesser extent, >100 ppb sulfate
- unconstrained plane stress crack tip conditions
- dynamic applied stress
- high yield stress, >800 MPa

Therefore, the extremely high propagation rates of the order of 10^{-4} mm/s that have been recorded in some laboratories (Figure 5.10) [36, 89, 102–104] approximate the predicted "high sulfur" propagation rate values that are maintained when combinations of the above system criteria under constant load or displacement conditions have been met.

It follows that sustained stress corrosion crack propagation is unlikely in low alloy RPV steels at the low corrosion potentials associated with PWR operations or BWRs operating under hydrogen

water chemistry conditions. Cracks may initially propagate at rates associated with the “low sulfur” rate [Equation (2)] in BWRs operating under “normal water chemistry conditions” but will be expected to arrest over time. Thus Equation (2) is predicted to be an upper limit (Figure 5.16) for stress corrosion under constant stress or displacement of low alloy steels in BWR systems operating according to the EPRI water chemistry guidelines. This disposition relationship has been adopted by EPRI [105] and accepted by the NRC.

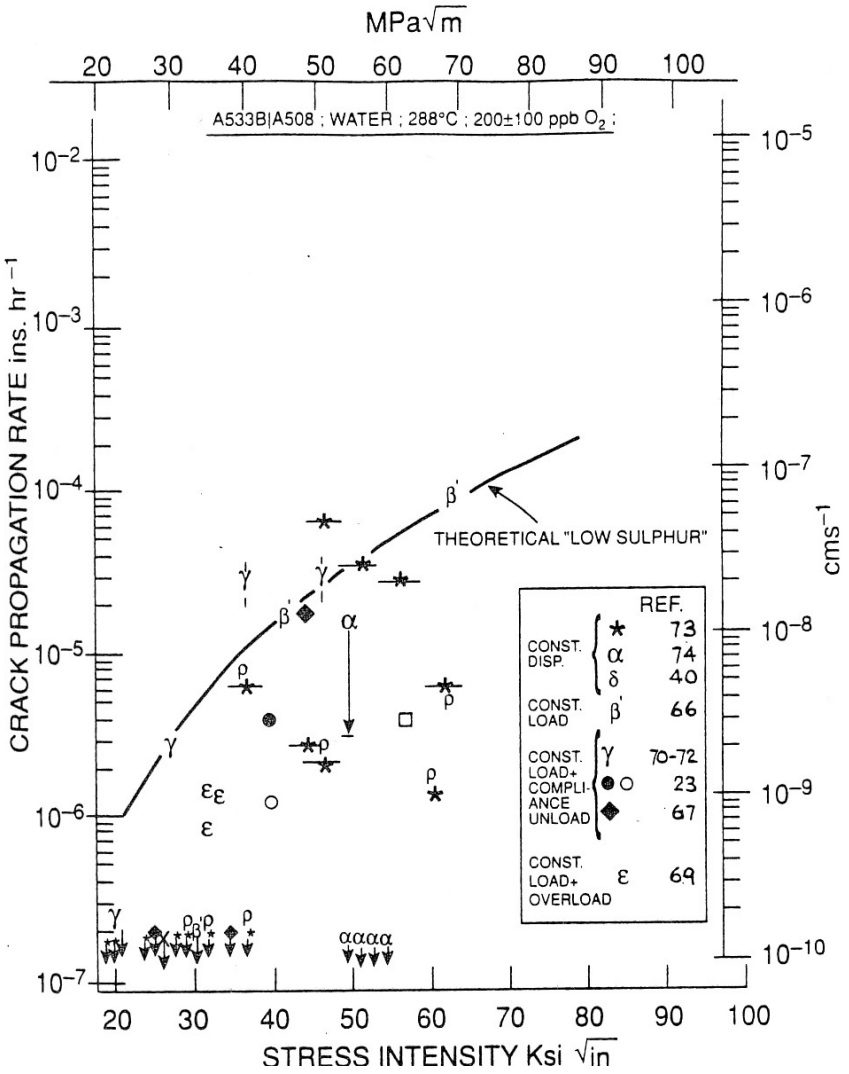

Figure 5.16. Theoretical “low-sulfur” crack propagation rate vs. stress intensity relationship [Equation (2)] compared with selected laboratory data obtained in 288 °C (550 °F) water containing 200 ppb oxygen, and stressed under constant load, constant displacement or constant load with periodic cycling conditions [94]. Copyright 1992 by the American Nuclear Society.

5.2.3.3 Concerns regarding SCC of carbon steels and low alloy steels beyond 60 years of operation

It is arguable, given the conjoint requirements for sustained SCC propagation discussed in the previous sections, that there is reasonable confidence that SCC will not be a major concern for carbon steels and low alloy steels for 40 to 60 year reactor operation, especially under the

current operating conditions where the corrosion potential is low in PWRs and in BWRs operating under hydrogen water chemistry, and where the reactors are not undergoing dynamic straining due to load following. However, there are concerns for extended operations beyond 60 years, where combinations of system variables may compromise the validity of current design and disposition criteria.

These concerns are described in the following subsections.

Stress corrosion cracking at dissimilar metal interfaces

Concern has been expressed about the possibility of a stress corrosion crack in 308 SS cladding or Alloy 182 weld continuing at a rapid, sustained, rate into the underlying low alloy steel. This would be a valid concern in BWRs (at, for instance, the H9 shroud support/pressure vessel joint) operating under “normal water chemistry” especially when the high local hardness [106, 107] and the complex metallurgical microstructure in the fusion zone adjacent to the weld are considered. It has been demonstrated that, in general, SCC in Alloy 182 in high-purity 288 °C (550 °F) water arrested [106–109] a propagating crack at or near the weld fusion line when the stress intensity factor was below 60 MPa√m (55 ksi√in) [107]. At that juncture the crack tip blunted into a pit or an oxide-plugged crack (Figure 5.17).

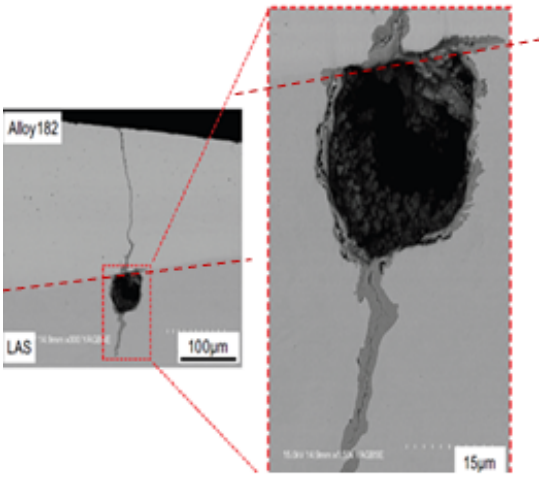

Figure 5.17. Cross-sectional view of low alloy steel bulk specimens after 1,500 h CBB exposure [108] illustrating the formation of a blunt pit in the low alloy steel, and a reactivated crack initiated after 1,500 h (but not 750 h) and propagating down a prior austenite grain boundary.

However, these arrested cracks can be reactivated as illustrated in Figure 5.17 from the pit in 2 ppm oxygenated water with an increase in sulfate to 20 ppb, or in 0.25 ppm oxygenated water with an increase in sulfate to 400 ppb [106]. As might be expected, there are combinations of stress intensity and anion concentration /corrosion potential that lead to sustained crack growth as the crack advanced into the A533B low alloy steel [107]. Transients in chloride concentration are markedly more detrimental than sulfate anions, as indicated in Figure 5.18(a). Indeed, in oxygenated water there is a very marked increase in sustained crack propagation rate to the upper theoretical value [Equation (1)] when the chloride concentration is of the order of 5 ppb [Figure 5.18(b)].

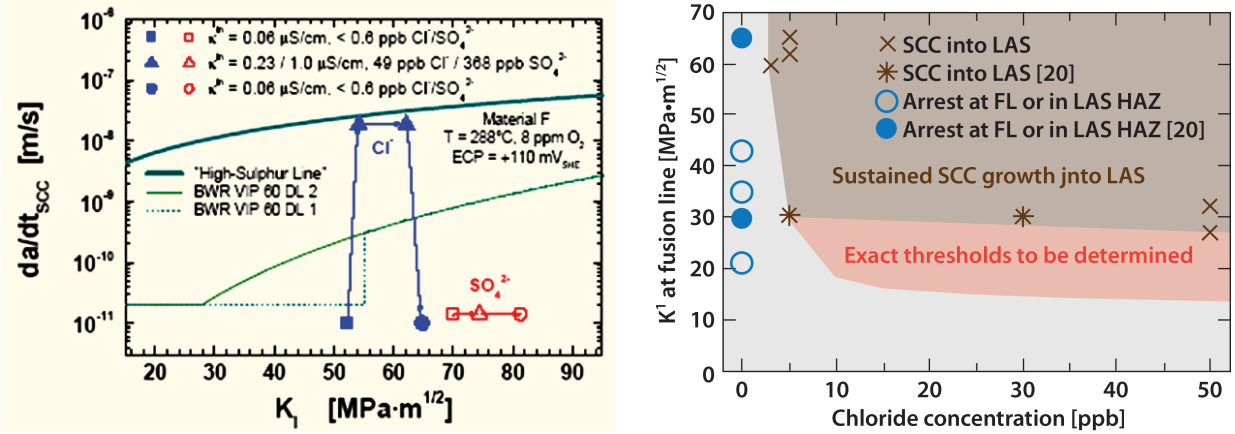

(a) (b)

Figure 5.18. (a) Effect of chloride and sulfate on the crack propagation rate of a low alloy steel in 8 ppm oxygenated water at 288 °C (550 °F) [110]. (b) Combinations of stress intensity factor and chloride concentration for sustained crack growth into the low alloy steel under BWR "normal water" chemistry conditions, after [107] (FL denotes “fusion line”).
Image (a) is copyright 2004 by the American Nuclear Society.

Presently, a consensus definition or mechanistic interpretation of these specific anionic effects is not available for the inclusion of these effects in life prediction models.

Although there is a reasonably acceptable, mechanisms-based rationale for the development of crack assessment and disposition relationships for SCC propagation, it is recognized that the framework is not complete and that the effects of several variables, in addition to the anionic specificity mentioned above, are not dealt with adequately. In order to assess potential material and component degradation for reactor operation beyond 60 years with reasonable certainty, the following factors need to be assessed and formulated:

Yield stress. It is widely acknowledged that increases in yield stress, or hardness, will increase the crack propagation rate in many alloy/environment systems. An example of this is given in Figure 5.19(a) for a Ni-Cr-Mo-V steam turbine disc alloy in water and in NaOH over the temperature range 100 °C (212 °F) to 110 °C (230 °F). A further example is illustrated in Figure 5.19(b) for a number of low alloy steels in oxygenated water at 288 °C (550 °F), where it is seen that at hardness levels >425 VHN the propagation rates for the “low sulfur” disposition value [equation (2)] are exceeded. Although the effects of hardness may be predicted in other alloys via formulation of the crack tip strain rate, such analyses have not yet been conducted for carbon steels and low alloy steels.

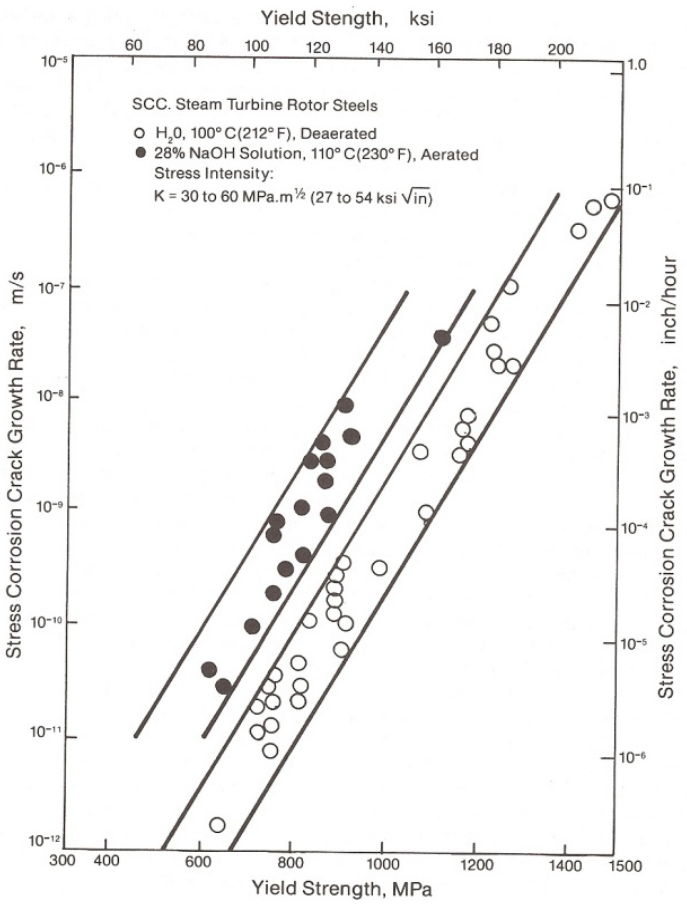

(a)

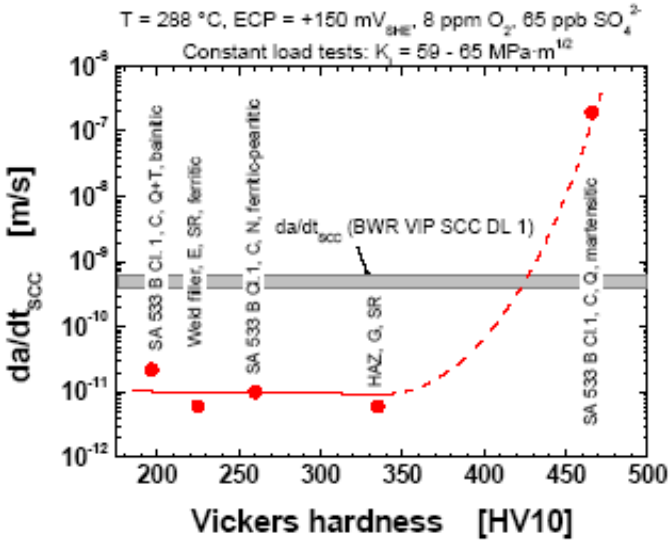

(b)

Figure 5.19. (a) Effect of yield stress and environment composition on crack propagation rate of Ni-Cr-Mo-V steel in deaerated water at 100 °C (212 °F) and aerated 28%NaOH at 110 °C (230 °F) [82]. (b) Effect of hardness on the crack propagation rate for various low alloy steels (e.g., weldments, plate) in 8 ppm oxygenated water containing 65 ppb SO_4^{2-} at 288 °C (550 °F) in comparison with the disposition propagation rate for the experimental conditions used [110].
Reproduced with permission of M. Speidel.

Periodic oxide rupture at an embryonic, as well as a mature, crack front is a common feature for a number of SCC hypotheses, and this dimensionally relates to the physical properties of the oxide (e.g., fracture strain) and the crack tip strain rate. However, the current crack tip strain rate algorithms as a function of engineering parameters (stress, stress intensity factor) do not take into account a number of physical phenomena, and hence there is epistemic uncertainty as to the completeness of the life prediction modeling (Figure 5.20).

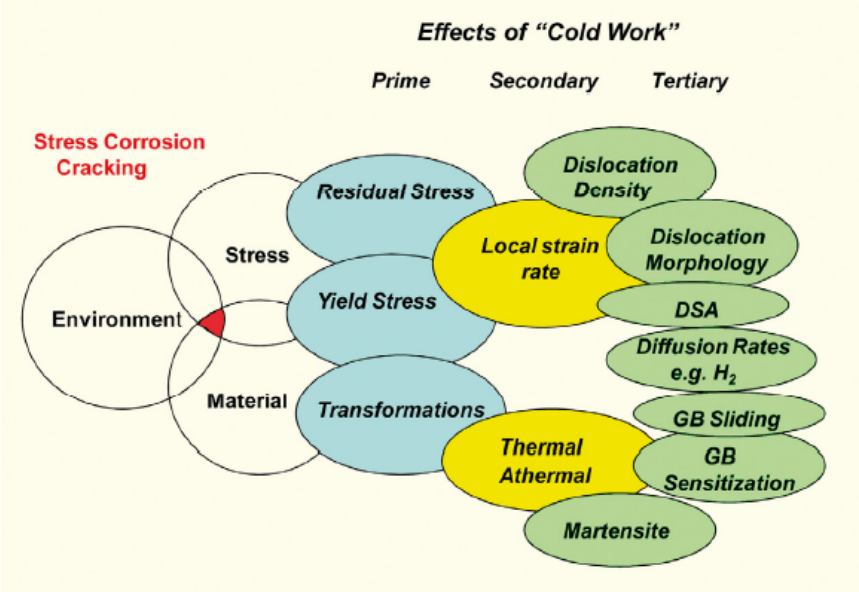

Figure 5.20. Interactions between the various parameters associated with "cold work" and their effect on the conjoint materials, environment and stress conditions for crack propagation.

These physical phenomena include the following:

- *Plasticity constraint.* Crack propagation rates markedly increase to values close to the upper theoretical limit associated with the "high sulfur" relationship when there is a significant degree of unconstrained plane stress rather than plane strain conditions. The practical impact for relatively thick carbon steel sections and low alloy steel sections is unclear at this time.

- *Ripple loading.* Small oscillations in stress on top of a high mean stress (ripple loading) or periodic unloading can under certain circumstances increase the crack propagation rate in a number of alloy/environment SCC systems, and this behavior has been noted for low alloy steels in BWR environments, to the extent that the "low sulfur" disposition propagation rate is exceeded. There are no crack tip strain rate algorithms that account for these dynamic loading effects, which could be important for reactor operations such as hot standby and thermal stress oscillations associated with increased coolant flow rates (e.g., power uprate).

- *Dynamic strain aging (DSA).* In recent years there has been an increasing number of observations that the stress corrosion and fatigue crack propagation rate is increased in those heats of low alloy steel having compositions that promote dynamic strain aging. Such an effect of discontinuous yielding, and the presumed effect on the crack tip strain rate, has again been observed in other alloy/environment systems (e.g., Al-Mg alloys in saline environments). There are no quantitative modifications to the current crack tip strain rate

algorithms that account for this physical metallurgical phenomenon, and there is no indication of the impact that such an understanding would have on the material composition specifications (Al, N). However, it is predicted (Figure 5.21) that the sensitivity of the crack propagation rate on dynamic strain aging (and yield stress) should be greater under constant load [Figure 5.21(a)] than under cyclic loading conditions [Figure 5.21(b)].

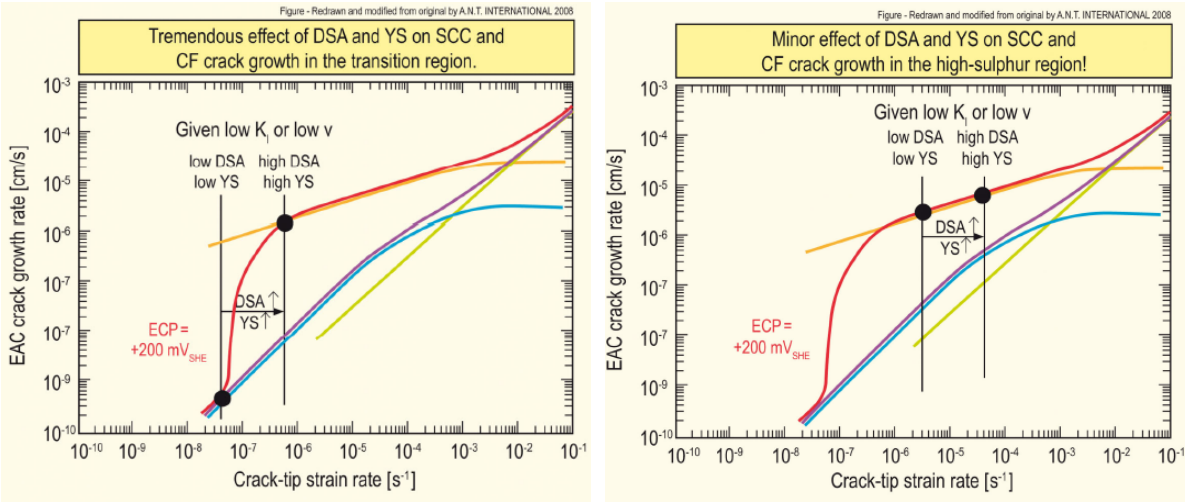

(a) (b)

Figure 5.21. Regions on the crack propagation rate/ crack tip strain rate diagram where dynamic strain aging and yield stress are likely to have (a) a large effect or (b) a small effect on EAC susceptibility of carbon steels and low alloy steels [100].

- *Residual stress profile (dK/da).* Andresen and coworkers have indicated that the stress corrosion crack propagation rate for stainless steels in high-temperature water can be markedly increased adjacent to weld fusion lines in the region where there is a positive dK/da residual stress profile. It is hypothesized that this stress intensity factor gradient effect may be related to an increase in the strain rate at the advancing crack tip. Such observations have not been conducted for carbon steels or low alloy steels but, if the hypothesis for the effect holds valid, then such phenomena could occur in other alloy/environment systems where the cracking depends on the prevailing strain rate at the crack tip.

In addition to these effects of specific material, environment, and stress variables on the SCC susceptibility of carbon and low alloys steels which need to be addressed for 60+ year operations, there is also concern of synergisms between SCC and other degradation modes whose influence may increase at extended operational times. These secondary degradation modes are as follows.

- *Creep/H_{ads}.* There have been several suggestions over the years relating SCC to the role of crack tip plasticity and the presence of absorbed hydrogen. Recently, Arioka and colleagues [111, 112] have demonstrated for cold-worked carbon steel that IGSCC in high-temperature, hydrogenated water and creep cracking in gaseous atmospheres have similar temperature dependence (Figure 5.22). Cavities were observed ahead of the crack tips, both in water and in air, and are believed to be the result of vacancy diffusion and coalescence to form crack embryos.

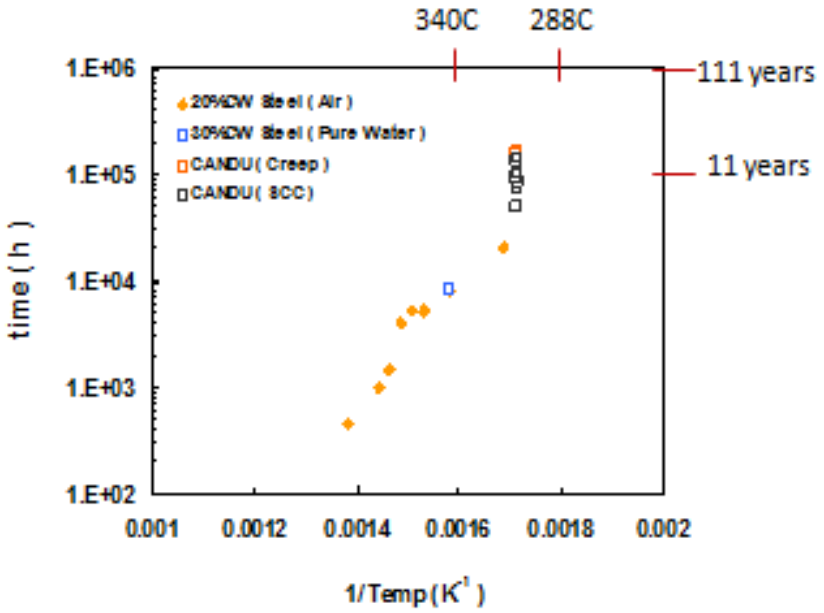

Figure 5.22. Temperature dependence for the crack initiation time in cold worked carbon steel due to creep in air or in high-temperature water [111, 112].

- *Irradiation hardening.* Irradiation embrittlement has long been of importance with respect to LWR operations and is the topic for discussion in another report. However, it is reasonable to propose that the increase in yield stress may well increase the EAC susceptibility of the RPV low alloy steel at regions where the steel has been exposed to the environment at the tips of cracks in the RPV cladding. Such a hypothesis has not been evaluated in terms of the increase in corrosion potential or in the degree of irradiation-induced residual stress relaxation.

- *Effect of the environment on fracture resistance.* An increasing number of investigators indicate that the fracture resistance maybe significantly decreased when testing is conducted in high-temperature water. This could have a measureable impact on safety analyses.

- *Temper embrittlement.* The impact toughness of ferritic steels varies as a function of tempering temperature, being concentrated in three temperature regions that are relevant to either the relatively short times associated with initial fabrication, or the extended time periods associated with plant operations.

  Intergranular fracture is possible in the temperature range of 200 °C (392 °F) to 400 °C (752 °F) in both carbon steels and low alloy steels with the sensitivity being markedly higher in martensitic rather than bainitic microstructures. A possible mechanism is associated with the formation of carbides due to the decomposition of martensite and, in particular, precipitation of the carbides in the form of films at grain boundaries.

  The embrittlement in the temperature range of 400–550 °C (752–1,022 °F) is confined to the bainitic structures of low alloy steels, particularly those containing higher Ni, Cr, and Mn compositions than the carbon steels (Table 5.1). The intergranular cracking is associated with the segregation of impurities such as Sn, Sb, As and, especially, P to the prior austenite

grain boundaries. Such embrittlement has received significant attention because it has been the cause for catastrophic failure of steam turbine discs. Intergranular fracture may occur along the ferrite grain boundaries of both carbon steels and low alloy steels after annealing at temperatures >650 °C for relatively short times (10 h).

The question arises as to whether temper embrittlement is possible in the carbon steels and low alloy steels used in LWR piping and RPVs either during fabrication or extended operational lives, and if it is possible, whether there can be a synergistic effect between the embrittlement and EAC. Temper embrittlement is possible (Figure 5.23) and may occur in the specified low alloy steel at relatively short times associated with fabrication PWHT. It is also possible [by extrapolation of data from 350 °C (662 °F) down to reactor operating temperatures] after extended operating times (>60 years). Caution is necessary, however, in making this conclusion because the steel investigated in Figure 5.23 had higher Ni, Cr, and P contents (which promote temper embrittlement) than those normal for RPVs such as A533B or 508. Some RPV steels, such as SA 508 Gr4N Class 1 [113], are the analogues of the 3.5NiCrMoV steam turbine steel that is prone to temper embrittlement, following stress relief heat treatments. Similarly, alloy 2Cr1Mo, which is used in cross-around piping for resistance to flow-accelerated corrosion, is similar to the steam turbine disc 3CrMo steel, which is prone to temper embrittlement.

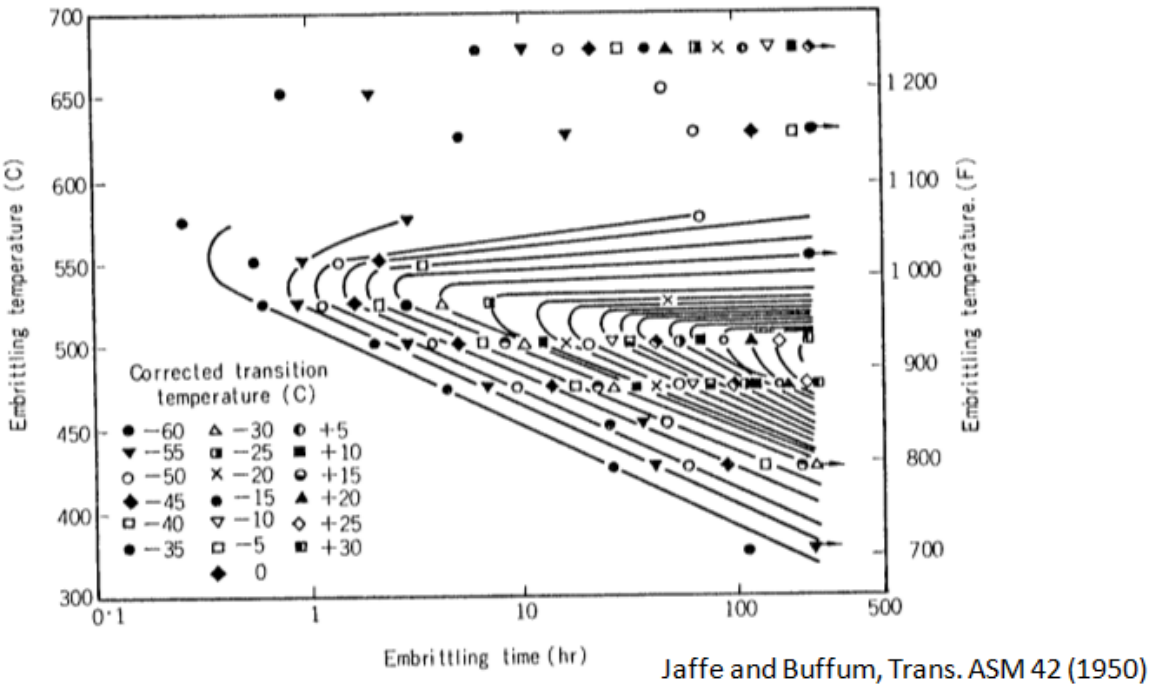

Figure 5.23. Effect of different tempering temperatures and times on the embrittlement of a low alloy steel (0.39C-0.79Mn-1.26Ni-0.77Cr-0.15P) where the different degrees of embrittlement are denoted by the changes in transition temperature [114].

Of interest in suggesting a synergistic interaction between SCC of low alloy steels in 288 °C water and temper embrittlement, is the observation of intergranular cracking down prior austenite grain boundaries of the low alloy steel in caustic environments [115].

5.3 SUMMARY

Carbon and low alloy steels are used for pressure-retaining components in the primary, secondary, and tertiary systems of both BWR and PWR systems. Corrosion and stress corrosion related forms of degradation have been noted in the past for these alloys. In the past, boric-acid corrosion, flow-accelerated corrosion, fatigue, and SCC under specific operating conditions have all been observed in service. In the original PMDA activity, most of carbon and low alloy steel issues in the RCS were expected to be manageable via current Aging Management Programs for the period of up to 60 years of operation. However for 60+ years of operation there is a need to take into account a changing "State of Knowledge" which challenges the original PMDA conclusions, especially with increased time for regulated Time Limited Aging Analyses (TLAA) such as fatigue, irradiation embrittlement and FAC. This is especially a factor given the fact that most U.S. reactors will be operating under power uprates, (water and steam flow rates, vibratory loading) and, potentially, load-following modes of operation.

Three specific areas of concern for 60+ years of operation were noted for carbon and low alloy steel. These include fatigue crack initiation, flow-accelerated corrosion, and stress corrosion cracking. Synergistic effects must also be considered.

- Fatigue crack initiation: The current RG 1.207 approach does not take into account the following factors, and therefore may impact the prediction capability out to 60-80 years. The fact that these factors are not addressed in the current approaches to CUF calculations raises some uncertainty about the quantification accuracy of corrosion fatigue crack initiation over extended operational times, when the number of actual cycles may be approaching the calculated maximum design value. Specific mechanistic elements that may be a factor include:
    - The MnS size and morphology are the parameters of importance not the sulfur content
    - The parameter of prime importance is the corrosion potential, not the dissolved oxygen content.
    - No account is given to the effect of water flow rate
    - No account is taken of the corrosion fatigue damage associated with complex strain /time patterns.
    - Of most importance, the water purity is not taken into account in spite of the very high sensitivity of the EAC sensitivity to sulphate, and especially chloride, concentrations.
- Flow-accelerated corrosion: Given the operating experience at Surry and Mihama, it is important to refine any prediction models to be accurate up to 80 years. Today, relatively accurate mechanisms–based FAC models exist and are used. However, a reassessment of the accuracy of empirically based models for 60+ years of service is needed.
- Stress corrosion cracking: SCC has occurred in closed coolant water systems, BWR feed water and steam lines, and PWR SG nozzles under very specific system conditions (e.g. oxygen, dynamic loading). There are number of observations coming to light since NUREG-6923 that have increased both the knowledge of the mode of degradation, but also the likelihood of environmentally assisted cracking concerns in extended operation.
    - *Stress corrosion Cracking at Dissimilar Metal Interfaces:* An increasing amount of data is indicating that crack propagation is arrested at a dissimilar metal weld when the crack (in e.g. Alloy182) reaches the LAS interface. However it is also apparent that the crack propagation may be reactivated under certain chemical conditions (Cl^-) very close to current Action Level 1.

- *Role of Yield Stress*: Increases in yield stress inevitably lead to increases in EAC susceptibility. There is some evidence for this in carbon and low alloy steels. The effect of irradiation damage and hardening at fluences associated with 80+ years on SCC is unknown.
- *Plasticity Restraint*: Transitions from plane strain to plane stress can give rise to increases in SCC propagation rate. It is unknown if this is a relevant factor for the geometries and loading in carbon steel piping.
- *Ripple Loading:* An increase in SCC susceptibility due to ripple loading is a well-recognized factor for carbon steels in lower temperature/ concentrated environments. This effect in higher temperature water is not clear, but could be of significance due to cyclic thermal stresses under power uprate conditions
- *Dynamic Strain Aging:* Dynamic strain aging has been increasingly implicated in SCC of LAS in accordance with similar effects of discontinuous yielding in other alloy/environment systems. It could become relevant to extended operations at reactor operating temperatures.

- *Synergistic effects:* There are possible synergies between EAC of carbon and low alloy steels and other degradation modes that become of significance as the operating time at LWR RCS temperatures increases towards 60+ years, apart from irradiation, mentioned earlier, there are the following possible interactions:
  - Creep and absorbed hydrogen/vacancy interactions that may increase the crack tip strain rate and/or introduce a component of hydrogen embrittlement
  - Temper-embrittlement, which can certainly play a synergistic role with SCC low alloy bainitic turbine disc steels. However, the role of temper-embrittlement associated in steels used in RPV and other LWR applications is less certain, particularly when the temper embrittlement may be associated with multiple stress relief treatments during fabrication or extended operational periods.

5.4 REFERENCES*

1. NRC, *Expert Panel Report on Proactive Materials Degradation Assessment,* NUREG Report CR-6923, U.S. Nuclear Regulatory Commission, February 2007.
2. EPRI, *EPRI Materials Degradation Matrix,* Document 3002000628, Electric Power Research Institute, May 2013.
3. NRC, *Generic Aging Lessons Learned (GALL) Report*, NUREG 1801, U.S. Nuclear Regulatory Commission, December 2010,
4. R. Pathania, "EPRI Materials Degradation Matrix Revision 1," EPRI Technical Report 1016486 Final Report, Electric Power Research Institute, May 2008.
5. Listing of conferences focused on the degradation of materials in water-cooled reactors:
   - *Proc. 1st Int. Symp. Environmental Degradation of Materials in Nuclear Power Systems—Water Reactors*, Myrtle Beach, Aug. 22–25, 1983, J. Roberts and W. Berry (eds.), National Association of Corrosion Engineers, 1984.
   - *Proc. 2nd Int. Symp. Environmental Degradation of Materials in Nuclear Power Systems—Water Reactors,* Monterey, Sept. 9–12, 1985, J. Roberts and J. Weeks (eds.), American Nuclear Society, 1986.

* Inclusion of references in this report does not necessarily constitute NRC approval or agreement with the referenced information.

- *Proc. 3rd Int. Symp. Environmental Degradation of Materials in Nuclear Power Systems—Water Reactors,* Traverse City, Aug. 30–Sept. 3, 1987, G.J. Theus and J. Weeks (eds.), The Metallurgical Society, 1987.
- *Proc. 4th Int. Symp. Environmental Degradation of Materials in Nuclear Power Systems—Water Reactors*, Jekyll Island, Aug. 6–10, 1989, D. Cubicciotti (ed.), National Association of Corrosion Engineers, 1990.
- *Proc. 5th Int. Symp. Environmental Degradation of Materials in Nuclear Power Systems—Water Reactors*, Monterey, Aug. 25–29, 1991, D. Cubicciotti and E. Simonen (eds.), American Nuclear Society, 1992.
- *Proc. 6th Int. Symp. Environmental Degradation of Materials in Nuclear Power Systems—Water Reactors,* San Diego, Aug. 1–5, 1993, E Simonen and R. Gold (eds.), The Minerals, Metals & Materials Society, 1993.
- *Proc. 7th Int. Symp. on Environmental Degradation of Materials in Nuclear Power Systems—Water Reactors*, Breckenridge, Aug. 7–12, 1995, R. Gold and A. McIlree (eds.), National Association of Corrosion Engineers, 1995.
- *Proc. 8th Int. Symp. Environmental Degradation of Materials in Nuclear Power Systems—Water Reactors*, Amelia Island, Aug. 10–14, 1997, A. McIlree and S. Bruemmer (eds.), American Nuclear Society, 1997.
- *Proc. 9th Int. Conf. Environmental Degradation of Materials in Nuclear Power Systems—Water Reactors*, Newport Beach, Aug. 1–5, 1999, S. Bruemmer, F. P. Ford and G. Was (eds.), The Minerals, Metals & Materials Society, 1999.
- *Proc. 10th Int. Conf. Environmental Degradation of Materials in Nuclear Power Systems—Water Reactors*, Lake Tahoe, Aug. 5–9, 2001, F. P. Ford and G. Was (eds.), National Association of Corrosion Engineers, 2002.
- *Proc. 11th Int. Conf. Environmental Degradation of Materials in Nuclear Power Systems—Water Reactors*, Stevenson, Aug. 10–14, 2003, G. Was and L. Nelson (eds.), American Nuclear Society, 2003.
- *Proc. 12th Int. Conf. Environmental Degradation of Materials in Nuclear Power Systems—Water Reactors*, Salt Lake City, Aug. 14–18, 2005, L. Nelson, P. King and T.R. Allen (eds.), The Minerals, Metals & Materials Society, 2007.
- *Proc. 13th Int. Conf. Environmental Degradation of Materials in Nuclear Power Systems,* Whistler, Aug. 19–23, 2007, P. King and T. Allen (eds.), The Canadian Nuclear Society, 2008.
- *Proc. 14th Int. Conf. Environmental Degradation of Materials in Nuclear Power Systems,* Virginia Beach, Aug. 23–27, 2009, T. Allen and J. Busby (eds.), American Nuclear Society, 2010.
- *Proc. 15th Int. Conf. Environmental Degradation of Materials in Nuclear Power Systems—Water Reactors,* Colorado Springs, Aug. 7–11, 2011, J. Busby and G. Ilevbare (eds.), The Minerals, Metals & Materials Society, 2012.
- *Proc. Fontevraud 1 Int. Symp.: Contribution of Materials Investigation to the Resolution of Problems Encountered in Pressurized Water Reactor Plants,* Société Française d'Energie Nucléaire, Paris, Sept. 2–6, 1985.
- *Proc. Fontevraud 2 Int. Symp.: Contribution of Materials Investigation to the Resolution of Problems Encountered in Pressurized Water Reactor Plants,* Société Française d'Energie Nucléaire, Paris, Sept. 10–14, 1990.
- *Proc. Fontevraud 3 Int. Symp.: Contribution of Materials Investigation to the Resolution of Problems Encountered in Pressurized Water Reactors*, F. de Keroulas and Ph. Berge (Meeting Chairs), Société Française d'Energie Nucléaire, Paris, Sept. 12–16, 1994.

- *Proc. Fontevraud 4 Int. Symp.: Contribution of Materials Investigation to the Resolution of Problems Encountered in Pressurized Water Reactors*, F. de Keroulas and Ph. Berge (Meeting Chairs), Société Française d'Energie Nucléaire, Paris, Sept. 14–18, 1998.
- *Proc. Fontevraud 5 Int. Symp.: Contribution of Materials Investigation to the Resolution of Problems Encountered in Pressurized Water Reactors,* F. de Keroulas and F. Hedin (Meeting Chairs), Société Française d'Energie Nucléaire, Paris, Sept. 23–27, 2002.
- *Proc. Fontevraud 6 Int. Symp.: Contribution of Materials Investigations to Improve the Safety and Performance of LWRs,* Société Française d'Energie Nucléaire, Paris, Sept. 18–22, 2006.
- *Proc. Fontevraud 7 Int. Symp.: Contribution of Materials Investigations to Improve the Safety and Performance of LWRs,* Société Française d'Energie Nucléaire, Avignon, Sept. 26–30, 2010.

6. T. G. Lian, Primary System Corrosion Research Program; EPRI Materials Degradation Matrix Revision 2, report 1020987, Electric Power Research Institute, August 2010.
7. R. Stark, *BWRVIP-167, BWR Vessel and Internals Project. Boiling Water Reactor Management Issue Tables,* Report 1014753, Electric Power Research Institute, January 2007.
8. D. Steininger, *Materials Reliability Program: Pressurized Water Reactor Issue Management Tables (MRP-205),* Report 1014446, Electric Power Research Institute, October 2006.
9. T. Shoji, Y. Takeda, J. Kuniya, P. Ford, and P. Scott, "Evaluation of Proactive Management Issues Associated with Materials Aging in Light Water Reactors," 3rd Int. Conf. on NPP Life Management (PLIM) for Long Term Operations, Salt Lake City, May 14–18, 2012, International Atomic Energy Agency.
10 W. Shack et al., *Fatigue Analysis of Components for 60-Year Plant Life,* NUREG/CR-6674 (PNNL-13227), U.S. Nuclear Regulatory Commission, June 2000.
11. W. E. Cooper, "The Initial Scope and Intent of the Section III Fatigue Design Procedure," *Technical Information from Workshop on Cyclic Life and Environmental Effects in Nuclear Applications,* Welding Research Council, Inc., 1992.
12. F. P. Ford, S. Ranganath, and D. Weinstein, *Environmentally-Assisted Cracking Fatigue Crack Initiation in Low Alloy Steels—A Review of the Literature and the ASME Code Requirements,* EPRI TR-102765, Electric Power Research Institute, 1993.
13. R. Kilian, J. Hickling, and R. Nickell, "Environmental Fatigue Testing of Stainless Steel Pipe Bends in Flowing, Simulated PWR Primary Water," *Proc. 3rd Int.Conf. Fatigue in Reactor Components,* Seville, Oct. 3–6, 2004, sponsored by EPRI, OECD, NEA/CSNI, and USNRC, MRP-151.
14. W. Alan Van Der Sluys, *PVRC's Position on Environmental Effects on Fatigue Life in LWR Applications*, Bulletin 487, Welding Research Council, Inc., December 2003.
15. H. S. Mehta, "An Update on the Consideration of Reactor Water Effects in Code Fatigue Initiation Evaluations for Pressure Vessels and Piping," pp. 45–51 in PVP Volume 410-2, ASME Pressure Vessels and Piping Conference, Seattle, 2000, American Society of Mechanical Engineers, 2000.
16. K. Iida, H. Kobayashi, and M. Higuchi, "Predictive Method of Low Cycle-Fatigue Life of Carbon and Low alloy Steels in High Temperature Water Environments," pp. 385–409 in

Vol. 2, *Proc. 2nd IAEA Specialists Meeting on Subcritical Crack Growth,* Sendai, Japan, May 15–17, 1985, International Atomic Energy Agency.

17. M. Higuchi and K. Iida, “Fatigue strength correction factors for carbon and low-alloy steels in oxygen-containing high-temperature water,” *Nuclear Engineering and Design* **129,** 293–306 (1991).

18. M. Higuchi and K. Iida, “Reduction in Low-Cycle Fatigue Life of Austenitic Stainless Steels in High–Temperature Water,” pp. 79–86 in *Pressure Vessel and Piping Codes and Standards,* PVP Vol. 353, D.P. Jones, B.R. Newton, W.J. O'Donnell, R. Vecchio, G.A. Antaki, D. Bhavani, N.G. Cofie, and G.L. Hollinger (eds.), American Society of Mechanical Engineers, New York, 1997.

19. M. Miksch, E. Lenz, and R. Lohberg, 9 MPA Seminar, Materialprüfungsanstalt Universität Stuttgart, Stuttgart, Germany, 1983.

20. F. Kassner, W. T. Ruther, H. M. Chung, P. D. Hicks, A. G. Hins, J. Y. Park, and W. J. Shack, “Fatigue and Environmentally-assisted Cracking in Light Water Reactors,” pp. 128–132 in *Proc. 19th Water Reactor Safety Information Meeting,* Bethesda, October 1991, NUREG/CP-0119, Vol. 1, U.S. Nuclear Regulatory Commission.

21. V. Philatov and A. Zelensky, “Low Cycle Fatigue of Structural Materials in Water Operating Environment,” pp. 215–221 in *Proc. 3rd International Atomic Energy Agency Specialists Meeting on Subcritical Crack Growth,* Moscow, May 1990, NUREG/CP-0112, Vol. 1, U.S. Nuclear Regulatory Commission.

22. J. B. Terrell and W. H. Cullen, “Fatigue Life Response of ASME SA 106-B Steel in Pressurized Water Environments,” pp. 155–172 and 215–221 in *Proc. 3rd International Atomic Energy Agency Specialists Meeting on Subcritical Crack Growth*, Moscow, May 1990, NUREG/CP-0112, Vol. 1, U.S. Nuclear Regulatory Commission.

23. D. A. Hale, S. A. Wilson, E. Kiss, and A. J. Gianuzzi, *Low Cycle Fatigue Evaluation of Primary Piping Materials in a BWR Environment,* Report GEAP 20244, General Electric, September 1977.

24. W. Shack et al., *Effects of LWR Coolant Environments on Fatigue Design Curves of Carbon and Low alloy Steels,* NUREG/CR-6583 (ANL-97/18), U.S. Nuclear Regulatory Commission, March 1998.

25. F. P. Ford, H. D. Solomon, L. M. Young, P. L. Andresen, D. Weinstein, A. Unruh, E. Tolksdorf, and R. Pathania, “Prediction of Corrosion Fatigue Crack Initiation in Low Alloy Pressure Vessel Steels,” pp. 315–325 in *Proc. Int. Symp. Plant Aging and Life Predictions of Corrodible Structures,* May 15–18, 1995, Sapporo, Japan.

26. O. K. Chopra and W. J. Shack, *Environmental Effects on Fatigue Crack Initiation in Piping and Pressure Vessel Steels,* NUREG/CR–6717, ANL–00/27, U.S. Nuclear Regulatory Commission, May 2001.

27. W. Shack et al., *Effects of LWR Coolant Environments on Fatigue Design Curves of Austenitic Stainless Steels,* NUREG/CR-5704 (ANL-98/31), U.S. Nuclear Regulatory Commission, April 1999.

28. H. Kanasaki et al., “Effect of Strain Rate and Temperature Change on the Fatigue Life of Stainless Steel in PWR Primary Water,” pp. 485–493 in *Trans. 14th Int. Conf. on Structural Mechanics in Reactor Technology (SMiRT 14)*, Lyon, France, 1997.

29. M. Higuchi, “Development of Evaluation Method of Fatigue Damage on Operating Plant Components in Considering Environmental Effect of LWR Coolant,” *Proc. 3rd Int. Conf.*

Fatigue of Reactor Components, Session 4: Code Rules and Guidelines, Seville, Spain, Oct. 3–6, 2004, OECD/EPRI.

30. O. K. Chopra and W. J. Shack, "Effects of Light Water Reactor Coolant Environments on Fatigue Crack Initiation in Carbon & Low–Alloy Steels and Austenitic Stainless Steels," *Proc. 3rd Int. Conf. Fatigue of Reactor Components*, NEA/CSNI/R(2004)21, Nuclear Energy Agency, 2005.
31. O. K. Chopra and W. J. Shack., *Effect of LWR Coolant on the Fatigue Life of Reactor Materials*, NUREG/CR-6909, U.S. Nuclear Regulatory Commission, February 2007.
32. NRC Regulatory Guide 1.207, *Guidelines for Evaluating Fatigue Analyses Incorporating the Life Reduction of Metal Components Due to the Effects of the Light Water Reactor Environment for New Reactors,* U.S. Nuclear Regulatory Commission, March 2007.
33. H. D. Solomon, R. DeLair, and E. Tolksdorf, "LCF Crack Initiation in WB 36 in High Temperature Water," pp. 865–874 in *Proc. 9th Int. Symp. Environmental Degradation of Materials in Nuclear Power Systems—Water Reactors,* Newport Beach, Aug. 1–5, 1999, S. Bruemmer, F. P. Ford, and G. Was (eds.), The Minerals, Metals & Materials Society, 1999.
34. C. J. Czajkowski, *Metallurgical Evaluation of an 18 inch Feedwater Line Failure at the Surry Unit 2 Power Station*, NUREG/CR-4868, Brookhaven National Laboratory, March 1987.
35. NISA, *Secondary Piping Rupture Accident at Mihama Power Station, Unit 3 of the Kansai Electric Power Co, Inc.—Final Report,* Nuclear and Industrial Safety Agency, Japan, 2005.
36. K. Kußmaul and B. Iskluth, "Environmentally Assisted Crack Growth in a Low Alloy Boiler Steel in High Temperature Water Containing Oxygen," *Nuclear Engineering and Design* **119,** 415–430 (1990).
37. R. L. Tapping, "Flow Accelerated Corrosion," Appendix B17 in *Expert Panel Report on Proactive Materials Degradation Assessment,* Report NUREG/CR-6923, U.S. Nuclear Regulatory Commission, 2007.
38. P. M. Scott, "Flow Accelerated Corrosion," in *Environmentally-Assisted Degradation of Carbon and Low Alloy Steels*, by P. Ford and P. Scott, Advanced Nuclear Technology International (ANTI), 2008.
39. B. Chexal, J. Horowitz, R. Jones, B. Dooley, and C. Wood, *Flow Accelerated Corrosion in Power Plants*, Report TR-106611, Electric Power Research Institute, June 1996.
40. C. Lemaignan, P. Scott, and B. Pierraggi, "La corrosion et l'oxydation des métaux dans les centrales nucléaires," pp. 415–420, Chapter 11 in *Oxydation de Matériaux Métalliques,* Lavoisier, 2003.
41. C. Wood, *BWR Water Chemistry Guidelines—2004 Revision*, Report TR-100819, Electric Power Research Institute.
42. R. K. Freier, "Operating Experiences with Protective Layers of Metal Oxides, Using Addition of Oxygen," *Vom Wasser,* Verlag Chemie Gmbh, Weinheim, Bergstr., vol. 38, 1971.
43. M. J. Davies, I. S. Woolsey, J. McGuigan, and T. Renwick, "Erosion-corrosion in AGR boilers," *Proc. Chimie 2002,* Societe Francaise d'Energie Nucleaire, 2002.
44. C. J. Bignold, C. H. de Whally, K. Garbett, and I. S. Woolsey, "Mechanistic aspects of erosion-corrosion under boiler feedwater conditions," pp. 219–226 in *Proc. Water Chemistry of Nuclear Reactor Systems III,* British Nuclear Energy Society, 1983.

45. J. Robertson, “The mechanism of high temperature aqueous corrosion of steel,” *Corrosion Science* **29,** 1275–1291(1989).

46. A. Bart, H. M. Crockett, L. F. Goyette, J. S. Horowitz, and R. Montgomery, “Flow accelerated corrosion—the entrance effect,” PVP2008-61185, *Proc. PVP2008, 2008 ASME Pressure Vessels and Piping Division Conference,* Chicago, 2008.

47. B. Poulson, “Advances in understanding hydrodynamic effects on corrosion,” *Corrosion Science* **35,** 655–665 (1993).

48. NRC*, Erosion/Corrosion-Induced Pipe Wall Thinning in U.S. Nuclear Power Plants*, NUREG-1344, U.S. Nuclear Regulatory Commission, April 1989.

49. EPRI, *CHECWORKS TM Computer Program Users Guide*, Report TR103198-P, Electric Power Research Institute, June 1998.

50. Y.S. Garud, “Issues and Advances in the Assessment of Flow Accelerated Corrosion,” Proc. 14th Int. Conf. Environmental Degradation in Nuclear Power Systems—Water Reactors, Virginia Beach, T. Allen and J. Busby (eds.), American Nuclear Society, 2010.

51. H. M. Crockett, N. Hiranuma, M. Honjin, and J. S. Horowitz, “A comparison of FAC programs in Japan and the United States,” PVP2008-61311, *Proc. 2008 ASME Pressure Vessels and Piping Division Conference*.

52. S. Uchida et al., "Evaluation of Wall Thinning Rate due to Flow Accelerated Corrosion with the Coupled Models of Electrochemical Analysis and Double Layer Oxide Analysis" *Proc. 14th Int. Conf. Environmental Degradation in Nuclear Power Systems—Water Reactors,* Virginia Beach, T. Allen and J. Busby (eds.), American Nuclear Society, 2010.

53 T. Satoh et al. "Effects of Alloy Composition of Carbon Steel on the Flow Accelerated Corrosion and Oxide Film Prperties in Neutral Water Condition", *Proc. 14th Int. Conf. Environmental Degradation in Nuclear Power Systems—Water Reactors,* Virginia Beach, T. Allen and J. Busby (eds.), American Nuclear Society, 2010.

54. A. Zander and H. Nopper, “The COMSY code for the detecting of piping degradation due to flow-accelerated corrosion,” PVP2008-61823, *Proc. PVP2008, 2008 ASME Pressure Vessels and Piping Division Conference,* July 27–31, 2008, Chicago.

55. M. Persoz, J-B. Bouvier, E. Ardillon, and S. Trévin, “Analysis of thickness measurements on secondary lines in EDF PWRs to evaluate the accuracy of the flow-accelerated corrosion monitoring software: BRT-CICERO,” pp.147–157 in *Proc. Fontevraud 6 Int. Symp.,* Société Française d'Energie Nucléaire, Paris, Sept. 18–22, 2006.

56. S. Trevin et al., “Flow accelerated corrosion mitigation at EDF with BRT-CICEROTM. Feedback of version 3 and process of validation,” *Proc. Fontevraud 7 Int. Symp.,* Société Française d'Energie Nucléaire, Avignon, Sept. 26–30, 2010, pp. A090 T07.

57. G. J. Bignold, K. Garbett, and L. S.Woolsey, “Mechanistic Aspects of the Temperature Dependence of Erosion–Corrosion,” *Proc. Conf. Corrosion Erosion of Steels in High Temperature Water and Wet Steam,* eds. Ph Berge, F. Kahn, Electricitie de France, 1982.

58. F. P. Ford, “A Mechanism of Environmentally Controlled Crack Growth for Structural Steels in High Temperature Water,” *IAEA Specialists Meeting on Crack Growth*, Freiburg, Germany, May 13–15, 1981.

59. J. Hickling and D. Blind*,* “Strain-induced corrosion cracking of low alloy steels in LWR systems—Case histories and identification of conditions leading to susceptibility,” *Nuclear Engineering and Design* **91,** 305–330 (1986).

60. R. N. Parkins, “The Stress Corrosion Cracking of Mild Steels in Nitrate Solution,” *Journal Iron and Steel Institute* **172,** 149 (1952).

61. R. N. Parkins, “Stress Corrosion Cracking of Low Carbon Steels,” p. 361 in *Fundamental Aspects of Stress-Corrosion Cracking,* R. W. Staehle, A. J. Forty, and D. VanRooyen (eds.), National Association of Corrosion Engineers, Houston, 1967.

62. J. A. S. Green and R. N. Parkins, “Electrochemical Properties of Ferrite and Cementite in Relation to Stress Corrosion of Mild Steels in Nitrate Solutions,” *Corrosion* **24,** 66 (1968).

63. R. N. Parkins “Stress Corrosion Spectrum,” *British Corrosion Journal* **7,** 15 (1972).

64. R. N. Parkins, R. W. Slatterly, W. R. Middleton, and M. J. Humphries, “Effects of quenching and tempering upon the stress corrosion cracking of ferritic steels,” *British Corrosion Journal* **8,** 117 (1973).

65. R. N. Parkins, “Environment Sensitive Fracture and its Prevention” *British Corrosion Journal* **14,** 5 (1975).

66. R. N. Parkins and B. S. Greenwell, “The interface between corrosion fatigue and stress corrosion cracking,” *Metal Science* **405** (August 1977).

67. R. N. Parkins and R. R. Fessler, “Stress corrosion cracking of high-pressure gas transmission pipelines,” *International Journal of Materials in Engineering Applications* **1,** 80 (1978).

68. R. N. Parkins, P. W. Slatterly, and B. S. Poulson, “The Effects of Alloying Additions to Ferritic Steels upon Stress Corrosion Cracking Resistance,” *Corrosion* **37**(11), 650–664 (1981).

69. R. N. Parkins, A. Alexandridou, and P. Majumdar, “Stress corrosion cracking of C–Mn steels in environments containing carbon dioxide,” *Materials Performance* **25,** 20 (1986).

70. R. N. Parkins and Z. A. Foroulis, “Stress corrosion cracking of mild steel in monoethanolamine solutions,” *Materials Performance* **27,** 19 (1988).

71. R. N. Parkins, “Stress Corrosion Cracking,” p. 1 in *Proc. 1st Int. Conf. Environment-Induced Cracking of Metals,* National Association of Corrosion Engineers, Houston, 1990.

72. R. N. Parkins and P. M. Singh, “Stress Corrosion Crack Coalescence,” *Corrosion* **26,** 485 (1990).

73. R. N. Parkins, “Mechanistic Aspects of SCC,” p. 3-42 in *Parkins Symp. Fundamental Aspects of Stress Corrosion Cracking,* S. M. Bruemmer et al. (eds.), American Institute of Mining, Metallurgical, and Petroleum Engineers, 1992.

74. R. N. Parkins, “Stress Corrosion Cracking of Ferritic Steels,” *Corrosion, Vol. 1, Metal/Environment Interactions,* 3rd ed., L. L.Shreir, R. A Jarman, and G. T. Burstein (eds.), 1994.

75. R. N. Parkins, “Stress Corrosion Cracking,” *Uhlig’s Corrosion Handbook, Second Edition,* R. Winston Revie (ed.), Wiley, 2000.

76. O. Jonas, *Stress Corrosion Cracking in PWR and BWR Closed Cooling Water Systems,* Report TR1009721, Electric Power Research Institute, October 2004.

77. J. M. Hodge and I. L. Mogford, “UK experience of stress corrosion cracking in steam turbine discs,” *Proceedings of the Insttution of Mechanical Engineers* **193,** 93–109 (1979).

78. R. E. Sperry, S. Toney, and D. J. Shade, “Some adverse effects of stress corrosion in steam turbines,” *Journal of Engineering for Power,* pp. 255–260, April 1977.

79. J. R. Weeks, *Stress Corrosion Cracking of Turbine Rotors in Nuclear Powered Reactors,* Report BNL-NUREG 22689-R, Brookhaven National Laboratory, 1978.

80. F. F. Lyle, A. J. Basche, H. C. Burghard, Jr., and G. R. Leverant, “Stress Corrosion Cracking of Steels in Low-Pressure Turbine Environments,” Corrosion 80, Chicago, March 1980, S. P. Lynch (ed.), *Metals Forum* **2,** 189 (1979).

81. B. W. Bussert, R. M. Curran, and G. C. Gould, “The Effect of Water Chemistry on the Reliability of Modern Large Steam Turbines,” *Journal of Engineering for Power* 1-6 (1978).

82. M. O. Speidel and J. E. Bertisson, “Stress Corrosion Cracking of Steam Turbine Rotors,” pp. 331–360 in *Corrosion in Power Generating Equipment,* M. O. Speidel and A. Atrens (eds.), Plenum Press, New York, 1984.

83. J. Hickling, H-P. Seifert, and S. Ritter, “Research and Service Experience with Environmentally Assisted Cracking of Low Alloy Steel,” *Power Plant Chemistry* **7,** 4–15 (2005).

84. H.-P. Seifert, S. Ritter, and J. Heldt, “Strain-Induced Corrosion Cracking of Low Alloy RPV Steels under BWR Conditions,” *Proc. 10th Int. Conf. Environmental Degradation of Materials in Nuclear Power Systems—Water Reactors,* Lake Tahoe, Aug. 5–9, 2001, F. P. Ford and G. Was (eds.), National Association of Corrosion Engineers, 2002.

85. T. Arai et al., “SCC Maps for low-alloy steels by SSRT method,” Paper 140, NACE Corrosion Conference, National Association of Corrosion Engineers, 1998.

86. W. J. Bamford, G. V. Rao, and J. L. Houtman, “Investigation of Service-Induced Degradation of Steam Generator Shell Materials,” *Proc. 5th Int. Symp. Environmental Degradation in Nuclear Power Systems–Water Reactors,* American Nuclear Society, 1991.

87. NRC, *Cracking of the Upper Shell to Transition Cone Girth Welds in Steam Generators*, Information Notice No. 90-04, U.S. Nuclear Regulatory Commission, 1990.

88. R. W. Staehle, “Variability in the Corrosion of Materials in LWR Environments,” Appendix B19 in J.X. Muscara, *Expert Panel Report on Proactive Materials Degradation Assessment,* NUREG/CR-6923, U.S. Nuclear Regulatory Commission, February 2007.

89. M. O. Speidel and R. Magdowski, “Stress corrosion cracking of nuclear reactor pressure vessel and piping steels,” *International Journal of Pressure Vessels Piping* **34,** 119–142 (1988).

90. V. Läpple, D. Blind, and P. Deimel, “Stand der Forschung zum Korrosionsgestützte Rißwachstum Niedriglegierter Ferritischer Stähle in Sauerstoffhaltigem Hochtemperaturwasser,” *VGB-Konferenz, Chemie im Kraftwerk 1996,* October 1996.

91. F. P. Ford, “Prediction of Corrosion Fatigue Initiation in Low Alloy Steel and Carbon Steel/Water Systems at 288 °C,” pp.9–16 in *Proc. 4th Int. Symp. Environmental Degradation in Nuclear Power Systems—Water Reactors,* Jekyll Island, Aug. 6–10, 1989, D. Cubicciotti and E. Simonen (eds.), National Association of Corrosion Engineers, 1990, ISBN 1-877914-04-5.

92. F. P. Ford, D. F. Taylor, P. L. Andresen, and R. G. Ballinger, *Corrosion-Assisted Cracking of Stainless Steel & Low alloy Steels in LWR Environments,* Report NP5064S, Electric Power Research Institute, 1987.

93. F. P. Ford and P. L. Andresen, “Corrosion Fatigue of A533B/A508 Pressure Vessel Steels in 288 °C Water,” pp.105–124 in *Proc. 3rd Int. Specialists Meeting on Sub Critical Crack Growth,* Moscow, USSR, 1990, W.Cullen (ed.), NUREG/CP-0112, Vol. 1, U.S. Nuclear Regulatory Commission.

94. F. P. Ford, P. L. Andresen, D. Weinstein, S. Ranganath, and R. Pathania, “Stress Corrosion Cracking of Low Alloy Steels in High Temperature Water,” pp. 561–568 in *Proc. 5th Int. Symp. Environmental Degradation in Nuclear Power Systems—Water Reactors,* Monterey, D. Cubicciotti and E. Simonen (eds.), American Nuclear Society, 1992.

95. P. L. Andresen and L. M. Young, “Crack Tip Microsampling and Growth Rate Measurements in Low Alloy Steel in High Temperature Water,” *Corrosion* **51**(3), 223–233 (1995).

96. L. Young and P. L. Andresen, “Crack Tip Microsampling and Growth Rate Measurements in a 0.01%S Low Alloy Steel,” pp.1193–1204 in *Proc. 7th Int. Symp. Environmental Degradation in Nuclear Power Systems—Water Reactors,* Breckenridge, R. Gold and A. McIlree (eds.), National Association of Corrosion Engineers, 1996.

97. F. P. Ford, “The Crack Tip System & Its Relevance to the Prediction of Cracking in Aqueous Environments,” pp. 139–165 in *Proc. 1st Int. Conf. Environmentally Assisted Cracking of Metals,* R. Gangloff and B. Ives (eds.), National Association of Corrosion Engineers, 1988.

98. P. L. Andresen, “Modelling of Water and Material Chemistry Effects on Crack Tip Chemistry and Resulting Crack Growth Kinetics,” pp. 301–314 in *Proc. 3rd Int. Symp. Environmental Degradation in Nuclear Power Systems–Water Reactors,* The Metallurgical Society, 1987.

99. P. L. Andresen, “Observation and Prediction of the Effects of Water Chemistry and Mechanics on Environmentally Assisted Cracking of Inconels 182 Weld Metal and 600,” *Corrosion* **44,** 376 (1988).

100. H.-P. Seifert and S. Ritter, *Environmentally-Assisted Cracking in Carbon and Low Alloy Steels in High Temperature Water*, SKI Report 2005:60, Statens Kärnkraftinspektion Swedish Nuclear Power Inspectorate, 2005.

101. V. Läpple, Einfluß von Probengeometrie und Belastungsart auf das Bedingungen, *Korrosionsgestützte Rißwachstum Niedriglegierter Ferritischer Stähle unter SWR-Zusatzauftrag: Auswertung des EPRI-Forschungsberichtes RPC 102-4, und Vergleich mit Korrosionsergebnissen der MPA Stuttgart*, MPA/VGB Forschungsvorhaben 3.1.2.5; MPA Auftrags Nr 944 703 700, February 1997.

102. K. Kussmaul et al., “Experience in the replacement of safety related piping in German boiling water reactors, *International Journal of Pressure Vessels Piping* **25,** 111–138 (1986).

103. E. Tenckhoff, M. Erve, E. Lenz, and G. Vazoukis, “Environmentally assisted crack growth in low alloy steels—results and their relevance to LWR components,” *Nuclear Engineering and Design* **119,** 371–378 (1990).

104. J. Matocha, V. Hluchan, J. Wozniak, I. Jiricek, and J. Vosta, “Environmentally-Assisted Cracking of Steam Generator Pressure Vessel Steel in High Temperature Water,” *Proc. 3rd International Atomic Energy Agency Specialists Meeting on Subcritical Crack Growth,* Moscow, USSR, May 1990.

105. EPRI, *Evaluation of Stress Corrosion Crack Growth in Low Alloy Steel Vessel Materials in BWR Environment,* BWR VIP-60, Report TR108709, Electric Power Research Institute, March 1999.

106. Q. Peng, H. Xue, J. Hou, Y. Takeda, J. Kuniya, and T. Shoji, “Stress Corrosion Cracking in the Fusion Boundary Region of an Alloy182-A533B Low Alloy Steel Dissimilar Weld Joint,” *Proc. Fontevraud 7 Int. Symp.,* Société Française d'Energie Nucléaire, Avignon, Sept. 26–30, 2010.

107. S. Ritter, H. P. Seifert, and H. J. Leber, “The Environmentally Assisted Cracking in the Transition Region of the Nickel-Base Alloy / Low Alloy Steel Dissimilar Metal Joints Under Simulated BWR Conditions," pp. A023 T02 in *Proc. Fontevraud 7 Int. Symp.,* Société Française d'Energie Nucléaire, Avignon, Sept. 26–30, 2010.

108. T. Kubo, M. Itow, N. Tanaka, and T. Saito, “SCC Retardation and Propagation Behaviour in Dissimilar Weldment of Alloy 182 and Low alloy Steel,” pp. 935–944 in *Proc. 14th Int. Conf. Environmental Degradation in Nuclear Power Systems—Water Reactors,* Virginia Beach, T. Allen and J. Busby (eds.), American Nuclear Society, 2010,.

109. H. Abe, M. Ishizawa, and Y. Watanabe, “Stress Corrosion Cracking Behaviour near the Fusion Line of Dissimilar Weld Joint with Alloy 182-A533B Low Alloy Steel,” pp. 791–802 in *Proc. 15th Int. Conf. Environmental Degradation in Nuclear Power Systems–Water Reactors,* J. Busby, G. Ilevbare, P. Andresen (eds.), The Metallurgical Society, Colorado Springs, 2011.

110. H.-P. Seifert and S. Ritter, “New Observations of the SCC Crack Growth Behaviors of Low alloy RPV Steels under BWR/NWC Conditions,” pp. 341–350 in *Proc. 11th Int. Conf. Environmental Degradation in Nuclear Power Systems—Water Reactors,* Skamania Lodge, G. Was and L. Nelson (eds.), American Nuclear Society, 2004.

111. K. Arioka, T. Miyamoto, T. Yamada, and T. Terachi, “Formation of Crack Embryos Prior to Crack Growth in High Temperature Water,” pp. 895–905 in *Proc. 14th Int. Conf. Environmental Degradation in Nuclear Power Systems–Water Reactors,* American Nuclear Society, 2010.

112. K. Arioka, T. Miyamoto, T. Yamada, and T. Terachi, “Role of Cavity Formation on Crack Growth of Cold-Worked Carbon Steel, TT 690 and MA 600 in High Temperature Water,” pp. 55–70 in J. T. Busby, G. Ilevbare, and P. L. Andresen (eds.), *15th International Conference on Environmental Degradation of Materials in Nuclear Power Systems-Water Reactors*, John Wiley & Sons, Inc., Hoboken, New Jersey, 2011.

113. D. B. Knorr, “An Evaluation of Temper Embrittlement in A508 Grade 4N Steel,” pp. 845–851 in *Proc. 9th Int. Symp. Environmental Degradation in Nuclear Power Systems—Water Reactors*, Newport Beach, S. Bruemmer and F. P. Ford (eds.), The Metallurgical Society, 2000.

114. L. D. Jaffe and D. C. Buffum, “Isothermal temper embrittlement,” *Transactions of the American Society of Metals* **42,** 604–614 (1950).

115. R. P. Harrison, D. deG. Jones, and J. F. Newman, “Caustic Cracking of Temper Embrittled Steels,” pp. 659–662 in *Proc. Stress-Corrosion Cracking and Hydrogen Embrittlement of Iron-Base Alloys,* National Association of Corrosion Engineers, Houston, 1977.

6. DEGRADATION OF CAST STAINLESS STEEL COMPONENTS UNDER EXTENDED SERVICE CONDITIONS

Jeremy Busby
Oak Ridge National Laboratory, Oak Ridge, Tennessee

6.1 BACKGROUND

Cast stainless steels are important class of materials in modern LWR facilities. Cast stainless steels are often chosen in areas for economic reasons. Historically, cast stainless steel grades have performed well in nuclear reactor applications and there are relatively few key degradation modes of concern.

Today, cast austenitic stainless steels (CASS) are used in a variety of applications in both BWRs and PWRs. Common alloys in service include the CF3 and CF8 series of alloys with the CF3, CF3A, CF3M, CF8, CF8A, and CF8M being the most prominent choices. Typical nuclear power plant applications and material grades of CASS include the use of CF8A, CF8M, and CPF3M for reactor coolant and auxiliary system piping. Reactor coolant pump casings are typically made from type CF8, CF8A, or CF8M CASS. Reactor coolant valve bodies and fittings often use CF8A or CF8M. In later construction and replacements, CF3s have been used rather than CF8s.

These alloys are exposed to elevated temperatures and corrosive environments. Piping and pump casings in BWRs may be exposed to NWC, HWC, and in some locations, lower level irradiation. In PWRs, these alloys experience the primary water environment.

Overall, degradation modes for CASS in reactor applications are relatively minor when compared to other alloy systems under normal operating conditions through 40 or 60 years of life. Thermal aging and irradiation effects are not considered to be areas of concern given the relatively low temperatures and fluences over that lifetime. There have been limited cases of SCC in CASS components in both BWRs and PWRs; however, these are attributed to irregularities in composition or microstructure rather than general vulnerabilities. In BWRs there is an increased susceptibility to SCC in areas of cold work or weldments. To date, there has been no record of IASCC in these components. Similarly, to date, there are no concerns for CASS components related to general or localized corrosion, fatigue, flow-accelerated corrosion, or wear for current lifetimes.

Under extended service scenarios, there may be additional degradation modes to consider. Thermal aging could lead to decomposition of key phases, resulting in increased susceptibility to embrittlement, irradiation-induced degradation, SCC, and general corrosion. This section will explore those degradation modes in more detail.

Cast austenitic stainless steels are typically grouped by their microstructure [1, 2]. There are fully austenitic grades such as grade CN7 (with up to 30 wt % Ni) and martensitic grades with lower Cr and Ni contents (13 and 4 wt % respectively). Duplex austenitic/ferritic alloys are also a major class of CASS. These include the CF family of cast grades which have approximately 19% Cr and 9% Ni. Common composition limits for these alloys are shown in Table 6.1 along with comparative composition limits for wrought equivalent steels.

Table 6.1. Comparison of ASTM chemistry specifications for cast stainless steel and wrought equivalents (compositions in wt %) [1, 2]

Grade	Type	C max	Mn max	Si max	P max	S max	Cr	Ni	Mo	Nb	Se	Cu	W max	V max	N
CF3	ASTM 743	0.03	1.50	1.50	0.04	0.04	17.0–21.0	8.0–12.0		--	--	--	--	--	
CF3A	ASTM 743	0.03	1.50	1.50	0.04	0.04	17.0–21.0	9.0–13.0	2.0–3.0	--	--	--	--	--	
CF3M	ASTM 743	0.03	1.50	1.50	0.040	0.040	17.0–22.0	9.0–13.0	2.0–3.0	--	--	--	--	--	0.10–0.20
CF8	ASTM 743	0.08	1.50	2.00	0.040	0.040	18.0–21.0	8.0–11.0							
CF8A	ASTM 743	0.08	1.50	2.00	0.040	0.040	18.0–21.0	8.0–11.0							
CF8M	ASTM 743	0.08	1.50	2.00	0.040	0.040	18.0–21.0	9.0–12.0	2.0–3.0						
304 SS	Wrought SS	0.08	2.00	1.00	0.045	0.03	18.0–20.0	8.0–11.0	--	--	--	--	--	--	0.00–0.10
304L SS	Wrought SS	0.03	2.00	1.00	0.045	0.03	18.0–20.0	8.0–12.0	--	--	--	--	--	--	0.00–0.10
316 SS	Wrought SS	0.08	2.00	1.00	0.045	0.03	16.0–18.0	10.0–14.0	2.0–3.0	--	--	--	--	--	0.00–0.10
316L SS	Wrought SS	0.03	2.00	1.00	0.045	0.03	16.0–18.0	10.0–14.0	2.0–3.0	--	--	--	--	--	0.00–0.10
321 SS[a]	Wrought SS	0.08	2.00	1.00	0.045	0.03	17.0–19.0	9.0–13.0	--	*a*	--	--	--	--	0.00–0.10
347 SS	Wrought SS	0.08	2.00	1.00	0.045	0.03	17.0–19.0	9.0–13.0	--	<1	--	--	--	--	0.00–0.10

[a] 0.70 wt % Ti.

Due to the chemical composition of CF3 and CF3M, the microstructures of these alloys can contain 3% to 30% ferrite in an austenite matrix, although CF-3 alloys typically contain 10 to 20% ferrite, while the CF-8 alloys typically have only 10% ferrite. The amount of ferrite varies strongly with composition and controlling the ferrite content can drive tensile strength higher.

These alloys are highly resistant to corrosion when exposed oxidizing acids such as nitric acid, similar to the wrought counterparts. ASME/ASTM SA/A 744 [2], "Specification for Castings, Iron-Chromium-Nickel, Corrosion Resistant, for Severe Service," provides the requirements for CF3 and CF3M castings that are subjected aggressive environments such as nitric acid solutions. It provides the requirement for chemical composition, heat-treating, weld repair, and product marking. Supplementary requirements include radiographic examination, liquid penetrant examination, examination of weld preparation, certification, a prior approval of weld repairs, corrosion testing, tension testing and surface carbon analysis.

6.2 THERMAL AGING

As noted above, CASS materials have optimized compositions and ferrite content in order to promote improved strength, castability, corrosion resistance, and weldability. However, the duplex nature of these alloys also creates the potential for thermal aging and decomposition of existing phases during extended time at temperature.

One area of potential concern is that CASS alloys are sensitive to thermal embrittlement at temperatures and times relevant to extended LWR service including up to and beyond 60 years of service. Under extended time at temperature, a variety of new phases may precipitate and lead to embrittlement. These phases are known to exist, but the rate at which they will form at lower temperatures is less certain. A schematic of the time-temperature transformation plot is shown in Figure 6.1, along with the potential influence of alloying elements on these curve shifts.

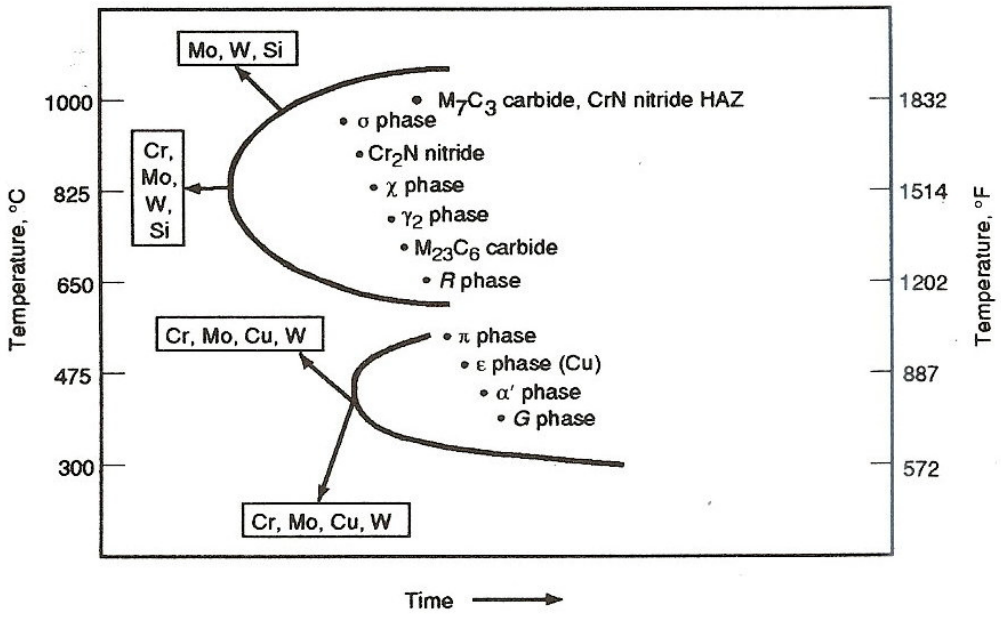

Figure 6.1. Time-temperature transformation diagram for CASS. The influence of alloying elements on precipitation reactions in duplex stainless steels is also shown [3].

6.2.1 Thermal Aging Considerations—Ferrite Phase

Thermal aging of the ferrite phase of CASS was discussed in detail in the original PDMA document by P. Scott [4]. As noted in that document,

> Thermal aging embrittlement of CASS at temperatures below about 400 °C (752 °F) arises primarily as a consequence of a thermally activated separation of chromium by diffusion in the Fe-Cr solid solution of the δ ferrite phase resulting in the formation of an iron rich α phase and a chromium rich α ' phase. This process is called 'spinodal decomposition' and occurs mainly at the higher chromium contents greater than ~23% in the δ ferrite (for temperatures <400 °C). The α' phase may also form by precipitate germination and growth, particularly at temperatures >400 °C, but can also contribute at lower temperatures depending on the precise combination of chromium content and temperature e.g. < 26%Cr at 400 °C and < 23%Cr at 300 °C (572 °F).
>
> The formation of α' during thermal aging can affect all Fe-Cr solid solutions with Cr contents in solution >10%. An "oscillation" in the resulting Cr distribution is observed by high-resolution microscopic techniques with "wavelength" (measured in nanometers) and amplitude increasing with aging time and temperature. The effect increases notably with the Cr and Mo content of the ferrite phase and consequently CF-8M is less resistant to aging than CF-8 or CF-3 without Mo. The formation of embrittling α' phase from δ ferrite is enhanced by other alloying elements such as silicon which, together with Cr and Mo, can be represented by the chrome equivalent. The presence of the adjacent austenite phase in CASS appears to exert a detrimental influence relative to purely ferritic alloys of similar composition.
>
> Other precipitation phenomena occur in the δ ferrite phase and at the ferrite-austenite interfaces above about 350 °C (662 °F), particularly the formation of the fcc Ni,Si,Mo rich G phase which can reach up to 12% by volume in Mo containing CASS. Carbon also enhances G phase precipitation. Nevertheless, G phase does not appear to contribute significantly to hardening and decrease in toughness. At higher temperatures between 400 °C (752 °F) and 500 °C (932 °F) other intermetallic phases precipitate but to a much lesser extent than G phase. However, extensive carbide (and sometimes nitride) precipitation, particularly at austenite-ferrite interfaces, occurs in the Mo-free CASS.
>
> Although solid-state diffusion processes fundamentally drive the microstructural evolution of CASS during thermal aging, the complexity and changing nature of the phenomena with temperature is such that extrapolation over large temperature ranges using Arrhenius type relations is very difficult. Accelerated thermal aging for PWR and BWR applications is generally only carried out up to 400 °C where hardening of the δ ferrite by α ' formation is the predominant aging process. Even with this restriction, the apparent activation energy observed for changes in mechanical properties such as hardness and toughness can be very variable and sometimes significantly below the activation energies of 210 to 260 kJ/mole associated with diffusion of metallic species, particularly Cr, in ferrite.

6.2.2 Thermal Aging Considerations—Austenite Phase

Even the fully austenitic matrix of 316 SS is thermodynamically unstable. During long-term exposure to elevated temperatures, the matrix will decompose into various carbide and intermetallic phases. These phases are often found at grain boundaries and other high-energy intragranular sites in the form of cubic or needle-like precipitates. In CASS, austenite/ferrite boundaries may also serve as precipitation sites.

These precipitates are responsible for the deterioration of mechanical properties, most notably a decrease in ductility, following high temperature exposure.

The microstructural evolution of CASS during thermal aging is extremely complex. For instance, one study identified at least 18 precipitate phases after exposure at 650 °C (1,202 °F) [4]. However, many of these phases are also present in as-cast or annealed material that is ductile. Therefore, the majority of studies have focused on primary precipitate phases that are believed to significantly affect material properties. These include two carbide phases ($M_{23}C_6$ and MC_6) and three intermetallic phases (Laves or η, σ, and χ).

Weiss and Stickler [5] developed time-temperature-transformation (TTT) diagrams between the temperatures of 400 and 900 °C and up to exposure time of 3,000 h. While these are at higher temperatures than LWR conditions, they are informative because LWR conditions will last hundreds of thousands of hours. Weiss and Sticker examined the effect of carbon content, solution treatment temperature, and cold work (CW) on the microstructural evolution of thermally annealed samples. The TTT diagram in Figure 6.2 has been extrapolated to 100,000 h (or approximately 11 years of operation) and altered to include the M_6C phase beyond 10,000 h observed by Stoter [4]. One should note that extrapolation to the end of service at 80 years would require additional extrapolation by a factor of 7 and should be considered with caution. The TTT diagram for a low carbon (>0.03% C) stainless steel is shown in Figure 6.3. Note that decreasing the carbon content (from ~0.07% in Figure 6.2) significantly accelerates the formation of intermetallic phases, but reduces the formation of carbides. Figure 6.4 is a similar TTT diagram for cold worked material. Note that CW prior to aging accelerates the formation of carbide and intermetallic phases, an effect, which is attributed to increased diffusion.

In each of the three TTT diagrams, it is apparent that the $M_{23}C_6$ carbide phase forms first, while the intermetallic phases appear only after much longer aging times. At temperatures below 900 °C (1,652 °F), the austenitic matrix is supersaturated with carbon. This condition leads to the rapid precipitation of $M_{23}C_6$ carbides, often in a matter of minutes at the aging temperature. As the carbides form, the carbon content in the matrix decreases, which leads to the formation of the intermetallic phases η, σ, and χ. Once the intermetallic phases form, the austenitic matrix is depleted of chromium and molybdenum, which increases the solubility limit of carbon and often leads to the dissolution of the $M_{23}C_6$ carbide precipitates.

Some general trends have been noted for the majority of precipitate phases. Thermal aging at higher temperatures causes precipitate particles to be coarser, whether on a grain boundary or within a grain. Smaller grains result in phase instability because they provide additional nucleating sites and decrease diffusion paths for precipitate forming elements [6].

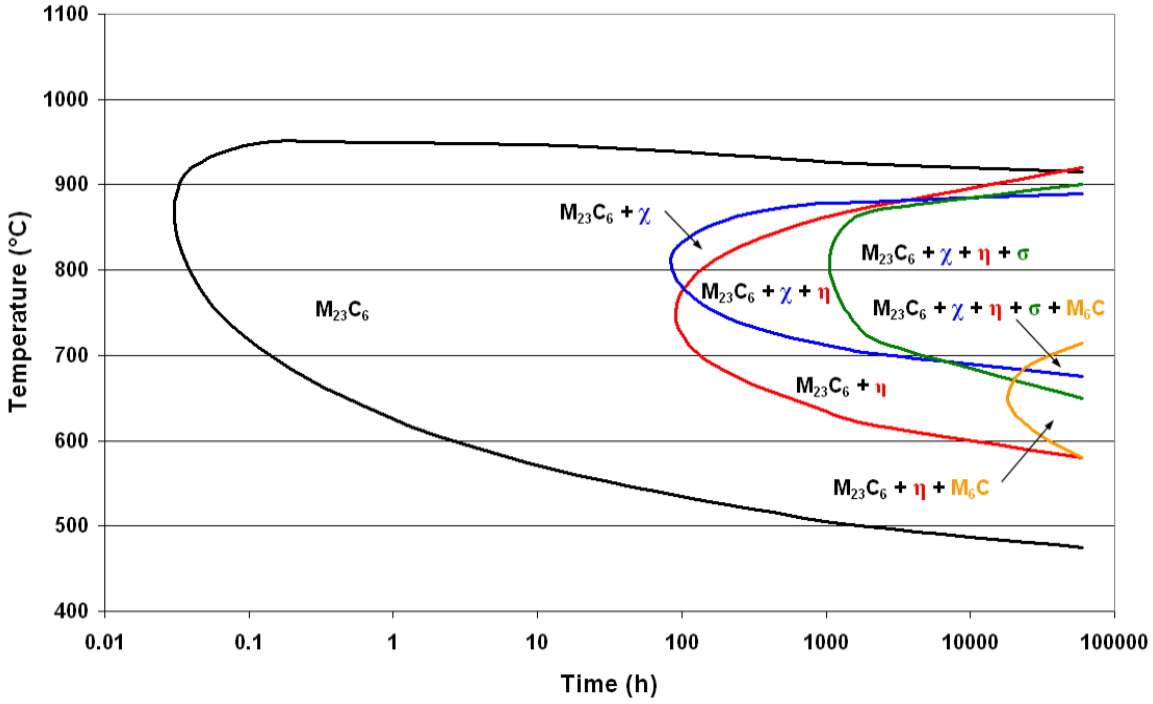

Figure 6.2. TTT diagram of CASS during thermal aging [5].
With kind permission from Springer Science+Business Media: L. P. Stoter, "Thermal ageing effects in AISI type 316 stainless steel," *Journal of Materials Science* 16, 1039 (1981).

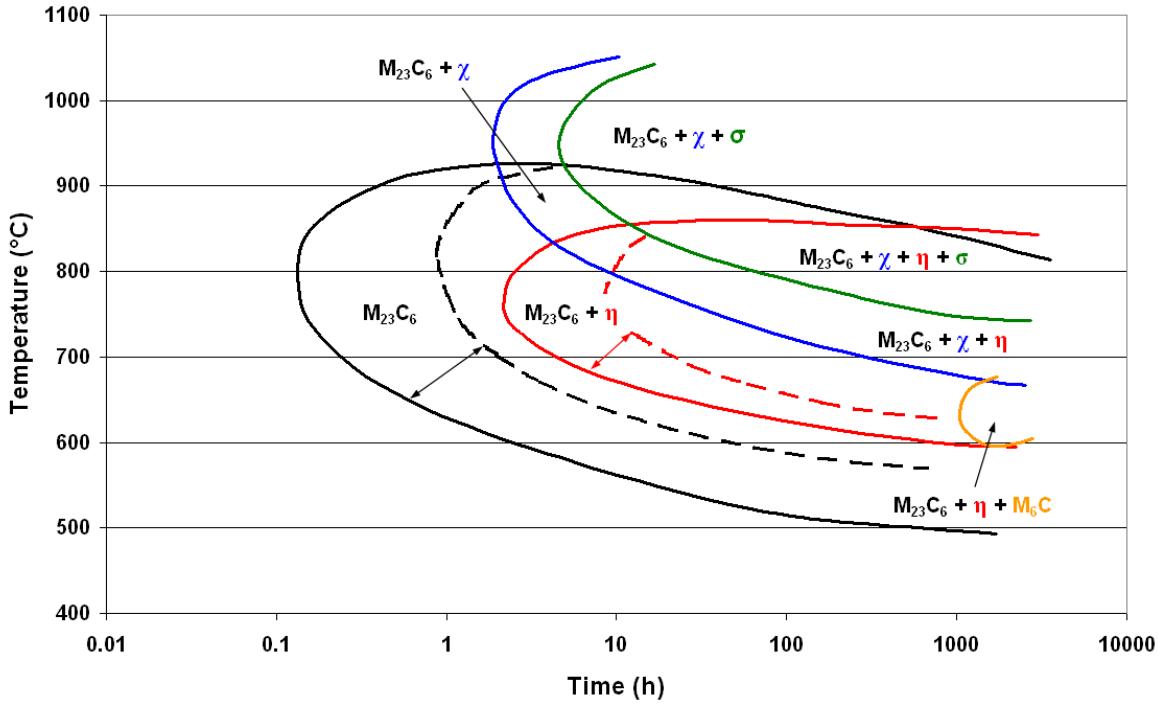

Figure 6.3. TTT diagram of low C CASS during thermal aging [5]. Dashed lines represent a lower solution anneal temperature [1,090 °C (1,994 °F) versus 1,560 °C (2,840 °F)].
With kind permission from Springer Science+Business Media: L. P. Stoter, "Thermal ageing effects in AISI type 316 stainless steel," Journal of Materials Science 16, 1039 (1981).

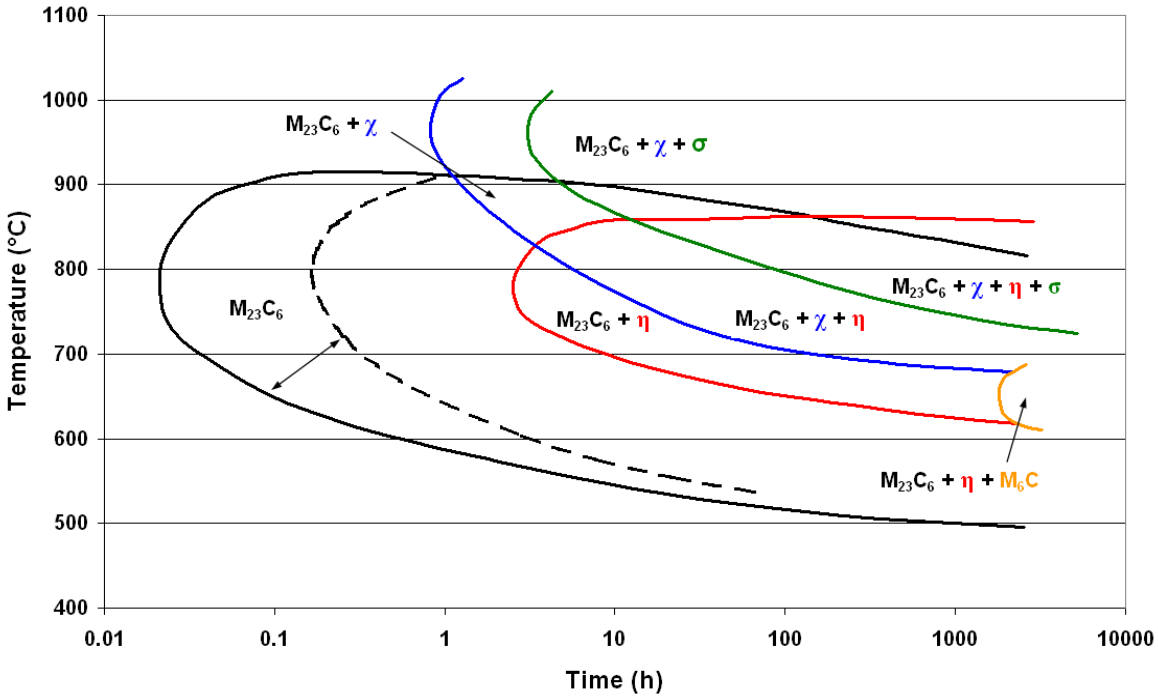

Figure 6.4. TTT diagram of cold worked SS during thermal aging [6]. Dashed line represents a lower solution anneal temperature [1,090 °C (1,994 °F) versus 1,260 °C (2,300 °F)]. Reprinted with permission of The Minerals, Metals & Materials Society.

6.2.2.1 $M_{23}C_6$ carbides

The most dominant precipitate in CASS is the $M_{23}C_6$ carbide phase, where the metal atom (M) is most likely to be chromium. The lattice parameters of face-centered cubic $M_{23}C_6$ tend to increase with aging temperature and time, reflecting an increase of the molybdenum content of the carbide [5] due to diffusion processes. The $M_{23}C_6$ carbide tends to precipitate successively on grain boundaries, incoherent twin boundaries, coherent twin boundaries, and intragranularly. The precipitates on grain boundaries are large and the number of precipitates increases with boron content [7]. Aging at 650 °C (1,202 °F) produces a uniform distribution of cubic precipitates on intragranular dislocations, while aging at higher temperatures resulted in large bulky precipitates on the grain boundaries with little precipitation within grains [5]. Cold working causes the $M_{23}C_6$ precipitates to form almost as readily at deformation bands as at grain boundaries [7].

Solution annealing at higher temperatures results in a larger $M_{23}C_6$ carbide size (the formation of which is shown in Figure 6.3). In general, high temperature annealing of an as-cast structure produces even larger grains, reduces the total volume of grain boundaries for precipitate formation. This, coupled with the higher quenched-in vacancy formation, results in higher solute-segregation along grain boundaries. Therefore, a shorter aging time is needed for $M_{23}C_6$ precipitation.

The precipitation of $M_{23}C_6$ is generally not desirable for good creep properties, except when precipitated in fine size intragranularly. Also, $M_{23}C_6$ is often associated with intergranular corrosion since its formation causes a local depletion of chromium along grain boundaries, thus losing the desirable “stainless” property on a local scale [7].

6.2.2.2 M_6C carbides

The M_6C precipitate is not very common in austenitic stainless steels. Weiss and Stickler observed M_6C in low carbon 316L SS for aging times of ~3,000 h, but not for 316 SS with a higher carbon content [5]. Stoter [5] identified M_6C after long-term aging (>28,000 h or nearly 3 years of operation) at 650 °C (1,202 °F). M_6C is diamond type face-centered cubic carbide. It is usually associated with very large $M_{23}C_6$ precipitates and has widely variable composition (with the exception that there is always 1% vanadium present). M_6C precipitates are predominantly found along grain boundaries and at triple point junctions [6].

6.2.2.3 Sigma (σ) phase

The sigma (σ) phase is a well-known intermetallic precipitate in Fe-Cr material systems that are often associated with embrittlement. Sigma phase is a tetragonal crystal composed of $(Cr,Mo)_x$ $(Ni,Fe)_y$. There are several theories concerning the formation of σ phase [8], but it always requires the presence of a high-energy interface to form. As expected, σ phase precipitates successively appear at triple points, grain boundaries, twin boundaries, and intragranularly at oxide inclusions. There is some evidence that σ phase precipitates only form on previous $M_{23}C_6$ sites or grow where $M_{23}C_6$ precipitates are dissolving [6]. The formation of σ phase can be retarded by solution annealing at high temperatures because the larger grains present a longer diffusion path for σ-forming elements to reach the grain boundaries. By contrast, cold working accelerates σ phase formation due to increased diffusion rates. However, it was found that recrystallization of the cold-worked microstructure had much greater effect on the amount and timing of the σ phase formation than did CW alone [7]. The σ phase has a detrimental effect on creep properties when located at grain boundaries, but little effect when it precipitates intragranularly [8, 9].

6.2.2.4 Chi (χ) phase

The chi (χ) phase is a body-centered cubic crystal that is typically thought of as a carbon-dissolving compound that behaves as either an $M_{18}C$ carbide or an intermetallic. The nucleation of χ phase typically follows the order of grain boundary, twin boundaries, and intragranular (within grain). The morphology of χ phase varies from large globular particles to rod-shaped crystals. Although a higher solution temperature will decrease the size of χ phase particles, it does not decrease the number of particles. Cold working causes χ-phase to precipitate within the grain in rod-shaped particles.

6.2.2.5 Laves (η) phase

Laves (η) phase particles are hexagonal crystals that are composed of Fe_2Mo in many molybdenum-containing alloys. Laves phase is often found as small equiaxed particles intragranularly, and occasionally found on the grain boundaries. High temperature annealing [above 1,400 °C (2,552 °F)] is effective at retarding the development of Laves phase particles because δ-ferrite forms, which favors the production of sigma and chi phases. Cold working accelerates Laves phase formation due to increased diffusion rates.

6.2.2.6 Thermal aging under extended service conditions

As noted above, one area of potential concern for service to 60 years is that CASS alloys are sensitive to thermal embrittlement at temperatures and times relevant to extended LWR service. Extending service to another 20 years provides additional time at temperature and increases the

potential for deleterious effects of aging. Detailed investigations (computational and experimental) could provide additional information on the potential and distribution of phase transformations as well as impacts on mechanical stability. The potential synergistic effects of thermal aging on general and localized corrosion may also be of increased concern.

6.3 MECHANICAL PERFORMANCE AND EMBRITTLEMENT

The potential for aging of CASS components under thermal conditions was recognized in the late 1980s, and several test and characterization programs were initiated [10–12]. In each of these studies, CASS materials were aged at service temperature or higher (to provide accelerated aging equivalent to longer lifetimes). In general, degradation of mechanical performance was observed, but there were differences in degree and nature of the embrittlement, which was tied to differences in composition and nature of the duplex cast structure. Several of these studies are discussed below.

Chopra and Sather's initial assessment [11], examined materials thermally aged up to 30,000 h at temperatures between 290 and 450 °C (~555 and 840 °F). They found that not only was aging condition important, but that ferrite morphology had a strong effect on the degree or extent of embrittlement. Embrittlement was tied to the formation of α' phase by spinodal decomposition of the ferrite. Precipitation and/or growth of phase boundary carbides or nitrides was also linked to a brittle failure.

In reference [13] the effect of thermal aging on tensile properties of CASS was examined. Several materials, including CF3, CF3M, and CF8M had aged up to 58,000 h at temperatures between 290 and 450 °C (554 and 842 °F). Aging at these temperatures and times was observed to increase hardness, yield stress (up 30%) with a concomitant decrease in ductility, fracture toughness, and impact strength. The study found that high-C Mo-bearing CF–8M steels were the most susceptible, while low-C Mo-free CF–3 steels were least susceptible to thermal aging.

In a separate study [14], Chopra and Shack examined material harvested from several components at the Shippingport reactor. These components had an actual service life of only 13 years with another 2 years of hot standby. The as-harvested material was examined while other materials were annealed and then aged in the laboratory. Comparison of these data sets allowed for assessment of the kinetics of the thermally induced phase transformations. The Shippingport materials exhibited modest degradation of mechanical properties, as would be expected at the relatively low operating temperatures. The room-temperature Charpy-impact energies of the materials were found to be relatively high, while the mid-shelf Charpy transition temperatures were very low. Interestingly, characterization of microstructures and mechanical performance of materials harvested from different locations also demonstrated the strong dependence of embrittlement on CASS microstructure. In this study, check valve materials were weaker than main valve materials because of the presence of phase-boundary carbides.

Some materials were aged further in the laboratory to determine the kinetics of embrittlement and the saturation or minimum fracture properties of a specific material. The results indicate that the Shippingport cast stainless steels were not very susceptible to thermal embrittlement at reactor operating temperatures. These findings are somewhat contradictory to the laboratory tests described previously and the difference may be due to one of two factors. First, the Shippingport materials only saw ~15 years of time at temperature, clearly lower than the laboratory tests. However, the laboratory tests also utilized higher temperatures, which may alter

the kinetics of the phase transformation process. These factors must be considered when extrapolating to a possible 80 years of service.

The studies listed support that CASS components may undergo thermally driven phase transformations and a potential change in mechanical performance. However, in the context of subsequent license renewal considerations, the studies described above were conducted for <60,000 hours. Potential extension to up to 80 years of life may require an order-of-magnitude increase in exposure to elevated temperatures. Further, while laboratory tests and accelerated aging will be required to evaluate 80 years of service, the potential influence of higher temperatures required for accelerated aging must also be considered. In this case, careful analysis of thermodynamic models will also be required.

6.4 GENERAL CORROSION

General (uniform) corrosion of CASS alloys is well studied and corrosion rates are typically very low, which is a prime driver for their use in this application. To date, there are no known service problems with CASS in the area of general corrosion.

Under extended service conditions, additional time will lead to opportunity for increased corrosion (weight loss or wall thinning); however, the rate of corrosion is so slow that this is unlikely to increase risk of component failure. The potential effects of thermal aging could lead to increased corrosion effects and this should be evaluated.

6.5 LOCALIZED CORROSION/PITTING

As with general corrosion, localized corrosion of CASS alloys is well studied and not a concern in modern LWR water chemistries. To date, there are no known service problems with CASS in the area of pitting or localized corrosion.

Under extended service conditions, additional time will lead to increased exposure to the coolant although pitting of CASS is expected to be unlikely to be a concern to service.

6.6 FLOW-ACCELERATED CORROSION

There are no known instances of flow-accelerated corrosion problems in today's fleet for CASS components. This is the expected behavior for these alloys. As above, while extended service conditions will lead to increased exposure to the coolant although FAC of CASS is unlikely to be a concern to service.

6.7 STRESS CORROSION CRACKING

6.7.1 SCC of CASS Components

Stress corrosion cracking has been observed in several cases in CASS in nuclear applications in both BWR and PWR environments. However, these observations are very limited [15]. In those cases, analysis of the cracked components revealed that the material was either higher in C or lower in ferrite than specified, leading to increased susceptibility.

There have also been limited observations of SCC in weldments of CASS components. However, as above, these have been attributed to improper heat treatment and/or cold-working rather than a general susceptibility.

Stress corrosion cracking of CASS has been identified as a knowledge gap in the most recent versions of the EPRI MDM and Issue Management Tables [15–17]. As noted in the MDM, this "is not intended to denote a significant concern at present, but rather to communicate the current lack of susceptibility data for CASS materials. A possible area warranting additional investigation is the potential effect of long-term thermal aging on the SCC susceptibility of CASS components having high ferrite content, considering that other materials (i.e., martensitic stainless steels) that embrittle with age also exhibit increased SCC susceptibility."

6.7.2 SCC of CASS Components under Extended Service

The positive service performance of CASS materials to date is encouraging when considering extended service conditions. However, the lack of susceptibility data for SCC and the potential influence of long-term aging may drive phase transformations must be considered. Thermal aging, as described above, could lead to increased SCC susceptibility. Additional studies on the dominant phase transformations and potential impacts on susceptibility are warranted.

6.8 IRRADIATION EFFECTS

6.8.1 Irradiation-Induced Effects in CASS

The evaluation of irradiation-induced degradation is a critical step in validating material service under any conditions. Nuclear reactor systems impose a harsh environment and radiation damage conditions on structural materials. While the exact materials and degradation mechanisms vary between the different applications, the fundamentals of radiation damage are the same. Irradiation of materials in reactors can lead to extensive changes in microstructure, microcomposition, and macroscopic properties.

Neutron irradiation can produce large property and dimensional changes in materials, primarily via one of five radiation damage processes:

- radiation-induced hardening and embrittlement (occurring predominantly at low exposure temperatures);
- phase instabilities from radiation-induced or -enhanced segregation and precipitation;
- irradiation creep due to unbalanced absorption of interstitials vs vacancies at dislocations;
- volumetric swelling from cavity formation; and
- high temperature helium embrittlement due to formation of helium-filled cavities on grain boundaries.

Many of these irradiation-induced degradation modes are discussed in detail in a later section. The key challenge for materials performance is to identify applicable degradation modes based on past history and exact range of irradiation conditions.

For CASS, irradiation effects are a minor concern in today's BWR fleet. Irradiation-induced hardening is the primary form of degradation associated with cast stainless steels and is closely related to the sensitivity to embrittlement observed in reactor pressure vessel materials.

Currently, CASS components are subjected to additional analysis and monitoring above a maximum fluence of 1×10^{17} n/cm^2. This limit was established by NRC guidance [18] to limit the potentially deleterious effects of radiation-induced hardening. As noted in the guidance, "If the neutron fluence is greater than 1×10^{17} n/cm^2 (E > 1.0 MeV), a mechanical loading assessment would be conducted for the component. This assessment will determine the maximum tensile loading on the component during ASME Code Level A, B, C and D conditions. If the loading is compressive or low enough to preclude fracture of the component, then the component would not require supplemental inspection. Failure to meet this criterion would require continued use of the supplemental inspection program."

In the same guidance letter [18], a program to systematically examine possible synergistic effects of irradiation on thermal aging processes was proposed. To date, there are no reports of irradiation-induced degradation limiting operation of these components.

6.8.2 Irradiation-Induced Effects under Extended Service Conditions

Clearly, extended service conditions will increase the total fluence to CASS components, although the total fluence will depend on a number of factors unique to each plant and component location in the reactor (e.g. service time, power-uprates, etc.) Careful consideration of maximum fluence and relation to the NRC guidance [18] is warranted.

6.8.3 Synergistic Effects of Irradiation-Induced Effects

The effects of irradiation on phase transformations and hardening may have synergistic effects on other forms of degradation. The potential influence of irradiation-induced hardening and decrease in fracture toughness may affect stress corrosion cracking susceptibility, analogous to that in wrought stainless steel components. In addition, the impact of irradiation-enhanced diffusion on thermal aging processes could accelerate that form of embrittlement. These forms of degradation may be less than in wrought steels due to the much larger grain size in CASS.

6.9 FATIGUE

As with general and localized corrosion, there are no known instances of (cyclic) fatigue problems in today's fleet for CASS components. Under extended service conditions, components will experience longer duration of service and additional cycles and, as with most materials, fatigue and environmental fatigue could become a greater concern simply due to the longer service life.

As discussed in previous sections, the largest uncertainty in fatigue behavior may be the result of synergistic effects related to thermal aging and possibly synergistic irradiation-induced effects. If phase transformations occur during extended lifetimes, decrease in fracture toughness could lead to increased concerns with fatigue and environmental fatigue.

6.10 SUMMARY

Cast stainless steels are important structural materials used in LWR facilities. Until now, the plants have experienced very limited failures related to material degradation. In the limited number of service observations of degradation, all have been attributed to high carbon contents, low ferrite contents, or improper heat treatment.

Under extended service scenarios, there may be additional degradation modes to consider for these alloys and components. Thermal aging could lead to the decomposition of key phases and formation of other deleterious phases. Such aging could result in the decrease in fracture toughness (analogous to that observed in other martensitic stainless steels). Additional surveys of potential phases and aging effects would help reduce the current gap and uncertainty in understanding of this mechanism.

Other forms of degradation such as general corrosion, localized corrosion, flow-accelerated corrosion, stress corrosion cracking, irradiation effects, and fatigue are not expected to limit operation under extended service conditions based on performance in the fleet to date. However, the synergistic effects of long-term thermal aging on these other forms of degradation must be considered in greater detail.

Key modes of degradation for extended service include:

- *Thermal aging.* Long-lifetimes at elevated temperatures may lead to changes in the cast microstructure. There is no data for performance at >600,000 hours. Changes in microstructure are lot a key concern on their own, however synergistic effects may lead to decrease in performance in other aspects.

- *Embrittlement and decrease in fracture toughness.* Laboratory data and studies to 60,000 hours indicate relatively little change in mechanical performance. However, in cases where embrittlement was observed, the change was correlated with changes in microstructure. Additional data may be required.

- *Corrosion and stress corrosion cracking.* As noted above, there are no examples of failure of cast stainless steel components in service to greater than 40 years of life. Changes in microstructure may lead to changes in corrosion performance. Additional data may be required.

6.11 REFERENCES*

1. *Specification for Castings, Iron-Chromium, Iron-Chromium-Nickel, Corrosion-Resistant, for General Application,* Standard ASME/ASTM SA/A 743/A 743M.
2. *Specification for Castings, Iron-Chromium-Nickel, Corrosion Resistant, for Severe Service,* Standard ASME/ASTM SA/A 744.
3. J. Charles, “Super Duplex Stainless Steels—Structure and Properties,” pp. 3–48 in *Proc. Duplex Stainless Steel Conference*, Vol. 1, Les Editions de Physique, Les Ulis Cedex,

* Inclusion of references in this report does not necessarily constitute NRC approval or agreement with the referenced information.

October 1991.

4. P. L. Andresen et al., *Expert Panel Report on Proactive Materials Degradation Analysis,* NUREG/CR-6923 (BNL-NUREG-77111-2006), U.S. Nuclear Regulatory Commission, February 2007.
5. L. P. Stoter, “Thermal ageing effects in AISI type 316 stainless steel,” *Journal of Materials Science* **16,** 1039 (1981).
6. B. Weiss and R. Stickler, “Phase Instabilities during High Temperature Exposure of 316 Austenitic Stainless Steel,” *Metallurgical Transactions* **3,** 851 (1972).
7. J. E. Spruiell et al., “Microstructural Stability of Thermal-Mechanically Pretreated Type 316 Austenitic Stainless Steel,” *Metallurgical Transactions* **4,** 1533 (1973).
8. T. Sourmail, “Precipitation in creep resistant austenitic stainless steels,” *Materials Science and Technology* **17,** 1 (2001).
9. J. Barcik, “Mechanism of σ phase precipitation in Cr-Ni austenitic steels,” *Materials Science and Technology* **4,** 5 (1988).
10. O. K. Chopra and H. M. Chung, “Initial Assessment of the Processes and Significance of Thermal Aging in Cast Stainless Steels,” p. 519 in Vol 3, *Proc. 16th Water Reactor Safety Information Meeting,* NUREG/CP–0097, U.S. Nuclear Regulatory Commission, March 1989.
11. O. K. Chopra and A. Sather, *Initial Assessment of the Mechanisms and Significance of Low-Temperature Embrittlement of Cast Stainless Steels in LWR Systems,* NUREG/CR-5385, U.S. Nuclear Regulatory Commission, 1990.
12. O. K. Chopra, *Estimation of Fracture Toughness of Cast Stainless Steels During Thermal Aging in LWR Systems,* NUREG/CR-4513, Rev. 1, U.S. Nuclear Regulatory Commission, August 1994.
13. W. F. Michaud, P. T. Toben, W. K. Soppet, and O. K. Chopra, *Tensile-Property Characterization of Thermally Aged Cast Stainless Steels,* NUREG/CR-6142, U.S. Nuclear Regulatory Commission, 1994.
14. O. K. Chopra and W. J. Shack, *Mechanical Properties of Thermally Aged Cast Stainless Steels from Shippingport Reactor Components,* NUREG/CR-6275, U.S. Nuclear Regulatory Commission, April 1995.
15. EPRI, *Primary System Corrosion Research Program: EPRI Materials Degradation Matrix, Revision 2,* EPRI Document 1020987, Electric Power Research Institute, August 2010.
16. EPRI, *Materials Reliability Program: Pressurized Water Reactor Issue Management Tables—Revision 2 (MRP-205),* Document 1021024, Electric Power Research Institute, October 2010.
17. EPRI, *BWRVIP-167NP, Revision 2: BWR Vessel and Internals Project, Boiling Water Reactor Issue Management Tables,* Document 1020995, Electric Power Research Institute, August 2010.
18. NRC, Staff Evaluation of License Renewal Issue No. 98-0030, “Thermal Aging Embrittlement of Cast Austenitic Stainless Steel Components,” U.S. Nuclear Regulatory Commission, May 2000.

7. CONTAINMENT LINER

Karen Gott
Swedish Nuclear Power Inspectorate* – Retired

The containment liners are either freestanding within a concrete shielding building or in contact with the concrete structure. The liners are made of 8–10 mm (0.31–0.39 in.) thick carbon steel sections welded together. Problems to date have been concentrated to liners in contact with the concrete and are related to corrosion both from the inside and outside surfaces [1]. On the inside, corrosion has been associated with damage to the protective coatings. From the outside, larger regions of corrosion have been found either because the corrosion had gone through the wall or had occurred in connection with holes being cut in the containment for component replacement.

The naturally alkaline environment on the outside of the liner is protective in that it promotes the formation of a stable oxide/hydroxide passive film. If the local environment becomes less alkaline (because of a reduction in the pH of the concrete pore water) or if the chloride concentration increases (because of concrete aging), the film can become disrupted, resulting in corrosion. There is also the possibility of intrusion of chlorides with the same result. The corrosion—galvanic, crevice, or pitting—is difficult to detect, and if it penetrates through the wall, the containment integrity is jeopardized. One contributing factor has been found to be foreign material left in the concrete from the construction phase (e.g., wood). The ingress of chlorides through cracks in the concrete and by diffusion through its pores is more likely to affect the environment in contact with the liner over time, but to date this has not been a problem.

The carbon steel material is subject to BAC but, with appropriate maintenance and protective coatings intact, there should be no problems. Most external corrosion events have been the result of foreign materials, such as wood or felt, in contact with the liner. If these materials decompose, microbiologically influenced corrosion could occur.

In the future, other degradation mechanisms should also be considered. One of the minerals formed during the curing of concrete is ettringite. If temperatures exceed 70 °C (158 °F) or the pH is lowered, then the ettringite can convert to its original phase, resulting in the release of sulfates in the form of $CaSO_4$, thereby increasing corrosion. Because the operating temperature of the containment is normally around 60 °C (140 °F) and operating times are long, it is possible that this transformation could occur.

Ettringite formation and other reactions that produce swelling (e.g., the alkali–silica reaction, if extensive) could lead to stresses on the external side of the liner. If these reactions are sufficiently high, this could lead to high stress states and stress corrosion cracking could be an issue. The containment liners are not subjected to cyclic stresses and will not result in fatigue damage. The stresses imposed during pressure tests are not sufficient to result in fatigue even if the frequency is increased considerably. Nor is the temperature difference between operating and shut down conditions sufficient in magnitude or total number to result in thermal fatigue. Degradation modes related to concrete and concrete/liner interactions are also covered in more detail in Volume 5 of this EMDA activity.

* Subsumed by the Swedish Radiation Safety Authority, Stockholm, in June 2008.

7.1 REFERENCE*

1. D. Dunn, A. Pulvirenti, and P. Klein, “Containment Liner Corrosion,” *Proc. 15th Int. Conf. Environmental Degradation in Nuclear Power Systems—Water Reactors,* Colorado Springs, J. Busby and G. Ilevbare (eds.), The Metallurgical Society, 2011 or http://pbadupws.nrc.gov/docs/ML1121/ML112140119.pdf.

* Inclusion of references in this report does not necessarily constitute NRC approval or agreement with the referenced information.

8. IRRADIATION EFFECTS

G. S. Was
University of Michigan, Ann Arbor, Mchigan

8.1 INTRODUCTION

Austenitic stainless steels and nickel (Ni)-base alloy steels are used for numerous core internal components in both BWRs and PWRs. These materials were chosen based on their good corrosion resistance, well-characterized mechanical properties, and ease of fabrication of components. Moreover, these alloys have been used extensively in other industries, such as petrochemical and fossil fuel. Table 8.1 lists the primary alloys used in BWR and PWR cores. This data has been given in earlier sections, but is also included here for convenience.

The core of a nuclear reactor is an extreme environment consisting of high temperature water, imposed service stresses and strains, intense radiation fields, and a corrosive medium. Most irradiated core components consist of austenitic stainless steels and Ni-base alloys exposed in environments that span oxygenated to hydrogenated water at ~270 °C (518 °F) to 340 °C (644 °F). While many aspects of radiation-induced degradation of metals were known at the time of construction of the current fleet, the doses and temperatures expected for the core components were judged to be within the range of tolerance for both irradiation and environmental effects. The primary effects of radiation on materials [1–11] include microcompositional effects (grain boundary chemistry) and microstructural changes (formation of dislocation loops, voids, void swelling, precipitates, and the resulting changes in hardening and deformation mode), and can be summarized as follows:

- *Radiolysis of water*, in which a variety of short- and long-lived radicals and species are produced.

- *Radiation-induced segregation*, which produces enrichment in some species (e.g., Ni and Si at grain boundaries and other defect sinks) and a depletion in other species (e.g., Cr at grain boundaries).

- *Radiation hardening and localized deformation*, which results from radiation damage and the creation of vacancy and interstitial loops, which impede dislocation motion. Once a few dislocations move along a given slip plane, they clear the “channel” of most of these barriers, and subsequent dislocation occurs primarily in these channels, resulting in localized deformation.

- *Radiation creep relaxation*, which reduces constant displacement stresses such as in bolts or associated with weld residual stress. During active irradiation, radiation creep can promote dynamic strain states.

- *Swelling*, which occurs to a limited extent at temperatures between ~300 °C (572 °F) and 360 °C (680 °F), but can be sufficient to produce reloading of components such as PWR baffle former bolts. Onset of swelling occurs at different times in different materials and is delayed in cold-worked materials versus solution-annealed alloys. Stresses due to swelling may be balanced by radiation creep relaxation.

Table 8.1. ASTM compositional specifications for austenitic stainless steel (304 SS, 304L SS, 316 SS, 316L SS, 316CW SS, 321 SS, 347 SS), A-286, and Ni-base alloys (600, 718, X-750) given in units of weight percent [1, 2]

Alloy	Carbon	Manganese	Chromium	Molybdenum	Nickel	Silicon	Phosphorus	Sulfur	Aluminum	Copper	Titanium	Iron	Other
304	0.08	2.0	18–20	-	8–10.5	1	0.45	0.03	-	-	-	Bal	-
304L	0.03	2.0	18–20	-	8–10.5	1	0.45	0.03	-	-	-	Bal	
316	0.08	2.0	16–18	2–3	10–14	1	0.45	0.03	-	-	-	Bal	
316L	0.08	2.0	16–18	2–3	10–14	1	0.45	0.03	-	-	-	Bal	
321	0.08	2.0	17–19	-	9–12	1	0.45	0.03	-	-	5× Cr min	Bal	-
347	0.08	2.0	17–19	0.75	9–13	1	0.45	0.03	-	0.5	-	Bal	
A-286	0.08	2.0	13–16	1–1.5	24–27	1	0.40	0.03	0.35	0.3	1.9–2.35	Bal	V, 0.1–0.5; boron (B), 0.001–0.1
600	0.15	1.0	14–17	-	72	0.5	-	0.015	-	0.5		6–10	
718	0.08	0.35	14–17	2.8–3.3	50–55	0.35	0.015	0.015	0.65–1.15	0.2–0.8	0.3	Bal	Niobium (Nb), 4.75–5.5; cobalt (Co), 1.0; B 0.006
X-750	0.08	1.0	14–17	-	70	0.5	-	0.01	0.4–1.0	.05	2.25–2.75	5–9	Co, <1; Nb+tantalum (Ta), 0.7–1.2

ASTM = American Society for Testing and Materials.

- Other *microstructural changes*, such as precipitation or dissolution of phases in materials.

- *Transmutation* of various elements in the alloy, which results in the production of helium (He) and hydrogen (H). Helium is known to have severe consequences on swelling and mechanical properties.

One of the major effects of irradiation is on stress corrosion cracking. The role of irradiation in stress corrosion cracking was not known, and neither was the importance of corrosion potential in this process at the time the current generation of plants was built. The SCC of reactor core components, which would not have undergone such degradation outside the core, implicated irradiation as a key effect in inducing premature degradation. Initially, the affected components were primarily small components (bolts, springs, etc.) or components designed for replacement (fuel rods, control blades, or instrumentation tubes). However, in the last ~20 years, irradiation-assisted stress corrosion cracking (IASCC) has been observed in structural components such as PWR baffle former bolts and BWR core shrouds and top guides. Table 8.2 summarizes the components that have experienced IASCC and are the focus of study on irradiation effects in LWR internals.

Table 8.2. IASCC service experience [9]

Component	Material	Reactor Type[a]	Possible Sources of Stress
Fuel cladding	304 SS	BWR	Fuel swelling
Fuel cladding	304 SS	PWR	Fuel swelling
Fuel cladding[b]	20%Cr/25%Ni/Nb	AGR	Fuel swelling
Fuel cladding ferrules	20%Cr/25%Ni/Nb	SGHWR	Fabrication
Neutron source holders	304 SS	BWR	Welding & Be swelling
Instrument dry tubes	304 SS	BWR	Fabrication
Control rod absorber tubes	304/304L/316L SS	BWR	B_4C swelling
Fuel bundle cap screws	304 SS	BWR	Fabrication
Control rod follower rivets	304 SS	BWR	Fabrication
Control blade handle	304 SS	BWR	Low stress
Control blade sheath	304 SS	BWR	Low stress
Control blades	304 SS	PWR	Low stress
Plate type control blade	304 SS	BWR	Low stress
Various bolts[c]	A-286	PWR & BWR	Service
Steam separator dryer bolts[c]	A-286	BWR	Service
Shroud head bolts[c]	600	BWR	Service
Various bolts	X-750	BWR & PWR	Service
Guide tube support pins	X-750	PWR	Service
Jet pump beams	X-750	BWR	Service
Various springs	X-750	BWR & PWR	Service
Various springs	718	PWR	Service

Table 8.2. IASCC service experience [9] (continued)

Component	Material	Reactor Type[a]	Possible Sources of Stress
Baffle former bolts	316 SS cold work	PWR	Torque, differential swelling
Core shroud	304/316/347/L SS	BWR	Weld residual stress
Top guide	304 SS	BWR	Low stress (bending)

[a] AGR, advanced gas-cooled reactor; BWR, boiling water reactor; PWR, pressurized water reactor; SGHWR, steam-generating heavy water reactor.
[b] Cracking in AGR fuel occurred during storage in spent fuel pond.
[c] Cracking of core internal occurs away from high neutron and gamma fluxes.

8.2 PRIMARY EFFECTS OF IRRADIATION ON LWR CORE COMPONENTS

Beyond IASCC, irradiation effects that produce only minor changes on dimensional or mechanical properties at 40 years may result in much more severe changes as lifetimes of 60–80 years are considered. The effects of irradiation on materials of core internal components (laboratory experiments) and actual components in service that have been documented to date are the following:

- Development of a dense dislocation loop network that saturates by several displacements per atom.
- Radiation hardening of core components by factors of up to 5 over the solution-annealed strength or hardness.
- Decrease in ductility typically concomitant with a large increase in strength. Ductility loss is accompanied by a reduction in strain hardening (and even strain softening) as well as a loss in total elongation.
- Change in the deformation mode to one in which plastic deformation is confined to intense, localized dislocation channels.
- Precipitation of second phases in austenitic stainless steels such as γ' and G-phase that may contribute to hardening and/or embrittlement.
- Radiation-induced segregation to grain boundaries resulting in depletion of Cr and Mo and enrichment of Ni, Si, and other elements.
- Reduction in fatigue life compared to the unirradiated material, which may be due to both a primary effect of irradiation or a synergistic effect of mechanical property changes due to irradiation.
- Irradiation creep leading to stress relaxation.
- Void formation resulting in swelling and dimensional changes in components.
- IASCC due to a combination of irradiation-induced changes to the material, high temperature, and a water environment.

For almost 30 years, many of these effects have been reported in conferences that have focused on the degradation of materials in water-cooled reactors (conferences through The Minerals,

Metals and Materials Society, ASTM, and others) as well as in various NRC publications (e.g., generic letters and periodic revisions of the Generic Aging Lessons (GALL) report). Of current interest are recent studies by both the NRC [12, 13] and EPRI [14, 15] to assess the future modes of material degradation of the reactor structural materials, including austenitic alloys used in core internal components.

The consequence of these material failures has been primarily economic, in that the failures have led to forced and extended plant outages, which entail only the cost of replacement power together with the cost of component repair/replacement without safety significance. Rarely has there been a significant safety issue quantified, for instance, by an actionable change associated with an increase in core damage frequency (ΔCDF). On the other hand, continued degradation could lead to more serious component damage that could affect safety.

Degradation modes for austenitic stainless steels and Ni-base alloys in reactor cores that are relevant to long-term operations (i.e., beyond 60 years) are discussed below in terms of (a) plant experience over the current license period; (b) current prediction capability (e.g., parametric dependency, mechanism-based models) that expand analysis time; and (c) longer term (80-year) concerns that address both new degradation modes and/or inadequacies in the current mitigation/plant management actions.

Subsequent sections address the following degradation modes for austenitic stainless steels and Ni base alloys:

- Radiation hardening
- Embrittlement (reduction in fracture toughness)
- Fatigue
- Radiation-induced creep and swelling
- IASCC
- Irradiation accelerated corrosion

8.3 RADIATION HARDENING

8.3.1 Past and Current Plant Experience

The microstructure of austenitic stainless steels changes rapidly under irradiation at LWR service temperatures. Point defect clusters (called “black dot damage” when electron microscopy is unable to resolve the details) begin to form at very low dose; dislocation loops and network dislocation densities evolve with dose over several displacements per atom; and the possibility exists for the formation and growth of He-filled bubbles, voids, and precipitates in core components in locations exposed to higher dose (greater than a few dpa) and temperatures [16–22]. Below 300 °C (572 °F), the microstructure is dominated by small clusters and dislocation loops. Near 300 °C, the microstructure contains larger faulted loops plus network dislocations from unfaulting of dislocation loops and cavities at higher doses.

The primary defect structures in LWRs are vacancy and interstitial clusters and Frank dislocation loops. The clusters are formed during the collapse of the damage cascade associated with primary and secondary atom collisions after interaction with a high-energy particle. The larger, faulted dislocation loops nucleate and grow as a result of the high mobility of interstitials. The loop population grows in size and number density until absorption of vacancies and interstitials

equalize, at which point the population has saturated. Figure 8.1 shows the evolution of loop density and loop size as a function of irradiation dose during LWR irradiation at 280 °C. Note that saturation of loop number density occurs very quickly, by ~1 dpa, while loop size continues to evolve up to ~5 dpa. The specific number density and size are dependent on irradiation conditions and alloying elements, but the loop size rarely exceeds 20 nm and densities are of the order 1×10^{23} m^{-3}.

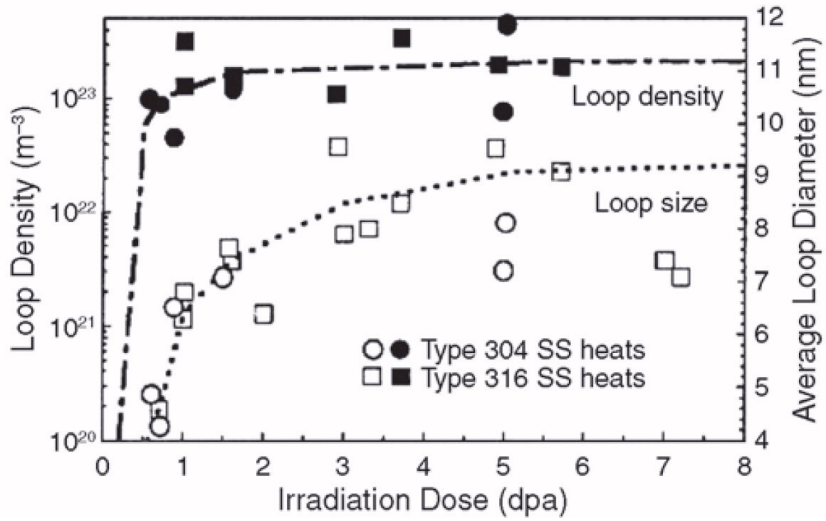

Figure 8.1. Measured change in density and size of interstitial loops as a function of dose during LWR irradiation of 300-SS at 275 °C (527 °F) to 290 °C (554 °F) [3]. Reprinted fromS. M. Bruemmer, E. P. Simonen, P. M. Scott, P. L. Andresen, G. S. Was, and J. L. Nelson, "Radiation-induced material changes and susceptibility to intergranular failure of light-water-reactor core internals," *Journal of Nuclear Materials* 274(3), 299–314 (1999), with permission from Elsevier.

In LWR materials, hardening is dominated by the dislocation microstructure, so it tends to follow a dose dependence similar to that for loops. Figure 8.2 shows radiation hardening in several 300-series stainless steels irradiated and tested near 300 °C. The hardening roughly follows a $dose^{1/2}$ dependence but the dependence on alloy composition is of secondary significance. However, cold work tends to suppress dislocation loop formation relative to the solution-annealed; therefore, hardening in cold-worked materials is less than that in solution-annealed materials.

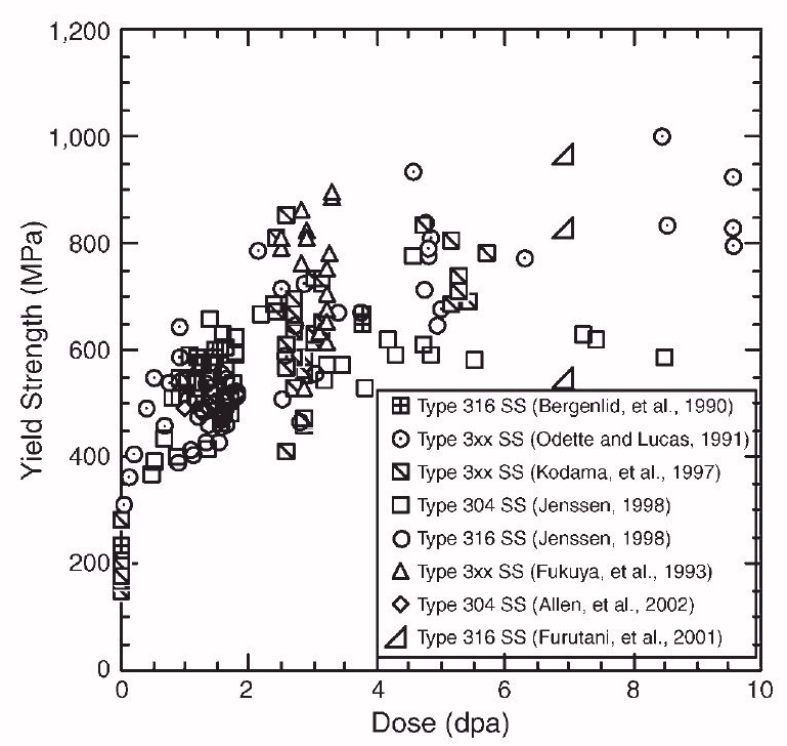

Figure 8.2. Irradiation dose effects on measured tensile yield strength for several 300-SS, irradiated and tested at a temperature of about 300 °C (572 °F) [23]. Copyright 2003 by the American Nuclear Society.

8.3.2 Mechanism and Parametric Dependencies

The hardening process and the IASCC susceptibility are influenced by small defects. The traditional view that small defect clusters are predominantly faulted interstitial loops and vacancy clusters [24] may be inaccurate. Analysis of recent postirradiation annealing experiments by Busby et al. [25] suggests that there are at least two types of defects with different annealing characteristics—vacancy and interstitial faulted loops, each with different annealing kinetics. The step change in hardness as a function of annealing time suggests that the density of vacancy loops is perhaps much higher than previously believed as well as higher than the density of interstitial loops [25].

Above 300 °C (572 °F), voids and bubbles may begin to form, aided by the increased mobility of vacancies at the higher temperature. The dislocation structure will evolve into a network structure as larger Frank loops unfault. The reduction in capacity to act as sinks of the dislocation loops aids in the growth of voids and bubbles. While their size and number densities increase with temperature, the dislocation microstructure continues to be the dominant microstructure component over the temperature range expected for LWR components <350 °C (662 °F)].

Irradiation can also accelerate or retard the growth of second phases, modify existing phases, or produce new phases. The phase microstructure can have important consequences for hardening. In stainless steels, the principal second phase is Cr carbides, which are relatively stable under irradiation. A key factor in phase formation in austenitic stainless steels under LWR operating conditions is radiation-induced segregation, which can induce the formation of phases by exceeding the local solubility limit. Precipitation of γ' was observed in cold-worked 316-SS baffle

bolts irradiated to 7 dpa at 299 °C (570 °F) [26]. Gamma prime is a coherent precipitate that can significantly strengthen the matrix and has the potential to alter the deformation behavior in the unirradiated and irradiated conditions. Was et al. [27] irradiated a high purity stainless steel containing 1 wt % Si with 3.2 MeV protons to 5.5 dpa at 360 °C (680 °F), and observed the formation of γ' (Ni_3Si) in the matrix. In addition to γ', G phase (Ni/Si rich) is frequently observed in irradiated stainless steel alloys [28]. In high strength Ni-base alloys, second phases can undergo several types of transformations: γ' can dissolve, γ'' can dissolve and re-precipitate, and Laves phase can become amorphous.

Oversize solutes can also affect the irradiated microstructure by mechanisms similar to radiation-induced segregation. Proton and Ni ion irradiations show that the addition of hafnium (Hf) to a 316 SS-base alloy increased loop density, decreased loop size, and eliminated voids [29]. Platinum addition to 316 SS resulted in no change in loop density and a small increase in loop size, but increased void size and density—all changes that can impact hardening under irradiation. The good agreement between proton and Ni ion irradiation results indicates that the major effect of the oversized solute is due not to the cascade (where there are large differences between proton and Ni ion irradiation), but rather to the post-cascade defect partitioning to the microstructure evolution. Electron irradiation experiments by Watanabe et al. [30] and proton irradiation experiments by Was et al. [27] showed that stainless steel with Ti additions had slightly lower dislocation loop densities and larger sizes compared to the base alloy. Addition of Nb increased only loop size. In contrast to the base alloy, neither the Ti- nor the Nb-doped alloys formed voids under the conditions tested. Addition of Zr to 304 SS resulted in reduced hardness and decreased loop density; loop size did not change in proton irradiation to 1.0 dpa at 400 °C (752 °F) and in comparison to the base alloy [31]. Samples containing Zr also had a lower void density with no change in void size as compared to the base alloy.

8.3.3 Long-Term Concerns for Radiation Hardening

The main concerns regarding radiation hardening at high doses involves the nucleation and growth of unanticipated precipitates and the increase in void swelling. The dislocation microstructure has been shown to be relatively unchanged up to very high doses [32]. Voids can contribute to hardness increases through a type of dispersed barrier-hardening mechanism and thus can further increase the hardness of alloys at high doses relative to that at low dose. The effect is additive and is governed by a root-mean-square law [33]; therefore, there is potential for significant increased hardening from loops.

In addition to loops and voids, radiation-induced precipitates can contribute to hardening. The role of γ' or G-phase in hardening of austenitic alloys has not yet been quantified, but is believed to contribute to the observed hardening behavior. Beyond these phases, the possibility exists that additional phases may be formed during irradiation. Ion irradiation of CP304 SS to 5 dpa at 360 °C (680 °F) has revealed the formation of copper precipitates of size 1.4 nm and density 1.55×10^{23} m^{-3} [34]. While the volume fraction is extremely small (0.005%), growth of these or other, unanticipated precipitates could contribute an additional hardening mechanism at high dose.

8.4 SWELLING AND IRRADIATION CREEP

8.4.1 Plant Experience

While swelling is more prevalent at high doses (>30 dpa) and high temperatures [>350 °C (662 °F)], certain locations in LWRs, such as the baffle bolt and baffle former plates, experience high temperatures (from gamma heating) and high doses. For example, swelling of baffle former plates bolted together with baffle former bolts produces a tensile stress along the axis of the bolt. While observations are still anecdotal, Figure 8.3 shows an example of swelling in a baffle bolt at modest doses and temperatures above 330 °C (626 °F). The bolt head in the figure was closest to the core, and the temperature distribution is caused by a combination of gamma heating and proximity to the coolant.

Measurements of irradiation creep and relaxation in LWR core internals is indirect, as direct observation is difficult. Figure 8.4 shows two examples of radiation-induced load relaxation. In Figure 8.4(a), load relaxation of a stainless steel bolt occurs under constant displacement conditions during irradiation at 288 °C. In Figure 8.4(b), radiation creep results in relaxation of an X-750 spring at 370 °C (698 °F). This process is quite reproducible over a wide range of materials and loading modes and generally produces sizeable (>50%) load relaxation within a few dpa. Thus, for example, in areas of the BWR shroud that receive a moderate neutron flux, if SCC initiation does not occur early in life (e.g., by 1 dpa), the relaxation in residual stress may diminish the likelihood of cracking later in life.

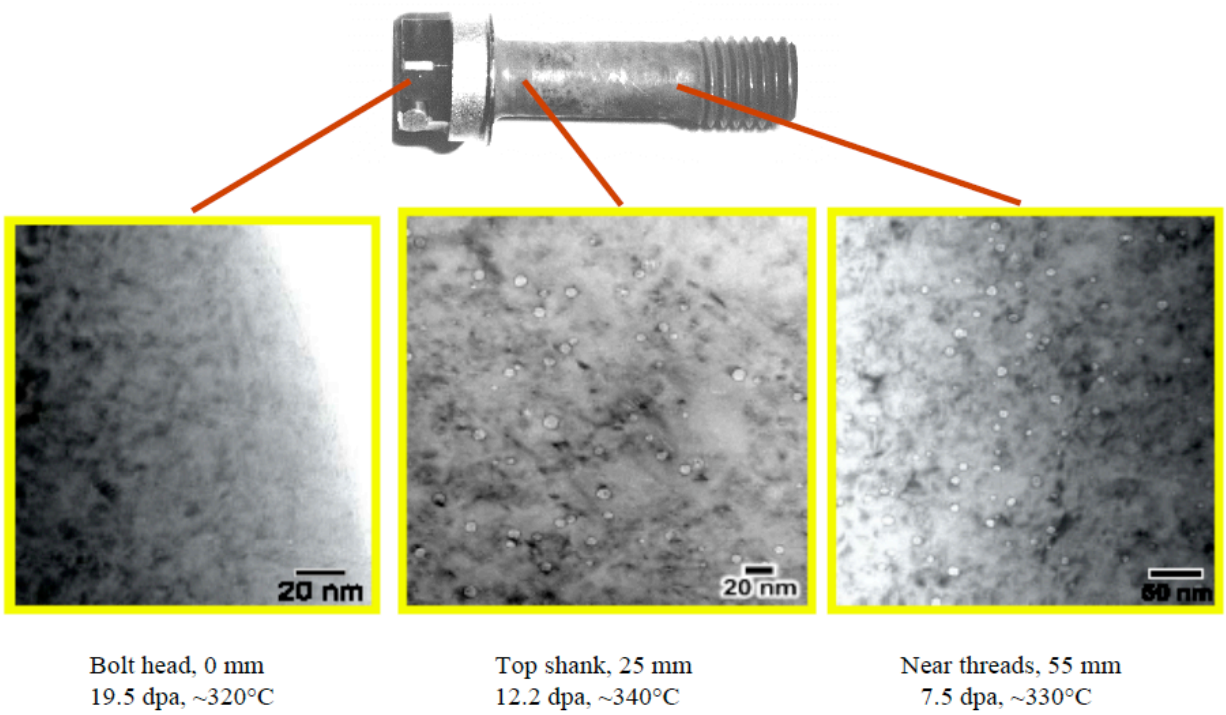

Figure 8.3. Swelling in a cold-worked 316 SS baffle bolt in a PWR as a function of position along the bolt length. The bolt head was closest to the core and the temperature distribution is caused by a combination of gamma heating and proximity to the coolant [33].
With kind permission from Springer Science+Business Media: G. S. Was, *Radition Materials Science: Metals and Alloys,* Springer, Berlin, 2007.

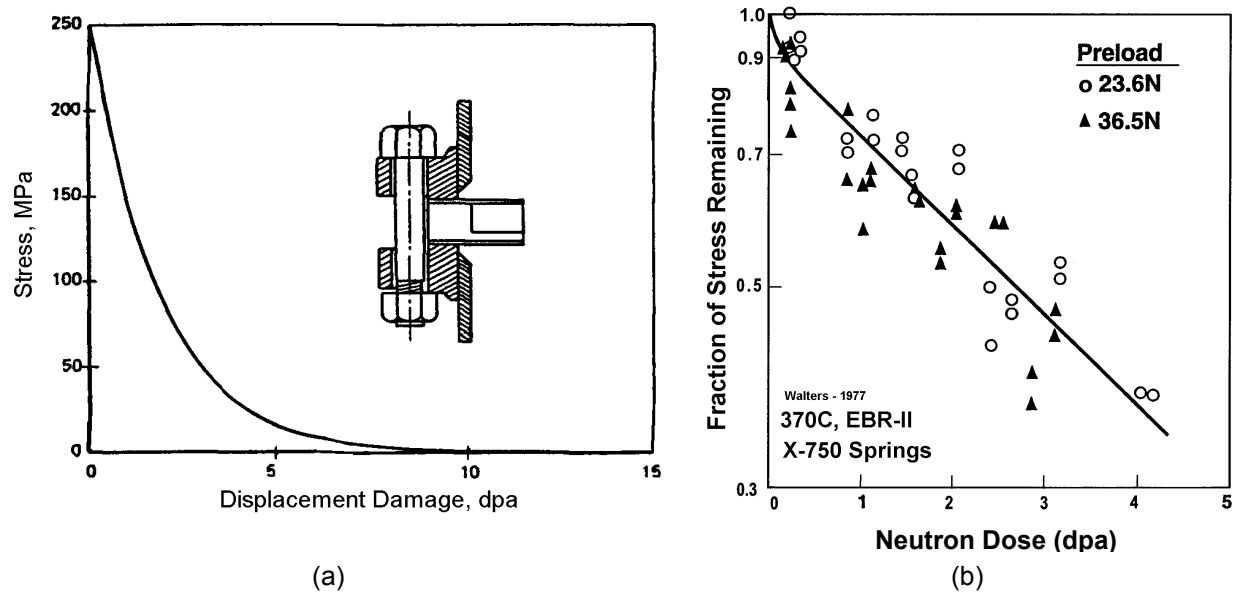

(a) (b)

Figure 8.4. (a) The effects of radiation-induced creep on load relaxation of stainless steel at 288 °C (550 °F) and (b) radiation creep relaxation of X-750 springs at 370 °C (698 °F) [35, 36]. Reprinted from *Journal of Nuclear Materials* 179–181(1), 130–134 (1991), Copyright 1991, with permission from Elsevier.

8.4.2 Mechanism and Parametric Dependencies

Swelling of SSs at the intermediate temperatures of an LWR core is reasonably well understood, though quantitative prediction remains a challenge. Nucleation of swelling is a strong function of damage rate, temperature, microstructure, and gas impurities. Void growth is a strong function of dose, dose rate, and temperature. The temperature dependence is best illustrated in Figure 8.5, which shows that over a wide range of doses, the demarcation between the swelling and the non-swelling regions in this Fe-Cr-Ni alloy is remarkably sharp, occurring over a 5 °C (41 °F) window. The lower dose rate in LWRs as compared to fast reactors enhances the nucleation of voids, and the higher production rate of He through transmutation reactions can stabilize void embryos. Thus, swelling can occur in core internal components in LWRs as long as the temperature is high enough. The result of swelling is an increase in volume of the component, which translates into an applied stress from surrounding components. Circumferential cracking in baffle former bolts has been observed at the intersection of the head and shank, and the sources of stress may well be swelling of the baffle plates. Reference [33] provides a more detailed treatment of the parametric dependencies of void growth.

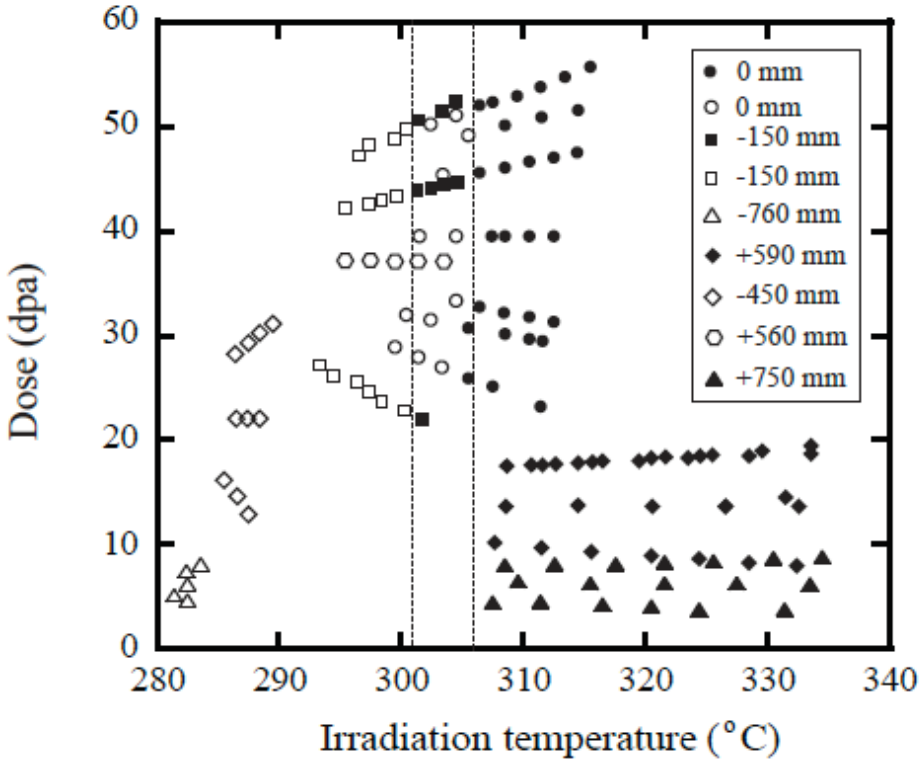

Figure 8.5. Dose-temperature plot of swelling in a Fe-Cr-Ni alloy irradiated in the BN-350 fast reactor showing the sharp temperature threshold for swelling [37]. Reprinted with permission of The Minerals, Metals & Materials Society.

At LWR temperatures, radiation creep results from diffusion of the radiation-produced vacancies and interstitial atoms to dislocations, enhancing the climb-to-glide process that controls time-dependent deformation. Radiation creep can be both beneficial and detrimental. Benefits accrue due to relaxation of constant displacement stresses (e.g., residual stress in welds and in loaded bolts and springs). However, under these conditions—and more so under constant load conditions—radiation creep also induces elevated creep rates, including grain boundary sliding, that may help to initiate and sustain SCC. Further, while the *average* magnitude of stress may be reduced by creep-induced stress relaxation, constraint in the polycrystal aggregate may result in high local stresses that could initiate a stress corrosion crack directly or cause large amounts of local grain boundary deformation that can rupture the oxide film locally, creating conditions for SCC initiation. Reference [33] provides a more comprehensive treatment of the creep mechanisms and dependencies.

While difficult to prove, the elevated and sustained deformation rates associated with radiation creep can also accentuate susceptibility to SCC. Estimates of crack tip deformation rates [2] indicate that radiation creep is not a large contributor to actively growing cracks, but rather it is expected to promote crack initiation and to sustain crack growth (or promote crack reinitiation, if an existing crack does arrest). It is important to factor radiation-creep relaxation into initial component design and subsequent SCC analysis. Its effect is significant and occurs in the same fluence range as radiation-induced segregation and radiation hardening.

As a specific example of this mechanism in service, radiation creep relaxation also affects PWR baffle bolts, which are subject to large variations in fluence and temperature [38, 39]. Baffle bolts

in high flux regions can accumulate more than 3 dpa per year; thus, the preload will rapidly decrease during the first several years. Therefore, SCC probably initiates early in life (before significant radiation creep relaxation occurs) or later in life when reloading occurs from differential swelling in the (annealed) baffle plates relative to the (cold-worked) baffle bolts.

8.4.3 Long-Term Concerns for Swelling and Creep

Concerns regarding the increased role of swelling and creep focus on the combination of dose, temperature, and gases produced by transmutation (He) or corrosion (H). The low temperature of most LWR internal components makes void nucleation difficult and the transition to steady-state void growth slow. With increasing years of operation, the higher doses reached could enable swelling to take hold and become more significant. The stability of voids will be enhanced by continued He production via the Ni reaction, as noted below. The role of hydrogen in void swelling remains uncertain, but there are indications that hydrogen can also stabilize voids. The implication is that dimensional stability will be reduced and stress on components will increase due to interaction of volume change in components (such as baffle plates and baffle bolts). A potential mitigating factor will be irradiation creep, which is dependent on many of the same parameters in much similar manner. Depending on the relative emergence of importance of these factors with increasing dose, risks of component degradation due to increased swelling and creep may be less, more, or much more severe than at lower doses.

Transmutation of various elements causes an increase in the He content of irradiated stainless steel and Ni alloys. At low fluence, transmutation of B produces He ($^{10}B + n \rightarrow {}^{6}Li + {}^{4}He$); the ^{10}B is consumed (burned out) within a few displacements per atom. While B segregates strongly to grain boundaries, the (n,α) reaction is energetic, and He is distributed throughout a region of ~10 µm around the grain boundary. A more prolific and persistent source of He occurs at higher fluence associated with $^{58}Ni(n,\gamma)$, ^{59}Ni, and ^{59}Ni (n,p and n,α) reactions. Because ^{59}Ni must be produced first, the production of He from this reaction is limited until 5–10 dpa. There is no evidence that He directly affects SCC behavior, but it can produce an increase in hardness and yield strength, and might affect fracture toughness. It is known to have a large effect on weld repairs because the thermal transient permits migration of He and the formation of bubbles along the grain boundaries. This can be managed to a certain extent by using low heat input processes, such as laser welding. Helium also stabilized void embryos, resulting in a shortening of the nucleation stage of voids. This also reduces the dose to reach steady-state (breakaway) swelling. Swelling can impact IASCC indirectly by causing isotropic strains, resulting in stresses in welded or bolted components, especially when swelling occurs at different rates in the fastened structures.

H is also produced by transmutation and proton injection during radiolysis of water, but these are small contributions in iron- and Ni-base alloys compared to the flux of H that occurs from exposure to the coolant. Unlike He, H is quite mobile, and readily permeates the material, entering and leaving voids, and other microstructural features. The hydrogen permeation rate is proportional to the square root of the coolant H_2 fugacity, so that H_2 inside a tube can dissociate and permeate back out of the tube into the coolant if the coolant H_2 level is reduced. Elevated H levels in metals are not evidence of extreme H fugacities in the metal; such elevations indicate only that there are more storage or trapping sites as the H permeates the metal.

8.5 EMBRITTLEMENT—DECREASE IN FRACTURE TOUGHNESS

8.5.1 Plant Experience

Chopra and Rao [40] reviewed the effect of neutron irradiation on the fracture toughness at 250–320 °C (482–608 °F) of austenitic stainless steels irradiated in LWRs [288–316 °C (550–601 °F)] up to about 17 dpa (Figure 8.6). The data show a rapid decrease in fracture toughness at a neutron dose of 1–5 dpa; this dose at the onset of the rapid decrease varies only somewhat with the alloy. In fact, the value of the fracture toughness, J_{Ic}, drops from values between 600–835 kJ/m^2 in the unirradiated condition to values as low as 20 kJ/m^2 for 304 SS irradiated to ~ 6 dpa and tested at 288 °C (550 °F) [41]. For the same irradiation conditions, the fracture toughness of thermally aged cast stainless steel (CF-8M) and weld metal (E308L SS) is lower than that for the HAZ material, which is lower than that for solution-annealed materials [42]. The fracture toughness values of welds and HAZ materials are consistently lower than those for the solution-annealed and even cold-worked materials. Some of the materials irradiated above 4 dpa at LWR temperatures show very low fracture toughness with J_{Ic} values near zero. For type 304 SS irradiated to 4.5–5.3 dpa (shown as cross in Figure 8.6), nine of ten compact tension (CT) specimens showed no ductile crack extension, and values of the plane strain fracture toughness, K_{Ic}, were 52.5–67.5 MPa m$^{1/2}$ (47.7–61.4 ksi in$^{1/2}$) [43]. The lowest fracture toughness, with K_{Jc} values in the range 36.8–40.3 MPa m$^{1/2}$ (33.5–36.6 ksi in.$^{1/2}$), was for a type 347 SS irradiated to 16.5 dpa in a PWR [43] and for a 304 SS irradiated to 7.4–8.4 dpa in a BWR [44].

Copra and Rao [40] note that the fracture toughness has also been observed to be orientation dependent. Fracture toughness *J–R* tests have been conducted on 304 SS control-rod and 304L SS top guide materials irradiated to 4.7–12 dpa and on 304 SS control-rod material irradiated to 7.4 and 8.4 dpa. The results show lower fracture toughness in the T–L orientation than in the L–T orientation [45]. The lower fracture toughness along the T–L orientation has been attributed to the presence of stringers consisting of long, narrow particles oriented in the rolling direction, which result in a long and narrow quasi-cleavage structure parallel to the crack advance, thereby accelerating the crack advance [45]. In addition, the 304 SS irradiated to 7.4–8.4 dpa showed very low fracture toughness (J_{Ic} of 40 kJ/m^2 in L–T and 7.5 kJ/m^2 in T–L orientation). The low J_Ic of this material was considered a special case of materials containing a high density of precipitates and inclusions aligned in the rolling direction. Nonetheless, these results show that very low fracture toughness values are possible for irradiated austenitic stainless steels.

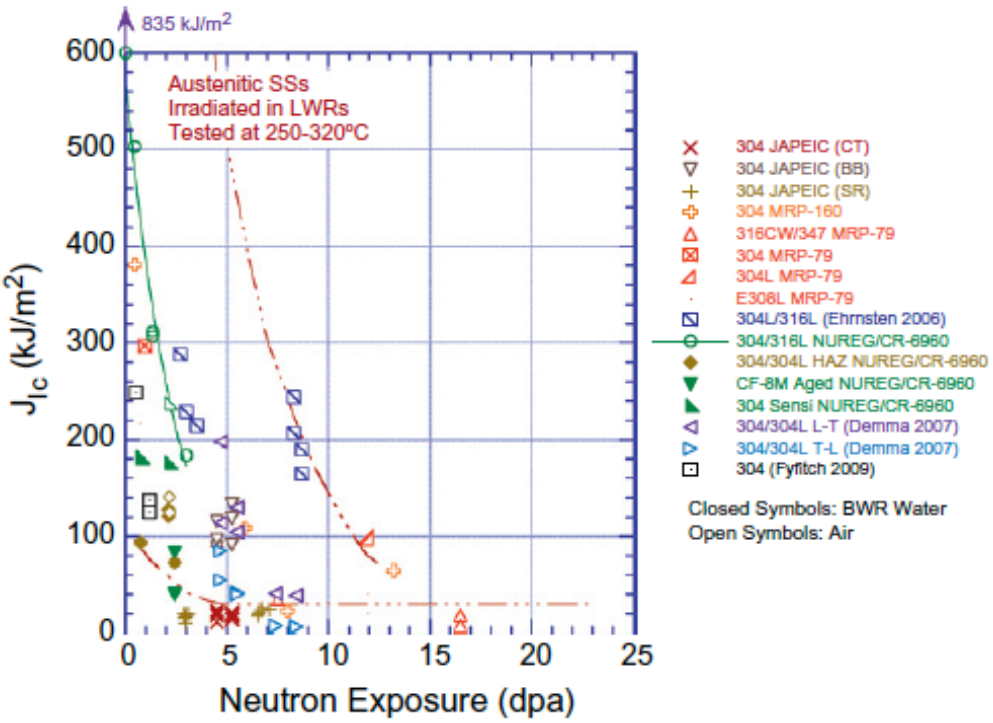

Figure 8.6. Fracture toughness as a function of neutron dose for austenitic alloys irradiated in LWRs [288–316 °C (550 °F–601 °F)] and tested in the temperature range 250 °C–320 °C (482 °F–608 °F) [40].
Reprinted from O. K. Chopra and A.S . Rao, "A review of irradiation effects on LWR core internal materials—neutron embrittlement," *Journal of Nuclear Materials* 412, 195–208 (2011), with permission from Elsevier.

8.5.2 Mechanism and Parametric Dependencies

Odette and Lucas [46] used a scaling relationship to describe the dependence of fracture toughness on irradiation:

$$\frac{K_{Ic}^{irr}}{K_{Ic}^{unirr}} = \sqrt{\frac{e_u^{irr}}{e_u^{unirr}} \frac{\sigma_0^{irr}}{\sigma_0^{unirr}}}, \quad (1)$$

where e_u is the uniform engineering strain. While it tracks the data well, this relation does not provide a physical basis for the reduction in toughness. Instead, it has been proposed that the decrease in fracture toughness with irradiation is due to a change in fracture mode from ductile-dimple rupture to cleavage. This process is described in more detail below.

In the unirradiated condition, ductile metals such as stainless steels fracture by ductile-dimple rupture in which voids nucleate and grow in the plastic region ahead of the crack tip until they eventually link up with the crack tip by necking of the remaining ligament [Figure 8.7(a)]. At low dose, irradiation may accelerate void linkage by work softening and localized deformation. In either case, the fracture toughness can be related to deformation parameters by [47]:

$$K_{Jc} = \sqrt{1.5\beta b \sigma_0 E'}, \quad (2)$$

where β is the ratio of crack opening to the distance to the next void at the point of crack-void linkage [$\beta = \delta/b$, and $E' = E/(1 - \nu^2)$, where δ represents crack tip opening displacement, E is Young's modulus and ν is Poisson's ratio]. The value of β decreases as deformation becomes increasingly localized. At high doses, crack advance is more likely controlled by heterogeneous deformation in the zone ahead of the crack due to intense dislocation channeling in the solid. In this case, fracture occurs by a decohesion process in which deformation is concentrated into a series of plastic ligaments behind the crack tip [Figure 8.7(b)]. Crack growth occurs when the displacement capacity of the last ligament, Δ_z, is reached under a local stress σ_z:

$$K_{Jc} = \sqrt{0.5\Delta_z \sigma_z E'}. \tag{3}$$

While these models are consistent with the role of the increased localization of plastic flow with irradiation dose, confirming experiments have yet to be conducted.

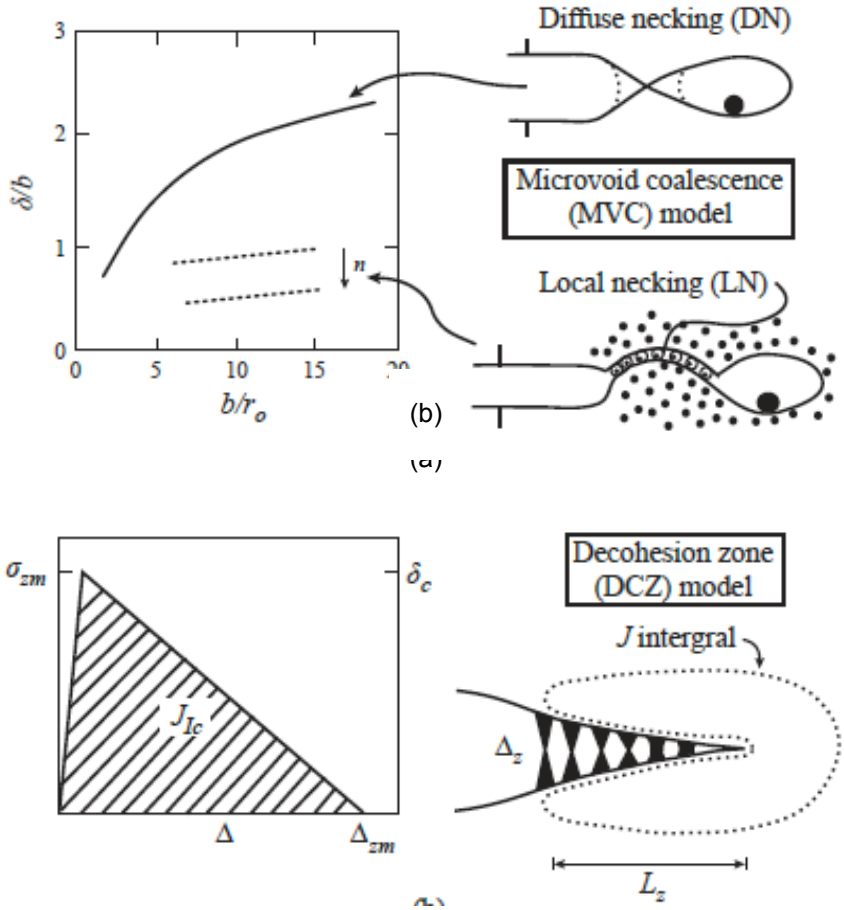

Figure 8.7. Models of ductile fracture. (a) Microvoid coalescence model: ratio of crack opening, δ to distance to the next void at the point of crack linkage, r^* vs the latter quantity normalized by the initial inclusion radius, r_0. (b) Decohesion zone model: crack growth by the failure of plastic ligaments bridging the faces of a virtual crack [47].
Reprinted from G. R. Odette and G. E. Lucas, *Journal of Nuclear Materials* 191-194, 50–57 (1992), with permission from Elsevier.

In addition to altering the ductile fracture process, irradiation may also result in a change in fracture mode from ductile-dimple rupture to cleavage. It is well known that plasticity can induce martensite formation in austenitic stainless steels that may fracture by a quasi-cleavage mechanism. However, such processes are unlikely when deformation occurs at temperatures $\geq$300 °C (572 °F).

Microstructural characterization of the 304 SS control-rod material has revealed a fine distribution of γ' phase with particle size in the range 2–10 nm and an average size of 4.4 nm [45]. The γ' phase has also been observed at dose levels above 4 dpa in cold-worked 316 SS irradiated under the PWR condition [48]. The presence of precipitates can change the strain-hardening behavior, and changes in material microchemistry due to radiation-induced segregation can change the deformation behavior, both of which can affect the fracture toughness of the material. The contribution of additional precipitate phases, voids, and cavities on fracture toughness needs to be investigated.

There is also evidence that the reduced fracture toughness may be correlated with void swelling. A classic example is a 316 SS alloy irradiated in EBR-II to 130 dpa at 400 °C (752 °F), resulting in 14% void swelling that fractured during handling at room temperature [49]. It has been proposed that the combination of radiation-induced segregation of Ni and Si to grain boundaries and void surfaces, and the formation of γ' reduces the stacking fault energy, resulting in greater slip planarity and an increase in the propensity for flow localization and fracture in the channels [40, 49].

8.5.3 Concern for Long-Term Embrittlement

While the exact processes by which irradiation induces embrittlement are not completely known, it is understood that the measured reduction in fracture toughness correlates with restriction or localization of plastic flow, formation of a distributed hard precipitates, and swelling. Localized deformation occurs after relatively low dose and, while the restriction of plastic flow becomes greater at higher dose, the degree of localized deformation should not change dramatically over the fluence interval between 60 and 80 years of life. However, the probability of second phase formation is much less well known, and it is possible that high doses could lead to the formation of precipitates that have not yet been observed. It is highly likely that void swelling will become more severe with extended operation. So if swelling has an effect on fracture toughness, then it will only worsen with age during extended operation.

8.6 FATIGUE

8.6.1 Plant Experience

There is a scarcity of data on the effect of neutron irradiation on fatigue in current LWRs. Chopra and Rao [50] reviewed the literature on the effect of neutron irradiation on fatigue crack growth and noted that most of the data have been generated under the fast breeder reactor program. In air, irradiation does not appear to enhance fatigue crack growth rates [50]. However, recent data have been collected on the crack growth rate (CGR) of solution-annealed 304 SS and 316 SS irradiated up to 3 dpa and tested in high- and low-dissolved oxygen (DO) environments. Figure 8.8 plots CGR in the environment against that in air for the same loading conditions. The data show that at low dose, there is little departure from the 45° line at low DO. However, increasing DO results in an increase in the CGR, and increasing dose causes the departure to increase still

further. Data on CGR of unirradiated HAZ weld material shows very similar CGRs and increases on CGR relative to air.

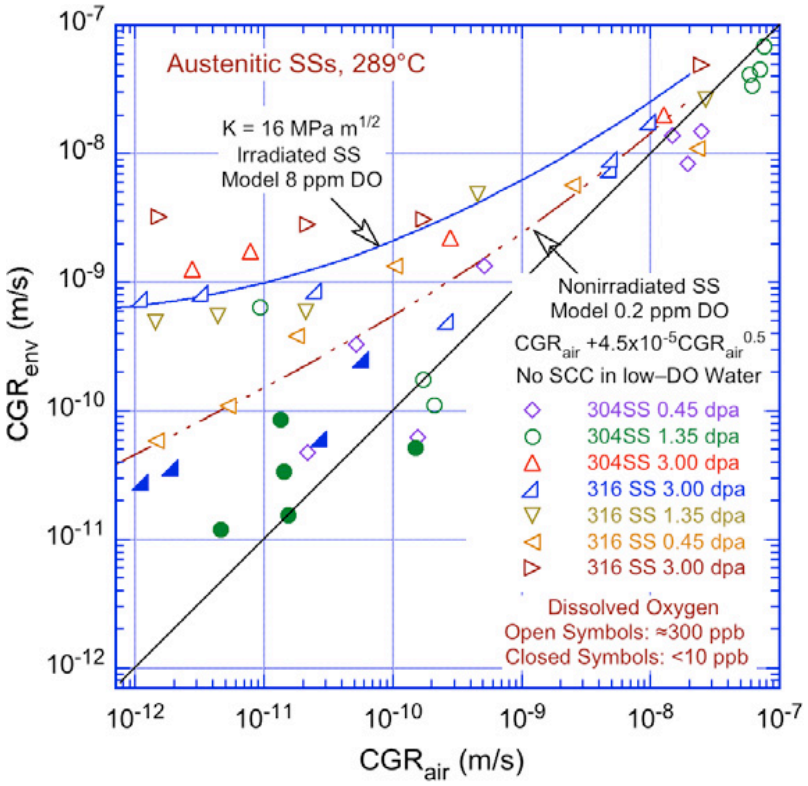

Figure 8.8. Fatigue crack growth rate for irradiated austenitic stainless steels tested in 289 °C (552 °F) water containing varying amounts of dissolved oxygen [50]. Reprinted from O. K. Chopra and A. S. Rao, "A review of irradiation effects on LWR core internal materials—neutron embrittlement," *Journal of Nuclear Materials* 412, 195–208 (2011), with permission from Elsevier.

8.6.2 Mechanism and Parametric Dependencies

The role of irradiation on fatigue is poorly understood, and existing data are minimal. Due to the reduced uniform strain and increasing localization of plastic deformation resulting from irradiation, it may be expected that fatigue crack growth should respond accordingly. In particular, in stage III fatigue crack growth, where the growth rate is limited by the fracture toughness, a reduction in fracture toughness due to irradiation will result in an increase in crack growth rate. In stage I, the threshold stress intensity range ΔK_{th} is sensitive to the chemical environment, the *R*-ratio, the grain boundary impurity segregation, and the tendency for high strength materials to undergo flow localization. This latter sensitivity is supported by empirical data showing that ΔK_{th} decreases with increasing yield strength in unirradiated 316 SS [51]. Consequently, the severe localization of plasticity caused by irradiation might lead to decreases in the threshold stress intensity.

However, the data on the effect of irradiation on fatigue in austenitic stainless steels in the low-to-intermediate temperature range is mostly in stage II as described by the Paris equation. In this regime, crack propagation is primarily dependent on the elastic constant of the material, and

less so on the microstructure and on plastic deformation processes. Limited data show that the crack growth rate is, in fact, relatively insensitive to irradiation to doses of up to about 30 dpa. Figure 8.9 shows that the crack growth rate of 316 SS irradiated to 2.03 × 10^{21} n/cm^2 at 380 °C (716 °F) is bounded by the high values for crack growth in mill-annealed plate and the low crack growth values for the 20% cold-worked plate, both in the unirradiated condition. As such, irradiation of austenitic stainless steels to low or intermediate doses does not result in measurable increases in fatigue crack growth. However, with increasing temperature, the generation and accumulation of He into bubbles can affect the nature and rate of fatigue crack propagation.

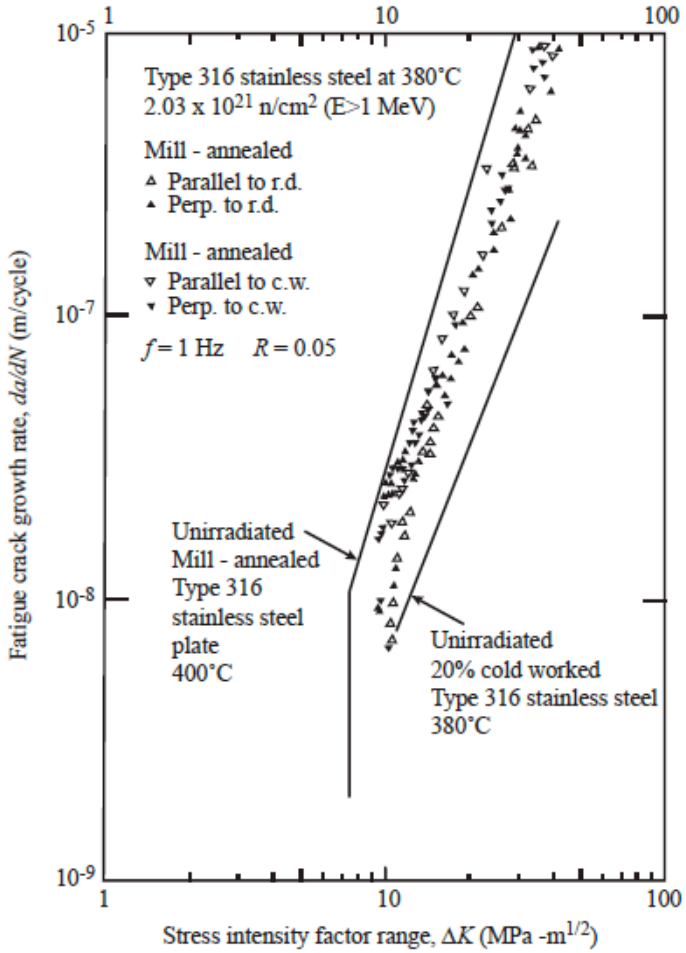

Figure 8.9. Effect of irradiation to 2.03 × 10^{21} n/cm^2 (E > 1 MeV) at 380 °C (716 °F) on fatigue crack propagation rate in mill-annealed and 20% cold-worked 316 SS [52]. Reprinted from G. Lloyd, *Journal of Nuclear Materials* 110, 20–27 (1982), with permission from Elsevier.

Nevertheless, it may be expected that under irradiation, low cycle fatigue life should decrease due to decreased ductility, and high cycle fatigue life should increase due to increased strength. This behavior was indeed measured for 304 SS at both room temperature and 325 °C (617 °F) following irradiation to 8 × 10^{22} n/cm^2 (E > 0.1 MeV) at a temperature of 400 °C (752 °F) [53]. The effect of irradiation in high cycle fatigue is less deleterious because despite significant hardening and a reduction in work hardening coefficient by a factor of 2.7, the alloy retained ductility to 4–5% elongation.

8.6.3 Long-Term Concern for Fatigue

Irradiation is important in influencing the high cycle fatigue, low cycle fatigue, and fatigue crack growth. The existing database for the effect of irradiation in LWRs on fatigue crack growth is limited to very low doses (about 3 dpa). There are no data on the role of irradiation at high doses encountered in LWR core components. Similarly, sparse data exists on irradiation effects on either low or high cycle fatigue in hot water. In all cases, hardening and flow localization are expected to play a role. While both tend to saturate at relatively modest doses (~5 dpa), hardening and localization can also be affected by precipitation reactions or the growth of voids or bubbles. Since these all tend to be higher dose phenomena in LWRs, the response of fatigue to such high dose processes is essentially unknown and represents significant opportunities for future study.

8.7 IRRADIATION-ASSISTED STRESS CORROSION CRACKING

8.7.1 Past and Current Plant Experience

Perhaps the single most important way in which irradiation can affect material performance in LWR core materials is in the inducement of SCC. Early plant (Figure 8.10) and laboratory (Figure 8.11) observations showed that the same basic dependencies existed for unirradiated and irradiated stainless steels, and that increasing fluence produces a well-behaved increase in SCC susceptibility (Figure 8.12). Intergranular SCC is promoted in austenitic stainless steels above a “threshold” fluence (Figures 8.11 and 8.12). This occurs in oxygenated (e.g., BWR) water above 2 to 5 × 10^{20} n/cm^2 (E > 1 MeV), which corresponds to about 0.3 to 0.7 dpa, and the fluence depends on the stress, water chemistry (especially sulfate and chloride), operating time, and other factors. (Therefore, it is not a true threshold, but rather indicates that a minimum fluence is required before IASCC is observed). Attempts to reproduce the same level of intergranular cracking in inert environments have been unsuccessful, confirming that it is an environmental cracking phenomenon, not simply a change in the microstructure, mechanical properties, and overall response of the irradiated material in an inert environment. Figure 8.10 shows a strong effect of water purity for both unirradiated and irradiated BWR components, and Figure 8.11 shows a very similar response to corrosion potential to that shown in Figure 8.13. As shown in Figure 8.13, dissolved oxygen strongly influences corrosion potential, which in turn affects crack chemistry and growth rate of sensitized stainless steels (two graphs at left) as well as cold-worked stainless steels and Alloy 600 (large rectangular symbols on right graph) and irradiated stainless steel (large triangular symbols). Cold-worked or irradiated materials have an elevated yield strength and exhibit an increase in growth rate at both low and high potential.

IASCC field experience is, perhaps, best summarized by the following trends and correlations [57]:

Water impurities: Impurities, especially chloride and sulfate, strongly and similarly affect IASCC in BWR water (Figure 8.10). This correlation applies equally to low and high flux regions and to laboratory experimental data on stainless steels [Figure 8.10(a) and (b)] and Ni-base alloys [Figure 8.10(b)], and closely parallels in the behavior observed in test specimens from out-of-core components. At higher concentration levels, the same impurities can affect SCC in PWRs. If high corrosion potential conditions form in the PWR primary (where B and Li are present), the crack chemistry is dramatically altered, and high growth rates can result.

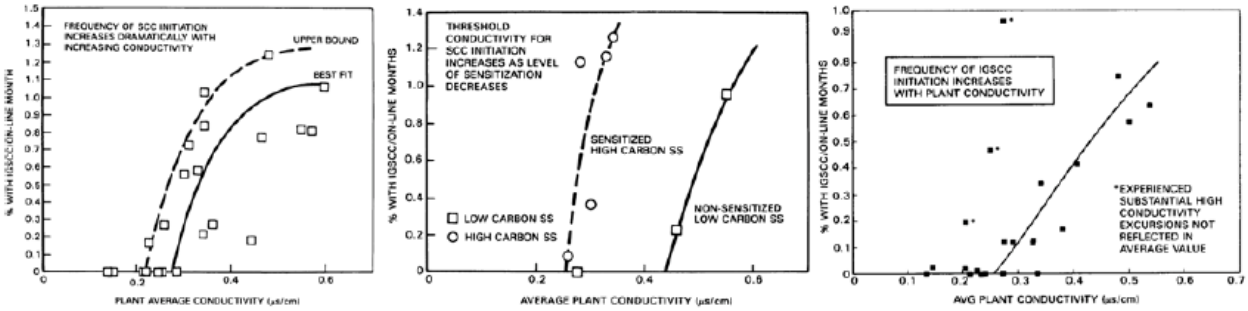

Figure 8.10. The effects of average plant water purity are shown in field correlations of the core component cracking behavior for (a) stainless steel intermediate and source range monitor dry tubes, (b) creviced stainless steel safe ends, and (c) creviced Alloy 600 shroud head bolts, which also shows the predicted response vs. conductivity [54, 55].
Reprinted with permission of The Minerals, Metals & Materials Society.

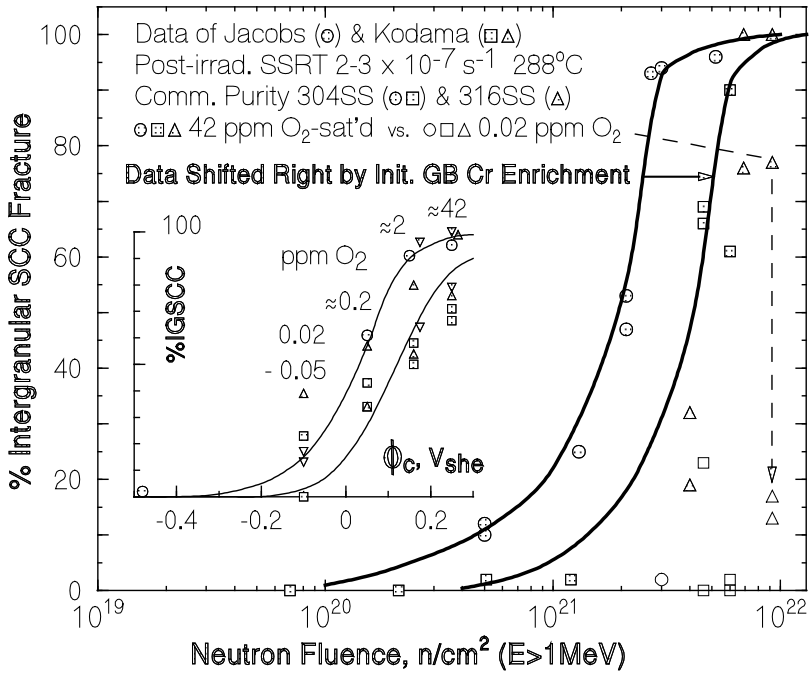

Figure 8.11. Dependence of IASCC on fast neutron fluence as measured in slow-strain rate tests at 3.7×10^{-7} s^{-1} on pre-irradiated 304 SS in 288 °C (550 °F) water [56]. The effect of corrosion potential via changes in dissolved oxygen is shown at a fluence of $\approx 2 \times 10^{21}$ n/cm^2.

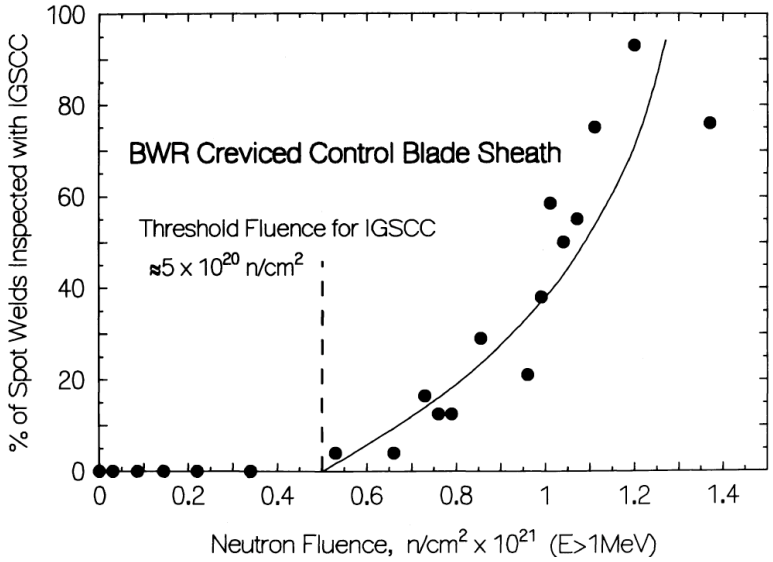

Figure 8.12. Dependence of IASCC on fast neutron fluence for creviced control blade sheath in high conductivity BWRs [54].

Corrosion potential: Field and laboratory data demonstrate that corrosion potential is a very important parameter, with its effect being consistent from zero to low to high fluence, except in some high fluence materials and/or under high stress intensity factor conditions where high growth rates are always observed. Materials prone to high radiation induced changes in grain boundary Si level may exhibit a very limited effect of corrosion potential. While corrosion potential usually affects crack initiation and growth, there is no evidence of *threshold* potential; indeed, it is not fully accepted that irradiated materials exhibit IASCC in deaerated water.

Crevices: Cracking is enhanced by crevices, primarily because of their ability to create a more aggressive crevice chemistry from the gradient in corrosion potential (in BWRs) or in temperature (most relevant to PWRs), which in turn can accelerate crack initiation. Stress and strain concentration can also occur in crevices, depending upon the severity (sharpness) of the tip of the crevice.

Temperature: Temperature increases both IASCC initiation and growth rate.

Fluence: IASCC of annealed stainless steel was once thought to occur only at fluences above $\approx 0.3 \times 10^{21}$ n/cm^2. However, significant intergranular cracking in BWR core shrouds (which have no thermal sensitization) occurs over a broad range of fluences, showing that a firm fluence threshold does not exist. The observations of SCC in unirradiated, unsensitized stainless steel (with or without cold work) also undermine the concept of a fluence *threshold* below which no SCC occurs. The use of concepts of thresholds in corrosion potential, water impurities, temperature, etc., has also been disproven.

Integration of fluence effects: Irradiation has a complex effect on SCC susceptibility. While radiation segregation and radiation hardening increase susceptibility, radiation creep relaxation of constant displacement loads (e.g., bolts and welds) tends to reduce susceptibility. For these reasons, SCC in BWR shrouds and PWR baffle bolts does not always correlate strongly with fluence. SCC can be interpreted and predicted only by accounting for the conjoint effects of multiple factors.

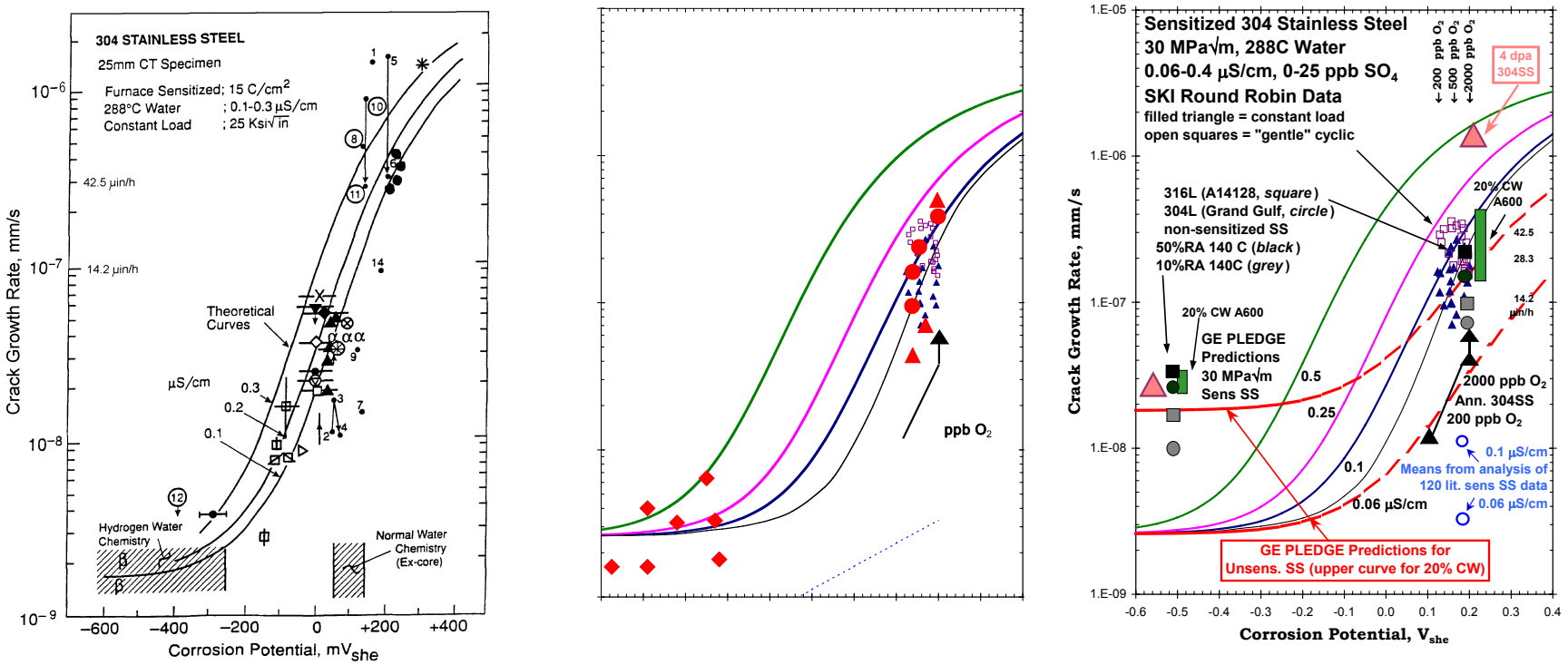

Figure 8.13. SCC growth rate vs. corrosion potential for stainless steels tested in 288 °C (550 °F) high-purity water containing 2,000 ppb O_2 and 95–3,000 ppb H_2.Dissolved oxygen strongly influences corrosion potential, which in turn affects crack chemistry and growth rate of sensitized stainless steels (two graphs at left) as well as cold-worked stainless steels and Alloy 600 (large rectangular symbols on right graph) and irradiated stainless steel (large triangular symbols). Cold-worked or irradiated materials have an elevated yield strength and show an increase in growth rate at both low and high potential [57].

Dynamic stress and strain: High stress and dynamic strains were responsible for the earliest incidents of IASCC, but cracking has since been observed at quite low stresses at high fluences during longer operating exposure. Laboratory and field data indicate that IASCC growth can occur at stress intensity factors well below 10 MPa√m, and initiation can occur at <20% of the irradiated yield stress.

Cold work: Bulk cold work, surface cold work (especially abusive surface grinding leading to a coarse surface and residual strains in the near-surface material), and weld residual strain in the heat affected zone tend to exacerbate all forms of SCC, although they can also delay the onset of some radiation effects (especially swelling) by creating more sinks for interstitials and vacancies.

Grain boundary Cr depletion: Preexisting grain boundary carbides and/or Cr depletion are not essential to IASCC, although furnace sensitized stainless steels are clearly highly susceptible to cracking in-core. Preexisting Cr depletion (e.g., from thermal sensitization) is magnified by irradiation and increases the IASCC susceptibility (primarily in pH-shifted environments, as can develop when potential or thermal gradients exist). In the absence of Cr depletion, the presence of grain boundary carbides or other particles is beneficial. The role of N, S, P, and other grain boundary segregants is less clear.

Interdependencies: The fluence at which IASCC is observed depends on applied stress and strain, corrosion potential, solution conductivity, crevice geometry, cold work, prior sensitization, etc. At sufficiently high conductivities, cracking has been observed in solution-annealed stainless steel in the field and in the laboratory. Thus, while potentially useful in an engineering context, the concept of a *threshold* fluence (or stress, corrosion potential, etc.) is scientifically misleading. IASCC initiation and growth must be understood in terms of the interdependent effects of many parameters.

8.7.2 Mechanisms and Parametric Dependencies

It is proposed that radiation enhances SCC primarily in four ways: segregation, hardening, relaxation, and radiolysis (Figure 8.14). At high fluence, differential swelling can produce reloading, and He generation and development or dissolution of phases in the microstructure can play a role. The neutron fluence where these processes have an effect is shown in Figure 8.15, along with the current end-of-life fluence projections for various BWR and PWR components. The primary radiation effects on materials operate in a similar range of fluence, and thus their individual contributions can be difficult to distinguish. An example of their interaction in altering SCC growth rate is shown in the prediction of cracking of a weld in a BWR core shroud (Figure 8.16), in which the individual effects are plotted along with the resulting crack length vs. time. As show in Figure 8.16, less aggressive water chemistry (corrosion potential and water purity) would result in less crack advance early in life, which would give a greater opportunity for radiation creep relaxation. The leak depth is the wall thickness of the shroud. While radiation hardening continues to increase the yield strength, its effect on crack growth tends to saturate. While many of the enhancements in SCC susceptibility from irradiation dose (neutron fluence) have been well established, it remains possible that additional factors will emerge at high fluence (e.g., >30 dpa). An extensive discussion of the possible mechanisms behind IASCC appears elsewhere [57] and will not be repeated in detail here. Rather, the processes believed to be important in the IASCC mechanism are summarized below.

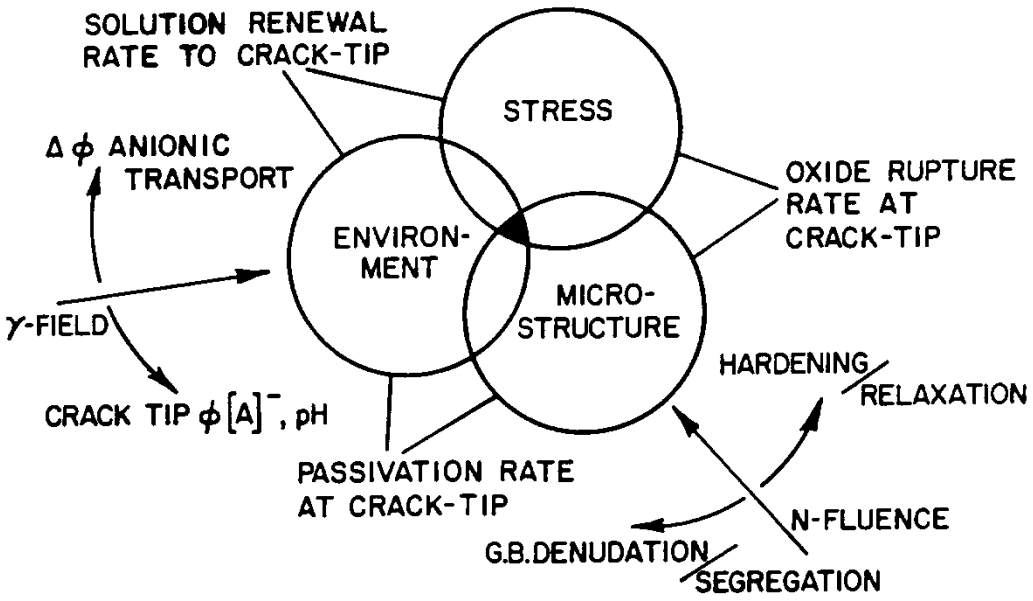

Figure 8.14. Schematic of the primary engineering parameters that effect SCC—stress, microstructure, and environment—and the underlying crack tip processes that control SCC [57]. The primary ways in which radiation affects SCC are also shown: segregation, hardening, relaxation and radiolysis. Radiolysis can increase the corrosion potential, which in turn increases the potential gradient ($\Delta\varphi$) and the crack tip potential φ, anion concentration [A], and pH.

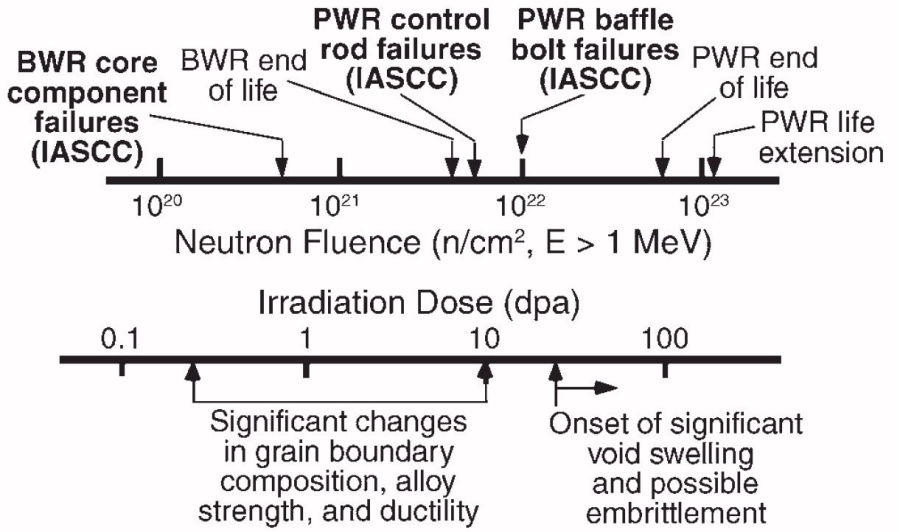

Figure 8.15. Neutron fluence effects on irradiation-assisted stress corrosion cracking susceptibility of 304 SS in BWR environments [3]. "End of life" above refers to end of 60 year operating period while "life extension" refers to end of 80 years.
Reprinted from S. M. Bruemmer, E. P. Simonen, P. M. Scott, P. L. Andresen, G. S. Was, and J. L. Nelson, "Radiation-induced material changes and susceptibility to intergranular failure of light-water-reactor core internals," *Journal of Nuclear Materials* 274(3), 299–314 (1999), with permission from Elsevier.

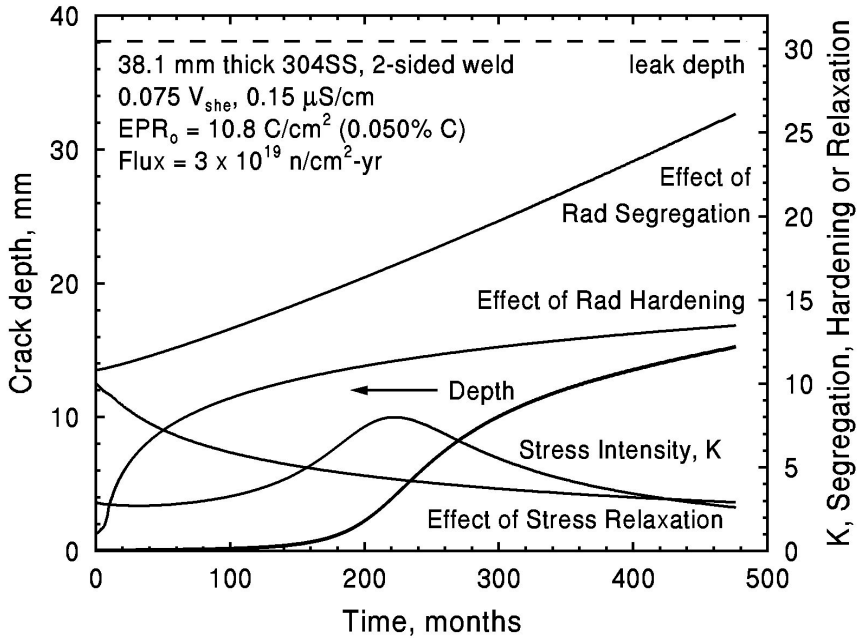

Figure 8.16. Predicted effect of radiation segregation, radiation hardening, and radiation creep relaxation on a BWR core shroud, where the through-wall weld residual stress profile is the primary source of stress [57]. Less aggressive water chemistry (corrosion potential and water purity) would result in less crack advance early in life, which would give a greater opportunity for radiation creep relaxation. The leak depth is the wall thickness of the shroud. While radiation hardening continues to increase the yield strength, its effect on crack growth tends to saturate.

- Dynamic strain is recognized as important in SCC in hot water, and it is widely considered to be a fundamental parameter, both by experimental observation and conceptually because the slip offsets caused by plastic strain disrupt the surface passive films that in turn impart corrosion resistance. Laboratory experiments, conducted with irradiated materials, and in-reactor data show that there is a strong effect of very slow straining or test perturbation on crack nucleation, short crack coalescence, and crack growth. Analysis of field data on PWR baffle former bolts showed a major influence of load following (daily reactor power changes) on incidence of SCC in bolts made from the same materials and used in multiple plants. If cyclic loading is present, the dynamic strain at the crack tip, or crack tip strain rate, results from the reversed slip processes that cause (inert) fatigue crack advance. In slow strain rate tests, the crack tip strain rate results from the applied strain rate, which is partitioned among the number of growing cracks. At constant load (or constant K), the dynamic strain results from the crack advance process itself, although thermal and irradiation creep can play a role. As the crack advances, the stress/strain field at the crack tip must be redistributed, which requires dislocation motion. This creates an interesting feedback circuit: dynamic strain causes crack advances, which sustain the dynamic strain. This is not non-physical, but it does make SCC much more difficult to study than, for example, corrosion fatigue.

- Radiation-induced segregation produces enrichment of some species (e.g., Ni and Si) at grain boundaries and other defect sinks, and depletion of other species (e.g., Cr). Even though the distance over which radiation-induced segregation occurs is very limited (a few nanometers), studies on unirradiated materials have shown that the narrow profiles can affect SCC. While Cr depletion is believed to be important only in the case of an oxidizing

environment, in low potential environments, segregation of other species, such as Si, could create deleterious results.

- Radiation hardening, which results from radiation damage and the creation of vacancy and interstitial loops, can impede dislocation motion. Once a few dislocations move along a slip plane, they clear the “channel” of most of these barriers, and subsequent dislocation motion occurs primarily along these channels. The localization of deformation into these channels creates very high local stresses and strains at their intersections with grain boundaries.

- Radiation creep relaxation reduces constant displacement stresses such as those that can occur in bolts or that are associated with weld residual stress. During active irradiation, however, radiation creep can promote dynamic strain, and thereby SCC.

- Swelling occurs to a limited extent at temperatures above ~300 °C (572 °F) but can be sufficient to produce reloading of components such as PWR baffle former bolts. Swelling occurs differently in different materials and is delayed in cold-worked materials. Stresses due to swelling are balanced by radiation creep relaxation, but the resulting stress can be sufficient to cause IASCC.

- Other microstructural changes include, for example, precipitation or dissolution of phases in materials. The lack of any clear evidence that such changes affect IASCC response may only be a reflection of the limited characterization and IASCC studies that have been performed on materials subjected to high fluence.

8.7.3 Long-Term Concern for IASCC

The lack of a clearer understanding and a consensus-mechanism for IASCC creates considerable difficulty in identifying long-term technical issues for IASCC for reactor components in service. However, given the physical, chemical, and mechanical processes that are believed to contribute to IASCC, it is possible to identify those likely to become more important. For example, the data suggest that, with the possible exception of Si, radiation-induced segregation at grain boundaries saturates at relatively modest doses (~5 dpa) and does not change much with increasing dose. Therefore, an increase in severity of IASCC driven by radiation-induced segregation seems unlikely. The same is true for the dislocation microstructure and the resulting hardening. However, precipitation of second phases remains an unknown at high doses. G-phase and γ’ are known to form at lower doses. Their behavior at high dose, however, is unknown. The observation of Cu precipitation in 304 SS suggests that other second phases may indeed form and become stable at higher doses.

Swelling is one such process that is very likely to become a bigger problem with longer reactor operating periods. The temperature range of core internals is at the lower edge of the swelling range, but with increasing dose, significant swelling could occur. Increased swelling of certain components, such as baffle plates, means increased stresses on the baffle bolts. So regardless of the mechanism, swelling will provide increasing stress that will drive IASCC. The role of irradiation creep in mitigating swelling is also relatively unknown. It may be that creep will mitigate swelling, but creep strains and swelling strains are not necessarily offsetting, so it is unlikely that they will completely cancel everywhere.

8.8 IRRADIATION ACCELERATED CORROSION

Irradiation can affect corrosion or oxidation in at least three different ways. First, radiation interaction with water can result in the decomposition of water (radiolysis) into radicals and oxidizing species that will increase the corrosion potential and lead to greater corrosion rates. Second, irradiation of the solid surface can produce excited states that can alter corrosion, such as in the case of photo-induced corrosion [58]. Displacement damage in the solid will result in a high flux of defects to the solid–solution interface that can alter and, perhaps, accelerate interface reactions. Defect fluxes to the oxide metal interface will also be increased by damage to the alloy. Third, radiation can affect oxide properties such as density, thermal conductivity, and crystal structure or phase fraction. Largely because of the difficulty in conducting controlled experiments, little data exist to provide an understanding of the role of irradiation of the solid in the corrosion process. However, experiments that *include* damage to the substrate show significantly larger increases in oxidation rate than those in which the effect is confined to the water. While irradiation is believed to affect corrosion of stainless steels, no experimental data exist to confirm such belief and enable the development of confirmatory models.

8.9 SUMMARY

Austenitic stainless steels and nickel (Ni)-base alloy steels are used for numerous core internal components in both BWRs and PWRs. The effect of irradiation on these core internal materials has been examined for decades. When considering an additional 20 years of service, the additional time will also result in increased neutron fluence (which may be compounded since power uprates may also increase the flux and fluence). Existing forms of irradiation-induced degradation are expected to become more severe with increased fluence, although new modes of degradation may also be observed at fluences corresponding to 80 years of service.

Key irradiation-induced degradation concerns for extended service include:

- Radiation hardening: Increases in the hardness of the material due to irradiation may change performance and reliability in service.
    - The main concerns regarding radiation hardening at high doses involves the nucleation and growth of unanticipated precipitates and the increase in void swelling. The dislocation microstructure has been shown to be relatively unchanged up to very high doses, although voids can contribute to hardness increases can further increase the hardness of alloys at high doses relative to that at low dose.
    - In addition to loops and voids, radiation-induced precipitates can contribute to hardening. The role of γ' or G-phase in hardening of austenitic alloys has not yet been quantified, but is believed to contribute to the observed hardening behavior. Beyond these phases, the possibility exists that additional phases may be formed during irradiation.

- Swelling and irradiation creep: The low temperature of most LWR internal components makes void nucleation difficult and the transition to steady-state void growth slow.
    - With increasing years of operation, the higher fluences will enable swelling to take hold and become more significant. The stability of voids will be enhanced by continued He production via the Ni reaction. The role of hydrogen in void swelling remains uncertain, but there are indications that hydrogen can also stabilize voids.
    - The implication is that dimensional stability will be reduced and stress on components will increase due to interaction of volume change in components (such as baffle

plates and baffle bolts). A potential mitigating factor will be irradiation creep, which is dependent on many of the same parameters in much similar manner. Depending on the relative emergence of importance of these factors with increasing dose, risks of component degradation due to increased swelling and creep may be less, more, or much more severe than at lower doses.

- Radiation-induced embrittlement: While the exact processes by which irradiation induces embrittlement are not completely known, it is understood that the measured reduction in fracture toughness correlates with restriction or localization of plastic flow, formation of a distributed hard precipitates, and swelling. Localized deformation occurs after relatively low dose and, while the restriction of plastic flow becomes greater at higher dose, the degree of localized deformation should not change dramatically over the fluence interval between 60 and 80 years of life. However, the probability of second phase formation is much less well known, and it is possible that high doses could lead to the formation of precipitates that have not yet been observed. With swelling, it is more certain that void swelling will become more severe with extended operation. So if swelling has an impact on fracture toughness, then it will only worsen with reactor age.

- Irradiation-effects on fatigue: Irradiation is important in influencing the high cycle fatigue, low cycle fatigue, and fatigue crack growth. The existing database for the effect of irradiation in LWRs on fatigue crack growth is limited to very low doses (about 3 dpa). There are no data on the role of irradiation at high doses encountered in core internal components. Similarly, sparse data are currently available for irradiation effects on either low or high cycle fatigue in hot water. In all cases, hardening and flow localization are expected to play a role.

- IASCC: The lack of a clearer understanding and a consensus-mechanism for IASCC creates considerable difficulty in identifying long-term technical issues for IASCC for reactor components in service. However, given the physical, chemical, and mechanical processes that are believed to contribute to IASCC, it is possible to identify those likely to become more important. The same is true for the dislocation microstructure and the resulting hardening. However, precipitation of second phases remains an unknown at high doses. G-phase and γ' are known to form at lower doses. Their behavior at high dose, however, is unknown. The observation of Cu precipitation in 304 SS suggests that other second phases may indeed form and become stable at higher doses, with unknown effects on IASCC.

8.10 REFERENCES*

1. P. L. Andresen and F. P. Ford, "Modeling and Prediction of Irradiation Assisted Stress Corrosion Cracking," pp. 893–908 in *Proc. 7th Int. Symp. Environmental Degradation of Materials in Nuclear Power Systems—Water Reactors,* Breckenridge, Aug. 7–12, 1995, R. Gold and A. McIlree (eds.), National Association of Corrosion Engineers, 1995.
2. P. L. Andresen, F. P. Ford, S. M. Murphy, and J. M. Perks, "State of Knowledge of Radiation Effects on Environmental Cracking in Light Water Reactor Core Materials," pp. 1–83 in *Proc. 4th Int. Symp. Environmental Degradation of Materials in Nuclear Power Systems—Water Reactors,* Jekyll Island, Aug. 6–10, 1989, D. Cubicciotti (ed.), National Association of Corrosion Engineers, 1990.

* Inclusion of references in this report does not necessarily constitute NRC approval or agreement with the referenced information.

3. S. M. Bruemmer, E. P. Simonen, P. M. Scott, P. L. Andresen, G. S. Was, and J. L. Nelson, "Radiation-induced material changes and susceptibility to intergranular failure of light-water-reactor core internals," *Journal of Nuclear Materials* **274**(3), 299–314 (1999).
4. F. P. Ford and P. L. Andresen, "Corrosion in Nuclear Systems: Environmentally Assisted Cracking in Light Water Reactors," pp. 501–546 in *Corrosion Mechanisms,* Marcel Dekker, New York, 1994.
5. H. Hanninen and I. Aho-Mantila, "Environment Sensitive Cracking of Reactor Internals," pp. 77–92 in *Proc. 3rd Environmental Degradation of Materials in Nuclear Power Systems—Water Reactors,* Traverse City, Aug. 30–Sept. 3, 1987, G. J. Theus and J. Weeks (eds.), The Metallurgical Society, 1987.
6. A. J. Jacobs and G. P. Wozadlo, "Irradiation Assisted Stress Corrosion Cracking as a Factor in Nuclear Power Plant Aging," p. 173 in *Proc. Int. Conf. Nuclear Power Plant Aging, Availability Factor and Reliability Analysis,* ASM International, Materials Park, OH, 1985.
7. P. Scott, "A Review of Irradiation Assisted Stress-Corrosion Cracking," *Journal of Nuclear Materials* **211**(2), 101–122 (1994).
8. G. S. Was and P. L. Andresen, "Irradiation-Assisted Stress-Corrosion Cracking in Austenitic Alloys," *Journal of the Minerals Metals & Materials Society* **44**(4), 8–13 (1992).
9. G. S. Was and P. L. Andresen, "Stress corrosion cracking behavior of alloys in aggressive nuclear reactor core environments," *Corrosion* **63**(1), 19–45 (2007).
10. P. L. Andresen, "Effects of Temperature on Crack Growth Rate in Sensitized Type 304 Stainless Steel and Alloy 600," *Corrosion* **49,** 714–725 (1993).
11. S. M. Bruemmer, B. W. Arey, and L. A. Charlot, "Grain Boundary Chromium Concentration Effects on the IGSCC and IASCC of Austenitic Stainless Steels," pp. 277–285 in *Proc. 6th Int. Symp. Environmental Degradation of Materials in Nuclear Power Systems—Water Reactors,* San Diego, Aug. 1–5, 1993, E Simonen and R. Gold (eds.), The Minerals, Metals & Materials Society, 1993.
12. P. L. Andresen et al., *Expert Panel Report on Proactive Materials Degradation Analysis,* NUREG/CR-6923 (BNL-NUREG-77111-2006), U.S. Nuclear Regulatory Commission, February 2007.
13. NRC, *Generic Aging Lessons Learned (GALL) Report*, NUREG 1801, U.S. Nuclear Regulatory Commission, December 2010.
14. EPRI, *EPRI Materials Degradation Matrix, Revision 3,* Document 3002000628, Electric Power Research Institute, May 2013.
15. R. Pathania, *EPRI Materials Degradation Matrix Revision 1,* Technical Report 1016486 Final Report, Electric Power Research Institute, May 2008.
16. .J. Edwards, E. P. Simonen, and S. M. Bruemmer, "Evolution of fine-scale defects in stainless steels neutron-irradiated at 275 °C," *Journal of Nuclear Materials* **317**(1), 13–31 (2003).
17. D. J. Edwards, B. A. Oliver, F. A. Garner, and S. M. Bruemmer, "Microstructural Evaluation of a Cold Worked 316SS Baffle Bolt Irradiated in a Commercial PWR," *Proc. 10th Int. Symp. Environmental Degradation of Materials in Nuclear Power Systems—Water Reactors,* Lake Tahoe, Aug. 5–9, 2001, F. P. Ford and G. Was (eds.), National Association of Corrosion Engineers, 2002.

18. D. J. Edwards, E. P. Simonen, F. A. Garner, L. R. Greenwood, B. M. Oliver, and S. M. Bruemmer, “Influence of irradiation temperature and dose gradients on the microstructural evolution in neutron-irradiated 316SS,” *Journal of Nuclear Materials* **317**(1), 32–45 (2003).

19. F. A. Garner, “Evolution of microstructure in face-centered cubic metals during irradiation,” *Journal of Nuclear Materials* **205,** 98–117 (1993).

20. P. J. Maziasz, “Overview of Microstructural Evolution in Neutron-Irradiated Austenitic Stainless-Steels,” *Journal of Nuclear Materials* **205,** 118–145 (1993).

21. P. J. Maziasz and C. J. McHargue, “Microstructural Evolution in Annealed Austenitic Steels during Neutron-Irradiation,” *Internation Materials Reviews* **32**(4), 190–219 (1987).

22. S. J. Zinkle, P. J. Maziasz, and R. E. Stoller, “Dose Dependence of the Microstructural Evolution in Neutron-Irradiated Austenitic Stainless-Steel,” *Journal of Nuclear Materials* **206**(2–3), 266–286 (1993).

23. G. S. Was, “Recent Developments in Understanding Irradiation Assisted Stress Corrosion Cracking,” pp. 965–985 in *Proc. 11th Int. Conf. Environmental Degradation of Materials in Nuclear Power Systems—Water Reactors,* Stevenson, Aug. 10–14, 2003, G. Was and L. Nelson (eds.), American Nuclear Society, 2003.

24. R. Stoller, “Primary damage formation in irradiated materials,” *Journal of the Minerals Metals & Materials Society* **48**(12), 23 (1996).

25. J. T. Busby, M. M. Sowa, G. S. Was, and E. P. Simonen, “Post-irradiation annealing of small defect clusters,” *Philosophical Magazine* **85**(4–7), 609–617 (2005).

26. D. J. Edwards, E. P. Simonen, and S. M. Bruemmer, “Radiation-induced Segregation Behavior in Austenitic Stainless Steels: Fast Reactor Versus Light Water Reactor Irradiations,” *Proc. 13th Int. Conf. on Environmental Degradation of Materials in Nuclear Power Systems,* Whistler, Aug. 19–23, 2007, P. King and T. Allen (eds.), The Canadian Nuclear Society, 2008.

27. J. T. Busby, E. A. Kenik, and G. S. Was, “Effect of Single Solute Additions on Radiation Induced Segregation and Microstructure of Model Austenitic Alloys,” *Journal of Nuclear Materials,* in press.

28. D. Edwards and S. M. Bruemmer, *Characterization of CIR II Irradiated Stainless Steels, Final Report,* EP-P19021/C9406, Electric Power Research Institute, 2008.

29. L. Fournier, B. H. Sencer, G. S. Was, E. P. Simonen, and S. M. Bruemmer, “The influence of oversized solute additions on radiation-induced changes and post-irradiation intergranular stress corrosion cracking behavior in high-purity 316 stainless steels,” *Journal of Nuclear Materials* **321**(2–3), 192–209 (2003).

30. H. Watanabe, T. Muroga, and N. Yoshida, “The temperature dependent role of phosphorus and titanium in microstructural evolution of Fe-Cr-Ni alloys irradiated in FFTF,” *Journal of Nuclear Materials* **228**(3), 261–274 (1996).

31. M. J. Hackett, J. T. Busby, M. K. Miller, and G. S. Was, “Effects of oversized solutes on radiation-induced segregation in austenitic stainless steels,” *Journal of Nuclear Materials* **389**(2), 265–278 (2009).

32. K. Fukuya, K. Fuji, H. Hishioka, and Y. Kitsunai, “Evolution of Microstructure and Microchemistry in Cold-worked 316 Stainless Steels under PWR Irradiation,” *Journal of Nuclear Science and Technology* **43**(2), 159–173 (2006).

33. G. S. Was, *Radition Materials Science: Metals and Alloys*, Springer, Berlin, 2007.

34. Z. Jiao and G. S. Was, “Novel Features of Radiation-Induced Segregation and Radiation-Induced Precipitation in Austenitic Stainless Steels,” *Acta Materialia* **59,** 1220–1238 (2011).

35. M. L. Grossbeck and L. K. Mansur, “Low-temperature irradiation creep of fusion reactor structural materials,” *Journal of Nuclear Materials* **179–181**(1), 130–134 (1991).

36. L. C. Walters and W. E. Ruther, “In-reactor stress relaxation of Inconel X75O springs,” *Journal of Nuclear Materials* **68,** 324 (1977).

37. F. A. Garner, S. I. Porollo, A. N. Norobjev, Yu. V. Konobeev, and A. M. Dvoriashin, *Proc. 9th Int. Symp. Environmental Degradation of Materials in Nuclear Power Systems—Water Reactors,* Newport Beach, Aug. 1–5, 1999, S. Bruemmer, F. P. Ford, and G. Was (eds.), The Minerals, Metals & Materials Society, 1999, p. 1051.

38. P. A. Heuze, O. Goltrant, and R. Cauvin, “Analysis of the Partition— Reinforcement Connecting Screws of the Tihange 1 Power Plant,” p. 195 in *Proc. Fontevraud 4 Int. Symp.,* Société Française d'Energie Nucléaire, Paris, Sept. 14–18, 1998 (in French).

39. P. M. Scott, M.-C. Meunier, D. Deydier, S. Silvestre, and A. Trenty, “An Analysis of Baffle/Former Bolt Cracking in French PWRs,” pp. 210–223 in *Environmentally Assisted Cracking: Predictive Methods for Risk Assessment and Evaluation of Materials, Equipment and Structures,* ASTM STP 1401, ASTM International, West Conshohocken, PA, 2000.

40. O. K. Chopra and A.S . Rao, “A review of irradiation effects on LWR core internal materials—neutron embrittlement,” *Journal of Nuclear Materials* **412,** 195–208 (2011).

41. NRC, *Fracture Toughness and Crack Growth Rates of Irradiated Austenitic Stainless Steels,* NUREG/CR-6826, U.S. Nuclear Regulatory Commission, 2003, p. 21.

42. O. K. Chopra and W. J. Shack, *Crack Growth Rates and Fracture Toughness of Irradiated Austenitic Stainless Steels in BWR Environments,* NUREG/CR-6960, ANL-06/58, U.S. Nuclear Regulatory Commission, March 2008.

43. EPRI, *A Review of Radiation Embrittlement for Stainless Steels, Materials Reliability Program (MRP-79),* Rev. 1, Report 1008204, Electric Power Research Institute, September 2004.

44. EPRI, *Fracture Troughness Testing of Decommissioned PWR Core Internals Material Samples, Materials Reliability Program (MRP-160),* Report 1012079, Electric Power Research Institute, September 2005.

45. A. Demma, R. Carter, A. Jenssen, T. Torimaru, and R. Gamble, Paper No. 114 in *Proc. 13th Int. Conf. Environmental Degradation of Materials in Nuclear Power Systems,* Whistler, Aug. 19–23, 2007, P. King and T. Allen (eds.), The Canadian Nuclear Society, 2008.

46. G. R. Odette and G. E. Lucas, “The effects of intermediate temperature irradiation on the mechanical behavior of 300-series austenitic stainless steels,” *Journal of Nuclear Materials* **179–181,** 572 (1991).

47. G. R. Odette and G. E. Lucas, “Deformation and fracture in irradiated austenitic stainless steels,” *Journal of Nuclear Materials* **191–194,** 50–57 (1992).

48. F. Fukuya, K. Fujii, H. Nishioka, and Y. Kitsunai, “Evolution of Microstructure and Microchemistry in Cold-worked 316 Stainless Steels under PWR Irradiation,” *Journal of Nuclear Science and Technology* **43**(2), 159–173 (2006).

49. D. L. Porter and F. A. Garner, “Irradiation creep and embrittlement behavior of AISI 316 stainless steel at very high neutron fluences,” *Journal of Nuclear Materials* **159,** 114–121 (1988).

50. O. K. Chopra and A. S. Rao, “A review of irradiation effects on LWR core internal materials—IASCC susceptibilty and crack growth rates of austenitic stainless steels,” *Journal of Nuclear Materials* **409,** 235–256 (2011).

51. W. G. Wolfer and R. H. Jones, “Flow and fracture of alloys in the fusion environment,” *Journal of Nuclear Materials* **103–104,** 1305–1314 (1981).

52. G. Lloyd, “Interpretation of the influences of irradiation upon fatigue crack propagation in austenitic stainless steels,” *Journal of Nuclear Materials* **110,** 20–27 (1982).

53. K. L. Murty and F. R. Holland, “Low Cycle Fatigue Characteristics of Irradiated Type 304 Stainless Steel,” *Nuclear Technology* **58,** 530–537 (1982).

54. G. M. Gordon and K. S. Brown, “Dependence of Creviced BWR Component IGSCC Behavior on Coolant Chemistry,” pp. 14-46–14-62 in *Proc. 4th Int. Conf. Environmental Degradation of Materials in Nuclear Power Systems—Water Reactors*, Jekyll Island, Aug. 6–10, 1989, D. Cubicciotti (ed.), National Association of Corrosion Engineers, 1990.

55. K. S. Brown and G. M. Gordon, “Effects of BWR Coolant Chemistry on the Propensity for IGSCC Initiation and Growth in Creviced Reactor Internals Components,” pp. 243–248 in *Proc. 3rd Environmental Degradation of Materials in Nuclear Power Systems—Water Reactors,* Traverse City, Aug. 30–Sept. 3, 1987, G. J. Theus and J. Weeks (eds.), Metallurgical Society, 1987.

56. A. J. Jacobs, D. A. Hale, and M. Siegler, Unpublished data on “SCC of Irradiated SS in 288 °C Water and Inert Gas,” GE Nuclear Energy, San Jose, CA, 1986.

57. G S. Was, Y. Ashida, and P. Andresen, “Irradiation-Assisted Stress Corrosion Cracking,” *Corrosion Review* **29,** 7–49 (2011).

58. D. D. Macdonald and D. F. Heaney, “Effect of Variable Intensity Ultraviolet Radiation on Passivity Breakdown of AISI Type 304 Stainless Steel,” *Corrosion Science* **42,** 1779–1799 (2000).

9. PIRT ANALYSIS AND ASSESSMENT OF KEY DEGRADATION MODES

An expanded PMDA activity benefits stakeholders in providing a comprehensive analysis of degradation modes and identifying potential gaps, which will need to be addressed by further research to provide data and information for assurance of safe and efficient extended reactor operation. Expansion of the PMDA to longer time frames and additional systems is a challenging assignment, involving experts from more disciplines and consideration of more experimental and operational experience information. The addition of new and distinct material and component systems such as cable insulation and concrete to the existing scope of NUREG/CR-6923 [1] was deemed too difficult to encompass in a single document or process given the divergence in materials systems, degradation modes, and the cognizant technical community. Thus, in addition to this panel on core internals and piping, separate and distinct expert panels were assembled to address key material issues for embrittlement of reactor pressure vessel steels, concrete, and cabling for long-term reactor operation. While each panel addressed very different materials and degradation modes, the overall methodology used for assessment was the same for each panel.

The expert elicitation process conducted for each panel is based on the Phenomena Identification and Ranking Table (PIRT) process. This process has been used in many industries for ranking and prioritizing any number of issues. This methodology is commonly used by NRC, including the original NUREG/CR-6923, which is the basis for this activity. Here, the PIRT process provides a systematic means of obtaining information from experts and involves generating lists (tables) of degradation phenomena that affect component lifetime and reliability. The process usually involves ranking of these phenomena using a series of scoring criteria. The results of the scoring can be assembled to lead to a quantitative ranking of issues or needs. This list is intended for use by stakeholders to prioritize research or other decision-making needs.

This Chapter focuses on the PIRT process associated with identifying those material degradation modes in BWRs and PWRs that might dominate in time periods >60 years and where there is currently insufficient knowledge to manage any potential problems. This time period is an extension of that addressed in current license renewal evaluations.

The degradation modes of interest in this EMDA analysis are broadly similar to those addressed in NUREG CR/6923, with a particular focus on any unexpected effects that may become apparent in 60 to 80 years of operation. For instance potential problems may be associated with

- The re-evaluation of Cumulative (fatigue) Usage Factors in complicated (but realistic) stress/time patterns
- Flow Assisted Corrosion
- Synergies between, for instance SCC and other degradation modes associated with irradiation hardening, temper embrittlement, strain aging, etc.

The physical nature of these phenomena was described in earlier Chapters addressing the degradation of various alloy groups.

This chapter of the EMDA presents the detailed results of the PIRT scoring. The PIRT process used here is described in detail in Section 9.1. Similarities and differences from the original PMDA process [1] are then described, along with cautions on the limitations of the PIRT process.

A high-level overview of the PIRT findings is given. The PIRT findings are then summarized for each material system described in the background assessments in Chapters 2–8. The trends and findings of this activity are also compared to other activities such as the PMDA and EPRI MDM [2, 3] results. Finally, a summary of key gaps in knowledge is presented along with other key concerns identified by the expert panel.

9.1 DESCRIPTION OF THE PIRT PROCESS

Each PIRT effort has been unique in some respect, which is also true of the current project. The current PIRT can be described in terms of several key elements. These are described for the generic process below, although each panel made minor adjustments based on the needs of that material system, and such adjustments will also be identified.

For NUREG/CR-6923, eight experts conducted the PIRT for core internals and piping. For the current EMDA activity described in this volume, nine experts participated in this exercise. To ensure a diverse set of background and expertise, the piping panel was assembled to include

- At least one member with regulatory experience
- At least two members representing industry (EPRI, vendors, etc.)
- At least one member from the DOE national laboratories
- At least one member from academia
- At least two members from outside the United States

Selection and assembly of panel experts was performed with NRC and DOE input and approval. The panelists selected for this core internals and piping panel had an average of over 40 years of experience in the field and the majority participated in developing the original PMDA report. Two members are also members of the U.S. National Academy of Engineers with another serving on the U.S. NRC Advisory committee on Reactor Safeguards. This broad and diverse expertise was a vital asset for this effort.

Initial technical background assessment documents of key degradation modes were then developed as a starting foundation for broader discussion, evaluation, and ranking. For the piping and core internal assessment, the existing NUREG/CR-6923 was used as a starting point and for additional discussion on the potential changes that might be experienced during subsequent operating periods. Each chapter of the technical background assessment was written by a single panelist and then peer reviewed by the entire panel. Subsequent discussion among the entire panel was also used to identify key themes, and revisions to the technical background assessments were made accordingly. These assessments are featured in Chapters 2 through 8 above. Each chapter included a summary of key concerns associated with long term operation.

It is important to note that these background assessments are not intended to be all-encompassing primers on particular degradation modes or material systems. Detailed primers and background assessments exist in other publications, and it is beyond the scope of this project to reproduce them here. Many of the key references are provided in the background assessment chapters above. Rather, the discussions presented are intended to introduce the

subject and context for the evaluation of key modes of degradation for extended operating periods, targeted to people with some familiarity of the topic.

Based on the input from the technical background assessments shown in Chapters 2–8, the expert panel then developed a PIRT matrix with a list of degradation scenarios to score. A degradation scenario generally encompasses a particular material, system, component, or subcomponent (the categorization scheme devised by the panel grouped together components and exposure conditions that were alike), the environmental condition to which that material is exposed; and the degradation mode that the material may experience, based on laboratory and operational data. If a certain material is exposed to multiple environments (that has a distinct effect) or may experience multiple degradation modes, those are listed and scored as distinct scenarios. The number of degradation scenarios was over one thousand for this panel.

For this volume on piping and core internals, a number of different aging mechanisms were considered for the alloy systems described previously, including:

- Wrought stainless steels in Chapter 2
- Alloy 600 and Alloy 182/82 weldments in Chapter 3
- Alloy 690 and Alloy 152/52 weldments in Chapter 4
- Carbon and Low alloy steels in Chapter 5
- Cast-austenitic stainless steels in Chapter 6
- Liner materials in Chapter 7
- Cross-cutting discussion of irradiation effects in Chapter 8

These modes of degradation are listed in Table 9.1 for both BWR and PWR systems. Also listed are the acronyms for each degradation mode. These acronyms are used extensively in the plots and analyses to follow. The number of times each mode of degradation was scored in BWR and PWR systems is also listed in Table 9.1.

Table 9.1. List of degradation modes considered for PIRT scoring of piping and core internals and number of categories scored as part of this EMDA activity for both PWR and BWR reactors

Degradation Mode	Degradation Acronym	PWR	BWR
Boric Acid Corrosion	BAC	6	--
Crevice Corrosion	CREV	26	47
Dealloying	DEALLOY	2	1
Debonding	DEBOND	1	2
Erosion–Corrosion (including steam cutting)	EC	1	4
Flow Accelerated Corrosion	FAC	11	6
Corrosion Fatigue	FAT	110	180
Fracture Resistance	FR	42	61
Galvanic Corrosion	GALV	0	1
General Corrosion	GC	12	44
Irradiation Creep	IC	21	0
Microbially Induced Corrosion	MIC	31	29
Pitting	PIT	36	58
Stress Corrosion Cracking	SCC	121	164
Swelling	SW	21	0
Fretting/Wear	WEAR	10	2

The reactor environment was a key variable for panelist consideration. The environment is a critical factor when considering both alloy/components and degradation modes in specific alloys and components. However, some generalization is required, as evaluating the exact water chemistry for each power plant or component over their operating history is not possible. For this exercise, reference water chemistries for PWR primary water, PWR secondary water, BWR Normal Water Chemistry (NWC) and BWR Hydrogen Water Chemistry (HWC) were considered. The reference conditions match those provided by industry [2, 3] and are the same as used in NUREG/CR-6923. These are summarized in Table 9.2.

Table 9.2. Reference water chemistry parameters assumed for PIRT scoring of piping and core internals[a]

	BWR-NWC	BWR-HWC	PWR Primary Water
Coolant temperature (°C)	288	288	320
Coolant pressure (MPa)	7.2	7.2	15.2 at 343 °C
pH (at 25 °C)	7.0	7.0	6.5-6.8
Oxygen (ppb)	+100–250	<10	<5
Hydrogen (ppm)		0.4–3	3–5 (35 cc/kg)
ECP (mV_{SHE})	+150	<-230	-770
Conductivity (µS/cm)	<0.1	<0.1	20–30
B content (ppm)			1,000
Li content (ppm)			2–3
SO_4^- content (ppb)	<3	<3	<3
Cl^- content (ppb)	<1	<1	<1

[a] Values listed in the table are not the EPRI Water Chemistry Guideline limits. Rather these represent common values achieved by the operating reactor fleet and were used as a representative baseline for this activity. Higher values were also considered if the panel deemed they had a very pronounced effect.

After the scoring matrix was developed, panelists independently scored the degradation scenarios in three categories: susceptibility, confidence, and Knowledge. These categories are the same as those used for NUREG/CR-6923. The definition of each factor and the meaning of each ranking score are reviewed below.

The **Susceptibility score** gages whether significant material degradation can develop under plausible conditions. Susceptibility was scored as 0, 1, 2, or 3, with the following definitions.

0 = not considered to be an issue

1 = conceptual basis for concern from data, or potential problems under unusual operating conditions, etc.

2 = strong basis for concern, or known but limited plant experience

3 = demonstrated, compelling evidence for occurrence, or multiple plant observations

Confidence is a measure of the expert's *personal* confidence in his or her judgment of Susceptibility.

1 = low confidence, little known phenomenon

2 = moderate confidence

3 = high confidence, compelling evidence, existing occurrences

Note, "3" is assumed if Susceptibility Factor is 0.

Finally, the **Knowledge score** is the expert's current belief of how adequately the relevant dependencies have been quantified either through laboratory studies, operating experience, or both. A "high Knowledge" score does not mean we know everything we might want to about underlying processes and mechanisms of SCC, or that guaranteed-effective mitigation approaches exist. As above, knowledge was scored as 1, 2, or 3.

1 = poor understanding, little and/or low-confidence data

2 = some reasonable basis to know dependencies qualitatively or semi-quantitatively from data, or extrapolation from similar "systems"

3 = extensive, consistent data covering all dependencies relevant to the component, perhaps with models, which provide clear insights into mitigation or management of the problem

Subsequent to the completion of panelists' scoring, all scores were compiled and the average of Susceptibility and Knowledge were separately calculated. Since Confidence is a measure of personal confidence, the average has little value in this exercise but is included as a reference for panelist confidence on their scores. Once compiled, any Susceptibility or Knowledge score that deviated from the average by a specified amount was flagged as an "outlier." This set amount is somewhat arbitrary, but a value of 0.7 was typically used. It is also important to note that the term "outlier" should not be interpreted as incorrect or of questionable value. Indeed, this identification of "outliers" was only performed to spur discussion on scoring among the panelists and allow individual "outlier" scores to be "verified after such discussion."

After completion of scoring and identification of "outliers," the panels discussed the scoring. In the core internal and piping panel, this was done in a face-to-face meeting. During this discussion, each degradation mode and related scoring was discussed, with the "outliers" being of highest priority. In these discussions, the scoring panelist presented their rationale for any scores that differed from the average. The primary goal was to foster debate and exchange differing points of view, not to develop a consensus score or force conformity among the panelists. In some cases, the "outlier" was changed based on the debate. In other cases, the other scores (and thus the over average score) were changed as new points of view were presented. This debate and discussion among panelists was an important part of the process to ensure that all points of view were considered, including information not previously considered, and accounted for in the final scoring.

After compiling any changes in scoring following this debate, the PIRT scoring was tabulated to determine relative needs and priorities. In this process, the average Susceptibility and average Knowledge scores were plotted versus each other on a simple plot. An example plot of Knowledge versus Susceptibility is shown in Figure 9.1. The left side of the plot with the lighter shading is indicative of low Knowledge, while the darker shading on the right side of the plot is indicative of high Knowledge. The labeled areas in the corners of the plot indicate the high Knowledge, low Susceptibility; high Knowledge, high Susceptibility; and low Knowledge, high Susceptibility areas discussed above. Moving from upper right to lower left can be accomplished via additional R&D to understand and predict key forms of degradation. The different domains of these plots highlight key areas of concern, including:

- Low Knowledge, high Susceptibility degradation modes are indicated by the pink shading in Figure 9.1 and are represent modes of degradation that could be detrimental to service with high Susceptibility scores (>2) and low Knowledge scores (<2). These scores indicate gaps in understanding for degradation modes that have been demonstrated in service. Low

Knowledge and moderate Susceptibility also indicate gaps in knowledge, although with lower consequences. These scoring regions are useful in identifying potential knowledge gaps and areas requiring further research into mechanisms and underlying causes to predict occurrence.

- High Knowledge, high Susceptibility degradation modes are shown in red in Figure 9.1 and represent areas that could be detrimental to service with high Susceptibility scores (>2) and high Knowledge scores (>2). These modes of degradation are well understood and have likely been observed in service. While there may be some mechanistic understanding of the underlying causes, re-confirmation for extended service and research into mitigation or detection technologies, and confirmation of the efficacy of the present aging management programs may be warranted.

- High Knowledge, low Susceptibility degradation modes (dark green in Figure 9.1) are those that are relatively well understood and of low consequence to service with low Susceptibility scores (<1) and high Knowledge scores (>2). These modes of degradation are adequately understood and may have been observed in service. Mitigation and maintenance can currently manage this form of degradation. Research on these modes of degradation is a lower priority.

Other combinations of Knowledge and Susceptibility are of course possible and fit between the cases listed above in terms of priority. Raw scores for each panelist are listed in Appendices A through K for every scoring category evaluated. In addition to the raw Knowledge, Susceptibility, and Confidence scores, panelist comments are also given. Each panelist is identified by number rather than name to retain anonymity. An example of the raw data shown in Appendix A is listed in Figure 9.2. An example Susceptibility versus knowledge plot for 347 SS in PWR primary water at low fluence is shown in Figure 9.3. In this example, five modes of degradation were considered, and the average scores for Susceptibility are shown. All five were considered to be high Knowledge with varying degrees of Susceptibility.

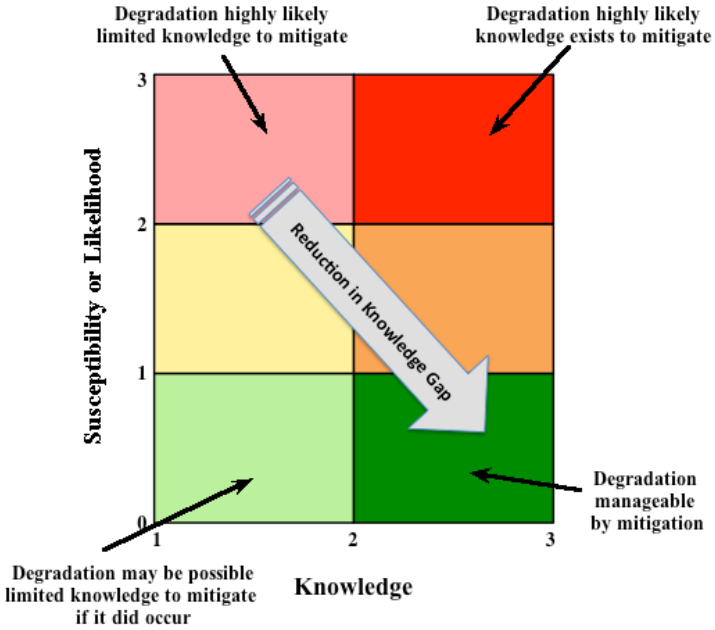

Figure 9.1. Schematic illustrating the combinations of Susceptibility and Knowledge scores suggesting various life management responses.

347 SS in Primary Water - Low fluence irradiation up to 0.5 dpa

Primary Water, 556 to 559°F, 2250 psia,

Stress Corrosion Cracking (includes IASCC)

Panelist	Susceptibility	Confidence	Knowledge	Rationale	Critical Factors
1	2	2	2	RP-256 notes SCC in reactor coolant and neutron flux environment	SCC vulnerability may increase with fluence but ECPs are low
2	2	3	2	Cold worked 347 used as alternative to CW 316 for high strength bolting. Experience base less than that for 316; hence lower knowledge score. The susceptibility score reflects behavior of CW 316	
3	2	2	2	At low fluences, SCC could be a factor with increasing lifetime	Specific loading and bolt location is important
4	2	2	2	Based on data of 20%CW 316/304 in PWR water up to 360C.	Time dependence of local stress due to stress relaxation and swelling of baffle former.
5	1	3	3	Good field experience, unlikely to get sufficient quantities of oxidants to provide right environment	
6	1	2	2	347 is susceptible, but weld residual strains are lower than in the SS HAZ, so it's more likely that initiation and most growth will occur in the HAZ. There is a limited effect of 0.5 dpa in PWR water, and such effects include some stress relaxation, so enhancement from irradiation is unlikely.	
7	1	3	2	Good field performance at low fluence	
8	2	2	2		
9	1	2	2	Should be minor issue at this low dose. Some uncertainty due to SCC response of cold-worked SS.	
Average:	1.56	2.33	2.1		

Relevant Components from PMDA (NUREG CR-6923):

Link	Parts and Components
NEW	Reactor Vessel-Internals

Figure 9.2. Example of PIRT scoring data for SCC of Type 347 SS in PWR primary water at low fluence (see Appendix A).

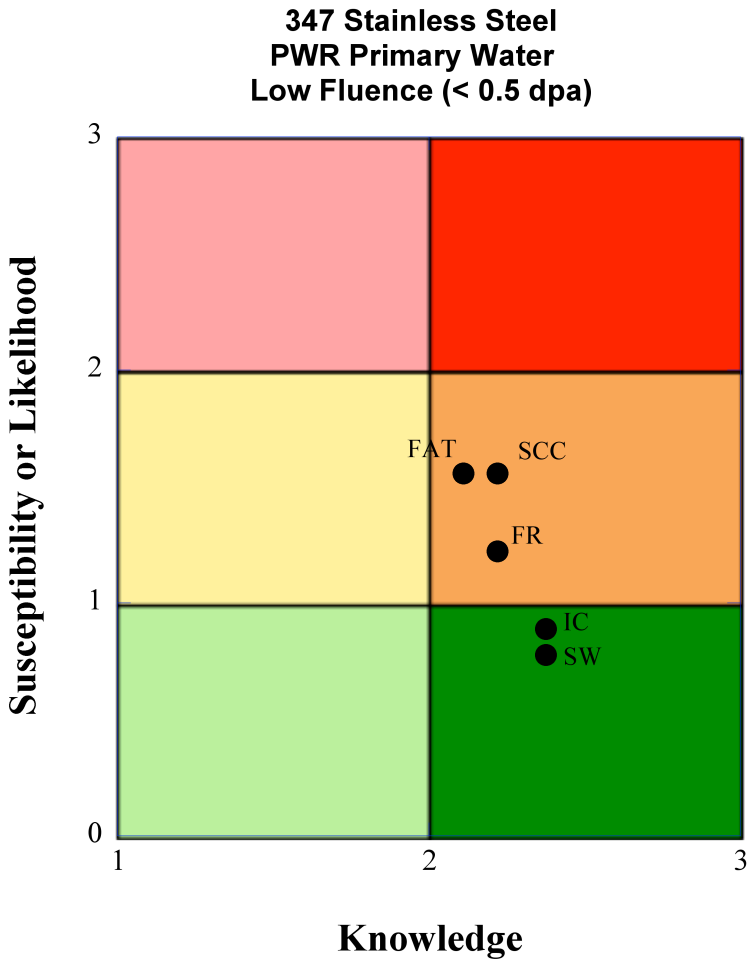

Figure 9.3. Example Susceptibility–Knowledge plot for Type 347 SS in PWR primary water at low fluence. [FAT = corrosion fatigue, FR = reduction in fracture resistance, IC = irradiation creep, SCC = stress corrosion cracking, and SW = swelling.]

Finally, the results of the PIRT scoring were compared to the background chapters to ensure that all-important modes of degradation and points were captured. Revisions were then made to the supporting chapters and analysis to ensure adequate discussion of key topics, outcomes, and underlying causes. Thus, the technical basis information for conducting PIRT and the results of the PIRT were re-iterated to ensure that coverage and consistency had been maintained in the various PIRT subject areas.

9.2 CAUTIONS AND LIMITATIONS OF THE PIRT PROCESS

One unintended consequence of identifying and scoring the degradation phenomena is that the simplified distillation of the color-coding may lead one to conclude that the problems are well understood and little investment is needed to resolve issues. Indeed, in the last decade, there has been a dramatic reduction in R&D funding and an alarming decline in critical scientific/engineering expertise, which would be needed to support developing scientific bases for reactor extended operation. This point will be discussed in more detail in a later section, however. Caution must be taken when examining the details of this PIRT process and the past PMDA described in NUREG/CR-6923 activity as all encompassing or representative of a specific

component in an individual plant. By necessity, environments, components, and alloys have been generalized for the PIRT scoring. Individual components may exist in specific operating conditions that are not bounded by the generalized conditions considered here. Indeed, all degradation phenomena occur preferentially at a small fraction of the possible locations where a combination of characteristics that make them the most susceptible.

There are inevitably a number of ambiguities in the interpretation of the scores from any individual panelist. For example, heat affected zones (HAZs) are often but not always explicitly scored, and in any event there are cases where a score for a base metal incorporates a concern for the weld HAZ (i.e., weld residual strains and stresses). Each panelist also weighs differently the importance of transient and off-normal conditions. For instance, the panelist may believe that degradation of a component is strongly influenced by effects of transient and off normal conditions, but when scoring, consider that such conditions are relatively uncommon. The diversity of the expert panel is intended to provide a broader perspective although each expert has material or degradation systems about which he or she is less familiar. This also underscores the value in examining the highest Susceptibility scores rather than only focusing on the average.

Caution must also be applied when examining the charts and results that follow because the combined PIRT scores may lead to misinterpretation of expert opinion. This is most likely for the following cases:

- Low Susceptibility scores do not necessarily mean no problems will occur. Rather the experts believed there would be either limited problems or a slow increase in evolution vs. time.

- Similarly, high Knowledge scores do not imply everything is known, but rather much is known and many dependencies are defined and/or modeled. However, an *adequate* understanding for effective prediction may not exist. A good example is the effects of ppb chloride on low alloy steel, which was unknown about a decade ago, and no work has yet been done on other impurities. Also, mitigation and management of the problems in the field may not be in hand, or the efficacy of the current aging management programs need to be validated over extended reactor operation.

- Low Knowledge, high Susceptibility scores are typically given the highest priority and visibility. However, it is important to note that this PIRT process makes no judgment or evaluation on the number of components or significance to structural integrity or safety for a given component, material, or degradation mode. For example, a form of degradation may be rated as low Knowledge, high Susceptibility but only affect a single component in service that is easily replaced and of limited safety consequence. Conversely, a high Knowledge, medium susceptibility mode of degradation may influence a key safety-related component that cannot be replaced. This work makes no attempt to include an additional factor for importance to the system, a caveat that should be considered when defining research priorities. As such, the components that fall in the red and yellow color regions (regardless of the knowledge level) should be considered for inclusion in research programs for mechanistic understanding, predictive modeling, mitigation, or detection.

- For all scored elements, the knowledge level scores ranged from low, indicating not enough knowledge is available to develop management and mitigation actions, to high, indicating such knowledge is available. It is important to note that since the scoring was performed by a relatively small number of experts (nine) using fixed integer scores, similar susceptibility and Knowledge scores can be achieved via different routes. For example, in cases where all nine

experts assigned a level of 2 (or when the average was 2), the average is the same as a case the panelist scoring is equally distributed among 1, 2, and 3 scoring. While the average score is the same, the agreement among panelists is considerably different. For this reason, panelist rationale for scoring is retained in Appendix A. These different scenarios are shown in Figures 9.4 through 9.6 for three different cases with varying degrees of panelist agreement. Note that since panelists scored with integer values, multiple symbols overlap on these plots. Figures 9.5 and 9.6 illustrate scoring with nearly identical average scores; however, the range of panelist opinions is considerably different.

- Finally, it must be recognized that the steady decrease in overall R&D funding over the last ~20 years limits capability to perform another evaluation of this type, or retain expertise for other purposes. Many of the experts involved in this evaluation are retired, and several will no longer remain active as consultants in future years. Others are likely to retire and may not be available to consult or transfer knowledge to their replacements. The combined experience and judgment represented by this panel may not be replaced in the next decade or two because the gap in expertise is so large. Further, the accumulated knowledge and judgment of the next generation of experts will be dramatically more difficult to acquire when the current leaders are no longer available.

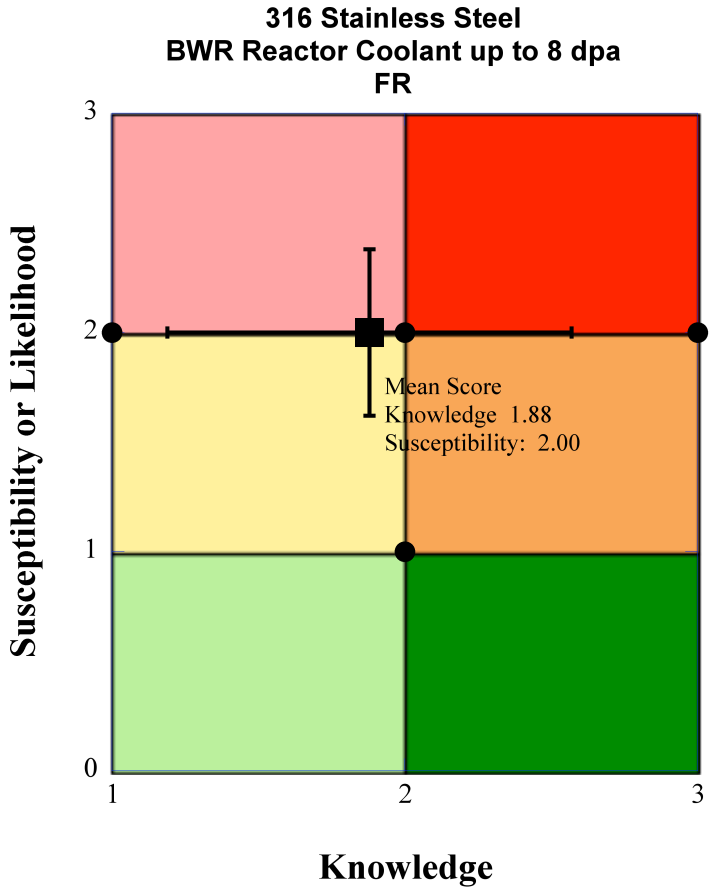

Figure 9.4. Susceptibility–knowledge plot for reduction of fracture toughness for 316 SS in PWR primary water at moderate fluence (up to 8 dpa). The individual panelist scores are shown (circles) along with the average score and standard deviation for both knowledge and susceptibility.

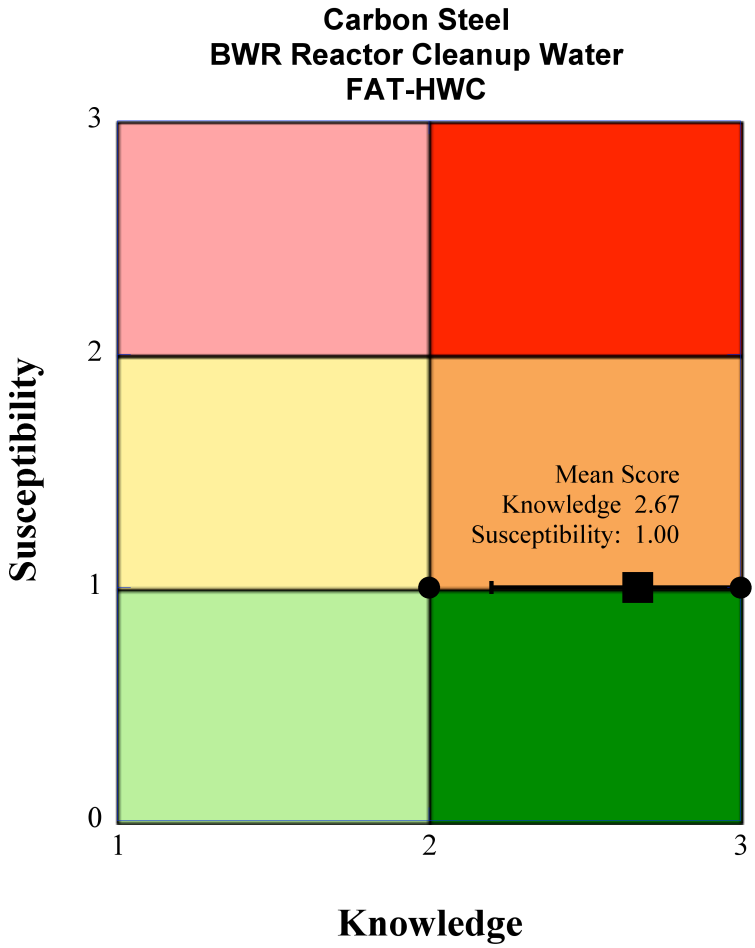

Figure 9.5. Susceptibility–knowledge plot for fatigue carbon steel in BWR-HWC cleanup water. The individual panelist scores are shown (circles) along with the average score and standard deviation for both knowledge and susceptibility.

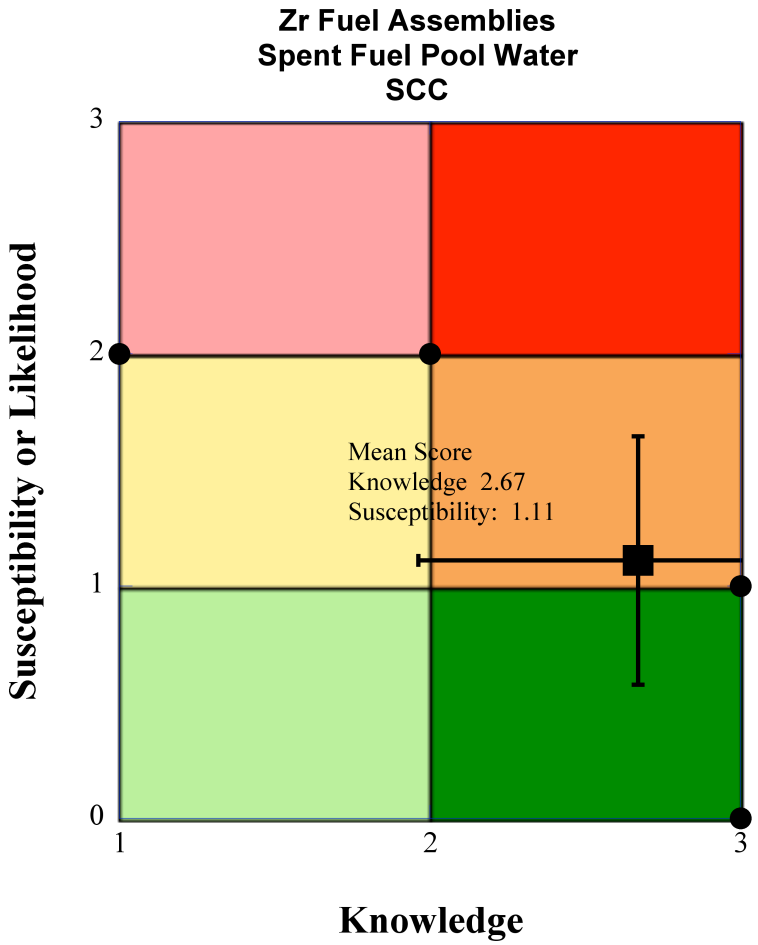

Figure 9.6. Susceptibility–knowledge plot for SCC of Zr-based fuel assemblies in BWR spent fuel pool water. The individual panelist scores are shown (circles) along with the average score and standard deviation for both knowledge and susceptibility.

9.3 KEY DIFFERENCES WITH THE PMDA

As noted above, the inspiration and methodology for this work is based on the past PMDA activity described in NUREG/CR-6923. However, there are also key differences in the PIRT assessment in this work versus the previous PMDA activity.

Of particular importance is the PIRT scoring. In NUREG/CR-6923 scoring was done on an individual component basis, or groups of components with similar characteristics. For a reference reactor design, a detailed component list was created for both a BWR and PWR plant. The environment was assessed for each component and then relevant degradation modes were considered. For NUREG/CR-6923, over 3,000 material/environment/degradation modes were considered and scored. However, upon analysis as part of this activity, many of the panelist scores were identical for common materials/environments despite different functions for the component.

For this current EMDA, considerable effort was made to reduce this scoring redundancy. The original scoring sheets from NUREG/CR-6923 were obtained and sorted by material and

environment. Common components/environments were then condensed into a common entry. For example, in NUREG/CR-6923, 316 SS HAZs in primary PWR with no irradiation appeared in 17 different entries, although the panelist scores were identical. In this EMDA, 316 SS HAZ in primary water was scored only a single time. This effort reduced the total number of scoring categories from >3,000 to 1,020 scoring categories, giving the panel more time to focus on substantive technical concerns.

As a result, this distillation of scoring categories provided a much more efficient process and reduced redundancy. However, it also precludes direct comparison of unique scores for an individual component between the two activities. To retain this capability, the part and component description from NUREG/CR-6923 were retained as a reference, and these cross-references can be found as part of the scoring summary for each category provided in Appendices A through K. Generic comparison between the results of NUREG/CR-6923 and this activity are provided in later sections.

9.4 SUMMARY OF RESULTS

As noted above, the panelists considered a total of 1,020 scoring categories (451 in PWR and 569 in BWR). This yielded a total of 27,450 raw scores to be compiled (three scores for each of the nine panelists in 1,020 categories). The data were entered into a database and compiled to yield average Susceptibility and Knowledge scores. While the scoring of individual categories was the ultimate goal of this effort, examining the trends for the entire data set also has some merit.

9.4.1 Trends Observed in Full Data Set

As noted above, 451 categories were scored for PWR degradation and 569 categories were scored for BWR degradation. Figure 9.7 shows the susceptibility–knowledge plot for all PWR categories, and Figure 9.8 shows the susceptibility–knowledge plot for all BWR categories. The numerical results are also tabulated in Table 9.3. It is important to note that, because of overlapping points, the plots contain more data than is readily visible. Since the limited number of panelists had to choose integer scores, only a finite number of possible averages are possible. As a result, many data points overlap and the data falls on “lines,” particularly on the Knowledge axis. Average scores exactly at a break point (i.e. 1.0 or 2.0) were rounded up to the more significant grouping. Several trends are readily apparent:

- Only a small fraction of scores fall into the low Knowledge regime for both PWR and BWR cases. Indeed, only 57 out of 1,020 categories were scored in the low Knowledge categories. The lowest Knowledge score observed for the 1.020 categories was 1.75; in that case, only two of the panelists scored knowledge less than a 2. This is, in part, likely due to the extensive research and field experience completed to date, even in the years since NUREG/CR-6923 was completed. This is also reflected in the personal confidence scores that are greater than 2.0 (greater than “low Knowledge”) in almost all low Knowledge categories. Individuals because of their extensive experience and judgment possess much of this Knowledge. It should not be assumed that such Knowledge is inherent in or automatically sustained by the industry, regulators, national labs, universities, etc. Indeed, a majority of the panelists expressed grave concerns about the ability to sustain expertise over the next half-decade.

- The vast majority of scores (>75% for both PWR and BWR) fall into the high Knowledge, moderate Susceptibility category. This indicates that the panelists felt the majority of degradation modes considered are well known and manageable to some extent.

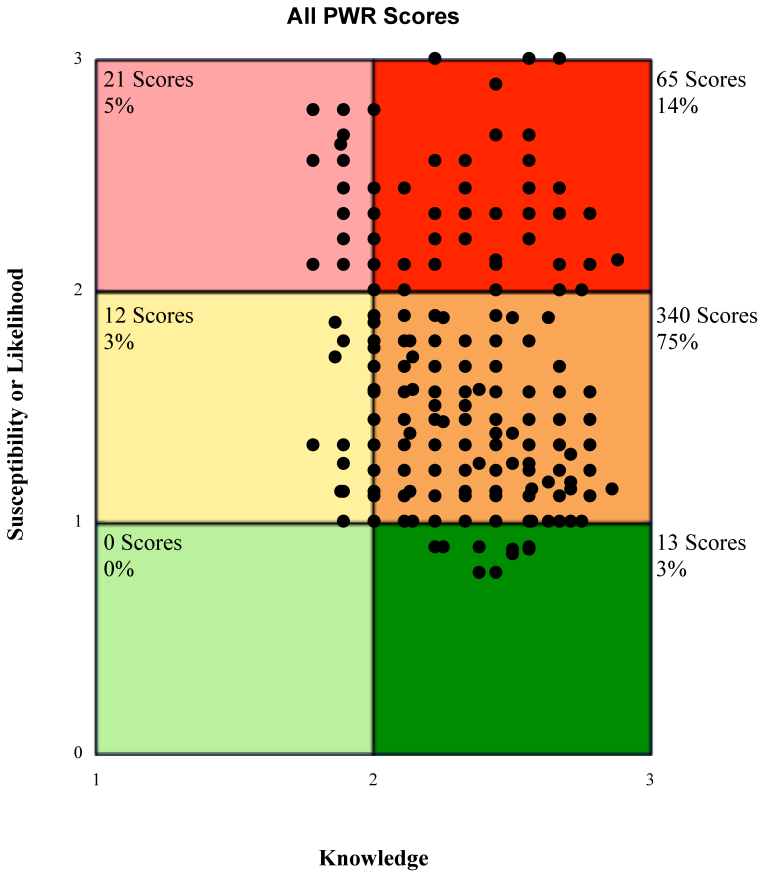

Figure 9.7. Susceptibility–Knowledge plot for all PWR categories.

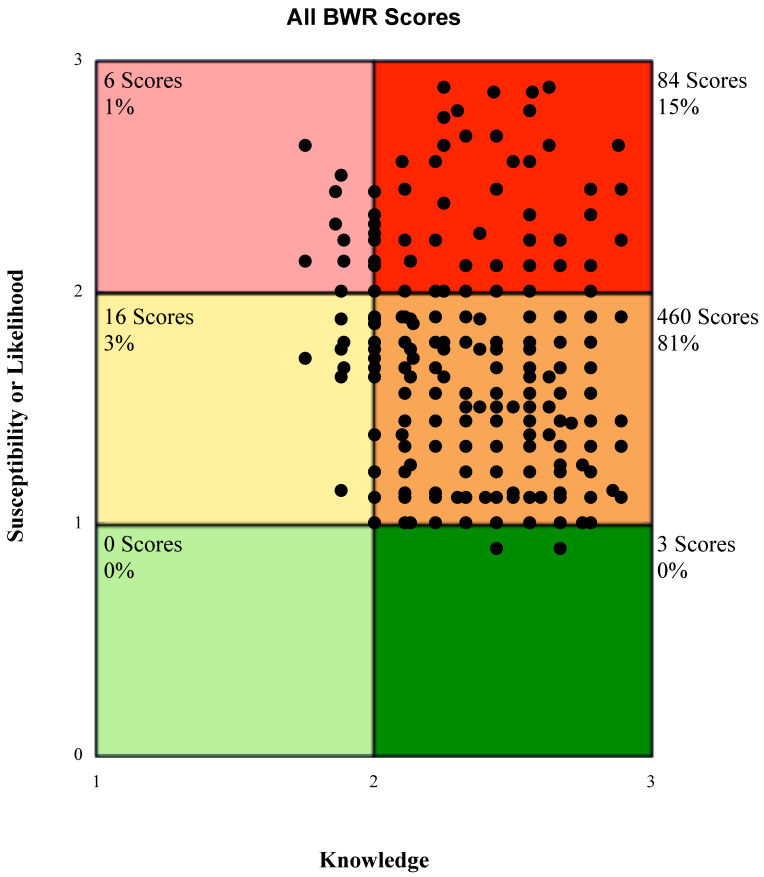

Figure 9.8. Susceptibility–Knowledge plot for all BWR categories.

Table 9.3. Comparison of PIRT findings for all PWR and BWR categories

		PWR		BWR	
		No. Scores	%	No. Scores	%
Low Susceptibility, low Knowledge		0	0.00	0	0.00
Low Susceptibility, high Knowledge		13	2.88	3	0.53
Moderate Susceptibility, low Knowledge		12	2.66	16	2.81
Moderate Susceptibility, high Knowledge		340	75.39	460	80.84
High Susceptibility, low Knowledge		21	4.66	6	1.05
High Susceptibility, high Knowledge		65	14.41	84	14.76

- The next largest grouping of scores is in the high Knowledge, high Susceptibility region of the rainbow plot. This grouping included 65 scores for PWR and 84 scores for BWR (14% and 15%, respectively). These forms of degradation, which are thought to have the greatest potential to occur during subsequent operating periods, are also all well known either through laboratory experience of observations in service. This leads to increased confidence in ability to predict the extent of degradation or mitigate their effects.

- For both PWR and BWR categories considered, none were found to be in low Susceptibility, low Knowledge categories. This is not unexpected as the LWR nuclear power fleet has

operated for over 40 years and many low Susceptibility categories were deemed irrelevant during the first PMDA activity (and thus not even scored).

9.4.2 Low Knowledge, High Susceptibility Categories

Low Knowledge, high Susceptibility degradation modes are those that could be detrimental to service with high Susceptibility (>2) scores and low Knowledge scores (<2). These scores indicate gaps in understanding and are areas requiring research into mechanisms and underlying causes to predict occurrence. As noted above, scores in this group are typically given the highest priority and visibility. The 21 scores in this category for PWR are listed in Table 9.4, and the six scores in this grouping for BWR are listed in Table 9.5. In addition, all other low Knowledge categories for PWR and BWR applications are also listed in Tables 9.4 and 9.5, although many have very low Susceptibility scores.

Table 9.4. Summary of all low Knowledge categories for categories for PWRs

Material/Environment	Degradation Mode	Average Knowledge	Average Susceptibility
High strength bolts internals in primary reactor water – moderate fluence irradiation up to 15 dpa	FR	1.89	2.00
High strength bolts internals in primary reactor water – high fluence irradiation over 15 dpa	FR	1.89	2.11
High strength bolts internals in primary reactor water – high fluence irradiation over 15 dpa	SW	1.88	2.11
304 SS core internals in primary water – high fluence irradiation over 15 dpa	SCC	1.89	2.33
304 SS core internals in primary water – high fluence irradiation over 15 dpa	FR	1.89	2.22
304 SS core internals in primary water – high fluence irradiation over 15 dpa	SW	1.89	2.33
304 SS core internal HAZ in primary water – high fluence irradiation over 15 dpa	SCC	1.89	2.33
304 SS core internal HAZ in primary water – high fluence irradiation over 15 dpa	FR	1.89	2.22
304 SS core internal HAZ in primary water – high fluence irradiation over 15 dpa	SW	1.89	2.33
316 SS core internals in primary water – moderate fluence irradiation up to 15 dpa	SCC	1.89	2.22
316 SS core internal HAZ in primary water – moderate fluence irradiation up to 15 dpa	SCC	1.89	2.22
316 SS core internals in primary water – high fluence irradiation over 15 dpa	SCC	1.78	2.22
316 SS core internals in primary water – high fluence irradiation over 15 dpa	FR	1.89	2.11
316 SS core internals in primary water – high fluence irradiation over 15 dpa	SW	1.89	2.22

Table 9.4. Summary of all low Knowledge categories for PWRs (continued)

Material/Environment	Degradation Mode	Average Knowledge	Average Susceptibility
316 SS core internal HAZ in primary water – high fluence irradiation over 15 dpa	SCC	1.78	2.22
316 SS core internal HAZ in primary water – high fluence irradiation over 15 dpa	FR	1.89	2.11
316 SS core internal HAZ in primary water – high fluence irradiation over 15 dpa	SW	1.89	2.22
Type 308 SS in primary water – moderate fluence irradiation up to 15 dpa	SCC	1.78	2.33
Type 308 SS in primary water – high fluence irradiation over 15 dpa	SCC	1.89	2.11
Type 308 SS in primary water – high fluence irradiation over 15 dpa	FR	1.89	2.11
Type 308 SS in primary water – high fluence irradiation over 15 dpa	SW	1.78	2.11
304 HAZ SS in Primary Water - No irradiation	FR	1.88	1.13
316 SS HAZ in borated demineralized water	MIC	1.89	1.25
52/152 Weldments in borated demin water	FR	1.89	1.00
Alloy 690 TT in Secondary Coolant	SCC	1.89	1.78
CASS HAZ in Primary Reactor Water - No irradiation	FR	1.86	1.71
CASS HAZ in Primary Water - Low fluence irradiation up to 0.5 dpa	SCC	1.86	1.86
CASS in Primary Reactor Water - No irradiation	SCC	1.89	1.33
CASS in Primary Water - Low fluence irradiation up to 0.5 dpa	SCC	1.78	1.33
High Strength Bolts in Reactor Primary Water - No Irradiation	FR	1.89	1.78
Type 308 in Primary Water - Moderate fluence irradiation up to 15 dpa	FR	1.89	1.78
Type 308 Weld Metals - Austenitic to Austenitic in borated demineralized water	MIC	1.89	1.13
Wrought 316 SS in borated demineralized water	MIC	1.89	1.25

Table 9.5. Summary of all low Knowledge categories for BWRs

Material/Environment	Degradation Mode	Average Knowledge	Average Susceptibility
X750 in reactor water – low fluence irradiation up to 0.5 dpa	FR	1.89	2.13
304 SS in reactor water – high fluence more than 8 dpa up to 20 dpa	SCC-HWC	1.86	2.43
304 SS in reactor water – high fluence more than 8 dpa up to 20 dpa	FR	1.86	2.29
304 SS HAZ in reactor water – high fluence more than 8 dpa up to 20 dpa	FR	1.86	2.29
316 SS in reactor water – moderate fluence up to 8 dpa	FR	1.88	2.00
316 SS HAZ in reactor water – high fluence more than 8 dpa up to 20 dpa	FR	1.75	2.13
CASS in Reactor Water - No irradiation	SCC	1.89	1.67
CASS in Reactor Water - No irradiation	FR	1.89	1.78
LAS weldments in Reactor Coolant	SCC	1.89	1.78
304 SS piping and component external surfaces	MIC	1.88	1.14
308SS piping and component external surfaces	MIC	1.88	1.14
316 SS piping and component external surfaces	MIC	1.88	1.14
304 SS in Reactor Water - Moderate Fluence up to 8 dpa	FR	1.88	1.75
304 HAZ SS in Reactor Water - Moderate Fluence up to 8 dpa	FAT	1.88	1.88
304 HAZ SS in Reactor Water - Moderate Fluence up to 8 dpa	FAT-HWC	1.88	1.63
304 HAZ SS in Reactor Water - Moderate Fluence up to 8 dpa	FR	1.88	1.75
316 SS in Reactor Water - High Fluence more than 8 dpa up to 20 dpa	FAT-HWC	1.88	1.75
316 HAZ SS in Reactor Water - Moderate Fluence up to 8 dpa	FAT-HWC	1.88	1.63
316 HAZ SS in Reactor Water - Moderate Fluence up to 8 dpa	SCC-HWC	1.88	1.88
316 HAZ SS in Reactor Water - Moderate Fluence up to 8 dpa	FR	1.88	1.88
316 HAZ SS in Reactor Water - High Fluence more than 8 dpa up to 20 dpa	FAT-HWC	1.88	1.75
XM-19 in Reactor Water - Low fluence irradiation up to 0.5 dpa	FR	1.75	1.71

An obvious conclusion from Tables 9.4 and 9.5 is that irradiation-induced phenomena dominate this grouping of low Knowledge, high Susceptibility categories. Further, many of the low Knowledge, moderate Susceptibility categories listed in Tables 9.4 and 9.5 also feature irradiation-induced degradation categories. As noted in Chapter 8, longer operating periods and

power uprates will lead to increased fluences that are beyond the current range of operating experience and laboratory datasets for LWR conditions, not to mention possible increases in vibration, flow rate, etc. that might affect degradation. The panelists also identified other experience (e.g., swelling experience with 316 SS in fast reactors) that supports the likelihood that these forms of degradation will occur in subsequent operating periods. While the average Knowledge scores for all 27 categories are <2, the lowest Knowledge score is 1.75 (for 316 SS HAZ in BWR-NWC at high fluence). In this specific case, two panelists scored 1 with the balance scoring a 2. The personal confidence is above 2 for all cases listed in Tables 9.4 and 9.5. This indicates that the panelists felt there was enough knowledge that these radiation effects will occur at longer lifetimes based on extrapolation of known data although the magnitude and impact of these changes on component performance is less certain.

Finally, as cautioned above, it is important to note that this PIRT process makes no judgment or evaluation on the number of components or significance to structural integrity or safety for a given component, material, or degradation mode. This caveat should be considered when making research priorities, and other high Knowledge categories should also be evaluated.

9.5 SCORING SUMMARY FOR WROUGHT STAINLESS STEELS

Stainless steels represent a significant class of alloys used in LWR applications, including piping, joints, liners, weldments, and structural supports. As discussed in Chapter 2, several grades of stainless steel are in wide use: 304 and 316 SS are widely used for piping and structural components in both BWRs and PWRs. Types 308 SS and 309 SS are utilized for weldments and cladding or liner applications. Type 347 SS is occasionally used for core internal components such as baffle bolts. As part of this EMDA activity, the expert panel scored 419 categories for different grades of stainless steel in different environmental conditions (216 for PWRs and 203 for BWRs).

This section presents the results of the PIRT scoring for wrought stainless steels. The section below is organized by reactor type, grade of stainless steel, and then degradation mode. This varies from the NUREG/CR-6923 activity where results were organized by reactor system. However, as discussed above, the PIRT was organized differently to streamline this activity, and direct comparisons for individual components are more difficult.

9.5.1 Wrought Stainless Steels in PWRs

Austenitic stainless steels are used for a broad range of applications in PWR applications and are exposed to a wide range of environments, spanning primary reactor coolant with high fluence irradiation to service water with different impurity levels to ambient air on the outside service of pipes. For the EMDA activity, the panelists scored 216 categories. The results are shown below with the data organized by alloy class and then degradation mode. For each degradation mode, scores are ranking the summary tables by Susceptibility score.

9.5.1.1 Type 304 SS in PWRs

Type 304 SS is a major component within modern PWR systems. It is used for piping, tubes, valves, and core internal structures. The scores for the major degradation modes considered are summarized below. Additional details on individual scores by panelists, their comments and

rationale, and parts and component numbers used in NUREG/CR-6923 are also shown in Appendix A.

Several knowledge gaps for 304 SS in PWR environments were identified via the PIRT process:

- Impact of irradiation on fracture toughness, irradiation creep, swelling, and SCC
- SCC susceptibility at very long lifetimes
- Impact of water chemistry control in service water on crevice corrosion, pitting, and MIC

Additionally, panelists noted that the cumulative impact of fatigue on corrosion and component integrity deserved additional examination due to possible changes and uncertainties in cyclic and flow-induced loading over extended service conditions.

Crevice Corrosion

Crevice corrosion of 304SS has been observed in service water and can occur for a variety of reasons. The panelists ranked 304 SS in service water in the high Knowledge, high Susceptibility grouping, noting that in this particular environment, water chemistry is not well controlled, potentially leading to increased susceptibility. All other environments for 304 SS were judged to be of lower susceptibility.

Table 9.6. Summary of CREV scores for 304 SS in PWR environments

Material/Environment	Degradation Mode	Average Knowledge	Average Susceptibility
304 SS in service water	CREV	2.44	2.11
304 SS in spent fuel pool water	CREV	2.50	1.38
304 SS in secondary water	CREV	2.11	1.33
304 SS HAZ racks and liners in spent fuel pool water	CREV	2.56	1.33
304 SS racks and liners in spent fuel pool water	CREV	2.56	1.22

Fatigue and Corrosion Fatigue

Fatigue and corrosion fatigue are known issues in reactor service. As service life increases, so does the total number of loading cycles experienced by a component. Further, power uprates may also increase cyclic loading and impact component lifetime. The cumulative fatigue usage factor (CUF) must be evaluated for extended service. Type 304 SS weldolets in primary water were scored in the high Knowledge, high Susceptibility grouping. This is based on broad service experience with these components. All other environments for 304 SS were judged to be of lower susceptibility.

Table 9.7. Summary of FAT scores for 304 SS in PWR environments

Material/Environment	Degradation Mode	Average Knowledge	Average Susceptibility
304 SS weldolets in primary water – no irradiation	FAT	2.56	2.33
304 SS core internals in primary water – high fluence irradiation over 15 dpa	FAT	2.11	1.89
304 SS core internal HAZ in primary water – high fluence irradiation over 15 dpa	FAT	2.11	1.89
304 SS socket welds in primary water at lower temperatures	FAT	2.22	1.89
304 SS core internals in primary water – moderate fluence irradiation up to 15 dpa	FAT	2.11	1.78
304 SS core internal HAZ in primary water – moderate fluence irradiation up to 15 dpa	FAT	2.11	1.78
304 SS socket welds in borated demineralized water	FAT	2.33	1.67
304 SS HAZ in stagnant saturated steam/condensate	FAT	2.22	1.56
Wrought 304 SS in primary water – no irradiation	FAT	2.22	1.44
304 SS HAZ in primary water – no irradiation	FAT	2.33	1.44
Forged 304 SS in primary water – no irradiation	FAT	2.22	1.44
304 SS core internals in primary water – low fluence irradiation up to 0.5 dpa	FAT	2.22	1.44
304 SS core internals HAZ in primary water – low fluence irradiation up to 0.5 dpa	FAT	2.11	1.44
Wrought 304 SS in stagnant saturated steam/condensate	FAT	2.22	1.44
Wrought 304 SS Springs in primary water – no irradiation	FAT	2.33	1.33
Wrought 304 SS in primary water at lower temperatures	FAT	2.33	1.11
Forged 304 SS in primary water at lower temperatures	FAT	2.22	1.11
304 SS HAZ in primary water at lower temperatures	FAT	2.33	1.00
Wrought 304 SS in borated demineralized water	FAT	2.33	1.00
304 SS HAZ in borated demineralized water	FAT	2.33	1.00
304 SS in spent fuel pool water	FAT	2.56	1.00
304 SS racks and liners in spent fuel pool water	FAT	2.71	1.00
304 SS HAZ racks and liners in spent fuel pool water	FAT	2.56	0.89

Fracture Resistance

Decrease in fracture resistance is a key issue for austenitic stainless steels serving as core internals. As service life increases, so does the fluence observed by a component. Further, power uprates may also increase flux and thus increase total radiation damage over a lifetime. As noted in an earlier section, decrease in fracture toughness for 304 SS and 304 SS HAZs in core primary water was scored in the low Knowledge, high Susceptibility category. This is primarily due to the smaller database of irradiation effects at such fluences under LWR-relevant conditions. The 304 SS HAZs were also scored at higher susceptibility for moderate irradiation fluences. Finally, it is worth noting that 304 SS HAZ also scored in the low Knowledge, moderate

Susceptibility grouping. The panelists noted that the long-term effects of hydrogen (from water environment) on fracture resistance over very long lifetimes are also relatively unknown. All other environments for 304 SS were judged to be of lower susceptibility.

Table 9.8. Summary of FR scores for 304 SS in PWR environments

Material/Environment	Degradation Mode	Average Knowledge	Average Susceptibility
304 SS core internals in primary water – high fluence irradiation over 15 dpa	FR	1.89	2.33
304 SS core internal HAZ in primary water – high fluence irradiation over 15 dpa	FR	1.89	2.33
304 SS core internal HAZ in primary water – moderate fluence irradiation up to 15 dpa	FR	2.00	2.00
304 SS HAZ in primary water – no irradiation	FR	1.88	1.13
304 SS core internals in primary water – moderate fluence irradiation up to 15 dpa	FR	2.00	1.78
304 SS core internals in primary water – low fluence irradiation up to 0.5 dpa	FR	2.33	1.11
304 SS core internals HAZ in primary water – low fluence irradiation up to 0.5 dpa	FR	2.33	1.11

Irradiation Creep

As above for irradiation effects, the higher fluence due to longer service life and power uprates increases potential for irradiation-creep effects and stress relaxation. As above, 304 SS and 304 SS HAZs in core primary water were scored in the high Knowledge, high Susceptibility category. All other environments for 304 SS were judged to be of lower susceptibility.

Table 9.9. Summary of IC scores for 304 SS in PWR environments

Material/Environment	Degradation Mode	Average Knowledge	Average Susceptibility
304 SS core internals in primary water – high fluence irradiation over 15 dpa	IC	2.22	2.56
304 SS core internal HAZ in primary water – high fluence irradiation over 15 dpa	IC	2.33	2.44
304 SS core internals in primary water – moderate fluence irradiation up to 15 dpa	IC	2.22	2.11
304 SS core internal HAZ in primary water – moderate fluence irradiation up to 15 dpa	IC	2.22	1.89
304 SS core internals in primary water – low fluence irradiation up to 0.5 dpa	IC	2.56	1.00
304 SS core internals HAZ in primary water – low fluence irradiation up to 0.5 dpa	IC	2.56	1.00

Microbially Induced Corrosion

Microbially induced corrosion has been observed in service and can occur for a variety of reasons. Type 304 SS in service water ranks in the high Knowledge, high Susceptibility grouping. The panelists noted that in this particular environment, water chemistry is not well controlled, potentially leading to increased susceptibility. All other environments for 304 SS were judged to be of lower susceptibility.

Table 9.10. Summary of MIC scores for 304 SS in PWR environments

Material/Environment	Degradation Mode	Average Knowledge	Average Susceptibility
304 SS in service water	MIC	2.11	2.11
304 SS piping and component external surfaces	MIC	2.71	1.17
304 SS racks and liners in spent fuel pool water	MIC	2.71	1.14
Wrought 304 SS in borated demineralized water	MIC	2.00	1.13
304 SS HAZ in borated demineralized water	MIC	2.00	1.13
304 SS in spent fuel pool water	MIC	2.44	1.13
304 SS HAZ racks and liners in spent fuel pool water	MIC	2.44	1.00

Pitting

Pitting has been observed in service and can also occur for a variety of reasons. Type 304 SS in service water ranks in the high Knowledge, high Susceptibility grouping. As above for crevice and MIC, the panelists noted that water chemistry is not well controlled in this particular environment, potentially leading to increased susceptibility in oxygenated, chloride-contaminated water. All other environments for 304 SS were judged to be of lower susceptibility.

Table 9.11. Summary of PIT scores for 304 SS in PWR environments

Material/Environment	Degradation Mode	Average Knowledge	Average Susceptibility
304 SS in service water	PIT	2.44	2.11
304 SS piping and component external surfaces	PIT	2.67	1.67
304 SS in spent fuel pool water	PIT	2.56	1.22
304 SS racks and liners in spent fuel pool water	PIT	2.67	1.22
304 SS HAZ racks and liners in spent fuel pool water	PIT	2.67	1.22

Stress Corrosion Cracking

As discussed in Chapter 2, SCC is a known issue for 304 SS, even in low corrosion-potential environments such as PWR primary coolant; this is especially the case when the yield stress has been increased by e.g. irradiation and/or cold work. Extended service will result in increased time at temperature while exposed to the environment and under stress. Further, for core internals, an increased fluence will be experienced due to longer service and power uprates. PIRT scoring for 304 SS and 304 SS HAZ in PWR environments is listed in Table 9.12. As noted in an earlier section, swelling of 304 SS and 304 SS HAZs in core primary water was scored in the low

Knowledge, high Susceptibility category. This is due to the increased fluence, unknown effects of irradiation on hardening and swelling, and increased exposure to H (primarily from H_2 in the water). Type 304 SS and the 304 SS HAZs were also scored at higher susceptibility for moderate irradiation fluences. All other environments, such as those associated with spent fuel pools or secondary side systems, were judged to be of lower susceptibility for 304 SS.

Table 9.12. Summary of SCC scores for 304 SS in PWR environments

Material/Environment	Degradation Mode	Average Knowledge	Average Susceptibility
304 SS core internal HAZ in primary water – high fluence irradiation over 15 dpa	SCC	1.89	2.78
304 SS core internals in primary water – high fluence irradiation over 15 dpa	SCC	1.89	2.67
304 SS core internal HAZ in primary water – moderate fluence irradiation up to 15 dpa	SCC	2.00	2.44
304 SS core internals in primary water – moderate fluence irradiation up to 15 dpa	SCC	2.00	2.22
304 SS HAZ in primary water – no irradiation	SCC	2.44	1.89
304 SS HAZ in stagnant saturated steam/condensate	SCC	2.11	1.78
304 SS core internals HAZ in primary water – low fluence irradiation up to 0.5 dpa	SCC	2.44	1.67
304 SS in service water	SCC	2.44	1.67
Wrought 304 SS springs in primary water – no irradiation	SCC	2.33	1.56
304 SS core internals in primary water – low fluence irradiation up to 0.5 dpa	SCC	2.44	1.56
304 SS in secondary water	SCC	2.22	1.56
304 SS piping and component external surfaces	SCC	2.78	1.56
Wrought 304 SS in primary water – no irradiation	SCC	2.44	1.44
Forged 304 SS in primary water – no irradiation	SCC	2.33	1.44
Wrought 304 SS in stagnant saturated steam/condensate	SCC	2.11	1.44
304 SS racks and liners in spent fuel pool water	SCC	2.67	1.22
304 SS HAZ racks and liners in spent fuel pool water	SCC	2.56	1.22
304 SS HAZ in borated demineralized water	SCC	2.44	1.11
304 SS in spent fuel pool water	SCC	2.67	1.11
Wrought 304 SS in primary water at lower temperatures	SCC	2.44	1.00
304 SS HAZ in primary water at lower temperatures	SCC	2.44	1.00
Forged 304 SS in primary water at lower temperatures	SCC	2.56	1.00
Wrought 304 SS in borated demineralized water	SCC	2.44	1.00

Swelling

Swelling is a known issue for 304 SS, particularly in the solution-annealed condition. This is known primarily from fast-reactor research programs, although it is expected at lower temperatures and

longer lifetimes for LWR applications based on model and theory predictions. The magnitude that may be expected for 80 years of service is not known, however. This may be a key issue as 304 SS PWR core internals experience additional fluence due to longer service life and power uprates. As noted in an earlier section, swelling of 304 SS and 304 SS HAZs in core primary water was scored in the low Knowledge, high Susceptibility category. This is primarily due to the smaller database of irradiation effects at such fluences under LWR-relevant conditions. Type 304 SS and the 304 SS HAZ were also scored at higher susceptibility for moderate irradiation fluences. All other environments for 304 SS were judged to be of lower susceptibility. This trend of increasing susceptibility and decreasing knowledge as a function of fluence can be observed in Figure 9.9.

Table 9.13. Summary of SW scores for 304 SS in PWR environments

Material/Environment	Degradation Mode	Average Knowledge	Average Susceptibility
304 SS core internals in primary water – high fluence irradiation over 15 dpa	SW	1.89	2.22
304 SS core internal HAZ in primary water – high fluence irradiation over 15 dpa	SW	1.89	2.11
304 SS core internals in primary water – moderate fluence irradiation up to 15 dpa	SW	2.22	1.44
304 SS core internal HAZ in primary water – moderate fluence irradiation up to 15 dpa	SW	2.11	1.33
304 SS core internals in primary water – low fluence irradiation up to 0.5 dpa	SW	2.44	0.78
304 SS core internals HAZ in primary water – low fluence irradiation up to 0.5 dpa	SW	2.44	0.78

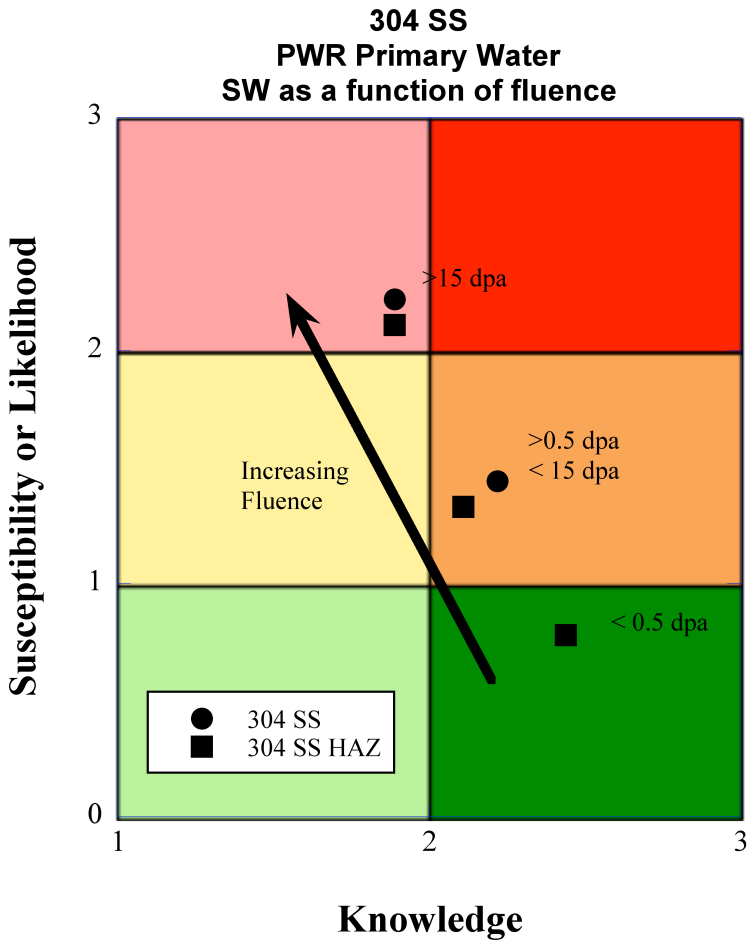

Figure 9.9. Susceptibility–Knowledge plot for swelling of 304 SS and 304 SS HAZ in PWR primary environment at different irradiation damage levels.

Wear

Wear was considered for springs and liners in the primary and spent fuel pool environments, respectively. The panelists scored susceptibility low (around 1) for both environments, citing no known service problems or significant concerns.

Table 9.14. Summary of WEAR scores for 304 SS in PWR environments

Material/Environment	Degradation Mode	Average Knowledge	Average Susceptibility
Wrought 304 SS springs in primary water – no irradiation	WEAR	2.33	1.13
304 SS racks and liners in spent fuel pool water	WEAR	2.56	0.88

9.5.1.2 Type 316 SS in PWRs

Type 316 SS is also a major alloy system used in modern PWR systems. The increased Ni and Mo content of this grade of steel improves corrosion resistance, and it has been shown to be more resistant to some forms of degradation such as irradiation-induced swelling. Like 304 SS, it is used for piping, tubes, valves, and core internal structures. The scores for the major degradation modes considered are summarized below. Additional details on individual scores by panelists, their comments and rationale, and parts and component numbers used in NUREG/CR-6923 are also shown in Appendix A.

Several knowledge gaps for 316 SS in PWR environments were identified via the PIRT process:

- Effect of irradiation on fracture toughness, irradiation creep, swelling, and SCC
- SCC susceptibility at very long lifetimes
- Effect of water chemistry control in service water on crevice corrosion, pitting, and MIC

Additionally, while scored in the high Knowledge category, the panelists noted that the cumulative effect of fatigue on corrosion and component integrity deserved additional examination due to possible changes and uncertainties in cyclic and flow-induced loading over extended service conditions.

Crevice Corrosion

Crevice corrosion has been observed in service and can occur for a variety of reasons. Type 316 SS in service water ranks in the high Knowledge, high Susceptibility grouping. The panelists noted that water chemistry is not well controlled, in this particular environment, potentially leading to increased susceptibility. All other environments for 316 SS were judged to be of lower susceptibility.

Table 9.15. Summary of CREV scores for 316 SS in PWR environments

Material/Environment	Degradation Mode	Average Knowledge	Average Susceptibility
316 SS in service water	CREV	2.44	2.00
316 SS in secondary water	CREV	2.22	1.56
316 SS in spent fuel pool water	CREV	2.56	1.33
316 SS liners in spent fuel pool water	CREV	2.56	1.33
316 SS HAZ in spent fuel pool water	CREV	2.71	1.14

Fatigue and Corrosion Fatigue

Fatigue and corrosion fatigue are known issues in reactor service. As service life increases, so does the total number of loading cycles experienced by a component. Further, power uprates may also increase flow-induced cyclic loading and impact component lifetime. The CUF must be evaluated for extended service. All environments for 316 SS were scored in the high Knowledge, moderate Susceptibility grouping. This is consistent with the majority of the 304 SS scoring described in the previous section.

Table 9.16. Summary of FAT scores for 316 SS in PWR environments

Material/Environment	Degradation Mode	Average Knowledge	Average Susceptibility
316 SS core internals in primary water – moderate fluence irradiation up to 15 dpa	FAT	2.11	1.78
316 SS core internal HAZ in primary water – moderate fluence irradiation up to 15 dpa	FAT	2.11	1.78
316 SS core internals in primary water – high fluence irradiation over 15 dpa	FAT	2.11	1.78
316 SS core internal HAZ in Primary water – high fluence irradiation over 15 dpa	FAT	2.11	1.78
316 SS socket welds in borated demineralized water	FAT	2.33	1.67
316 SS HAZ in primary water – no irradiation	FAT	2.44	1.56
Forged 316 SS in primary water – no irradiation	FAT	2.33	1.56
Wrought 316 SS in primary water – no irradiation	FAT	2.33	1.44
316 SS core internals in primary water – low fluence irradiation up to 0.5 dpa	FAT	2.22	1.44
316 SS core internals HAZ in primary water – low fluence irradiation up to 0.5 dpa	FAT	2.11	1.44
316 SS HAZ in stagnant saturated steam/condensate	FAT	2.11	1.44
Forged 316 SS in primary water at lower temperatures	FAT	2.11	1.22
Wrought 316 SS in stagnant saturated steam/condensate	FAT	2.11	1.22
Wrought 316 SS in primary water at lower temperatures	FAT	2.22	1.11
316 SS HAZ in primary water at lower temperatures	FAT	2.22	1.11
Wrought 316 SS in borated demineralized water	FAT	2.22	1.00
316 SS HAZ in borated demineralized water	FAT	2.22	1.00
316 SS in spent fuel pool water	FAT	2.56	1.00
316 SS HAZ in spent fuel pool water	FAT	2.71	1.00

Fracture Resistance

As noted in the previous section for 304 SS, decrease in fracture resistance is a key issue for austenitic stainless steels serving as core internals. As service life increases, so does the fluence observed by a component. Further, power uprates may also increase flux and thus increase total radiation damage over a lifetime. As noted in an earlier section, decrease in fracture toughness for 316 SS and 316 SS HAZs in core primary water was scored in the low Knowledge, high Susceptibility category. This is primarily due to the smaller database of irradiation effects at such fluences under LWR-relevant conditions. The 304 SS HAZ was also scored at higher susceptibility for moderate irradiation fluences. All other environments for 316 SS were judged to be of lower susceptibility, although the panelists again noted that the long-term effects of H (from water environment) on fracture resistance over very long lifetimes are also relatively unknown.

Table 9.17. Summary of FR scores for 316 SS in PWR environments

Material/Environment	Degradation Mode	Average Knowledge	Average Susceptibility
316 SS core internal HAZ in primary water – high fluence irradiation over 15 dpa	FR	1.89	2.56
316 SS core internals in primary water – high fluence irradiation over 15 dpa	FR	1.89	2.33
316 SS core internal HAZ in primary water – moderate fluence irradiation up to 15 dpa	FR	2.00	2.22
316 SS core internals in primary water – moderate fluence irradiation up to 15 dpa	FR	2.00	2.00
316 SS core internals HAZ in primary water – low fluence irradiation up to 0.5 dpa	FR	2.33	1.11
316 SS HAZ in primary water at lower temperatures	FR	2.22	1.11
316 SS core internals in primary water – low fluence irradiation up to 0.5 dpa	FR	2.33	1.00

Irradiation Creep

As noted above for 304 SS, the higher fluence due to longer service life and power uprates increases the potential for irradiation-creep (IC) effects and stress relaxation. Type 316 SS and 316 SS HAZs in core primary water were scored in the high Knowledge, high Susceptibility category. All other environments for 316 SS were judged to be of lower susceptibility.

Table 9.18. Summary of IC scores for 316 SS in PWR environments

Material/Environment	Degradation Mode	Average Knowledge	Average Susceptibility
316 SS core internals in primary water – high fluence irradiation over 15 dpa	IC	2.22	2.56
316 SS core internal HAZ in primary water – high fluence irradiation over 15 dpa	IC	2.22	2.56
316 SS core internal HAZ in primary water – moderate fluence irradiation up to 15 dpa	IC	2.22	2.11
316 SS core internals in primary water – moderate fluence irradiation up to 15 dpa	IC	2.22	1.89
316 SS core internals in primary water – low fluence irradiation up to 0.5 dpa	IC	2.67	1.11
316 SS core internals HAZ in primary water – low fluence irradiation up to 0.5 dpa	IC	2.67	1.11

Microbially Induced Corrosion

As noted previously, MIC has been observed in operation and can occur for a variety of reasons. Identical to 304 SS, 316 SS in service water ranks in the high Knowledge, high Susceptibility grouping. The panelists noted that water chemistry is not well controlled, in this particular

environment, potentially leading to increased susceptibility. All other environments for 316 SS were judged to be of lower susceptibility.

Table 9.19. Summary of MIC scores for 316 SS in PWR environments

Material/Environment	Degradation Mode	Average Knowledge	Average Susceptibility
316 SS in service water	MIC	2.00	2.11
Wrought 316 SS in borated demineralized water	MIC	1.89	1.25
316 SS HAZ in borated demineralized water	MIC	1.89	1.25
316 SS piping and component external surfaces	MIC	2.63	1.17
316 SS HAZ in spent fuel pool water	MIC	2.86	1.14
316 SS in spent fuel pool water	MIC	2.44	1.13

Pitting

Pitting has been observed in service and can also occur for a variety of reasons. As a result, 316 SS in service water ranked in the high Knowledge, high Susceptibility grouping. Once again, the panelists noted water chemistry is not well controlled, that in this particular environment, potentially leading to increased susceptibility. All other environments for 316 SS were judged to be of lower susceptibility.

Table 9.20. Summary of PIT scores for 316 SS in PWR environments

Material/Environment	Degradation Mode	Average Knowledge	Average Susceptibility
316 SS in service water	PIT	2.44	2.00
316 SS piping and component external surfaces	PIT	2.56	1.33
316 SS HAZ in spent fuel pool water	PIT	2.71	1.14
316 SS in spent fuel pool water	PIT	2.56	1.11

Stress Corrosion Cracking

As discussed in Chapter 2, 316 SS may be more resistant to SCC than 304 SS grades, although the growing database shows that SCC can occur in 316 SS even in low corrosion-potential environments. Extended service will result in increased time under temperature while exposed to the high temperature water environment and under stress. Further, for core internals, an increased fluence will be experienced due to longer service and power uprates. PIRT scoring for 316 SS and 316 SS HAZ in PWR environments is listed in Table 9.21. As noted in an earlier section, SCC of 316 SS and 316 SS HAZs in core primary water were scored in the low Knowledge, high Susceptibility category. This is due to the increased fluence, unknown effects of irradiation on hardening and swelling, and increased exposure to H (primarily due to H_2 in the water environment). All other environments for 316 SS and 316 SS HAZ were judged to be of lower susceptibility and higher knowledge.

Table 9.21. Summary of SCC scores for 316 SS in PWR environments

Material/Environment	Degradation Mode	Average Knowledge	Average Susceptibility
316 SS core internal HAZ in primary water – high fluence irradiation over 15 dpa	SCC	1.78	2.78
316 SS core internals in primary water – high fluence irradiation over 15 dpa	SCC	1.78	2.56
316 SS core internal HAZ in primary water – moderate fluence irradiation up to 15 dpa	SCC	1.89	2.44
316 SS core internals in primary water – moderate fluence irradiation up to 15 dpa	SCC	1.89	2.22
316 SS HAZ in primary water – no irradiation	SCC	2.33	1.78
316 SS core internals HAZ in primary water – low fluence irradiation up to 0.5 dpa	SCC	2.22	1.78
316 SS in secondary water	SCC	2.22	1.67
Wrought 316 SS in stagnant saturated steam/condensate	SCC	2.00	1.67
316 SS HAZ in stagnant saturated steam/condensate	SCC	2.00	1.67
316 SS core internals in primary water – low fluence irradiation up to 0.5 dpa	SCC	2.33	1.56
316 SS in service water	SCC	2.33	1.56
Wrought 316 SS in primary water – no irradiation	SCC	2.33	1.44
Forged 316 SS in primary water – no irradiation	SCC	2.33	1.44
316 SS piping and component external surfaces	SCC	2.78	1.33
316 SS HAZ in spent fuel pool water	SCC	2.71	1.29
316 SS liners in spent fuel pool water	SCC	2.56	1.22
316 SS HAZ in borated demineralized water	SCC	2.33	1.11
Wrought 316 SS in primary water at lower temperatures	SCC	2.44	1.00
316 SS HAZ in primary water at lower temperatures	SCC	2.44	1.00
Forged 316 SS in primary water at lower temperatures	SCC	2.56	1.00
Wrought 316 SS in borated demineralized water	SCC	2.33	1.00
316 SS in spent fuel pool water	SCC	2.56	1.00

Swelling

Swelling is typically lower in 316 SS when compared to 304 SS, primarily due to its increased Ni content. This has been observed extensively in fast-reactor research programs, although it could still occur at lower temperatures and longer lifetimes in LWR applications based on model and theory predictions. The magnitude that may be expected for 80 years of service is not known, however. This may be an issue as 316 SS core internals experience additional fluence due to longer service life and power uprates. As noted in an earlier section, swelling of 316 SS and 316 SS HAZs in core primary water were scored in the low Knowledge, high Susceptibility category. This is primarily due to the smaller database of irradiation effects at such fluences under LWR-relevant conditions. Type 316 SS and 316 SS HAZ were also scored at higher

susceptibility for moderate irradiation fluences. All other environments for 316 SS were judged to be of lower susceptibility and higher knowledge.

Table 9.22. Summary of SW scores for 316 SS in PWR environments

Material/Environment	Degradation Mode	Average Knowledge	Average Susceptibility
316 SS core internals in primary water – high fluence irradiation over 15 dpa	SW	1.89	2.33
316 SS core internal HAZ in primary water – high fluence irradiation over 15 dpa	SW	1.89	2.33
316 SS core internal HAZ in primary water – moderate fluence irradiation up to 15 dpa	SW	2.11	1.56
316 SS core internals in primary water – moderate fluence irradiation up to 15 dpa	SW	2.11	1.44
316 SS core internals in primary water – low fluence irradiation up to 0.5 dpa	SW	2.44	1.11
316 SS core internals HAZ in primary water – low fluence irradiation up to 0.5 dpa	SW	2.44	1.11

9.5.1.3 Type 347 SS in PWRs

Type 347 SS is not as widely used in U.S. reactors as 304 SS or 316 SS. This grade of steel is used primarily for baffle bolt applications. The scores for the major degradation modes considered are summarized below. Additional details on individual scores by panelists, their comments and rationale, and parts and component numbers used in NUREG/CR-6923 are also shown in Appendix A.

The effect of irradiation on fracture toughness, irradiation creep, swelling, and SCC was identified as a potential knowledge gap for 347 SS in PWR environments.

Fatigue and Corrosion Fatigue

As noted above, fatigue and corrosion fatigue are known issues in reactor service. As service life increases, so does the total number of loading cycles experienced by a component. Further, power uprates may also increase cyclic loading and impact component lifetime. Baffle bolts at moderate to high fluence were both scored in the high Knowledge, high Susceptibility category. Lower fluences for 347 SS were judged to be of lower susceptibility, based on good service experience.

Table 9.23. Summary of FAT scores for 347 SS in PWR environments

Material/Environment	Degradation Mode	Average Knowledge	Average Susceptibility
347 SS in primary water – high fluence irradiation over 15 dpa	FAT	2.00	2.00
347 SS in primary water – moderate fluence irradiation up to 15 dpa	FAT	2.00	2.00
347 SS in primary water – low fluence irradiation up to 0.5 dpa	FAT	2.22	1.56

Fracture Resistance

Decrease in fracture resistance is a key issue for austenitic stainless steels serving as core internals. As service life increases, so does the fluence observed by a component. Further, power uprates may also increase flux and thus increase total radiation damage over a lifetime. Decrease in fracture toughness for 347 SS baffle bolts in core primary water was scored in the high Knowledge, high Susceptibility grouping. The panelists noted that the long-term effects of H (from H_2 in the water environment) on fracture resistance over very long lifetimes are also relatively unknown. All other environments for 347 SS were judged to be of lower susceptibility.

Table 9.24. Summary of FR scores for 347 SS in PWR environments

Material/Environment	Degradation Mode	Average Knowledge	Average Susceptibility
347 SS in primary water – high fluence irradiation over 15 dpa	FR	2.00	2.33
347 SS in primary water – moderate fluence irradiation up to 15 dpa	FR	2.11	1.89
347 SS in primary water – low fluence irradiation up to 0.5 dpa	FR	2.22	1.22

Irradiation Creep

As above for 304 SS and 316 SS, the higher fluence due to longer service life and power uprates increases potential for irradiation-creep effects and stress relaxation. Components of 347 SS in core primary water were scored in the high Knowledge, high Susceptibility category at moderate and high fluence. All other environments for 347 SS were judged to be of lower susceptibility.

Table 9.25. Summary of IC scores for 347 SS in PWR environments

Material/Environment	Degradation Mode	Average Knowledge	Average Susceptibility
347 SS in primary water – high fluence irradiation over 15 dpa	IC	2.33	2.56
347 SS in primary water – moderate fluence irradiation up to 15 dpa	IC	2.22	2.11
347 SS in primary water – low fluence irradiation up to 0.5 dpa	IC	2.38	0.89

Stress Corrosion Cracking

Similar to rationale for irradiation creep scoring, the higher fluence due to longer service life and power uprates increases susceptibility for SCC. Components of 347 SS in core primary water were scored in the high Knowledge, high Susceptibility grouping at moderate and high fluence. All other environments for 347 SS were judged to be of lower susceptibility and higher knowledge.

Table 9.26. Summary of SCC scores for 347 SS in PWR environments

Material/Environment	Degradation Mode	Average Knowledge	Average Susceptibility
347 SS in primary water – high fluence irradiation over 15 dpa	SCC	2.00	2.78
347 SS in primary water – moderate fluence irradiation up to 15 dpa	SCC	2.00	2.44
347 SS in primary water – low fluence irradiation up to 0.5 dpa	SCC	2.11	1.56

Swelling

As for the other degradation modes, the higher fluence due to longer service life and power uprates increases the potential for swelling. Components of 347 SS in core primary water were scored in the high Knowledge, high Susceptibility category at high fluence. All other environments for 347 SS were judged to be of lower susceptibility and higher knowledge.

Table 9.27. Summary of SW scores for 347 SS in PWR environments

Material/Environment	Degradation Mode	Average Knowledge	Average Susceptibility
347 SS in primary water – high fluence irradiation over 15 dpa	SW	2.22	2.33
347 SS in primary water – moderate fluence irradiation up to 15 dpa	SW	2.22	1.33
347 SS in primary water – low fluence irradiation up to 0.5 dpa	SW	2.38	0.78

9.5.1.4 Type 308 SS Weldments and Clad in PWRs

Types 308 SS and 309 SS serve an important function in LWR applications, being used for weldments and clad applications. The scores for the major degradation modes considered are summarized below. Additional details on individual scores by panelists, their comments and rationale, and parts and component numbers used in NUREG/CR-6923 are also shown in Appendix A.

Several knowledge gaps for 308/309 SS in PWR environments were identified via the PIRT process:

- Impact of irradiation on fracture toughness, irradiation creep, swelling, and SCC
- SCC susceptibility at very long lifetimes
- Impact of water chemistry control in borated and demineralized water on MIC

Crevice Corrosion and Debonding

Crevice corrosion was considered for 308 SS weld metals in spent fuel pool water and found to be high Knowledge, moderate Susceptibility by the expert panel. Debonding of 308 SS cladding

was also evaluated in the PIRT and also scored in the high Knowledge, moderate Susceptibility grouping.

Table 9.28. Summary of CREV and DEBOND scores for 308 SS in PWR environments

Material/Environment	Degradation Mode	Average Knowledge	Average Susceptibility
308 SS weld metals – austenitic to austenitic in spent fuel pool water	CREV	2.44	1.22
308 SS cladding – in primary water	DEBOND	2.11	1.11

Fatigue and Corrosion Fatigue

As noted above, fatigue and corrosion fatigue are known issues in reactor service. As service life increases, so does the total number of loading cycles experienced by a component. Further, power uprates may also increase cyclic loading and impact component lifetime. The CUF must be evaluated for extended service. Type 308 SS weld metals in all PWR environments were scored in the high Knowledge, moderate Susceptibility grouping.

Table 9.29. Summary of FAT scores for 308 SS in PWR environments

Material/Environment	Degradation Mode	Average Knowledge	Average Susceptibility
308 SS in primary water – high fluence irradiation over 15 dpa	FAT	2.11	1.78
308 SS in primary water – moderate fluence irradiation up to 15 dpa	FAT	2.11	1.44
308 SS weld metals – austenitic to austenitic in primary water – no irradiation	FAT	2.22	1.22
308 SS in primary water – low fluence irradiation up to 0.5 dpa	FAT	2.11	1.22
308 SS weld metals – austenitic to austenitic in stagnant saturated steam condensate	FAT	2.22	1.22
308/309 SS weld metals – austenitic to C and LAS in primary water – no irradiation	FAT	2.22	1.11
308 SS cladding – in primary water	FAT	2.44	1.00
308 SS weld metals – austenitic to austenitic in primary water at lower temperature	FAT	2.22	1.00
308 SS weld metals – austenitic to austenitic in borated demineralized water	FAT	2.33	1.00
308 SS weld metals – austenitic to austenitic in spent fuel pool water	FAT	2.33	1.00

Fracture Resistance

Similar to the other grades of wrought stainless steel described above, decrease in fracture resistance is a key issue in 308 and 309 SS serving as core internals. As service life increases, so does the fluence observed by a component. Further, power uprates may also increase flux

and thus increase total radiation damage over extended reactor operation. As noted in an earlier section, decrease in fracture toughness for type 308 SS weldments in core primary water was scored in the low Knowledge, high Susceptibility category for high fluence and in the low Knowledge, moderate Susceptibility for moderate fluence. This is primarily due to the smaller database of irradiation effects at such fluences under LWR-relevant conditions. All other environments for 308 weld metals and cladding were judged to be of lower susceptibility and higher knowledge, although the panelists again noted that the long-term effects of H (from water environment) on fracture resistance are relatively unknown.

Table 9.30. Summary of FR scores for 308 SS in PWR environments

Material/Environment	Degradation Mode	Average Knowledge	Average Susceptibility
308 SS in primary water – high fluence irradiation over 15 dpa	FR	1.89	2.11
308 SS in primary water – moderate fluence irradiation up to 15 dpa	FR	1.89	1.78
308 SS in primary water – low fluence irradiation up to 0.5 dpa	FR	2.22	1.22
308 SS weld metals – austenitic to austenitic in stagnant saturated steam condensate	FR	2.00	1.22
308/309 SS weld metals – austenitic to C and LAS in primary water – no irradiation	FR	2.00	1.22
308 SS weld metals – austenitic to austenitic in primary water – no irradiation	FR	2.11	1.11
308 SS cladding – in primary water	FR	2.33	1.00

Irradiation Creep

As stated above for the wrought stainless steels, the higher fluence due to longer service life and power uprates increases the potential for irradiation-creep effects and stress relaxation. Type 308 SS weldments in core primary water were scored in the high Knowledge, high Susceptibility category at high fluence. All other environments for 308 were judged to be of lower susceptibility.

Table 9.31. Summary of IC scores for 308 SS in PWR environments

Material/Environment	Degradation Mode	Average Knowledge	Average Susceptibility
308 SS in primary water – high fluence irradiation over 15 dpa	IC	2.11	2.44
308 SS in primary water – moderate fluence irradiation up to 15 dpa	IC	2.33	1.56
308 SS in primary water – low fluence irradiation up to 0.5 dpa	IC	2.67	1.00

Microbially Induced Corrosion and Pitting

For 308 SS weld metals, MIC in borated and demineralized water was scored in the low Knowledge, moderate Susceptibility grouping. The panelists noted that in this particular environment, water chemistry is not well controlled, potentially leading to increased susceptibility. All other environments for 308 weldments for both MIC and pitting were judged to be of lower susceptibility.

Table 9.32. Summary of MIC scores for 308 SS in PWR environments

Material/Environment	Degradation Mode	Average Knowledge	Average Susceptibility
308 SS weld metals – austenitic to austenitic in borated demineralized water	MIC	1.89	1.13
308 SS piping and component external surfaces	MIC	2.63	1.00
308/309 SS weld metals – austenitic to C and LAS in air	PIT	2.44	1.67
308 SS weld metals – austenitic to austenitic in spent fuel pool water	PIT	2.44	1.11
308 SS cladding – in primary water	PIT	2.56	0.89

Stress Corrosion Cracking

As discussed in Chapter 2, stainless steel is susceptible to SCC, even in low corrosion-potential environments. Extended service will result in increased time under temperature while exposed to the environment and under stress. Further, for core internal weldments, an increased fluence will be experienced due to longer service and power uprates. PIRT scoring for 308 SS weldments in PWR environments is listed in Table 9.33. As noted in an earlier section, SCC of 308 SS weldments in core primary water was scored in the low Knowledge, high Susceptibility category for both moderate and high fluences. This is due to the increased fluence, unknown impacts of irradiation on hardening and swelling, and increased exposure to H (primarily due to H_2 in the water coolant). All other environments for 308 SS were judged to be of lower susceptibility and higher knowledge.

Table 9.33. Summary of SCC scores for 308 SS in PWR environments

Material/Environment	Degradation Mode	Average Knowledge	Average Susceptibility
308 SS in primary water – high fluence irradiation over 15 dpa	SCC	1.89	2.44
308 SS in primary water – moderate fluence irradiation up to 15 dpa	SCC	1.78	2.11
308/309 SS weld metals – austenitic to C and LAS in air	SCC	2.33	1.67
308 SS weld metals – austenitic to austenitic in stagnant saturated steam condensate	SCC	2.00	1.33
308/309 SS weld metals – austenitic to C and LAS in primary water – no irradiation	SCC	2.11	1.33
308 SS in primary water – low fluence irradiation up to 0.5 dpa	SCC	2.33	1.22
308 SS weld metals – austenitic to austenitic in primary water – no irradiation	SCC	2.11	1.11

Table 9.33. Summary of SCC scores for 308 SS in PWR environments (continued)

Material/Environment	Degradation Mode	Average Knowledge	Average Susceptibility
308 SS cladding – in primary water	SCC	2.22	1.00
308 SS weld metals – austenitic to austenitic in primary water at lower temperature	SCC	2.33	1.00
308 SS weld metals – austenitic to austenitic in borated demineralized water	SCC	2.33	1.00
308 SS weld metals – austenitic to austenitic in spent fuel pool water	SCC	2.56	1.00

Swelling

As for the other degradation modes, the higher fluence due to longer service life and power uprates increases the potential for swelling, among other forms of irradiation-induced degradation. Type 308 SS weldments in core primary water were scored in the low Knowledge, high Susceptibility category at high fluence. Lower fluence levels were scored at lower susceptibility and higher knowledge.

Table 9.34. Summary of SW scores for 308 SS in PWR environments

Material/Environment	Degradation Mode	Average Knowledge	Average Susceptibility
308 SS in primary water – high fluence irradiation over 15 dpa	SW	1.78	2.11
308 SS in primary water – moderate fluence irradiation up to 15 dpa	SW	2.11	1.22
308 SS in primary water – low fluence irradiation up to 0.5 dpa	SW	2.50	0.88

9.5.2 Wrought Stainless Steels in BWRs

Austenitic stainless steels are also used for a broad range of applications in BWR systems and serve in a wide range of environments. These include the boiling water reactor coolant with high fluence irradiation and steam inside the reactor vessel. Service water, steam condensate, and even ambient air on the outside service of pipes are also considered. Where relevant, both normal water chemistry and hydrogen water chemistry environments were considered. For the EMDA activity, the panelists scored 203 categories. The results are shown below with the data organized by alloy class and then degradation mode. Within each degradation mode, scores are ranked the summary tables by Susceptibility score.

9.5.2.1 Type 304 SS in BWRs

Type 304 SS is used for major components in modern BWR systems. It is used for piping, tubes, valves, and core internal support structures and as key structures in the upper core internals. The scores for the major degradation modes considered by the expert panel are summarized below. Additional details on individual scores by panelists, their comments and rationale, and parts and component numbers used in NUREG/CR-6923 are also shown in Appendix B.

Several knowledge gaps for 304 SS in BWR environments were identified via the PIRT process:

- Impact of irradiation on fracture toughness and SCC in both NWC and HWC environments
- SCC susceptibility at very long operation periods, particularly in NWC environments
- Cumulative impact of fatigue on corrosion and component integrity, particularly weldolets, sockolets, and components in the upper core internals

Crevice Corrosion

Crevice corrosion has been observed in service and can occur for a variety of reasons. This localized corrosion of 304 SS all BWR environments high Knowledge, moderate Susceptibility grouping. The PIRT scores were very consistent in both knowledge and susceptibility across all BWR environments.

Table 9.35. Summary of CREV scores for 304 SS in BWR environments

Material/Environment	Degradation Mode	Average Knowledge	Average Susceptibility
304 SS in suppression pool water	CREV	2.56	1.78
304 SS in circulating water (treated or sea/lake/pond)	CREV	2.56	1.67
304 SS in reactor water at lower temperature	CREV	2.44	1.44
304 SS HAZ in reactor water at lower temperature	CREV	2.44	1.44
304 SS in reactor water at lower temperature, normally stagnant	CREV	2.44	1.33
304 SS in feedwater	CREV	2.56	1.33
304 SS in demineralized water	CREV	2.56	1.33

Fatigue and Corrosion Fatigue

Fatigue and corrosion fatigue are known issues in BWR service. As service life increases, so does the total number of loading cycles experienced by a component. Further, power uprates may also increase cyclic loading and impact component lifetime. This is particularly true for 304 SS serving in the reactor coolant steam in the upper reactor core. The expert panel noted that flow patterns, irradiation effects, and cyclic stress could all be impacted by uprates and extended service and that the CUF must be evaluated for extended service for all these components. Type 304 SS in reactor coolant steam was scored in the high Knowledge, high Susceptibility grouping, as were 304 SS weldolets and sockolets in BWR NWC environments. This is based on broad service experience with these components. All other environments for 304 SS were judged to be of lower susceptibility and higher knowledge.

Similar trends were found in analysis of the PIRT scoring for 304 SS in BWR HWC environments. The 304 SS weldolets and sockolets scored in the high Knowledge, high Susceptibility grouping. All other HWC environments for 304 SS were judged to be of lower susceptibility or higher knowledge.

Table 9.36. Summary of FAT scores for 304 SS in BWR environments

Material/Environment	Degradation Mode	Average Knowledge	Average Susceptibility
304 SS in reactor coolant steam	FAT	2.22	2.22
304 SS weldolets and sockolets in reactor water	FAT	2.67	2.11
304 SS sockolet in reactor water at lower temperature	FAT	2.22	2.00
304 SS HAZ in reactor water – moderate fluence up to 8 dpa	FAT	1.88	1.88
304 SS in reactor water – high fluence more than 8 dpa up to 20 dpa	FAT	2.14	1.86
304 SS HAZ in reactor water – high fluence more than 8 dpa up to 20 dpa	FAT	2.00	1.86
304 SS HAZ in reactor coolant steam	FAT	2.33	1.78
304 SS in reactor water – moderate fluence up to 8 dpa	FAT	2.13	1.75
304 SS HAZ core internals in reactor water – no irradiation	FAT	2.56	1.67
304 SS HAZ core internals in reactor water – low fluence irradiation up to 0.5 dpa	FAT	2.44	1.67
304 SS in reactor water – low fluence up to 0.5 dpa and vibration	FAT	2.56	1.56
304 SS HAZ in piping in reactor water – no irradiation	FAT	2.56	1.44
304 SS in deoxygenated reactor water	FAT	2.67	1.44
304 SS piping in reactor water – no irradiation	FAT	2.56	1.33
304 SS core internals in reactor water – no irradiation	FAT	2.67	1.33
304 SS in reactor water – low fluence up to 0.5 dpa	FAT	2.56	1.33
304 SS in feedwater	FAT	2.67	1.33
304 SS in reactor water at lower temperature	FAT	2.56	1.22
304 SS HAZ in reactor water at lower temperature	FAT	2.56	1.22
304 SS in circulating water (treated or sea/lake/pond)	FAT	2.56	1.22
304 SS in reactor water at lower temperature, normally stagnant	FAT	2.67	1.11
304 SS in condensate storage water	FAT	2.67	1.00
304 SS HAZ in condensate storage water	FAT	2.67	1.00
304 SS in suppression pool water	FAT	2.44	1.00
304 SS in demineralized water	FAT	2.78	1.00
304 SS weldolets and sockolets in reactor water	FAT-HWC	2.33	2.11
304 SS HAZ in reactor water – moderate fluence up to 8 dpa	FAT-HWC	1.88	1.63
304 SS in reactor water – high fluence more than 8 dpa up to 20 dpa	FAT-HWC	2.14	1.71
304 SS HAZ in reactor water – high fluence more than 8 dpa up to 20 dpa	FAT-HWC	2.00	1.71
304 SS HAZ core internals in reactor water – no irradiation	FAT-HWC	2.22	1.67
304 SS in reactor water – moderate fluence up to 8 dpa	FAT-HWC	2.25	1.63
304 SS in reactor water – low fluence up to 0.5 dpa and vibration	FAT-HWC	2.33	1.56

Table 9.36. Summary of FAT scores for 304 SS in BWR environments (continued)

Material/Environment	Degradation Mode	Average Knowledge	Average Susceptibility
304 SS HAZ core internals in reactor water – low fluence irradiation up to 0.5 dpa	FAT-HWC	2.33	1.56
304 SS piping in reactor water – no irradiation	FAT-HWC	2.44	1.33
304 SS core internals in reactor water – no irradiation	FAT-HWC	2.33	1.33
304 SS in reactor water – low fluence up to 0.5 dpa	FAT-HWC	2.67	1.33
304 SS HAZ in piping in reactor water – no irradiation	FAT-HWC	2.33	1.33

Fracture Resistance

Decrease in fracture resistance is a key issue for austenitic stainless steels serving as core internals in both PWR and BWR applications. As service life increases, so does the fluence observed by a component. Further, power uprates may also increase flux and thus increase total radiation damage over a lifetime. As noted in an earlier section, decrease in fracture toughness for 304 SS and 304 SS HAZs in NWC was scored in the low Knowledge, high Susceptibility grouping. This is primarily due to the smaller database of irradiation effects at such fluences under LWR-relevant conditions. Similarly, 304 SS and 304 SS HAZs in BWR NWC environment at moderate fluence were scored in the low Knowledge, moderate Susceptibility grouping. The 304 SS HAZ was also scored at higher susceptibility for moderate irradiation fluences. All other environments for 304 SS were judged to be of lower susceptibility and higher knowledge.

Table 9.37. Summary of FR scores for 304 SS in BWR environments

Material/Environment	Degradation Mode	Average Knowledge	Average Susceptibility
304 SS in reactor water – high fluence more than 8 dpa up to 20 dpa	FR	1.86	2.29
304 SS HAZ in reactor water – high fluence more than 8 dpa up to 20 dpa	FR	1.86	2.29
304 SS in reactor water – moderate fluence up to 8 dpa	FR	1.88	1.75
304 SS HAZ in reactor water – moderate fluence up to 8 dpa	FR	1.88	1.75
304 SS in reactor water – low fluence up to 0.5 dpa and vibration	FR	2.33	1.33
304 SS HAZ core internals in reactor water – low fluence irradiation up to 0.5 dpa	FR	2.11	1.33
304 SS in reactor water – low fluence up to 0.5 dpa	FR	2.11	1.22
304 SS HAZ in piping in reactor water – no irradiation	FR	2.22	1.11
304 SS HAZ core internals in reactor water – no irradiation	FR	2.22	1.11
304 SS in reactor coolant steam	FR	2.44	1.11
304 SS HAZ in reactor coolant steam	FR	2.33	1.11

Table 9.37. Summary of FR scores for 304 SS in BWR environments (continued)

Material/Environment	Degradation Mode	Average Knowledge	Average Susceptibility
304 SS piping in reactor water – no irradiation	FR	2.22	1.00
304 SS core internals in reactor water – no irradiation	FR	2.22	1.00
304 SS in reactor water at lower temperature	FR	2.67	1.00
304 SS HAZ in reactor water at lower temperature	FR	2.67	1.00

General Corrosion

General corrosion is well understood and not generally an issue for 304 SS or 304 SS HAZ if water chemistry is maintained. There have been few instances of issues in service. The panelists scored susceptibility very low (near 1) for all environments and noted that corrosion was unlikely to occur in these environments.

Table 9.38. Summary of GC scores for 304 SS in BWR environments

Material/Environment	Degradation Mode	Average Knowledge	Average Susceptibility
304 SS in feedwater	GC	2.56	1.11
304 SS in circulating water (treated or sea/lake/pond)	GC	2.67	1.11
304 SS in reactor water at lower temperature	GC	2.56	1.00
304 SS HAZ in reactor water at lower temperature	GC	2.56	1.00
304 SS in suppression pool water	GC	2.67	1.00
304 SS in deoxygenated reactor water	GC	2.67	0.89

Microbially Induced Corrosion

Microbially induced corrosion can occur for a variety of reasons in service, particularly if the environment is not well controlled. Type 304 SS and external piping surfaces scored in the low Knowledge, moderate Susceptibility grouping, although it should be noted that it is narrowly in the low-knowledge grouping and susceptibility falls below most other environments. The panelists noted that a wide variety of environments could be expected. All other environments for 304 SS were judged to be of lower susceptibility and higher knowledge.

Table 9.39. Summary of MIC scores for 304 SS in BWR environments

Material/Environment	Degradation Mode	Average Knowledge	Average Susceptibility
304 SS piping and component external surfaces	MIC	1.88	1.14
304 SS in suppression pool water	MIC	2.56	1.63
304 SS in circulating water (treated or sea/lake/pond)	MIC	2.33	1.50
304 SS in condensate storage water	MIC	2.11	1.13
304 SS HAZ in condensate storage water	MIC	2.22	1.13

Pitting

Pitting can also occur for a variety of reasons and has been observed in BWR service. For all BWR environments, 304 SS was scored in the high Knowledge, moderate Susceptibility grouping. In fact, the average knowledge and Susceptibility scores are almost constant for all environments considered.

Table 9.40. Summary of PIT scores for 304 SS in BWR environments

Material/Environment	Degradation Mode	Average Knowledge	Average Susceptibility
304 SS in suppression pool water	PIT	2.67	1.67
304 SS in circulating water (treated or sea/lake/pond)	PIT	2.67	1.67
304 SS external surfaces	PIT	2.56	1.44
304 SS HAZ in reactor water at lower temperature	PIT	2.63	1.38
304 SS in reactor water at lower temperature, normally stagnant	PIT	2.67	1.33
304 SS in feedwater	PIT	2.67	1.33
304 SS in reactor water at lower temperature	PIT	2.67	1.22
304 SS in deoxygenated reactor water	PIT	2.67	1.22
304 SS in demineralized water	PIT	2.67	1.22

Stress Corrosion Cracking

As discussed in Chapter 2, SCC is a known issue for 304 SS, especially in BWR higher corrosion-potential environments. Extended service will result in increased time under temperature while exposed to the high-temperature water environment and under stress. Further, for core internals, an increased fluence will be experienced due to longer service and power uprates. PIRT scoring for 304 SS and 304 SS HAZ in BWR environments is listed in Table 9.41. The susceptibility of 304 SS and 304 SS HAZ in higher corrosion-potential environments is reflected in the panelist scores, as 11 environmental categories were in the high Knowledge, high Susceptibility grouping. SCC expectations in other environments with lower temperatures or no irradiation were deemed to be of lower susceptibility, consistent with both laboratory and service experience.

Similar trends were observed in HWC. Type 304 SS and the 304 SS HAZs in BWR NWC at high fluence were scored in the low Knowledge, high Susceptibility grouping. In part, this is due to the increased fluence, unknown impacts of irradiation on hardening and swelling, and increased exposure to H (due to higher H_2 in the BWR HWC environment). All other environments for 304 SS were judged to be of lower susceptibility. The scoring for the HWC environment yielded lower Susceptibility scores than the NWC environment for the same materials. This is expected given the difference in susceptibilities in these two environments and experience from both operating environments and laboratory testing.

Table 9.41. Summary of SCC scores for 304 SS in BWR environments

Material/Environment	Degradation Mode	Average Knowledge	Average Susceptibility
304 SS in reactor water – high fluence more than 8 dpa up to 20 dpa	SCC	2.43	2.86
304 SS HAZ in reactor water – high fluence more than 8 dpa up to 20 dpa	SCC	2.57	2.86
304 SS in reactor water – moderate fluence up to 8 dpa	SCC	2.88	2.63
304 SS HAZ in reactor water – moderate fluence up to 8 dpa	SCC	2.63	2.63
304 SS HAZ in piping in reactor water – no irradiation	SCC	2.89	2.44
304 SS HAZ core internals in reactor water – low fluence irradiation up to 0.5 dpa	SCC	2.78	2.44
304 SS HAZ core internals in reactor water – no irradiation	SCC	2.78	2.33
304 SS HAZ in reactor coolant steam	SCC	2.67	2.22
304 SS in reactor water – low fluence up to 0.5 dpa	SCC	2.78	2.11
304 SS in reactor coolant steam	SCC	2.78	2.00
304 SS HAZ in reactor water at lower temperature	SCC	2.44	2.00
304 SS core internals in reactor water – no irradiation	SCC	2.89	1.89
304 SS in reactor water at lower temperature, normally stagnant	SCC	2.67	1.67
304 SS in feedwater	SCC	2.44	1.67
304 SS in reactor water at lower temperature	SCC	2.44	1.56
304 SS piping in reactor water – no irradiation	SCC	2.89	1.44
304 SS HAZ in condensate storage water	SCC	2.56	1.44
304 SS in circulating water (treated or sea/lake/pond)	SCC	2.56	1.44
304 SS in suppression pool water	SCC	2.67	1.33
304 SS external surfaces	SCC	2.78	1.33
304 SS in deoxygenated reactor water	SCC	2.67	1.22
304 SS in condensate storage water	SCC	2.56	1.22
304 SS in demineralized water	SCC	2.78	1.00
304 SS in reactor water – high fluence more than 8 dpa up to 20 dpa	SCC-HWC	1.86	2.43
304 SS HAZ in reactor water – high fluence more than 8 dpa up to 20 dpa	SCC-HWC	2.00	2.43
304 SS in reactor water – moderate fluence up to 8 dpa	SCC-HWC	2.38	1.88
304 SS HAZ in reactor water – moderate fluence up to 8 dpa	SCC-HWC	2.00	1.88
304 SS HAZ core internals in reactor water – low fluence irradiation up to 0.5 dpa	SCC-HWC	2.44	1.78
304 SS HAZ in piping in reactor water – no irradiation	SCC-HWC	2.56	1.67
304 SS HAZ core internals in reactor water – no irradiation	SCC-HWC	2.56	1.56

Table 9.41. Summary of SCC scores for 304 SS in BWR environments (continued)

Material/Environment	Degradation Mode	Average Knowledge	Average Susceptibility
304 SS in reactor water – low fluence up to 0.5 dpa	SCC-HWC	2.56	1.33
304 SS core internals in reactor water – no irradiation	SCC-HWC	2.56	1.22
304 SS Piping in reactor water – no irradiation	SCC-HWC	2.56	1.11

Wear

Wear was considered for the jet pump assembly. The panelists scored susceptibility moderate (around 2), generally citing flow-induced vibration as a potential concern over long operating periods and if operating conditions change.

Table 9.42. Summary of WEAR scores for 304 SS in BWR environments

Material/Environment	Degradation Mode	Average Knowledge	Average Susceptibility
304 SS in reactor water – low fluence up to 0.5 dpa and vibration	WEAR	2.22	1.89

9.5.2.2 Type 316 SS in BWRs

Type 316 SS is also a major alloy used in modern BWR systems. The increased Ni content of this grade of steel improves corrosion resistance and has been shown to be more resistant to some forms of degradation such as irradiation-induced swelling. Like 304 SS, it is used for piping, tubes, valves, and core internal structures. The scores for the major degradation modes considered are summarized below. Additional details on individual scores by panelists, their comments and rationale, and parts and component numbers used in NUREG/CR-6923 are also shown in Appendix B.

Several knowledge gaps for 316 SS in BWR environments were identified via the PIRT process:

- Impact of irradiation on fracture toughness and SCC in both NWC and HWC environments
- SCC susceptibility during extended reactor operation, particularly in NWC environments
- Cumulative impact of fatigue on corrosion and component integrity

Fatigue and Corrosion Fatigue

Fatigue and corrosion fatigue are known issues for 316 SS in BWR service. As service life increases, so does the total number of loading cycles experienced by a component. Further, power uprates may also increase cyclic loading and impact component lifetime. The CUF must be evaluated for extended service. The 316 SS HAZ in reactor water scored in the high Knowledge, high Susceptibility grouping although it should be noted that it scored at the minimum (2.00) for inclusion in the high Susceptibility grouping and is not significantly different than the other categories. All environments for 316 SS were scored in the high Knowledge,

moderate Susceptibility grouping. This is consistent with the 304 SS scoring described in the previous section.

In the HWC environment, 316 SS and 316 SS HAZ scored in the low Knowledge, moderate Susceptibility grouping. The panelists noted a lower knowledge base on the long-term effects of H (both from water chemistry and increased H generated via irradiation processes when compared to 304 SS). All other environments were scored with higher knowledge rankings.

Table 9.43. Summary of FAT scores for 316 SS in BWR environments

Material/Environment	Degradation Mode	Average Knowledge	Average Susceptibility
316 SS HAZ in reactor water – high fluence more than 8 dpa up to 20 dpa	FAT	2.00	2.00
316 SS in reactor water – high fluence more than 8 dpa up to 20 dpa	FAT	2.13	1.88
316 SS HAZ in reactor water – moderate fluence up to 8 dpa	FAT	2.00	1.88
316 SS HAZ in reactor water	FAT	2.33	1.78
316 SS HAZ in reactor water – low fluence irradiation up to 0.5 dpa	FAT	2.67	1.78
316 SS in reactor water – moderate fluence up to 8 dpa	FAT	2.13	1.75
316 SS in reactor water – no irradiation	FAT	2.78	1.22
316 SS in reactor water – low fluence irradiation up to 0.5 dpa	FAT	2.67	1.22
316 SS in deoxygenated reactor water	FAT	2.78	1.11
316 SS in reactor water – high fluence more than 8 dpa up to 20 dpa	FAT-HWC	1.88	1.75
316 SS HAZ in reactor water – high fluence more than 8 dpa up to 20 dpa	FAT-HWC	1.88	1.75
316 SS HAZ in reactor water – moderate fluence up to 8 dpa	FAT-HWC	1.88	1.63
316 SS HAZ in reactor water	FAT-HWC	2.22	1.78
316 SS HAZ in reactor water – low fluence irradiation up to 0.5 dpa	FAT-HWC	2.22	1.67
316 SS in reactor water – moderate fluence up to 8 dpa	FAT-HWC	2.00	1.63
316 SS in reactor water – no irradiation	FAT-HWC	2.44	1.22
316 SS in reactor water – low fluence irradiation up to 0.5 dpa	FAT-HWC	2.56	1.22

Fracture Resistance

As noted previously, decrease in fracture resistance is a key issue for austenitic stainless steels serving as core internals. As service life increases, so does the fluence observed by a component. Further, power uprates may also increase flux and thus increase total radiation damage over a lifetime. As noted in an earlier section, decrease in fracture toughness for 316 SS and 316 SS HAZs was scored in the low Knowledge, high Susceptibility grouping. This is

primarily due to the smaller database of irradiation effects at such fluences under LWR-relevant conditions. Type 316 SS and the 316 SS HAZ at moderate fluence were also scored at higher susceptibility or lower knowledge. All other environments for 316 SS were judged to be of higher knowledge.

Table 9.44. Summary of FR scores for 316 SS in BWR environments

Material/Environment	Degradation Mode	Average Knowledge	Average Susceptibility
316 SS HAZ in reactor water – high fluence more than 8 dpa up to 20 dpa	FR	1.75	2.13
316 SS in reactor water – moderate fluence up to 8 dpa	FR	1.88	2.00
316 SS in reactor water – high fluence more than 8 dpa up to 20 dpa	FR	2.00	2.29
316 SS HAZ in reactor water – moderate fluence up to 8 dpa	FR	1.88	1.88
316 SS HAZ in reactor water – low fluence irradiation up to 0.5 dpa	FR	2.00	1.22
316 SS in reactor water – low fluence irradiation up to 0.5 dpa	FR	2.00	1.11
316 SS HAZ in reactor water	FR	2.00	1.11
316 SS in reactor water – no irradiation	FR	2.22	1.00

General Corrosion, Microbially Induced Corrosion and Pitting

General corrosion, MIC, and pitting can occur for a variety of reasons. All scores for these modes of degradation for 316 SS in BWR environments were very low in susceptibility, consistent with the alloy's good corrosion resistance.

Table 9.45. Summary of MIC scores for 316 SS in BWR environments

Material/Environment	Degradation Mode	Average Knowledge	Average Susceptibility
316 SS in deoxygenated reactor water	GC	2.78	1.00
316 SS piping and component external surfaces	MIC	1.88	1.14
316 SS external surfaces	PIT	2.67	1.44
316 SS in deoxygenated reactor water	PIT	2.67	1.11

Stress Corrosion Cracking

As noted earlier, 316 SS is more resistant to SCC than 304 SS, although it is still susceptible in higher corrosion-potential environments. Extended service will result in increased time under temperature while exposed to the environment and under stress. Further, for core internals, an increased fluence will be experienced due to longer service and power uprates. PIRT scoring for 316 SS and 316 SS HAZ in BWR environments is listed in Table 9.46. The susceptibility of 316 SS and 316 SS HAZ in higher corrosion-potential environments is reflected in the panelist scores, as seven environmental categories were in the high Knowledge, high Susceptibility grouping.

SCC expectations in other environments with lower temperatures or no irradiation were scored to be of lower susceptibility, consistent with both laboratory and service experience.

Similar trends were observed in HWC. Type 316 SS and 316 SS HAZs in BWR NWC at moderate fluence were scored in the low Knowledge, high Susceptibility grouping in BWR NWC environments. In part, this is due to the increased fluence, unknown impacts of irradiation on hardening and swelling, and increased exposure to H (primarily due to higher H_2 concentrations in the coolant). All other environments for 316 were judged to be of lower Susceptibility.

The scoring for the HWC environment yielded lower Susceptibility scores than the NWC environment for 316 SS. This is expected given the difference in susceptibilities in these two environments and experience in both operating environments and laboratory settings.

Table 9.46. Summary of SCC scores for 316 SS in BWR environments

Material/Environment	Degradation Mode	Average Knowledge	Average Susceptibility
316 SS HAZ in reactor water – high fluence more than 8 dpa up to 20 dpa	SCC	2.63	2.88
316 SS in reactor water – high fluence more than 8 dpa up to 20 dpa	SCC	2.57	2.86
316 SS in reactor water – moderate fluence up to 8 dpa	SCC	2.88	2.63
316 SS HAZ in reactor water – moderate fluence up to 8 dpa	SCC	2.63	2.63
316 SS HAZ in reactor water – low fluence irradiation up to 0.5 dpa	SCC	2.78	2.33
316 SS HAZ in reactor water	SCC	2.89	2.22
316 SS in reactor water – low fluence irradiation up to 0.5 dpa	SCC	2.78	2.00
316 SS in reactor water – no irradiation	SCC	2.89	1.33
316 SS external surfaces	SCC	2.78	1.33
316 SS in deoxygenated reactor water	SCC	2.78	1.11
316 SS in reactor water – high fluence more than 8 dpa up to 20 dpa	SCC-HWC	2.00	2.29
316 SS HAZ in reactor water – high fluence more than 8 dpa up to 20 dpa	SCC-HWC	2.00	2.25
316 SS HAZ in reactor water – moderate fluence up to 8 dpa	SCC-HWC	1.88	1.88
316 S in reactor water – moderate fluence up to 8 dpa	SCC-HWC	2.25	1.75
316 SS HAZ in reactor water – low fluence irradiation up to 0.5 dpa	SCC-HWC	2.33	1.56
316 SS HAZ in reactor water	SCC-HWC	2.44	1.44
316 SS in reactor water – low fluence irradiation up to 0.5 dpa	SCC-HWC	2.56	1.22
316 SS in reactor water – no irradiation	SCC-HWC	2.56	1.11

9.5.2.3 Type 309 SS as Cladding in BWRs

Type 309 SS is used in BWR applications as cladding to protect carbon or low alloy steel from the aggressive water environments. The scores for the major degradation modes considered are summarized below. Additional details on individual scores by panelists, their comments and rationale, and parts and component numbers used in NUREG/CR-6923 are also shown in Appendix B. No knowledge gaps for 309 SS cladding in BWR environments were identified via the PIRT process.

Debonding

The expert panel considered debonding of the clad layer from the low alloy steel structures. All scores for this mode of degradation for 309 SS in BWR environments were very low in susceptibility.

Table 9.47. Summary of DEBOND scores for 309 SS cladding in BWR environments

Material/Environment	Degradation Mode	Average Knowledge	Average Susceptibility
309 SS in reactor water – no irradiation	DEBOND	2.22	1.11
309 SS in reactor water – low fluence up to 0.5 dpa	DEBOND	2.22	1.11

Fatigue and Corrosion Fatigue

As noted above, fatigue and corrosion fatigue are known issues in reactor service. The expert panel considered fatigue damage of the clad layer. All scores for this mode of degradation for 309 SS in BWR environments were very low in susceptibility, as a source of fatigue in a clad component was not apparent to the panel.

Table 9.48. Summary of FAT scores for 309 SS cladding in BWR environments

Material/Environment	Degradation Mode	Average Knowledge	Average Susceptibility
309 SS in reactor water – no irradiation	FAT	2.78	1.00
309 SS in reactor water – low fluence up to 0.5 dpa	FAT	2.78	1.00
309 SS in reactor water – no irradiation	FAT-HWC	2.56	1.11
309 SS in reactor water – low fluence up to 0.5 dpa	FAT-HWC	2.56	1.11

Fracture Resistance

The expert panel also considered a decrease in fracture toughness of the clad layer. All scores for this mode of degradation for 309 SS in BWR environments were very low in susceptibility, as neutron fluences, even in extreme conditions, were relatively low for significant changes to manifest.

Table 9.49. Summary of FR scores for 309 SS cladding in BWR environments

Material/Environment	Degradation Mode	Average Knowledge	Average Susceptibility
309 SS in reactor water – no irradiation	FR	2.22	1.00
309 SS in reactor water – low fluence up to 0.5 dpa	FR	2.22	1.00

Stress Corrosion Cracking

The expert panel also considered SCC of the clad layer in both NWC and HWC environments. All scores for this mode of degradation for 309 SS in BWR environments were very low in susceptibility. Low stress, low fatigue, and relatively low neutron fluence were all cited as reasons by the expert panel for the low Susceptibility scores.

Table 9.50. Summary of SCC scores for 309 SS cladding in BWR environments

Material/Environment	Degradation Mode	Average Knowledge	Average Susceptibility
309 SS in reactor water – no irradiation	SCC	2.56	1.33
309 SS in reactor water – low fluence up to 0.5 dpa	SCC	2.56	1.33
309 SS in reactor water – no irradiation	SCC-HWC	2.44	1.00
309 SS in reactor water – low fluence up to 0.5 dpa	SCC-HWC	2.44	0.89

9.5.2.4 Types 308 and 309 SS Weldments in BWRs

Types 308 SS and 309 SS serve an important function in LWR applications, being used for weldments and clad applications. The scores for the major degradation modes considered are summarized below. Additional details on individual scores by panelists, their comments and rationale, and parts and component numbers used in NUREG/CR-6923 are also shown in Appendix B.

While no specific low-knowledge gaps for 308 SS and 309 SS weldments in BWR environments were identified via the PIRT process, the panelists did note the impact of irradiation on fracture resistance, and SCC for 308L SS in steam in some environments and SCC susceptibility at very long lifetimes as potential issues deserving additional consideration for long term reactor operation.

Crevice Corrosion and Debonding

Crevice corrosion was considered for 308 SS and 309 SS weld metals and found to be high Knowledge, moderate Susceptibility by the expert panel. The scores for this mode of degradation for 309 SS in BWR environments were very low in susceptibility.

Table 9.51. Summary of CREV scores for 308 SS and 309 SS weldments in BWR environments

Material/Environment	Degradation Mode	Average Knowledge	Average Susceptibility
308/309 SS in lower temperature reactor coolant, normally stagnant	CREV	2.56	1.33

Fatigue and Corrosion Fatigue

With increasing service duration or changes in flow conditions, the total number of loading cycles experienced by a component will also change. The CUF must be evaluated for extended service. Types 308 and 309 weld metals in all BWR wet steam were scored in the high Knowledge, high Susceptibility grouping, which was primarily driven by the higher flow rates and increased loading cycles over a lifetime. All other environments for were scored in the high Knowledge, moderate Susceptibility grouping for both NWC and HWC environments.

Table 9.52. Summary of FAT scores for 308 SS and 309 SS weldments in BWR environments

Material/Environment	Degradation Mode	Average Knowledge	Average Susceptibility
308L SS in wet steam	FAT	2.56	2.22
308 SS weldments in reactor water – high fluence more than 7 dpa up to 20 dpa	FAT	2.00	1.75
308 SS weldments in reactor water – moderate fluence up to 8 dpa	FAT	2.13	1.63
308/309 SS weldments in reactor water – no irradiation	FAT	2.56	1.33
308/309 SS weldments in reactor water – low fluence irradiation up to 0.5 dpa	FAT	2.56	1.33
308 and 309 SS in lower temperature reactor coolant, normally stagnant	FAT	2.56	1.11
308 SS in deoxygenated reactor water	FAT	2.78	1.00
308 SS weldments in reactor water – high fluence more than 7 dpa up to 20 dpa	FAT-HWC	2.00	1.75
308 SS weldments in reactor water – moderate fluence up to 8 dpa	FAT-HWC	2.00	1.63
308/309 SS weldments in reactor water – no irradiation	FAT-HWC	2.33	1.22
308/309 SS weldments in reactor water – low fluence irradiation up to 0.5 dpa	FAT-HWC	2.33	1.22

Fracture Resistance

Similar to the other stainless steels noted above for both PWR and BWR environments, a decrease in fracture resistance is a key issue for in 308 SS and 309 SS weldments. As service life increases, so does the fluence observed by a component. Further, power uprates may also increase flux and thus increase total radiation damage over a lifetime. Weldments in the reactor core at high fluence were graded with a score of 2.0 for knowledge and susceptibility. The higher susceptibility was a result of less experience at the higher fluence level and expectation of radiation damage at that fluence. Fracture resistance was scored in the high Knowledge, moderate Susceptibility grouping for all other environments considered.

Table 9.53. Summary of FR scores for 308 SS and 309 SS weldments in BWR environments

Material/Environment	Degradation Mode	Average Knowledge	Average Susceptibility
308 SS weldments in reactor water – high fluence more than 8 dpa up to 20 dpa	FR	2.00	2.00
308 SS weldments in reactor water – moderate fluence up to 8 dpa	FR	2.00	1.75
308/309 SS weldments in reactor water – no irradiation	FR	2.22	1.11
308/309 SS weldments in reactor water – low fluence irradiation up to 0.5 dpa	FR	2.11	1.11
308L SS in wet steam	FR	2.33	1.11

General Corrosion, Microbially Induced Corrosion and Pitting

General corrosion, MIC, and pitting can occur for a variety of reasons. All scores for these modes of degradation for 308 SS and 309 SS in BWR environments were very low in susceptibility, consistent with the alloys' good corrosion resistance.

Table 9.54. Summary of GC, MIC, and PIT scores for 308 SS and 309 SS weldments in BWR environments

Material/Environment	Degradation Mode	Average Knowledge	Average Susceptibility
308 SS in deoxygenated reactor water	GC	2.67	1.00
308 SS piping and component external surfaces	MIC	1.88	1.14
308/309 SS in lower temperature reactor coolant, normally stagnant	PIT	2.56	1.33
308 SS in deoxygenated reactor water	PIT	2.56	1.11

Stress Corrosion Cracking

PIRT scoring for 308 SS and 309 SS weldments in BWR environments is listed in Table 9.55. The susceptibility of 308 SS and 309 SS weldments at higher fluences in NWC was scored in high Knowledge, high Susceptibility grouping. SCC expectations in other environments with lower temperatures or no irradiation were lower susceptibility, consistent with both laboratory and service experience.

For 308 SS and 309 SS weldments at high fluence in HWC, SCC was scored in the high Knowledge, high Susceptibility grouping. The increased exposure to H (primarily due to additional H_2 in the coolant under HWC environments) was noted as a factor for the higher Susceptibility score. All other environments for 308 SS and 309 SS weldments were judged to be of lower susceptibility.

Table 9.55. Summary of SCC scores for 308 SS and 309 SS weldments in BWR environments

Material/Environment	Degradation Mode	Average Knowledge	Average Susceptibility
308 SS weldments in reactor water – high fluence more than 8 dpa up to 20 dpa	SCC	2.25	2.63
308 SS weldments in reactor water – moderate fluence up to 8 dpa	SCC	2.25	2.00
308L SS in wet steam	SCC	2.56	1.89
308/309 SS weldments in reactor water – low fluence irradiation up to 0.5 dpa	SCC	2.44	1.67
308/309 SS weldments in reactor water – no irradiation	SCC	2.56	1.56
308 SS in deoxygenated reactor water	SCC	2.56	1.22
308/309 SS in lower temperature reactor coolant, normally stagnant	SCC	2.56	1.11
308 SS weldments in reactor water – high fluence more than 8 dpa up to 20 dpa	SCC-HWC	2.00	2.13
308 SS weldments in reactor water – moderate fluence up to 8 dpa	SCC-HWC	2.00	1.63
308/309 SS weldments in reactor water – no irradiation	SCC-HWC	2.33	1.11
308/309 SS weldments in reactor water – low fluence irradiation up to 0.5 dpa	SCC-HWC	2.22	1.11

9.5.3 Summary of PIRT Findings for Wrought Stainless Steels

Stainless steels represent significant class of alloys used for LWR applications, such as piping, joints, liners, weldments, and structural supports. The previous sections presented the results of the PIRT scoring for wrought stainless steels starting with PWR conditions and then followed by BWR environments.

The PIRT scoring process for PWR environments identified several knowledge gaps, covering alloy/environment combinations that scored in the “pink” and “yellow” regions of the rainbow charts, like those shown in Figure 9.1. These potential gaps included:

- Impact of irradiation on fracture toughness, irradiation creep, swelling, and SCC for 304 SS, 316 SS, 347 SS, and 308/309 SS weldments
- SCC susceptibility at very long lifetimes for 304 SS, 316 SS, and 308/309 SS weldments
- Potential impact of poor water chemistry control in service water on crevice corrosion, pitting, and MIC for 304 SS, 316 SS, and 308/309 SS weldments
- Cumulative impact of fatigue on corrosion and component integrity for 304 SS and 316 SS structures

In BWR environments, a similar series of gaps were identified and included the following items:

- Impact of irradiation on fracture toughness and SCC in both NWC and HWC environments for 304 SS, 316 SS, and 308/309 SS weldments
- SCC susceptibility at very long lifetimes, particularly in NWC environments for 304 SS, 316 SS, and 308/309 SS weldments
- Cumulative impact of fatigue on corrosion and component integrity, particularly weldolets, sockolets, and components in the upper core internals.

The extent of these knowledge gaps is impacted by unknowns associated with synergisms between different degradation modes; for instance, the effect on SCC of irradiation damage, thermal embrittlement, etc. which are very time dependent. These concerns were covered in more detail in earlier alloy-specific chapters. Recent data on corrosion fatigue crack initiation of wrought stainless steels in BWR-HWC and PWR primary environments indicate, contrary to intuition, the corrosion fatigue resistance may be reduced under these reducing water chemistry conditions.

9.6 SCORING SUMMARY FOR ALLOY 600 AND ALLOY 182/82 WELD METALS

Nickel alloys and weld metals were chosen for LWR components because their low corrosion rate, resistance to SCC, and thermal expansion coefficient are similar to those of low alloy RPV steel. PWR components include nozzles, piping, control rod drive mechanisms, and steam generator tubing among others. BWR components containing Alloy 600 and Alloys 182 and 82 as weld metals include RPV attachment welds, head bolts, feedwater nozzles, safe end butters, and supports.

As noted in Chapter 3, degradation modes and related concerns in Ni alloys and weld metals include:

- SCC
- corrosion fatigue
- reduction in fracture resistance

For weld metals, potential issues also include:

- welding defects, such as hot cracking, ductility dip cracking, and lack of fusion
- thermal aging which may lead to secondary microstructural changes and increased susceptibility to other forms of degradation
- dilution effects (and cracking along the weld interface)
- stress corrosion cracking through weld metal attachment pads that interfaces with and penetrates the underlying low alloy steel

Significant cracking of Ni-base alloys was discovered in BWR components in the 1970s, and SCC has become the primary materials issue for these alloys in LWRs. Although cracking occurred initially in crevices and/or cold-worked components, it has spread to other areas and components and has especially manifested in Alloy 182 welds.

As part of the EMDA activity, the expert panel scored 76 categories for Alloy 600 and 182/82 weldments in different environmental conditions (42 for PWRs and 34 for BWRs).

This section presents the results of the PIRT scoring for Alloy 600 and its weldments. The section below is organized by reactor type and then degradation mode. This varies from the NUREG/CR-6923 activity where results were organized by reactor system. However, as discussed above, the PIRT was arranged differently for this EMDA activity, and direct comparisons for individual components are more difficult.

9.6.1 Alloy 600 and Alloy 182/82 Weldments in PWRs

Alloy 600 is used in important components in PWR systems, particularly as nozzles and steam generator tubing. The scores for the major degradation modes considered are summarized below. For long-term reactor operation, several areas for additional consideration for Alloy 600 and 182/82 in PWR environments were identified by the expert panel:

- SCC was identified as a high Knowledge, high Susceptibility mode of degradation in all primary and secondary environments. This is a known issue for these alloys.

- Wear was identified as a high Knowledge, high Susceptibility mode of degradation in secondary coolant environments. This is a known form of degradation.

- Fracture resistance in Alloy 182/82 welds at lower temperatures has been noted in laboratory testing although the mechanism has not been clearly established.

9.6.1.1 Alloy 600 in PWRs

The scores for the major degradation modes considered are summarized below. Additional details on individual scores by panelists, their comments and rationale, and parts and component numbers used in NUREG/CR-6923 are also shown in Appendix C. Alloy 600 exists in service in several different metallurgical states, including mill annealed, thermally treated, and solution annealed. All are considered as separate categories in this PIRT activity.

Several potential areas for future consideration for Alloy 600 in PWR environments were identified by the expert panel:

- SCC was identified as a high Knowledge, high Susceptibility mode of degradation in all primary and secondary environments, as expected based on service experience

- Wear was identified as a high Knowledge, high Susceptibility mode of degradation in secondary coolant environments, as expected based on service experience.

Fatigue and Corrosion Fatigue

Fatigue and corrosion fatigue are known issues in reactor service and may increase with increased cyclic loading over longer reactor operation periods. The expert panel considered

twelve different alloy/environment categories and all were scored in the high Knowledge, moderate Susceptibility grouping. The expert panelists noted that corrosion fatigue damage is directly related to operational conditions and changes in flow rates or other conditions due to power uprates may reduce useful life.

Table 9.56. Summary of FAT scores for Alloy 600 in PWR environments

Material/Environment	Degradation Mode	Average Knowledge	Average Susceptibility
Alloy 600 TT forged components in primary reactor water	FAT	2.33	1.78
Alloy 600 TT tubes in primary reactor water	FAT	2.33	1.78
Alloy 600 TT in secondary coolant	FAT	2.11	1.78
Alloy 600 MA in secondary coolant	FAT	2.11	1.78
Alloy 600 MA HAZ in secondary coolant	FAT	2.22	1.78
Alloy 600 TT HAZ in primary reactor water	FAT	2.33	1.67
Alloy 600 MA tubes in primary reactor water	FAT	2.33	1.67
Alloy 600 SA in primary reactor water	FAT	2.33	1.67
Alloy 600 TT HAZ in secondary coolant	FAT	2.22	1.67
Alloy 600 SA in secondary coolant	FAT	2.11	1.67
Alloy 600 MA forged components in primary reactor	FAT	2.22	1.56
Alloy 600 MA HAZ in primary reactor	FAT	2.22	1.44

Pitting

Pitting of Alloy 600 tubing has been observed in specific service conditions and is known to occur for a variety of reasons. All pitting categories for Alloy 600 in PWR environments were scored in the high Knowledge, moderate Susceptibility grouping with nearly identical scoring. The expert panelists noted that pitting damage is directly controlled by good water chemistry control. As long as water chemistry is maintained, pitting damage is expected to be minimal in these alloys.

Table 9.57. Summary of PIT scores for Alloy 600 in PWR environments

Material/Environment	Degradation Mode	Average Knowledge	Average Susceptibility
Alloy 600 TT in secondary coolant	PIT	2.44	1.56
Alloy 600 MA in secondary coolant	PIT	2.33	1.44
Alloy 600 TT HAZ in secondary coolant	PIT	2.67	1.44
Alloy 600 SA in secondary coolant	PIT	2.33	1.44
Alloy 600 MA HAZ in secondary coolant	PIT	2.67	1.33

Stress Corrosion Cracking

SCC is a known issue for Alloy 600 in all alloy forms. SCC has been observed in both primary- and secondary-side applications for all forms of Alloy 600 in service. The expert panel scored all twelve categories of SCC in the high Knowledge, high Susceptibility grouping. Alloy 600 in the

MA form was given the highest possible Susceptibility score, consistent with operational experience. Most plants have or will be performing steam generator replacements and in the process are upgrading from Alloy 600 to Alloy 690.

Table 9.58. Summary of SCC scores for Alloy 600 in PWR environments

Material/Environment	Degradation Mode	Average Knowledge	Average Susceptibility
Alloy 600 MA tubes in primary reactor water	SCC	2.67	3.00
Alloy 600 MA in secondary coolant	SCC	2.56	3.00
Alloy 600 SA in secondary coolant	SCC	2.56	3.00
Alloy 600 MA HAZ in secondary coolant	SCC	2.44	2.89
Alloy 600 TT forged components in primary reactor water	SCC	2.56	2.67
Alloy 600 TT HAZ in primary reactor water	SCC	2.56	2.67
Alloy 600 TT Tubes in primary reactor water	SCC	2.56	2.67
Alloy 600 MA Forged components in primary reactor	SCC	2.56	2.67
Alloy 600 MA HAZ in primary reactor	SCC	2.44	2.67
Alloy 600 SA in primary reactor water	SCC	2.56	2.67
Alloy 600 TT in secondary coolant	SCC	2.56	2.67
Alloy 600 TT HAZ in secondary coolant	SCC	2.56	2.44

Wear

Wear was considered for Alloy 600 tubes and supports on the secondary coolant side of the steam generators. All forms of Alloy 600 were scored between 1.78 and 2.00 on susceptibility. The Alloy 600 MA and SA were given scores of 2.00, placing them in the high Knowledge, high Susceptibility grouping rather than high Knowledge, moderate Susceptibility although the difference in the scoring is not significant from the Alloy 600TT.

Table 9.59. Summary of WEAR scores for Alloy 600 in PWR environments

Material/Environment	Degradation Mode	Average Knowledge	Average Susceptibility
Alloy 600 MA in secondary coolant	WEAR	2.11	2.00
Alloy 600 SA in secondary coolant	WEAR	2.11	2.00
Alloy 600 TT in secondary coolant	WEAR	2.00	1.89
Alloy 600 TT HAZ in secondary coolant	WEAR	2.33	1.78
Alloy 600 MA HAZ in secondary coolant	WEAR	2.44	1.78

9.6.1.2 Alloy 182/82 Weldments in PWRs

The scores for the major degradation modes considered are summarized below. Additional details on individual scores by panelists, their comments and rationale, and parts and component numbers used in NUREG/CR-6923 are also shown in Appendix C.

The expert panel identified only one potential knowledge need for Alloy 182/82 in PWR environments. Specifically, fracture resistance in Alloy 182/82 welds at lower temperatures has been noted in laboratory testing although limited mechanistic understanding has been established. .

Fatigue and Corrosion Fatigue

Fatigue and corrosion fatigue are known issues for all material systems, particular as the total number of loading cycles experienced by a component increases. The CUF must be evaluated for extended service. Two different alloy/environment categories were considered by the expert panel, and all were scored in the high Knowledge, moderate Susceptibility grouping.

Table 9.60. Summary of FAT scores for Alloy 182/82 weldments in PWR environments

Material/Environment	Degradation Mode	Average Knowledge	Average Susceptibility
Alloy 82/182 weldments in primary reactor water	FAT	2.22	1.89
Alloy 82/182 weldments in borated demin water	FAT	2.33	1.33

Fracture Resistance

Fracture resistance was evaluated for the Alloy 182/82 weldments for extended service operations. The expert panel scored both categories of FR in the high Knowledge, moderate Susceptibility grouping. The experts noted that low temperature cracking under very specific conditions requires further analysis in terms of mechanism and of practical significance.

Table 9.61. Summary of FR scores for Alloy 182/82 weldments in PWR environments

Material/Environment	Degradation Mode	Average Knowledge	Average Susceptibility
Alloy 82/182 weldments in primary reactor water	FR	2.00	1.56
Alloy 82/182 weldments in borated demin water	FR	2.00	1.56

Stress Corrosion Cracking

As above for Alloy 600, SCC is a known issue for Alloy 182/82 weldments. Extensive SCC has been observed for Alloy 182 in primary water environments during PWR service. The expert panel scored Alloy 182/82 SCC in primary water in the high Knowledge, high Susceptibility grouping. SCC in borated demineralized water environments and on external surfaces has a much lower susceptibility due to lower temperatures and less aggressive environments.

Table 9.62. Summary of SCC scores for Alloy 182/82 weldments in PWR environments

Material/Environment	Degradation Mode	Average Knowledge	Average Susceptibility
Alloy 82/182 weldments in primary reactor water	SCC	2.67	3.00
Alloy 82/182 weldments in borated demineralized water	SCC	2.56	1.56
Alloy 82/182 weldments on external surfaces	SCC	2.11	1.11

9.6.2 Alloy 600 and Alloy 182/82 Weldments in BWRs

Alloy 600 is also an important component in BWR systems, particularly as RPV attachment welds, head bolts, feedwater nozzles, safe end butters, and supports. The scores for the major degradation modes considered are summarized below. Where relevant, both NWC and HWC environments were considered. For the EMDA activity, the panelists scored 34 categories. The results are shown below with the data organized by alloy class and then degradation mode. Within each degradation mode, scores are ranked in the summary tables by Susceptibility score. Additional details on individual scores by panelists, their comments and rationale, and parts and component numbers used in NUREG/CR-6923 are also shown in Appendix D.

No low Knowledge categories for Alloys 600 and 182/82 in BWR environments were identified via the PIRT process. However, the panelists noted two areas for additional consideration, including:

- SCC was identified as a high Knowledge, high Susceptibility mode of degradation in NWC environments. This is a known issue for these alloys in service.

- Decrease in fracture resistance in Alloy 182/82 welds at lower temperatures has been noted in laboratory testing although the mechanism is not well understood.

9.6.2.1 Alloy 600 in BWRs

The scores for the Alloy 600 major degradation modes in BWRs considered are summarized below. Additional details on individual scores by panelists, their comments and rationale, and parts and component numbers used in NUREG/CR-6923 are also shown in Appendix D. Alloy 600 is present in several different metallurgical states including MA, TT, and SA conditions. All are considered as separate categories in this PIRT activity.

SCC was identified as a high Knowledge, high Susceptibility mode of degradation for Alloy 600 in BWR NWC environments by the expert panel. This is a known issue for these alloys in high potential environments.

Fatigue and Corrosion Fatigue

Eight different alloy/environment categories for corrosion fatigue were considered by the expert panel, and all were scored in the high Knowledge, moderate Susceptibility grouping with Susceptibility scores near 1 for all categories, indicating very low susceptibility. As with PWR scoring for this alloy, the expert panelists noted that FAT damage is directly related to operational conditions and changes in flow rates or other conditions due to power uprates may reduce useful life.

Table 9.63. Summary of FAT scores for Alloy 600 in BWR environments

Material/Environment	Degradation Mode	Average Knowledge	Average Susceptibility
Alloy 600 in reactor coolant – low fluence irradiation up to 0.2 dpa	FAT	2.44	1.22
Alloy 600 in reactor coolant – no irradiation	FAT	2.56	1.11
Alloy 600 HAZ in reactor coolant – no irradiation	FAT	2.56	1.11

Table 9.63. Summary of FAT scores for Alloy 600 in BWR environments (continued)

Material/Environment	Degradation Mode	Average Knowledge	Average Susceptibility
Alloy 600 HAZ in reactor coolant – low fluence irradiation up to 0.2 dpa	FAT	2.50	1.11
Alloy 600 in reactor coolant – no irradiation	FAT-HWC	2.44	1.11
Alloy 600 HAZ in reactor coolant – no irradiation	FAT-HWC	2.44	1.11
Alloy 600 HAZ in reactor coolant – low fluence irradiation up to 0.2 dpa	FAT-HWC	2.50	1.11
Alloy 600 in reactor coolant – low fluence irradiation up to 0.2 dpa	FAT-HWC	2.44	1.00

Fracture Resistance

Fracture resistance was evaluated for the Alloy 600 components used in BWR core internal applications. The expert panel scored all categories of FR in the high Knowledge, moderate Susceptibility grouping. The experts unanimously scored susceptibility at the lowest possible susceptibility, noting good field experience and lack of significant loading for these components as factors for the low scoring.

Table 9.64. Summary of FR scores for Alloy 600 in BWR environments

Material/Environment	Degradation Mode	Average Knowledge	Average Susceptibility
Alloy 600 in reactor coolant – no irradiation	FR	2.00	1.00
Alloy 600 in reactor coolant – low fluence irradiation up to 0.2 dpa	FR	2.00	1.00
Alloy 600 HAZ in reactor coolant – no irradiation	FR	2.11	1.00
Alloy 600 HAZ in reactor coolant – low fluence irradiation up to 0.2 dpa	FR	2.13	1.00

Stress Corrosion Cracking

SCC is a known issue for Alloy 600 in all forms. SCC has been observed in BWR service and is a known issue. The expert panel scored all categories of SCC in NWC environments in the high Knowledge, high Susceptibility grouping. However, all categories for Alloy 600 in HWC were ranked in the high Knowledge, moderate Susceptibility grouping, as the lower potential mitigates crack initiation and crack growth.

Table 9.65. Summary of SCC scores for Alloy 600 in BWR environments

Material/Environment	Degradation Mode	Average Knowledge	Average Susceptibility
Alloy 600 HAZ in reactor coolant – no irradiation	SCC	2.33	2.67
Alloy 600 HAZ in reactor coolant – low fluence irradiation up to 0.2 dpa	SCC	2.50	2.56
Alloy 600 in reactor coolant – no irradiation	SCC	2.44	2.11

Table 9.65. Summary of SCC scores for Alloy 600 in BWR environments (continued)

Material/Environment	Degradation Mode	Average Knowledge	Average Susceptibility
Alloy 600 in reactor coolant – low fluence irradiation up to 0.2 dpa	SCC	2.44	2.11
Alloy 600 HAZ in reactor coolant – no irradiation	SCC-HWC	2.33	1.78
Alloy 600 HAZ in reactor coolant – low fluence irradiation up to 0.2 dpa	SCC-HWC	2.25	1.78
Alloy 600 in reactor coolant – no irradiation	SCC-HWC	2.44	1.67
Alloy 600 in reactor coolant – low fluence irradiation up to 0.2 dpa	SCC-HWC	2.44	1.67

9.6.2.2 Alloy 182/82 Weldments in BWRs

The scores for the major degradation modes considered are summarized below. Additional details on individual scores by panelists, their comments and rationale, and parts and component numbers used in NUREG/CR-6923 are also shown in Appendix D.

No low-Knowledge categories were identified for Alloy182/82 in BWR environments. However, the panelists noted two areas for additional consideration, including:

- SCC was identified as a high Knowledge, high Susceptibility mode of degradation for Alloy 182/82 weldments in BWR NWC environments. This is a known issue for these alloys at high potential.

- Reduced fracture resistance in Alloy 182/82 welds at lower temperatures has been noted in laboratory testing although additional mechanistic understanding is needed.

Fatigue and Corrosion Fatigue

Fatigue and corrosion fatigue are known issues in reactor service. As service life increases, so does the total number of loading cycles experienced by a component. Further, power uprates may also increase cyclic loading and impact component lifetime. Three different alloy/environment categories were considered by the expert panel in NWC with another two categories evaluated for HWC environments. All were scored in the high Knowledge, moderate Susceptibility grouping with Susceptibility scores near 1 for all categories. As with PWR scoring for this alloy, the expert panelists noted that FAT damage is directly related to operational conditions and that changes in flow rates or other conditions due to power uprates may reduce useful life.

Table 9.66. Summary of FAT scores for Alloy 182/82 weldments in BWR environments

Material/Environment	Degradation Mode	Average Knowledge	Average Susceptibility
Alloy 82/182 welds in reactor coolant – no irradiation	FAT	2.44	1.22
Alloy 182 in reactor water – low fluence irradiation up to 0.2 dpa	FAT	2.30	1.11

Table 9.66. Summary of FAT scores for Alloy 182/82 weldments in BWR environments (continued)

Material/Environment	Degradation Mode	Average Knowledge	Average Susceptibility
Alloy 82/182 welds in reactor coolant steam	FAT	2.60	1.11
Alloy 82/182 welds in reactor coolant – no irradiation	FAT-HWC	2.44	1.22
Alloy 182 in reactor water – low fluence irradiation up to 0.2 dpa	FAT-HWC	2.4	1.11

Fracture Resistance

A decrease in fracture resistance was evaluated for the Alloy 182/82 weldments for extended service operations. The expert panel scored both categories of FR in the high Knowledge, moderate Susceptibility grouping. The experts noted that microstructural changes might occur over very long lifetimes although there is relatively little data and understanding of the mechanisms.

Table 9.67. Summary of FR scores for Alloy 182/82 weldments in BWR environments

Material/Environment	Degradation Mode	Average Knowledge	Average Susceptibility
Alloy 82/182 welds in reactor coolant – no irradiation	FR	2.00	1.38
Alloy 182 in reactor water – low fluence irradiation up to 0.2 dpa	FR	2.1	1.38
Alloy 82/182 welds in reactor coolant steam	FR	2.1	1.38

Stress Corrosion Cracking

As discussed above for Alloy 600, SCC is a known issue for Alloy 182/82 weldments, particularly in higher corrosion-potential environments like NWC and has been observed in BWR operation for particularly for Alloy 182 welds. The expert panel scored all categories of SCC in NWC environments in the high Knowledge, high Susceptibility grouping. However, all categories for Alloy 182/82 in HWC were ranked in the high Knowledge, moderate Susceptibility grouping as the lower potential mitigates crack initiation and crack growth, consistent with operating experience.

Table 9.68. Summary of SCC scores for Alloy 182/82 weldments in BWR environments

Material/Environment	Degradation Mode	Average Knowledge	Average Susceptibility
Alloy 182 in reactor water – low fluence irradiation up to 0.2 dpa	SCC	2.3	2.78
Alloy 82/182 welds in reactor coolant – no irradiation	SCC	2.56	2.56
Alloy 82/182 welds in reactor coolant steam	SCC	2.1	2.56
Alloy 182 in reactor water – low fluence irradiation up to 0.2 dpa	SCC-HWC	2.1	1.89
82/182 welds in reactor coolant – no irradiation	SCC-HWC	2.33	1.78

9.6.3 Summary of PIRT Findings for Alloy 600 and Alloy 182/82 Weldments

Nickel-base alloys and weld metals were chosen for LWR components because of low corrosion rate, resistance to SCC, and thermal expansion coefficient that is similar to that of low alloy RPV steel. PWR components include nozzles, piping, control rod drive feedthroughs, and steam generator tubing among others. BWR components containing Alloy 600 and Alloy 182 and 82 weld metals include RPV attachment welds, head bolts, feedwater nozzles, safe end butters, and supports.

As discussed above, no specific low Knowledge categories for Alloys 600 and 182/82 in BWR or PWR environments were identified via the PIRT scoring. However, the panelists noted two areas for additional consideration under extended operation, including:

- SCC was identified as a high Knowledge, high Susceptibility mode of degradation in all primary and secondary environments for Alloy 600 and 182/82 weldments. This is a known issue for these alloys.

- Wear was identified as a high Knowledge, high Susceptibility mode of degradation in secondary coolant environments for Alloy 600. This is a known form of degradation and is typically a result of design issues rather than specific material conditions. However, if conditions for wear develop, this material will be susceptible to this form of degradation, although this is not unique to extended operating periods.

- Reductions in fracture resistance in Alloy 182/82 welds at lower temperatures has been noted in laboratory testing although the mechanistic understanding is limited.

For BWR environments, similar trends were identified via the PIRT process:

- SCC was identified as a high Knowledge, high Susceptibility mode of degradation for Alloy 600 and Alloy 182/82 weldments in NWC environments. This is a known issue for these alloys at high potential.

- Reduced fracture resistance issues in Alloy 182/82 welds at lower temperatures have been noted in laboratory testing although the mechanistic understanding is limited.

9.7 SCORING SUMMARY FOR ALLOY 690 AND ALLOY 152/52 WELD METALS

As discussed in Chapter 4, wrought Alloy 690 and its associated weld metals (Alloys 152, 52, 52M, and other variants) have become the common replacement and repair materials for Alloy 600 and Alloy 182/82 weld metals with lower chromium content in PWRs, primarily due to their superior resistance to primary side SCC. The previous section described the PIRT findings for Alloy 600 and 182/82 weldments, which included SCC susceptibility in all water chemistries for both PWR and BWR use. Alloy 690 was selected as the replacement material for the nozzles; Alloys 152, 52, and 52M were used as associated welds. To date, Alloy 690 and its weld metals have not experienced significant degradation in service. On the contrary, successful performance of these alloys in PWRs has been noticed for about two decades as effective replacement materials for Alloys 600, 182, and 82 in PWRs. In addition, the high-Cr weld metals

have also been used extensively and without incident as a corrosion-resistant overlay for component repair.

In general, potential degradation modes of concern for Alloy 690 are similar to Alloy 600, including SCC, corrosion fatigue, and environment-induced fracture at high and low temperatures. The high-Cr weld metals encounter similar issues along with a susceptibility to ductility dip and hot cracking during welding plus significant dilution effects for dissimilar metal welds. Vulnerabilities to corrosion and cracking have only been identified in laboratory experiments, and typically during testing in off-normal material conditions and/or in severe environments.

As part of the EMDA activity, the expert panel scored 22 categories for Alloy 690 and 152/52 weldments in different PWR conditions. This section presents the results of the PIRT scoring for Alloy 690 and 152/52 weldment degradation modes. The section below is organized by reactor type and then degradation mode. This varies from the NUREG/CR-6923 activity where results were organized by reactor system. As discussed earlier, this PIRT is arranged differently from the NUREG/CR-6923 activity and direct comparisons for individual components are more difficult.

9.7.1 Alloy 690 and Alloy 152/52 Weldments in PWRs

Alloy 690 is an important material used in components in PWR systems, particularly as a replacement for Alloy 600. The scores for the major degradation modes considered are summarized below. Additional details on individual scores by panelists, their comments and rationale, and parts and component numbers used in NUREG/CR-6923 are also shown in Appendix E.

No significant knowledge gaps for Alloys 690 and Alloy 152/52 in PWR environments were identified, although good water chemistry must be maintained to minimize SCC, fatigue damage, and pitting.

9.7.1.1 Alloy 690 in PWRs

The scores for the major degradation modes of Alloy 690 and Alloy 152/52 weldments considered are summarized below. Additional details on individual scores by panelists, their comments and rationale, and parts and component numbers used in NUREG/CR-6923 are also shown in Appendix E.

No knowledge gaps were identified for Alloy 690 under subsequent operating periods in PWR environments following the PIRT scoring activity. The panelists did note that SCC, fatigue cracking, and pitting should be minimal for Alloy 690 in service, although good water chemistry must be maintained.

Fatigue and Corrosion Fatigue

Fatigue and corrosion fatigue are known issues in reactor service. As service life increases, so does the total number of loading cycles experienced by a component. Further, power uprates may also increase cyclic loading and impact component lifetime. The CUF must be evaluated for extended service. The expert panel considered five different alloy/environment categories and all were scored in the high Knowledge, moderate Susceptibility grouping. The panelists viewed

fatigue loading as inconsequential and a key factor in the scoring, although if operational conditions change, corrosion fatigue damage is possible.

Table 9.69. Summary of FAT scores for Alloy 690 in PWR environments

Material/Environment	Degradation Mode	Average Knowledge	Average Susceptibility
Alloy 690 TT in secondary coolant	FAT	2.33	1.22
Alloy 690 TT HAZ in secondary coolant	FAT	2.33	1.22
Alloy 690 TT forged components in primary reactor water	FAT	2.22	1.11
Alloy 690 TT tubes in primary reactor water	FAT	2.33	1.11
Alloy 690 TT HAZ in primary reactor	FAT	2.22	1.11

Pitting

Pitting can also occur for a variety of reasons. Both pitting categories for Alloy 690 in PWR were scored in the high Knowledge, moderate Susceptibility grouping with nearly identical scoring. The expert panelists noted that pitting damage is directly controlled by good water chemistry control. As long as water chemistry is maintained, particularly during shutdown, pitting damage is expected to be minimal in both the base alloy and HAZ.

Table 9.70. Summary of PIT scores for Alloy 690 in PWR environments

Material/Environment	Degradation Mode	Average Knowledge	Average Susceptibility
Alloy 690 TT HAZ in secondary coolant	PIT	2.38	1.25
Alloy 690 TT in secondary coolant	PIT	2.44	1.22

Stress Corrosion Cracking

SCC is a known issue for Alloy 690 in all its forms. SCC has not been observed to date in actual service, although it has been observed in some laboratory experiments. The expert panel scored Knowledge for SCC of Alloy 690 slightly lower than the other categories, but it is near 2.0 for all categories. All other SCC categories were scored in the high Knowledge, moderate Susceptibility grouping. The experts noted laboratory experiments demonstrating the effects of other species (e.g., Pb in particular) on SCC resistance, although water chemistry control should also be better because of knowledge of the potential issues with poor water chemistry control are recognized. The differences in scoring between Alloy 600 and Alloy 690 are consistent with expectations based on operating experience and the expert assessments described in Chapters 3 and 4 above.

Table 9.71. Summary of SCC scores for Alloy 690 in PWR environments

Material/Environment	Degradation Mode	Average Knowledge	Average Susceptibility
Alloy 690 TT in secondary coolant	SCC	1.89	1.78
Alloy 690 TT HAZ in secondary coolant	SCC	2.00	1.56
Alloy 690 TT HAZ in primary reactor water	SCC	2.22	1.44
Alloy 690 TT forged components in primary reactor water	SCC	2.00	1.33
Alloy 690 TT tubes in primary reactor water	SCC	2.00	1.33

Wear

Wear was considered for Alloy 690 tubes on the secondary coolant side of the steam generators. Alloy 690 TT was scored in the high Knowledge, moderate Susceptibility grouping. The expert panel noted that wear is typically a result of design issues rather than specific material conditions. However, if conditions for wear develop, this material will be susceptible to this form of degradation.

Table 9.72. Summary of WEAR scores for Alloy 690 in PWR environments

Material/Environment	Degradation Mode	Average Knowledge	Average Susceptibility
Alloy 690 TT HAZ in secondary coolant	WEAR	2.44	1.78
Alloy 690 TT in secondary coolant	WEAR	2.44	1.67

9.7.1.2 Alloy 152/52 Weldments in PWRs

The scores for the major degradation modes for Alloy 152/52 weldments considered are summarized below. Additional details on individual scores by panelists, their comments and rationale, and parts and component numbers used in NUREG/CR-6923 are also shown in Appendix E.

No potential gaps for Alloy 152/52 in PWR environments were identified via the PIRT process.

Fatigue and Corrosion Fatigue

Fatigue was evaluated for Alloy 152/52 weldments in several categories. Like Alloy 690 above, corrosion fatigue damage for Alloy 152/52 weldments were scored in the high Knowledge, moderate Susceptibility grouping. The panelists viewed fatigue loading as inconsequential and a key factor in the scoring, although if operational conditions change, corrosion fatigue damage is possible.

Table 9.73. Summary of FAT scores for Alloy 152/52 weldments in PWR environments

Material/Environment	Degradation Mode	Average Knowledge	Average Susceptibility
Alloy 52/152 weldments in primary reactor water	FAT	2.22	1.11
Alloy 52/152 weldments in borated demin water	FAT	2.11	1.11

Fracture Resistance

Fracture resistance was evaluated for the 152/52 weldments for extended service operations. The expert panel scored both categories of FR with virtually the same scores. The difference in knowledge listed in Table 9.74 is not statistically significant. The experts noted that fracture resistance should not be an issue at the temperatures considered.

Table 9.74. Summary of FR scores for Alloy 152/52 weldments in PWR environments

Material/Environment	Degradation Mode	Average Knowledge	Average Susceptibility
Alloy 52/152 weldments in borated demin water	FR	1.89	1.00
Alloy 52/152 weldments in primary reactor water	FR	2.00	1.11

Stress Corrosion Cracking

As indicated for Alloy 690, SCC has not been observed to date in actual service, but it has been documented for cold-worked materials in some laboratory experiments. The expert panel scored SCC of Alloy 152/52 weldments in the high Knowledge, moderate Susceptibility grouping. The average knowledge and Susceptibility scores were very similar to the data for Alloy 690, as well as the rationale for scoring given by the expert panelists. The panelists did note that the database is more limited than for Alloy182/82, but this is not surprising given the difference in time in operating experience.

Table 9.75. Summary of SCC scores for Alloy 152/52 weldments in PWR environments

Material/Environment	Degradation Mode	Average Knowledge	Average Susceptibility
Alloy 52/152 weldments in primary reactor water	SCC	2.00	1.44
Alloy 52/152 weldments on external surfaces	SCC	2.22	1.11
Alloy 52/152 weldments in borated demin water	SCC	2.00	1.00

9.7.2 Summary of PIRT Findings for Alloy 690 and Alloy 152/52 Weldments

Wrought Alloy 690 and its associated weld metals (Alloys 152, 52, 52M, and other variants) have become the common replacement and repair materials for Alloy 600 and Alloy 182/82 weld metals, primarily due to their superior resistance to primary side SCC. During the PIRT process, the expert panel considered 22 different alloy/environment categories. No knowledge gaps were identified for Alloy 690 or Alloy 152/52 weldments under subsequent operating periods in PWR environments via the PIRT process. The panelists did note that SCC, fatigue cracking, and pitting should be minimal for Alloy 690, although good secondary-side water chemistry must be maintained. The differences in scoring and knowledge gaps identified between Alloy 600 and Alloy 690 are consistent with expectations based on operating experience. Indeed, this improved resistance to corrosion and SCC is a driving factor in replacement of Alloy 600 with Alloy 690.

9.8 SCORING SUMMARY FOR CARBON AND LOW ALLOY STEELS

Carbon and low alloy steels serve in a variety of locations within the LWR fleet. These ductile structural materials are used in pressure boundary components, such as pressure vessels and piping in the RCS, ECCS, secondary water, and service water systems of LWRs. These alloys are used due to their relatively low cost, good mechanical properties in thick sections, and excellent weldability. In reactor coolant system components, such as the pressure vessel, pressurizer, and some piping, the carbon and low alloy steels are clad on the inside wetted surface with corrosion-resistant materials such as austenitic stainless steels or nickel-base alloys.

These steels are used in the reactor in a variety of forms, including seamless piping, forgings, castings, plate, and bolting. The specific carbon or low alloy steel/component combinations that are used in a particular reactor vary among reactor designs and manufacturers, but, in general, the reactor components include the reactor pressure vessel, top and bottom heads, steam generator shells, steam generator tube sheets, steam generator channel heads, pressurizer shells in PWRs, and a variety of piping applications.

A number of key aging and degradation issues are possible for these components. Carbon and low alloy steels are susceptible to irradiation damage, even at low fluence. These materials are also susceptible to fatigue damage, pitting, flow-accelerated corrosion, and MIC in some piping and water chemistry environments. These alloys are also highly susceptible to BAC in the event of PWR primary-side leaks.

As part of the EMDA activity, the expert panel scored 364 categories for different grades of carbon and low alloy steels (95 for PWRs and 269 for BWRs).

This section presents the results of the PIRT scoring for carbon and low alloy steels. The section below is organized by reactor type and then degradation mode. This varies from the NUREG/CR-6923 activity where results were organized by reactor system. However, as discussed above, the PIRT was arranged differently for this activity, and direct comparisons for individual components are more difficult. The detailed scores and comments for each panelist for all categories are shown in Appendices F and G, including links to the components scored in NUREG/CR-6923. It is important to note that irradiation effects for these alloys are considered in the EMDA volume on RPV degradation. More details on this form of degradation can be found there.

9.8.1 Carbon and Low Alloy Steels in PWRs

Carbon and low alloy steels are critical materials for PWR reactors. These steels are used for the reactor pressure vessel including the top and bottom sections. In addition, these alloys are used as steam generator shells, steam generator tube sheets, and steam generator channel heads. The pressurizer shells are generally made of low alloy steels with stainless steel cladding (see previous sections on 308/309 SS cladding). Reactor coolant piping for PWR primary circuits may be seamless carbon steel with, in some designs, austenitic stainless steel cladding.

The scores for the major degradation modes considered are summarized below. Additional details on individual scores by panelists, their comments and rationale, and parts and component numbers used in NUREG/CR-6923 are also shown in Appendix F.

No significant knowledge gaps were identified for carbon and low alloy steels in PWR environments following analysis of the PIRT scoring. However, several trends and common themes were identified by the expert panel, including:

- Carbon and low alloy steels are highly susceptible to BAC of carbon steel in the event of a leak of primary coolant, regardless if this occurs in current or future operating periods. This is a well-known form of degradation.

- Crevice corrosion, pitting, MIC, and general corrosion of carbon steel and low alloy steel were identified as high-knowledge modes of degradation, but only in the event of loss of water chemistry control or failure of protective features such as liners or cathodic protection. These are well-known forms of degradation.

- Flow-accelerated corrosion is a well-known form of degradation for low alloy and carbon steels, but can be exacerbated in elbows; changing water chemistry and flow conditions as well as longer service life and exposure to FAC conditions may increase susceptibility.

- Stress corrosion cracking and fatigue are possible for these alloys, but unlikely in service. Changes in loading or increases in chemical conditions (such as chloride content) may drive increased susceptibility over a long operating period.

9.8.1.1 Carbon Steels in PWRs

The PIRT scores for the major degradation modes for carbon steels are summarized below. Additional details on individual scores by panelists, their comments and rationale, and parts and component numbers used in NUREG/CR-6923 are also shown in Appendix F. Carbon steels are used in a variety of environments and applications. As noted above, irradiation effects for these alloys are considered in the EMDA volume on RPV degradation.

Several trends for carbon steels in PWR environments were identified via the PIRT process:

- BAC of carbon steel was identified as a high Knowledge, high Susceptibility mode of degradation, but only in the event of a leak of primary coolant. This is a well-known form of degradation.

- Crevice corrosion, pitting, MIC, and general corrosion of carbon steel were identified as high Knowledge, high Susceptibility modes of degradation, but only in the event of a breach of the liner material or loss of water chemistry control. These are well-known forms of degradation.

- Three categories (saturated steam, demineralized water, and saturated water) scored in the high Knowledge, high Susceptibility grouping for flow-accelerated corrosion. This form of degradation is well known, but can be exacerbated in elbows; changing water chemistry and flow conditions as well as longer service life and exposure to FAC conditions may increase susceptibility.

- Stress corrosion cracking and fatigue are possible for these alloys, but unlikely in service. Changes in loading or increases in chemical conditions (such as chloride content) may result in increased susceptibility over a long operating period.

Boric Acid Corrosion

Carbon and low alloy steels are highly susceptible to BAC, although these steels are clad with stainless steel to avoid these conditions. However, in the event of a leak, BAC can occur in

carbon and low alloy steels if boric acid is leaking from the PWR primary pressure boundary. This has been observed in multiple power plants in recent years. The expert panel considered BAC in the event of a leak, which is different than normal operating conditions. In this scenario, carbon and low alloy steels were placed in the high Knowledge, high Susceptibility grouping based on past experience. External surfaces in high temperature air were also considered. The expert panel scored this category as a high Knowledge, moderate Susceptibility, but noted this form of degradation is only possible in the presence of boric acid.

Table 9.76. Summary of BAC scores for carbon and low alloy steels in PWR environments

Material/Environment	Degradation Mode	Average Knowledge	Average Susceptibility
Carbon and low alloy steel – external surfaces in high temperature air, in event of leak	BAC	2.33	2.33
Carbon steel, welds, and HAZ – external surfaces in high temperature air	BAC	2.56	1.56

Crevice Corrosion

Crevice corrosion of carbon steels has been observed in service and can occur for a variety of reasons. The expert panel scored this form of degradation in ten different environments. Crevice corrosion in salt water, secondary coolant, and pond water was scored in the high Knowledge, high Susceptibility grouping, although this requires a break in the lining of the piping to be a serious issue. All other categories were found to be of lower susceptibility.

Table 9.77. Summary of CREV scores for carbon steels, weldments, and HAZ in PWR environments

Material/Environment	Degradation Mode	Average Knowledge	Average Susceptibility
Carbon steel, welds, and HAZ in salt water	CREV	2.67	2.33
Carbon steel and weldments in secondary coolant	CREV	2.78	2.33
Carbon steel, welds, and HAZ in pond water	CREV	2.67	2.00
Carbon steels in treated, stagnant surge water	CREV	2.56	1.44
Cast carbon steel components in treated stagnant surge water	CREV	2.56	1.33
Carbon steel and weldments in treated heat exchanger water	CREV	2.56	1.33
Carbon steel, welds, and HAZ in condensate water	CREV	2.67	1.22
Carbon steel in spent fuel pool cooling water	CREV	2.67	1.22
Carbon and low steel in air at ambient conditions	CREV	2.56	1.22
Carbon steel and weldments in main steam feed water	CREV	2.67	1.11

Flow-Accelerated Corrosion

Flow-accelerated corrosion is an important form of degradation for carbon and low alloy steels. High-profile incidents of FAC at Surry and Mihama have led to a greater understanding and monitoring of FAC in service. Flow-accelerated corrosion in carbon steels is highly dependent on water chemistry and flow-rate conditions. The expert panelists scored nine categories of FAC for

carbon steel and weldments. Three categories (saturated steam, demineralized water, and saturated water) scored in the high Knowledge, high Susceptibility grouping. This form of degradation is well known, but can be exacerbated in elbows and from changing water chemistry and flow conditions. All other categories were found to be of lower susceptibility, although longer service life and exposure to FAC conditions may increase susceptibility.

Table 9.78. Summary of FAC scores for carbon steels, weldments, and HAZ in PWR environments

Material/Environment	Degradation Mode	Average Knowledge	Average Susceptibility
Carbon steel and weldments in saturated steam	FAC	2.56	2.56
Carbon steel and weldments in demineralized water	FAC	2.78	2.33
Carbon steel in saturated water from steam generator	FAC	2.67	2.33
Carbon steel and weldments in secondary coolant	FAC	2.33	1.67
Carbon steel and weldments in treated heat exchanger water	FAC	2.44	1.22
Carbon steel in spent fuel pool cooling water	FAC	2.78	1.11
Carbon steel, welds, and HAZ in pond water	FAC	2.56	1.11
Carbon steels in treated, stagnant surge water	FAC	2.67	1.00
Cast carbon steel components in treated stagnant surge water	FAC	2.56	0.89

Fatigue and Corrosion Fatigue

Fatigue and corrosion fatigue have been observed in service for carbon steels in specific situations. As service life increases, so does the total number of loading cycles experienced by a component. All 17 categories for carbon steel corrosion fatigue were scored in the high Knowledge, moderate Susceptibility grouping. The panelists viewed fatigue loading as inconsequential, although if operational conditions over extended service change, corrosion fatigue damage is possible.

Table 9.79. Summary of FAT scores for carbon steels, weldments, and HAZ in PWR environments

Material/Environment	Degradation Mode	Average Knowledge	Average Susceptibility
Carbon steel and weldments in demineralized water	FAT	2.44	1.89
Carbon steel weldments in treated heat exchanger water	FAT	2.22	1.89
Carbon steel in saturated water from steam generator	FAT	2.44	1.89
Carbon steel weldments in treated, stagnant surge water	FAT	2.33	1.67
Carbon steel and weldments in saturated steam	FAT	2.44	1.56
Carbon steel, welds, and HAZ in condensate water	FAT	2.78	1.44

Table 9.79. Summary of FAT scores for carbon steels, weldments, and HAZ in PWR environments (continued)

Material/Environment	Degradation Mode	Average Knowledge	Average Susceptibility
Carbon steels in treated, stagnant surge water	FAT	2.67	1.33

Carbon steel and weldments in treated heat exchanger water	FAT	2.56	1.33
Carbon steel and weldments in main steam feed water	FAT	2.44	1.11
Cast carbon steel components in treated stagnant surge water	FAT	2.56	1.11
Carbon steel in spent fuel pool cooling water	FAT	2.56	1.11
Carbon steel, welds, and HAZ in pond water	FAT	2.44	1.11
Carbon steel, welds, and HAZ – buried external surfaces	FAT	2.78	1.11
Carbon and low alloy steel – external surfaces in high temperature air, in event of leak	FAT	2.56	1.11
Carbon steel, welds, and HAZ – external surfaces in high temperature air	FAT	2.67	1.11
Carbon and low steel in air at ambient conditions	FAT	2.67	1.11
Carbon steel and weldments in secondary coolant	FR	2.11	1.11

General Corrosion

General corrosion has been observed in operation in carbon steels and can occur for a variety of reasons. The expert panel scored this form of degradation in eight different environments. General corrosion in pond water and buried external surfaces were scored in the high Knowledge, high Susceptibility grouping. The panelists noted that corrosion susceptibility is strongly affected by oxygen concentration, temperature, and pH, (which could be unfavorable in pond water). External buried surfaces should also be resistant to general corrosion, provided the cathodic protection systems are functioning as designed. All other categories were found to be of lower susceptibility.

Table 9.80. Summary of GC scores for carbon steels, weldments, and HAZ in PWR environments

Material/Environment	Degradation Mode	Average Knowledge	Average Susceptibility
Carbon steel, welds, and HAZ in pond water	GC	2.67	2.11
Carbon steel, welds, and HAZ – buried external surfaces	GC	2.78	2.11
Carbon steels in treated, stagnant surge water	GC	2.44	1.44
Cast carbon steel components in treated stagnant surge water	GC	2.44	1.44
Carbon steel in spent fuel pool cooling water	GC	2.56	1.33
Carbon steel and weldments in treated heat exchanger water	GC	2.56	1.33
Carbon and low steel in air at ambient conditions	GC	2.56	1.22
Carbon steel and weldments in main steam feed water	GC	2.78	1.11

Microbially Induced Corrosion

Microbially induced corrosion can occur for a variety of reasons in service and has been observed in operation. The expert panel scored this form of degradation in 12 different environments. MIC in pond water, salt water, and buried external surfaces were scored in the high Knowledge, high

Susceptibility grouping. The panelists noted that MIC could be extensive in raw pond water. As above for general and crevice corrosion, MIC in salt and on external buried surfaces should also be minimal, provided piping liners and the cathodic protection systems, respectively, are functioning as designed. All other categories were found to be of lower susceptibility, but the panel again noted that this is dependent upon the water being properly treated.

Table 9.81. Summary of MIC scores for carbon steels, weldments, and HAZ in PWR environments

Material/Environment	Degradation Mode	Average Knowledge	Average Susceptibility
Carbon steel, welds, and HAZ in pond water	MIC	2.67	2.44
Carbon steel, welds, and HAZ in salt water	MIC	2.44	2.33
Carbon steel, welds, and HAZ – buried external surfaces	MIC	2.44	2.13
Carbon steel, welds, and HAZ in condensate water	MIC	2.25	1.88
Carbon steel and weldments in demineralized water at lower temperatures	MIC	2.22	1.50
Carbon steels in treated, stagnant surge water	MIC	2.33	1.50
Cast carbon steel components in treated stagnant surge water	MIC	2.44	1.38
Carbon and low steel in air at ambient conditions	MIC	2.44	1.38
Carbon steel and weldments in treated heat exchanger water	MIC	2.56	1.25
Carbon steel in spent fuel pool cooling water	MIC	2.33	1.13
Carbon steel and weldments in main steam feed water	MIC	2.75	1.00
Carbon steel, welds, and HAZ – external surfaces in high temperature air	MIC	2.44	1.00

Pitting

Pitting of carbon steels can occur for a variety of reasons and has been observed in service. The expert panel scored this form of degradation in 13 different environments. Pitting corrosion in pond water, salt water, and buried external surfaces were scored in the high Knowledge, high Susceptibility grouping. As noted above for crevice corrosion, general corrosion, and MIC, pitting in salt and on external buried surfaces should also be minimal, provided piping liners and the cathodic protection systems, respectively, are functioning as designed. All other categories were found to be of lower susceptibility, but the panel again noted that this is dependent upon the water being properly treated.

Table 9.82. Summary of PIT scores carbon steels, weldments, and HAZ in PWR environments

Material/Environment	Degradation Mode	Average Knowledge	Average Susceptibility
Carbon steel, welds, and HAZ in pond water	PIT	2.67	2.33
Carbon steel, welds, and HAZ in salt water	PIT	2.78	2.33
Carbon steel, welds, and HAZ – buried external surfaces	PIT	2.88	2.13
Carbon steel and weldments in demineralized water at lower temperatures	PIT	2.67	1.56
Carbon Steel, welds, and HAZ in condensate water	PIT	2.67	1.56
Carbon steel and weldments in treated heat exchanger water	PIT	2.44	1.56
Carbon steels in treated, stagnant surge water	PIT	2.56	1.44
Cast carbon steel components in treated stagnant surge water	PIT	2.67	1.33
Carbon steel and weldments in main steam feed water	PIT	2.78	1.22
Carbon steel in spent fuel pool cooling water	PIT	2.67	1.22
Carbon steel, welds, and HAZ – external surfaces in high temperature air	PIT	2.44	1.22
Carbon and low alloy steel in air at ambient conditions	PIT	2.56	1.22
Carbon and low alloy steel – external surfaces in high temperature air, in event of leak	PIT	2.33	1.11

Stress Corrosion Cracking

Extended service will result in increased time under temperature while exposed to the high temperature water environment and under stress. The expert panel considered 16 different categories of SCC for carbon steels in PWR environments. All categories were ranked in the high Knowledge, moderate Susceptibility grouping. In most categories, the panel noted that SCC should not be an issue if good water chemistry and protective features (e.g., lining or cathodic protection) are being utilized. SCC is possible for these alloys, but unlikely in service. Changes in loading or increases in chemical conditions (such as chloride content) may drive increased susceptibility over a long operating period.

Table 9.83. Summary of SCC scores for carbon steels, weldments, and HAZ in PWR environments

Material/Environment	Degradation Mode	Average Knowledge	Average Susceptibility
Carbon steel, welds, and HAZ – buried external surfaces	SCC	2.33	1.67
Carbon steel and weldments in demineralized water	SCC	2.11	1.56
Carbon steel in saturated water from steam generator	SCC	2.11	1.56
Carbon steel and weldments in main steam feed water	SCC	2.44	1.44
Carbon steel and weldments in treated heat exchanger water	SCC	2.44	1.44
Carbon steel and weldments in saturated steam	SCC	2.22	1.44
Carbon steel, welds, and HAZ in pond water	SCC	2.44	1.33

Table 9.83. Summary of SCC scores for carbon steels, weldments, and HAZ in PWR environments (continued

Material/Environment	Degradation Mode	Average Knowledge	Average Susceptibility
Carbon and low alloy steel – external surfaces in high temperature air, in event of leak	SCC	2.44	1.33
Carbon steel in spent fuel pool cooling water	SCC	2.56	1.22
Carbon steel, welds, and HAZ – external surfaces in high temperature air	SCC	2.56	1.22
Carbon steel and weldments in demineralized water at lower temperatures	SCC	2.67	1.11
Carbon steel, welds, and HAZ in condensate water	SCC	2.33	1.11
Carbon steels in treated, stagnant surge water	SCC	2.56	1.11
Cast carbon steel components in treated stagnant surge water	SCC	2.67	1.11
Carbon steel and weldments in secondary coolant	SCC	2.11	1.11
Carbon and low steel in air at ambient conditions	SCC	2.56	1.00

9.8.1.2 Low Alloy Steels in PWRs

The PIRT scores for the major degradation modes for low alloy steels are summarized below. Some generic categories were scored and listed in the above tables along with carbon steels due to their similar response. Additional categories were scored specifically for low alloy steels. Additional details on individual scores by panelists, their comments and rationale, and parts and component numbers used in NUREG/CR-6923 are also shown in Appendix F. Low alloy steels are used in a variety of environments and applications. As noted above, irradiation effects for these alloys are considered in the EMDA volume on RPV degradation. More details on this form of degradation can be found there.

Several trends for low alloy steels in PWR environments were identified via the PIRT process:

- BAC of low alloy steel was identified as a high Knowledge, high Susceptibility mode of degradation, but only in the event of a leak of primary coolant. This is a well-known form of degradation.

- Crevice corrosion, pitting, and FAC of low alloy steel were identified as high Knowledge, moderate Susceptibility modes of degradation, but only in the event of a loss of water chemistry control. These are well-known forms of degradation.

- Stress corrosion cracking and fatigue are possible for these alloys, but unlikely in service. Changes in loading or increases in chemical conditions may drive increased susceptibility over a long operating period.

Boric Acid Corrosion

Low alloy steels are highly susceptible to BAC should a leak of primary coolant occur. This has been observed in multiple power plants in recent years. The expert panel considered BAC in the event of a leak, which is different than normal operating conditions. In this scenario, carbon and

low alloy steels were placed in the high Knowledge, high Susceptibility grouping based on past experience.

Table 9.84. Summary of BAC scores for low alloy steels in PWR environments

Material/Environment	Degradation Mode	Average Knowledge	Average Susceptibility
Low alloy steel in primary water	BAC	2.56	2.22

Crevice Corrosion

The expert panel scored crevice corrosion in a single category resulting in a high Knowledge, moderate Susceptibility ranking. However, the panel noted there should not be crevice corrosion in a low-oxygen, low corrosion-potential environment.

Table 9.85. Summary of CREV scores for low alloy steels in PWR environments

Material/Environment	Degradation Mode	Average Knowledge	Average Susceptibility
Low alloy steel in primary water	CREV	2.44	1.11

Flow-Accelerated Corrosion

Flow-accelerated corrosion in low alloy steels is highly dependent on water chemistry and flow-rate conditions. The expert panel considered two categories of FAC for low alloy steels. Both were ranked in the high Knowledge, moderate Susceptibility grouping. This form of degradation is well known, but can be exacerbated in elbows and by changing water chemistry and flow conditions.

Table 9.86. Summary of FAC scores for low alloy steels in PWR environments

Material/Environment	Degradation Mode	Average Knowledge	Average Susceptibility
Low alloy steel in saturated steam	FAC	2.56	1.78
Low alloy steel in primary water	FAC	2.44	1.33

Fatigue and Corrosion Fatigue

Fatigue and corrosion fatigue for low alloy steels were scored in the high Knowledge, moderate Susceptibility grouping. The panelists viewed fatigue loading as inconsequential, although if operational conditions over extended service change, corrosion fatigue damage is possible.

Table 9.87. Summary of FAT scores for low alloy steels in PWR environments

Material/Environment	Degradation Mode	Average Knowledge	Average Susceptibility
Low alloy steel in primary water	FAT	2.56	1.11

Pitting

The expert panel scored this form of degradation in a single category for low alloy steels. Like crevice corrosion above, pitting was scored in the high Knowledge, moderate Susceptibility grouping, although the panel noted there should not be pitting in a low-oxygen, low corrosion-potential environment.

Table 9.88. Summary of PIT scores for low alloy steels in PWR environments

Material/Environment	Degradation Mode	Average Knowledge	Average Susceptibility
Low alloy steel in primary water	PIT	2.33	1.11

Stress Corrosion Cracking

Extended service will result in increased time of exposure to the high-temperature water environment and under stress, increasing the potential factors for SCC degradation. The expert panel considered two different categories of SCC for low alloy steels in PWR environments. All categories were ranked in the high Knowledge, moderate Susceptibility grouping. As with carbon steels, the panel noted that SCC should not be an issue if good water chemistry is maintained. SCC is possible for these alloys, but unlikely in service. Changes in loading or increases in chemical conditions (such as chloride content) may drive increased susceptibility over a long operating period.

Table 9.89. Summary of SCC scores for low alloy steels in PWR environments

Material/Environment	Degradation Mode	Average Knowledge	Average Susceptibility
Low alloy steel in saturated steam	SCC	2.11	1.33
Low alloy steel in primary water	SCC	2.44	1.22

9.8.2 Carbon and Low Alloy Steels in BWRs

Carbon and low alloy steels are used in critical BWR components, including the vertical, top, and bottom sections of the reactor pressure vessel. The recirculation piping in BWRs is usually stainless steel (Types 304 SS, 316 SS, 304L SS, 316L SS), although A333 Gr 6 carbon steel piping without cladding may be used in the main steam and the feedwater lines. The piping in the lower-temperature emergency core cooling and auxiliary/support systems is usually seamless A105 or A106 Gr B carbon steel.

The scores for the major degradation modes considered are summarized below. Additional details on individual scores by panelists, their comments and rationale, and parts and component numbers used in NUREG/CR-6923 are also shown in Appendix G.

No significant knowledge gaps were identified for carbon and low alloy steels in PWR environments following analysis of the PIRT scoring. However, several trends and common themes were identified:

- Crevice corrosion, pitting, MIC, and general corrosion of carbon steel and low alloy steel were identified as high Knowledge modes of degradation, occurring only in the event of loss of water chemistry control.

- Flow-accelerated corrosion is a well-known form of degradation for low alloy and carbon steels, but can be exacerbated in elbows; changing water chemistry and flow conditions. Longer service life and continued exposure to FAC conditions may increase susceptibility.

- Stress corrosion cracking and fatigue are possible for these alloys, but unlikely in service. Changes in loading or increases in chemical conditions (such as chloride content) may drive increased susceptibility over a long operating period.

9.8.2.1 Carbon Steels in BWRs

The PIRT scores for the major degradation modes for carbon steels are summarized below. Additional details on individual scores by panelists, their comments and rationale, and parts and component numbers used in NUREG/CR-6923 are also shown in Appendix G. Carbon steels are used in a variety of environments and applications. As noted above, irradiation effects for these alloys are considered in the EMDA volume on RPV degradation. More details on this form of degradation can be found there.

Several trends for carbon steels in BWR environments were identified via the PIRT process:

- Crevice corrosion, pitting, MIC, and general corrosion of carbon steel were identified as high Knowledge, moderate Susceptibility modes of degradation for almost all cases considered. These are well-known forms of degradation, and susceptibility is mitigated with good water chemistry control.

- Several categories scored in the high Knowledge, high Susceptibility grouping for flow-accelerated corrosion. This form of degradation is well known, but can be exacerbated in elbows; changing water chemistry and flow conditions as well as longer service life and exposure to FAC conditions may increase susceptibility. Predictive models based on empirical observation or mechanistic understanding have been developed in the United States, Europe, and Japan.

- Stress corrosion cracking and fatigue are possible for these alloys, but is relatively rare in service. The reasons for this rarity are reasonably well understood and are discussed in some detail in Chapter 5. Changes in loading or increases in water chemistry conditions (such as chloride content) may drive increased susceptibility over a long operating period. Further aspects needing confirmation are synergistic effects between SCC susceptibility and other degradation modes associated with irradiation hardening and embrittlement, temper embrittlement and dynamic strain aging, which may dominate over long term operation.

Crevice Corrosion

Crevice corrosion has been observed in service for carbon steels in this environment and can occur for a variety of reasons. The expert panel scored this form of degradation in 32 different environments. As shown in Table 9.90, 10 of those modes were scored in the high Knowledge, high Susceptibility grouping, although it should be noted that the average Susceptibility score is not significantly different than the other 22 categories. All other categories were found to be of

lower susceptibility. The panelists noted that susceptibility to crevice corrosion could increase due to a loss of water chemistry control, specifically for higher oxygen concentrations.

Table 9.90. Summary of CREV scores for carbon steels, weldments, and HAZ in BWR environments

Material/Environment	Degradation Mode	Average Knowledge	Average Susceptibility
Carbon steel in suppression/storage pool water	CREV	2.78	2.11
Carbon steel weldments in suppression/storage pool water	CREV	2.78	2.11
Carbon steel HAZ in suppression/storage pool water	CREV	2.78	2.11
Carbon steel in stagnant suppression pool water	CREV	2.78	2.11
Carbon steel weldments in stagnant suppression pool water	CREV	2.78	2.11
Carbon steel HAZ in stagnant suppression pool water	CREV	2.78	2.11
Carbon steel in condensate storage water	CREV	2.78	2.00
Carbon steel weldments in condensate storage water	CREV	2.78	2.00
Carbon steel HAZ in condensate storage water	CREV	2.78	2.00
Carbon steel in drywell environment	CREV	2.78	2.00
Carbon steel in stagnant reactor water at lower temperature	CREV	2.67	1.89
Carbon steel weldments in stagnant reactor water at lower temperature	CREV	2.67	1.89
Carbon steel HAZ in stagnant reactor water at lower temperature	CREV	2.67	1.89
Carbon steel weldments in drywell environment	CREV	2.78	1.89
Carbon steel HAZ in drywell environment	CREV	2.78	1.89
Carbon steel in treated service water	CREV	2.78	1.89
Carbon steel in stagnant reactor water	CREV	2.78	1.67
Carbon steel weldments in stagnant reactor water	CREV	2.78	1.67
Carbon steel HAZ in stagnant reactor water	CREV	2.78	1.67
Carbon steel in lower temperature reactor water	CREV	2.56	1.56
Carbon steel weldments in lower temperature reactor water	CREV	2.56	1.56
Carbon steel HAZ in lower temperature reactor water	CREV	2.56	1.56
Carbon steel HAZ in feedwater	CREV	2.78	1.44
Carbon steel in stagnant wet steam	CREV	2.78	1.33
Carbon steel HAZ in stagnant wet steam	CREV	2.78	1.33
Carbon steel in reactor cleanup water	CREV	2.78	1.33
Carbon steel weldments in reactor cleanup water	CREV	2.78	1.33
Carbon steel in feedwater	CREV	2.78	1.33
Carbon steel weldments in feedwater	CREV	2.78	1.33

Table 9.90. Summary of CREV scores for carbon steels, weldments, and HAZ in BWR environments (continued)

Material/Environment	Degradation Mode	Average Knowledge	Average Susceptibility
Carbon steel weldments in stagnant wet steam	CREV	2.75	1.25
Carbon steel in stagnant steam condensate	CREV	2.78	1.22
Carbon steel external surfaces in high temperature air	CREV	2.78	1.11

Flow-Accelerated Corrosion

The expert panelists scored six categories of FAC for carbon steel and weldments. Three categories in lower temperature reactor water were scored in the high Knowledge, high Susceptibility grouping. However, it should be noted that the average Susceptibility score is not significantly different than the other 22 categories. This form of degradation is well known, but can be exacerbated in elbows and by changing water chemistry and flow conditions. All other categories were found to be of lower susceptibility, although longer service life and exposure to continuing FAC conditions may increase susceptibility.

Table 9.91. Summary of FAC scores for carbon steels, weldments, and HAZ in BWR environments

Material/Environment	Degradation Mode	Average Knowledge	Average Susceptibility
Carbon steel in lower temperature reactor water	FAC	2.56	2.22
Carbon steel weldments in lower temperature reactor water	FAC	2.56	2.11
Carbon steel HAZ in lower temperature reactor water	FAC	2.56	2.11
Carbon steel in feedwater	FAC	2.78	1.33
Carbon steel weldments in feedwater	FAC	2.78	1.22
Carbon steel HAZ in feedwater	FAC	2.78	1.22

Fatigue and Corrosion Fatigue

Fatigue and corrosion fatigue for carbon steel, weldments, and HAZ were considered for a wide variety of environmental conditions in BWR service. In total, 56 categories for carbon steel FAT were scored. Five were ranked in the high Knowledge, high Susceptibility grouping. As mentioned above, it should be noted that the average Susceptibility score is not significantly different than that for the rest of the categories. The panelists viewed fatigue loading as inconsequential, although if operational conditions over extended service change, corrosion fatigue damage is possible.

Table 9.92. Summary of FAT scores for carbon steels, weldments, and HAZ in BWR environments

Material/Environment	Degradation Mode	Average Knowledge	Average Susceptibility
Carbon and carbon steel weldolets and sockolets in lower temperature reactor water	FAT	2.11	2.22
Carbon weldolet steel in feedwater	FAT	2.67	2.22
Carbon and carbon steel weldolets and sockolets in reactor water	FAT	2.44	2.11
Carbon steel weldolet in stagnant wet steam	FAT	2.44	2.00
Carbon steel weldolet in drywell environment	FAT	2.22	2.00
Carbon steel in stagnant wet steam	FAT	2.56	1.89
Carbon steel weldolet in condensate storage water	FAT	2.33	1.89
Carbon steel weldments in stagnant wet steam	FAT	2.56	1.78
Carbon steel HAZ in stagnant wet steam	FAT	2.56	1.78
Carbon steel weldolet in stagnant suppression pool water	FAT	2.22	1.78
Carbon steel weldolet in suppression/storage pool water	FAT	2.22	1.67
Carbon steel in stagnant steam condensate	FAT	2.78	1.56
Carbon steel in reactor coolant	FAT	2.78	1.44
Carbon steel weldments in reactor coolant	FAT	2.78	1.44
Carbon steel HAZ in reactor coolant	FAT	2.78	1.44
Carbon steel weldments in reactor cleanup water	FAT	2.78	1.33
Carbon steel weldments in feedwater	FAT	2.67	1.33
Carbon steel HAZ in feedwater	FAT	2.78	1.33
Carbon steel in lower temperature reactor water	FAT	2.67	1.22
Carbon steel weldments in lower temperature reactor water	FAT	2.67	1.22
Carbon steel HAZ in lower temperature reactor water	FAT	2.67	1.22
Carbon steel in stagnant reactor water	FAT	2.78	1.22
Carbon steel weldments in stagnant reactor water	FAT	2.78	1.22
Carbon steel HAZ in stagnant reactor water	FAT	2.78	1.22
Carbon steel in deoxygenated reactor water	FAT	2.67	1.22
Carbon steel weldments in deoxygenated reactor water	FAT	2.67	1.22
Carbon steel HAZ in deoxygenated reactor water	FAT	2.67	1.22
Carbon steel in reactor cleanup water	FAT	2.78	1.22
Carbon steel in feedwater	FAT	2.67	1.22
Carbon steel in treated service water	FAT	2.78	1.22
Carbon steel in stagnant reactor water at lower temperature	FAT	2.78	1.11
Carbon steel weldments in stagnant reactor water at lower temperature	FAT	2.78	1.11
Carbon steel HAZ in stagnant reactor water at lower temperature	FAT	2.78	1.11

Table 9.92. Summary of FAT scores for carbon steels, weldments, and HAZ in BWR environments (continued)

Material/Environment	Degradation Mode	Average Knowledge	Average Susceptibility
Carbon steel in suppression/storage pool water	FAT	2.67	1.11
Carbon steel weldments in suppression/storage pool water	FAT	2.67	1.11
Carbon steel HAZ in suppression/storage pool water	FAT	2.67	1.11
Carbon steel in stagnant suppression pool water	FAT	2.67	1.11
Carbon steel weldments in stagnant suppression pool water	FAT	2.67	1.11
Carbon steel HAZ in stagnant suppression pool water	FAT	2.67	1.11
Carbon steel in condensate storage water	FAT	2.67	1.11
Carbon steel weldments in condensate storage water	FAT	2.67	1.11
Carbon steel HAZ in condensate storage water	FAT	2.67	1.11
Carbon steel in drywell environment	FAT	2.67	1.11
Carbon steel weldments in drywell environment	FAT	2.67	1.11
Carbon steel HAZ in drywell environment	FAT	2.67	1.11
Carbon steel external surfaces in high temperature air	FAT	2.89	1.11
Carbon steel external surfaces in containment air	FAT	2.89	1.11
Carbon and carbon steel weldolets and sockolets in reactor water	FAT-HWC	2.44	1.78
Carbon steel in reactor coolant	FAT-HWC	2.56	1.11
Carbon steel weldments in reactor coolant	FAT-HWC	2.56	1.11
Carbon steel HAZ in reactor coolant	FAT-HWC	2.56	1.11
Carbon steel in stagnant reactor water	FAT-HWC	2.67	1.11
Carbon steel weldments in stagnant reactor water	FAT-HWC	2.67	1.11
Carbon steel HAZ in stagnant reactor water	FAT-HWC	2.67	1.11
Carbon steel weldments in reactor cleanup water	FAT-HWC	2.67	1.11
Carbon steel in reactor cleanup water	FAT-HWC	2.67	1.00

Fracture Resistance

Fracture resistance was evaluated for carbon steel and weldments for extended service operations. The expert panel scored all categories of fracture resistance in the high Knowledge, moderate Susceptibility grouping. The experts noted that there are minimal mechanistic changes over very long lifetimes although there is relatively little data and understanding of the mechanisms. Irradiation-induced embrittlement is considered separately in the RPV volume of this work.

Table 9.93. Summary of FR scores for carbon steels, weldments, and HAZ in BWR environments

Material/Environment	Degradation Mode	Average Knowledge	Average Susceptibility
Carbon steel in reactor coolant	FR	2.44	1.00
Carbon steel weldments in reactor coolant	FR	2.44	1.00
Carbon steel HAZ in reactor coolant	FR	2.44	1.00

General Corrosion

General corrosion can occur in carbon steels for a variety of reasons in service and has been observed in operation. The expert panel scored this form of degradation in 32 different environments. General corrosion in suppression pool and stagnant suppression pool water were scored in the high Knowledge, high Susceptibility grouping. The panelists noted that corrosion susceptibility is strongly affected by water chemistry and should not be an issue if good water chemistry guidelines are followed. All other categories were ranked in the high Knowledge, moderate Susceptibility grouping with similar cautions on good water chemistry control.

Table 9.94. Summary of GC scores for carbon steels, weldments, and HAZ in BWR environments

Material/Environment	Degradation Mode	Average Knowledge	Average Susceptibility
Carbon steel in stagnant suppression pool water	GC	2.78	2.11
Carbon steel weldments in stagnant suppression pool water	GC	2.78	2.11
Carbon steel HAZ in stagnant suppression pool water	GC	2.78	2.11
Carbon steel weldments in suppression/storage pool water	GC	2.78	1.89
Carbon steel in condensate storage water	GC	2.78	1.89
Carbon steel weldments in condensate storage water	GC	2.78	1.89
Carbon steel HAZ in condensate storage water	GC	2.78	1.89
Carbon steel in drywell environment	GC	2.67	1.89
Carbon steel weldments in drywell environment	GC	2.67	1.89
Carbon steel HAZ in drywell environment	GC	2.67	1.89
Carbon steel in treated service water	GC	2.78	1.89
Carbon steel in suppression/storage pool water	GC	2.78	1.78
Carbon steel HAZ in suppression/storage pool water	GC	2.78	1.78
Carbon steel in lower temperature reactor water	GC	2.67	1.67
Carbon steel weldments in lower temperature reactor water	GC	2.67	1.67
Carbon steel HAZ in lower temperature reactor water	GC	2.67	1.67
Carbon steel HAZ in deoxygenated reactor water	GC	2.78	1.56
Carbon steel in deoxygenated reactor water	GC	2.78	1.44
Carbon steel weldments in deoxygenated reactor water	GC	2.78	1.44

Table 9.94. Summary of GC scores for carbon steels, weldments, and HAZ in BWR environments (continued)

Material/Environment	Degradation Mode	Average Knowledge	Average Susceptibility
Carbon steel in reactor cleanup water	GC	2.78	1.33
Carbon steel weldments in reactor cleanup water	GC	2.67	1.33
Carbon steel in stagnant wet steam	GC	2.78	1.22
Carbon steel weldments in stagnant wet steam	GC	2.78	1.22
Carbon steel HAZ in stagnant wet steam	GC	2.78	1.22
Carbon steel in feedwater	GC	2.78	1.22
Carbon steel weldments in feedwater	GC	2.78	1.22
Carbon steel HAZ in feedwater	GC	2.78	1.22
Carbon steel in stagnant steam condensate	GC	2.78	1.11
Carbon steel external surfaces in containment air	GC	2.78	1.11
Carbon steel weldments in reactor coolant	GC	2.67	1.56
Carbon steel in reactor coolant	GC	2.67	1.44
Carbon steel HAZ in reactor coolant	GC	2.67	1.44

Microbially Induced Corrosion

Microbially induced corrosion has been observed in operation for carbon steels. The expert panel scored this form of degradation in 20 different environments. MIC in suppression pool and stagnant suppression pool water categories were scored in the high Knowledge, high Susceptibility grouping. The panelists noted that MIC could be extensive in water with acceptable environments for microbes. As noted above for general and crevice corrosion, water chemistry control was identified as important to mitigate MIC by the expert panel. All other categories were found to be of lower susceptibility, but the panel again noted that this is dependent upon the water being properly treated.

Table 9.95. Summary of MIC scores for carbon steels, weldments, and HAZ in BWR environments

Material/Environment	Degradation Mode	Average Knowledge	Average Susceptibility
Carbon steel in suppression/storage pool water	MIC	2.44	2.00
Carbon steel weldments in suppression/storage pool water	MIC	2.44	2.00
Carbon steel HAZ in suppression/storage pool water	MIC	2.44	2.00
Carbon steel in stagnant suppression pool water	MIC	2.56	2.00
Carbon steel weldments in stagnant suppression pool water	MIC	2.56	2.00
Carbon steel HAZ in stagnant suppression pool water	MIC	2.56	2.00
Carbon steel in condensate storage water	MIC	2.56	1.75
Carbon steel weldments in condensate storage water	MIC	2.56	1.75
Carbon steel HAZ in condensate storage water	MIC	2.56	1.75

Table 9.95. Summary of MIC scores for carbon steels, weldments, and HAZ in BWR environments (continued)

Material/Environment	Degradation Mode	Average Knowledge	Average Susceptibility
Carbon steel in drywell environment	MIC	2.44	1.75
Carbon steel weldments in drywell environment	MIC	2.44	1.75
Carbon steel HAZ in drywell environment	MIC	2.44	1.75
Carbon steel in stagnant reactor water	MIC	2.56	1.50
Carbon steel weldments in stagnant reactor water at lower temperature	MIC	2.56	1.50
Carbon steel HAZ in stagnant reactor water at lower temperature	MIC	2.56	1.50
Carbon steel in treated service water	MIC	2.44	1.50
Carbon steel weldments in stagnant reactor water	MIC	2.56	1.38
Carbon steel HAZ in stagnant reactor water	MIC	2.56	1.38
Carbon steel in stagnant reactor water at lower temperature	MIC	2.56	1.38
Carbon steel external surfaces in containment air	MIC	2.67	1.25

Pitting

Pitting of carbon steels has also been observed in service. The expert panel scored this form of degradation in 40 different environments. Pitting corrosion in suppression pool and stagnant suppression pool water categories was scored in the high Knowledge, high Susceptibility grouping, although the average Susceptibility score was only 2.11. All other categories were found to be of lower susceptibility, but the panel again noted that this is dependent upon the water being properly treated.

Table 9.96. Summary of PIT scores for carbon steels, weldments, and HAZ in BWR environments

Material/Environment	Degradation Mode	Average Knowledge	Average Susceptibility
Carbon steel in suppression/storage pool water	PIT	2.67	2.11
Carbon steel weldments in suppression/storage pool water	PIT	2.67	2.11
Carbon steel HAZ in suppression/storage pool water	PIT	2.67	2.11
Carbon steel in stagnant suppression pool water	PIT	2.78	2.11
Carbon steel weldments in stagnant suppression pool water	PIT	2.78	2.11
Carbon steel HAZ in stagnant suppression pool water	PIT	2.78	2.11
Carbon steel in condensate storage water	PIT	2.78	2.00
Carbon steel weldments in condensate storage water	PIT	2.78	2.00
Carbon steel HAZ in condensate storage water	PIT	2.78	2.00
Carbon steel in drywell environment	PIT	2.78	2.00

Table 9.96. Summary of PIT scores carbon steels, weldments, and HAZ in BWR environments (continued)

Material/Environment	Degradation Mode	Average Knowledge	Average Susceptibility
Carbon steel in stagnant reactor water at lower temperature	PIT	2.67	1.89
Carbon steel weldments in stagnant reactor water at lower temperature	PIT	2.67	1.89
Carbon steel HAZ in stagnant reactor water at lower temperature	PIT	2.67	1.89
Carbon steel weldments in drywell environment	PIT	2.78	1.89
Carbon steel HAZ in drywell environment	PIT	2.78	1.89
Carbon steel in treated service water	PIT	2.78	1.89
Carbon steel in lower temperature reactor water	PIT	2.67	1.67
Carbon steel weldments in lower temperature reactor water	PIT	2.67	1.67
Carbon steel HAZ in lower temperature reactor water	PIT	2.67	1.67
Carbon steel in stagnant reactor water	PIT	2.78	1.67
Carbon steel weldments in stagnant reactor water	PIT	2.78	1.67
Carbon steel HAZ in stagnant reactor water	PIT	2.78	1.67
Carbon steel HAZ in deoxygenated reactor water	PIT	2.78	1.67
Carbon steel in deoxygenated reactor water	PIT	2.78	1.56
Carbon steel weldments in deoxygenated reactor water	PIT	2.78	1.56
Carbon steel HAZ in feedwater	PIT	2.78	1.56
Carbon steel in stagnant steam condensate	PIT	2.78	1.44
Carbon steel in reactor coolant	PIT	2.78	1.33
Carbon steel weldments in reactor coolant	PIT	2.78	1.33
Carbon steel HAZ in reactor coolant	PIT	2.78	1.33
Carbon steel in stagnant wet steam	PIT	2.67	1.33
Carbon steel weldments in reactor cleanup water	PIT	2.78	1.33
Carbon steel weldments in feedwater	PIT	2.78	1.33
Carbon steel external surfaces in containment air	PIT	2.78	1.33
Carbon steel weldments in stagnant wet steam	PIT	2.67	1.22
Carbon steel HAZ in stagnant wet steam	PIT	2.67	1.22
Carbon steel in reactor cleanup water	PIT	2.67	1.22
Carbon steel in feedwater	PIT	2.78	1.22
Carbon steel external surfaces in high temperature air	PIT	2.86	1.14
Carbon steel external surfaces in high temperature air	PIT	2.67	1.11

Stress Corrosion Cracking

The expert panel considered 46 different categories of SCC for carbon steels in BWR environments. All categories were ranked in the high Knowledge, moderate Susceptibility

grouping. In most categories, the panel noted that SCC should not be an issue at lower temperatures for most categories and if good water chemistry and protective features (e.g., lining) are maintained. However, changes in loading or increases in chemical conditions (such as chloride content) may drive increased susceptibility during long-term operation.

Table 9.97. Summary of SCC scores for carbon steels, weldments, and HAZ in BWR environments

Material/Environment	Degradation Mode	Average Knowledge	Average Susceptibility
Carbon steel HAZ in reactor coolant	SCC	2.56	1.67
Carbon steel HAZ in feedwater	SCC	2.67	1.67
Carbon steel HAZ in stagnant reactor water	SCC	2.67	1.56
Carbon steel in stagnant wet steam	SCC	2.67	1.56
Carbon steel weldments in reactor cleanup water	SCC	2.33	1.56
Carbon steel weldments in feedwater	SCC	2.67	1.56
Carbon steel weldments in reactor coolant	SCC	2.56	1.44
Carbon steel HAZ in lower temperature reactor water	SCC	2.67	1.44
Carbon steel HAZ in stagnant reactor water at lower temperature	SCC	2.67	1.44
Carbon steel weldments in stagnant wet steam	SCC	2.67	1.44
Carbon steel HAZ in stagnant wet steam	SCC	2.78	1.44
Carbon steel in reactor cleanup water	SCC	2.44	1.44
Carbon steel in feedwater	SCC	2.67	1.44
Carbon steel in reactor coolant	SCC	2.44	1.33
Carbon steel in lower temperature reactor water	SCC	2.67	1.33
Carbon steel weldments in lower temperature reactor water	SCC	2.67	1.33
Carbon steel in stagnant reactor water	SCC	2.67	1.33
Carbon steel weldments in stagnant reactor water	SCC	2.67	1.33
Carbon steel weldments in stagnant reactor water at lower temperature	SCC	2.67	1.33
Carbon steel HAZ in suppression/storage pool water	SCC	2.78	1.33
Carbon steel HAZ in stagnant suppression pool water	SCC	2.78	1.33
Carbon steel in condensate storage water	SCC	2.78	1.33
Carbon steel weldments in condensate storage water	SCC	2.78	1.33
Carbon steel HAZ in condensate storage water	SCC	2.78	1.33
Carbon steel in treated service water	SCC	2.78	1.33
Carbon steel in stagnant reactor water at lower temperature	SCC	2.67	1.22
Carbon steel in deoxygenated reactor water	SCC	2.78	1.22
Carbon steel weldments in deoxygenated reactor water	SCC	2.78	1.22
Carbon steel HAZ in deoxygenated reactor water	SCC	2.78	1.22
Carbon steel in stagnant steam condensate	SCC	2.78	1.22
Carbon steel in suppression/storage pool water	SCC	2.78	1.22

Table 9.97. Summary of SCC scores for carbon steels, weldments, and HAZ in BWR environments (continued)

Material/Environment	Degradation Mode	Average Knowledge	Average Susceptibility
Carbon steel weldments in suppression/storage pool water	SCC	2.78	1.22
Carbon steel in stagnant suppression pool water	SCC	2.78	1.22
Carbon steel weldments in stagnant suppression pool water	SCC	2.78	1.22
Carbon steel in drywell environment	SCC	2.78	1.22
Carbon steel weldments in drywell environment	SCC	2.78	1.11
Carbon steel HAZ in drywell environment	SCC	2.78	1.11
Carbon steel external surfaces in high temperature air	SCC	2.78	1.00
Carbon steel weldments in reactor coolant	SCC-HWC	2.44	1.22
Carbon steel HAZ in reactor coolant	SCC-HWC	2.44	1.22
Carbon steel in stagnant reactor water	SCC-HWC	2.56	1.22
Carbon steel weldments in stagnant reactor water	SCC-HWC	2.56	1.22
Carbon steel HAZ in stagnant reactor water	SCC-HWC	2.56	1.22
Carbon steel in reactor cleanup water	SCC-HWC	2.56	1.22
Carbon steel weldments in reactor cleanup water	SCC-HWC	2.56	1.22
Carbon steel in reactor coolant	SCC-HWC	2.44	1.11

9.8.2.2 Low Alloy Steels in BWRs

The PIRT scores for the major degradation modes for low alloy steels in BWR environments are summarized below. Additional details on individual scores by panelists, their comments and rationale, and parts and component numbers used in NUREG/CR-6923 are also shown in Appendix G. Low alloy steels are used in a variety of environments and applications. As noted above, irradiation effects for these alloys are considered in the EMDA volume on RPV degradation. More details on this form of degradation can be found there.

Several trends for low alloy steels in BWR environments were identified via the PIRT process:

- Crevice corrosion, pitting, general, and MIC of low alloy steel were identified as high Knowledge, moderate Susceptibility modes of degradation for most environments. However, these are expected to be operational issues only in the event of a loss of water chemistry control. These are well-known forms of degradation.

- Stress corrosion cracking and fatigue are possible for these alloys, but SCC is relatively rare in service. The reasons for this rarity are reasonably well understood and are discussed in some detail in Chapter 5. Changes in loading or increases in water chemistry conditions (such as chloride content) may drive increased susceptibility over a long operating period. Further aspects needing confirmation are synergistic effects between SCC susceptibility and other degradation modes associated with irradiation hardening and embrittlement, temper embrittlement and dynamic strain aging, which may dominate over long operational times.

Crevice Corrosion

The expert panel scored this form of degradation in a single category. It was scored in the high Knowledge, high Susceptibility grouping, although the Susceptibility score is not statistically different from the moderate Susceptibility grouping. The panel noted that crevice corrosion could occur under deposits or with loss of water chemistry control.

Table 9.98. Summary of CREV scores for low alloy steels in BWR environments

Material/Environment	Degradation Mode	Average Knowledge	Average Susceptibility
LAS in suppression/storage pool water	CREV	2.78	2.11

Fatigue and Corrosion Fatigue

Fatigue and corrosion fatigue for low alloy steels in both BWR NWC and BWR HWC environments was scored in the high Knowledge, moderate Susceptibility grouping for all 12 categories. The panelists viewed fatigue loading as inconsequential with good service experience, although if operational conditions over extended service change, corrosion fatigue damage is possible.

Table 9.99. Summary of FAT scores for low alloy steels in BWR environments

Material/Environment	Degradation Mode	Average Knowledge	Average Susceptibility
LAS HAZ in reactor coolant	FAT	2.67	1.56
LAS in reactor coolant	FAT	2.78	1.44
LAS weldments in reactor coolant	FAT	2.67	1.44
LAS in reactor coolant steam	FAT	2.56	1.44
LAS weldments in reactor coolant steam	FAT	2.67	1.44
LAS HAZ in reactor coolant steam	FAT	2.67	1.44
LAS in suppression/storage pool water	FAT	2.67	1.00
LAS in containment air	FAT	2.78	1.00
LAS in reactor coolant	FAT-HWC	2.44	1.11
LAS weldments in reactor coolant	FAT-HWC	2.44	1.11
LAS HAZ in reactor coolant	FAT-HWC	2.44	1.11
LAS in reactor coolant steam	FAT-HWC	2.56	1.11

Fracture Resistance

Fracture resistance was evaluated for low alloy steel, HAZ, and weldments for extended service operations. The expert panel scored all categories of fracture resistance in the high Knowledge, moderate Susceptibility grouping with very low Susceptibility scores. The experts noted that there are minimal mechanistic changes over very long-term reactor operation although there is relatively little data and understanding of the mechanisms. Irradiation-induced embrittlement was considered separately in the RPV volume of this work.

Table 9.100. Summary of FR scores for low alloy steels in BWR environments

Material/Environment	Degradation Mode	Average Knowledge	Average Susceptibility
LAS in reactor coolant	FR	2.33	1.33
LAS weldments in reactor coolant	FR	2.22	1.33
LAS HAZ in reactor coolant	FR	2.22	1.11
LAS in reactor coolant steam	FR	2.11	1.11
LAS weldments in reactor coolant steam	FR	2.11	1.11
LAS HAZ in reactor coolant steam	FR	2.11	1.11
LAS in containment air	FR	2.56	1.00

General Corrosion

General corrosion has been observed in operation for low alloy steels. The expert panel scored this form of degradation in the high Knowledge, moderate Susceptibility grouping. The panelists noted that corrosion susceptibility is strongly affected by water chemistry and should not be an issue if good water chemistry guidelines are followed.

Table 9.101. Summary of GC scores for low alloy steels in BWR environments

Material/Environment	Degradation Mode	Average Knowledge	Average Susceptibility
LAS in suppression/storage pool water	GC	2.78	1.33

Microbially Induced Corrosion

Microbially induced corrosion can occur in BWR environments for low alloy steels. The expert panel scored this form of degradation in the high Knowledge, high Susceptibility grouping, although the Susceptibility score is not statistically different from the moderate Susceptibility grouping. The panel noted that, like CREV or GC above, MIC could occur with loss of water chemistry control.

Table 9.102. Summary of MIC scores for low alloy steels in BWR environments

Material/Environment	Degradation Mode	Average Knowledge	Average Susceptibility
LAS in suppression/storage pool water	MIC	2.44	2.00

Pitting

The expert panel scored this form of degradation in a single category for low alloy steels. Like MIC above, the expert panel scored this form of degradation in the high Knowledge, high Susceptibility grouping, although the Susceptibility score is not statistically different from the moderate Susceptibility grouping. The panel noted that, like crevice corrosion, MIC, or general corrosion, pitting could occur with loss of water chemistry control.

Table 9.103. Summary of PIT scores for low alloy steels in BWR environments

Material/Environment	Degradation Mode	Average Knowledge	Average Susceptibility
LAS in suppression/storage pool water	PIT	2.67	2.11

Stress Corrosion Cracking

The expert panel considered 11 categories of SCC for low alloy steels in both NWC and HWC environments. All categories were ranked in the high Knowledge, moderate Susceptibility grouping. As with carbon steels, the panel noted that SCC should not be an issue if good water chemistry is maintained. SCC is possible for these alloys, but unlikely in service, consistent with operating experience. Changes in loading or chemical conditions (such as chloride content) may drive increased susceptibility over a long operating period.

Table 9.104. Summary of SCC scores for low alloy steels in BWR environments

Material/Environment	Degradation Mode	Average Knowledge	Average Susceptibility
LAS weldments in reactor coolant	SCC	1.89	1.78
LAS in reactor coolant	SCC	2.22	1.78
LAS HAZ in reactor coolant	SCC	2.11	1.78
LAS in reactor coolant steam	SCC	2.22	1.67
LAS HAZ in reactor coolant steam	SCC	2.22	1.67
LAS weldments in reactor coolant steam	SCC	2.22	1.56
LAS in suppression/storage pool water	SCC	2.67	1.00
LAS in reactor coolant	SCC-HWC	2.44	1.22
LAS weldments in reactor coolant	SCC-HWC	2.33	1.22
LAS HAZ in reactor coolant	SCC-HWC	2.44	1.22
LAS in reactor coolant steam	SCC-HWC	2.33	1.22

9.8.3 Summary of PIRT Findings for Carbon and Low alloy Steels

Carbon and low alloy steels are used in a variety of components with varying environmental conditions, depending upon locations within the reactor. These ductile structural materials are used as pressure boundary materials in pressure vessels and piping in the RCS, ECCS, secondary water, and service water systems of LWRs. These alloys are attractive for this use due to their relatively low cost, good mechanical properties in thick sections, and good weldability. In reactor coolant system components, such as the pressure vessel, pressurizer, and some piping, the carbon and low alloy steels are clad on the inside wetted surface with corrosion-resistant materials such as austenitic stainless steels or nickel-base alloys. A number of key technical aging degradation issues are possible for these components. Carbon and low alloy steels are susceptible to irradiation damage, even at low fluence. These materials are also susceptible to fatigue damage, pitting, flow-accelerated corrosion, and MIC in some piping and water chemistry environments. These alloys are also highly susceptible to BAC in the event of leaks in PWR environments.

No significant knowledge gaps were identified for carbon and low alloy steels in PWR environments following analysis of the PIRT scoring. However, several trends and common themes were identified:

- Carbon and low alloy steels are highly susceptible to BAC in the event of a leak of primary coolant. This is a well-known form of degradation and is not unique to extended service conditions.

- Crevice corrosion, pitting, MIC, and general corrosion of carbon steel and low alloy steel were identified as high-knowledge modes of degradation, occurring only in the event of loss of water chemistry control or failure of protective features such as liners or cathodic protection. These are well-known forms of degradation.

- Flow-accelerated corrosion is a well-known form of degradation for low alloy and carbon steels, but can be exacerbated in elbows; changing water chemistry and flow conditions as well as longer service life and exposure to FAC conditions may increase susceptibility. Predictive models based on empirical observation or mechanistic understanding have been developed in the United States, Europe, and Japan.

- Stress corrosion cracking and fatigue are possible for these alloys, but is relatively rare in service. The reasons for this rarity are reasonably well understood and are discussed in some detail in Chapter 5. Changes in loading or increases in water chemistry conditions (such as chloride content) may drive increased susceptibility over a long operating period. Further aspects needing confirmation are synergistic effects between SCC susceptibility and other degradation modes associated with irradiation hardening and embrittlement, temper embrittlement and dynamic strain aging, which may dominate over long operational times.

Like in PWR environments, no significant knowledge gaps were identified for carbon and low alloy steels in BWR environments based on analysis of the PIRT scoring. However, several trends and common themes were identified:

- Crevice corrosion, pitting, general, flow-accelerated, and MIC of low alloy steel were identified as high Knowledge, moderate Susceptibility modes of degradation for most environments. However, these are expected to be operating and technical safety issues only in the event of a loss of water chemistry control. These are well-known forms of degradation.

- Stress corrosion cracking and fatigue are possible for these alloys, but unlikely in service. Changes in loading or chemical conditions may drive increased susceptibility over a long operating period.

9.9 SCORING SUMMARY FOR CAST AUSTENITIC STAINLESS STEELS

Cast austenitic stainless steel is an important material used for components in modern LWR facilities. Cast stainless steels are often chosen in nuclear components for economic reasons. Historically, cast stainless steel grades have performed well in nuclear reactor applications, and there are relatively few key degradation modes of concern.

Today, CASS are used in a variety of applications of BWR and PWR applications including for reactor coolant, auxiliary system piping, reactor coolant pump casings, and reactor coolant valve

bodies and fittings. Several grades of CASS employed today include the CF8 and CF3 family of alloys. These alloys are exposed to elevated temperatures and corrosive environments. Piping and pump casings in BWRs may be exposed to NWC or HWC environments and be exposed to low neutron fluxes in some locations. These alloys serve in the primary water environment in PWR applications.

As discussed in Chapter 6, degradation modes for CASS in reactor applications are relatively minor when compared to other alloy systems under normal operating conditions through 40 or 60 years of life. Thermal aging and irradiation effects are not considered an area of concern given the relatively low temperatures and fluences over that lifetime. There have been limited cases of SCC in CASS components in both BWRs and PWRs; however, these are attributed to irregularities in composition or microstructure rather than general vulnerabilities.

An increased susceptibility to SCC has been identified for BWRs in areas of cold work or weldments. As a result of the very low irradiation fluence, there has been no record of irradiation-assisted SCC in CASS components. Finally, there are no concerns for CASS components related to general or localized corrosion, fatigue, flow-accelerated corrosion, or wear for current lifetimes.

Under extended service scenarios, there may be additional degradation modes to consider. Thermal aging could lead to decomposition of key phases, resulting in increased susceptibility to embrittlement, irradiation-induced degradation, SCC, and general corrosion. This section will explore those degradation modes in more detail.

This section presents the results of the PIRT scoring for CASS materials. The section is organized by reactor type, grade of stainless steel, and degradation mode. This differs from the NUREG/CR-6923 activity where results were organized by reactor system. However, as discussed above, the PIRT was arranged differently for this activity, and direct comparisons for individual components are more difficult.

9.9.1 Cast Austenitic Stainless Steels in PWRs

In PWR systems, CASS are used for a variety of applications. Common alloys in service include the CF3 and CF8 series of alloys with CF3, CF3A, CF3M, CF8, CF8A, and CF8M being the most prominent choices. Typical nuclear power plant applications and material grades of CASS include the use of CF8A, CF8M, and CPF3M for reactor coolant and auxiliary system piping. Reactor coolant pump casings are typically made from types CF8, CF8A, or CF8M CASS. Reactor coolant valve bodies and fittings often use CF8A or CF8M. In later construction applications and replacements, CF3s have been used rather than CF8s.

For the EMDA activity, the panelists scored 24 categories. The results are shown below with the data organized by degradation mode. For each degradation mode, scores are ranking the summary tables by Susceptibility score. Additional details on individual scores by panelists, their comments and rationale, and parts and component numbers used in NUREG/CR-6923 are also shown in Appendix H.

One knowledge gap for CASS materials in PWR environments was identified via the PIRT process. Specifically, the effects of long-term thermal aging for extended operating periods may drive changes in mechanical or corrosion performance that are relatively unknown.

Fatigue and Corrosion Fatigue

Eight categories for fatigue of CASS materials were scored in the high Knowledge, moderate Susceptibility grouping. The panelists viewed fatigue loading as inconsequential, although if operational conditions over extended service change, corrosion fatigue damage is possible.

Table 9.105. Summary of FAT scores for CASS in PWR environments

Material/Environment	Degradation Mode	Average Knowledge	Average Susceptibility
CASS in primary water – low fluence irradiation up to 0.5 dpa	FAT	2.22	1.33
CASS in primary reactor water – no irradiation	FAT	2.11	1.11
CASS HAZ in primary water – low fluence irradiation up to 0.5 dpa	FAT	2.71	1.00
CASS HAZ in primary reactor water – no irradiation	FAT	2.57	1.00
CASS in borated demineralized water	FAT	2.11	1.11
CASS in primary reactor water at lower temperature	FAT	2.44	1.00
CASS HAZ in primary reactor water at lower temperature	FAT	2.71	1.00
CASS HAZ in borated demineralized water	FAT	2.57	1.00

Fracture Resistance

Fracture resistance was evaluated CASS alloys and HAZ in eight different categories. The expert panel scored the CASS HAZ in primary water in the low Knowledge, moderate Susceptibility category. This was driven by uncertainty in the effects of thermal aging over an extended operating period on microstructure and mechanical performance. Scores for CASS and HAZ in primary water at low fluence were statistically the same, although they ranked in the high Knowledge, medium susceptibility grouping. Thermal aging effects were considered by the panel as the key factor for this mode of degradation in all environments.

Table 9.106. Summary of FR scores for CASS in PWR environments

Material/Environment	Degradation Mode	Average Knowledge	Average Susceptibility
CASS HAZ in primary reactor water – no irradiation	FR	1.86	1.71
CASS HAZ in primary water – low fluence irradiation up to 0.5 dpa	FR	2.00	1.86
CASS in primary water – low fluence irradiation up to 0.5 dpa	FR	2.00	1.78
CASS in primary reactor water – no irradiation	FR	2.00	1.67
CASS HAZ in primary reactor water at lower temperature	FR	2.00	1.57
CASS HAZ in borated demineralized water	FR	2.14	1.57
CASS in borated demineralized water	FR	2.22	1.11
CASS in primary reactor water at lower temperature	FR	2.22	1.00

Stress Corrosion Cracking

While CASS components have an excellent performance record, extended service will result in increased exposure time to the primary water environment and stress. The expert panel considered eight different categories of SCC for cast austenitic alloys in PWR environments. The panel scored the CASS and HAZ in primary water in the low Knowledge, moderate Susceptibility category. As above, this was driven by uncertainty in the effects of thermal aging over an extended operating period on microstructure and mechanical performance. Other categories were ranked at lower susceptibility, although thermal aging effects were considered by the panel as the key factor for this mode of degradation in all environments.

Table 9.107. Summary of SCC scores for CASS in PWR environments

Material/Environment	Degradation Mode	Average Knowledge	Average Susceptibility
CASS HAZ in primary water – low fluence irradiation up to 0.5 dpa	SCC	1.86	1.86
CASS in primary water – low fluence irradiation up to 0.5 dpa	SCC	1.78	1.33
CASS in primary reactor water – no irradiation	SCC	1.89	1.33
CASS HAZ in primary reactor water – no irradiation	SCC	2.14	1.71
CASS in borated demineralized water	SCC	2.33	1.11
CASS HAZ in primary reactor water at lower temperature	SCC	2.14	1.00
CASS HAZ in borated demineralized water	SCC	2.14	1.00
CASS in primary reactor water at lower temperature	SCC	2.22	0.89

9.9.2 Cast Austenitic Stainless Steels in BWRs

In BWR systems, CASS materials are used for a variety of applications, primarily piping and pump housings. For the EMDA activity, the panelists scored 19 categories. The results are shown below with the data organized by degradation mode. For each degradation mode, scores are ranking the summary tables by Susceptibility score. Additional details on individual scores by panelists, their comments and rationale, and parts and component numbers used in NUREG/CR-6923 are also shown in Appendix I.

The general results for CASS in BWRs are very similar to that found for PWRs. There is an increased susceptibility to SCC in areas of cold work or weldments. In addition, there are no concerns for CASS components related to general or localized corrosion, fatigue, FAC or wear for current operating periods to 60 years. The expert panel assessment showed little concern for these modes of degradation for service to 80 years.

One knowledge gap for CASS components in BWR environments was identified via the PIRT process. Specifically, the effects of long-term thermal aging for extended operating periods may drive changes in mechanical or corrosion performance that are relatively unknown.

Crevice Corrosion

Crevice corrosion can occur in service, although it has not been observed in BWR applications for CASS. This mode of degradation for CASS was scored in the high Knowledge, moderate Susceptibility grouping.

Table 9.108. Summary of CREV scores for CASS in BWR environments

Material/Environment	Degradation Mode	Average Knowledge	Average Susceptibility
CASS in saturated wet steam	CREV	2.33	1.00

Erosion Corrosion

Erosion corrosion can occur for CASS components, although it has not been observed in BWR service to date. This mode of degradation in wet steam was scored in the high Knowledge, moderate Susceptibility grouping.

Table 9.109. Summary of EC scores for CASS in BWR environments

Material/Environment	Degradation Mode	Average Knowledge	Average Susceptibility
CASS in saturated wet steam	EC	2.44	1.22

Fatigue and Corrosion Fatigue

Six categories for CASS FAT were scored in the high Knowledge, moderate Susceptibility grouping. The panelists viewed fatigue loading as inconsequential, although if operational conditions over extended service change, corrosion fatigue damage is possible and the CUF must be evaluated for extended service conditions.

Table 9.110. Summary of FAT scores for CASS in BWR environments

Material/Environment	Degradation Mode	Average Knowledge	Average Susceptibility
CASS in reactor water – no irradiation	FAT	2.44	1.56
CASS in reactor water – low fluence irradiation up to 0.5 dpa	FAT	2.44	1.44
CASS in saturated wet steam	FAT	2.22	1.33
CASS in deoxygenated reactor water	FAT	2.33	1.11
CASS in reactor water – no irradiation	FAT-HWC	2.33	1.56
CASS in reactor water – low fluence irradiation up to 0.5 dpa	FAT-HWC	2.33	1.44

Fracture Resistance

Fracture resistance was evaluated CASS alloys and HAZ in three different categories. The panel scored the CASS HAZ in primary water in the low Knowledge, moderate Susceptibility category.

This was driven by uncertainty in the effects of thermal aging over an extended operating period on microstructure and mechanical performance. Similar scores for CASS and HAZ in reactor water at low fluence were statistically the same and ranked in the high Knowledge, medium susceptibility grouping. Thermal aging effects were considered by the panel as the key factor for this mode of degradation in all environments.

Table 9.111. Summary of FR scores for CASS in BWR environments

Material/Environment	Degradation Mode	Average Knowledge	Average Susceptibility
CASS in reactor water – no irradiation	FR	1.89	1.78
CASS in reactor water – low fluence irradiation up to 0.5 dpa	FR	2.00	1.78
CASS in saturated wet steam	FR	2.11	1.56

General Corrosion

General corrosion can occur for CASS materials, although it has not been observed in service for CASS. This mode of degradation for CASS was scored as high Knowledge, moderate Susceptibility grouping.

Table 9.112. Summary of GC scores for CASS in BWR environments

Material/Environment	Degradation Mode	Average Knowledge	Average Susceptibility
CASS in saturated wet steam	GC	2.22	1.00

Pitting

Pitting of CASS has not been observed in service, although it is possible under conditions. This mode of degradation for CASS was scored in the high Knowledge, low Susceptibility grouping.

Table 9.113. Summary of PIT scores for CASS in BWR environments

Material/Environment	Degradation Mode	Average Knowledge	Average Susceptibility
CASS in saturated wet steam	PIT	2.44	0.89

Stress Corrosion Cracking

The panel considered five different categories of SCC for cast austenitic alloys in BWR environments and scored the CASS and HAZ in NWC reactor water in the low Knowledge, moderate Susceptibility category. As stated above for PWR environments, this was driven by uncertainty in the effects of thermal aging on microstructure and mechanical performance over an extended operating period. Other categories were ranked at higher Knowledge, although thermal aging effects were considered by the panel as the key factor for this mode of degradation in all environments.

Table 9.114. Summary of SCC scores for CASS in BWR environments

Material/Environment	Degradation Mode	Average Knowledge	Average Susceptibility
CASS in reactor water – no irradiation	SCC	1.89	1.67
CASS in reactor water – low fluence irradiation up to 0.5 dpa	SCC	2.00	1.89
CASS in deoxygenated reactor water	SCC	2.00	1.22
CASS in reactor water – low fluence irradiation up to 0.5 dpa	SCC-HWC	2.11	1.33
CASS in reactor water – no irradiation	SCC-HWC	2.00	1.00

Wear

The expert panel scored wear for CASS components in the reactor core. The category was ranked with high Knowledge and lower Susceptibility scores as conditions for wear should not exist for these components.

Table 9.115. Summary of WEAR scores for CASS in BWR environments

Material/Environment	Degradation Mode	Average Knowledge	Average Susceptibility
CASS in reactor water – low fluence irradiation up to 0.5 dpa	WEAR	2.11	1.13

9.9.3 Summary of PIRT Findings for Cast Austenitic Stainless Steels

Cast austenitic stainless steels are used in both BWRs and PWRs including for reactor coolant, auxiliary system piping, reactor coolant pump casings, and reactor coolant valve bodies and fittings. A variety of different degradation modes were considered for these alloys in BWR and PWR environments.

One potential knowledge gap for CASSs was identified for both PWR and BWR environments using the PIRT data. Specifically, the effects of long-term thermal aging for extended operating periods may drive changes in mechanical or corrosion performance that are relatively unknown. This is consistent with the conclusions of the background assessment presented in Chapter 6.

9.10 SCORING SUMMARY FOR OTHER MATERIALS

Previous sections of the PIRT analysis focused on major alloy groups including wrought and CASS, Alloy 600 and its weldments, Alloy 690 and its weldments, carbon steels, and low alloy steels. While these materials comprise the majority of LWR components, other materials are also in use in a variety of environments. These material systems are also subject to degradation and were considered here. As part of the EMDA activity, the expert panel scored 95 categories for other materials in different environmental conditions (52 for PWRs and 43 for BWRs).

This section presents the results of the PIRT scoring for these other important materials. The section below is organized by reactor type, material class, and degradation mode. This differs

from the NUREG/CR-6923 activity where results were organized by reactor system. However, as discussed above, the PIRT was arranged differently for this activity, and direct comparisons for individual components are more difficult. In some cases where a material has one single use, degradation modes are discussed collectively.

9.10.1 Other Materials in PWRs

Many additional alloys and materials are important in PWR systems, including high strength bolting alloys (precipitation hardened Ni-base alloys) in the core internals, closure studs (carbon and low alloy steel alloys, but were considered as a separate group for this and the past PMDA activity), CuZn and CuNi tubes, Zr-based fuel assemblies, and ferritic steels. The scores for the major degradation modes considered are summarized below. Additional details on individual scores by panelists, their comments and rationale, and parts and component numbers used in NUREG/CR-6923 are also shown in Appendix J.

Several knowledge gaps were identified via the PIRT process for high strength bolting:

- Impact of irradiation on fracture toughness, irradiation creep, swelling, and SCC of high strength bolting materials used in core internal applications
- SCC susceptibility of high strength bolting over very long operating periods due to potential microstructure changes

No significant gaps in knowledge for extended service were identified for closure studs in PWRs. Further, no significant gaps were identified for CuZn tubes, CuNi tubes, BORAL® panels, Zr-fuel assemblies, or 405/409 steels although the importance of maintaining good water chemistry control was noted for each material system.

9.10.1.1 High Strength Bolting

High-strength, precipitation-hardened Ni-base alloys are frequently used for core internal bolting applications in PWRs, but these materials can also be used as fasteners and springs for fuel assemblies. These alloys are subject to primary reactor coolant and irradiation damage. The scores for the major degradation modes considered are summarized below. Additional details on individual scores by panelists, their comments and rationale, and parts and component numbers used in NUREG/CR-6923 are also shown in Appendix J.

Several knowledge gaps for high strength bolting applications in PWR environments were identified via the PIRT process. Specifically:

- Impact of irradiation on fracture toughness, irradiation creep, swelling, and SCC
- SCC susceptibility for long reactor operation

Fatigue and Corrosion Fatigue

High strength bolts were scored high Knowledge, moderate Susceptibility grouping for four different environmental categories. This is based on broad service experience with these components.

Table 9.116. Summary of FAT scores for high-strength bolting in PWR environments

Material/Environment	Degradation Mode	Average Knowledge	Average Susceptibility
High strength bolts internals in primary reactor water – high fluence irradiation over 15 dpa	FAT	2.00	1.67
High strength bolts internals in primary reactor water – moderate fluence irradiation up to 15 dpa	FAT	2.00	1.67
High strength bolts internals in primary reactor water – low fluence irradiation up to 0.5 dpa	FAT	2.13	1.38
High strength bolts in reactor primary water – no irradiation	FAT	2.57	1.14

Fracture Resistance

Decrease in fracture resistance is a key issue for most alloys serving as core internals, including high strength Ni-based alloys. As service life increases, so does the fluence accumulated over service life. Further, power uprates may also increase flux and thus increase total radiation damage over a long operating period. As noted in an earlier section, decrease in fracture resistance for these materials in core primary water was scored in the low Knowledge, high Susceptibility category. This is primarily due to the smaller database of irradiation effects at such fluences under LWR-relevant conditions. Changes in mechanical performance are expected due to possible changes in microstructure under irradiation. The panelists noted that the long-term effects of hydrogen (from water environment) on fracture resistance over very long reactor operation periods are also relatively unknown. All other environments were judged to be of lower susceptibility or higher knowledge.

Table 9.117. Summary of FR scores for high-strength bolting in PWR environments

Material/Environment	Degradation Mode	Average Knowledge	Average Susceptibility
High strength bolts internals in primary reactor water – high fluence irradiation over 15 dpa	FR	1.89	2.56
High strength bolts internals in primary reactor water – moderate fluence irradiation up to 15 dpa	FR	1.89	2.44
High strength bolts internals in primary reactor water – low fluence irradiation up to 0.5 dpa	FR	2.00	1.89
High strength bolts in reactor primary water – no irradiation	FR	1.89	1.78

Irradiation Creep

As discussed above for irradiation effects on these alloys and wrought stainless steels, the higher fluence due to longer service life and power uprates increases the potential for the onset of irradiation-creep effects and stress relaxation. As previously mentioned, high strength bolting in core primary water was scored in the high Knowledge, high Susceptibility category. All other environments were judged to be of lower susceptibility.

Table 9.118. Summary of IC scores for high-strength bolting in PWR environments

Material/Environment	Degradation Mode	Average Knowledge	Average Susceptibility
High strength bolts internals in primary reactor water – high fluence irradiation over 15 dpa	IC	2.22	3.00
High strength bolts internals in primary reactor water – moderate fluence irradiation up to 15 dpa	IC	2.33	2.22
High strength bolts internals in primary reactor water – low fluence irradiation up to 0.5 dpa	IC	2.44	1.33

Stress Corrosion Cracking

SCC is a known issue for high-strength Ni alloys in PWR primary water and has, been observed in service. Extended service will result in increased time under temperature while exposed to the environment and under stress. Further, for core internals, an increased fluence will be experienced due to longer service and power uprates. High strength bolting in PWR environments was scored in the high Knowledge, high Susceptibility category. This is due to the increased fluence, impacts of irradiation on hardening and swelling, and increased exposure to H (primarily due to higher H_2 concentrations in the primary water).

Table 9.119. Summary of SCC scores for high-strength bolting in PWR environments

Material/Environment	Degradation Mode	Average Knowledge	Average Susceptibility
High strength bolts internals in primary reactor water – high fluence irradiation over 15 dpa	SCC	2.11	2.44
High strength bolts internals in primary reactor water – moderate fluence irradiation up to 15 dpa	SCC	2.11	2.44
High strength bolts internals in primary reactor water – low fluence irradiation up to 0.5 dpa	SCC	2.22	2.22
High strength bolts in reactor primary water – no irradiation	SCC	2.22	2.11

Swelling

Swelling is a known issue for austenitic alloys, although information for precipitation-hardened Ni-base alloys is relatively limited. The existing database is primarily from fast-reactor research programs, although it is expected at lower temperatures and longer operational periods based on model and theory predictions. The magnitude that may be expected for 80 years of service is not known, however. This may be a key issue as core internals experience additional fluence due to longer operational periods and power uprates. As noted in an earlier section for 304 SS and 316 SS, Susceptibility and Knowledge increase and decrease, respectively, with increasing service duration. Additional research to determine the possible magnitudes of the effects of swelling may be required.

Table 9.120. Summary of SW scores for high-strength bolting in PWR environments

Material/Environment	Degradation Mode	Average Knowledge	Average Susceptibility
High strength bolts internals in primary reactor water – high fluence irradiation over 15 dpa	SW	1.88	2.63
High strength bolts internals in primary reactor water – moderate fluence irradiation up to 15 dpa	SW	2.00	1.75
High strength bolts internals in primary reactor water – low fluence irradiation up to 0.5 dpa	SW	2.50	0.86

Wear

The expert panel scored wear degradation for PWR high strength bolting components. The category was ranked in the high Knowledge, moderate Susceptibility grouping as conditions for wear should not exist for these components.

Table 9.121. Summary of WEAR scores for high-strength bolting in PWR environments

Material/Environment	Degradation Mode	Average Knowledge	Average Susceptibility
High strength bolts in reactor primary water – no irradiation	WEAR	2.13	1.13

9.10.1.2 Closure Studs in PWRs

Closure studs serve an important function in both PWR and BWR applications. These components are typically made of carbon and low alloy steels, which were examined in previous sections. Closure studs were scored and considered separately for the EMDA and past PMDA activity.

No significant gaps in knowledge for extended service were identified for closure studs in PWRs.

Boric Acid Corrosion

As noted previously, carbon and low alloy steels are highly susceptible to BAC. However, BAC can occur in carbon and low alloy steels if the boric acid is leaking from the PWR primary pressure boundary. This has been observed in multiple power plants in recent years. The expert panel ranked three categories of BAC for closure studs in the high Knowledge, moderate Susceptibility grouping based on past experience.

Table 9.122. Summary of BAC scores for closure studs in PWR environments

Material/Environment	Degradation Mode	Average Knowledge	Average Susceptibility
SA-193 Gr B7 in primary water (in case of flange leak)	BAC	2.33	1.78
SA-540 Gr B24 in hot air environment	BAC	2.33	1.56
SA-193 Gr B7 in air environment	BAC	2.56	1.44

Erosion Corrosion

Erosion corrosion can occur for carbon and low alloys steel closure studs in the event of a flange leak and was ranked in the high Knowledge, moderate Susceptibility grouping.

Table 9.123. Summary of EC scores for closure studs in PWR environments

Material/Environment	Degradation Mode	Average Knowledge	Average Susceptibility
SA-193 Gr B7 in primary water (in case of flange leak)	EC	2.13	1.78

Fatigue and Corrosion Fatigue

Corrosion fatigue for closure studs was scored in the high Knowledge, moderate or low Susceptibility groupings. The panelists viewed fatigue loading as inconsequential, although if operational conditions over extended service change, corrosion fatigue damage is possible.

Table 9.124. Summary of FAT scores for closure studs in PWR environments

Material/Environment	Degradation Mode	Average Knowledge	Average Susceptibility
SA-193 Gr B7 in primary water (in case of flange leak)	FAT	2.11	1.00
SA-193 Gr B7 in air environment	FAT	2.44	1.00
SA-194 Gr B16 in air environment	FAT	2.44	1.00
SA-540 Gr B24 in hot air environment	FAT	2.25	0.89
SA-453 Gr 660 in air environment	FAT	2.38	0.89

Fracture Resistance

Fracture resistance was evaluated for carbon steel closure studs under extended service operations. The expert panel scored all categories of FR in the high Knowledge, moderate Susceptibility grouping with very low Susceptibility scores. The experts noted that there are minimal material changes even over very long lifetimes although there is relatively little data and understanding of the mechanisms.

Table 9.125. Summary of FR scores for closure studs in PWR environments

Material/Environment	Degradation Mode	Average Knowledge	Average Susceptibility
SA-193 Gr B7 in air environment	FR	2.22	1.11

General Corrosion

The expert panel scored general corrosion of carbon steel closure studs in the high Knowledge, moderate Susceptibility grouping. The panelists noted that corrosion susceptibility is strongly affected by environmental conditions and should not be an issue in air environments.

Table 9.126. Summary of GC scores for closure studs in PWR environments

Material/Environment	Degradation Mode	Average Knowledge	Average Susceptibility
SA-193 Gr B7 in air environment	GC	2.67	1.11

Stress Corrosion Cracking

The expert panel scored SCC of carbon closure studs in the high Knowledge, moderate Susceptibility grouping. The panelists noted that corrosion susceptibility is strongly affected by environmental conditions and should not be an issue in air environments, but could occur if the surfaces remain wetted.

Table 9.127. Summary of SCC scores for closure studs in PWR environments

Material/Environment	Degradation Mode	Average Knowledge	Average Susceptibility
SA-193 Gr B7 in Primary Water (in case of flange leak)	SCC	2.22	1.33
SA-193 Gr B7 in air environment	SCC	2.67	1.22
SA-194 Gr B16 in air environment	SCC	2.67	1.22
SA-540 Gr B24 in hot air environment	SCC	2.44	1.22
SA-453 Gr 660 in air environment	SCC	2.56	1.22

9.10.1.3 Copper–Zinc Tubes in PWRs

Copper–zinc tubes are used in service water discharge piping in modern PWRs. Several degradation modes were considered by the expert panel. These included SCC, pitting, crevice corrosion, MIC and dealloying. In all cases, the panelists noted the importance of specific water conditions, which will drive susceptibility for these alloys. The color score indication for pitting moved into the red category, but its susceptibility score was not significantly higher than the other four degradation modes. Brass is more susceptible to these forms of degradation than other CuZn alloys, although these forms of degradation can also occur in other CuZn alloys given the proper water conditions.

Table 9.128. Summary of PIRT scores for CuZn Tubes in PWR environments

Material/Environment	Degradation Mode	Average Knowledge	Average Susceptibility
Copper–zinc tubes in service water	SCC	2.25	1.88
Copper–zinc tubes in service water	PIT	2.75	2.00
Copper–zinc tubes in service water	CREV	2.50	1.88
Copper–zinc tubes in service water	MIC	2.38	1.57
Copper–zinc tubes in service water	DEALLOY	2.63	1.88

9.10.1.4 Copper–Nickel Tubes in PWRs

Copper–nickel tubes are used in service water discharge piping in PWRs. The degradation modes considered by the panel included SCC, pitting, crevice corrosion, MIC and dealloying. In all cases, the panelists noted the importance of specific water conditions, which will drive susceptibility for these alloys. The higher Ni content in these tubes offers greater resistance to corrosion degradation than that exhibited by the CuZn tubes discussed in the previous section.

Table 9.129. Summary of PIRT scores for CuNi Tubes in PWR environments

Material/Environment	Degradation Mode	Average Knowledge	Average Susceptibility
Copper–nickel tubes in service water	SCC	2.67	1.11
Copper–nickel tubes in service water	PIT	2.44	1.33
Copper–nickel tubes in service water	CREV	2.44	1.56
Copper–nickel tubes in service water	MIC	2.67	1.44
Copper–nickel tubes in service water	DEALLOY	2.25	1.43

9.10.1.5 BORAL® Panels in PWRs

BORAL® panels are used in spent fuel pools as criticality control. The expert panel considered a number of degradation modes, including general corrosion, pitting and crevice corrosion. All categories were ranked in the high Knowledge, moderate Susceptibility grouping. There are known observations of degradation of this material in service, although these components are readily replaceable.

Table 9.130. Summary of PIRT scores for BORAL® panels in PWR environments

Material/Environment	Degradation Mode	Average Knowledge	Average Susceptibility
BORAL® panels in spent fuel pool water	GC	2.56	1.33
BORAL® panels in spent fuel pool water	CREV	2.56	1.56
BORAL® panels in spent fuel pool water	PIT	2.44	1.56

9.10.1.6 Zircaloy-Based Fuel Assemblies in PWRs

Zircaloy-fuel cladding and fuel assembly structures are stored in spent fuel pools following use in the reactor core. While not structural or safety components, the expert panel considered SCC and general corrosion degradation mechanisms. All categories were ranked in the high Knowledge, moderate Susceptibility grouping. In all cases, the panelists noted that service observations of problems (particularly general corrosion) with these components in spent fuel pools is likely due to loss of water chemistry control rather than a generic vulnerability of the Zircaloy. However, material state in the fuel pool will depend upon the burn-up, degree of oxidation, and adhesion of the oxide layer.

Table 9.131. Summary of PIRT scores for Zr-based fuel assemblies in PWR environments

Material/Environment	Degradation Mode	Average Knowledge	Average Susceptibility
Zr-based fuel assemblies in spent fuel pool water	SCC	2.67	1.11
Zr-based fuel assemblies in spent fuel pool water	GC	2.56	1.11

9.10.1.7 Ferritic Stainless Steels in PWRs

Ferritic stainless steel alloys 405 and 409 are also used in the secondary side of steam generators in PWRs. The expert panel rated these materials in the secondary environment for SCC and crevice corrosion. In both cases, the panelists noted the importance of specific water conditions, which will drive susceptibility for these alloys.

Table 9.132. Summary of PIRT scores for 405 and 409 ferritic SS in PWR environments

Material/Environment	Degradation Mode	Average Knowledge	Average Susceptibility
405 and 409 SS in secondary water	SCC	2.50	1.25
405 and 409 SS in secondary water	CREV	2.50	1.25

9.10.2 Other Materials in BWRs

As described above for PWRs, many other metallic alloys play important roles in BWR systems. These include high strength bolting alloys in the core internals, closure studs (carbon and low alloy steels, again considered as a separate group for this and the past PMDA activity), brass tubes, titanium tubes and aluminum alloys. The scores for the major degradation modes considered are summarized below. Additional details on individual scores by panelists, their comments and rationale, and parts and component numbers used in *NUREG/CR-6923* are also shown in Appendix K.

Two knowledge gaps for high strength bolting applications in BWR environments were identified via the PIRT process. These included the impact of irradiation on fracture resistance and SCC, particularly for X-750 used in core internal applications and SCC susceptibility at very long lifetimes for XM-19 and X-750.

No significant gaps in knowledge for extended service were identified for closure studs in BWRs. Further, no significant gaps were identified for brass tubes, Ti-tubing, or 6061-T6 components although the importance of maintaining good water chemistry control was noted for each material system.

9.10.2.1 High Strength Bolting in BWRs

High-strength, precipitation-hardened Ni-base alloys are frequently used for core internal bolting applications in PWRs, including fasteners and springs. These alloys are exposed to primary reactor coolant and irradiation damage. The scores for the major degradation modes considered are summarized below. Additional details on individual scores by panelists, their comments and rationale, and parts and component numbers used in NUREG/CR-6923 are also shown in Appendix K.

Two knowledge gaps for high strength bolting applications in BWR environments were identified via the PIRT process including a reduction in fracture resistance and SCC susceptibility for X-750 and XM-19.

Fatigue and Corrosion Fatigue

High strength bolts in BWR applications were scored in the high Knowledge, moderate Susceptibility grouping for three categories of FAT in both NWC and HWC environments. This is based on broad service experience with these components. Potential ripple loading and changes in flow conditions may needto be considered for more component-specific evaluation of conditions.

Table 9.133. Summary of FAT scores for high-strength bolting in BWR environments

Material/Environment	Degradation Mode	Average Knowledge	Average Susceptibility
XM-19 in reactor water – low fluence irradiation up to 0.5 dpa	FAT	2.38	1.75
X-750 in reactor water – low fluence irradiation up to 0.5 dpa	FAT	2.44	1.67
X-750 in reactor water – no irradiation	FAT	2.44	1.56
XM-19 in reactor water – low fluence irradiation up to 0.5 dpa	FAT-HWC	2.38	1.50
X-750 in reactor water – no irradiation	FAT-HWC	2.22	1.44
X-750 in reactor water – low fluence irradiation up to 0.5 dpa	FAT-HWC	2.22	1.44

Fracture Resistance

As noted in several sections previously, decrease in fracture resistance is a key issue for most alloys serving as core internals, including high strength Ni-based alloys. As service life increases, so does the fluence accumulated over service life. Further, power uprates may also increase flux and thus increase total radiation damage over a lifetime. Decrease in fracture resistance for these materials in reactor water was scored in the low Knowledge, high Susceptibility category for X-750 due to service observations and a lack of relevant laboratory data. Similarly, fracture resistance of XM-19 in reactor water was scored in the low Knowledge, moderate Susceptibility grouping. Changes in mechanical performance are expected due to possible changes in microstructure under irradiation.

Table 9.134. Summary of FR scores for high-strength bolting in BWR environments

Material/Environment	Degradation Mode	Average Knowledge	Average Susceptibility
X-750 SS in reactor water – low fluence irradiation up to 0.5 dpa	FR	1.89	2.13
XM-19 in reactor water – low fluence irradiation up to 0.5 dpa	FR	1.75	1.71
X-750 SS in reactor water – no irradiation	FR	2.00	1.88

Stress Corrosion Cracking

SCC is a known issue for these high-strength Ni alloys, even in low corrosion-potential environments, and has been observed in service. Extended service will result in increased time exposed to the high-temperature water environment and under stress. Further, for core internals, an increased fluence will be experienced due to longer service and power uprates. PIRT scoring for X-750 in BWR environments were scored in the high Knowledge, high Susceptibility category due to problems identified in service, while XM-19 was judged to be of lower susceptibility due its better field experience.

Table 9.135. Summary of SCC scores for high-strength bolting in BWR environments

Material/Environment	Degradation Mode	Average Knowledge	Average Susceptibility
X-750 SS in reactor water – low fluence irradiation up to 0.5 dpa	SCC	2.44	2.44
X-750 SS in reactor water – no irradiation	SCC	2.56	2.33
XM-19 SS in reactor water – low fluence irradiation up to 0.5 dpa	SCC	2.25	1.75
X-750 SS in reactor water – no irradiation	SCC-HWC	2.44	2.11
X-750 SS in reactor water – low fluence irradiation up to 0.5 dpa	SCC-HWC	2.33	2.00
XM-19 SS in reactor water – low fluence irradiation up to 0.5 dpa	SCC-HWC	2.25	1.75

9.10.2.2 Closure Studs in BWRs

Closure studs also serve an important function in BWR applications. These components are typically made of carbon and low alloy steels, which were discussed in previous sections. These components were scored and considered separately for the EMDA and past PMDA activity.

No significant gaps in knowledge for extended service were identified for closure studs in BWRs.

Crevice Corrosion

Crevice corrosion of carbon and low alloy steel closure studs was scored in the high knowledge, moderate susceptibility grouping, but significant problems are only anticipated when the environment is poorly controlled.

Table 9.136. Summary of CREV scores for closure studs in BWR environments

Material/Environment	Degradation Mode	Average Knowledge	Average Susceptibility
SA-540 Gr B21 in suppression pool water	CREV	2.67	1.67
SA-193 Gr B7 in containment air	CREV	2.56	1.11

Erosion Corrosion

Erosion corrosion of closure studs, which only occurs in case of a flange leak was scored in the

high knowledge, moderate susceptibility grouping.

Table 9.137. Summary of EC scores for closure studs in BWR environments

Material/Environment	Degradation Mode	Average Knowledge	Average Susceptibility
SA-540 carbon steel in containment air	EC	2.44	1.44

Fatigue and Corrosion Fatigue

Fatigue and corrosion fatigue for closure studs was scored in the high Knowledge, moderate Susceptibility groupings. The panelists viewed fatigue loading as inconsequential, although if operational conditions over extended service change, corrosion fatigue damage is possible.

Table 9.138. Summary of FAT scores for closure studs in BWR environments

Material/Environment	Degradation Mode	Average Knowledge	Average Susceptibility
SA-540 Gr B21 in suppression pool water	FAT	2.22	1.00
SA-540 carbon steel in containment air	FAT	2.67	1.00
SA-193 Gr B7 in containment air	FAT	2.56	1.00

Fracture Resistance

Fracture resistance was evaluated for closure studs under extended service operations. The expert panel scored all categories in the high Knowledge, moderate Susceptibility grouping with very low Susceptibility scores. The experts noted that there are minimal material changes over long operational periods although there is relatively little data and understanding of the mechanisms.

Table 9.139. Summary of FR scores for closure studs in BWR environments

Material/Environment	Degradation Mode	Average Knowledge	Average Susceptibility
SA-540 carbon steel in containment air	FR	2.13	1.25
LAS lug welds SFA5.5:15-308 in containment air	FR	2.22	1.00

General Corrosion

The expert panel scored general corrosion of closure studs in the high Knowledge, moderate Susceptibility grouping. The panelists noted that corrosion susceptibility is strongly affected by water chemistry control.

Table 9.140. Summary of GC scores for closure studs in BWR environments

Material/Environment	Degradation Mode	Average Knowledge	Average Susceptibility
SA-540 Gr B21 in suppression pool water	GC	2.33	1.56

Pitting

The expert panel scored pitting of closure studs in BWR service in the high Knowledge, moderate Susceptibility grouping. The panelists noted that pitting susceptibility is strongly affected by water chemistry control and temperature, which should be low for this environment.

Table 9.141. Summary of PIT scores for closure studs in BWR environments

Material/Environment	Degradation Mode	Average Knowledge	Average Susceptibility
SA-540 Gr B21 in suppression pool water	PIT	2.56	1.89

Stress Corrosion Cracking

SCC can occur in carbon and low alloy steels for a variety of reasons in service. For suppression pool water, SCC was ranked in the high Knowledge, high Susceptibility grouping due to the potential for different stress states, different levels of cold work, and potential poor water control. The expert panel scored this form of degradation in the high Knowledge, moderate Susceptibility grouping for containment air. The panelists noted that stress corrosion cracking susceptibility is strongly affected by environmental conditions and should not be an issue in air environments, but could occur if the surfaces remain wetted.

Table 9.142. Summary of SCC scores for closure studs in BWR environments

Material/Environment	Degradation Mode	Average Knowledge	Average Susceptibility
SA-540 Gr B21 in suppression pool water	SCC	2.38	2.25
SA-193 Gr B7 in containment air	SCC	2.67	1.11

9.10.2.3 Brass in BWRs

Brass is used in BWR applications as spray piping for the spray header in the drywell environment. As such, this alloy experiences suppression pool water environments. A number of degradation modes were considered by the expert panel, including fatigue/corrosion fatigue, SCC, pitting, general corrosion, crevice corrosion, MIC, and dealloying. In all cases, the panelists noted the importance of specific water conditions, which will drive susceptibility for these alloys. All categories were scored in the high Knowledge, moderate Susceptibility grouping.

Table 9.143. Summary of PIRT scores for brass in BWR environments

Material/Environment	Degradation Mode	Average Knowledge	Average Susceptibility
Brass in suppression pool water	FAT	2.75	1.00
Brass in suppression pool water	SCC	2.50	1.13
Brass in suppression pool water	MIC	2.71	1.43
Brass in suppression pool water	PIT	2.63	1.63

Table 9.143. Summary of PIRT scores for brass in BWR environments (continued)

Material/Environment	Degradation Mode	Average Knowledge	Average Susceptibility
Brass in suppression pool water	GC	2.63	1.50
Brass in suppression pool water	CREV	2.63	1.50
Brass in suppression pool water	DEALLOY	2.50	1.50

9.10.2.4 Titanium Tubes in BWRs

Titanium tubes are utilized in the BWR main condenser and may be exposed to seawater on the inside of the tube. Several degradation modes were considered by the expert panel including fatigue, SCC, erosion corrosion and galvanic corrosion. All categories were scored in the high Knowledge, moderate Susceptibility grouping. The panelists noted that hydrides from loss of cathodic protection for the Ti alloy may drive embrittlement and performance issues. Erosion corrosion is also a known issue for the main condenser tubing, but Ti alloys are not as susceptible.

Table 9.144. Summary of PIRT scores for Ti-tubes in BWR environments

Material/Environment	Degradation Mode	Average Knowledge	Average Susceptibility
Titanium tubes in seawater	FAT	2.67	1.00
Titanium tubes in seawater	SCC	2.78	1.00
Titanium tubes in seawater	EC	2.67	1.78
Titanium tubes in seawater	GALV	2.67	1.67
Titanium tubes in wet steam	EC	2.67	1.89

9.10.2.5 Aluminum Alloy 6061-T6 in BWRs

Aluminum alloy 6061-T6 is used in the cycled condensate storage tank in the form of plates, pipes, supports, shells, flanges, vents, and nozzles. The expert panel considered a number of degradation modes, including fatigue/corrosion fatigue, SCC, pitting and crevice corrosion. All categories were scored in the high Knowledge, moderate Susceptibility grouping.

Table 9.145. Summary of PIRT scores for Al 6061-T6 in BWR environments

Material/Environment	Degradation Mode	Average Knowledge	Average Susceptibility
6061-T6 in demineralized water	FAT	2.67	1.13
6061-T6 in demineralized water	SCC	2.67	1.11
6061-T6 in demineralized water	PIT	2.78	1.22
6061-T6 in demineralized water	CREV	2.78	1.33

9.10.3 Summary of PIRT Findings for Other Materials

Previous sections of the PIRT analysis focused on major alloy groups including wrought and CASS, Alloy 600 and its weldments, Alloy 690 and its weldments, carbon steels, and low alloy steels. While these materials comprise the majority of LWR components, other materials are also in use in a variety of environments.

Several knowledge gaps were identified via the PIRT process for high strength bolting in both BWR and PWR systems:

- Impact of irradiation on fracture toughness, irradiation creep, swelling, and SCC of high strength bolting materials used in core internal applications

- During long operational periods, SCC susceptibility of high strength bolting due to potential microstructure changes.

No significant gaps in knowledge for extended service were identified for closure studs in PWRs or BWRs. Further, no significant gaps were identified for CuZn tubes, CuNi tubes, BORAL® panels, Zr-fuel assemblies, or 405/409 steels in PWRs nor were gaps found for brass tubes, Ti-tubing, or 6061-T6 components in BWRs. The importance of maintaining good water chemistry control was noted for each material system.

9.11 SUMMARY LISTING OF KEY PIRT FINDINGS

In the previous seven sections, the PIRT data was analyzed in considerable detail for each alloy system in both PWRs and BWRs. A number of knowledge gaps were identified, consistent with the findings of the background chapters developed *a priori* and presented earlier. While this material has been presented in earlier sections, a summary review is offered here for convenience.

9.11.1 Wrought Stainless Steels

Stainless steels represent a significant class of alloys used for LWR applications, including piping, joints, liners, weldments, and structural supports. Previous sections presented the results of the PIRT scoring for wrought stainless steels starting with PWR conditions and then BWR environments.

The PIRT scoring process for PWR environments identified several knowledge gaps, including:

- Impact of irradiation on fracture toughness, irradiation creep, swelling, and SCC for 304 SS, 316 SS, 347 SS, and 308/309 SS weldments

- SCC susceptibility for up to 80 years of service for 304 SS, 316 SS, and 308/309 SS weldments. The extent of these knowledge gaps is impacted by unknowns associated with synergisms between different degradation modes; for instance, the effect on SCC of irradiation damage and thermal embrittlement, which are very time-dependent. These concerns were covered in more detail in earlier alloy-specific chapters

- Potential impact of poor water chemistry control in service water on crevice corrosion, pitting, and MIC for 304 SS, 316 SS, and 308/309 SS weldments

- Cumulative impact of fatigue on component integrity for 304 SS and 316 SS structures. Recent data on corrosion fatigue crack initiation of wrought stainless steels in BWR-HWC and PWR primary environments indicate, contrary to intuition, the corrosion fatigue resistance may be reduced under these reducing water chemistry conditions.

In BWR environments, a similar series of gaps was identified, specifically, the following items:

- Impact of irradiation on fracture toughness and SCC in both NWC and HWC environments for 304 SS, 316 SS, and 308/309 SS weldments

- SCC susceptibility at long reactor operation periods, particularly in NWC environments for 304 SS, 316 SS, and 308/309 SS weldments

- Cumulative impact of fatigue on component integrity, particularly weldolets, sockolets, and components in the upper core internals

9.11.2 Alloy 600 and Alloy 182/82 Weldments

Nickel alloys and weld metals were chosen for LWR components because of low corrosion rate, resistance to SCC, and thermal expansion coefficient that is similar to that of low alloy RPV steel. PWR components include nozzles, piping, control rod drive feedthroughs, and steam generator tubing among others. BWR components containing Alloy 600 and Alloy 182 and 82 weld metals include RPV attachment welds, head bolts, feedwater nozzles, safe end butters, and supports.

In PWR environments, no low-Knowledge areas were identified. However, several outstanding issues were raised by the expert panel for additional consideration, including:

- SCC was identified as a high Knowledge, high Susceptibility mode of degradation in all primary and secondary environments for Alloy 600 and Alloy182/82 weldments. This is a known issue for these alloys.

- Wear was identified as a high Knowledge, high Susceptibility mode of degradation in secondary coolant environments for Alloy 600. This is a known form of degradation.

- Fracture resistance in 182/82 welds at lower temperatures has been noted in laboratory testing although the mechanism is not completely understood.

As stated above, in BWR environments, all scoring was in the high Knowledge category but the panelists did identify several areas for further consideration. Specifically:

- SCC was identified as a high Knowledge, high Susceptibility mode of degradation for Alloy 600 and Alloy 182/82 weldments in NWC environments. This is a known issue for these alloys at high potential.

- Fracture resistance issues in Alloy 182/82 welds at lower temperatures have been noted in laboratory testing although the mechanism is not entirely understood.

9.11.3 Alloy 690 and Alloy 152/52 Weldments

Wrought Alloy 690 and its associated weld metals (Alloys 152, 52, 52M, and other variants) have become the common replacement and repair materials for Alloy 600 and Alloy 182/82 weld metals, primarily due to their superior resistance to primary-side SCC. During the PIRT process, the expert panel considered 22 different alloy/environment categories. No knowledge gaps were identified for Alloy 690 or Alloy 152/52 weldments under subsequent operating periods in PWR environments via the PIRT process. The panelists did note that SCC, fatigue cracking, and pitting should be minimal for Alloy 690, although good water chemistry must be maintained. The differences in scoring and knowledge gaps identified between Alloy 600 and Alloy 690 are consistent with expectations based on service experience. Indeed, this improved resistance to corrosion is a driving factor in replacement of Alloy 600 with Alloy 690.

9.11.4 Carbon and Low Alloy Steels

Carbon and low alloy steels are used for various components subjected to different environments (temperature, stress, and water of different chemistry) within the nuclear power plant. These ductile structural materials are used as pressure boundary materials in pressure vessels and piping in the RCS, ECCS, secondary water, and service water systems of LWRs. These alloys are attractive for this use owing to their relatively low cost, good mechanical properties in thick sections, and good weldability. In reactor coolant system components, such as the pressure vessel, pressurizer, and some piping, the carbon and low alloy steels are clad on the inside wetted surface with corrosion-resistant materials such as austenitic stainless steels or nickel-base alloys. A number of key issues are possible for these components. Carbon and low alloy steels are susceptible to irradiation damage, even at low fluence. These materials are also susceptible to fatigue damage, pitting, FAC, and MIC in some piping and water chemistry environments. These alloys are also highly susceptible to BAC in the event of leaks in PWR environments.

No significant knowledge gaps were identified for carbon and low alloy steels in PWR environments following analysis of the PIRT scoring. However, several trends and common themes were identified:

- Carbon and low alloy steels are highly susceptible to BAC but only in the event of a leak of primary coolant. This is a well-known form of degradation.

- Crevice corrosion, pitting, MIC, and general corrosion of carbon steel and low alloy steel were identified as high-knowledge modes of degradation, but only in the event of loss of water chemistry control or failure of protective features such as liners or cathodic protection. These are well-known forms of degradation.

- Flow-accelerated corrosion is a well-known form of degradation for low alloy and carbon steels, but can be exacerbated in elbows; changing water chemistry and flow conditions as well as longer service life and exposure to FAC conditions may increase susceptibility. Predictive models based on empirical observation or mechanistic understanding have been developed in the United States, Europe, and Japan.

- Stress corrosion cracking and corrosion fatigue are possible for these alloys, but SCC is relatively rare in service. The reasons for this rarity are reasonably well understood and are discussed in some detail in Chapter 5. Changes in loading or increases in water chemistry

conditions (such as chloride content) may drive increased susceptibility over a long operating period. Further aspects needing confirmation are synergistic effects between SCC susceptibility and other degradation modes associated with irradiation hardening and embrittlement, temper embrittlement and dynamic strain aging, which may dominate over long-term operation.

Similar to the PWR assessment, no significant knowledge gaps were identified for carbon and low alloy steels in BWR environments following analysis of the PIRT scoring. However, several trends and common themes were identified:

- Crevice corrosion; pitting; general corrosion, FAC, and MIC of low alloy steel were identified as high Knowledge, moderate Susceptibility modes of degradation for most environments. However, these are expected to be an issue only in the event of a loss of water chemistry control. These are well-known forms of degradation.

- Stress corrosion cracking and corrosion fatigue are possible for these alloys, but unlikely in service. Changes in loading or increases in chemical conditions may drive increased susceptibility over a long operating period.

9.11.5 Cast Austenitic Stainless Steels

Cast austenitic stainless steel is used in a variety of components in both BWRs and PWRs including for reactor coolant, auxiliary system piping, reactor coolant pump casings, and reactor coolant valve bodies and fittings. Piping and pump casings in BWRs may be exposed to NWC and HWC conditions. Low-level irradiation is also possible in some core internal locations. In PWRs, these alloys experience the primary water environment.

One potential knowledge gap for CASS materials was identified for both PWR and BWR environments using the PIRT data. Specifically, the effects of long-term thermal aging for extended operating periods may drive changes in mechanical or corrosion performance that are relatively unknown. This is consistent with the conclusions of the background assessment presented in Chapter 6.

9.11.6 Other Material Systems

Previous sections of the PIRT analysis focused on major alloy groups. While these materials comprise the majority of LWR components, other materials are also very important. Tubes of CuZn or CuNi alloys are used in both BWR and PWR applications. Precipitation-hardened Ni-base alloys are used for high strength bolting application in LWRs. Closure studs of carbon and low alloy steel also serve a very specific function in both BWR and PWR applications. BORAL® panels and Zircaloy systems are found in spent fuel pools and degradation has been observed in service. Titanium and Al-based tubing are utilized in BWR applications. The expert panel considered a number of different degradation modes for these other important materials.

Several knowledge gaps were identified via the PIRT process for high strength bolting in both BWR and PWR systems:

- Impact of irradiation on fracture toughness, irradiation creep, swelling, and SCC of high strength bolting materials used in core internal applications

- SCC susceptibility of high strength bolting during long-term operation due to potential microstructure changes.

No significant gaps in knowledge for extended service were identified for closure studs in PWRs or BWRs. Further, no significant gaps were identified for CuZn tubes, CuNi tubes, BORAL® panels, Zr-fuel assemblies, or 405/409 SS in PWRs nor any gaps identified for brass tubes, Ti-tubing, or Al 6061-T6 components in BWRs. The importance of maintaining good water chemistry control was noted for each material system.

9.12 OTHER POTENTIAL GAPS IDENTIFIED BY THE EXPERT PANEL

In addition to the specific technical issues for specific material degradation modes and material systems, the expert panel also felt strongly about several other key potential considerations. The items below are not specific material degradation issues and represent the personal opinion of the majority (if not entirety) of the expert panel. While not technical, the expert panel felt strongly that these topics may also ultimately be gaps for extended operation and should be mentioned here.

Knowledge retention and transfer is a key factor in capturing knowledge from past generations to future operators, regulators, and researchers who will support extended service operations. Knowledge" represents the subset of information which is known with some certainty, and "expertise" involves greater subtlety associated with the much larger myriad of information that is a combination of complex, not well distilled, ambiguous, and even conflicting. Sustaining expertise is a much more challenging process than transferring knowledge. Similarly, a loss of laboratory capacity could be limiting when trying to close knowledge gaps. Each is briefly addressed below.

9.12.1 Expertise

Knowledge (information) transfer is important, but is a miniscule part of maintaining the expertise necessary to understand and interpret degradation, not to mention advancing the state of understanding. Expertise is broadly acknowledged to require one or more decades of focused experience, and all recognized international experts in this particular field have come from a background of laboratory experience, presumably because it has given them an opportunity to directly observe degradation and the effects of key variables, in addition to observing and interpreting field problems. At all levels and in all organizations, the investment in expertise has diminished for a quarter century, and existing expertise has been mined with little consideration for the future. There is little encouragement or opportunity for people to build deep and broad expertise, and pressures to move into management or shift into other areas of research are great. Most experts on this panel are retired, and several more are at retirement age. The gap in expertise between experts on this panel and the next, much smaller generation of researchers cannot be understated. This could leave a population of fewer experts whose knowledge and experience represents a small fraction of that acquired by acknowledged experts today. This is the *overriding concern* for the majority of the expert panelists and will take immediate and considerable action to correct. The loss of knowledge, experience, intuition, and judgment of the current experts is transferable for a limited time. Once the "expert" retires and does not keep up with the technology then his ability to transfer his knowledge effectively is limited to 5 years at the most. If that experience is lost it could require ten or twenty times as much time and money to regenerate from scratch.

9.12.2 Laboratory Capability

The dramatic drop in R&D funding in the last decade or two has considerably reduced the availability of high quality, proven laboratory capability to address the key, complex issues that are crucial to quantify for long-term operation. This is directly related to knowledge transfer of expertise.

9.13 REFERENCES*

1. P. L. Andresen et al., *Expert Panel Report on Proactive Materials Degradation Analysis,* NUREG/CR-6923 (BNL-NUREG-77111-2006), U.S. Nuclear Regulatory Commission, February 2007.
2. EPRI, *EPRI Materials Degradation Matrix,* Document 3002000628, Electric Power Research Institute, May 2013.
3. EPRI, *EPRI Materials Reliability Program: Pressurized Water Reactor Issue Management Tables—Revision 2 (MRP-205),* Document 1021024, Electric Power Research Institute, October 2010.

* Inclusion of references in this report does not necessarily constitute NRC approval or agreement with the referenced information.

10. RECOMMENDATIONS AND CONCLUSIONS

A systematic assessment of degradation mechanisms that could impact passive long-lived systems, structures, and components is a valuable tool to help prioritize research needs to support possible license renewal decisions for beyond 60 years. A panel of international experts was assembled to examine and rank degradation modes for possible extended operation up to 80 years. This volume detailed the results of expert panel assessment of the aging and degradation of core internals and piping components of light-water reactors. The main objectives were to identify core internal and primary piping components of LWRs where degradation is likely to occur, to define relevant aging and degradation modes and mechanisms, and to perform systematic assessment of the aging effects on the future integrity of those components. The approach adopted by the panel is based on the Phenomena Identification and Ranking Table process.

Materials degradation phenomena in the core internals and primary piping components is complex processes and involves many material and operational variables including different alloys, environments, stress states, irradiation levels, and operating times. Past degradation ranking efforts provided a systematic and detailed assessment of the susceptibility and knowledge for many of those material, environment, and degradation combinations.

The expert panel deliberated and identified key forms of degradation and potential concerns for extended service operations. Volume 2 of the EMDA report provided expert background assessments of corrosion, stress corrosion cracking, thermal effects, and irradiation for key material systems in core internal and piping systems. Based on the technical background assessments, the panel then developed a PIRT matrix with a list of degradation scenarios to score. Panelists independently scored each of 1,020 distinct degradation scenarios in three categories: susceptibility, confidence, and knowledge. Subsequent debate and discussion among panelists was an important part of the process to ensure all points of view were considered. Finally, the results of the PIRT scoring were compiled and used to identify potential knowledge gaps for extended service conditions.

As part of the PIRT analysis, 451 categories were scored for PWR degradation and 569 categories were scored for BWR degradation. Only a small fraction of scores fall into the low Knowledge regime for both PWR and BWR cases. Indeed, only 57 out of 1,020 categories were scored in the low Knowledge categories. The vast majority of scores (>75% for both PWR and BWR) fall into the high Knowledge, moderate Susceptibility category. This indicates that the panelists agreed that the majority of degradation modes considered are well known and manageable to some extent.

Low Knowledge, high Susceptibility degradation modes are those that could be detrimental to service with high Susceptibility (>2) scores and low Knowledge scores (<2). These scores indicate gaps in understanding and can be considered to be identified research to inform degradation mechanisms and underlying causes to predict occurrence during long-term operation. A total of 27 categories were scored in this grouping as part of the PIRT analysis (less than 3%). All of these categories were related to high fluence irradiation effects on core internals. It is important to note that this PIRT process makes no judgment or evaluation on the number of components or significance to structural integrity or safety for a given component, material, or degradation mode. This caveat should be considered when making research priorities and other high Knowledge categories should also be evaluated in that process.

The technical background assessment for irradiation effects identified several modes of degradation that could be key during the subsequent operating period. These included the influence of more direct irradiation effects such as hardening, potential phase transformations, swelling and irradiation creep, which may play more significant roles at high fluences. These changes may also have a significant effect on irradiation-induced embrittlement and stress corrosion cracking although the understanding of the interdependencies and synergies at high fluences are yet to be fully developed. These assessments were confirmed following analysis of the PIRT scoring. All 27 low Knowledge, high Susceptibility categories (summarized in Tables 9.4 and 9.5 of Volume 2) are related to fracture resistance, swelling, and SCC effects at high fluence for stainless steels and high strength bolting in core internal applications. The panelists also identified other experience (e.g. swelling experience with 316 SS in fast reactors) that supports the possibility that these forms of degradation will occur in subsequent operating periods.

For stainless steel components, the assessment of background information identified a number of possible knowledge gaps including SCC effects in low-potential environments, effect of stagnant and off-normal water chemistries, crack growth in weld metals, and crack initiation effects under different loading conditions over long-life times. These were similar gaps as identified by the PIRT scoring process for PWR and BWR environments, which included:

- Effect of irradiation on fracture toughness, irradiation creep, swelling, and SCC for Type 304, 316, 347, and 308/309 SS weldments

- SCC susceptibility at very long lifetimes for 304, 316, and 308/309 weldments, particularly in BWR normal water chemistry (NWC) environments

- Potential impact of poor water chemistry control in service water on crevice corrosion, pitting, and MIC for 304, 317, and 308/309 SS weldments

- Cumulative impact of corrosion and fatigue on component integrity for 304 and 316

Alloy 600 has been used for LWR components and piping applications due to low corrosion rate, general resistance to SCC, and thermal expansion coefficient that is similar to that of low-alloy RPV steel. Over the last two decades, there have been numerous incidents of stress corrosion cracking and that is expected to continue with extended service. No low-Knowledge areas were identified in either PWR or BWR environments. However, several outstanding issues were raised by the expert panel for additional consideration, including:

- SCC was identified as a high Knowledge, high Susceptibility mode of degradation in all primary and secondary PWR environments and in BWR NWC and hydrogen water chemistry (HWC) environments for Alloy 600 and Alloy182/82 weldments. This is a known issue for these alloys.

- Wear was identified as a high Knowledge, high Susceptibility mode of degradation in secondary coolant environments for Alloy 600. This is a known form of degradation.

- A reduction in fracture resistance in 182/82 welds at lower temperatures has been noted in laboratory testing although the mechanism is not completely understood.

Today, wrought Alloy 690 and its associated weld metals (Alloy 152, 52, 52M, and other variants) have become the common replacement and repair materials for Alloy 600 and Alloy 182/82 weld

metals, primarily due to their superior resistance to primary side SCC. No knowledge gaps were identified for Alloy 690 or 152/52 weldments under subsequent operating periods in PWR environments via the PIRT process. The panelists did note that SCC, fatigue cracking, and pitting should be minimal for Alloy 690, although good water chemistry must be maintained.

Carbon and low alloy steels are widely used, important materials and were the focus of considerable discussion in the expert assessment and PIRT scoring activities. Three specific areas of concern were noted. These include potential lack of understanding in key driving factors and predictive tools for fatigue crack initiation, flow-accelerated corrosion, and stress corrosion cracking. Synergistic effects must also be considered when evaluating long service life integrity. No significant knowledge gaps were identified for carbon and low-alloy steels in PWR or BWR environments following analysis of the PIRT scoring. However, several trends and common themes were identified. These are consistent with the background assessment and included:

- Carbon and low-alloy steels are highly susceptible to BAC of carbon steel but only in the event of a leak of primary coolant. This is a well-known form of degradation.

- Crevice corrosion, pitting, microbial-induced corrosion, and general corrosion of carbon steel and low-alloy steel was identified as a high Knowledge mode of degradation, but only in the event of loss of water-chemistry control or failure of protective features such as liners or cathodic protection. These are well-known forms of degradations.

- Flow-accelerated corrosion is a well-known form of degradation for low-alloy and carbon steels, but can be exacerbated in elbows and changing water chemistry and flow conditions and longer service life and exposure to FAC conditions may increase susceptibility.

- Stress corrosion cracking and fatigue are possible for these alloys, but the Susceptibility was scored low (near 1) for most environments considered. Changes in loading or increases in chemical conditions (such as chloride content) may drive increased susceptibility over a long operating period. Other synergistic effects should also be evaluated as noted in the technical background assessment in Chapter 5.

Today, cast austenitic stainless steels (CASS) are used in a variety of applications in both BWRs and PWRs including for reactor coolant, auxiliary system piping, reactor coolant pump casings, reactor coolant valve bodies and fittings. The expert background assessment identified the effects of long-term thermal aging and subsequent degradation on mechanical properties, fracture resistance, and/or corrosion properties as a research need. The PIRT process also identified the effects of long-term thermal aging for extended operating as a knowledge gap.

Other materials beyond these major classes are also in use in a variety of environments and were evaluated as part of the PIRT process. While these materials comprise the majority of LWR components, other materials are also very important. Several knowledge gaps were identified for high strength bolting in both BWR and PWR systems. Specifically, the impact of irradiation on fracture toughness, irradiation creep, swelling, and SCC of high strength bolting materials used in core internal applications and SCC susceptibility over very long lifetimes were noted. No significant gaps in knowledge for extended service were identified for closure studs in PWRs or BWRs. Further, no significant gaps were identified for CuZn tubes, CuNi tubes, BORAL® panels, Zr-fuel assemblies, or 405/409 SS in PWRs nor any gaps identified for brass tubes, Ti-tubing, or Al 6061-T6 components in BWRs. The importance of maintaining good water chemistry control was noted for each material system.

In addition to the specific technical issues for specific material degradation modes and material systems, the expert panel also felt strongly about several other key potential considerations. The items below are not specific material degradation issues and represent the personal opinion of the majority (if not entirety) of the expert panel. While not technical, the expert panel felt strongly that these topics might also ultimately be gaps for extended operation and should be mentioned here. Knowledge retention and transfer is a key factor in capturing knowledge from past generations to future operators, regulators, and researchers who will support extended service operations. Knowledge" represents the subset of information which is known with some certainty, and "expertise" involves greater subtlety associated with the much larger myriad of information that is a combination of complex, not well distilled, ambiguous, and even conflicting. Sustaining expertise is a much more challenging process than transferring knowledge. Similarly, a loss of laboratory capacity could be limiting when trying to close knowledge gaps.

NRC FORM 335
(12-2010)
NRCMD 3.7

U.S. NUCLEAR REGULATORY COMMISSION

BIBLIOGRAPHIC DATA SHEET

(See instructions on the reverse)

1. REPORT NUMBER
(Assigned by NRC, Add Vol., Supp., Rev., and Addendum Numbers, if any.)
NUREG/CR-7153,
Volumes 1 - 5

2. TITLE AND SUBTITLE
Expanded Materials Degradation Assessment (EMDA)

3. DATE REPORT PUBLISHED

MONTH	YEAR
October	2014

4. FIN OR GRANT NUMBER

5. AUTHOR(S)
J. Busby, ORNL

6. TYPE OF REPORT
Technical

7. PERIOD COVERED (Inclusive Dates)

8. PERFORMING ORGANIZATION - NAME AND ADDRESS (If NRC, provide Division, Office or Region, U. S. Nuclear Regulatory Commission, and mailing address; if contractor, provide name and mailing address.)
Oak Ridge National Laboratory
Reactor and Nuclear Systems Division
PO Box 2008
Oak Ridge, TN 37831

9. SPONSORING ORGANIZATION - NAME AND ADDRESS (If NRC, type "Same as above", if contractor, provide NRC Division, Office or Region, U. S. Nuclear Regulatory Commission, and mailing address.)
Office of Nuclear Regulatory Research
Division of Engineering
U.S. Nuclear Regulatory Commission
Washington, DC 20555

10. SUPPLEMENTARY NOTES

11. ABSTRACT (200 words or less)
Most nuclear power plants in the United States are currently licensed for up to 60 years of operation. The nuclear industry is assessing the feasibility of operation for up to 80 years. The U.S. Nuclear Regulatory Commission (NRC) and U.S. Department of Energy (DOE) co-sponsored the Expanded Materials Degradation Assessment (EMDA) to identify information gaps and research priorities for aging related degradation of reactor components for up to 80 years. Expert panels were convened to examine four main component groups using the phenomena identification and ranking technique: reactor core internals and piping systems, the reactor pressure vessel, concrete and civil structures, and electrical cables. Panelists included participants from NRC, DOE national laboratories, industry, academia, and international organizations. The EMDA reports include a ranking of degradation scenarios according to the probability of occurrence and level of knowledge, along with a summary of the current state of knowledge for each component group.

12. KEY WORDS/DESCRIPTORS (List words or phrases that will assist researchers in locating the report.)
Light water reactors
Long term operation
Corrosion
Aging

13. AVAILABILITY STATEMENT
unlimited

14. SECURITY CLASSIFICATION
(This Page)
unclassified
(This Report)
unclassified

15. NUMBER OF PAGES

16. PRICE

Federal Recycling Program

UNITED STATES
NUCLEAR REGULATORY COMMISSION
WASHINGTON, DC 20555-0001

OFFICIAL BUSINESS